PGC-1α in neurodegeneration and ageing

Thesis

Li Li, M.Sc., M.B.B.S.

PhD in Ageing and neurodegeneration

Institute of Healthy Ageing

Institute of Neurology

University College London

Gower Street, London. 20th of November 2016

Declaration

I confirm that the work presented in this thesis is my own. Where information has been derived from other sources, I confirm that this has been indicated in the thesis.

_____

Li Li

PGC-1α in neurodegeneration and ageing

Li Li, M.Sc., M.B.B.S.

PhD Committee:

Prof. Dame Linda Partridge, DBE, FRS, FMedSci

Prof. John Hardy, FRS, FMedSci

Funded by: Parkinson's UK and the Wellcome Trust

PARKINSON'S UK
CHANGE ATTITUDES. FIND A CURE. JOIN US.

wellcome trust

I delicate this work to my beloved family:

my father Yujun Li,
my mother Jingfen Sun,
my father in-law Jian Fu,
my mother in-law Suping Sheng,
my husband Shan Fu, and
my son Li Fu

I am thankful for your love and support.
You are my strong fortress and inspiration.

I would like to delicate this work to the pillars of our family

My grandparents:

Guojie Qin†
Wenfang Li†
Yalan Zhang†
Gui Sun†

Thanks to my cousin Dr. Chong Han for all of your advice and support in the UK.

To my extensive family and friends.

Acknowledgements

First of all I would like to thank my mentors Linda Partridge and John Hardy for their support and guidance. It was a definite pleasure to learn from you both. You are great examples of what I would like to achieve in the future.

Both my master's work and the work presented here would not have been possible without the trust, guidance and support of Kerri Kinghorn. Thanks for taking a chance on me and showing me the road to becoming a great scientist. I truly admire you and I hope I can work together again in the near future.

To my dearest friend Jorge Iván Castillo-Quan who was always there for me to guide me, assist me and keep me grounded and focused. I truly enjoyed your mentorship and support.

Thanks to Teresa Niccoli, Nazif Alic, Dobril Ivanov, Anna Tillmann, Yifan Yu, Yuan Zhao, Nikoleta Vavouraki and Vassilios N Kotiadis for helping me when I needed it the most. You are true stars.

A special thank you to my PhD examiners Dr. Alex Whitworth and Dr. Lazaros Foukas for reading and improving the thesis with your comments, suggestions and corrections.

Thanks to Professors Michael Duchen and Andrey Abramov for their advice and support.

Thanks to my office mates, Thanet Sornda, Thomas Moens, Rubika Balendra, Hongyuan Wang, Peter Rennert, Helena Cochemé, Oyinkan Sofola- Adesakin, Fiona Kerr, and Ann Gilliat. It was a great pleasure to share laughter, stress and frustration and overall the good times.

Thanks to the extensive family at the Institute of Healthy Ageing (past and present): Mobina Khericha, Adam Dobson, Nathan Woodling, Anqi Yan, Mingyao Yang, Xiaoli He, Yan Kong, Matthew Piper, Cathy Slack, Hrovje Augustin, Pedro Martinez†, Giovanna Vinti, Ekin Bolukbasi, David Gems, Jenny Regan, James Catterson, Melissa Cabecinha, Jennifer Addcott, Marcia Merrick, Arj Rajasingam, Inge Snoeren, Mumtaz Ahmad, Michael Wright, Julie Black, Danny Filer, Catherine Au, Marina Ezcurra, Daniel Pearce. Fly pushing, molecular lab work, lunch, all those cakes and desserts, and Christmas parties were special because of you. Thanks!

My Chinese Family in and out of London have played an important part in keeping me sane. Thanks to Xi Wang, Joyce Chen, Tianyi Bu, Ge Zhan, Congcong Wang, Yanjie Zhao, Clare Yu and her family, Gloria, Sue, Sophie, Tailin Xu, Josi, Qiang Gang, Yu Tao, Li Li, and Tiandi Yang. Thanks for all the amazing times together.

Contents

Abstract

Alzheimer's disease (AD) and Parkinson's disease (PD) are the most common age-related neurodegenerative disorders, affecting millions of people worldwide. There are currently no effective or curative therapies for the treatment of these diseases. Genetic studies have demonstrated that mitochondrial dysfunction and oxidative stress play key roles in the pathogenesis of both AD and PD. Therefore, genetic or pharmacological interventions targeting these effectors may prove to be useful therapeutic strategies. In my thesis, I focus on the transcriptional cofactor PGC-1α, a key modulator in many biological processes, including mitochondrial biogenesis, the oxidative stress defence system, the circadian clock, and protein quality control. The possible relevance of this gene in the pathogenesis of AD and PD came to light with the demonstration that PGC-1α gene expression levels are decreased in the post-mortem brain tissues of both AD and PD patients.

Consistent with this, I have shown that up-regulation of PGC-1α in the neurons of a *Drosophila* model of Aβ toxicity rescues lifespan, the behavioural phenotypes and circadian rhythm disruption. I demonstrated that amelioration of Aβ toxicity is associated with improved mitochondrial homeostasis and activation of the ER unfolded protein response (UPR^{ER}). In keeping with this, I also found that rifampicin, an antibiotic used in the treatment of tuberculosis and leprosy, also activated the UPR^{ER} and rescued the neurotoxicity in Aβ-expressing flies. These findings suggest that stimulating the UPR^{ER}, either by increasing intraneuronal PGC-1α levels or through oral administration of rifampicin, may offer significant therapeutic benefits in AD.

Contrary to the results seen using Aβ-expressing flies, I demonstrated that over-expression of PGC-1α did not rescue the neurotoxic phenotypes in *Drosophila* models of familial PD, lacking *PINK1* or *parkin.*

Given an increasing ageing population coupled with the high prevalence of age-related diseases there is an urgent need for the development of pharmacological agents that can improve healthy aging. PGC-1α has been identified as a novel

modulator of fly ageing. The precise mechanisms involved however have not been fully elucidated.

Here I also identified the transcription factor GA-binding protein (*dGABPα*), downstream of PGC-1α, as a key modulator of fly ageing. *dGABPα* gain-of-function extends female lifespan via mechanisms beyond dietary restriction (DR), with an associated reduction in IIS/mTOR signalling. In addition, over-expression of *dGABPα* improved gut homeostasis by delaying age-related over-proliferation of intestinal stem cells. Additionally, *dGABPα* gain-of-function flies showed resistance to xenobiotic stress. Finally, I demonstrated that *dGABPα* up-regulated *ImpL2*, the insulin ligand binding protein, which down-regulates IIS and extends lifespan. Given the evolutionary conserved effects of reduced IIS/mTOR signalling, these findings suggest that GABPα may be an important modulator of mammalian ageing and a potential therapeutic target in the treatment of age-related diseases.

Research impact

Alzheimer's disease (AD) is a progressive brain disorder that causes cellular dysfunction and eventually neuronal loss. Clinically this results in memory loss as well as more widespread cognitive dysfunction. In America alone, more than 5 million people are living with AD, and this number is predicted to triple by 2050. AD is the 6th leading cause of death in the U.S., and there is currently no cure or disease-modifying therapy available.

The main objective of this project was to investigate the neuroprotective properties of PGC-1α using the fruit fly *Drosophila melanogaster* models of Aβ toxicity. PGC-1α, the captain of the mitochondrion, is the key modulator of energy metabolism. The possible relevance of this protein in AD pathogenesis was highlighted by work demonstrating that human post-mortem brains display reduced PGC-1α levels. These findings suggest that elevating PGC-1α expression or activity pharmacologically, or via other means, may prove to be an useful therapeutic strategy.

My work demonstrated that up-regulation of PGC-1α may be neuroprotective, with overexpression of PGC-1α rescuing the neurotoxic phenotypes in Aβ-expressing flies *in vivo*. My study also elucidated the mechanisms associated with the neuroprotective effect of PGC-1α, including improved mitochondrial homeostasis, activation of the unfolded protein response, both of which have been implicated in AD pathogenesis. I also found that metformin and rifampicin, two drugs already licensed for human use, rescued Aβ toxicity through similar mechanisms of activation as PGC-1α. My findings thus highlight the potential therapeutic benefits of either increasing the intraneuronal levels of PGC-1α, or pharmacologically targeting the UPR^{ER} by oral administration of metformin or rifampicin, in treating AD. Future studies are now warranted in mammalian models and in clinical trials.

Genetic manipulations and dietary restriction (DR) in model organisms have proven that lifespan extension is achievable. Most importantly, these same interventions offer protection against a number of age-related diseases and therefore improve general health. Considerable current research efforts are being made to identify novel modulators that mimic healthy lifespan. PGC-1α is one such novel modulator of

ageing that has been shown to extend lifespan in *Drosophila*. In this project, I identified *dGABPα*, as a downstream effector of PGC-1α and a novel modulator of ageing in the fly. I demonstrated that *dGABPα* extended lifespan via mechanisms beyond DR, with an associated reduction in IIS/mTOR signalling. Moreover, activation of *dGABPα* also improved healthy lifespan, including gut homeostasis and resistance to xenobiotic stress. Given the evolutionary conserved effects of reducing IIS/mTOR, this finding suggests that GABPα may prove to be an important modulator of mammalian ageing.

List of Figures

List of Tables

Publications arising from this thesis

Sofola-Adesakin, O., Castillo-Quan, J.I., Rallis, C., Tain, L.S., Bjedov, I., Rogers, I., **Li, L**., Martinez, P., Khericha, M., Cabecinha, M., et al. (2014). Lithium suppresses Abeta pathology by inhibiting translation in an adult Drosophila model of Alzheimer's disease. Front Aging Neurosci *6*, 190.

Kinghorn, K.J., Castillo-Quan, J.I., Bartolome, F., Angelova, P.R., **Li, L**., Pope, S., Cocheme, H.M., Khan, S., Asghari, S., Bhatia, K.P., et al. (2015). Loss of PLA2G6 leads to elevated mitochondrial lipid peroxidation and mitochondrial dysfunction. Brain *138*, 1801-1816.

Castillo-Quan, J.I., **Li, L**., Kinghorn, K.J., Ivanov, D.K., Tain, L.S., Slack, C., Kerr, F., Nespital, T., Thornton, J., Hardy, J., et al. (2016). Lithium Promotes Longevity through GSK3/NRF2-Dependent Hormesis. Cell Rep *15*, 638-650.

Kinghorn, K.J., Castillo-Quan, J.I., **Li, L**., Bhatia, K.P., Abramov, A.Y., Hardy, J., and Partridge, L. (2016). Reply: Glial mitochondropathy in infantile neuroaxonal dystrophy: pathophysiological and therapeutic implications. Brain.

Niccoli, T., Cabecinha, M., Tillmann, A., Kerr, F., Wong, C.T., Cardenes, D., Vincent, A.J., Bettedi, L., **Li, L**., Gronke, S., et al. (2016). Increased Glucose Transport into Neurons Rescues Abeta Toxicity in *Drosophila*. Curr Biol.

Kinghorn, K.J., Gronke, S., Castillo-Quan, J.I., Woodling, N.S., **Li, L.**, Sirka, E., Gegg, M., Mills, K., Hardy, J., Bjedov, I., et al. (2016). A Drosophila Model of Neuronopathic Gaucher Disease Demonstrates Lysosomal-Autophagic Defects and Altered mTOR Signalling and Is Functionally Rescued by Rapamycin. J Neurosci *36*, 11654-11670.

Abbreviations

AD	Alzheimer's disease
4E-BP1	Eukaryotic initiation 4E binding protein 1
ABAD	Aβ-binding alcohol dehydrogenase
ActGS	Actin-GenesWitch
AKT	Protein kinase B
AMPK	5' adenosine monophosphate-activated protein kinase
AP	Antagonistic pleiotropic
APP	Amyloid precursor protein
ARJP	Autosomal recessive juvenile Parkinsonism
ASK1	Apoptotic signal-regulating kinase 1
ATF6a	Transcription factor 6a
Atg	Autophagy related gene
ATP	Adenosine triphosphate
Aβ	Amyloid β
BAT	Brown adipose tissue
Bip	Binding immunoglobulin protein
cAMP	Cyclic adenosine monophosphate
CCCP	Carbonylcyanide m-chlorophenylhydrazone
CHOP	C/ebpβ homology protein
CncC	Cap'n'collar C
CNS	Central nerve system
CREB	Camp response element binding protein
Cyt-c-p	Cytochrome c proximal
DA	Dopaminergic neurons
daGS	Daughterless-GeneSwitch
DILPs	Drosophila insulin like peptides
DN	Dominant negative
DR	Dietary restriction
eIF2a	Eukaryotic translation initiation factor 2a
elavGS	Embryonic lethal abnormal vision-GeneSwitch
ELISA	Enzyme-linked immunoabsorbent assay
ER	Endoplasmic reticulum
ERAD	ER associated degradation
ETC	Electoral transport chain
FOXO	FOrkhead boX subgroup O transcription factor
FRET	Fluorescence resonance energy transfer
GABPα	GA binding protein α
GADD34	DNA damage-inducible 34
GFP	Green fluorescent protein
Glut	Glucose transporter
Grp78	Glucose regulated protein 78
GS	Gene switch
GSK3	Glycogen synthase kinase 3
GWAS	Genome-wide association studies
H_2O_2	Hydrogen peroxide
HD	Huntington's disease
HNF-4α	Hepatocyte nuclear factor 4α
HSR	Heat shock response
IF	Intermittent fasting
IIS	IGF-1-like signaling
InR	Insulin receptor

IRE1	Inositol-requiring enzyme 1
IRS1	Insulin receptor substrate 1
JNK	JUN amino-terminal kinase
LB	Lewy body
LC3-I/II	Microtubule associated protein A 1A/1B-light chain 3
LiCl	Lithium chloride
LRRK2	Leucine-rich repeat kinase 2
M	Molar
MAPK	Mitogen-activated protein kinase
MEF2	Myocyte enhancer factor-2
miRNAs	Micro Ribonucleic Acids
Mitophagy	Mitochondrial autophagy
mL	Mililitre
mM	Milimolar
mNSCs	Median neurosecretory cells
mtDNA	Mitochondrial DNA
mTOR	Mechanistic Target of Rapamycin
mTORC1	Mtor complex 1
mTORC2	Mtor complex 2
mtTFA	Mitochondrial transcription factor A
NF-kB	Nuclear factor kappa-light-chain-enhancer of activated B cells
NFTs	Neurofibrillary tangles
NMJ	Neuromuscular junction
NRF2	NF-E2-related factor
NRF2	Nuclear respiratory factor 2
OCR	Oxygen consumption rate
OXPHOS	Oxidative phosphorylation
PBS	Phosphate buffered saline
PCR	Polymerase chain reaction
PD	Parkinson's disease
PDP1ε	Par Domain Protein 1ε
PERK	Protein kinase RNA-like ER kinase
PGC-1α	Peroxisome proliferator-activated receptor (PPAR)-γ coactivator-1α
PI	Performance index
PI3K	Phosphatidylinositide 3-kinases
PINK1	PTEN-induced putative kinase 1
PPARγ	Peroxisome proliferator-activated receptor
PRC	PGC-1-related co-activator
Proteostasis	Proteome homeostasis
PSEN	Presenilin
qRT-PCR	Quantitative real time PCR
RNAi	Ribonucleic Acid interference
ROS	Reactive oxygen species
RU/RU486	Mifepristone
S6Ks	S6 kinases
SEM	Standard error of the mean
SN	Substantia nigra
SNCA	Alpha-synuclein
SOD	Superoxide dismutase
SY	Sugar yeast
TBST	Tris-buffered saline with Tween 20
TF-EB	Transcription factor-EB
TFs	Transcription factors
TOR	Target of rapamycin

UAS	Upstream activation sequence
UCP-1	Uncoupling protein-1
UPR	Unfolded protein response
UPR^{ER}	Unfolded protein response ER
UPR^{mt}	Mitochondrial unfolded protein response
UPS	Ubiquitin proteasome system
w^{1118}	White 1118
WAT	White adipose tissue
w^{Dah}	White Dahomey
XBP1	X-box binding protein 1
$\Delta\Psi_M$	Mitochondrial membrane potential

Chapter 1 Introduction

1.1 Alzheimer's disease

1.1.1 Overview of Alzheimer's disease

Alzheimer's disease (AD) is the most common form of dementia in the ageing population, affecting millions of people worldwide. Clinical symptoms of AD include but are not limited to memory loss and cognitive decline, including temporal-spatial disorientation, impairment of judgment and problem solving, and deterioration of language abilities (Faber-Langendoen et al., 1988). Behavioral and personality changes may also be observed with disease progression. In the severe stages of the disease, movement abnormalities often develop, which along with dementia, leave patients often bedridden and dependent on caregivers.

In 1907, Alois Alzheimer first described a dementing illness and identified senile plaques and neurofibrillary tangles (NFTs) in the post-mortem brain tissue (Alzheimer, 1907), the two neuropathogical hallmarks still utilized by neuropathologists today to make the histological diagnosis of AD. In 1927, Divry used Congo red staining to describe the senile plaques in the AD brain as extracellular aggregates of amyloid-β (Aβ) (Divry and Florkin, 1927), various species of which are derived from the amyloid precursor protein (APP) (Kang et al., 1987). NFTs, the other classic hallmark of AD pathology, are intracellular aggregates of paired helical filaments composed of hyperphosphorylated tau protein (Brion et al., 1985). NFTs are mainly found in the hippocampus, entorhinal cortex and neocortex (Hyman et al., 1984). Since both Aβ and tau are normal proteins found in healthy neurons, there is a great deal of interest in understanding what triggers their conversion into the abnormal and aggregated forms found in AD.

1.1.2 Molecular genetics of AD

The majority of AD cases are sporadic, while only a small proportion of AD cases (<1%) result from the autosomal dominant inheritance of gene mutations. Since familial cases share similar symptoms and pathology with sporadic AD (Harvey et al., 2003), the identification of the genes involved in these rare forms of AD provides a

powerful tool for the elucidation of disease pathogenesis and therapeutic strategy. Mutations in three genes cause autosomal dominant AD, including the amyloid precursor protein (*APP*) and the *presenilin* genes (*PSEN1* and *PSEN2*) (Goate et al., 1991, Levy-Lahad et al., 1995, Rogaev et al., 1995), all of which show altered Aβ production through APP processing (Figure 1.1) (Charier-Harlin, 1991, Citron et al., 1992, Price and Sisodia, 1998, Suzuki et al., 1994). APP is a type I transmembrane protein with a large amino-terminal extracellular domain. To produce Aβ, the extracellular domain is first removed by β-secretase. The remaining carboxy-terminal fragment is then cleaved within the membrane by γ-secretase, which is composed of presenilin and other components (De Strooper et al., 1998, Edbauer et al., 2003). γ-secretase can cleave APP at different sites, producing Aβ peptides of 40 or 42 amino acids. *APP* gene mutations found in a Swedish family result in increased β-secretase cleavage and thus increased production of both Aβ40 and Aβ42. Among the different species of Aβ, Aβ42 is more prone to oligomerization and is believed to be more toxic than Aβ40 (McGowan et al., 2005). Mutations at the γ-secretase cleavage site found in the familial cases lead to production of more the toxic Aβ42 compared to Aβ40 (Charier-Harlin, 1991, Price and Sisodia, 1998). Moreover, *APP* mutations found in the Dutch and Arctic families result in increased fibrillogenesis or resistance to proteolysis (Massi et al., 2002, Nilsberth et al., 2001). Identification of these mutants demonstrated a fundamental role of Aβ peptides, especially Aβ42, in the pathogenesis of AD. In addition to point mutations, multiplication in the *APP* gene can also cause early-onset AD (Cabrejo et al., 2006), indicating the importance of protein aggregation and mis-folding in disease progression. Other disease-related gene mutations have been identified in the *presenilin* genes, which encode the catalytic subunit of γ-secretase (Levy-Lahad et al., 1995, Rogaev et al., 1995). AD-associated *presenilin* mutations increase the Aβ42/Aβ40 ratio (Rogaev et al., 1995, Duff, 1997, Oyama et al., 1998), also indicating that Aβ42 is the more toxic species of the Aβ peptides. Taken together, genetic findings from familial AD have helped to establish a basic understanding of the aetiology of AD, in which increased levels of Aβ peptides, especially with an increased ratio of Aβ42/Aβ40 resulting from AD-related gene mutations or duplication, are the main cause of pathogenesis in AD.

Most cases of AD do not exhibit autosomal-dominant inheritance and are termed sporadic AD, in which genetic differences may act as risk factors. The best-known genetic risk factor for AD is the inheritance of the ε4 allele of the apolipoprotein E (APOE) (Strittmatter et al., 1993, Mahley et al., 2006). The APOE4 allele increases the risk of the AD by three times in heterozygotes and by 15 times in homozygotes (Blennow et al., 2006). How the APOE proteins mediate their effect in AD is not fully elucidated, however the previous studies using APP transgenic mice model that harboured the human *APOE* genes suggest that APOE4 show reduced efficiency in the clearance of Aβ (Kim et al., 2009).

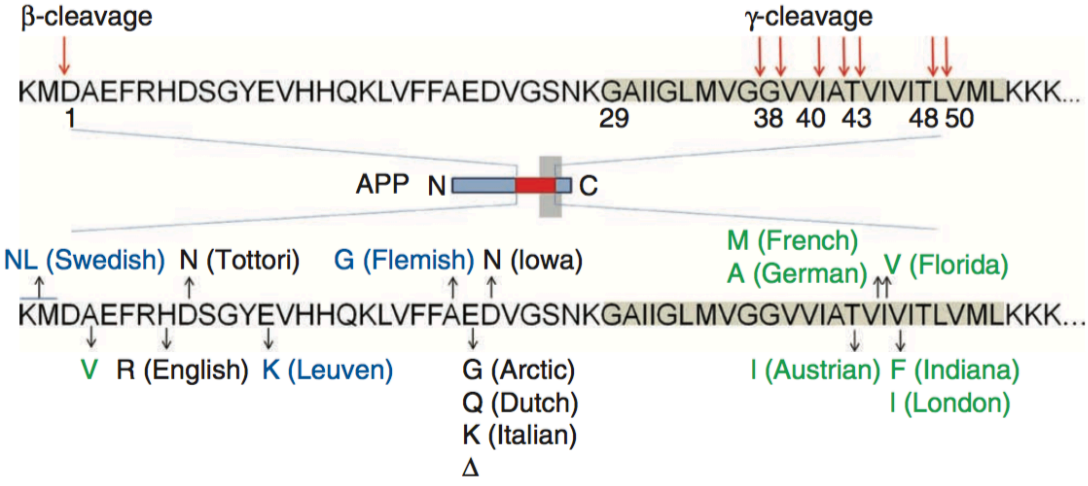

Figure 1.1 Generation of Aβ from the amyloid precursor protein.

The sites of β- and γ-secretase–mediated cleavage are indicated with arrows, and the transmembrane domain of APP is highlighted in gray. γ-cleavage produces a pool of Aβ fragments that vary in length and hydrophobicity. The mutations in the Aβ region of APP increase the total Aβ production (in blue), alter Aβ biophysical properties (in black), or affect the Aβ spectrum in both quantitative and qualitative ways (in green). Taken from (Benilova et al., 2012).

1.1.3 The amyloid cascade hypothesis

The evidence from pathology, phenotypes mediated by genetic mutations in familiar cases and risk factors conferred by the *APOE* gene metioned above appears to facilitate Aβ in the central position of AD pathogenesis. The amyloid cascade hypothesis was first proposed in 1992 by Hardy and Higgins, who postulated that "Aβ peptides are the causative agent in AD pathology, and then give rise to a complex network of downstream events, including neurofibrillary tangles, cell loss, vascular

damage and dementia" (Hardy and Higgins, 1992). Although the majority of research data still supports a role for Aβ as the primary initiator of AD pathogenesis (Musiek and Holtzman, 2015), this hypothesis has subsequently been subject to some criticism.

Firstly, it has become clear that the correlation between dementia or other cognitive alteration and the accumulation of amyloid plaques in the brain is not linear, neither in humans (Price et al., 2009) nor in mice (Games et al., 1995). According to this observation, there is now increasing data to support the modified hypothesis that it is the soluble toxic oligomeric forms of the Aβ peptide that account for the neurotoxicity of Aβ peptide in AD, rather than the monomer or fibrillar aggregates. A variety of cytotoxic oligomeric Aβ species have been identified in AD brain lysates, with pathogenic effects *in vitro* and *in vivo* in animal models (Shankar et al., 2008, Walsh et al., 2002, Mucke and Selkoe, 2012). In humans, Aβ oligomers accumulate with age, and directly initiate tau phosphorylation *in vitro* and *in vivo* (Jin et al., 2011, Zhang et al., 2014). Mouse models displaying accumulation of Aβ oligomers developed synaptic damage, inflammation, glial activation, cognitive impairment and neuronal loss (Zhang et al., 2014, Tomiyama et al., 2010). Although the precise neurotoxicity of Aβ oligomers *in vivo* is still unknown, studies have revealed that Aβ can cause oxidative stress, lipid peroxidation, mitochondrial dysfunction and inflammation (Pratico et al., 2001, Benzing et al., 1999, Calkins et al., 2011). Interestingly, abnormal stress responses that can be induced by Aβ, such as oxidative stress (Guix et al., 2012), mitochondrial dysfunction (Kukreja et al., 2014) and inflammation (Liu et al., 2014), can also directly influence APP metabolism and Aβ accumulation, suggesting a confounding feed-forward mechanism to exacerbate Aβ production and toxicity. However, there is still little evidence in humans that genetic mutations that increase mitochondrial dysfunction, oxidative stress, or inflammation cause Aβ pathology. Since the aforementioned pathogenic markers are also seen in other neurological disease, it is likely that these risk factors influence the pathogenic mechanisms downstream of Aβ, but are not unique to AD (Musiek and Holtzman, 2015). Factors that affect Aβ production or aggregation or suppress Aβ clearance can contribute to disease progression. The accumulation of Aβ oligomers is predicted to affect the ability of the brain to maintain proper protein quality control, including autophagy failure, imbalance in protein degradation and protein synthesis. This

eventually prompts further aggregation of Aβ, tau and other intracellular proteins in association with an exacerbation of neurotoxicity (Dasuri et al., 2013, Nixon and Yang, 2011). The sleep disturbance observed in AD patients may also increase neuronal Aβ release via an impaired sleep-wake cycle, thereby leading to abnormal oscillations of extracellular Aβ levels (Kang et al., 2009). Moreover, ageing is a major risk factor for AD. Since proteostatic and cytoprotective pathways in the central nervous system decline with age (Taylor and Dillin, 2011, Lu et al., 2014), age-related disturbances in proteostasis and neuronal stress response signalling pathways may also shift the balance of Aβ metabolism towards aggregation. In addition, age-related disorders such as vasculopathy and atherosclerosis, diabetes, head trauma, or sleep disruption may also affect Aβ accumulation and aggregation, exacerbating AD pathology and stimulating the onset of dementia (Kang et al., 2009, Musiek and Holtzman, 2015). A full understanding of the complex interplay between these processes and Aβ aggregation is still awaited, but it is likely that these cellular pathways may prove to be excellent therapeutic targets in the treatment of AD.

Secondly, the relationship between Aβ plaques and neurofibrillary tangles of tau remains unclear and therefore has been of considerable debate for many years. Previous studies showed that tau pathology occurs first in the transentorhinal cortex, often in the absence of plaque pathology. Moreover, the patten of tau pathology is highly regular, whereas Aβ plaque pathology is much more varied (Braak and Braak, 1991). In order population, there is significant increase in the presence of neurofibrillary tangles, but no association between age and Aβ plaque was observed (Price et al., 2009). In addition, Gomes-Isla *et al.* measured the total number of neurons in AD braisn compared to age-matched controls, and found that there was a statistically significant correlation between the loss of neurons and the increased in the presence of neurofibrillary tangles with disease progression; however, no correlation was observed between Aβ load and either disease duration or neuronal loss (Gomez-Isla et al., 1997). All the evidence discussed above suggest that there is considerable gaps in our understanding of AD pathology, therefore to some extent debate amyloid hypothesis. The hypothesis that accommodates most of the known data is that Aβ aggregation and deposition triggers a process that leads to neuronal

loss via the formation of neurofibrillary tangles of tau, although the mechanisms are not fully understood.

Thirdly, there are currently three main therapeutic interventions strategies amied at Aβ: reducing Aβ production, facilitating Aβ clearance and preventing Aβ aggregation. However, all of the Aβ-centric approaches that reached Phase III clinical trials have failed. For example, semagacestat, a well-characterzed γ-secretase inhititor, effectively reduced Aβ deposition in both APP transgenic mouse model (Ness et al., 2004) and human volunteers (Bateman et al., 2009). However, Phase III trails demonstrated that patients who were treated with semagacestat displayed an increased deterioration in cognition and daily activity compared to controls. This failure again challenged the amyloid hypothesis, and also remain questions unanswered: by how much should Aβ production be lowered, and at what stage of the disease process would an Aβ-directed therapeutic approach be likely to show clinical efficacy? Recently, aducanumab, a human monoclonal antibody that selectively targets aggregated forms of Aβ, was reported to reduce both soluble and insoluble Aβ in a transgenic mice model (Sevigny et al., 2016). In addition, AD patients in the early stages of disease injected with aducanumab showed reduced Aβ levels, which was accompanied by a slowing in clinical decline. These ongoing clinical trials, as well offering great promise for the future treatment of AD, also provide compelling support for the amyloid hypothesis.

1.1.4 Animal models of Alzheimer's disease

A number of genetic models have been developed in the study of AD, including a large number of mouse models, many of which have failed to recapitulate all of the histopathological and behavioral features of AD. Transgenic mice harboring human *APP* mutations develop amyloid pathology and memory defects without neuronal loss (Mucke et al., 2000, Cheng et al., 2004). In order to isolate the effects of Aβ, transgenic Aβ mouse models were generated, but only amyloid pathology was observed (McGowan et al., 2005). Transgenic mice with mutant *presenilin* expression demonstrated increased Aβ42 levels, while no AD pathology or cognitive deficits developed (Holcomb et al., 1999, Dewachter et al., 2008). Moreover, a transgenic

mutant tau mouse model demonstrated hyperphosphorylated tau, neurofibrillary lesions and cell loss (Lewis et al., 2000, Andorfer et al., 2003).

In addition, non-mammalian experimental models have been used to study the biology of AD. They are excellent genetic tools suited for drug screening and the study of toxic molecular cascades involved in disease progression. Furthermore they offer advantages over mammalian models with a quick generation time and low cost. The most commonly used invertebrate model organism in neurodegeneration is the fruit fly *Drosophila melanogaster* given their complex brains, short lifespan and relative ease of genetic manipulation. Several fly models already exist to study AD biology. Flies that over-express *Drosophila* or human tau have been developed that display several neuronal dysfunction phenotypes, including disrupted neuronal and synaptic function and climbing defects (Mershin et al., 2004, Wittmann et al., 2001, Ubhi et al., 2007). Fly models expressing Aβ peptides have also been developed that show neurodegeneration, reduced lifespan and amyloid deposition (Finelli et al., 2004, Crowther et al., 2005, Iijima et al., 2004). Although an *APP* orthologue exists in flies, the Aβ sequence is not conserved (Rosen et al., 1989). In keeping with this limitation, the only abnormal phenotypes seen in a fly model of *APP* over-expression were axonal transport phenotypes (Gunawardena and Goldstein, 2001). Therefore in summary, *Drosophila* models directly expressing Aβ allow investigation of Aβ toxicity in the absence of any endogenous amyloid production. It is a simple model to study the downstream effects of Aβ neurotoxicity and the potential mechanisms of Aβ degradation, independent of APP processing.

1.1.5 Mitochondrial dysfunction and oxidative stress in Alzheimer's disease

Mitochondrial dysfunction and oxidative damage have been implicated in the pathogenesis of AD. Studies have shown that oxidative damage and lipid peroxidation occur early in the pathogenesis of AD brains and in an APP mouse model (Nunomura et al., 2001, Pratico et al., 2001). Moreover the genes responsible for mitochondrial metabolism and apoptosis were up-regulated in neurons undergoing oxidative stress, suggesting early cellular change before Aβ deposition (Reddy et al., 2004). Deficiency in cytochrome c oxidase and α-ketoglutarate dehydrogenase has been

observed in AD patients, suggesting the involvement of mitochondrial dysfunction in AD pathogenesis (Gibson et al., 1988, Parker et al., 1990).

In addition, mitochondrial dysfunction and oxidative damage also contribute causally to AD-related pathology. Indeed treating neurons with hydrogen peroxide, a potent oxidizer, increases intracellular levels of Aβ (Ohyagi et al., 2000). Furthermore, treatment of astrocytes with the mitochondrial uncoupler CCCP (carbonylcyanide m-chlorophenylhydrazone), an inhibitor of oxidative phosphorylation (OXPHOS), promotes amyloidogenic APP processing and intracellular Aβ accumulation (Busciglio et al., 2002). APP mouse models lacking the mitochondrial antioxidant enzyme, MnSOD, or treated with inhibitors of energy metabolism, have also shown dramatically increased levels of β-secretase, Aβ, and senile plaques (Li et al., 2004, Velliquette et al., 2005).

Several studies have suggested that AD pathology can directly affect mitochondria and mitochondrial proteins. APP can directly target mitochondria, and clog the mitochondrial protein importation machinery, leading to mitochondrial dysfunction and metabolic defects (Anandatheerthavarada et al., 2003). Aβ can bind to a mitochondrial-matrix protein named ABAD (Aβ-binding alcohol dehydrogenase), leading to Aβ-induced apoptosis and free-radical generation in neurons (Lustbader et al., 2004). Moreover, Aβ can physically interact with mitochondria, inhibiting cytochrome c oxidase activity, impairing mitochondrial respiration, and increasing free radical generation and oxidative damage in AD neurons (Crouch et al., 2005, Manczak et al., 2006, Casley et al., 2002).

Mitochondrial DNA (mtDNA) is particularly sensitive to free radical damage. Deletions and mutations in mtDNA have been observed in post mortem AD brains (Bender et al., 2008, Coskun et al., 2004), highlighting the likely role of mitochondrial dysfunction in AD pathogenesis. Moreover, oxidative stress has been implicated in AD pathology, with alterations in several signalling pathways identified in AD brain tissue. For example, oxidative damage can increase the levels of β-secretase through activation of p38 mitogen-activated protein kinase (MAPK) and C-Jun amino-terminal kinase (Tamagno et al., 2005), leading to excessive tau

hyperphosphorylation through the activation of glycogen synthase kinase 3 (GSK3) (Lovell et al., 2004).

1.1.6 The unfolded protein response (UPR) in neurodegeneration

Cells are faced with a variety of stressors throughout their lifetime, which leads to protein mis-folding and aggregation (Balch et al., 2008). Maintaining protein homeostasis (proteostasis) requires the appropriate coordination of efficient folding and assembly of proteins and protein quality control systems, in order to minimize the load of unfolded or mis-folded proteins, and to reduce abnormal protein aggregation. Protein folding and assembling occur mainly in the endoplasmic reticulum (ER), where chaperones are induced to ensure the proper folding of proteins. Mis-folded proteins are then recognized by the quality control mechanisms, triggering degradation by the ubiquitin-proteasome machinery or the lysosome-autophagy pathway. Under conditions of cellular stress or pathogenic conditions that alter the protein-folding process, accumulation of mis-folded protein in the ER lumen causes ER stress. In response to ER stress, the folding and degrading capacity of the ER is adjusted by induction of a complex signalling network, known as the unfolded protein response (UPR^{ER}).

Whether the UPR restores proteostasis or induces apoptosis depends on the intensity and duration of the stress stimuli. Moderate accumulation of mis-folded proteins can activate the UPR to augment protein folding, quality control and protein degradation mechanisms (Hetz, 2012, Walter and Ron, 2011, Wang and Kaufman, 2012). Mis-folded proteins can also be re-translocated to the cytosol, where they are cleared via the ER-associated protein degradation (ERAD) pathway, including ubiquitin-proteosome mediated or lysosome-autophagy degradation.

The UPR consists of two central components, a group of ER transmembrane sensors and downstream signalling cascades that enable adaptation to stress or the induction of apoptosis (Figure 1.2). Three well-characterized signalling branches mediate this response: PERK (protein kinase RNA-like ER kinase), inositol-requiring enzyme 1 (IRE1), and transcription factor 6α (ATF6α) (Wu and Kaufman, 2006, Hetz and Mollereau, 2014). Under normal physiological conditions, these three trans-

membrane signaling components are bound and inhibited by Grp78. During ER stress, mis-folded proteins titrate down Grp78, thus activating signaling cascades downstream of the UPR. PERK directly phosphorylates and inhibits ubiquitous eukaryotic translation initiation factor 2α (eIF2α), leading to a rapid and transient attenuation of translation. A reduction in global translation relieves the stress of mis-folded proteins in the ER by reducing the total load of newly synthesized proteins in the ER lumen. Moreover, phosphorylated eIF2α selectively induces the translation of the mRNA encoding the transcription factor ATF4, which then translocates into nucleus and induces the expression of ER chaperones and genes involved in autophagy, redox control and amino acid metabolism (Walter and Ron, 2011). The most conserved UPR signalling branch is initiated by IRE1. Activated IRE1 catalyzes splicing of the mRNA encoding the transcription factor X-box binding protein 1 (Xbp1), leading to a stable and active transcription factor that controls UPR target genes involved in protein folding, ERAD, lipid synthase, ER chaperones, and ER translation (Hetz et al., 2011). Upon ER stress, ATF6α is transported to the Golgi where it is processed to produce a cytosolic fragment, which operates as a transcription factor that regulates *Xbp1*, ER chaperones, and ERAD genes (Walter and Ron, 2011).

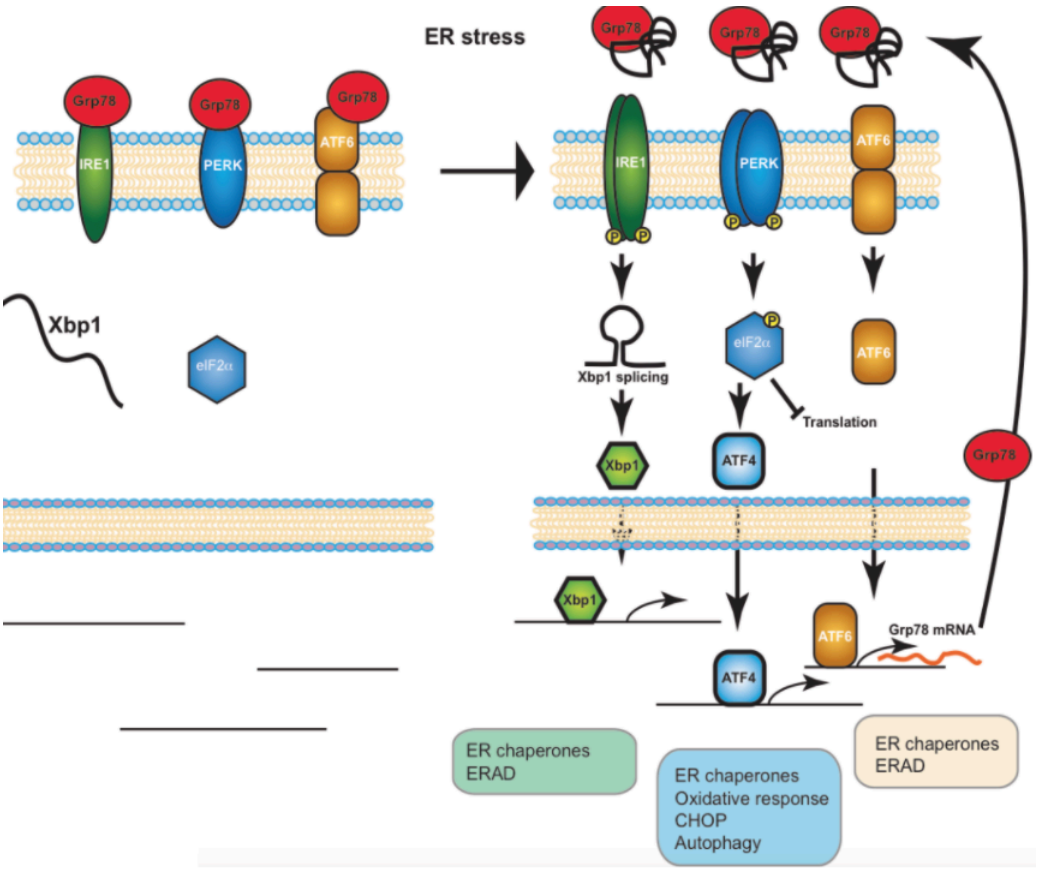

Figure 1.2 A schematic representation of the UPR

The UPR is mediated by 3 trans-membrane signalling components. Under normal physiological conditions, these are bound and inhibited by Grp78. During ER stress, mis-folded proteins titrate down Grp78, thus activating signalling cascades downstream of the UPR. Taken from (Niccoli et al., 2016).

Moreover, chronic or irreversible ER stress in neurodegenerative disease can trigger apoptosis via signalling mechanisms that overlap with those activated in the adaptive response (Figure 1.3). Sustained activation of PERK signalling triggers a series of transcriptional responses mediated by ATF4, which induce C/EBP-homologous protein (CHOP) and its downstream targets, leading to increased DNA damage-inducible 34 (GADD34), BAX-and BAK-dependent caspases. In turn the survival protein BCL-1 is inhibited, leading to cells entering apoptosis (Tabas and Ron, 2011, Shore et al., 2011, Urra et al., 2013). Moreover, the IRE1 pathway also contributes to apoptosis and cell death by inducing the activity of JUN amino-terminal kinase (JNK) and the apoptotic signal-regulating kinase 1 (ASK1) (Urano et al., 2000). In addition, IRE1 can also degrade microRNAs (miRNAs), thereby negatively regulating the expression of ER chaperones (Urra et al., 2013). In summary, the UPR is a complex

signalling network that coordinates adaptation to ER stress or elimination of damaged cells by apoptosis, depending on the intensity and temporal exposure to stress.

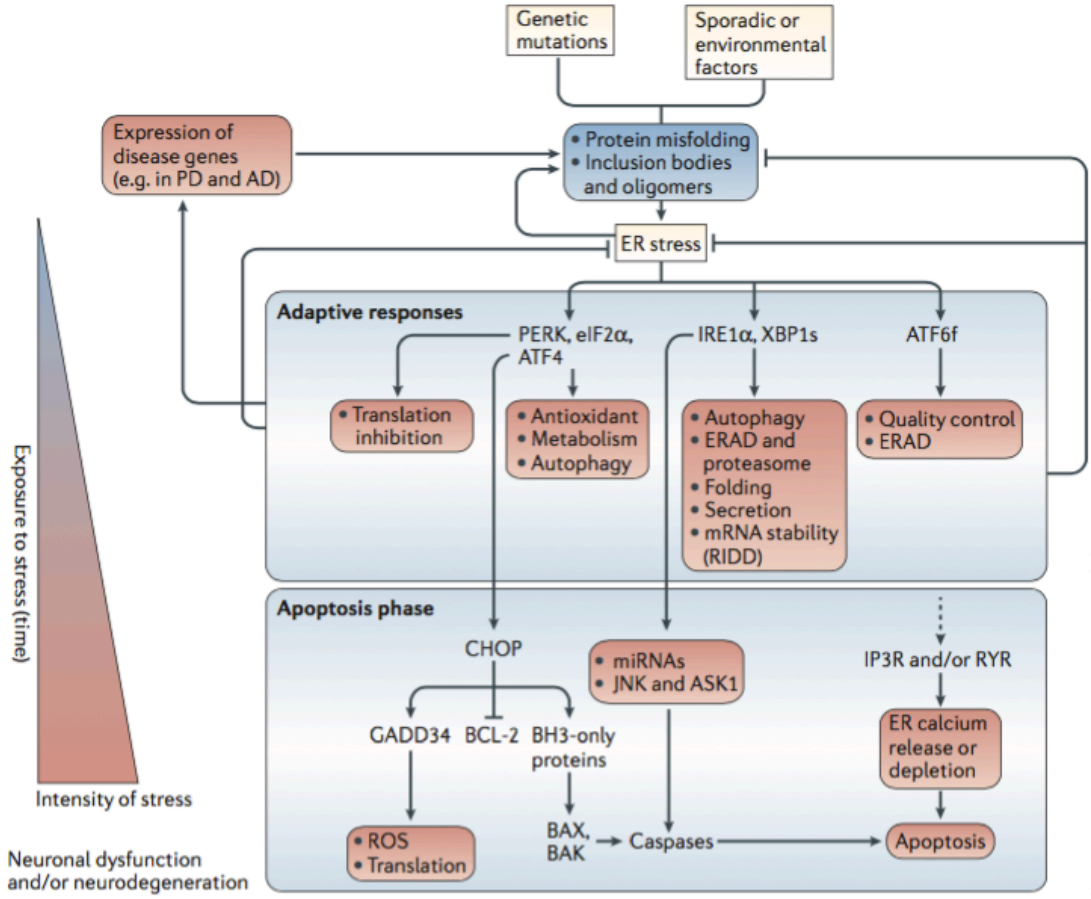

Figure 1.3 The UPR signalling outputs in neurodegeneration

Disease-related genes can trigger the mis-folding of a particular protein, which can then form different types of aggregates, ranging from small oligomeric species to inclusion bodies. This abnormal aggregation process results in ER stress. Prolonged ER stress overcomes the adaptive responses of the UPR and apoptosis is induced. Various apoptotic pathways have been described, including up-regulation of CHOP through ATF4. This pathway also inhibits the expression of BCL-2 family members, and the up-regulation of BH3-only proteins results in BAK- and BAX-dependent apoptosis. CHOP also induces the expression of growth arrest and GADD34, which increases the levels of ROS and protein synthesis. IRE1α also induces activation of JNK and ASK1, which contributes to cell death. In addition, IRE1α can degrade miRNAs that negatively control the expression of caspases. UPR signalling events can also modulate the expression of various genes involved in the aetiology of disease. Taken from (Hetz and Mollereau, 2014).

The UPR also contributes to ageing and age-related neurodegeneration. The ability of cells to ensure proteostasis by the UPR declines with age (Taylor and Dillin, 2011).

Damaged, mis-folded, and aggregated proteins progressively accumulate with age. At the same time ER chaperones are down-regulated, and activation of the UPR^{ER} and ER stress is limited during ageing, leading to an overall decline in the capacity of the cell to adapt and protect its proteome against age-related disease (Ben-Zvi et al., 2009).

Neurodegeneration is characterized by the accumulation of mis-folded pathological proteins in the central nervous system (CNS). For example, amyloid plaques and neurofibrillary tangles, the two hallmark pathological lesions in AD, and *α-synuclein*, the main component of Lewy Bodies (LB) in PD, all arise from protein mis-folding. The involvement of ER stress in neurodegenerative disease is well known but the role of the UPR in neurodegeneration is complex and yet to be fully determined. Activation of the UPR can either enhance or reduce neurodegeneration depending on the specific UPR-signalling mechanisms activated. In PD, chronic ER stress has been identified as a pathological event that contributes to dopaminergic neuronal loss (Hoozemans et al., 2007). However, activation of UPR components (ATF6) protects against PD-induced neurotoxicity in cells (Egawa et al., 2011), and up-regulation of GRP78 or eIF2α phosphorylation has shown neuroprotective effects in PD mouse models (Gorbatyuk et al., 2012, Boyce et al., 2005).

In AD, neurons expressing phosphorylated tau show activated PERK signalling, suggesting up-regulation of the UPR (Hoozemans and Scheper, 2012). In addition, Xbp1, the downstream effector in the IRE1 branch of the UPR, has been found to be a risk factor in sporadic AD (Liu et al., 2013). Reduced levels of Xbp1 are also found in AD patients' brains (Reinhardt et al., 2014), suggesting that elevating Xbp1 may represent an excellent therapeutic avenue. Indeed, over-expression of active *Xbp1* rescues the neurotoxic phenotypes in a *Drosophila* model of Aβ toxicity (Casas-Tinto et al., 2011). Moreover, a *C. elegans* model of AD confirmed that Xbp1 is critically important for maintaining ER homeostasis in the presence or absence of ER stress (Safra et al., 2013). Moreover, we recently demonstrated that down-regulation of glucose-regulated protein 78 (Grp78; also know as Bip-binding immunoglobulin protein) in fly neurons can ameliorate Aβ-induced neurotoxicity. In addition this correlated with increased activation of the UPR (Niccoli et al., 2016). Grp78 is the

master negative regulator of the UPR, and binds and inhibits the UPR trans-membrane sensors under normal physiological conditions. Under ER stress, mis-folded proteins titrate down Grp78, leading to activation of UPR sensors and their downstream targets. Our study therefore suggests that decreasing Grp78 protein levels, leading to activation of the UPR, may be neuroprotective in AD.

In addition to the up-regulation of the adaptive response of the UPR in AD, the apoptosis phase of the UPR has been also implicated in AD pathogenesis. JNK3, the downstream effector of IRE1, which activates apoptosis, and eIF2α phosphorylation, the downstream effector in PERK activity, have both been shown to be up-regulated in AD brain and APP mouse models (Yoon et al., 2012, Ma et al., 2013). Activation of JNK3 increases Aβ levels by promoting APP processing, while suppression of eIF2α kinase ameliorates AD-related memory defects, suggesting that chronic or irreversible activation of the UPR could also exacerbate AD pathology. Indeed, down-regulation of Grp78 in fly neurons ameliorates Aβ toxicity via activation of the UPR, to the extent that eIF2α phosphorylation is not detectable (Niccoli et al., 2016). This supports the hypothesis that moderate activation of the UPR may be beneficial in preventing AD pathology. In summary, the impact of the UPR on AD depends on the strength and duration of the stress stimulus. However, a better understanding of this pathway awaits more *in vivo* studies.

1.2 Parkinson's Disease

1.2.1 Overview of Parkinson's disease

Parkinson disease (PD) is the commonest movement disorder and the second most prevalent neurodegenerative disease after AD. The typical clinical presentation of PD includes tremor, bradykinesia, rigidity, gait and balance impairment (Lees et al., 2009). Although the cause of PD is not fully explored, it is believed to involve both genetic and environmental factors. There is an increased risk in people exposed to certain pesticides including rotenone and paraquat (Moretto and Colosio, 2013, Tanner et al., 2011). Moreover, MPTP is a pro-drug to the neurotoxin MPP+, which inhibits Complex 1 activity, leads to mitochondrial dysfunction and causes permanent symptoms of PD by destroying DA neurons in the SN of the brain (Langston et al.,

1983). There is also a reduced risk in tobacco smokers and those who drink coffee (Kalia and Lang, 2015). The predominant pathological features of PD are the selective loss of dopaminergic neurons in the substantia nigra (SN) of the mid brain, in association with intraneuronal inclusions called Lewy bodies (LB), composed of insoluble aggregates of the presynaptic protein α-synuclein (Spillantini et al., 1997, Dickson et al., 2009). The finding of α-synuclein gene (*SNCA*) mutations in familial PD patients, together with the identification of *SNCA* as a genetic risk factor for sporadic PD in two genome-wide association studies (GWAS) and a meta-analysis, confirmed the fundamental role of α-synuclein in the pathogenesis of PD (Polymeropoulos et al., 1997, International Parkinson Disease Genomics et al., 2011, Simon-Sanchez et al., 2009, Satake et al., 2009, Martin et al., 2011).

Over the past few years, a number of genes linked to Parkinsonism, known as the *PARK* genes, have been characterized. Currently 16 *PARK* loci have been identified, with autosomal dominant genes such as *SNCA* (*PARK*1), and leucine-rich repeat kinase 2 (*LRRK2*) (*PARK*8) (Paisan-Ruiz et al., 2004), and autosomal recessive genes such as *parkin* (*PARK2*) (Kitada et al., 1998), PTEN-induced putative kinase 1 (*PINK1*) (*PARK*6) (Valente et al., 2004), *DJ-1* (*PARK*7) (Bonifati et al., 2003), *ATP13A2* (Ramirez et al., 2006) and *PLA2G6* (*PARK*14) (Paisan-Ruiz et al., 2009). Unraveling the link between mutations in these genes and neurodegeneration has greatly aided our understanding of the pathogenic mechanisms underlying familial and sporadic PD pathology.

1.2.2 *Drosophila* models of Parkinson's disease

Recent research has focused on the development of genetic animal models, including organisms as diverse as yeast, worms, *Drosophila* and mice, in order to model the cellular and phenotypic features of human PD. Such models allow the dissection of the critical events leading to α-synuclein accumulation and neurodegeneration in PD. Among these animal models, the fruit fly *Drosophila melanogaster* has produced some of the most significant advances in our understanding of the cellular pathways in PD.

Drosophila is a widely used genetic tool to study neurological and genetic disorders, including PD and AD. One of the greatest advantages of using *Drosophila* to model PD is that it can recapitulate some of the characteristic phenotypes of patients, such as inclusion-like formation and dopaminergic neuronal loss (Feany and Bender, 2000). Moreover, PD *Drosophila* models also show locomotor defects that parallel the motor disability of patients. In fact, the climbing phenotype has become one of the best approaches to evaluating neurodegeneration in flies. In addition, the other advantages of using the fruit fly as a model organism, is that it is fast breeding, has rapid growth and easy genetic manipulation, as well as substantial genetic stocks. In addition, approximately 60% of the genes in *Drosophila* overlap with those of human genes. Therefore, *Drosophila* has become an important organism for the study of neurodegeneration.

1.2.2.1 Gain-of-function fly models of PD

Drosophila models exist for the study of many of the genetic variants of PD. Of the classic genes involved in PD, *SNCA* is the only one not conserved in *Drosophila*. However, by over-expressing human *SNCA* in the fly neuronal tissue, it has been possible to model the neurotoxicity of α-synuclein in PD in *Drosophila*. The fly models display LB-like aggregates (Figure 1.4), movement phenotypes, and dopaminergic neuronal loss (Feany and Bender, 2000). Although work in cell and mouse models suggest that mutant α-synuclein leads to the development of LB-like inclusions, as well as mitochondrial dysfunction and increased oxidative stress (Conway et al., 2000, Greenbaum et al., 2005, Masliah et al., 2000), the precise mechanisms by which α-synuclein species result in neurotoxicity is still unclear (Cookson and van der Brug, 2008).

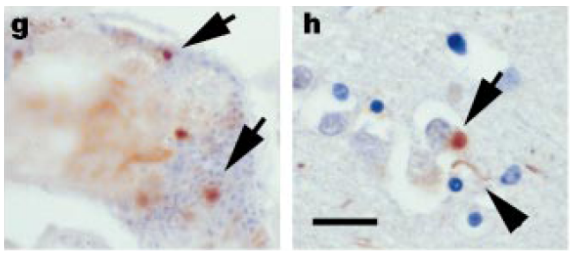

Figure 1.4 Alpha-synuclein pathology

Left: aggregated α-synuclein in a LB-like inclusion in the brain of *Drosophila*. Right: a human LB composed of α-synuclein. Images taken from (Feany and Bender, 2000).

Work in *Drosophila* has shown that over-expression of both wild type and pathogenic forms of α-synuclein leads to dopaminergic neuronal loss and neurodegeneration (Feany and Bender, 2000, Karpinar et al., 2009, Chen and Feany, 2005, Periquet et al., 2007). Furthermore expression of mutant forms of α-synuclein, which increase the generation of oligomeric species, leads to greater toxicity, confirming the preferential toxicity of α-synuclein oligomers *in vivo* (Karpinar et al., 2009).

However, so far all of these PD-like phenotypes are induced through the use of the UAS-GAL4 system in *Drosophila*, which results in the expression of α-synuclein throughout development as well as adulthood. One concern is that developmental effects may significantly alter brain physiology and neurodegeneration measured in adulthood. It is therefore impossible to disentangle developmental effects from secondary neurodegenerative effects in these models. Similar to other animal models such as rats or monkeys, specific over-expression of α-synuclein in adult neurons avoids any deleterious effects of developmental expression and the possibility of compensatory mechanisms (Waxman and Giasson, 2009). It is therefore necessary to model late-onset sporadic PD through the temporal expression of α-synuclein using the inducible GeneSwitch system. I have shown that over-expression of different variants of α-synuclein (Karpinar et al., 2009) in adult neurons do not shorten lifespan, and only cause climbing defects to a very limit extent (unpublished results). Moreover, I found that mutations that increase the generation of oligomeric species of α-synuclein increase the amount of total α-synuclein protein. It is therefore impossible to conclude whether the toxic phenotypes are due to increased oligomeric species or a greater total load of α-synuclein.

1.2.2.2 Knockout fly models of PD

Unlike *SNCA*, *PARK2* is well conserved in *Drosophila*. Flies lacking *parkin* display a wide variety of phenotypes, including locomotor defects, DA neurodegeneration and muscle degeneration, in addition to clear mitochondrial phenotypes (Greene et al., 2003, Cha et al., 2005). In addition, *Drosophila PINK1* mutants show almost all of the phenotypes of *parkin* mutants, presenting with decreased climbing ability, flight

disability, flight muscle degeneration as well as DA neuronal loss (Park et al., 2006, Clark et al., 2006, Whitworth and Pallanck, 2009). Moreover, epistasis experiments using the fruit fly have shown that PINK1 and parkin are linked in a common pathway with parkin acting downstream of PINK1 (Park et al., 2006). The link between PINK1 and parkin and their role in mitochondrial disease will be described in detail in Chapter 4.

Recently we generated the first *PLA2G6* knockout fly model, which showed reduced survival, locomotor defects, increased sensitivity to oxidative stress, mitochondrial lipid peroxidation and mitochondrial defects (Kinghorn et al., 2015, Kinghorn et al., 2016). Another known causative gene, *DJ-1*, is also conserved in *Drosophila*, and has been shown to mediate a protective role against oxidative stress. *DJ-1 alpha* and *DJ-1 beta* double knockout flies have a normal lifespan, but exhibit locomotor defects and increased sensitivity to environmental stressors, including paraquat and rotenone, demonstrating the involvement of *DJ-1* in stress response pathways (Menzies et al., 2005, Meulener et al., 2005). All of these genetic fly models enable us to study the pathogenesis of PD, and also provide a useful platform for drug discovery.

1.2.3 Mitochondrial dysfunction in PD

Mitochondrial dysfunction was first implicated in the pathogenesis of PD more than 2 decades ago. The first evidence came from a postmortem study, which described abnormalities of mitochondrial function in complex I and increased free radical mediated damage in the PD brains (Schapira et al., 1989). Since then a number of gene mutations causing familial PD have been identified. The study of how these genes cause dopaminergic neuronal loss has significantly aided our understanding of the mechanisms of pathogenesis of PD. Studies have shown that mitochondrial dysfunction and oxidative damage play an important role in PD pathology. Although proteostatic failure due to protein mis-folding and aggregation is undoubtedly crucial to PD pathogenesis, the importance of mitochondrial dysfunction has been specifically highlighted by work studying PD causing genes. Mutations in *SNCA*, *PINK1*, *PARK2*, and *PLA2G6* have all been shown to cause alterations in mitochondrial function, further confirming the role of mitochondrial dysfunction in PD (Schapira and Gegg, 2011, Gadd et al., 2006, Singleton et al., 2003).

As mentioned above, α-synuclein is one of the major components of LB in PD and other synucleinopathies. The finding that point mutations or multiplications in the *SNCA* gene were associated with PD provided important insights into the role of α-synuclein in neurodegeneration (Polymeropoulos et al., 1997, Kruger et al., 1998, Farrer et al., 2004, Zarranz et al., 2004, Spillantini et al., 1997). Although the majority of α-synuclein was found localized to the cytoplasm, a small part of the protein was identified localized to the membrane of mitochondria in a mouse brain (Li et al., 2007a). Studies from cell and animal models demonstrated that α-synuclein could directly interact with the mitochondrial membrane to inhibit Complex I activity, reducing ATP synthase and the mitochondrial membrane potential, resulting in mitochondrial dysfunction (Liu et al., 2009, Devi et al., 2008, Nakamura et al., 2008, Banerjee et al., 2010, Kamp et al., 2010, Martin et al., 2006). In turn these mitochondrial abnormalities lead to increased oxidative stress, synaptic defects and eventual cell loss and neurodegeneration.

Autosomal recessive mutations in the *PINK1* gene can cause an early onset juvenile parkinsonism. The PINK1 protein, encoded by *PINK1* gene, is a serine/threonine kinase possessing a mitochondrial targeting sequence at its N-terminus and has an intra-mitochondrial location (Valente et al., 2004). *PINK1* pathology in humans and animal models includes mitochondrial dysfunction, defective oxidative phosphorylation (OXPHOS), and increased free radical damage (Hoepken et al., 2007, Piccoli et al., 2008, Gautier et al., 2008, Gandhi et al., 2009, Gegg et al., 2009). Mutations found in *PINK1* lead to the abnormal phosphorylation of PINK1-targeted mitochondrial proteins, which in turn leads to mitochondrial respiratory and metabolic defects, oxidative damage and neuronal death (Valente et al., 2004).

PARK2 mutations are the commonest cause of autosomal recessive juvenile parkinsonism (ARJR), with an age of onset around 40 years. This form of PD displays a benign disease course and a good response to L-DOPA. *Parkin*-associated PD is associated with pure dopaminergic neuronal loss in the SN without LB formation, in contrast to *PINK1*-associated PD neuropathology in which LBs are seen (Kitada et al., 1998, Farrer et al., 2001, Pramstaller et al., 2005). Parkin functions as an E3 ligase,

ubiquitinating proteins for degradation by the proteasome (Shimura et al., 2000, Zhang et al., 2000, Chin et al., 2010). Cell studies have revealed that parkin can translocate and associate with the mitochondrial outer membrane to regulate mitochondrial function (Darios et al., 2003). Human and animal model studies have identified reduced complex I and IV activities in *parkin* mutants, which lead to reduced ATP production, impaired electron transport chain (ETC) activity, and apoptotic neuronal death (Greene et al., 2003, Darios et al., 2003, Muftuoglu et al., 2004, Mortiboys et al., 2008, Grunewald et al., 2010). Cell studies have demonstrated that PINK1, together with parkin, plays a crucial role in the turnover of mitochondria by autophagy (mitophagy), a mitochondrial quality control program that maintains mitochondrial dynamics and homeostasis (Zhang and Ney, 2010). Damaged mitochondria were firstly recognized by PINK1. PINK1 builds up on the outer membrane of the mitochondria and recruits parkin to target the damaged mitochondria for degradation by lysosomes-autophagy pathway (Zhang and Ney, 2010, Poole et al., 2008, Narendra et al., 2008, Vives-Bauza et al., 2010).

The *PLA2G6* gene encodes an 85-kDa group VI calcium-independent phospholipase A2 beta enzyme. *PLA2G6*, at the *PARK14* locus, has been characterized as the causative gene in a subgroup of patients with autosomal recessive early-onset dystonia-parkinsonism. Neuropathological examination of the post mortem brains of affected individuals revealed widespread LB pathology and the accumulation of hyperphosphorylated tau (Paisan-Ruiz et al., 2009, Paisan-Ruiz et al., 2012). PLA2G6 localizes to the mitochondria, and is required for the remodeling of membrane phospholipids and calcium signalling (Gadd et al., 2006). Loss-of-function mutations lead to abnormalities in mitochondrial morphology and synaptic membranes (Beck et al., 2011). In addition, we recently showed that knockout of the *Drosophila* homologue of *PLA2G6* leads to elevated mitochondrial lipid peroxidation and reactive oxygen species (ROS), mitochondrial respiratory chain dysfunction, reduced ATP synthesis and abnormal mitochondrial morphology (Kinghorn et al., 2015). In summary, studies of the mechanisms of pathogenesis of the *PARK* genes in causing neurodegeneration highlight the central role of mitochondrial dysfunction in PD.

In conclusion, the mechanisms of pathogenesis of both AD and PD described above are tightly linked to mitochondrial dysfunction. Therefore, targeting mitochondrial biogenesis may potentially ameliorate neurotoxicity in these neurodegenerative conditions. In Chapters 3 and 4, I will focus on dissecting the role of PGC-1α, the key regulator of mitochondrial biogenesis, in the pathogenesis of AD and PD using *Drosophila* models.

1.3 PGG-1α: an overview

Transcription factors (TFs) regulate gene transcription in the control of the myriad of biological signalling pathways necessary for the effective functioning of our cells. Gene transcription must be temporally coordinated through the interplay of protein complexes including TFs, RNA polymerases and related factors. TFs are proteins that bind DNA around the 5' end at the transcription start site in a sequence-specific manner. Transcriptional coactivators are proteins that can increase the rate of transcription by interacting with TFs, but do not themselves bind to DNA in a sequence-specific manner. Transcriptional coactivators coordinate RNA polymerase recruitment and orientation, and the unwinding of DNA to initiate transcriptional activity. The work in this thesis will focus on Peroxisome proliferator-activated receptor (PPAR)-γ coactivator-1α (PGC-1α), which is a well-know transcriptional coactivator involved in multiple biological processes in different tissues and physiological states.

The PGC-1α gene is located on chromosome 4 in humans, and encodes a protein containing 798 amino acids. It is mainly located in the cell nucleus and expressed at a high level in metabolically active tissues, where mitochondria are abundant and oxidative metabolism is active, such as in skeletal muscle, brown adipose tissue (BAT), the heart, the brain and kidneys. It is involved in a wide variety of biological functions, including adaptive thermogenesis, mitochondrial biogenesis, glucose/fatty acid metabolism, fibre type switching in skeletal muscle, as well as in the development of the heart.

1.3.1 Adaptive thermogenesis

PGC-1α was first discovered as a transcriptional coactivator in studies that distinguished white and brown fat pathways in adaptive thermogenesis. Adaptive thermogenesis involves the activation of a number of physiological mechanisms to increase heat production in response to environmental challenges such as cold, diet or infections, particularly in brown fat and muscle (Cannon et al., 1998, Rothwell and Stock, 1979). This process is important for energy homeostasis and metabolic defense against obesity. BAT, containing multiple small lipid droplets and a high number of mitochondria, is the main metabolic site for energy dissipation, in contrast to white adipose tissue (WAT), which primarily stores energy. Uncoupling protein-1 (UCP-1), which is exclusively expressed in BAT, is the main component in diet/cold-induced thermogenesis (Enerback et al., 1997), where its gene transcription is controlled by the transcription factors cAMP response element binding protein (CREB) (Kozak et al., 1994), thyroid hormone receptor (Cassard-Doulcier et al., 1994), and nuclear hormone receptor PPARγ (Sears et al., 1996). Interestingly, PGC-1α, whose mRNA levels are dramatically increased in response to cold stress, can elevate the transcriptional activity of PPARγ and the thyroid hormone receptor on the UCP-1 promoter (Puigserver et al., 1998). Indeed, ectopic expression of PGC-1α in brown fat cells activates UCP-1 and the expression of a number of genes necessary for mitochondrial respiratory chain activity. It also leads to the up-regulation of mitochondrial density, and thus has a central role in adaptive thermogenesis and energy metabolism.

1.3.2 Mitochondrial biogenesis

Enhanced mitochondrial biogenesis in skeletal muscle, in which PGC-1α is highly expressed and up-regulated by cold, adrenergic stimuli and exercise, is an important component of adaptive thermogenesis (Figure 1.5). Ectopic expression of PGC-1α in myotubes results in elevated mitochondrial biogenesis, including increased respiration and mtDNA copy number, as well as increases in genes involved in OXPHOS (Wu et al., 1999). In a mouse model of amyotrophic lateral sclerosis (ALS), a disease characterized by loss of motor neurons, over-expression of PGC-1α maintained mitochondrial biogenesis and muscle function, and delayed muscle atrophy, in the absence of any effect on lifespan (Da Cruz et al., 2012). Scarpulla and collaborators

have identified two transcription factors, nuclear respiratory factor (NRF)-1 and -2, that can bind to the promoter regions of nuclear-encoded mitochondrial genes, including ATP synthase, cytochrome-c, cytochrome-c-oxidase subunit IV, and mitochondrial transcription factor A (mtTFA). It is of particular interest that mtTFA can translocate to the mitochondrion and activate mitochondrial DNA (mtDNA) replication and mtDNA-encoded mitochondrial protein expression (Virbasius et al., 1993, Evans and Scarpulla, 1990). This suggests that the NRFs are key nuclear receptors for mitochondrial biogenesis and respiration. Interestingly, PGC-1α physically interacts with NRF-1, therefore co-regulating its transcriptional activity in mitochondrial biogenesis. In addition to NRF-1, transcription factors YY1 and ERRα were later also identified as being co-activated by PGC-1α in mitochondrial biogenesis (Scarpulla, 2008, Cunningham et al., 2007). Moreover, PGC-1α can dramatically induce gene expression of NRF-1 and -2, and ERRα, forming a double –positive–feedback loop that drives the expression of many OXPHOS genes (Wu et al., 1999, Mootha et al., 2004).

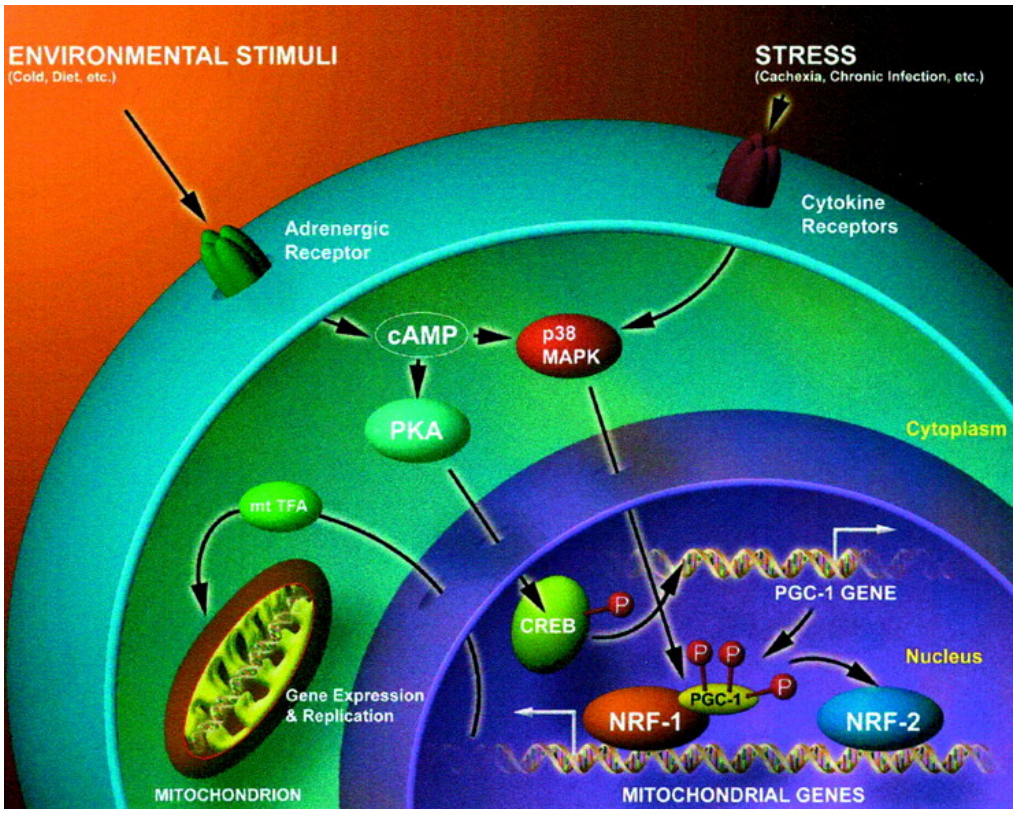

Figure 1.5 Adaptive thermogenesis and mitochondrial biogenesis

Mitochondrial biogenesis is highly induced by environmental stressors including cold, diet and infections in adaptive thermogenesis. PGC-1α, the key regulator in mitochondrial biogenesis is

activated by a cytokine signalling pathway through direct phosphorylation by p38 MAPK. In addition, the expression level of PGC-1α is directly controlled by the cAMP-CREB pathway. PGC-1α interacts with the transcription factors NRF-1 and NRF2 which in turn control the expression of genes for mitochondrial function. Taken from (Puigserver and Spiegelman, 2003).

PGC-1α plays a central role in mitochondrial biogenesis, and itself is regulated by several signalling cascades. It is activated by the cytokine signalling pathway through direct phosphorylation by p38 mitogen-activated protein kinase (MAPK) (Puigserver et al., 2001). Moreover, CREB- a transcription factor activated by cAMP, directly activates the expression of PGC-1α by binding to its promoter in hepatic gluconeogenesis (Herzig et al., 2001). In addition, PGC-1α activity can also be directly regulated by insulin-stimulated AKT phosphorylation in hepatic metabolism (Li et al., 2007b).

1.3.3 Hepatic gluconeogenesis

The study of PGC-1α is increasingly an area of interest in diabetes. Blood glucose levels are normally tightly controlled by the balance between peripheral glucose uptake and hepatic gluconeogenesis. The exact role of PGC-1α in the control of glucose uptake and metabolism is controversial. Studies using cultured muscle cells suggest that PGC-1α regulates glucose uptake and metabolism by co-activating the muscle transcriptional regulator MEF2 (myocyte enhancer factor-2), up-regulating the endogenous level of the insulin-sensitive glucose transporter (Glut4), and increasing glucose uptake (Michael et al., 2001). However, another study reported that over-expression of PGC-1α in skeletal muscle down-regulated Glut4 transcription and impaired the glycemic control after insulin administration (Miura et al., 2003). Indeed, it has been demonstrated that glucose uptake and metabolism do not necessarily reflect insulin sensitivity, which is most likely controlled by hepatic gluconeogenesis.

The liver is the major producer of glucose, mainly through gluconeogenesis, which occurs during fasting and is aberrantly activated in diabetes mellitus. PGC-1α is highly induced in type I (insulin-deficient) and type II (profound insulin resistance with a relative lack of insulin) diabetic mouse models, suggesting a key role for insulin as a suppressor of PGC-1α expression in the liver. The diabetic state is also

associated with low insulin-stimulated cAMP-CREB signalling, which directly controls the gene expression of PGC-1α (Herzig et al., 2001, Yoon et al., 2001). Moreover, insulin can suppress PGC-1α activity directly through AKT phosphorylation. This prevents the recruitment of PGC-1α to the cognate promoters, impairing its ability to bind and co-activate the forkhead transcription factor FOXO1 or the hepatocyte nuclear factor 4α (HNF-4α), to promote gluconeogenesis and fatty acid oxidation (Puigserver et al., 2003, Li et al., 2007b). Therefore, insulin inhibits PGC-1α activity, leads to a reduction in hepatic gluconeogenesis and reduced blood glucose levels. However, in type II diabetes, where patients exhibit high blood glucose levels, insulin resistance, and a low level of insulin, activation of PGC-1α and the associated up-regulation of hepatic gluconeogenesis lead to a further increase in glucose production and release. This phenomenon eventually leads to a further reduction in insulin sensitivity and exacerbates insulin resistance.

1.3.4 The role of PGC-1α in neurodegeneration

The physiological functions of PGC-1α have been studied in metabolically active tissues. However, there is an increasing interest in dissecting its role in neurodegeneration. PGC-1α null mice show hyperactivity and other movement disorders representative of basal ganglia pathology, such as stimulus-induced myoclonus, dystonic posturing and frequent limb clasping. They also develop spongiform lesions with axonal loss in the striatum, and exhibit neuronal cell death, suggesting a neuroprotective role for PGC-1α (Lin et al., 2004, Lucas et al., 2014, Leone et al., 2005). Moreover, PGC-1α plays a role in the defence against oxidative stress, a system that is known to contribute to neurodegeneration in ageing cells. Indeed, PGC-1α null mice display a more severe loss of dopaminergic neurons compared to controls when challenged with MPTP (1- methyl-4-phenyl-1, 2, 3, 6-tetrahydropyridine), a complex I inhibitor that induces PD in humans and animal models (St-Pierre et al., 2006).

PGC-1α has been shown to be a neuroprotective therapeutic target in animal models of several neurodegenerative diseases caused by abnormal protein aggregation, including Huntington's disease (Cui et al., 2006, Weydt et al., 2006, Tsunemi et al., 2012) and ALS (Zhao et al., 2011, Liang et al., 2011). Furthermore, amelioration of

neurotoxicity by PGC-1α activation is associated with the improvement in mitochondrial and lysosomal-autophagy function. Human studies have shown that PGC-1α activity negatively correlates with the age of onset of AD (Helisalmi et al., 2008) and PD (Clark et al., 2011). Indeed, human post-mortem studies demonstrated that PGC-1α levels are remarkably decreased in AD and PD patients' brains (Qin et al., 2009, Shin et al., 2011), suggesting that neuronal up-regulation of this factor may offer therapeutic benefits. However, the effects of elevating PGC-1α in AD animal models are elaborate (Sheng et al., 2012, Katsouri et al., 2011, Dumont et al., 2014), and its precise function *in vivo* in the pathogenesis of AD awaits further investigation. PGC-1α over-expression has been shown to rescue dopaminergic neuronal loss in primary neuronal cultures expressing mutant α-synuclein, in association with up-regulation of mitochondrial respiratory chain complex genes (Zheng et al., 2010). The role of PGC-1α in PD *in vivo*, however, is yet to be studied. In my thesis, I will focus on dissecting the role of PGC-1α in AD and PD using *Drosophila* models. A comprehensive review of what is already known with regards to the role of PGC-1α in AD and PD is provided in Chapters 3 and 4 respectively.

1.3.5 The *Drosophila* homologue of the PGC-1 family

Mammalian PGC-1α is a member of the PGC-1 family, which also includes the closely related homolog PGC-1ß (Lin et al., 2002), and PGC-1-related coactivator (PRC) (Andersson and Scarpulla, 2001). All of these proteins have significant functional overlap in mitochondrial biogenesis, and a high degree of homology in the transcriptional activation domain, RNA-binding motif, and serine-arginine-rich motif, which makes it difficult to tease apart their relative roles *in vivo*. Among invertebrate models, *Drosophila* carries a single *PGC-1* homolog in its genome (Gershman et al., 2007), whereas other invertebrate models such as yeast and *C. elegans* do not carry any *PGC-1* homologous sequences (Lin et al., 2005). The *Drosophila* homologue of *PGC-1α*, *spargel* (CG9808), is the only homologue of the mammalian PGC-1 family, therefore providing a system in which PGC-1 function can be assessed without interference from redundancy.

Drosophila larvae lacking *dPGC-1* show that there is 44% of the nuclear encoded mitochondrial proteins have been reduced the expression compared to wild type

controls, together with mitochondrial respiratory chain defects, demonstrating that *dPGC-1* is required for mitochondrial biogenesis in a similar manner to its mammalian counterpart (Tiefenböck et al., 2010). Moreover, *dPGC-1* null flies show reduced lipid storage and glycogen levels in association with a lean body phenotype. These results confirm that the main metabolic functions of PGC-1α described in mammals, including mitochondrial biogenesis, fatty acid oxidation and energy metabolism, are all conserved in *Drosophila*.

dPGC-1 has been reported to be a downstream target of the insulin/TOR signalling pathway involved in cellular growth, metabolism and nutrition (Tiefenböck et al., 2010, Mukherjee and Duttaroy, 2013). Insufficiency of either insulin or TOR results in developmental growth defects due to low ATP levels. Reduced expression of *dPGC-1* results in growth retardation with smaller body size and developmental delay, while *dPGC-1* gain-of-function has no immediate effect on *Drosophila* growth (Rera et al., 2011, Mukherjee and Duttaroy, 2013). *dPGC-1* acts to increase mitochondrial activity, cell growth and the transcription of target genes in response to insulin signalling, and over-expression of *dPGC-1* can overcome insulin/TOR-mediated cell growth defects. However, *dPGC-1* does not mediate all of the effects of TOR, since *dPGC-1* has been shown to have no effect on 4E-BP phosphorylation, the key regulator of mTOR-mediated mitochondrial activity and biogenesis (Morita et al., 2013). In addition, epistasis analysis has shown that over-expression of *dPGC-1* does not ameliorate the negative effects of over-expression of FOXO, the main IIS downstream effector responsible for cellular growth. This thus suggests that *dPGC-1* either works in parallel with FOXO or up-stream of FOXO. Therefore, the exact mechanisms linking *dPGC-1*-mediated cellular growth and mitochondrial function under the control of insulin/TOR are yet to be elucidated, though the overall effect of *dPGC-1* on growth is positive, like other members of the insulin/TOR signalling pathway.

An earlier study claimed that activation of insulin signalling is important for the transport of the *dPGC-1* protein from the cytoplasm to the nucleus (Tiefenböck et al., 2010). However, reduced insulin signalling by starvation failed to sequester the protein to the cytosol (Mukherjee et al., 2014), suggesting that the cellular localization

of *dPGC-1* might occur independently of insulin signalling. Interestingly, *dPGC-1* has also been found to form a negative feedback loop in the regulation of insulin signalling, suggesting a complex network between *dPGC-1* and IIS (Tiefenböck et al., 2010). In addition, a recent study suggested that *dPGC-1* can be directly up-regulated by Mitf, the *Drosophila* homologue of the transcription factor EB (TFEB) (Bouche et al., 2016). Inhibition of mTORC1 induces Mitf translocation to the nucleus and regulates the expression of genes involved in lysosomal biogenesis and lipid metabolism. This therefore highlights a novel role of *dPGC-1* in the mTOR-signalling pathway.

Mammalian PGC-1α and its relationship with insulin/mTOR signalling have become more tissue-specific during the course of evolution. In the absence of insulin, PGC-1α expression is elevated in the liver and gluconeogenesis is subsequently initiated (Puigserver et al., 2003). Therefore, liver-specific knock down of PGC-1α in mice results in higher insulin sensitivity (Koo et al., 2004). Conversely, the absence of PGC-1α in skeletal muscles has no effect on insulin sensitivity (Zechner et al., 2010). *In vivo* studies have demonstrated the functions of *dPGC-1* in several distinct fly tissues. Eye-specific knock down of *dPGC-1* results in eye phenotypes, including abnormal ommatidia and bristle formation (Merzetti and Staveley, 2015), suggesting a role in neurodegeneration. Over-expression of *dPGC-1α* in *Drosophila* muscle tissue improved the climbing ability of the flies (Tinkerhess et al., 2012), although the precise mechanisms underlying these effects require further investigation. With respect to longevity, reduced IIS/mTOR signalling extends lifespan in different species (Fontana et al., 2010). The action of *dPGC-1* on longevity is apparent as reduced *dPGC-1* expression causes significant shortening of lifespan in *Drosophila* (Mukherjee et al., 2014). The most comprehensive study of *dPGC-1* gain-of-function *in vivo* to date was that performed by Walker and colleagues. They demonstrated that over-expression of *dPGC-1* in the fly gut improved gut homeostasis and extended lifespan (Rera et al., 2011). Improved mitochondrial function and reduced ROS production were cited as the two major underlying mediators of the lifespan extension, however this has yet to be fully proven.

Interestingly, over-expression of *dPGC-1* in intestinal stem cells also prevented age-related over-proliferation of cells in maintaining gut homeostasis (Rera et al., 2011). Although this mechanism is not fully elucidated, it is known that a moderate reduction in IIS/mTOR signalling can also reduce age-related cell proliferation (Biteau et al., 2010). Previous studies have suggested that *dPGC-1* forms a negative feedback loop in the regulation of insulin signalling (Tiefenböck et al., 2010), which potentially explains why *dPGC-1* gain-of-function mimics reduced IIS/mTOR in regulating stem cell proliferation. Further work is required in this area to dissect the precise mechanisms of action of *dPGC-1* in insulin/mTOR signalling. It is still controversial as to whether up-regulation of *dPGC-1* in animal models is beneficial to lifespan (Tinkerhess et al., 2012), depending on the tissues and the experimental conditions. Research in *Drosophila* has significantly aided our understanding of the role of the PGC-1 group of proteins in ageing. Since both PGC-1α and IIS are involved in many physiological metabolic processes that contribute to obesity, diabetes, ageing and neurodegeneration, understanding how *dPGC-1* modulates IIS is likely to provide new insights into our understanding of mammalian ageing and age-related diseases. It may also lead to the identification of novel biomarkers and therapeutic targets in the treatment of these diseases.

1.4 The problem of ageing

The need to understand the ageing process and to discover new strategies to improve healthy lifespan is becoming more urgent in light of the increasing ageing population and the higher prevalence of age-related diseases (Fontana and Partridge, 2015). By 2050, the number of people over the age of 60 globally will triple (Figure 1.6) (Fontana et al., 2014).

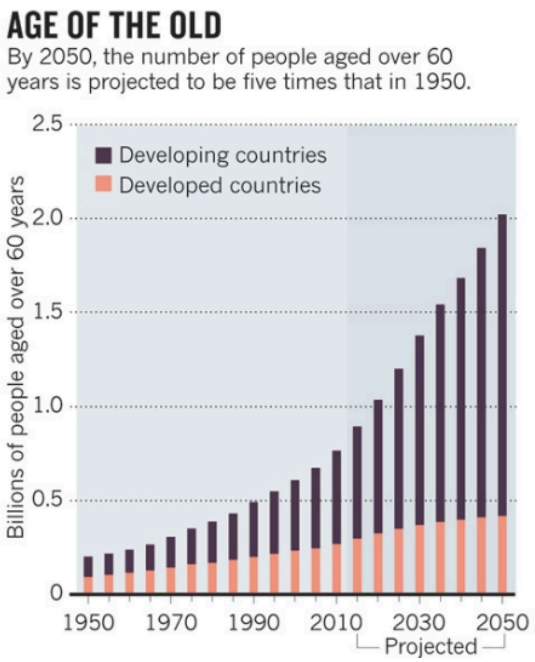

Figure 1.6 The prevalence of the ageing population

The prevalence of people over the age of 60 in developing and developed countries will dramatically increase by 2050. Taken from (Fontana et al., 2014).

The majority of people over the age of 65 years already report suffering from one or more chronic disorders, such as diabetes, cancer, heart disease, stroke and neurodegeneration (Hung et al., 2011). With an ever-increasing aged population the prevalence of ageing-associated diseases has increased (Figure 1.7). These demographics are increasingly becoming a central issue for public health in developed countries, and bring considerable costs to the individuals as well at the population level. Moreover, studies using animal models suggest that delaying one age-related disease could potentially reduce the prevalence of others (Fontana et al., 2014), suggesting that ageing and age-related disorders are tightly linked.

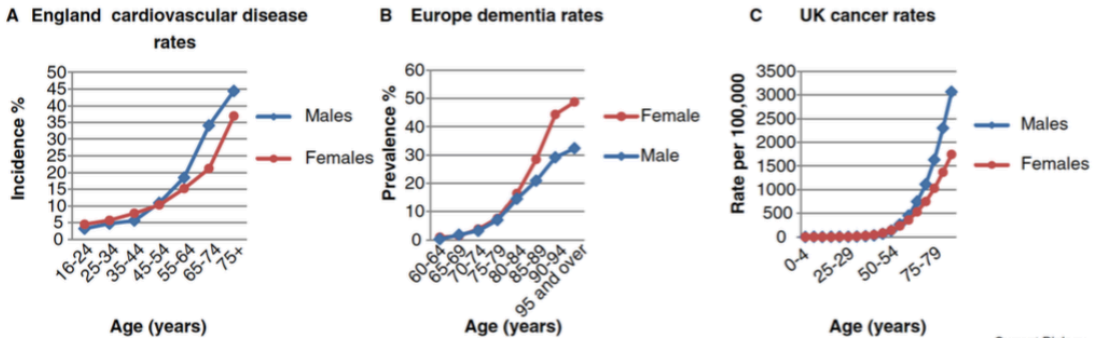

Figure 1.7 The incidence of age-related disease in 2006

(A) The incidence of cardiovascular disease in England. (B) The prevalence of dementia in European countries. (C) The UK cancer rate per 100,000 population. Taken from (Niccoli and Partridge, 2012).

1.4.1 The theories of ageing

Ageing is a complex process, involving genetic and environmental factors. Many theories of ageing have been developed to explain why we age and how we age. The altruistic theory of ageing proposes that the existence of ageing is beneficial, since decreasing the burden of older individuals may benefit the young and healthy individuals when natural resources are limited (Kirkwood and Austad, 2000). However it does not explain why ageing exists in the first place.

The evolutionary theory of ageing comes from the observation that the force of natural selection declines with age (Figure 1.8). The variation within the population exists, because random mutations will occur in the genome of individuals. Natural selection is the evolutionary mechanism that determines whether these mutations persist or are eliminated, depending on their contribution to reproductive capacity. If the mutations have a negative impact on development or reproductive ability, they would tend to be removed from the population and will not pass on to the next generation. However, the mutations that do not affect reproductive capacity will persist, and the offspring can inherit such mutations. In other words, harmful mutations that occur during childhood before the age of reproductive capacity are under strong natural selection, and thus are less likely to be passed on. However, the force of natural selection starts to decline after reproduction commences, which means that mutations that occur later will be under low or no natural selection, and will continue to accumulate. Accumulation of late-acting deleterious mutations over the course of the evolution of a population causes what we now understand as ageing, and this is called the mutation accumulation theory of ageing (Medawar, 1957).

This can be better understood by a comparison between progeroid syndromes and Huntington's disease (De Strooper et al.). Patients with progeroid show phenotypes in early life, limiting their reproductive capacity, giving rise to a low prevalence of this disorder in the population. Conversely, HD is a late-onset neurodegenerative disorder, which enables the defective gene to be passed on to the next generation, giving rise to

a higher prevalence (Rose, 1999, Haldane, 1941). This illustrates how deleterious disease-causing genes are not removed by natural selection.

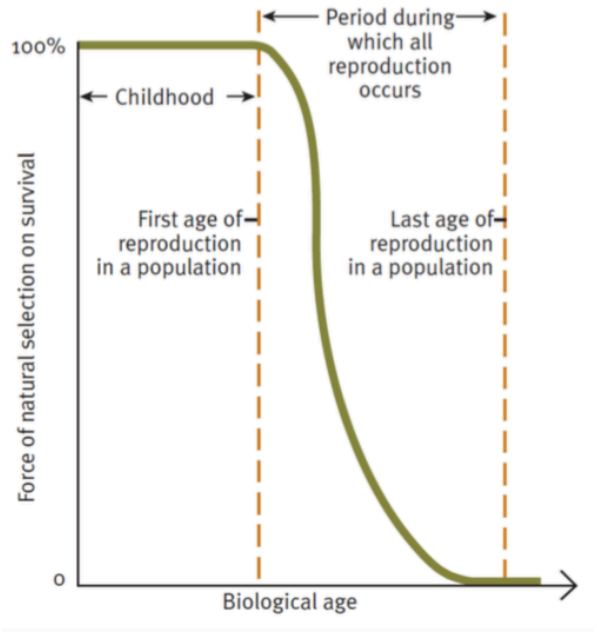

Figure 1.8 The force of natural selection declines with age

Mutations arising during childhood before the onset of reproductive fitness are under strong natural selection. Mutations whose phenotypes manifest after sexual maturity are under less selective pressure. Therefore, late-manifesting mutations are able to pass on to the next generation. Taken from (Rose, 1999).

The evolutionary theory of ageing arising from the concept of natural selection has been further developed into several differential explanations. George Williams proposed that mutations that ensure reproductive capacity would be favored by natural selection even if they pose a disadvantage later in life, which is referred to as the antagonistic pleiotropic (AP) theory of ageing (Williams, 1957). The AP theory highlights the dual early benefit and late negative effect of such mutations, and provides guidance on translating developmental studies into ageing research. Researchers must bear in mind that genes that are required during development will affect reproductive fitness by natural selection, and their contribution to ageing will therefore remain unknown. Insulin and the mTOR signalling pathways provide good proofs of principle of the AP theory. These two pathways are very important for development and growth, as they promote energy metabolism and protein synthesis. Meanwhile, these pathways are now known to contribute to ageing, as down-

regulation of the insulin/mTOR signalling pathways extends lifespan in diverse organisms (Fontana and Partridge, 2015), highlighting the pleiotropic functions of the insulin/mTOR pathways. They are also important for reproduction and therefore they persist after natural selection

1.4.2 The study of ageing in model organisms

To understand the biological processes that drive ageing, laboratory animal models have been used to investigate different pharmacologic or genetic interventions. In order to assess the effects of such interventions on lifespan, the median and maximum lifespan of groups of animals are often measured. Median lifespan refers to the time at which 50% of the population remains alive. Maximum lifespan refers to the time when the last individual dies. Each model organism has its advantages and disadvantages for studying ageing and age-related diseases. However, interventions in any specific cellular pathway have to be at least evolutionary conserved in order to effectively translate research findings from these animal model species to humans (Partridge, 2001). In mammalian models, the mouse is the preferred organism with an average lifespan of 3 years and the availability of well-characterised genetic tools. Although mice are costly and require considerable maintenance, especially for lifespan experiments requiring large population numbers (Swindell, 2012), their use is important when testing successful interventions discovered in less complex organisms.

Simple model organisms like *C. elegans* and *Drosophila melanogaster* offer many advantages for ageing research, due to their relatively short lifespan and well-known genomes. *Drosophila* (the fruit fly) is a powerful genetic tool for studying genetic inheritance, development, behaviour, disease and ageing. Moreover, the distinct brain structure with cell types analogous to the human brain, and the presence of a blood brain barrier, make it an excellent model to study neurodegeneration (McGurk et al., 2015, Fernandez-Funez et al., 2015). *Drosophila* has a short life cycle, which is approximately 10 days from egg laying to the eclosion of adult flies at 25°C (Figure 1.9). Under laboratory conditions, *Drosophila* can live for around 3 months, and female flies live slightly longer than male flies. The *Drosophila* genome contains 4 pairs of chromosomes: an X/Y pair, and three autosomes named 2, 3, and 4.

Determination of the sex in *Drosophila* depends on the ratio of X chromosomes to autosomes, which is different from that in humans. Moreover, 60% of the *Drosophila* genes are conserved in the human genome, and 75% of known human disease genes have a recognizable homologue in the *Drosophila* genome. Therefore, *Drosophila* has been successfully used as a genetic model for several human diseases including PD and AD, some of which I have utilized in my research.

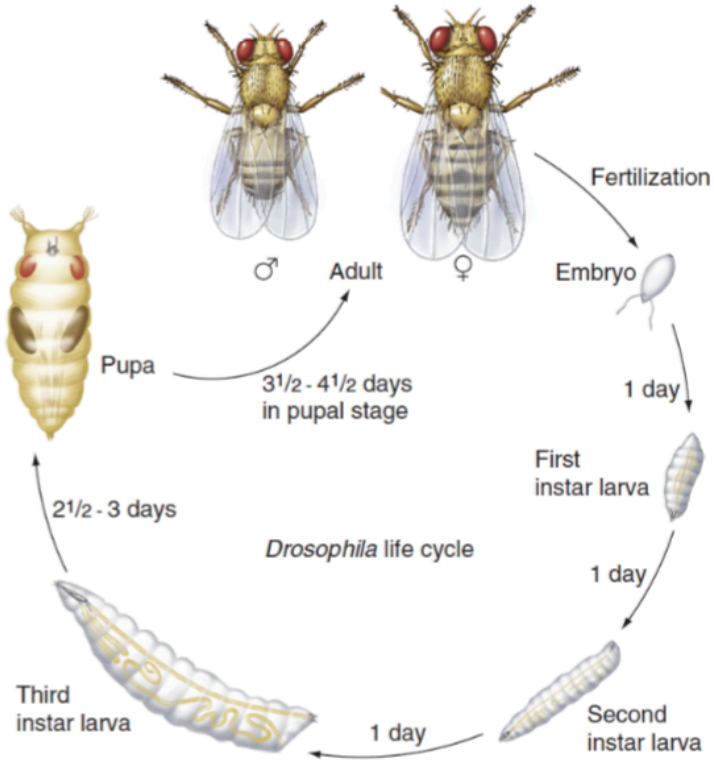

Figure 1.9 The *Drosophila* life cycle

Fertilized females store sperm in storage organs, and fertilize their eggs just before laying the embryo (egg). The embryo completes its development within 24 hours and hatches as a first instar larva and progresses to a third instar larva. Just before pupariation the third instar larva crawls up the side of the housing bottle and undergoes metamorphosis inside the protective pupal case. During this four-day period most larval tissues are replaced with adult-like tissues. After flies emerge from their pupae, their wings expand, and their exoskeleton hardens and becomes pigmented. Taken from (Hartwell et al., 2011).

1.4.3 The molecular basis of the ageing process

Ageing is the progressive loss of physiological integrity, leading to dysfunction and increased vulnerability to death. This deterioration is the main risk factor for human diseases, including cancer, diabetes and neurodegeneration. Ageing research has

achieved huge success during the past few decades, particularly with the discovery that ageing process can, to a certain extent, be delayed or ameliorated. The hallmarks of ageing include mitochondrial dysfunction, dysregulated nutrient sensing, proteostatic failure, alterations in epigenetics, telomere attrition, genomic instability, alterations in intercellular communication, stem cell exhaustion and cellular senescence (Figure 1.10) (Lopez-Otin et al., 2013). The ageing process is complex: not only do the individual components contribute to ageing, but also there is considerable crosslink between different components. Here I will describe the role of mitochondrial dysfunction and proteostatic failure in the ageing process.

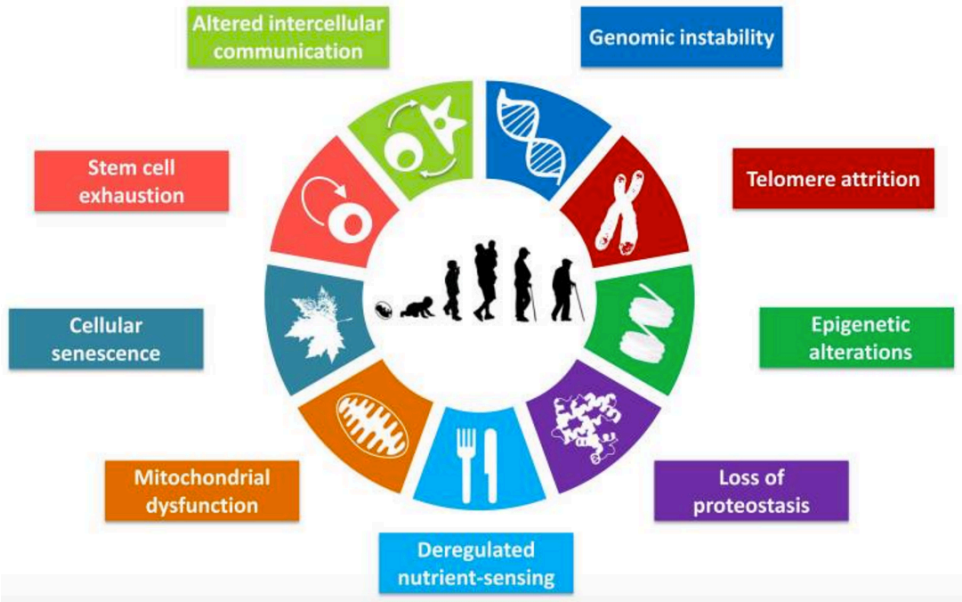

Figure 1.10 The hallmarks of ageing

This diagram depicts the 9 hallmarks of ageing, including mitochondrial dysfunction, deregulated nutrient sensing, proteostatic failure, alterations in epigenetics, telomere attrition, genomic instability, alterations in intercellular communication, stem cell exhaustion and cellular senescence. Taken from (Lopez-Otin et al., 2013).

1.4.4 Mitochondrial dysfunction in ageing

The mitochondrion is the energy factory of living cells, playing an important role in maintaining intracellular homeostasis. The role of mitochondrial dysfunction in neurodegeneration has been addressed above. Its involvement in the ageing process, however, is complex and controversial. The physiological functions of mitochondria

include energy metabolism and respiration, which is essential for development and cell growth. The mitochondrial respiratory chain, as well aiding the production of ATP, is also the main site of ROS production. The mitochondrial free radical theory of ageing states that the accelerated mitochondrial dysfunction that occurs with age causes increased ETC leakage and production of ROS. In turn this accumulation of ROS results in free radical damage, including mtDNA mutations or deletions, increased lipid peroxidation, calcium deregulation, further mitochondrial deterioration and eventually cell death (Harman, 1965, Green et al., 2011). However, many studies have suggested that free radical damage and lifespan can be uncoupled. Mitochondrial ROS and oxidative damage in mice did not accelerate ageing (Zhang et al., 2009), while reduction of ROS by increasing antioxidant defence in mice failed to extend lifespan (Van Raamsdonk and Hekimi, 2009). Indeed, several studies showed that moderate increases in ROS can be beneficial and extend lifespan in yeast and *C. elegans* (Doonan et al., 2008, Mesquita et al., 2010, Van Raamsdonk and Hekimi, 2009). Therefore, the role of ROS in ageing requires re-evaluation: rather than being a direct contributor to ageing, it is more likely a response modulator for stress-elicited survival signalling (Sena and Chandel, 2012).

Mutations and deletions in aged mtDNA may also contribute to ageing (Park and Larsson, 2011). mtDNA is considerably vulnerable to ageing-associated stress and mutation due to the lack of protective histones and the limited efficiency of repair mechanisms (Linnane et al., 1989). Interestingly, most mtDNA mutations in aged cells appear to be caused by replication errors early in life rather than oxidative damage. These mutations may undergo polyclonal expansion and result in ETC dysfunction and mitochondrial ageing (Ameur et al., 2011, Payne et al., 2011). Moreover, mice lacking mitochondrial polymerase gamma showed accumulation of mtDNA mutations and deletions, impaired mitochondrial function, and shortened lifespan (Kujoth et al., 2005, Trifunovic et al., 2004, Vermulst et al., 2008). Therefore, it would be interesting to know whether genetic manipulations that decrease the load of mtDNA mutations can extend lifespan.

PGC-1α, the captain of the mitochondrion, has dual effects in increasing mitochondrial mass and activity and defending against oxidative damage (St-Pierre et

al., 2006). A lack of PGC-1α leads to mitochondrial dysfunction and can cause premature ageing and age-related diseases. Recently a study showed that over-expression of PGC-1 in *Drosophila* could extend lifespan, improve mitochondrial function, including increasing ETC activity and mitochondrial mass, as well as reduce ROS (Rera et al., 2011). Given the controversial roles of these effectors in ageing, further studies are warranted to investigate whether genetic manipulation of the above effectors can directly extend lifespan.

1.4.5 Proteostatic failure in ageing

A decline in proteome homeostasis (proteostasis) leads to ageing and age-related neurodegeneration (Hetz et al., 2011). Maintenance of proteostasis requires proper protein folding and assembly and protein quality control. To protect against proteotoxicity, cells have evolved several independent stress responses that result in the induction of chaperones and degradation machineries within selected organelles. Three well-characterized stress response pathways are the endoplasmic reticulum unfolded protein response (UPR^{ER}) (Ron and Walter, 2007), the mitochondrial unfolded protein response (UPR^{mt}) (Haynes and Ron, 2010) and the heat shock response (HSR) (Akerfelt et al., 2010). The UPR is the stress response pathway that is activated by the accumulation of mis-folded proteins in the ER or mitochondria, in order to either re-establish proteostasis or induce apoptosis. However, the ability to maintain proteostasis by activating the UPR^{ER} declines with age (Casas-Tinto et al., 2011). Activation of the UPR^{ER} by over-expression of an active *Xbp1*, the downstream effector of the IRE1 branch of the UPR^{ER} promotes ER stress resistance, and extends lifespan in *C. elegans* (Taylor and Dillin, 2013). The questions of whether activating the UPR^{ER} can extend lifespan in more complex organisms remains unanswered.

In addition, deleterious mitochondrial stress caused by excessive ROS production may be detrimental to the maintenance of the mitochondrial proteome, with elevated mitochondrial lipid peroxidation (Kinghorn et al., 2015), calcium deregulation (Du et al., 2010), and eventually abnormal assembly of the ETC components (Tatsuta and Langer, 2008). Interestingly, mild mitochondrial stress has been shown to be beneficial in terms of lifespan (Merkwirth et al., 2016). The UPR^{mt} is a stress-response pathway that adapts and activates the folding capacity of the mitochondrial

matrix in response to mitochondrial dysfunction, leading to up-regulation of nuclear-encoded, mitochondrial-localized chaperones. These in turn promote both protein folding and degradation to either restore mitochondrial proteostasis or to trigger apoptosis (Neupert and Herrmann, 2007, Haynes and Ron, 2010). In mammalian cells, activation of the UPR^{mt} correlates with increased JNK2 signalling, leading to induction of the transcription factors CHOP and C/EBPβ, thus up-regulating the mitochondrial chaperone HSP60 (Aldridge et al., 2007, Zhao et al., 2002).

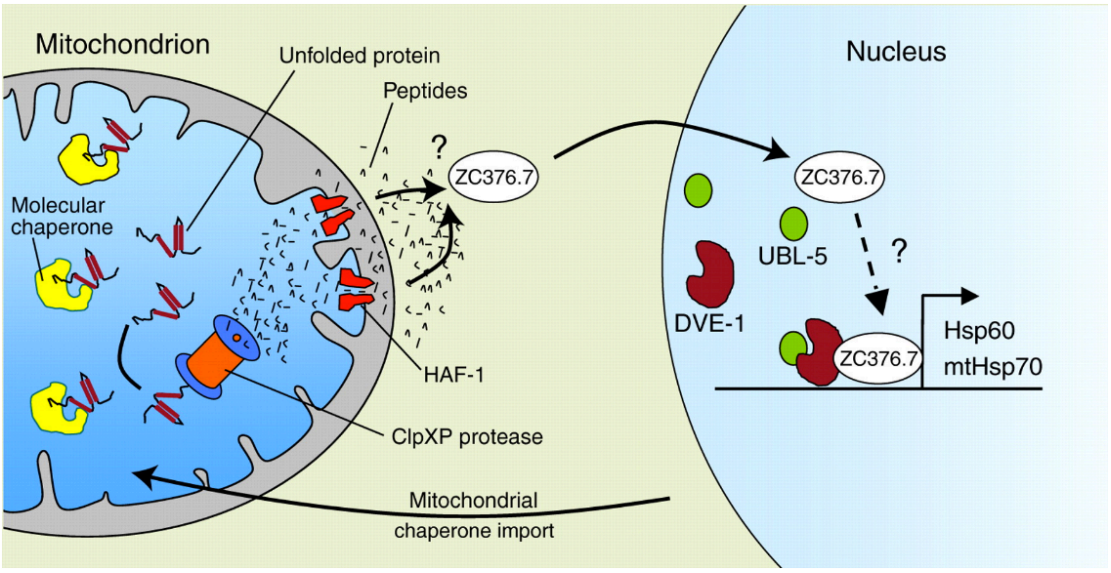

Figure 1.11 A model of mitochondrial UPR signalling in *C. elegans*

The mitochondrial UPR is initiated when mis-folded proteins in the mitochondrial matrix exceed the capacity of the mitochondrial chaperones. The ClpXP protease degrades the unfolded protein into peptides, which is then released to the cytosol by the HAF-1 transporter. This peptide efflux activates the translocation of the transcription factor ZC376.7 into the nucleus by unknown mechanisms. ZC376.7, together with UBL-5 and DVE-1, form a transcriptional complex to drive gene expression of nuclear-encoded but mitochondrial-localized chaperones. Transcriptional up-regulation of mitochondrial chaperones in turn relieves the stress and re-establishes homeostasis. Taken from (Haynes and Ron, 2010)

In *C. elegans* (Figure 1.11), the protease ClpXP degrades mis-folded proteins into peptides, which are then exported into the cytosol through the HAF-1a transporter, leading to translocation of the transcription factor ZC376.7 into the nucleus. This leads to the up-regulation of the mitochondrial chaperones HSP60 and mtHSP70/Glucose regulated protein 75 (Grp75), thus relieving stress and re-establishing homeostasis (Haynes et al., 2007, Yoneda et al., 2004). Recent studies

found that an early perturbation of mitochondria leads to remodelling and silencing of chromatin, and extends lifespan in *C. elegans* (Tian et al., 2016). Therefore, the role of UPR^{mt} in ageing is complex and awaits further investigation.

Another biological stress response pathway involved in ageing is the UPS (Ubiquitin proteasome system), which is also implicated in age-related neurodegenerative diseases such as AD and PD (Morimoto, 2008, Lopez-Otin et al., 2013). The UPS, together with the lysosome-autophagy system and chaperone network, acts to maintain cellular protein homeostasis by removing unwanted or damaged proteins that may become toxic to cells (Jung et al., 2009, Glickman and Ciechanover, 2002). UPS activity is ATP-dependent, which supports the hypothesis that improving energy metabolism may suppress the age-related decline in proteasome activity (Fontana and Partridge, 2015).

1.4.6 Anti-ageing interventions

Since ancient times individuals have been seeking ways to prolong youth and avoid the ageing process. The most successful findings in ageing research to date come from the discovery that ageing can be ameliorated by diet, genetic or pharmacological interventions in the nutrient-sensing pathway. Multiple molecular pathways appear to set the pace of physiological ageing. Interventions in these pathways prolong lifespan and healthy ageing in rodents and mammals. Reduced food/caloric intake, simultaneously avoiding malnutrition, can delay ageing and age-related disease in different organisms from yeast to humans (Fontana et al., 2010).

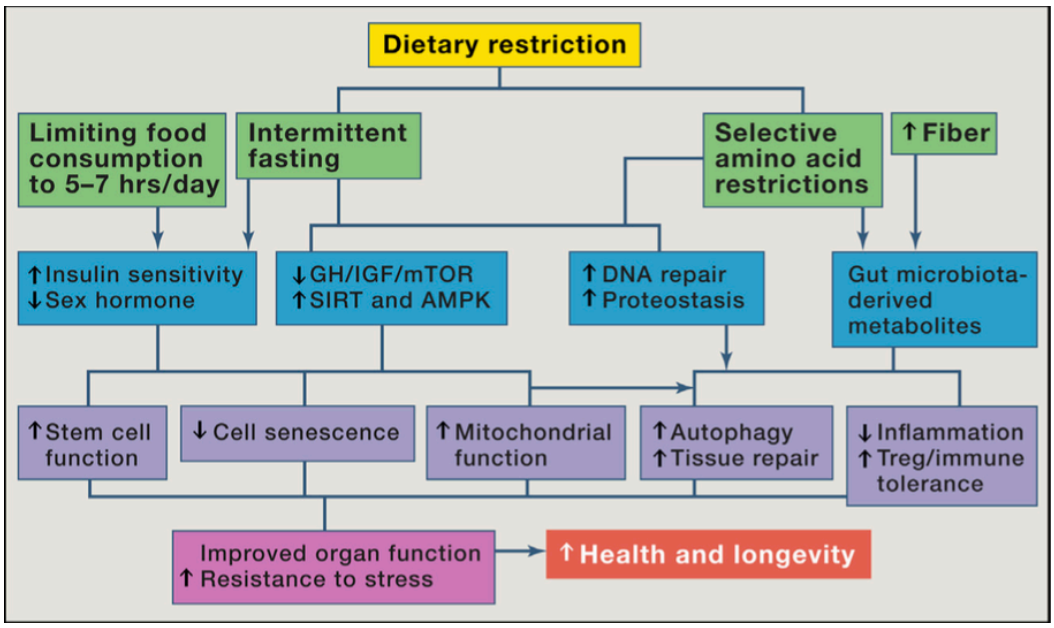

Figure 1.12 The role of DR in ageing

DR improves healthy lifespan through multiple systemic, neuronal, and cellular mechanisms. Taken from (Fontana and Partridge, 2015).

DR in mice and rats improves healthy lifespan, in association with a reduction in the prevalence of age-related pathologies (Fontana et al., 2010, Ikeno et al., 2006, Maeda et al., 1985). Young monkeys subjected to DR show improved metabolism and a lower prevalence of type-2 diabetes, cancer and cardiovascular disease (Colman et al., 2014, Mattison et al., 2012). In humans, long-term DR results in similar metabolic and molecular changes to those seen in animals. DR improves several markers of health and reduces the risk of developing cardiovascular diseases, neurodegeneration, and cancer (Heilbronn et al., 2006, Cava and Fontana, 2013, Masoro, 2003). Due to its robustness and strong conservation across different species, the discovery of the molecular mechanisms involved in DR will provide useful insights into the mechanisms of ageing. The mechanisms by which DR improves healthy lifespan are not fully understood in any species. One of the best known mechanisms of DR that is evolutionarily conserved across species is that, under the conditions of nutrient limitation, there is an adaptive switch in metabolic state from reproduction and growth toward somatic maintenance to ensure survival (Holliday, 1989). DR also extends lifespan in many less-complex and shorter-lived organisms including *S. cerevisiae*, *C. elegans* and *Drosophila*. The wide use of yeast and invertebrates has

enabled researchers, through genetic and pharmacological interventions, to discover the evolutionarily conserved mechanisms that extend healthy lifespan.

One of the molecular mediators of DR on longevity is the mTOR (mechanistic target of rapamycin), which is an evolutionarily conserved nutrient-sensing protein kinase that responds to amino acid levels. It thus regulates growth and metabolism in all eukaryotic cells (Johnson et al., 2013). mTOR functions in two distinct complexes: mTOR complex 1 (mTORC1) and mTOR complex 2 (mTORC2). Rapamycin inhibits mTORC1 activity, extending lifespan across species from yeast to mammals. It mediates its longevity effects via mechanisms including reduced mRNA translation and induction of autophagy through at least two mTORC1 substrates, ribosomal protein S6 kinases (S6Ks) and eukaryotic translation initiation factor 4E-binding protein 1 (4E-BP1) (Bjedov et al., 2010, Powers et al., 2006, Robida-Stubbs et al., 2012, Harrison et al., 2009, Medvedik et al., 2007, Miller et al., 2011). Moreover, inhibition of mTORC1 also improves proteostasis and enhances stem cell function (Kapahi et al., 2010, Johnson et al., 2013). mTORC2 is not sensitive to inhibition by rapamycin, and is usually considered not relevant in nutrient sensing. However it is necessary for the phosphorylation and activation of AKT downstream of the IIS (Guertin and Sabatini, 2009). In addition, mTORC1 extends lifespan in mechanisms overlapping with IIS. mTORC1 is activated by insulin through PI3K (phosphatidylinositide 3-kinases) and AKT kinase signalling, while mTORC1 negatively regulates IIS though S6K, which inhibits insulin receptor substrate 1 (IRS 1) (Laplante and Sabatini, 2012, Takano et al., 2001). Additional studies have indicated that the mTORC1 target 4E-BP is also a transcriptional target of FOXO in fruit flies (Tettweiler et al., 2005). mTORC1 has also been implicated in several ageing processes including inflammation and mitochondrial dysfunction (Johnson et al., 2013). Hyper-activation of mTOR is often associated with inflammation, and rapamycin has been shown to have anti-inflammatory effects via NF-kB (nuclear factor kappa-light-chain-enhancer of activated B cells) (Liu, 2006, Nuhrenberg et al., 2005). The activity of NF-kB signalling increases with age (Ren et al., 2007, Libert et al., 2006), and imbalanced NF-kB signalling is a major risk factor underlying ageing and age-related disease (Chung et al., 2009). This highlights the potential therapeutic benefits of limiting NF-kB signalling to improve tissue homeostasis in ageing (Guo et

al., 2014). In addition, regulation of mitochondrial function by mTORC1 is complex. mTOR complex actively promotes mitochondrial biogenesis and metabolism through PGC-1α and YY1 (Cunningham et al., 2007). However, yeast and mouse studies have demonstrated that inhibition of mTORC1 results in a metabolic shift towards greater mitochondrial respiration, thereby increasing chronological longevity (Bonawitz et al., 2007, Polak et al., 2008).

It has been shown in *S. cerevisiae* that decreased mTOR signalling mediates the pro-longevity effects of DR (Kaeberlein et al., 2005). Moreover, the first *C. elegans* model to show a DR-like response with lifespan extension was that carrying an *eat-2* mutation, which directly causes pharyngeal pumping defects (Lakowski and Hekimi, 1998). Several components in the mTOR signalling networks have been shown to mediate the lifespan extension of DR in *C. elegans*. Late-onset knockdown of mTOR using RNAi extends lifespan (Vellai et al., 2003), in a FOXO-independent manner. This suggests that mTOR mediates lifespan regulation through mechanisms other than reduced insulin signalling pathway activity (Vellai et al., 2003, Guarente and Kenyon, 2000). Down-regulation of the components in the mTOR complex or the downstream effectors in the mTOR signalling pathway have been found to mediate lifespan extension by reducing bacterial food concentration in the diet, suggesting a DR-like mechanism (Chen et al., 2009b, Honjoh et al., 2009, Jia et al., 2004). Moreover, inhibition of the mTOR pathway in the DR mimetic *eat-2* mutant background does not further extend lifespan, suggesting that mTOR signalling pathway inhibition and DR share overlapping mechanisms in regulating lifespan (Hansen et al., 2008, Chen et al., 2009b).

DR also extends lifespan in *Drosophila* (Clancy et al., 2002, Mair et al., 2003, Rogina et al., 2002). In *Drosophila*, the method of restricting food intake is different from that in yeast or worms. The diet used in *Drosophila* usually contains a carbohydrate source (sucrose), yeast as a source of amino acids, vitamins, minerals, cholesterol and essential fatty acids. Previous studies showed that it was modulation of the yeast in the diet that mediated the DR-associated lifespan extension, rather than the carbohydrate content or water (Kapahi et al., 2004, Mair et al., 2005). Therefore, the diet in *Drosophila* DR studies is manipulated by reducing the yeast component

without changing the carbohydrate load. Therefore, the evaluation of DR on lifespan is usually performed by varying the amount of yeast from low to high, using at least 3 different concentrations. With an increased gradient of yeast concentration, lifespan gradually increases to a maximum, after which the lifespan drops with any further increases in yeast concentration. When the values of the median or maximum lifespan are plotted against the concentration of yeast, the graph appears as a tent-shaped curve. The DR condition therefore refers to the yeast concentration that shows the highest lifespan (either median lifespan or maximum lifespan). Lower yeast concentrations limit lifespan by malnourishment, while higher concentration limits lifespan by over-nourishment (Bass et al., 2007, Grandison et al., 2009, Metaxakis and Partridge, 2013). The practical use of a DR-tent is to test the potential interactions between different interventions and diet on lifespan (Figure 1.13). When the intervention is truly a DR mimetic, the flies should behave as though they are already to some extent subjected to DR. They should therefore be more prone than controls to starvation at low levels of nutrition. At the food dilution that maximizes control lifespan, the flies with intervention would be malnourished and less long-lived. Lifespan of those flies should peak at a higher food concentration than that of controls dose, and at this and higher food concentrations, the flies with intervention should be longer lived than controls (Clancy et al., 2002) (Figure 1.13A). If the intervention is not a DR mimetic, lifespan extension will occur to a similar degree regardless of the yeast conditions (Figure 1.13B). In addition, if an intervention shares some mechanisms with DR, it might still further extend lifespan under DR conditions, however the response to different yeast conditions will differ and the maximum benefit for this intervention might be within full-feeding (Figure 1.13C). Cox proportional hazard (CPH) analysis makes this comparison much easier, and simply evaluates the effect of an intervention across all the different yeast levels. In other words, CPH will establish whether the shape of the DR-tent is different between interventions and related-controls. A significant interaction suggests that the intervention and DR share similar mechanisms. A non-significant difference suggests that the intervention is a non-DR mimetic or acts beyond DR.

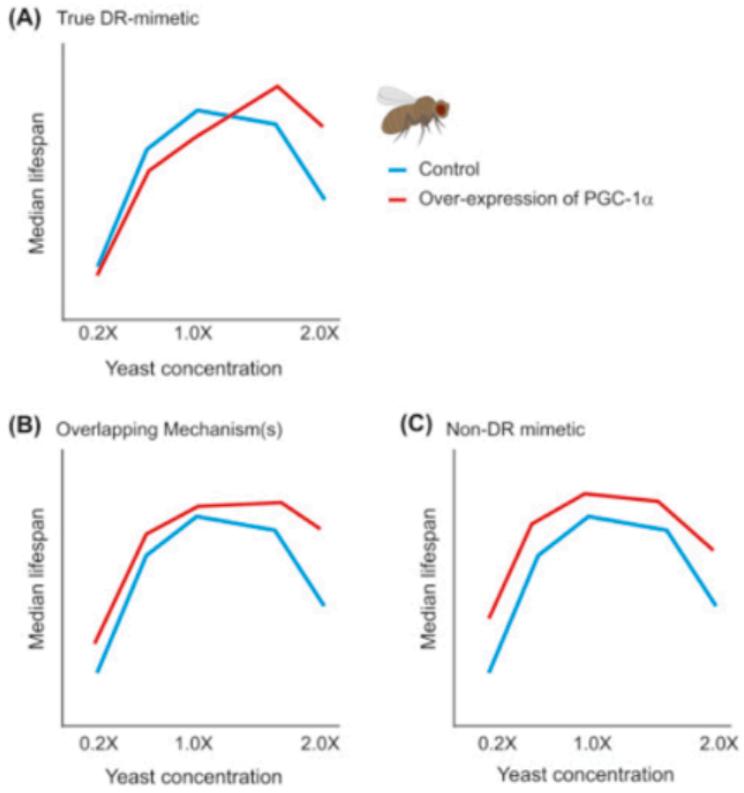

Figure 1.13 Testing a genetic intervention that extends lifespan and its interaction with DR

PGC-1α, the transcriptional coactivator in mitochondrial biogenesis, has previously been shown to extend lifespan in *Drosophila* (Rera et al., 2011). However its mechanisms of lifespan extension are not fully understood. (A) The DR-tent if over-expression of *dPGC-1* is a true DR-mimetic. (B) The DR-tent if over-expressing *dPGC-1* is partially overlapped with DR. (C) The DR-tent if *dPGC-1* over-expression extends lifespan beyond DR. Taken from (Castillo-Quan et al., 2015).

Inhibition of mTOR signalling components extend lifespan in *Drosophila,* but not to a greater extent than that seen with DR, supporting the idea that mTOR mediates the lifespan extension by DR-related mechanisms (Kapahi et al., 2004). Moreover, feeding flies with rapamycin, which inhibits mTORC1 activity, extends lifespan in *Drosophila* (Bjedov et al., 2010). Rapamycin further increases the lifespan of *Drosophila* under different yeast concentrations. However, the responses to diet are different between controls and rapamycin-treated flies across the different food conditions, in which the largest increase in lifespan by rapamycin is under the full feeding. This result suggests that pharmacological inhibition of mTOR signalling by rapamycin shares overlapping mechanisms with DR in lifespan regulation.

In addition, mTOR signalling also mediates mammalian longevity. The long-lived

Ames dwarf mice show reduced protein synthesis via inhibition of mTOR activity (Bartke and Brown-Borg, 2004, Sharp and Bartke, 2005). Moreover, administration of the mTORC1 inhibitor rapamycin extends lifespan in mice, further demonstrating the beneficial effect on lifespan of inhibiting mTOR signalling (Harrison et al., 2009, Chen et al., 2009a).

Insulin/IGF-1-like signalling (IIS) also mediates the lifespan extension of DR, although comprehensive studies are very limited. Reduced insulin/IIS increases longevity in *C. elegans*, fruit flies and mice (Fontana et al., 2010, Kenyon, 2010). Lifespan extension and stress resistance resulting from reduced IIS is mediated by the FOXO family of transcription factors through PI3K and AKT kinase signalling (Laplante and Sabatini, 2012, Tullet et al., 2008). Inhibition of AKT activates FOXO, which then up-regulates several "longevity pathways" controlling DNA repair, autophagy, antioxidant activity, stress resistance and cell proliferation (Webb and Brunet, 2014, Wang et al., 2014). Reducing IIS via partial ablation of the insulin-like peptide-producing median neurosecretory cells (mNSCs) in the adult *Drosophila* brain, which produce three of the seven *Drosophila* insulin-like peptides (dilp2, 3 and 5), reduces IIS signalling and extends lifespan (Broughton et al., 2010). Moreover, a study using $chico^{1}$ mutants, a long-lived insulin mutant in *Drosophila* showed that reduced IIS and DR extended lifespan via overlapping mechanisms (Clancy et al., 2002). Although the nature of the mechanisms by which $chico^{1}$ acts like DR requires further analysis, reduced IIS and DR may interact in determination of lifespan because they both alter some common downstream process. Indeed, reduced IIS signalling can inhibit mTORC1 activity through AKT phosphorylation in *Drosophila*, suggesting that mTOR may be one of the common pathways downstream of both interventions.

The other two nutrient sensors, AMPK (5' adenosine monophosphate-activated protein kinase) and sirtuins, act in the opposite direction to IIS and mTOR. They therefore sense nutrient scarcity and catabolism instead of nutrient abundance and anabolism (Lopez-Otin et al., 2013). In general, activation of AMPK and sirtuins promotes longevity. AMPK activation has multiple effects on metabolism. Activation of AMPK can down-regulate mTORC1 activity, therefore controlling cell growth, autophagy and translation (Alers et al., 2012). Activation of AMPK also activates

PGC-1α, antioxidant defences and fatty acid oxidation (Wu et al., 1999, St-Pierre et al., 2006). Moreover, AMPK mediates longevity induced by DR in *C. elegans* (Burkewitz et al., 2014, Greer et al., 2007). Administration of metformin to worms and mice show lifespan extension mediated by activation of AMPK (Anisimov et al., 2011, Mair et al., 2011, Onken and Driscoll, 2010). In addition metformin does not further extend lifespan in *Drosophila* on DR food, further confirming the idea that it mimics the DR effect in lifespan extension (Slack et al., 2012).

Over-expression of some sirtuins (i.e., SIRT1, 3, and 6) increases lifespan via mechanisms overlapping with DR (Guarente, 2013). Activation of SIRT increases genomic stability, reduces NF-kB signalling, and improves metabolic homeostasis through histone deacetylation (Mouchiroud et al., 2013, Guarente, 2013). Moreover, SIRT1 can deacetylate and activate PGC-1α to regulate glucose homeostasis (Rodgers et al., 2005), therefore sharing similar downstream effectors with AMPK.

Another characterized effector mediating DR in mice is the transcription factor NF-E2-related factor (NRF2), which is the key regulator in several enzymatic pathways involved in anti-oxidant responses (Martin-Montalvo et al., 2011). The beneficial effect of calorie restriction in mice is partially mediated by NRF2. In addition, we recently published research demonstrating that lithium, the most commonly prescribed drug for the treatment of bipolar disorder, extends lifespan in *Drosophila* through inhibition of GSK-3 and activation of NRF-2. Furthermore this lifespan extension was mediated at least partially through DR (Castillo-Quan et al., 2016).

Heat shock factors (HSFs) have been also implicated in the effects of DR on health and longevity (Akerfelt et al., 2010). HSFs mediate the stress responses to environmental/pathological stressors by activating molecular chaperones such as HSP70 and stress proteins. These proteins are therefore essential for all organisms to survive exposure to acute stress. Furthermore the heat shock responses become impaired with age, in addition to numerous other cellular defense systems including the UPR and the removal of mis-folded proteins by the cellular degradation machinery, leading to cellular ageing and neurodegeneration (Powers et al., 2009, Ben-Zvi et al., 2009). Down-regulation of HSF in *C. elegans* leads to lifespan shortening and accelerated protein aggregation. On the other hand, reduced IIS can activate HSF,

improve proteostasis, and extend lifespan (Hsu et al., 2003, Morley and Morimoto, 2004). In addition, age-related proteostatic failure can be ameliorated by over-expression of HSF or daf-16 (FOXO), suggesting an important role of these stress-responsive transcription factors in maintaining global proteome homeostasis (Ben-Zvi et al., 2009). Moreover, HSF1 can be directly deacetylated by SIRT1, which then becomes activated for DNA binding. Indeed a decrease in SIRT1 levels during ageing is also associated with an inhibition of HSF1 DNA-binding activity (Westerheide et al., 2009). Furthermore, an age-related decrease in the HSF1 DNA-binding activity and reduced transcripts of HSP70 are reversed by caloric restriction (Heydari et al., 1996). These results suggest that HSF1 and SIRT1 function together to protect cells from stress stimuli, thereby promoting survival and extending lifespan.

In addition to reducing food intake, the timing of a meal also appears to be important. During evolution, animals and humans ate intermittently. For many invertebrates, long periods of starvation are normal and they have developed conserved responses against starvation (Fontana and Partridge, 2015). For example, intermittent fasting (IF), with 2 days of normal feeding followed by 2 days of fasting extends lifespan in *C. elegans* through reduced IIS/mTOR signalling (Honjoh et al., 2009). Chronic starvation even extends lifespan in *C. elegans* with shared mechanisms with IF that include reduced IIS/mTOR signalling and activation of FOXO family transcription factors (Kaeberlein et al., 2006, Lee et al., 2006, Uno et al., 2013, Honjoh et al., 2009). Short-term every-other-day feeding/fasting mimics many positive outcomes of DR, improving the healthy lifespan by up to 30% in mice (Brown-Borg and Rakoczy, 2013). However, the age of initiation of the fasting seems also to be crucial, as old-aged mice are more sensitive to fasting than younger ones, suggesting they are more likely starvation-sensitive (Goodrick et al., 1990). In addition to its pro-longevity effects, IF may also prevent age-related chronic disorders, such as diabetes, neurodegeneration, obesity, cardiovascular disease and hypertension (Mattson et al., 2014). Human trials on the effects of IF are ongoing and appear to show promising results, including reduced body weight, fat mass, serum concentrations of total and LDL cholesterol, triglycerides and arterial blood pressure. Biomarkers for cancer risk were reduced, but total and free IGF-1 did not change (Harvie et al., 2011). In rodents, several molecular changes appear to mediate the benefits of fasting, including a metabolic shift to fat metabolism and ketone production, enhanced adaptive cellular

and molecular stress responses that prevent and repair molecular damage, reduced inflammation and oxidative stress (Mattson et al., 2014). In addition, fasting can also improve mitochondrial function, elevate stress responses by increasing production of the chaperones HSP70 and Grp78. It also leads to the inhibition of the nutrient sensing network AKT/mTOR pathway, increases autophagy and stimulates the DNA repair pathway in different cell types (Brown-Borg and Rakoczy, 2013, Mattson et al., 2014). Prolonged fasting in mice reduced circulating IGF-1, improved stem cell protection, self-renewal and regeneration (Cheng et al., 2014).

However, the effect of IF in cancer or other cachexia disease states is controversial. One study reported that fasting could initiate and promote liver carcinogenesis in rats with increased production of TGF-beta1 (Tessitore and Bollito, 2006). Moreover, *Drosophila* models of tumours secreted ImpL2, the antagonist of insulin signalling, leading to a sustained and dramatic reduction of insulin activity and tissue loss, suggesting that excessive reduction of IIS/mTOR signalling pathway might be causative for the pathogenesis and progression of tumours (Figueroa-Clarevega and Bilder, 2015, Kwon et al., 2015). This cachexia mimics malnourishment and further reducing the insulin signalling by IF will deteriorate this situation. Wasting, starvation, IF, and DR therefore share similar molecular mechanisms in controlling the physiological and pathological state in response to nutrient limitation, although the levels of reduction and outcomes are varied.

1.5 Thesis outline

My PhD work was mainly focused on dissecting the role of PGC-1α in neurodegenerative diseases, including AD and PD, in *Drosophila* models. This work also involved the identification of the interaction partners of PGC-1α in regulating metabolic processes in disease states. Moreover, I also characterised the downstream effectors of PGC-1α in the regulation of ageing in the fly. This work provides significant insights into the role of PGC-1α and its interactors in both ageing and neurodegeneration. It also highlights a number of potential therapeutic strategies for promoting healthy ageing and preventing age-related diseases such as neurodegeneration.

Most of my PhD work is yet to be published. However, I have already been a co-author on a number of publications and these can be found in the Appendix.

A summary of each results chapter is detailed below.

1.5.1 PGC-1 regulates the ER-unfolded protein response and ameliorates Aβ toxicity. (Chapter 3)

AD is the most common neurodegenerative disorder affecting millions of people worldwide. Ageing is the greatest risk factor for developing AD (Niccoli and Partridge, 2012). Therefore there is an urgent need to develop therapeutic strategies for AD in the ever-increasing ageing world population. Mitochondrial dysfunction, oxidative stress, proteostatic failure, and circadian rhythm disruption have all been implicated in the pathogenesis of AD (Hetz and Mollereau, 2014, Bender et al., 2008, Nunomura et al., 2001, Harper et al., 2005), suggesting that these processes may provide excellent therapeutic targets for preventing AD. PGC-1α is a key regulator in many biological processes, including mitochondrial biogenesis, oxidative stress responses, circadian clock control, and protein quality control (Puigserver and Spiegelman, 2003, St-Pierre et al., 2006, Liu et al., 2007, Wu et al., 2011). It has also been found to be present at reduced levels in AD post mortem brains (Qin et al., 2009), suggesting that elevating the levels of PGC-1α in neurons might be beneficial in AD. In Chapter 3, I demonstrated for the first time *in vivo* that up-regulation of PGC-1α in neurons can prevent the neurotoxic phenotypes in a *Drosophila* model of Aß toxicity. I then investigated the mechanisms by which activation of *dPGC-1* in neurons ameliorates Aß induced neurotoxicity.

To further explore the downstream effectors of *dPGC-1* in ameliorating Aß neurotoxicity, I performed a small-scale screen of transcription factors previously reported to co-activate *dPGC-1* in regulating many metabolic processes. We have previously shown that Aß neurotoxicity leads to an arrhythmic sleep pattern (Niccoli et al., 2016). I confirmed this by demonstrating that over-expression of Aß disrupts the circadian clock via increasing the period *tau*. I also demonstrated that over-expression of *dPGC-1* ameliorates this neurotoxic phenotype. Mammalian PGC-1α

has been implicated in a second feedback loop of circadian clock control by co-activating a transcription factor RORα (Liu et al., 2007). However its role in the *Drosophila* in a similar loop is still unknown. In order to examine this further I investigated the Par Domain Protein 1ε (PDP1ε), the transcription factor involved in second feedback loop of the circadian clock in *Drosophila* (Cyran et al., 2003). I demonstrated that *dPGC-1* and PDP1ε interact to form a complex by Fluorescence Resonance Energy Transfer. Using genetic manipulation, I further showed that over-expression of *Pdp1ε* in neurons can ameliorate Aß neurotoxic phenotypes in flies.

Activation of *dPGC-1* or *Pdp1ε* in neurons can ameliorate Aß neurotoxicity through activation of the UPR^{ER}. Therefore compounds potentially targeting the UPR^{ER} may offer therapeutic avenues for the treatment of AD. I therefore tested three compounds in Aß-expressing fly models. In collaboration with Dr. Sofola-Adesakin, we found that lithium, the main drug used in the treatment of bipolar disorder, rescued the toxic phenotypes in Aß-expressing flies by reducing protein synthesis (Sofola-Adesakin et al., 2014). I also found that metformin, the drug for treating type-2 diabetes, could rescue the shortened lifespan of Aß-expressing flies. I then collaborated with Dr Niccoli to investigate the mechanisms of this amelioration, and found that metformin reduces Grp78 protein levels, leading to activation of the UPR^{ER} (Niccoli et al., 2016). Another drug I tested in collaboration with Dr. Castillo-Quan and Dr. Kinghorn is rifampicin, a well-known antibiotic used for the treatment of tuberculosis and leprosy. Previous studies have suggested that rifampicin can reduce Aß oligomerization and improve the memory defects in an APP mouse model via improved autophagy-lysosomal function (Umeda et al., 2016). In keeping with this I describe the neuroprotective effects of rifampicin in Aß-expressing flies.

1.5.2 The role of PGC-1α in *Drosophila* models of Parkinson's disease (Chapter 4)

One of the main aims of my PhD work was to investigate the role of PGC-1α in familial PD. This work followed on from extensive studies suggesting that PGC-1α and mitochondrial dysfunction might play a central role in PD pathogenesis (Whitworth and Pallanck, 2009, Shin et al., 2011). In Chapter 4, I describe my work assessing the role of PGC-1α in *Drosophila* null mutants of *parkin* and *PINK1*.

1.5.3 PGC-1α-GABPα modulates ageing in *Drosophila.* (Chapter 5)

Drosophila models that over-express *dPGC-1* in the intestinal system show extended lifespan with improved intestinal homeostasis and mitochondrial function (Rera et al., 2011). However the mechanisms of lifespan extension by *dPGC-1* have not been fully explored. Mammalian GABPα is induced by PGC-1α in the regulation of mitochondrial biogenesis in skeletal muscle (Yang et al., 2014, Mootha et al., 2004). *Drosophila* GABPα is required for proper mitochondrial gene expression together with *dPGC-1* in a nutrient-sensing manner (Tiefenböck et al., 2010, Baltzer et al., 2009), suggesting the *Drosophila* homologue may share a conserved molecular function with its mammalian counterpart. I hypothesised that *dGABPα* may be regulated by *dPGC-1* and therefore responsible for *dPGC-1*-mediated lifespan extension. In Chapter 5, I describe my work investigating the role of *dGABPα*, the homologue of human GA-binding protein α subunit (also called Nuclear respiratory factor 2α, NRF2α), in regulating longevity and healthy lifespan. I used a genome-wide unbiased approach to interrogate the transcriptomes in response to over-expression of *dGABPα,* in order to aid our understanding of the molecular mechanisms underlying lifespan extension. I performed RNAseq analyses, to assess how the transcriptional response of *dGABPα* activation correlates with other interventions that promote longevity in *Drosophila*.

Chapter 2 General methodology

2.1 *Drosophila* melanogaster: strains and genetics

One of the major advantages of working with the fruit fly *Drosophila melanogaster* is that there is a huge wealth of different laboratory stains and mutants. The Partridge laboratory has a large inventory of genetic stocks allowing appropriate use of and generation of different crosses. All stocks were kept at 18°C, while experimental crosses and transgenic flies were kept at 25°C and 65% humidity on a 12:12 light: dark cycle using standard sugar/yeast (SY) medium. Flies were reared at standard larval density (around 300 flies per 200 mL bottles) and eclosing adults were collected over a 4-hour period after which they were mated for 48 hours, before collecting females or males for experiments (Bass et al., 2007).

2.1.1 *White Dahomey* (w^{Dah})

The background control stock white *Dahomey* (w^{Dah}) has been maintained in large population cages with overlapping generations since 1970. The w^{Dah} stock was derived by the incorporation of the w^{1118} mutation into the outbred *Dahomey* background by backcrossing (Bass et al., 2007). The w^{Dah} strain is naturally infected by the intra-cytoplasmic bacterium *Wolbachia*, which modulates the lifespan effects of the IIS pathway (Gronke et al., 2010, Ikeya et al., 2009, Negri, 2011).

2.1.2 *White 1118* (w^{1118})

The w^{1118} *Drosophila* stock is an inbred and isogenic strain often used for neurodegeneration studies. This strain is also often used as a control in ageing studies to demonstrate that pro-longevity effects found in the w^{Dah} strain are independent of genetic background (Bjedov et al., 2010).

2.1.3 Backcrossing

Backcrossing of the transgenic lines was necessary to ensure that any differences between mutant and control flies are due to the expression of the transgene alone, and

not due to confounding mutations or insertional mutagenic effects (Partridge and Gems, 2007). Previous studies have demonstrated that insufficient standardization of the genetic background, and inappropriate backcrossing or use of inappropriate controls, produces artificial lifespan extension (Burnett et al., 2011, Toivonen et al., 2007). For this reason, before the transgenic stocks could be used for experiments, they were backcrossed at least 6 generations into the desired background strain. In the first cross, transgenic males were mated with wild type female virgins, which results in the wild type cytoplasmic content (including the mitochondrial genome) being pass to the offspring. The offspring then were selected either by their visible phenotype (eye colour for example) or by PCR analysis following transgene/construct-specific sequences. After this initial cross virgin females were collected and crossed to wild type males, and this cross was repeated at least another five times until six backcrossing events were completed. Transgenic lines were then made homozygous or balanced and kept as a stock for experiments. Transgenic lines were normally refreshed by three generations following a similar protocol before re-use after extended periods of time.

2.1.4 The GAL4-UAS system

The GAL4-UAS system is considered one of the most powerful genetic tools to study gene expression and function in the fruit fly (Brand and Perrimon, 1993). Its major advantage is that it can restrict the expression of genes of interest in a cellular or tissue-specific manner using native gene promoters. The system has two parts: the *GAL4* gene, encoding the yeast *Saccaromyces cervisiae* transcriptional activator protein GAL4, and the UAS (Upstream Activation Sequence), an enhancer to which GAL4 specifically binds to activate gene transcription. The *GAL4* transgene is placed under the control of a native gene promoter, or driver gene, which is then only expressed in cells where the driver gene is usually active. For example, the *elav-GAL4* fly line will express the GAL4 protein under the elav promoter. *Elav* encodes for embryonic lethal abnormal vision, a pan-neuronal protein and is therefore a neuronal driver. Therefore GAL4 should only activate gene transcription where a UAS has been introduced. For example, when green fluorescent protein (GFP) is placed under UAS control, i.e. *UAS-GFP*, and this line is crossed with an *elav-GAL4* line, the

offspring genotype *elavGAL4>UAS-GFP* will express GFP only in neurons (Osterwalder et al., 2001).

2.1.5 The gene-switch system

The gene-switch (GS) system uses the GAL4/UAS system with the restriction that the transcriptional activity depends on the presence of a steroid hormone or a chemically related compound (Osterwalder et al., 2001, Ford et al., 2007, Roman et al., 2001). In the GAL4/UAS system, the binding of the transcription factor GAL4 to UAS, results in the transcription of the UAS-linked transgene (Brand and Perrimon, 1993). In the GS system, GAL4 is fused with the regulatory domain of the human progesterone receptor (Osterwalder et al., 2001, Ford et al., 2007, Roman et al., 2001, Poirier et al., 2008). In the absence of the activator mifepristone (RU486), the GAL4 protein and UAS transgene can coexist in the fly with only leaky weak expression of the transgene under the control of UAS. Only when these flies are fed with RU486, the GAL4-GS is able to bind to the UAS and therefore the transgene is induced (Figure 2.1) (Osterwalder et al., 2001, Roman et al., 2001).

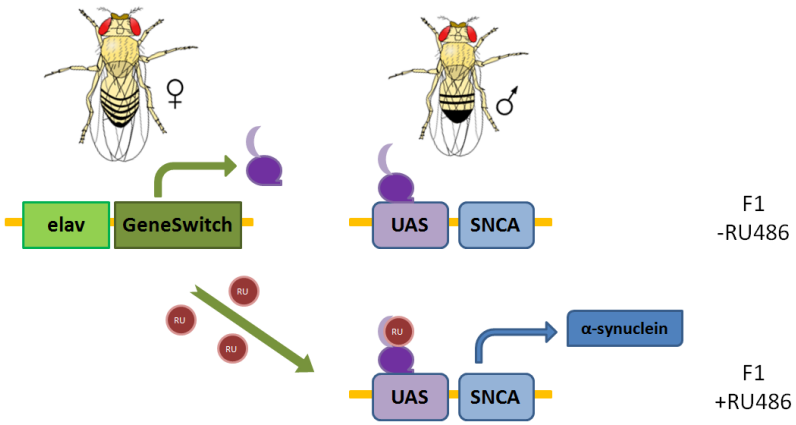

Figure 2.1 The GeneSwitch expression systems

This diagram illustrates the cross between a gene-switch driver (*elavGS*) and a UAS construct linked to the *SNCA* gene (*UAS-SNCA*) to obtain a line carrying both the driver and UAS line, which results in the following line: *elavGS/+>UAS-SNCA/+*. Flies only express the α-synuclein protein in the nervous system following ingestion of medium supplemented with RU486 (RU+). Flies with the same genotypes, but not fed RU486 (RU-), are used as genetic controls.

2.2 *Drosophila* food medium

2.2.1 Sugar-yeast medium (SY)

Our standard laboratory medium (SY) was used for the development and maintenance of all flies, unless otherwise stated. The SY medium was made in the following way: 15 g of agar were dissolved in 700 mL distilled water by heating until boiling. After this, 100 g of autolysed yeast powder and 50 g of sugar were added until boiling. 170 mL of distilled water were added to the mixture and it was then left to cool down. When the temperature of the mixture was between 50-60°C, 30 mL of nipagin (100 g/L) and 3 mL propionic acid (both anti-fungal preservatives) were added. The food was then dispensed (4 mL per vial) into plastic vials and allowed to set at room temperature before storing at 4°C (Bass et al., 2007).

2.2.2 Grape juice medium

Grape plates were used as a surface for egg laying and collection. Collected eggs were subsequently dispensed into bottles containing SY medium. Grape plates were made as follows: 25 g agar were dissolved in 500 mL distilled water and brought to the boil. To this, 300 mL of red grape juice were added and the medium was brought to the boil again. After adding an additional 50 mL of distilled water the medium was allowed to cool to below 60°C. As with the SY medium 21 mL of nipagin (100 g/L) were added. The medium was dispensed into plastic petri dishes and allowed to set at room temperature before storing at 4°C.

2.2.3 Starvation medium

The starvation medium was prepared by adding 15 g of agar to 700 mL of distilled water. This was brought to the boil and cooled down before dispensing into vials. No additional ingredients (including anti-fungal) were added to avoid any potential source of nutrients.

2.2.4 Dietary restriction

For DR experiments a yeast dilution protocol was established as detailed below:
Recipe for SY preparation for DR tent (1 litre of medium)

Ingredient	0.0 SY	0.1SY	0.5SY	1.0SY	1.5SY	2.0SY
ddH_2O (mL)	700	700	700	700	700	700
Agar (g)	15	15	15	15	15	15
Sucrose (g)	50	50	50	50	50	50
Yeast (g)	0	10	50	100	150	200
Addional ddH_2O (mL)	223	218	196	170	144	118
Nipagin (mL)	30	30	30	30	30	30
Propionic acid (mL)	3	3	3	3	3	3

1. Agar was added to the initial volume of water (ddH_2O) just before heating. Stirring was continuous throughout the preparation process to prevent any of the ingredients sticking to the saucepan.
2. Just after boiling, sucrose was added and the mixture was brought to the boil again.
3. The yeast was added and the mixture was brought to the boil again. The saucepan was then removed from the heating source and the additional ddH_2O was added to cool down the medium.
4. Only after the medium reached a temperature below 60°C (preferably between 50 and 58°C), nipagin and propionic acid were added.
5. The medium was then ready for dispensing.

2.3 Fly husbandry and culturing

2.3.1 Male and female separation

Some anti-ageing interventions that extend lifespan are sex-specific, and are often confined to females in both *Drosophila* (Clancy et al., 2001) and mice (Selman et al., 2009). In other cases the responses show some dimorphism, with the response attenuated in males (Bjedov et al., 2010, Miller et al., 2014). Therefore, it is a common practice in ageing studies to test males and females separately (Partridge and Gems, 2007). Additionally, continuous mating can impact several physiological parameters, including survival (Barnes et al., 2008, Chapman and Partridge, 1996). Female and male flies can be distinguished very easily under a microscope whilst flies are anesthetized with CO_2 (Greenspan, 2004). For most experiments only the female flies were used, though some phenotypes were also corroborated in males to ensure sex-independent effects. Female and male flies were sorted using a fine paintbrush while anesthetized. Flies were usually separated at day 2 post-eclosion after a 48-hour mating period.

2.3.2 Virgin collection

To obtain the desired genotypes, it was often necessary to cross male and female flies of different genotypes. This ensured the transfer of at least one copy of the chosen transgene to the progeny. This was achieved by collecting unmated female flies (or virgins). Virgin collection was carried out for backcrossing and to obtain the desired genotypes for experiments. Female *Drosophila* flies do not respond to courting males during the first 6 hours after eclosion at 25°C (Greenspan, 2004). Therefore newly emerged female flies were collected within 6 hours after clearing rearing bottles.

2.4 *Drosophila* handling and survival

2.4.1 Lifespan assays

An important determinant for ageing analysis is to ensure that the parents of the experimental flies were the same age at egg laying and reared under the same conditions. In this way the effects of parental age on lifespan were controlled (Priest et al., 2002). 'Egg squirt' protocols were undertaken to ensure that all flies in the experiment were raised at similar larval densities (~300 eggs per bottle containing 70 mL of food), thereby avoiding any effects of larval density on lifespan (Priest et al., 2002). Flies were allowed to lay eggs for less than 24 hours on grape medium plates, with live yeast paste to encourage mating. The eggs were then collected from the plate by washing with phosphate buffered saline (PBS) solution and collected into falcon tubes. The eggs were allowed to settle to the bottom of the tube. Using a 100 μL Gilson pipette, ~18-20 μL of egg suspension was dispensed into 200 mL glass bottles containing 70 mL SY medium. This equated to ~300 eggs per bottle.

After 10 days of development flies emerged from their pupae and were then transferred into fresh bottles. The flies were then allowed to mate in these new bottles for 48 hours. After this flies were sorted using a paintbrush under CO_2 anesthesia, and divided into vials (15 flies per vial).

Flies were then transferred to fresh food vials three times a week throughout life. The number of dead flies found during each transfer was recorded. Accidental death and escapees were distinguished from deaths, and were censored from the experiment.

From these data, a survivorship graph was generated, making it possible to compare survival curves over time between different genotypes or experimental conditions. Lifespan curves were analyzed using a log-rank test.

2.4.2 Stress assays

For stress assays lifespan experiments were performed using different chemicals to induce cellular stress.

2.4.2.1 Paraquat

Flies were kept under pre-determined conditions similar to those in the lifespan assays for a fixed period of time, after which they were transferred onto food containing paraquat. 1 M paraquat containing food was prepared by dissolving *N*, *N*′-dimethyl-4, 4′-bipyridinium dichloride (paraquat, Sigma 856177) into ddH_2O. This was then was added to a 0.0 SY (agar/sugar) medium to achieve a final concentration of 10 mM. All stress assays were tested without yeast in the medium to avoid interaction between yeast and the stressor. The medium used has all the other components of the standard medium including sucrose. Flies were typically assayed with 15 flies per vial. Deaths were scored every 4 hours after the detection of the initial wave of death. Data was plotted as a survival curve and analysed using a log-rank test.

2.4.2.2 Hydrogen Peroxide (H_2O_2)

For the preparation of H_2O_2 containing medium, a 30% H_2O_2 stock solution from Sigma was diluted into a 0.0 SY medium to give a final concentration of 2.5% or 5%. Flies were typically assayed with 15 flies per vial. Deaths were scored at least 3 times per day, plotted as a survival curve and analyzed using a log-rank test.

2.4.2.3 Phenobarbital

Phenobarbital (Sigma P1636) was prepared by directly adding the salt to 0.0 SY medium to obtain a final concentration of 6%.

2.4.2.4 Tunicamycin

Flies were tipped into vials containing 1% agar, 1.5% sucrose, and 10 mg/l of tunicamycin. Dead flies were scored at regular intervals, and lifespan curves were compared using a log-rank test.

2.4.3 Mifepristone (RU486)

As explained above the GeneSwitch system uses mifepristone (RU486) as an inducer of gene expression in the presence of the GeneSwitch driver (Osterwalder et al., 2001, Poirier et al., 2008). Our laboratory has optimised the dose of RU486 that produces effective transgene expression without impairing longevity, fecundity or metabolism. RU486 (Sigma, M8046) was dissolved in 100% ethanol and supplemented to standard SY medium before dispensing into vials. Food supplemented with RU486 was stored at 4°C until use.

2.5 Behavioural investigations

2.5.1 Fecundity assay

Fecundity has historically been heavily linked to longevity (Partridge et al., 2005). Although this association has been uncoupled (Grandison et al., 2009), interventions to prolong lifespan without affecting fecundity are still limited. To assess fecundity female flies were allowed to lay eggs for a period of 24 hours in vials containing standard medium. Vials containing eggs were frozen and kept at -20°C for a short time until eggs were counted using a hand held counter. The total number of eggs laid was divided by the number of flies per vial and a t-test was used to determine statistical value.

2.5.2 Climbing assay (negative geotaxis)

Age-related decline in locomotor ability represents a behavioural measurement of neuronal health. It is an insightful measurement read-out of the functional capacity of flies that is also sensitive to some anti-ageing interventions (Gargano et al., 2005, Jones et al., 2009). The climbing assay involved the placement of 15 flies in a 35 cm

column (1.5 cm diameter) with a conic bottom end. Flies were tapped down and observed during a 45 second period. The column was separated into three areas: top, middle, and bottom by two lines: one was 10 cm from top and the other was 3 cm from bottom. After 45 seconds the flies located in each of these three sections were recorded. Each column was evaluated three times to minimized trial error and a minimum of three vials per genotype/condition was assessed. The numbers of flies in the top (ntop) and at the bottom (nbottom) were used to obtain a motor performance index (PI). This was calculated as ½ (ntot + ntop –nbottom /ntot). The PI was plotted against time per each genotype and condition. Statistical analysis was performed in R using ordinal logistical regression, using the individual heights for each fly as data points.

2.6 Biochemistry and molecular biology methods

2.6.1 DNA extraction and Single-Fly Polymerase Chain Reaction (PCR)

To analyse single flies for specific mutations one fly was placed in a 1.5 mL eppendorf and squashed with a blue pestle. 50 µL of squish buffer (990 µL of squish buffer (10 mM Tris-HCl pH 8.0, 1 mM EDTA, 25 mM NaCl) + 10 µL of proteinase K) were then added. The liquid was transferred to a PCR tube and incubated for 1 hour at 37°C and then at 95°C for 10 min. The sample was spun, after which it was either stored at 4°C or prepared for PCR.

The PCR reaction consisted of (per fly) 2 µL of extracted DNA, 2.5 µL 10X PCR buffer (15 mM $MgCl_2$), 0.5 µL dNTPs (10 mM), 0.5 µL of each primer (10 mM), 0.25 µL TAQ polymerase and 18.75 µL of ddH_2O. All reagents were obtained from Qiagen, UK. The PCR cycles were run using a thermal cycler (Eppendorf UK limited), with the following protocol: 1 cycle of 94 °C for 15 min (initial melting step to denature the hot-start TAQ polymerase), 30 to 35 cycles of 95 °C for 30 sec (for denaturing DNA), 50-60 °C for 30 sec (to anneal the primers), and 72 °C for 2 min (elongation step). Finally, 1 cycle of 72 °C for 10 min was performed for the final elongation phase. Samples were then either stored at 4 °C, -20 °C or run on an agarose gel.

2.6.2 Gel electrophoresis

1 to 2 grams of agarose (Sigma, UK) were dissolved in 100 mL of TAE (Tris base, acetic acid, EDTA) buffer and heated in a microwave, until close to boiling, after which it was slowly cooled down. Once cooled 5 μL of ethidium bromide was added to the agar solution. The mixture was placed in a gel tray and a comb was added to create wells for the sample. The gel was allowed to set for 1 hour. A marker was added to the first well and samples were added in conjunction with 6X loading dye (40% glycerol, 6X TBE buffer, and 0.25% bromophenol blue) at a final volume of 20-25 μL. Electrophoresis was performed between 70-100 V as necessary to separate the DNA bands. The samples were then visualized under the UV light using a UV trans-illuminator.

2.6.3 Quantitative Real Time PCR (qRT-PCR)

Total RNA was extracted from 15 whole flies or 25 fly heads using TRIzol® (GIBCO) according to the manufacturer's instructions. The concentration of total RNA purified for each sample was measured using Nano Drop2000 (Thermo Scientific). 5 μg of total RNA was then subjected to DNA digestion using DNAse I (Ambion), immediately followed by reverse transcription using the Superscript II system (Invitrogen) with oligo (dT) primers. Quantitative PCR was performed using the PRISM 7000 sequence-detection system (Applied Biosystems) and SYBR Green (Molecular Probes) by following the manufacturer's instructions. Each sample was analyzed in duplicate with both target and reference (*RP49*) gene primers in parallel. The values are the mean of three or four independent biological repeats ± SEM.

2.6.4 Western blotting

10 female flies/15 fly heads were homogenized in 200 uL/40 uL of 2X SDS Laemmli loading sample buffer (120mM Tris-HCl pH6.8, 20% glycerol, 4% SDS) containing 5% β-mercaptoethanol. Samples were heated at 95 °C for 5 minutes after which extracts were cleared by centrifugation. 10 μL of protein extract were loaded and

separated on pre-cast 4%-12% Invitrogen Bis-Tris gels (NP0322). After separation, the proteins were transferred to a nitrocellulose membrane in Tris-glycine buffer supplemented with 10% ethanol. Membranes were saturated in 5% milk in TBS-T (Tris-buffered saline with 0.05% Tween-20) for 1 hour at room temperature (RT) and then incubated with a selected primary antibody in saturation solution overnight. After 5x washes in TBS-T, they were then incubated with an appropriate secondary antibody for 1 hour at RT. Bands were visualized with Luminata Forte (Millipore) and imaged with ImageQuant LAS4000 (GE Healthcare Life Sciences). Quantification was carried out with ImageJ.

2.6.5 Protein Quantification

The Bicinchoninic acid protein (BCA) assay from Thermo Sciencific (23225) was used to determine the protein concentration of biological samples. BSA albumin standards were diluted using the same diluent as the samples. The following standard concentrations were prepared: 2000, 1500, 1000, 750, 500, 250, 125, 25, 0 μg/mL. The working reagent (WR) was prepared by mixing 50 parts of BCA reagent A with 1 part of BCA reagent B. 25 μL of each standard and sample was dispensed twice into a microplate well. To each well 200 μL of the WR was added by using a multi-channel pipette and mixed thoroughly on a plate shaker for 30 seconds. The plate was then covered and incubated at 37 °C for 30 mins. The plate was then allowed to cool to room temperature. The absorbance was then measured at 562 nm on a plate reader.

Chapter 3 PGC-1 regulates the ER-unfolded protein response and ameliorates Aβ toxicity

3.1 Summary

Alzheimer's disease (AD) is the most common neurodegenerative disorder and is neuropathologically characterised by the extracellular deposition of aggregates of the Aβ protein. The misfolding of Aβ is associated with cellular defects in brain energy metabolism, hypersensitivity to stress and proteostatic failure (Musiek and Holtzman, 2015). Peroxisome proliferator-activated receptor gamma coactivator 1-alpha (PGC-1α) is a transcriptional coactivator that regulates energy homeostasis within the cell, and is the master regulator of mitochondrial biogenesis (Puigserver and Spiegelman, 2003). The possible relevance of this gene in the pathogenesis of AD was identified with the demonstration that PGC-1α gene expression levels are decreased in the post-mortem brain tissue of AD patients (Qin et al., 2009). Consistent with this I have shown that up-regulation of *dPGC-1* in the neurons of a *Drosophila* model of Aβ toxicity rescues lifespan, behavioral phenotypes and circadian rhythm disruption. Moreover I demonstrated that the amelioration of Aβ toxicity is associated with improved mitochondrial homeostasis and activation of the unfolded protein response (UPR). Specifically, *dPGC-1* increased electron transport chain (ETC) activity and ATP production. Moreover, expression of *dPGC-1* also protected Aβ-expressing flies against oxidative stress and was shown to regulate the levels of mitochondrial chaperones in response to Aβ, thereby modulating mitochondrial UPR (UPR^{mt}). In addition, over-expression of *dPGC-1* negatively regulated Grp78 protein levels, indicative of increased endoplasmic reticulum UPR (UPR^{ER}). Therefore through UPR activation in the mitochondrial matrix and up-regulation of ER-mediated protein homeostasis and quality control, *dPGC-1* over-expression ameliorated the Aβ associated neurotoxic phenotypes. Lastly I demonstrated that *dPGC-1* physically interacted with Par Domain Protein 1ε (PDP1ε) in the *Drosophila* brain, and that genetic activation of *Pdp1ε* in neurons partially rescued the shortened lifespan of Aβ-

expressing flies via activation of UPR^{ER}. In keeping with this, I demonstrated that rifampicin, a well-known antibiotic, also activated the UPR^{ER} and rescued neurotoxicity in Aβ flies. These findings suggest that either increasing intraneuronal PGC-1α levels, or oral administration of rifampicin, could offer therapeutic benefits in AD by increasing the UPR^{ER}.

3.2 Introduction

AD is a progressive neurological disorder characterized by memory loss, cognitive decline and neuronal death predominantly in the cerebral cortex and hippocampus. Typical neuropathology includes extracellular deposits of amyloid-ß aggregates and intracellular inclusions of hyper-phosphorylated tau aggregates (Crews and Masliah, 2010). The disease progression is thought to be triggered by accumulation of Aß oligomer peptides, generated through the abnormal processing of the amyloid precursor protein (APP). This results in a neurotoxic cascade of events, including mitochondrial dysfunction, oxidative stress, proteostatic failure, circadian disruption, inflammation, tau hyper-phosphorylation, and eventual neuronal death. Some of these pathways also directly influence APP metabolism and Aß accumulation (Hardy and Higgins, 1992, Musiek and Holtzman, 2015). Whether these pathogenic processes are the main drivers of disease in AD is controversial, however, what is clear, is that they all represent possible therapeutic targets in the treatment of AD. Genetic or pharmacological interventions targeting these modulators may provide excellent therapeutic avenues.

Neurodegenerative diseases are characterized by the neuronal accumulation of insoluble aggregates of mis-folded proteins in the endoplasmic reticulum (ER) (Hetz and Mollereau, 2014). Activation of the UPR^{ER} allows cells to either restore protein homeostasis or to enter apoptosis as a protective response. Three well-characterized UPR sensors mediate this response: PERK (protein kinase RNA-like ER kinase), inositol-requiring enzyme 1 (IRE1), and transcription factor 6α (ATF6α) (Wu and Kaufman, 2006, Hetz and Mollereau, 2014). Under normal physiological conditions, these trans-membrane signalling components are bound and inhibited by GRP78. During ER stress, mis-folded proteins titrate down the levels of Grp78, thus activating

the signalling cascades downstream of ATF6α, IRE1 and PERK. ATF6α is transported to the Golgi where it is processed to produce a cytosolic fragment, which operates as a transcription factor, regulating *X-box binding protein 1* (*Xbp1*) and *Grp78* mRNA levels. Active IRE1 induces the splicing of *Xbp1* mRNA, leading to the expression of the active transcription factor Xbp1. PERK phosphorylates eukaryotic translation initiation factor 2α (elF2α), and induces the expression of ATF4. All of the above leads to the up-regulation of ER chaperones, ER-associated protein degradation, autophagy, redox reactions, and eventually apoptosis.

Increasingly evidence has indicated that disruptions in brain energy metabolism are critically involved in the pathogenesis of AD (Kapogiannis and Mattson, 2011), including mitochondrial damage (Galindo et al., 2010, Wu et al., 1999, Calkins et al., 2011), a decline in glucose metabolism (Mosconi et al., 2008), and oxidative damage (Siegel et al., 2007, Head et al., 2001). The PGC-1 family of transcriptional co-activators, including the founding member PGC-1α (PPARγ co-activator 1), and its homologue PGC-1ß and PRC (PGC-1-related co-activator), are important for the normal functioning of mitochondrial biogenesis (Mootha et al., 2004, Scarpulla, 2008), adaptive thermogenesis (Puigserver and Spiegelman, 2003), hepatic metabolism (Puigserver and Spiegelman, 2003, Li et al., 2007b), stress defence (Valle et al., 2005, St-Pierre et al., 2006), and circadian rhythms in metabolically active organs (Liu et al., 2007). Moreover, PGC-1α has been show to modulate ageing and diabetes, the two main risk factors for developing AD (Rogers et al., 2012, Willette et al., 2015). The PGC-1 family was reported in animal models as a novel modulator of lifespan (Rera et al., 2011). Furthermore, PGC-1α-responsive genes involved in oxidative phosphorylation have been shown to be reduced in the muscles of patients with type 2 diabetes mellitus (Mootha et al., 2003, Patti et al., 2003), suggesting its importance in ageing, human diabetes, and possibly in the development of AD. Indeed, the age-related decline in protein homeostasis and neuronal stress response signalling might contribute to AD progression (Taylor and Dillin, 2011, Hipp et al., 2014), and PGC-1α, which has been implicated in the stress defence system, and in protein quality control (St-Pierre et al., 2006, Wu et al., 2011), might therefore represent a promising therapeutic target.

PGC-1α mutant mouse models display neurodegenerative pathology in the brain and behavioural abnormalities, highlighting its protective role in neurons (Leone et al., 2005, Lin et al., 2004, Lucas et al., 2014, St-Pierre et al., 2006). Indeed, PGC-1α is neuroprotective in animal models of several neurodegenerative diseases characterised by abnormal protein aggregation, including Huntington's disease (Cui et al., 2006, Weydt et al., 2006, Tsunemi et al., 2012) and amyotrophic lateral sclerosis (Zhao et al., 2011, Liang et al., 2011). Human studies report that PGC-1α activity negatively correlates with the age of onset of AD (Helisalmi et al., 2008) and PD (Clark et al., 2011). In addition, PGC-1α and ATP are remarkably decreased in AD patient brains (Kapogiannis and Mattson, 2011, Hoyer, 1996, Qin et al., 2009). However, the effect of elevating PGC-1α in AD animal models is not well established, with some studies showing a protective role of PGC-1α in mitochondrial dysfunction (Sheng et al., 2012) and Aß accumulation (Katsouri et al., 2011), while another study demonstrated opposite effects (Dumont et al., 2014).

The question of whether reduced PGC-1α is causal in the neurodegeneration of AD is yet to be determined. A reduction in PGC-1α could contribute to disease progression in several ways. It may cause mitochondrial dysfunction and reduced ATP, as PGC-1α is the master regulator of the electron transport chain to generate ATP synthesis. Reduced PGC-1α also leads to increased sensitivity to stressors by ROS, thereby impairing mitochondrial homeostasis (St-Pierre et al., 2006, Lu et al., 2014, Haynes and Ron, 2010). PGC-1α deficiency may also exacerbate age-related disturbances in proteostasis and neuronal stress response pathways (Taylor and Dillin, 2011, Hipp et al., 2014, Wu et al., 2011). Mammalian PGC-1α regulates the circadian clock and therefore a reduction in this transcription factor may contribute to circadian rhythm disruption (Liu et al., 2007). I therefore investigated these pathways to dissect the role of PGC-1α in the pathogenesis of AD.

I studied the role of PGC-1α in the pathogenesis of AD, using a model of Aß toxicity in the fruit fly *Drosophila melanogaster* (Sofola et al., 2010). *Drosophila* is a powerful genetic tool to study neurodegeneration (McGurk et al., 2015, Fernandez-Funez et al., 2015), with distinct brain structures and analogous cell types to those in the human brain, as well as a blood brain barrier. I utilised the fly AD model that

expresses pathogenic Arctic $Aß_{1-42}$, which displays a shortened lifespan, behaviour defects as well as neurodegeneration (Sofola et al., 2010). Moreover, *Drosophila* possesses a single homologue of the mammalian PGC-1 family, *Spargel* (*dPGC-1*), (Tiefenböck et al., 2010), therefore providing a system in which PGC-1 function can be analysed in the absence of redundancy.

In order to determine whether neuronal PGC-1 contributes to the pathogenic cascades downstream of toxic Aß, I genetically over-expressed *dPGC-1* in the neurones of flies over-expressing Arctic $Aß_{1-42}$ also in neuronal tissue. I demonstrated that *dPGC-1* over-expression partially rescued the Aß-induced neurotoxic phenotypes, including lifespan, climbing ability and circadian rhythm, without affecting the levels of Aß peptides. In addition, over-expression of *dPGC-1* increased mitochondrial membrane potential and ATP levels, compensating for the mitochondrial defects mediated by Aß. Furthermore, activation of *dPGC-1* ameliorated Aß-induced hypersensitivity to oxidative stress, and regulated mitochondrial chaperones in response to Aß, suggesting improved mitochondrial proteostasis. *dPGC-1* also down-regulated the expression of Grp78, the negative master regulator of UPR^{ER}, suggesting activation of the UPR^{ER}, leading to improved proteostasis and restoration of ER function. In addition, I identified a novel transcriptional complex of PGC-1, the Par Domain Protein 1ε (PDP1ε), and demonstrated that they physically interact in fly brain using FRET (Fluorescence Resonance Energy Transfer). Activation of *Pdp1ε* ameliorated the shortened lifespan of Aß-expressing flies, likely through activation of the UPR^{ER}. Consistent with this, treatment of Aß flies with the antibiotic rifampicin, induced the UPR^{ER} by decreasing Grp78 levels, and rescued the toxic phenotypes associated with Aß *in vivo*. Taken together, our results highlight the potential therapeutic benefits of up-regulating the UPR^{ER} in AD, either via increasing intraneuronal PGC-1α or PDP1ε or via the use of pharmacological activators such as rifampicin.

3.3 Results:

3.3.1 *dPGC-1* over-expression ameliorated Aβ42 toxicity

To investigate the role of *dPGC-1* in Aβ-mediated neurotoxicity I assessed the effect of over-expression of *dPGC-1* on a number of Aβ-induced neurotoxic phenotypes.

Firstly I confirmed the over-expression of *dPGC-1* in the heads of Aβ-expressing flies using qRT-PCR (Figure 3.1**)**. In order to confirm that *dPGC-1* was not mediating its effect through a change in Aβ load, I demonstrated that *dPGC-1* over-expression did not affect Aβ protein or mRNA levels in fly heads (Figure 3.2 and 3.3)

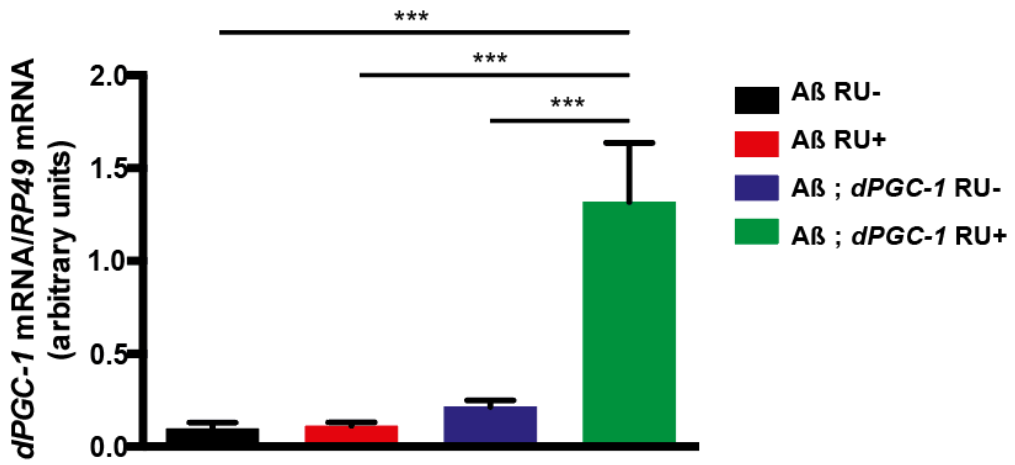

Figure 3.1 mRNA expression levels of *dPGC-1* in Aß-expressing flies

qRT-PCR analysis revealed that 30-day-old flies co-expressing Aβ + *dPGC-1* in the neural tissue using the inducible *elav-GS* driver (*Aβ; dPGC-1 RU+)* displayed *dPGC-1* mRNA levels (relative to a control endogenous gene, *RP49*) are significantly higher than in non-expressing Aβ + *dPGC-1* flies (*Aβ; dPGC-1 RU-*) and induced and non-induced Aβ-expressing flies (*Aβ; RU+* and *Aβ RU-*). The bars represent the mean ± SEM (n=4, ***p<0.001 by two-way ANOVA Newman-Keuls test).

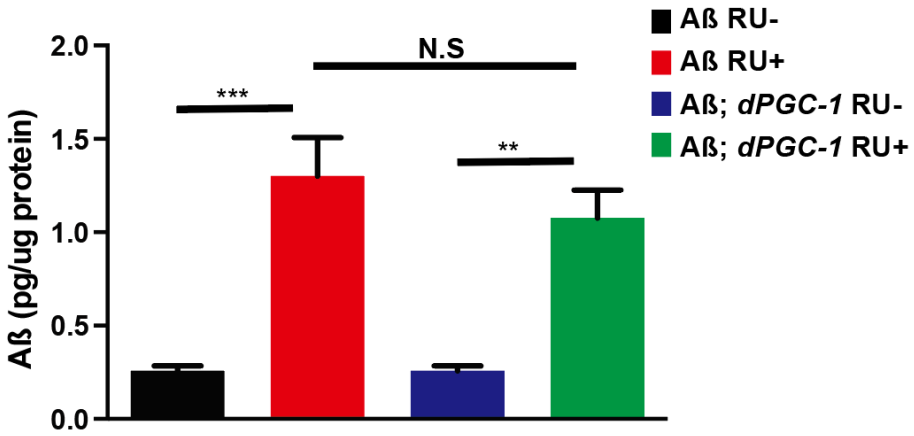

Figure 3.2 Aß protein levels were not significantly reduced by *dPGC-1* over-expression

dPGC-1 over-expression had no significant effect on Aß protein levels as measured by an ELISA assay on the heads of 30-day-old flies expressing Aß (*Aß*, red bar, *RU+*) compared with Aß + *dPGC-1* co-expressing flies (*Aß; dPGC-1*, green bar, *RU+*). Bars represent the means ±SEM (n=3, **p<0.01; ***P<0.001 by two-way ANOVA Newman-Keuls test).

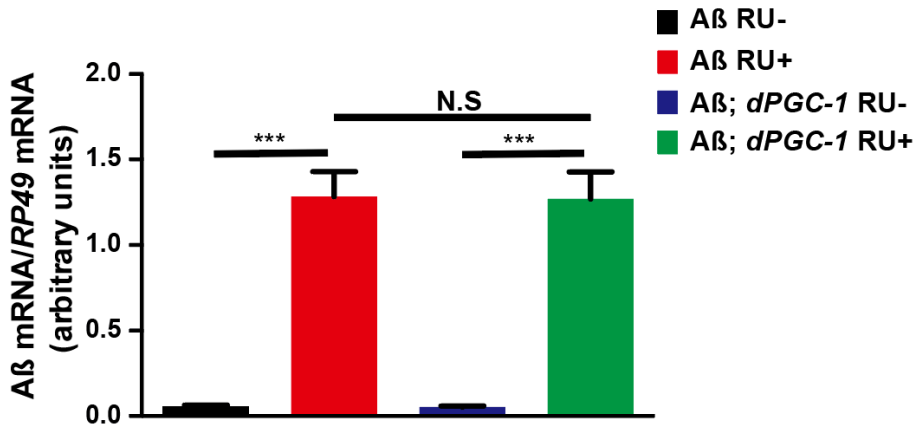

Figure 3.3 Over-expression of *dPGC-1* did not affect Aß mRNA levels

Over-expression of *dPGC-1* did not alter Aß mRNA levels (relative to an internal control gene *RP49*) in the heads of 30-day-old flies compared to controls as measured by qRT-PCR. Bars represent the means ±SEM (n=3, ***p<0.001 by two-way ANOVA Newman-Keuls test).

Over-expression of *dPGC-1* in the neural tissue of adult flies using an inducible *elavGS* driver significantly extended the lifespan of both female and male Aβ-expressing flies (Figure 3.4 A and B) (median lifespan was extended by 28% in females, $p = 1.22354 \times 10^{-17}$ and 8% in males, p<0.001). *dPGC-1* over-expression also protected against Aβ-induced climbing defects, a behavioral measurement for neuronal health (Figure 3.5).

Circadian rhythms, which have been found disrupted in AD patients and *Drosophila* Aβ-expressing models (Harper et al., 2005, Blake et al., 2015, Long et al., 2014), are directly controlled by neuronal activity. Circadian rhythm is a biological process that displays an endogenous, entrainable oscillation that completes one cycle (*tau*) in 24 hours and is driven by the circadian clock located in the suprachiasmatic nucleus in humans. I demonstrated, in keeping with previous work (Long et al., 2014, Blake et al., 2015), that Aβ-expressing flies show an increase in the period *tau* compared to non-induced controls, suggesting an impaired circadian clock. Over-expression of *dPGC-1*, however, restored the period to control levels (Figure 3.6), suggesting an improved circadian clock. Taken together our results suggest that increasing *dPGC-1* in neurons ameliorates Aβ-induced toxicity.

A

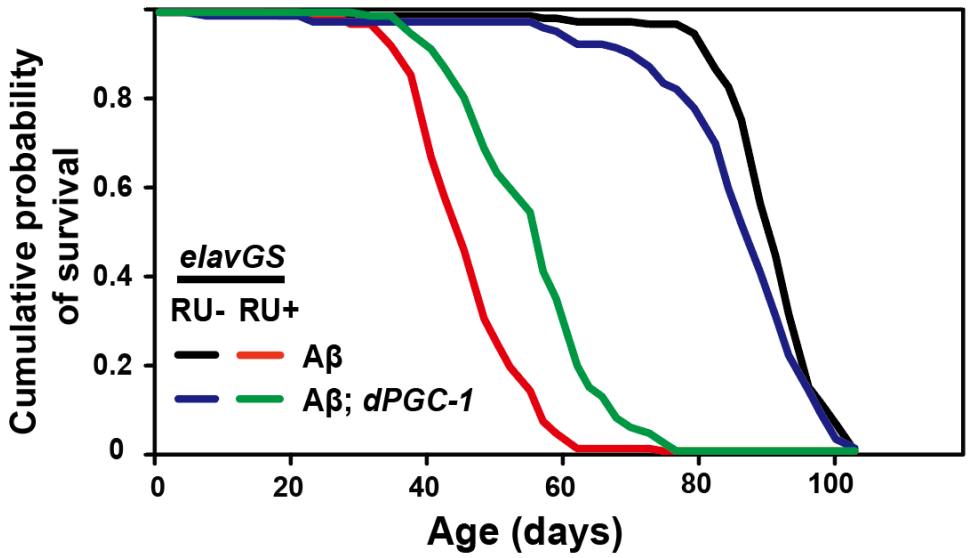

B

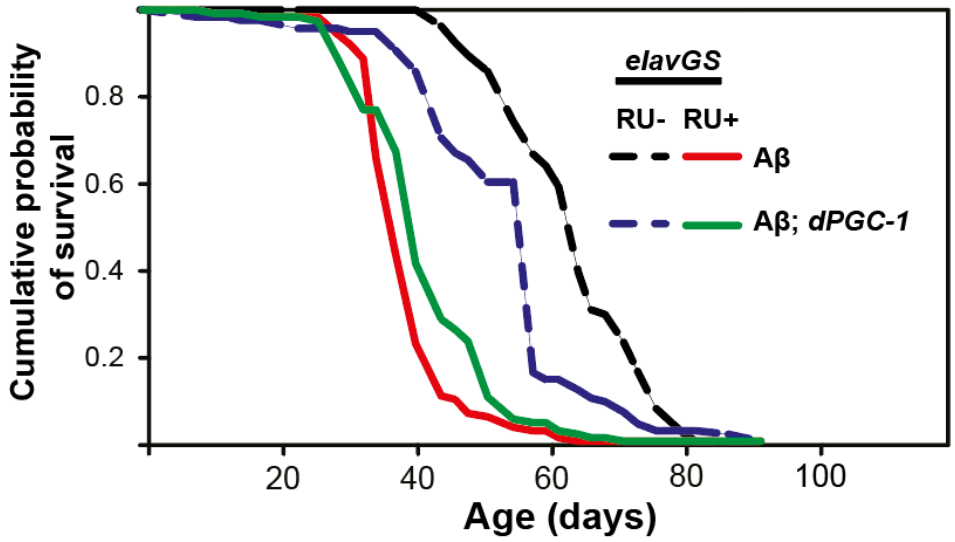

Figure 3.4 Over-expression of *dPGC-1* in neurons extended the lifespan of Aß-expressing flies.

Survival curves of female (A) and male (B) flies expressing Aß or Aß + *dPGC-1* in adult neurons (RU+) and non-induced controls (RU-) ($p < 2 \times 10^{-17}$ vs. *Aß RU+* and *Aß; dPGC-1 RU+* female flies by log-rank test; $p < 0.001$ vs. *Aß RU+* and *Aß; dPGC-1 RU+* male flies by log-rank test), n=150 flies per conditions.

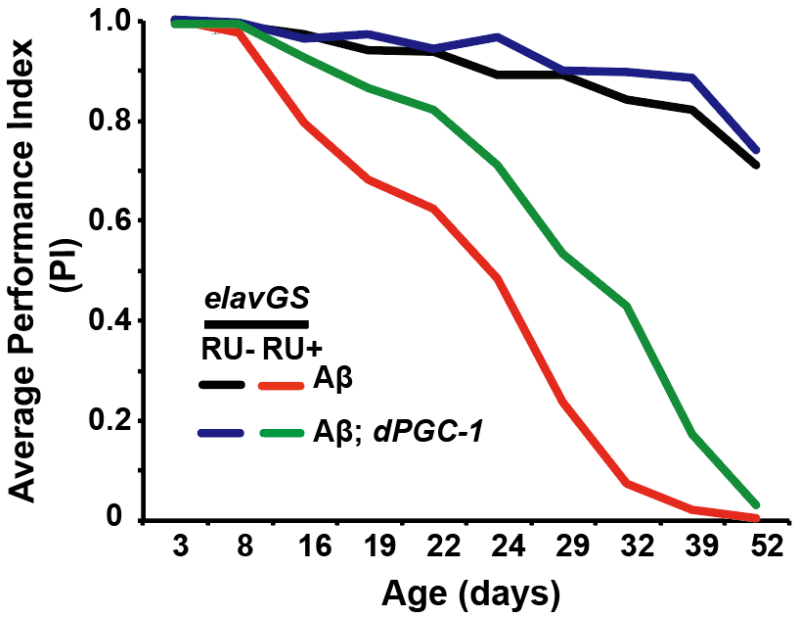

Figure 3.5 Over-expression of *dPGC-1* in Aß-expressing flies partially ameliorated the age-dependent climbing defects.

Co-expression of *dPGC-1* in Aß-expressing female flies results in greater climbing ability than in non-induced controls. ($P < 2 \times 10^{-16}$ *Aβ RU+* vs. *Aβ; dPGC-1 RU+* by ordinal logistic regression).

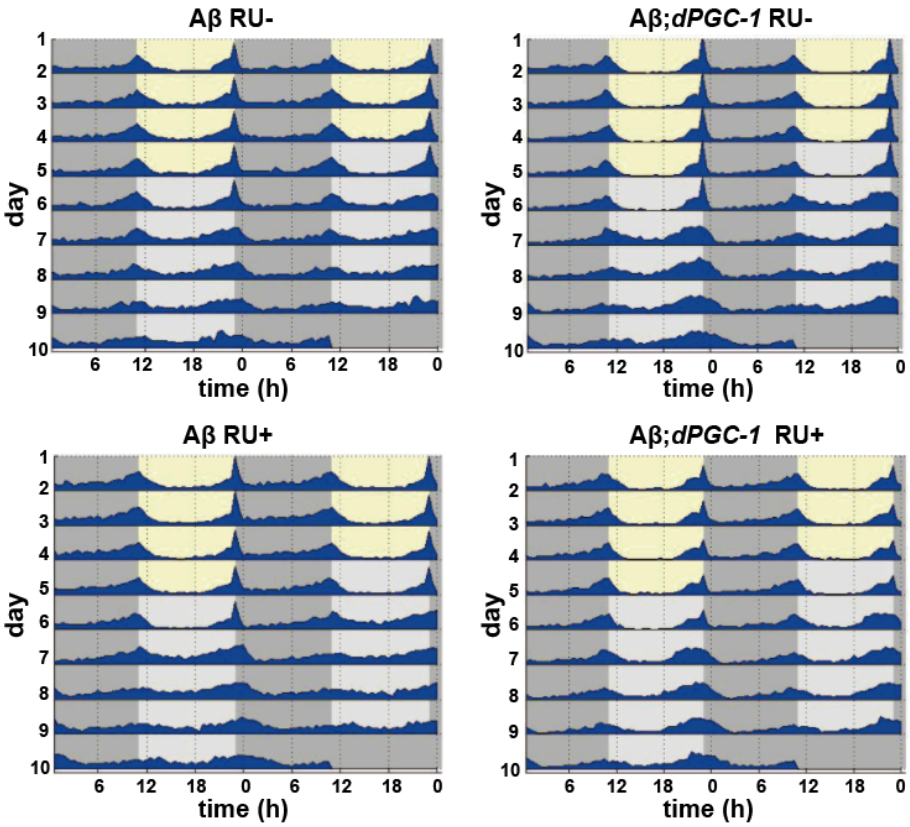

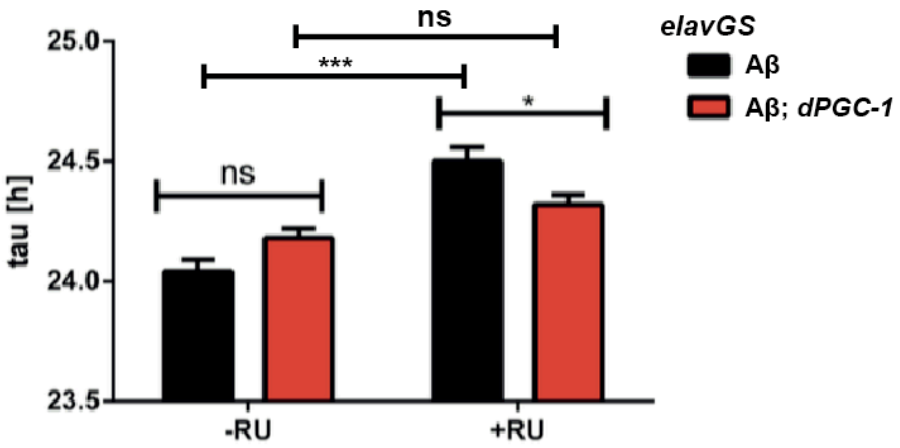

Figure 3.6 Over-expression of *dPGC-1* in Aß-expressing flies rescued the defects in circadian rhythm

(Above) Actograms for the locomotor activity rhythms of 21-day-old male flies expressing Aß or Aß + *dPGC-1* in adult neurons (RU+) and un-induced controls (RU-). This data was recorded over 5 days under 12:12 LD conditions followed by 5 days in DD conditions in Trikinetics *Drosophila* Activity monitors. (Below) Mean free-running periods under DD conditions of the same flies were calculated using autocorrelation, plotted as means ±SEM (n=32, *p < 0.05, ***p < 0.001 by Two-way ANOVA Newman-Keuls test). This experiment was performed in collaboration with Dr Anna Tillman.

To further explore the mechanisms by which *dPGC-1* improves the health-span of Aβ-expressing flies, I measured the ATP concentrations in whole flies. I found reduced ATP levels in Aβ-expressing flies, with restoration towards control levels when *dPGC-1* was co-expressed (Figure 3.7), suggesting an improvement in steady state of homeostasis.

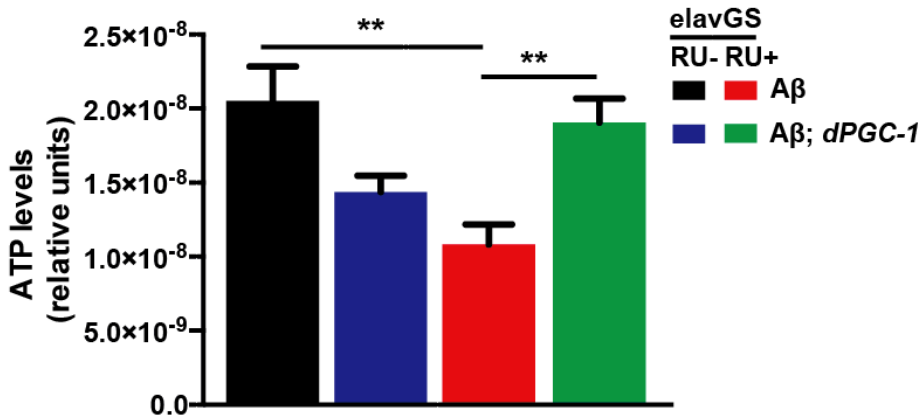

Figure 3.7 Over-expression of *dPGC-1* in Aß-expressing flies ameliorated the reduction in ATP

ATP levels were reduced in 15-day-old whole flies expressing Aß in neurons using the *elavGS* driver (*elavGS>UAS-Aß*, red bar, RU+) compared with control non-induced flies (*elavGS>UAS-Aß*, black bar RU-). ATP levels measured in flies co-expressing Aß and *dPGC-1* (*elavGS>UAS-Aß/UAS-dPGC-1,* green bar, RU+) in adult neurons demonstrated that *dPGC-1* gain-of-function partially ameliorated the decreased ATP levels associated with Aß-expression. The bars are plotted as the means ±SEM (n=7), **p<0.01 by two-way ANOVA Newman-Keuls test. The genotypes used were: *elavGS>UAS-Aß; elavGS>UAS-Aß/UAS-dPGC-1*.

3.3.2*dPGC-1* extended the lifespan of Aβ flies beyond the maximum achieved by DR

DR, an intervention involving the chronic reduction of food intake without malnourishment, is the most robust environmental method known to extend lifespan in a wide range of evolutionarily diverse organisms from yeast to mammals (Fontana et al., 2010, Katewa and Kapahi, 2010, Colman et al., 2009). In addition to its pro-longevity effects, DR has also been shown to improve healthy lifespan in mice, monkeys and humans (Fontana et al., 2010, Ikeno et al., 2006, Maeda et al., 1985, Colman et al., 2014, Mattison et al., 2012). Long-term DR results in an improvement in several markers of health, and reduces the risk of developing age-related disorders such as neurodegeneration (Heilbronn et al., 2006, Cava and Fontana, 2013, Masoro, 2003). As a result of the robust effects of DR, and its strong conservation across different species, unravelling the precise mechanisms linking this intervention to lifespan extension will provide useful insights into the mechanisms of ageing and age-related neurodegeneration.

I showed that over-expression of *dPGC-1* in fly neurons extended lifespan in Aβ-expressing flies (Figure 3.4). Other studies also suggested *dPGC-1* is a modulator for longevity in *Drosophila* (Rera et al., 2011), however the mechanism has not been fully elucidated. To investigate whether lifespan extension mediated by *dPGC-1* in Aβ-expressing flies involves a DR-like mechanism, I carried out a lifespan analysis using a DR-tent (varying concentrations of yeast in the food). If over-expression of *dPGC-1* in Aβ expressing neurons extends lifespan like a true DR mimetic, the lifespan under the dietary conditions where lifespan has already been maximized will not be further extended or may even be shortened. If on the other hand *dPGC-1*

extends lifespan through overlapping mechanisms with DR, it might still further extend lifespan in the optimised DR condition, however, the maximum benefit on lifespan may occur with full feeding. Interestingly I found that over-expression of *dPGC-1* in neurons extends both median and maximum lifespan in all yeast conditions compared to Aβ-expressing flies (Figure 3.8), suggesting that *dPGC-1* extends lifespan via an additive effect to DR. Interestingly, *dPGC-1* over-expression achieved the maximum lifespan extension in full-feeding, indicating an overlapping mechanism with DR. Taken together, *dPGC-1* over-expression in neurons ameliorates the shortened lifespan of Aβ flies through mechanisms partially overlapping with those of DR.

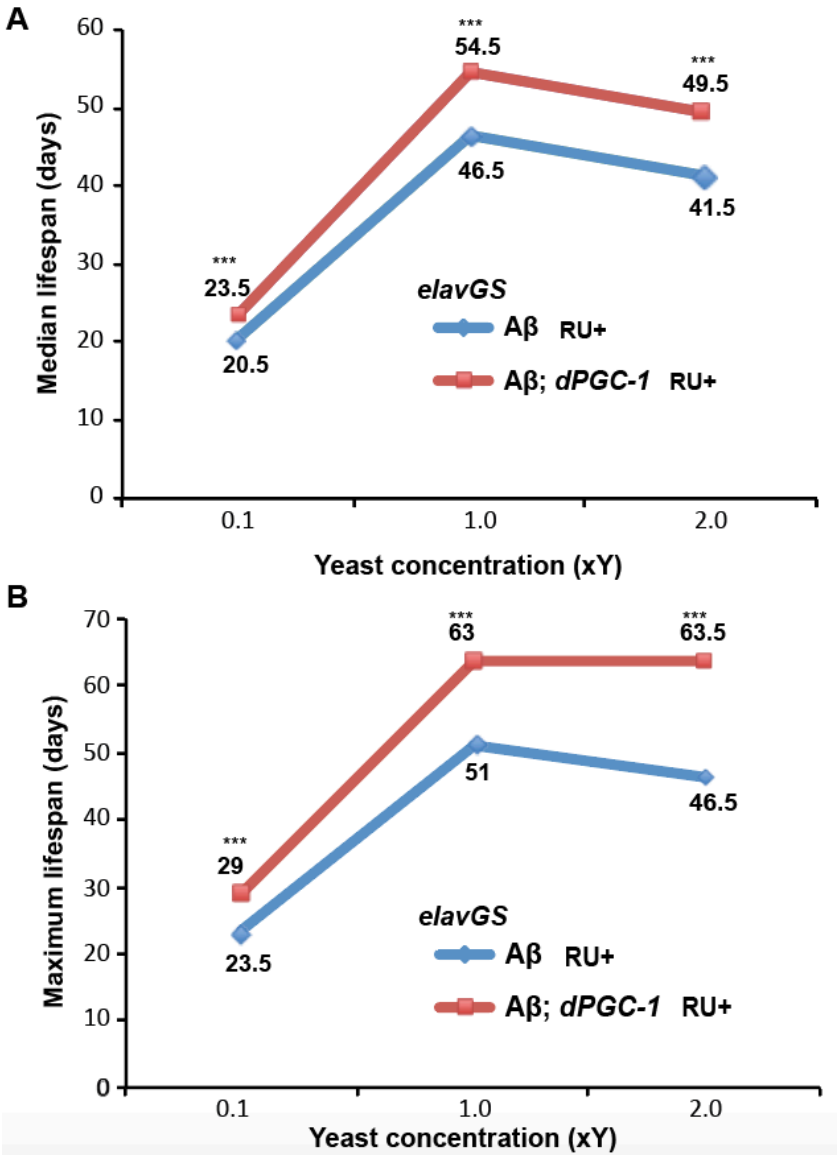

Figure 3.8 Over-expression of *dPGC-1* increased the lifespan of Aβ flies irrespective of food concentration

Over-expression of *dPGC-1* in neurons increased (A) the median and (B) the maximum lifespan in Aβ-expressing female flies across different yeast concentrations in SY food. Plotted are median lifespan values for Aβ-expressing flies (blue line) and Aβ + *dPGC-1* co-expressing flies (red line) against yeast concentration (0.1 x, 1.0 x, and 2.0 x yeast) in SY food supplemented with 200 μM RU. Flies co-expressing Aβ + *dPGC-1* had significantly increased lifespan at each yeast concentration compared to Aβ-expressing flies (***p<0.001, log-rank test). For example, expression of *dPGC-1* increased the median lifespan of Aβ-expressing flies by 17% and maximum lifespan by 24% in 1.0 x SY DR food, and increased median lifespan by 19% and maximum lifespan by 37% under 2 x SY full feeding food. The genotypes used were: *elavGS>UAS-Aβ; elavGS>UAS-Aβ/UAS-dPGC-1*.

3.3.3 *dPGC-1* over-expression improved mitochondrial function in Aβ flies

PGC-1α affects many cellular processes, and therefore may rescue Aβ toxicity through a number of different mechanisms. Aβ toxicity has been linked to mitochondrial dysfunction, impaired energy metabolism and oxidative damage (Garcia-Escudero et al., 2013, Lustbader et al., 2004, Abramov et al., 2004). PGC-1α is the master regulator of mitochondrial biogenesis and oxidative phosphorylation through co-activation of nuclear receptors (Mootha et al., 2004, Tiefenböck et al., 2010, Rera et al., 2011, Puigserver and Spiegelman, 2003). PGC-1 regulates mitochondrial density in mammalian primary neurons (Wareski et al., 2009), the fly fat body (Tiefenböck et al., 2010), and the fly gut (Rera et al., 2011). I therefore asked whether *dPGC-1* induction increases mitochondrial biogenesis in fly neurons by measuring the amount of mitochondrial DNA (mtDNA) relative to that of nuclear DNA (nDNA). I demonstrated that Aβ expression lead to a significant reduction in mtDNA (Figure 3.9). This result parallels the observation of mtDNA deletions or mutations in AD patients' brains (Bender et al., 2008, Coskun et al., 2004). Over-expression of *dPGC-1* in neurons did not rescue this phenotype (Figure 3.9).

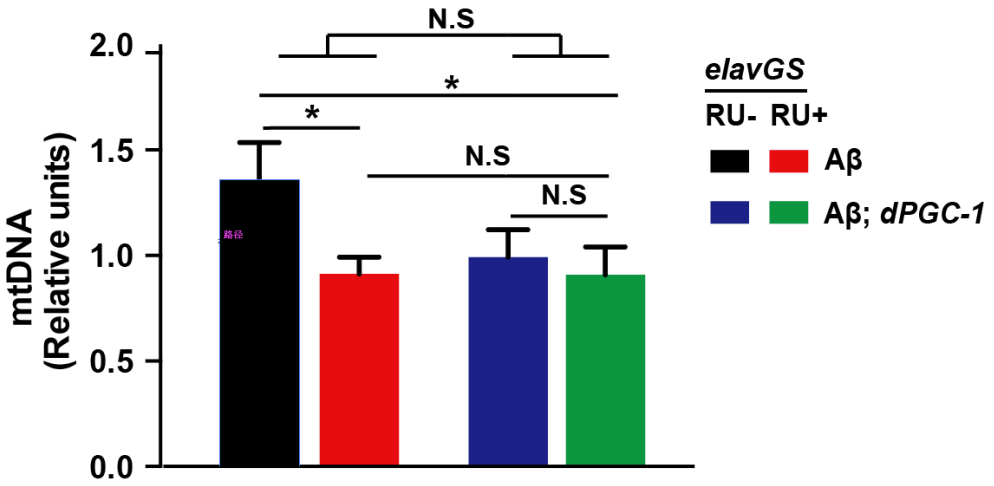

Figure 3.9 Mitochondrial DNA was reduced in Aβ and *dPGC-1* expressing flies

Mitochondrial DNA (mtDNA), relative to the nuclear DNA (nDNA) amplicon was measured by qRT-PCR in fly heads expressing Aß or Aß + *dPGC-1* in adult neurons (RU+) and in un-induced controls (RU-) at 30-days of age. The bars represent the means ± SEM (n=4, *p<0.05 by ANOVA Newman-Keuls test, two-way ANOVA shows p>0.05 when comparing Aß response to RU relative to Aß; *dPGC-1* response to RU). The genotypes used were: *elavGS>UAS-Aβ; elavGS>UAS-Aβ/UAS-dPGC-1*.

Changes in mitochondrial DNA copy number do not necessarily reflect changes in the activity of the electron transport chain (ETC) (Tiefenböck et al., 2010). I therefore investigated whether up-regulation of *dPGC-1* in neurons can increase ETC activity in Aβ-expressing flies. The ETC consists of a series of enzymes that transfer electrons from donors to acceptors via redox reactions, to create an electrochemical proton gradient, the mitochondrial membrane potential ($\Delta\Psi_M$), which is the driving force for the synthesis of adenosine triphosphate (ATP) by the F1F0-ATP synthase. To assess the mitochondrial membrane potential, I measured TMRM fluorescence in Aβ-expressing fly brains, and found a significant increase in $\Delta\Psi_M$ compared to controls (Figure 3.10). Hyperpolarization of mitochondria has previously been described in many neurodegenerative disorders, as a compensatory response to certain deficiencies in ETC enzymatic activity. For example, this has been observed in PD patient fibroblasts carrying a *PINK1* mutation (Abramov et al., 2011) and in neurons carrying a severe mtDNA mutation, leading to defective complex I of the ETC (Abramov et al., 2010). In our study, mitochondria from Aβ-expressing flies display hyperpolarized mitochondrial membranes, likely in response to Aβ toxicity and reduced mtDNA, which encodes the subunits of the ETC components. Surprisingly,

dPGC-1 over-expression increased brain tissue TMRM fluorescent intensity even more than in flies expressing Aß alone (Figure 3.10), suggesting that *dPGC-1* acts to rescue Aβ toxicity by increasing the hyperpolarising compensatory response.

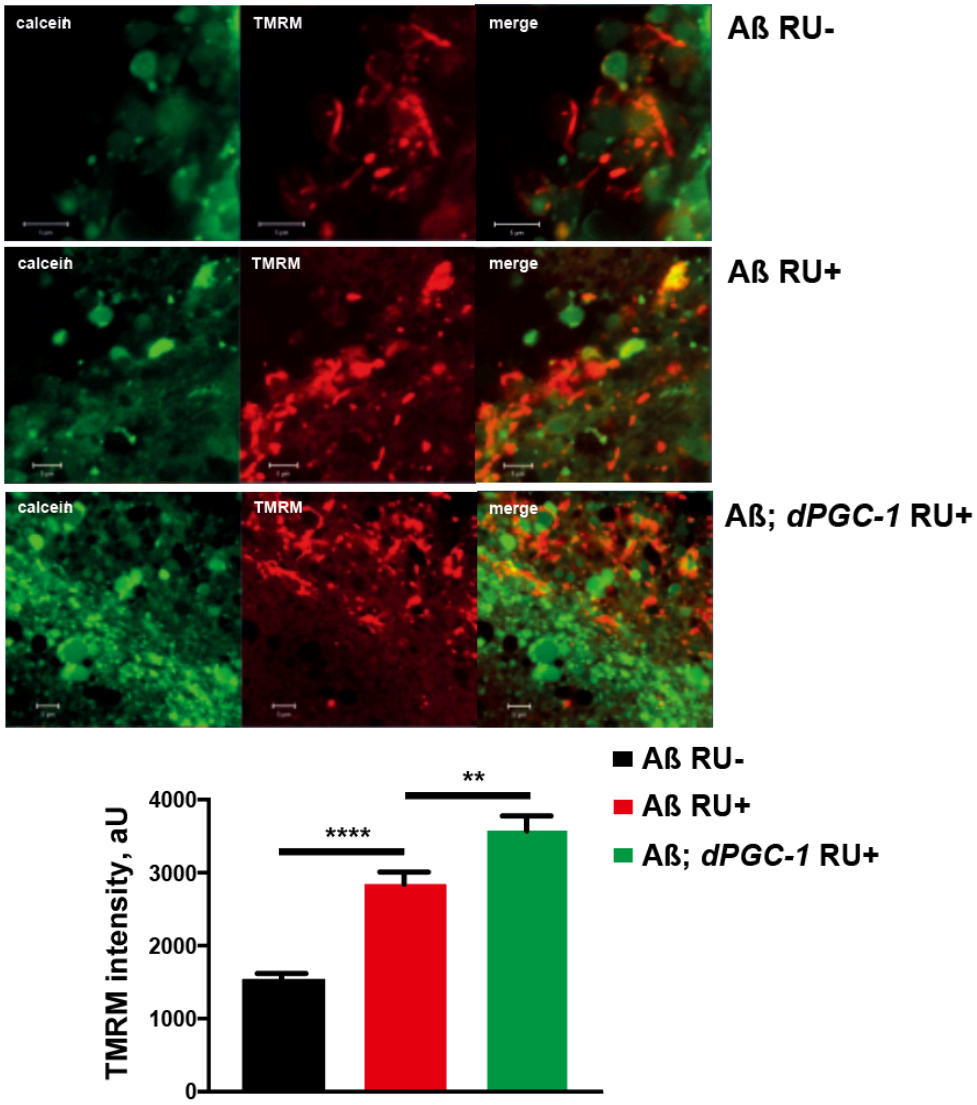

Figure 3.10 Both Aβ and *dPGC-1* over-expression increased the mitochondrial membrane potential in the fly brain

Aß-expressing fly brains displayed increased mitochondrial membrane potential at 30-day of age. *dPGC-1* over-expression in Aß co-expressing flies lead to further hyperpolarization of the mitochondrial membrane. The ΔΨm is represented as arbitrary units of TMRM intensities. Data are shown as the mean ± SEM (n=11 for *Aβ RU-*, n=10 for *Aβ RU+* and n=11 for *Aβ; dPCG-1 RU+*; **p<0.01, ***p<0.001 by ANOVA Newman-Keuls test). In collaboration with Dr. Plamena R. Angelova.

dPGC-1 is required for the proper expression of many mitochondrial ETC genes, including *cytochrome c proximal* (*cyt-c-p*), which encodes one of the enzymes in

cytochrome c that participates in the creation of the mitochondrial membrane potential (Tiefenböck et al., 2010). Aβ has been shown to directly inhibit cytochrome c activity *in vitro* (Crouch et al., 2005, Casley et al., 2002), suggesting that elevating *dPGC-1* in neurons might rescue toxicity be increasing expression of *cyt-c-p*. Therefore, I assessed the mRNA transcript levels of *cyt-c-p* in Aβ-expressing fly heads by qRT-PCR, and found that as predicted, mRNA levels of *cyt-c-p* were reduced in response to Aβ-expression, while co-expression with *dPGC-1* significantly rescued this effect (Figure 3.11). These findings suggest that the induction of *dPGC-1* in fly neurons might lead to the elevation of ETC enzymes in association with mitochondrial membrane hyperpolarization.

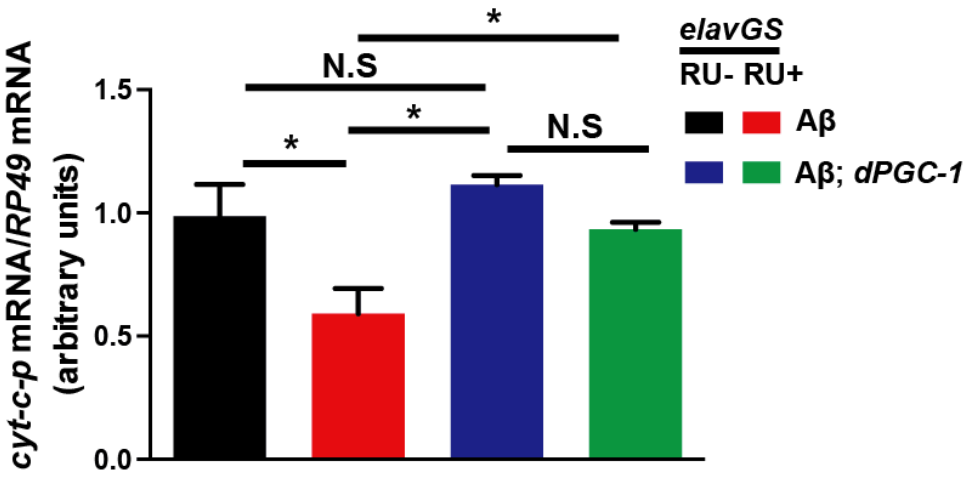

Figure 3.11 Aß and *dPGC-1* had opposing effects on *cyt-c-p* transcription.

qRT-PCR demonstrated that *cyt-c-p* mRNA levels (relative to *RP49*) in the heads of 30-day-old flies expressing Aß (RU+) were lower compared to controls (RU-). Co-expression of *dPGC-1* in adult neurons had the opposite effect, increasing *cyt-c-p* mRNA levels. Bars represent means ± SEM (n=3, *p<0.05 by ANOVA Newman-Keuls test). The genotypes used were: *elavGS>UAS-Aß; elavGS>UAS-Aß/UAS-dPGC-1*.

To determine whether these changes in *cyt-c-p* had functional consequences, I measured ATP concentrations in fly heads and observed a significant increase in ATP levels in *dPGC-1* flies (Figure 3.12). Although I observed a trend towards a reduction in ATP in response to Aβ, this did not reach statistical significance. Therefore, activation of *dPGC-1* in neurons elevated ATP production by increasing the

membrane potential, through up-regulation of the genes responsible for ETC activity in Aβ-expressing flies.

Taken together my results demonstrated that Aβ reduces mitochondrial DNA copy number and cytochrome c activity, in association with a compensatory increase in the mitochondrial membrane potential. In addition, *dPGC-1* may partially ameliorate the Aβ–phenotypes through the compensatory increase in mitochondrial membrane potential, an increase in ATP production, as well as the up-regulation of ETC enzymes.

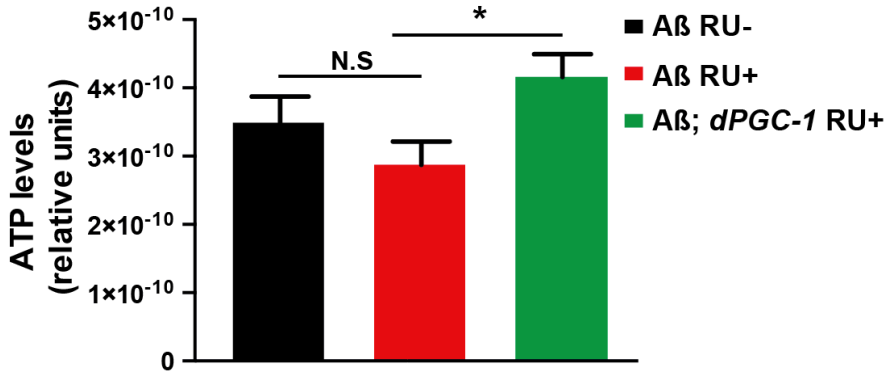

Figure 3.12 *dPGC-1* over-expression increased ATP levels in Aß-expressing fly heads

dPGC-1 over-expression in Aß-expressing flies leads to an increase in ATP levels in adult neurons at 30 days of age (genotypes: *Aß RU-; Aß RU+; and Aß; dPGC-1 RU+*). Bars represent the means ± SEM (n=5, *p<0.05 by ANOVA Newman-Keuls test).

3.3.4 *dPGC-1* over-expression regulated the mitochondrial stress response to Aβ toxicity and protected Aβ flies against oxidative stress

Mitochondrial DNA depletion and increases in mitochondrial membrane potential can lead to excessive production of ROS and deleterious mitochondrial stress. This in turn is detrimental to the maintenance of the mitochondrial proteome and can lead to apoptosis (Haynes and Ron, 2010, Kinghorn et al., 2015). UPR^{mt} is a stress-response pathway that adapts and activates the folding capacity of the mitochondrial matrix in response to mitochondrial dysfunction. It also leads to up-regulation of nuclear-encoded mitochondrial-localized chaperones to promote both protein folding and

degradation, to either restore mitochondrial proteostasis or enter apoptosis (Neupert and Herrmann, 2007, Haynes and Ron, 2010).

I next asked whether the amelioration of the neurotoxic phenotypes associated with Aß by *dPGC-1* over-expression is accompanied by improved mitochondrial proteostasis. Immunoblot analyses against mitochondrial chaperones HSP60 and Grp75 showed a significant reduction in response to Aβ (Figure 3.13 and 3.14), suggesting an impaired UPR^{mt} and proteostastic failure. Interestingly, flies co-expressing both *dPGC-1* and Aβ in neurons returned the levels of HSP60 and Grp75 to control levels seen in their un-induced counterparts. Since there was significantly different basal levels of mitochondrial chaperones in the corresponding transgenic control lines, we confirmed our findings by statistical analysis using a two-way ANOVA. This demonstrated a significant interaction between the induction of RU (indicative of gene expression) and the genotypes, suggesting that over-expression of neuronal *dPGC-1* reverses the reduction in mitochondrial chaperones seen in Aβ-expressing flies (Figure 3.13 and 3.14). These results suggest that over-expression of *dPGC-1* leads to an increase in UPR^{mt} activity, ameliorating Aβ toxicity.

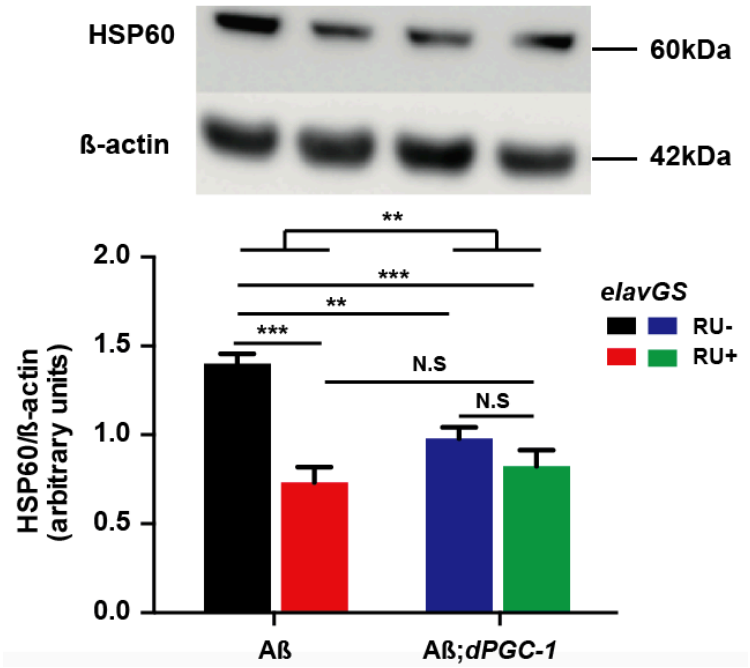

Figure 3.13 Aß-expressing flies displayed reduced levels of the HSP60 protein

Western blot analysis on 22-day-old Aß-expressing fly heads (*Aß RU+*) showed reduced HSP60 protein levels compared to controls (*Aß RU-*). Co-expression of Aß + *dPGC-1* in adult neurons (*Aß;*

dPGC-1 RU+) did not show significant difference in HSP60 protein levels compared to controls (*Aß; dPGC-1 RU-*). The HSP60 levels are shown normalized to ß-actin. Bars represent means ± SEM (n=4). The image is a representative gel from one biological repeat (**p<0.01, ***p<0.001 by ANOVA Newman-Keuls test. two-way ANOVA analysis shows **p<0.01 when comparing Aß response to RU relative to Aß; *dPGC-1* response to RU). The genotypes used were: *elavGS>UAS-Aß; elavGS>UAS-Aß/UAS-dPGC-1*.

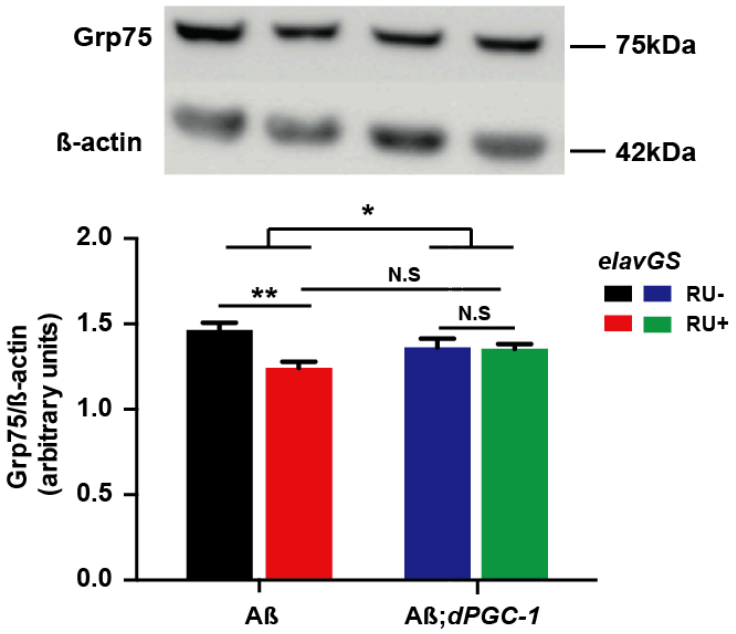

Figure 3.14 Aß-expressing flies displayed reduced levels of the Grp75 protein

Aß-expressing fly heads display reduced levels of the Grp75 protein as assessed by Western blot analysis on the heads of 22-day-old flies. The Grp75 protein levels were normalized to ß-actin. Bars represent means ± SEM (n=3-4). The image is a representative gel from one biological repeat (**p<0.01 by ANOVA Newman-Keuls test, two-way analysis shows *p<0.05 when comparing Aß response to RU relative to Aß; *dPGC-1* response to RU).

Aß-induced mitochondrial stress is similar to that caused by exposure to the potent oxidizer paraquat (Cocheme and Murphy, 2008). I therefore determined the effect of *dPGC-1* over-expression on the sensitivity of Aβ-expressing flies to paraquat. A single injection of the redox-cycler paraquat, which produces superoxide in part through the mitochondria (Cocheme and Murphy, 2008), caused a significant reduction in the survival of Aβ-expressing flies compared to controls (Figure 3.15). Interestingly, co-expression of Aβ with *dPGC-1* restored survival to control levels (Figure 3.15), suggesting that activation of *dPGC-1* in neurons protects Aβ-

expressing flies from oxidative stress, likely through an improved mitochondrial stress response.

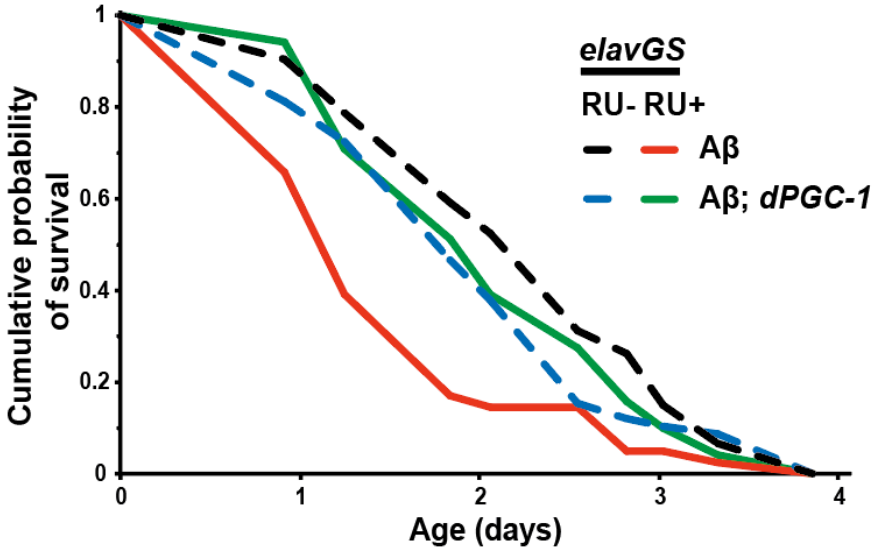

Figure 3.15 Over-expression of *dPGC-1* rescued the survival of Aß-expressing female flies injected with paraquat

The survival curves of flies expressing Aß or Aß + *dPGC-1* in adult neurons (RU+) and un-induced controls (RU-) demonstrated a rescuing effect of *dPGC-1* on the survival of Aß-expressing flies when injected with paraquat ($p<0.0001$ when comparing *Aß RU+* and *Aß; dPGC-1 RU+* by log-rank test). This work was performed in collaboration with Dr. Anna Tillmann.

Activation of *dPGC-1* in neurons further increases the mitochondrial membrane potential in Aβ flies, which is assumed to increase the ETC leakage, the ROS production and the free radical damage (Green et al., 2011). However, the free radial damage and lifespan can be uncoupled (Zhang et al., 2009, Van Raamsdonk and Hekimi, 2009). Rather than a direct contributor to disease pathology, ROS is more likely a response modulator for mitochondrial stress-elicited survival signal (Sena and Chandel, 2012). Our findings suggest a model in which over-expression of Aß leads to mtDNA deletion, increased oxidative damage, and impaired mitochondrial stress response and proteostatic failure. However, over-expression of *dPGC-1* in neurons switches on a compensatory mechanism involving the further increase in mitochondrial membrane potential to drive ATP synthase. In addition, *dPGC-1* protects Aß flies from mitochondrial stress likely through improvement in the UPR^{mt}.

3.3.5 *dPGC-1* regulated the UPR^{ER} in flies expressing Aβ

PGC-1 activates the UPR^{ER} in mammalian skeletal muscle as an adaptive response to exercise, partially though co-activation of ATF6a (Wu et al., 2011). I therefore assessed whether *dPGC-1* activation in neurons can protect Aβ flies from ER stress. The Grp78 protein is a negative master regulator of the UPR and binds and maintains the downstream cascades in an inactive state (Carrara et al., 2013, Bertolotti et al., 2000, Gorbatyuk et al., 2012, Li et al., 2008), and increases in response to Aβ (Niccoli et al., 2016). Immunoblot analyses confirmed that the levels of the Grp78 protein were increased in Aβ-expressing flies, and that co-expression of *dPGC-1* restored Grp78 expression back to control levels (Figure 3.16). In keeping with this we recently showed that genetic down-regulation of Grp78 protects flies from Aβ toxicity (Niccoli et al., 2016), suggesting that *dPGC-1* could ameliorate Aβ toxicity by modulating the UPR^{ER}.

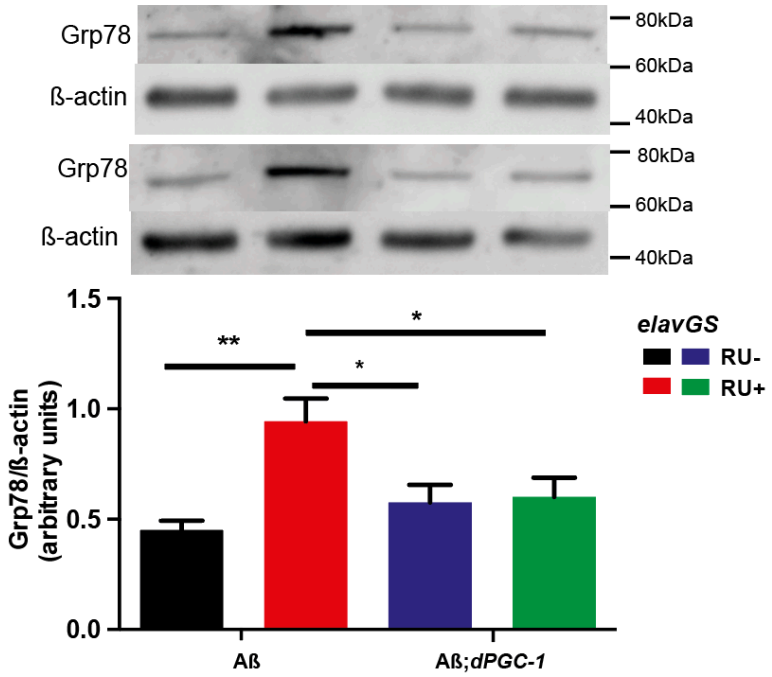

Figure 3.16 The levels of the Grp78 protein were elevated in Aβ-expressing fly heads but returned towards control levels with co-expression of *dPGC-1*

Western blot analysis of the protein levels of the ER chaperone Grp78 in the heads of 22-day-old flies expressing Aß or Aß + *dPGC-1* in neurons (RU+) and un-induced controls (RU-). Protein levels were normalized to ß-actin and the bars represent the means ± SEM (n=4, *p<0.05, **p<0.01 by ANOVA Newman-Keuls test). The image is a representative gel of two biological repeats.

Low levels of Grp78 would be predicted to be associated with increased activation of the UPR^{ER}. To confirm this, I analysed the levels of *Xbp1* splicing, a marker of IRE1 activation. Over-expression of Aβ in the fly brain resulted in a trend towards an increase in *Xbp1* splicing, but this did not reach significance. Other studies have however shown an increase in *Xbp1* splicing in response to Aβ (Casas-Tinto et al., 2011, Niccoli et al., 2016). As predicted, co-expression of Aβ with *dPGC-1* increased the levels of spliced *Xbp1* three-fold, suggesting over-expression of *dPGC-1* in neurons increases IRE1 activity (Figure 3.17).

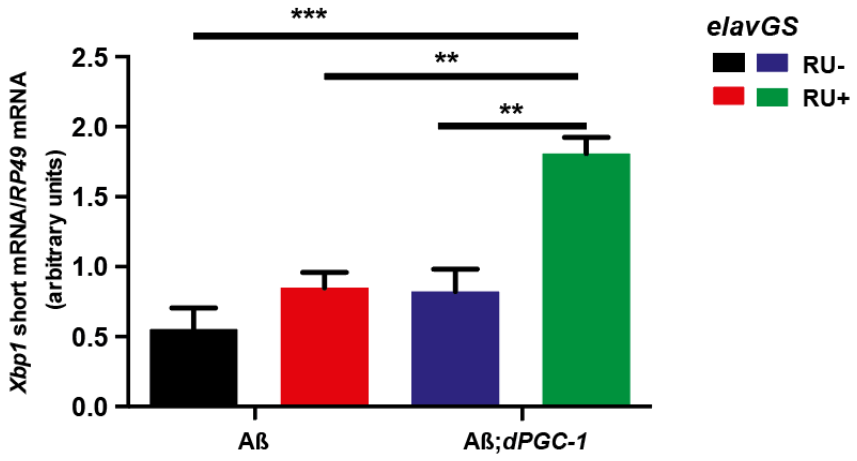

Figure 3.17 The mRNA levels of *Xbp1* splicing were increased in the heads of Aβ-expressing flies co-expressing *dPGC-1*

Spliced *Xbp1* mRNA levels in heads of 15-day-old flies expressing Aß or Aß + *dPGC-1* in neurons (RU+) and un-induced controls (RU-), as measured by qRT-PCR (relative to *RP49*). The bars represent the means ± SEM (n=3, ** P<0.01, ***p<0.001 by ANOVA Newman-Keuls test).

Similarly, *Grp78* mRNA levels, a marker of ATF6a activation, increased in response to Aβ over-expression (Figure 3.18), and co-over-expression of *dPGC-1* resulted in an even greater increase than that seen with Aβ alone (Figure 3.18). Grp78 protein levels are tightly controlled at the levels of translation (Gulow et al., 2002), and an increase in the mRNA, therefore, does not necessarily indicate higher protein levels, suggesting that *dPGC-1* reduced either Grp78 translation or stability. Taken together, these findings suggest that Aβ activates the UPR^{ER}, and that *dPGC-1* further activates it, by reducing the protein levels of Grp78 and hence activating the IRE1 and ATF6α pathways, resulting in the amelioration of Aß toxicity.

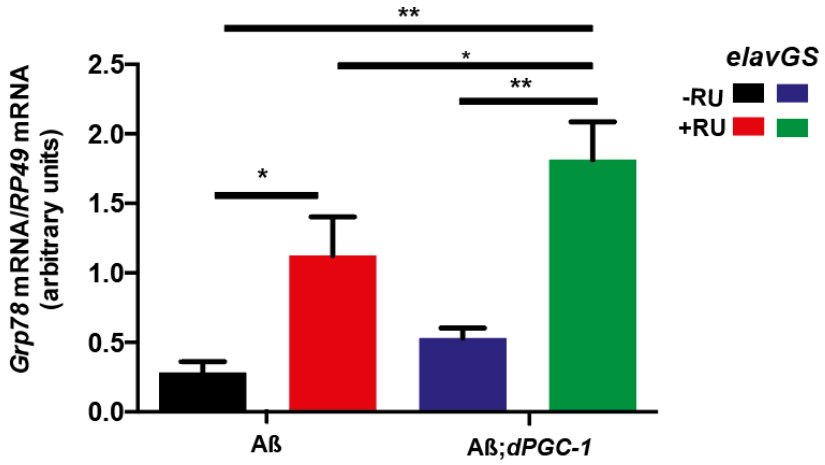

Figure 3.18 The mRNA levels of *Grp78* were increased in Aβ-expressing fly heads and further increased by the co-expression of *dPGC-1*

Grp78 mRNA levels in the heads of 15-day-old flies expressing Aß or Aß + *dPGC-1* in neurons (RU+) and un-induced controls (RU-), measured by qRT-PCR (relative to *RP49*). The bars represent the means ± SEM (n=3, *p<0.05, **p<0.01, ***p<0.001 by ANOVA Newman-Keuls test). The genotypes used were: *elavGS>UAS-Aß; elavGS>UAS-Aß /UAS-dPGC-1*.

As described above, I demonstrated that over-expression of *dPGC-1* in neurons modulates the levels of chaperones in both the UPR^{ER} and the UPR^{mt} in response to Aß toxicity. I therefore addressed the question of whether *dPGC-1* regulates the basal levels of these chaperones in the absence of Aß. Interestingly, activation of *dPGC-1* in neurons did not change the basal levels of Grp75 and Grp78, and even down-regulated the level of HSP60 compared to non-RU treated young control flies (Figure 3.19). This therefore demonstrated that the effect of *dPGC-1* on the chaperones involved in the UPR^{ER} and the UPR^{mt} is specific to Aß-mediated pathogenesis. It also highlights the potential therapeutic benefits of modulating these chaperones in the treatment of AD.

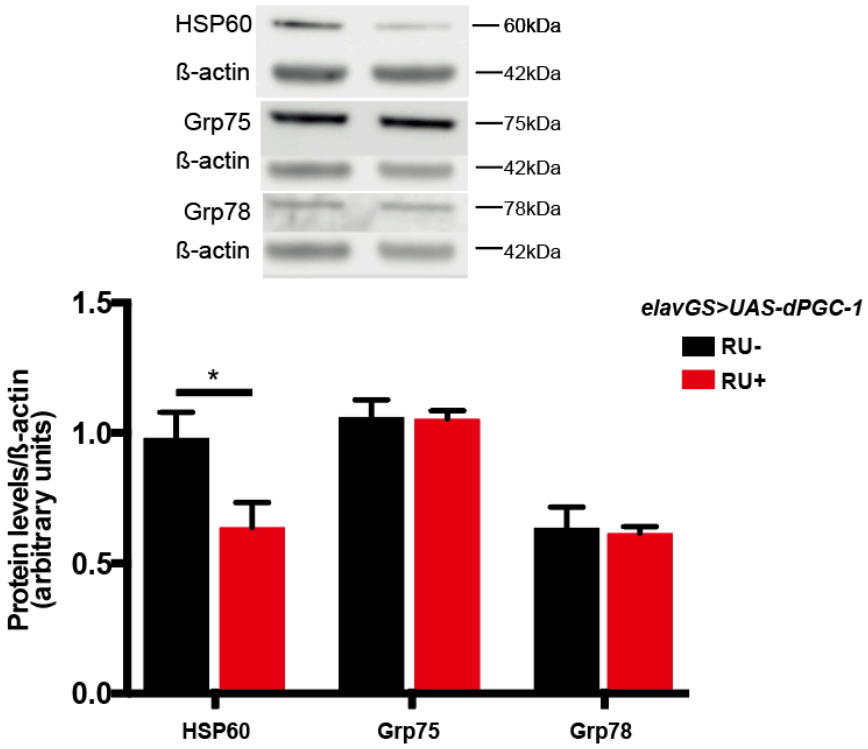

Figure 3.19 Over-expression of *dPGC-1* in neurons did not change the basal levels of chaperones in young flies

Western blot analysis of the protein levels of the mitochondrial chaperones HSP60, Grp75, and the ER chaperone Grp78 in the heads of 15-day-old flies over-expressing *dPGC-1* (RU+) and un-induced controls (RU-). Protein levels were normalized to ß-actin. The bars are plotted below as the means ± SEM (n=4, *p<0.05 by t-test). The image is a representative gel from one biological repeat.

3.3.6 Rifampicin ameliorated Aß neurotoxicity via activation of the UPR^{ER}

Since *dPGC-1* ameliorates Aβ toxicity through activation of UPR^{ER}, pharmacological targeting of the UPR^{ER} may represent a potential therapeutic avenue for the treatment of AD. Rifampicin, a well-known antibiotic used to treat tuberculosis and leprosy, is known to cross the blood brain barrier following oral administration (Umeda et al., 2016). Interestingly it has been shown that leprosy patients treated with rifampicin show a lower incidence of dementia and a reduction in senile plaques compared to the general population (Mcgeer et al., 1992, Chui et al., 1994, Namba et al., 1992). Rifampicin has also been shown to have neuroprotective effects in a number of animal models of neurodegenerative diseases (Tomiyama et al., 1994, Umeda et al., 2016, Oida et al., 2006, Kilic et al., 2004), but the mechanisms involved have not

been fully elucidated. Rifampicin reduced Aβ oligomerization and improved memory in an APP mice model through improved autophagy-lysosomal function (Umeda et al., 2016). It was also shown to activate the UPR and offer protection against rotenone-induced cytotoxicity *in vitro* (Jing et al., 2014).

I therefore treated our Arctic Aβ over-expressing flies with rifampicin to determine whether it can protect against Aß neurotoxicity *in vivo*. Indeed, feeding Aβ flies with 200 μM of rifampicin statistically extended lifespan (Figure 3.20, p=0.002 by log-rank test), and improved climbing ability (Figure 3.22) without altering Aß levels (Figure 3.21). 200 μM of rifampicin did not improve either the lifespan (Figure 3.20, p=0.06 by log-rank test) or the climbing ability in non-induced control flies, suggesting that the effects of rifampicin are specific to AD pathology. Although 500 μM rifampicin increased the lifespan of both Aβ-expressing flies and non-induced controls (Figure 3.20, p=0.0009 and p=0.0006 respectively), their climbing ability was not affected (Figure 3.22), suggesting that the effects on climbing ability and lifespan can be uncoupled. Cox proportional hazard analysis confirmed that there is no significant interaction between the response to RU and the response to rifampicin (500 μM) treatment (Table 1, p=0.89), suggesting that high dose (500 μM) rifampicin extends lifespan regardless of whether Aß is present or not. Rifampicin may therefore have broad-spectrum effects on lifespan when administrated at high concentrations, but a specific protective effect against Aß-induced neurotoxicity when administrated at lower concentrations. Rifampicin treatment, similar to *dPGC-1* over-expression, also reversed the increase in Grp78 levels associated with Aβ-expression (Figure 3.23), suggesting activation of the UPR^{ER}. Rifampicin is therefore a promising ready-to-use medicine for the treatment of AD pathology, through its activation of the UPR^{ER}.

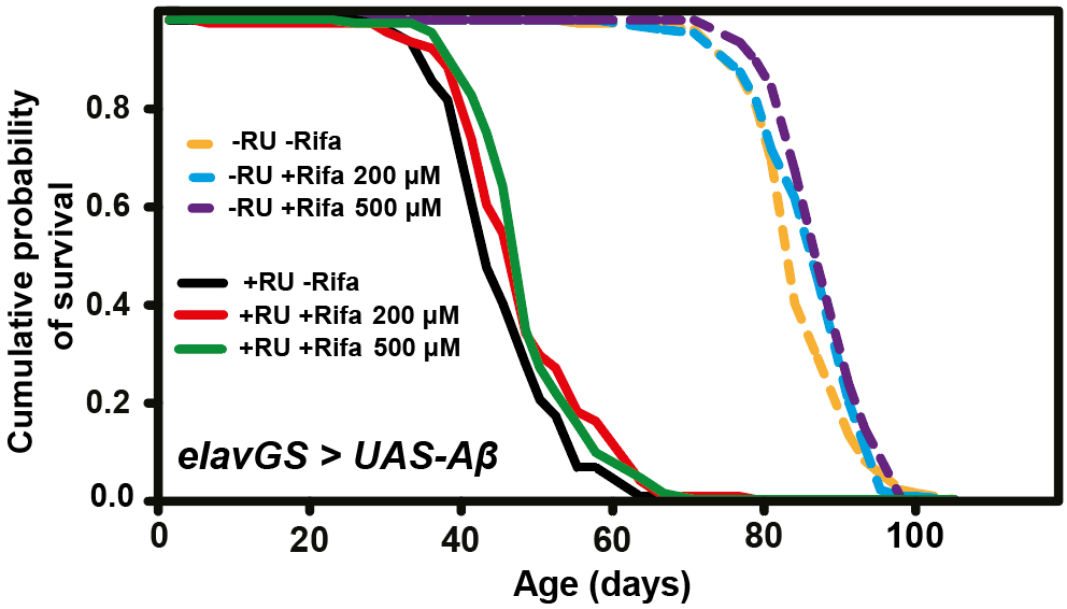

Figure 3.20 Rifampicin increased the lifespan of Aβ-expressing female flies

Survival curves of flies expressing Aß in adult neurons (RU+) and un-induced controls (RU-) using inducible *elavGS* driver with or without rifampicin treatment at 200 µM (P=0.002 when comparing *Aβ RU+* Rifampicin 0 µM and *Aβ RU+* Rifampicin 200 µM by log-rank test; p=0.06 when comparing *Aβ RU-* Rifampicin 0 µM and *Aβ RU-* Rifampicin 200 µM by log-rank test) and 500 µM (P=0.0009 when comparing *Aβ RU+* 0 µM and *Aβ RU+* Rifampicin 500 µM by log-rank test; p=0.0006 when comparing *Aβ RU-* Rifampicin 0 µM and *Aβ RU-* Rifampicin 500 µM by log-rank test. N= 150 flies per conditions. This work was performed in collaboration with Dr. Jorge Iván Castillo-Quan.

```
coxph(formula = Surv(time = dataC$DAY, event = dataC$CENSOR,
    type = c("right"), origin = 0) ~ dataC$RU * dataC$RIFAMPICIN)

  n= 607, number of events= 601

                              coef exp(coef)  se(coef)      z Pr(>|z|)
dataC$RU                   6.54502 695.76983   0.61510 10.641  < 2e-16 ***
dataC$RIFAMPICIN          -0.33977   0.71193   0.11702 -2.904  0.00369 **
dataC$RU:dataC$RIFAMPICIN -0.02155   0.97868   0.16472 -0.131  0.89591
---
Signif. codes:  0 '***' 0.001 '**' 0.01 '*' 0.05 '.' 0.1 ' ' 1
```

Table 1 CPH analysis of the survival of Aß-expressing flies on treatment with 500 µM rifampicin

CPH analysis showed that there was no interaction between the response to RU and the response to rifampicin 500µM (p=0.89). This suggests that treatment with 500µM rifampicin extends lifespan regardless of whether Aß is present or not.

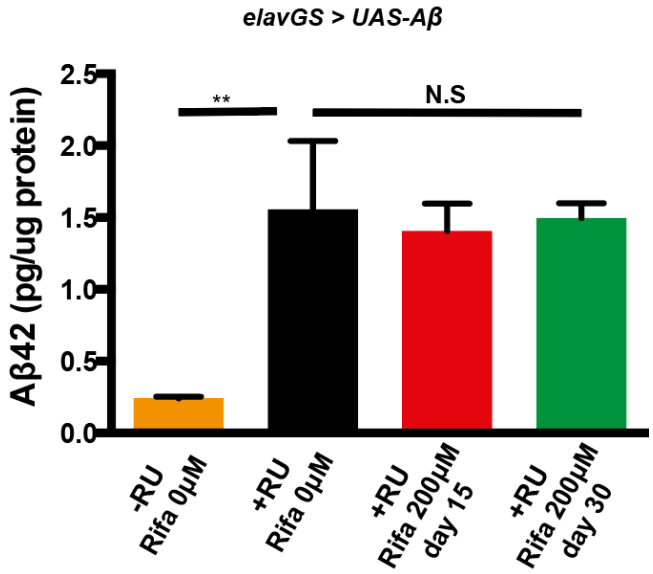

Figure 3.21 Rifampicin treatment had no effect on Aβ protein levels.

Aß protein levels, measured by ELISA, in the heads of 15- or 30-day old Aß- expressing flies (+RU) and un-induced controls (-RU) treated with or without 200uM rifampicin. Bars represent the means ±SEM (n=3, **p<0.01 by ANOVA Newman-Keuls test).

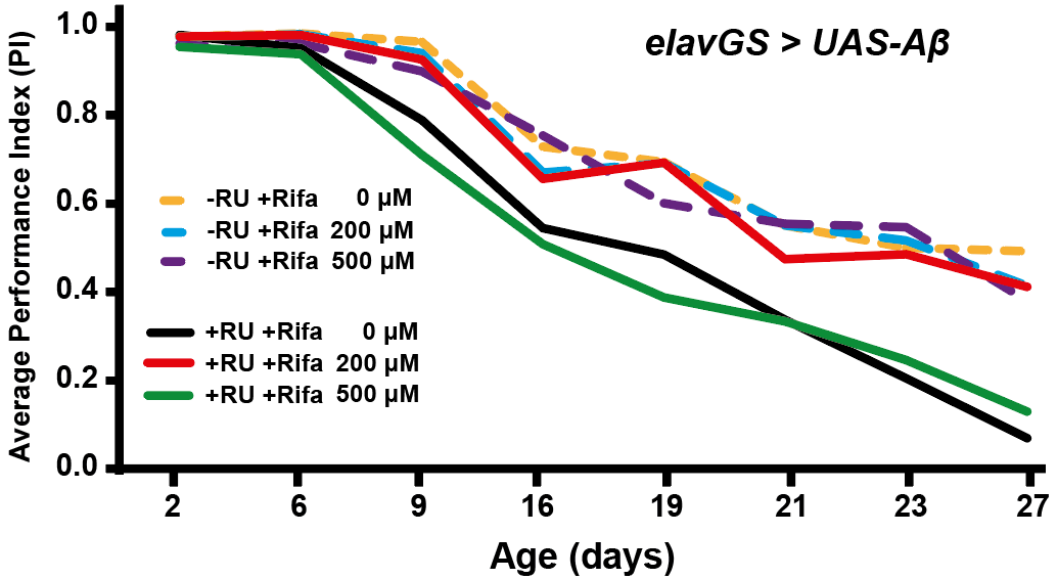

Figure 3.22 Rifampicin rescued the locomotor ability of Aβ-expressing flies

The climbing assay Performance Index (PI) of Aß-expressing flies in the absence and presence of rifampicin. P<0.001 when comparing the Aß response to RU relative to the Aß response to RU + rifampicin 200μM by ordinal logistic regression. There is no significant difference between *Aß RU+* rifampicin 0 μM and *Aß RU+* rifampicin 500 μM.

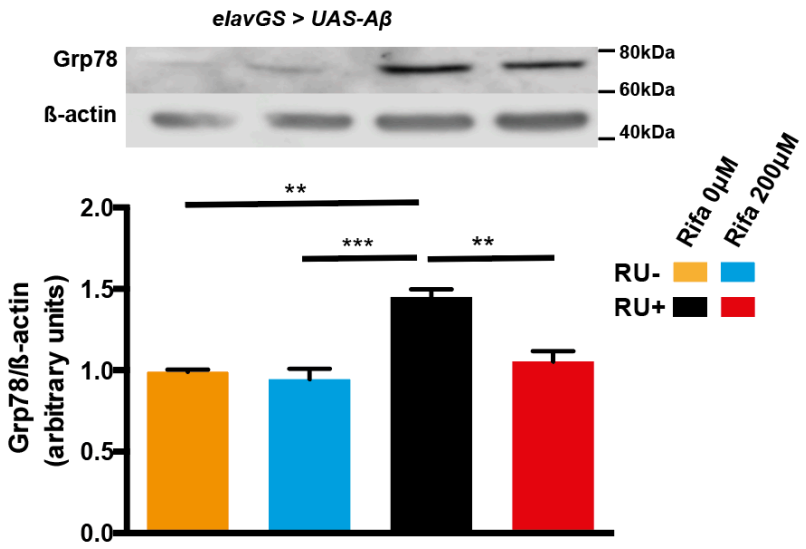

Figure 3.23 Rifampicin reduced the increased levels of the Grp78 protein in Aß-expressing fly heads

Western blot of Grp78 in the heads of 15-day-old flies expressing Aß in neurons (RU+) and un-induced controls (RU-) with or without 200μM rifampicin treatment. The bars are plotted below as the means ± SEM (n=3, **p<0.01, ***p<0.001 ANOVA Newman-Keuls test). The image is a representative gel of one biological repeat.

3.3.7 Over-expression of *dGABPα* or *dYY1* did not rescue Aß toxicity

PGC-1α is a transcriptional coactivator involved in mitochondrial biogenesis (Cunningham et al., 2007, Mootha et al., 2004) and the regulation of the circadian clock (Liu et al., 2007). To further explore the downstream effectors of *dPGC-1* involved in the amelioration of Aß neurotoxicity, I performed a small-scale screen of transcription factors previously reported to be required for the co-activation of *dPGC-1*. I tested the transcription factor PDP1ϵ, which is involved in the regulation of the circadian clock (Cyran et al., 2003), and two other transcription factors, YY1 and GABPα, known to play a role in mitochondrial biogenesis.

Mammalian PGC-1α has been shown to regulate mitochondrial oxidative phosphorylation by co-activating the transcription factor YY1 (Cunningham et al., 2007). I therefore investigated whether *dPGC-1* over-expression ameliorates Aß toxicity through YY1. Surprisingly, up-regulation of neuronal *dYY1* (*pho*, CG17743) in neurons shortened the lifespan of the Aß-expressing flies (Figure 3.24).

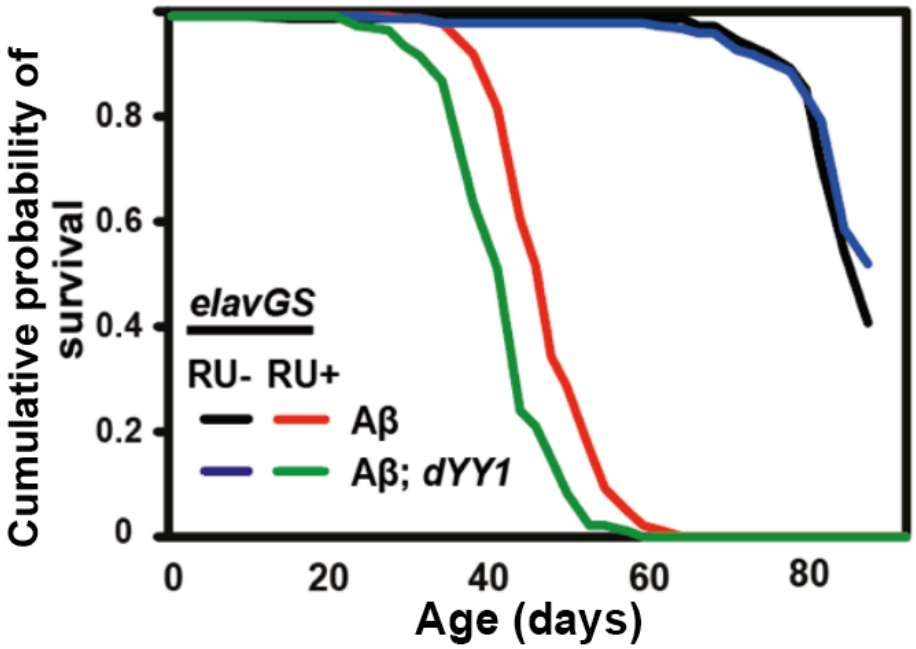

Figure 3.24 The co-expression of *dYY1* in the neurons of Aß-expressing flies lead to a decrease in lifespan

The survival curves of female flies expressing Aß or Aß + *dYY1* in adult neurons (RU+) and un-induced controls (RU-). The genotypes used were: *elavGS>UAS- Aß; elavGS>UAS- Aß/UAS-dYY1*.

Mammalian PGC-1α has been also shown to regulate mitochondrial biogenesis through the transcription factor GABPα (also known as Nuclear respiratory factor 2a, NRF2a) (Mootha et al., 2004, Virbasius et al., 1993). Animal models lacking GABPα exhibit mitochondrial dysfunction (Yang et al., 2014, Baltzer et al., 2009). I therefore considered whether *dPGC-1* over-expression reduced Aß-mediated toxicity by acting through *dGABPα*. Up-regulation of *dGABPα* (*delg*, CG6338) in neurons was not sufficient to the extend lifespan of Aß-expressing flies (Figure 3.25), and therefore it does not appear to be an important downstream mediator of PGC-1α in extending lifespan.

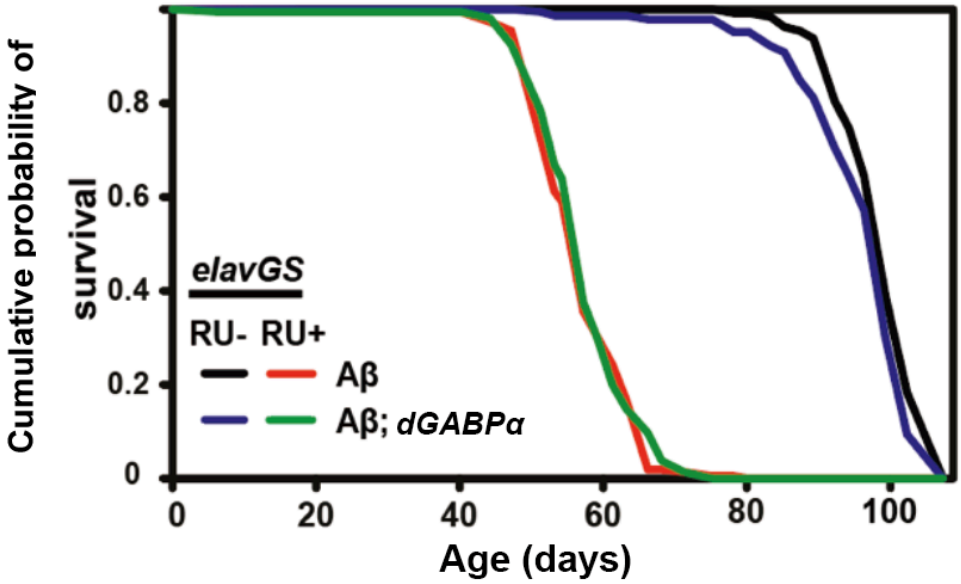

Figure 3.25 Co-expression of *dGABPα* in neurons did not rescue the shortened lifespan of Aß-expressing flies

The survival curves of female flies expressing Aß or Aß + *dGABPα* in adult neurons (RU+) and un-induced controls (RU-). The genotypes used were: *elavGS>UAS- Aß; elavGS>UAS- Aß/UAS-dGABPα*.

3.3.8 PDP1ϵ ameliorated Aß neurotoxicity via activation of the UPR^{ER}

We recently demonstrated that Aß-expressing flies display an arrhythmic sleep pattern (Niccoli et al., 2016). I confirmed the finding that over-expression of Aß can disrupt the circadian clock via increasing the period *tau*. In agreement with previous human and animal studies, our results suggest that Aβ-induced neurotoxicity might directly contribute to circadian rhythm disruption (Harper et al., 2005, Blake et al., 2015, Long et al., 2014). Moreover, metabolic defects and disturbance in redox state can lead to an alteration of circadian rhythm. This in turn has been found not only to occur as a consequence of AD pathology, but may also contribute to APP processing and Aβ accumulation (Kang et al., 2009, Xie et al., 2013, Musiek et al., 2013). Therefore, Aβ-induced defects in circadian rhythm might also lead to a further increase in disease progression.

Circadian clocks coordinate physiological, neurological, and behavioral functions into approximately 24-hour rhythms, and the molecular mechanisms underlying circadian clock oscillation are conserved from *Drosophila* to humans. *Drosophila* have a well

studied circadian clock, consisting of two interlocked transcriptional feedback loops (Figure 3.26). In the first feedback loop, dCLOCK/CYCLE activates *period* expression, and the PERIOD protein then inhibits dCLOCK/CYCLE activity. In the second feedback loop, dCLOCK/CYCLE activates *Pdp1ϵ* and *vri* expression, and then PDP1ϵ activates *dClock* while VRI inhibits *dClock* expression (Cyran et al., 2003). Flies lacking *Pdp1ϵ* have impaired circadian clocks, demonstrating that it is important for the rhythmic expression of dCLOCK. Moreover, flies lacking *Pdp1ϵ* also exhibit increased sensitivity to oxidative damage (Beaver et al., 2010), suggesting its role in maintaining the redox state and circadian rhythm.

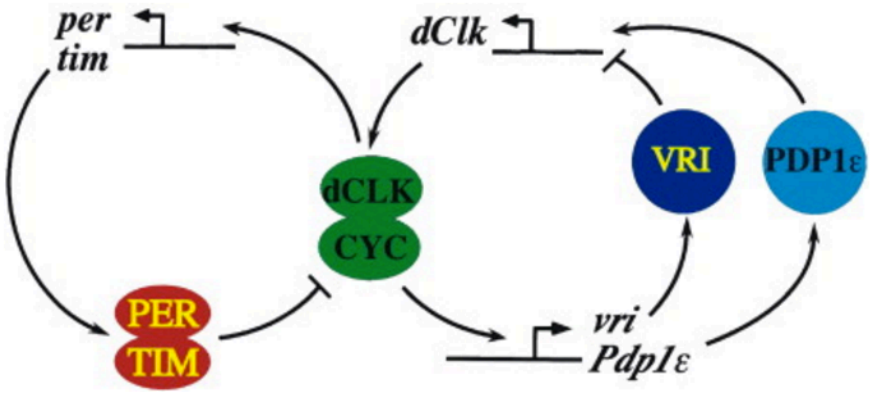

Figure 3.26 The circadian loop model for the *Drosophila* clock

Two interconnected transcription feedback loops lie at the core of the *Drosophila* molecular clock. In one loop, dCLOCK and CYCLE directly activate the transcription of *per* and *tim* by binding their promoters. Inhibition of dCLOCK/CYCLE activity is mediated by TIM transporting PER into the nucleus. dCLOCK/CYCLE also directly activate *vri* and *Pdp1ϵ* transcription. *dClock* transcription is first repressed by VRI, and then activated by PDP1ϵ. Repression and activation of *dClock* are separated by the different phases of VRI and PDP1ϵ proteins.

Mammalian PGC-1α has been found to co-activate the transcription factor RORα to activate *Bmal/CLOCK* gene expression. It is therefore involved in the second feedback loop of the circadian clock (Liu et al., 2007). Whether its *Drosophila* counterpart also controls circadian clock awaits investigation. Work in our research group has however shown that *dPGC-1* is rhythmically expressed (unpublished data). Therefore, I hypothesised that *dPGC-1* is a clock gene, regulating the circadian clock in *Drosophila*. As described above I have shown that over-expression of *dPGC-1* in neurons ameliorates Aβ-induced circadian clock disruption, namely the increased period *tau*, suggesting that *dPGC-1* might directly participate in the feedback loop.

Using FRET (Fluorescence Resonance Energy Transfer), a sensitive method to study protein interactions *in vivo*, I sought to determine whether *dPGC-1* and PDP1ϵ physically interact in the fly brain. Briefly, FRET involves the non-radioactive transfer of energy from an excited state donor fluorophore to a nearby acceptor, which can be detected when two labelled molecules are separated by a distance of 2-10 nm. FRET acceptor photo bleaching is a method that measures the donor "de-quenching" in the presence of an acceptor by comparing donor fluorescence intensity in the same sample/region before and after destroying the acceptor by photobleaching. If FRET was initially present, a resultant increase in donor fluorescence will occur on photobleaching of the acceptor. FRET efficiency is considered positive when the fluorescence intensity of the donor after acceptor photobleaching ($\mathbf{D_{post}}$) > fluorescence intensity of the donor before acceptor photobleaching ($\mathbf{D_{pre}}$). I generated transgenic flies carrying both GFP-tagged PDP1ϵ and HA-tagged *dPGC-1* as a donor-acceptor pair for FRET analysis (Figure 3.27). HA-tagged *dPGC-1* protein were immune-stained and labelled with RFP as acceptor fluorophore. After acceptor photobleaching in region of interest (ROI), I observed an increase in $\mathbf{D_{post}}$ compared to $\mathbf{D_{pre}}$ (Figure 3.28), suggesting the FRET efficiency was positive. It should be noted that this was a single experiment and more repeats are required to confirm this interaction. Therefore, I can conclude that *dPGC-1* and PDP1ϵ may physically interact in the fly brain.

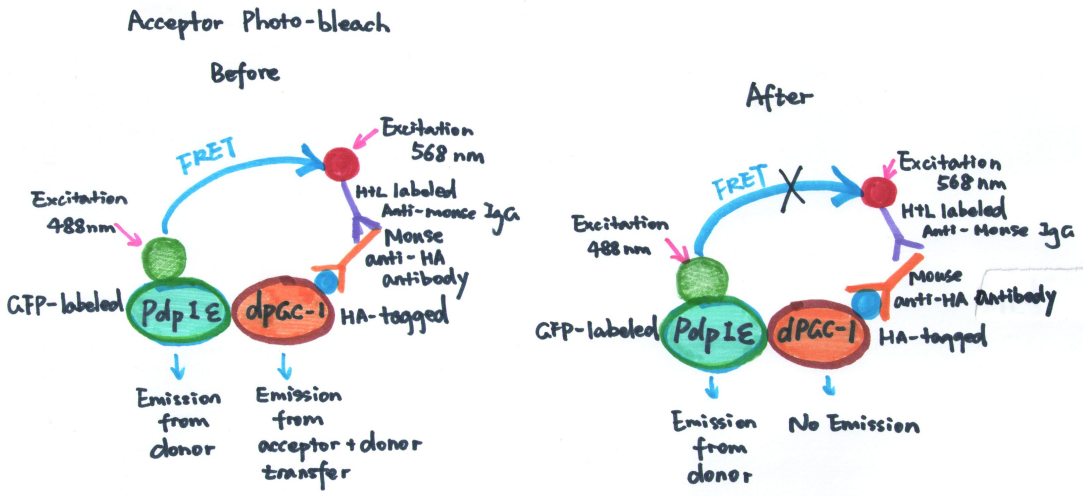

Figure 3.27 A model for the FRET donor-acceptor pair

Double mutant flies carried both GFP-tagged PDP1ϵ and HA-tagged *dPGC-1*. GFP labeled protein was excited at 488nm as the donor, and HA-labeled protein was stained and labeled by RFP and excited at

568nm as the acceptor. When two molecules are very close to each other (<10nm), then energy will transfer from the excited donor to the acceptor. The emission from the acceptor will include the part transferred from the donor. Acceptor photobleaching is used to stop the energy transfer from the excited donor and involves bleaching the acceptor. The emission of the donor will be increased after photobleaching as energy will no longer be transferred.

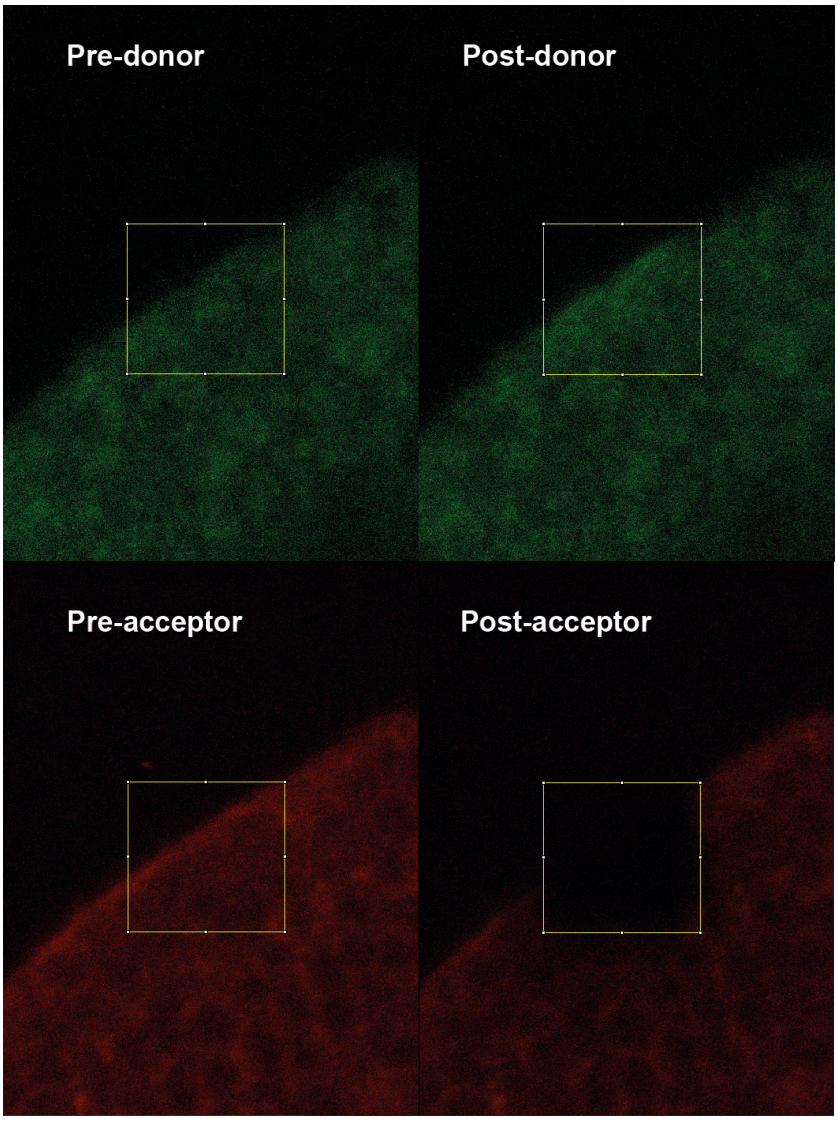

Figure 3.28 Acceptor photobleaching within the regions of interest (ROI)

FRET photobleaching was conducted using confocal microscopy. The mean fluorescence intensities in the same ROI (see boxes) in the brains before (36.7) and after (10.6) acceptor photobleaching with the 555-nm laser line are shown. The mean fluorescence intensity of the donor after acceptor photobleaching (30.578) is higher than that before acceptor photobleaching (25.481), suggesting a positive FRET efficiency. Fluorescence intensity was measured using ImageJ. This demonstrates that *dPGC-1* and PDP1ϵ may physically interact in the fly brain.

I then explored whether genetic manipulation of *Pdp1ϵ* may prevent Aβ neurotoxicity. Neuronal over-expression of *Pdp1ϵ* in adult flies using the inducible *elavGS* driver significantly extended the lifespan of Aβ-expressing flies (Figure 3.29), although the effects were much less than those seen with *dPGC-1* over-expression. However, over-expression of *Pdp1ϵ* in neurons was unable to rescue the climbing defects (Figure 3.30).

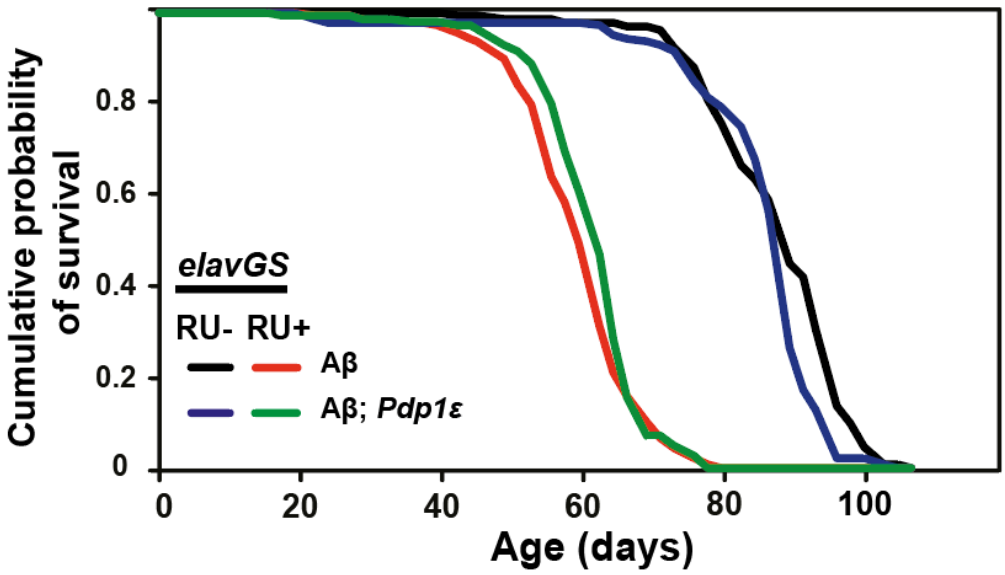

Figure 3.29 Over-expression of *Pdp1ϵ* in neurons extended the lifespan of Aß flies

The survival curves of female flies expressing Aß or Aß + *Pdp1ϵ* in adult neurons (RU+) and un-induced controls (RU-). P<0.01 when comparing the Aß response to RU relative to the Aß + *Pdp1ϵ* response to RU by Cox proportional hazard model using JMP and software R. The genotypes used were: *elavGS>UAS-Aß; elavGS>UAS-Aß/UAS-Pdp1ϵ*. This work was performed in collaboration with Miss. Nikoleta Vavouraki.

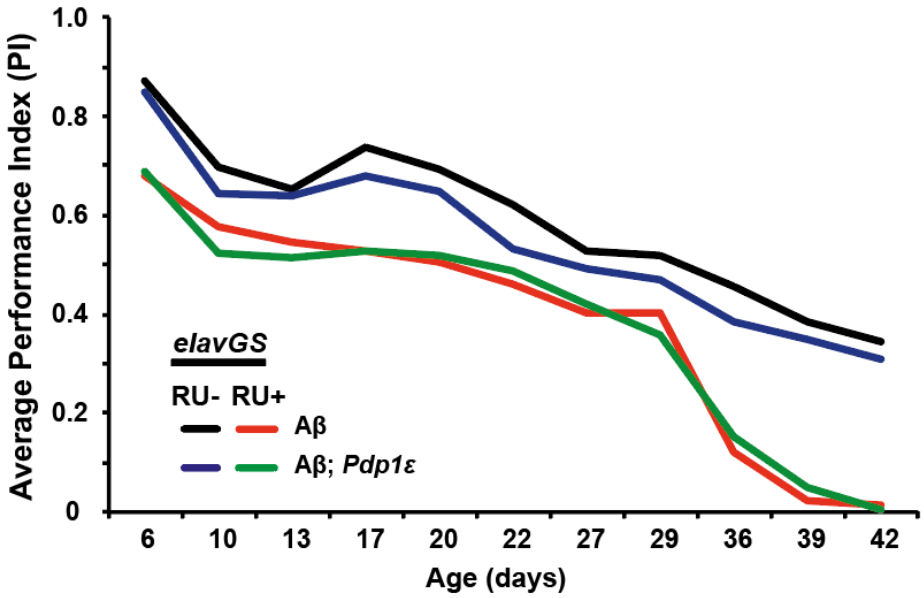

Figure 3.30 Co-expression of *Pdp1ϵ* did not rescue the locomotor ability of Aß-expressing flies

The climbing ability shown as the PI of flies of the same genotypes. P>0.05 when comparing the Aß response to RU relative to the Aß; *Pdp1ϵ* response to RU, by ordinal logistics regression. This work was also performed in collaboration with Miss. Nikoleta Vavouraki.

I confirmed that *Pdp1ϵ* over-expression was not modulating Aβ toxicity via a direct effect on Aβ levels, by demonstrating that total Aβ protein levels were not significantly different in flies co-expressing Aβ and *Pdp1ϵ* compared to those expressing Aβ alone (Figure 3.31). There was however a slight increase in Aβ mRNA levels in response to *Pdp1ϵ* over-expression (Figure 3.32), but since this was not correlated with increased protein expression, the significance of this is not clear. Therefore, I demonstrated that over-expression of *Pdp1ϵ* reduced the toxicity of Aβ, independently of Aβ protein levels.

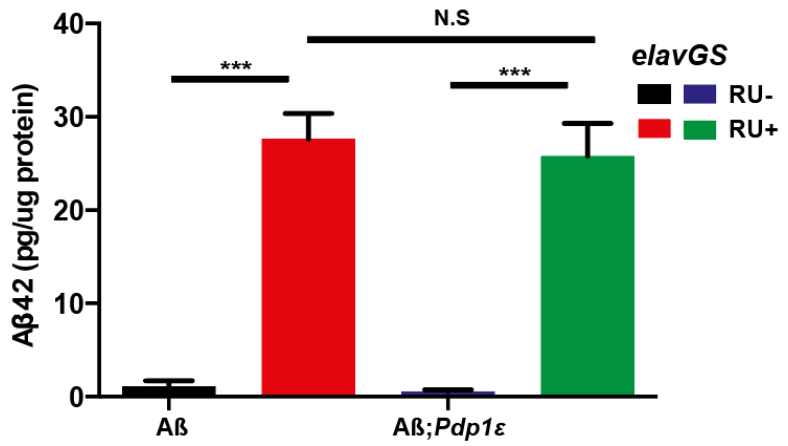

Figure 3.31 Co-expression of *Pdp1ϵ* in Aß-expressing flies did not alter Aß protein levels

Aß protein levels were measured by ELISA in the heads of 30-day-old flies expressing Aß or Aß + *Pdp1ϵ* in neurons (RU+) and un-induced controls (RU-). The bars are plotted as the means ±SEM (n=3, ***P<0.001 by ANOVA Newman-Keuls test). This work was performed in collaboration with Miss. Nikoleta Vavouraki.

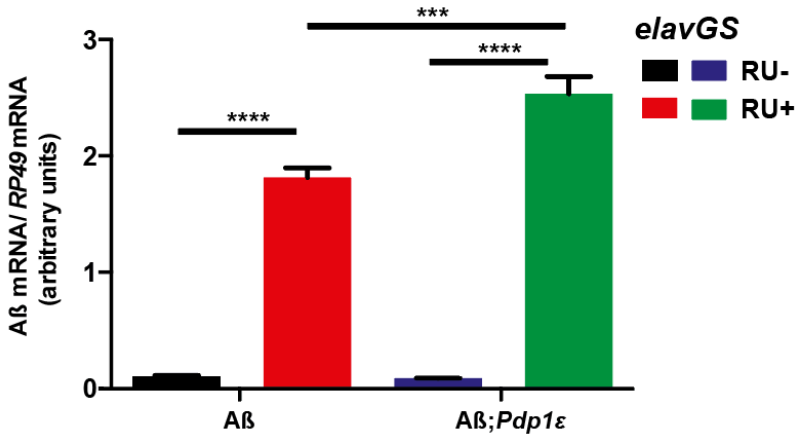

Figure 3.32 The mRNA levels of Aß were increased by the co-expression of *Pdp1ϵ in* Aß-expressing flies

Aß mRNA levels (relative to the internal control gene *RP49*) in heads of 15-day-old flies were measured by qRT-PCR. The bars are plotted as the means ±SEM (n=4, ***p<0.001, ****p<0.0001 by ANOVA Newman-Keuls test). The genotypes used were: *elavGS>UAS-Aß; elavGS>UAS-Aß/UAS-Pdp1ϵ.* This work was performed in collaboration with Miss. Nikoleta Vavouraki.

Previous studies demonstrated that *Pdp1ϵ* could regulate the expression of genes involved in the detoxification pathway (Beaver et al., 2010). Loss of *Pdp1ϵ* leads to reduced levels of *cyp6a2* and *DHR96*, suggesting that over-expression of *Pdp1ϵ* might increase the expression of these genes. I therefore measured the transcript levels of

cyp6a2 and *DHR96* in flies co-expressing Aβ and *Pdp1ϵ*, and found that over-expression of *Pdp1ϵ* increased the mRNA levels of *DHR96* compared to the non-induced controls or flies expressing Aβ alone, confirming an increase in the activity of *Pdp1ϵ* (Figure 3.33). In addition, over-expression of *Pdp1ϵ* did not change the mRNA levels of *cyp6a2*. However *cyp6a2* transcript levels were significantly reduced in response to Aβ, suggesting that Aβ may impair the detoxification pathway (Figure 3.34). Our results confirm that *Pdp1ϵ* over-expression in flies activates the appropriate downstream molecular pathways.

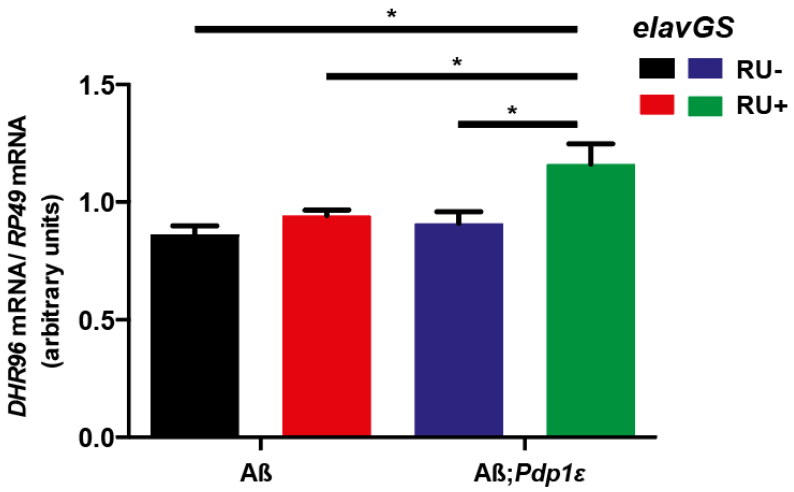

Figure 3.33 Over-expression of *Pdp1ϵ* in Aβ-expressing flies lead to increased *DHR96* levels in fly heads

DHR96 mRNA levels in the heads of 15-day-old flies expressing Aß or Aß + *Pdp1ϵ* in neurons (RU+) and un-induced controls (RU-), measured by qRT-PCR (relative to the internal control gene *RP49*). The bars represent the means ± SEM (n=4, *p<0.05 by ANOVA Newman-Keuls test). The genotypes used were: *elavGS>UAS-Aß; elavGS>UAS-Aß/UAS-Pdp1ϵ*. This work was performed in collaboration with Miss. Nikoleta Vavouraki.

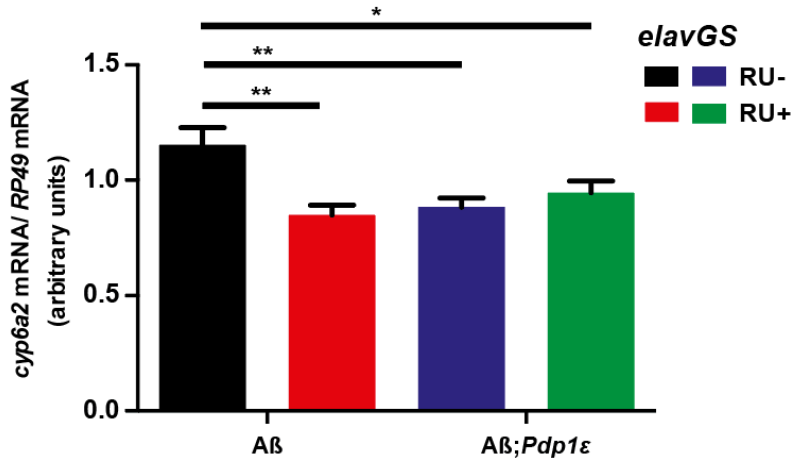

Figure 3.34 Over-expression of Aβ, but not *Pdp1ϵ*, reduced *cyp6a2* mRNA levels in fly heads

cyp6a2 mRNA levels in the heads of 15-days-old flies expressing Aß or Aß + *Pdp1ϵ* in neurons (RU+) and un-induced controls (RU-), measured by qRT-PCR (relative to the internal control gene *RP49*). The bars represent the means ± SEM (n=4, *p<0.05, ** p<0.01 by ANOVA Newman-Keuls test). The genotypes used were: *elavGS>UAS-Aß; elavGS>UAS-Aß/UAS- Pdp1ϵ*. This study was performed in collaboration with Miss. Nikoleta Vavouraki.

Since *dPGC-1* ameliorates Aβ toxicity through activation of the UPR^{ER}, I assessed whether *Pdp1ϵ* activation in neurons can protect Aβ flies against ER stress. I first analysed the levels of *Xbp1* splicing, a marker of IRE1 activation. Expression of Aβ significantly increased *Xbp1* splicing in agreement with previous studies (Casas-Tinto et al., 2011, Niccoli et al., 2016). Co-expression with *Pdp1ϵ* lead to a trend towards an increase in *Xbp1* splicing, but this did not reach statistical significance, suggesting that over-expression of *Pdp1ϵ* in neurons is not sufficient to increase IRE1 activity (Figure 3.35). I next assessed *Grp78* mRNA levels, a marker of ATF6α activation, and found that in addition to their increase in response to Aβ, there was an even further increase in *Pdp1ϵ*-co-expressing flies (Figure 3.36), suggesting activation of the ATF6α branch of the UPR^{ER}. Taken together, over-expression of *Pdp1ϵ* activates the UPR^{ER} through activation of the ATF6α branch, in a similar manner to *dPGC-1*, therefore leading to re-establishment of ER homeostasis in Aβ-expressing flies.

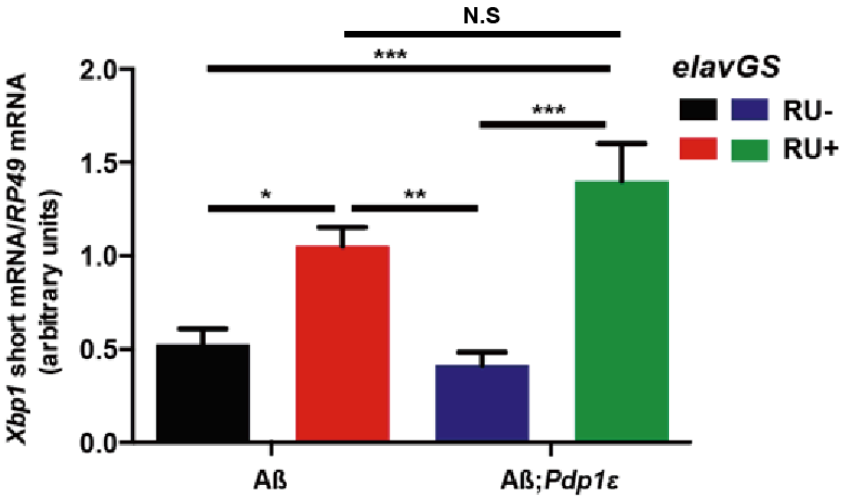

Figure 3.35 mRNA levels of *Xbp1* splicing were increased by the expression of Aβ and *Pdp1ϵ* in fly heads

Spliced *Xbp1* mRNA levels in heads of 15-day-old flies expressing Aß or Aß + *Pdp1ϵ* in neurons (RU+) and un-induced controls (RU-), measured by qRT-PCR (relative to *RP49*). Bars are plotted as the means ± SEM (n=3, *p<0.05, **p<0.01, ***p<0.001 by ANOVA Newman-Keuls test). This experiment was performed in collaboration with Miss. Nikoleta Vavouraki.

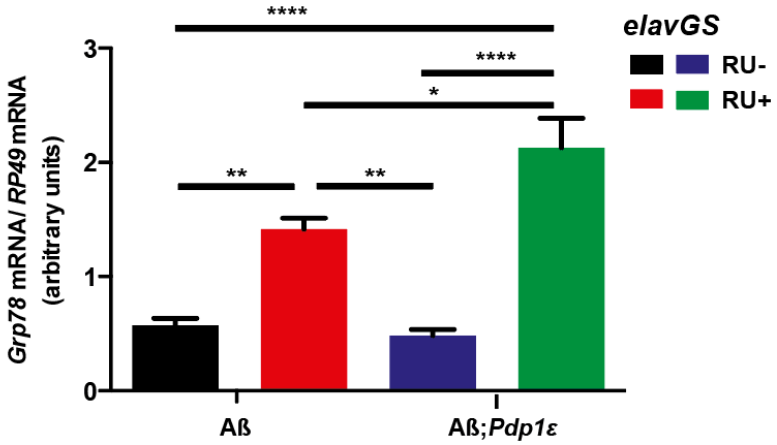

Figure 3.36 mRNA levels of *Grp78* were increased in flies expressing Aβ and *Pdp1ϵ* in their heads

Grp78 mRNA levels in the heads of 15-day-old flies expressing Aß or Aß + *Pdp1ϵ* in neurons (RU+) and un-induced controls (R-U), measured by qRT-PCR (relative to the internal control gene *RP49*). The bars are plotted below as the means ± SEM (n=3, *p<0.05, **p<0.01, ***p<0.001, ****p<0.0001 by ANOVA Newman-Keuls test). The genotypes used were: *elavGS>UAS-Aß; elavGS>UAS-Aß/UAS-Pdp1ϵ.* This work was performed in collaboration with Miss. Nikoleta Vavouraki.

3.4 Discussion

AD, triggered by the accumulation of Aß oligomers or aggregates, causes a neurotoxic cascade including oxidative stress, mitochondrial dysfunction, proteostatic failure, and eventual cell death (Hardy and Higgins, 1992, Musiek and Holtzman, 2015). Ageing-related disturbances in protein homeostasis, neuronal stress response pathways, and circadian rhythm also contribute and exacerbate disease progression (Musiek et al., 2013, Taylor and Dillin, 2011, Hipp et al., 2014). Therefore, genetic or pharmacological interventions targeting these modulators may provide excellent therapeutic avenues.

PGC-1α has been implicated in AD pathology in both human and animal studies (Qin et al., 2009, Helisalmi et al., 2008). However the effects of elevating PGC-1α in animal models of AD are controversial (Sheng et al., 2012, Katsouri et al., 2011, Dumont et al., 2014). Acting as a transcriptional co-activator, PGC-1α has been broadly implicated in many cellular processes and it is therefore regarded as the master regulator of energy metabolism (Mootha et al., 2004, Scarpulla, 2008, Puigserver and Spiegelman, 2003, Li et al., 2007b). Here I demonstrated that neuronal activation of *dPGC-1* can extend lifespan and ameliorate Aβ induced neurotoxicity, including climbing defects and circadian rhythm disruption. This improvement was associated with a compensatory mitochondrial response, namely increased ETC activity and ATP production, and improved mitochondrial proteostasis. Mitochondrial dysfunction plays a central role in disease progression, since it is the energy factory for cells. Damaged mitochondria lead to metabolic defects, including reduced glucose metabolism and ATP production in AD brains (Mosconi et al., 2008, Willette et al., 2015, Winkler et al., 2015, Kapogiannis and Mattson, 2011). In our flies, Aβ over-expression in neurons lead to a trend in ATP reduction. Conversely, *dPGC-1* activation in neurons increased the ATP levels in Aβ-expressing flies, suggesting an increase in steady-state homeostasis.

In AD patients, mitochondrial dysfunction has been reported in association with mutations or deletions in mtDNA (Bender et al., 2008, Coskun et al., 2004). I showed that Aβ accumulation in the brain leads to the loss of mtDNA, and a compensatory response involving increased mitochondrial membrane potential. This is consistent

with the hyperpolarization of mitochondrial membranes seen in PD patient fibroblasts carrying *PINK1* mutations (Abramov et al., 2011), and in neurons carrying a severe mtDNA mutation (Abramov et al., 2010). I demonstrated that *dPGC-1* up-regulation potentiates this compensatory response via up-regulation of the cytochrome c, which leads to a further increase in mitochondrial membrane potential and ATP synthase.

The ETC is the main site of premature electron leakage to oxygen, generating superoxide and reactive oxygen species (ROS). Inefficient electron transport chain activity of mitochondria also produces excessive ROS and mitochondrial-driven apoptosis, which both exacerbate AD pathology (Head et al., 2001, Siegel et al., 2007). In keeping with this I demonstrated that flies over-expressing Aβ in neurons exhibit increased sensitivity to paraquat-induced oxidative stress. Over-expression of *dPGC-1* in neurons protected Aβ –expressing flies against paraquat-induced oxidative stress. Our results are consistence with a previous study (St-Pierre et al., 2006), suggesting that PGC-1α suppresses ROS to prevent neurodegeneration.

The mechanisms by which PGC-1α suppresses ROS and protects against oxidative damage have not been fully elucidated. However, it is already known that increased mitochondrial ROS and lifespan can be uncoupled (Zhang et al., 2009). Indeed, in the context of age-related pathology, ROS is likely a response modulator of stress-elicited survival signals (Sena and Chandel, 2012) and therefore has beneficial roles. Several studies have shown that a moderate increase in ROS or mitochondrial stress may be beneficial and extend lifespan in *S. cerevisiae* and *C. elegans* via modulation of stress response pathways, including up-regulation of mitochondrial chaperones and chromatin remodelling (Doonan et al., 2008, Mesquita et al., 2010, Van Raamsdonk and Hekimi, 2009, Merkwirth et al., 2016, Tian et al., 2016).

Mitochondrial stress, similar to paraquat-induced oxidative stress (Cocheme and Murphy, 2008), activates the UPR^{mt}. This is a stress signalling pathway designed to ensure mitochondrial homeostasis through up-regulation of mitochondrial chaperones (Merkwirth et al., 2016, Haynes et al., 2007). Recent studies demonstrated that early activation of the UPR^{mt}, prior to mitochondrial dysfunction, can be beneficial for the organism and may extend lifespan in *C. elegans* (Merkwirth et al., 2016). This

suggests that a moderate increase in the UPR^{mt} is essential for the maintenance of mitochondrial proteostasis. In our model, Aβ over-expression leads to a reduction in mitochondrial chaperones and therefore down-regulation of the UPR^{mt}, leading to an imbalance in mitochondrial homeostasis. Co-expression of *dPGC-1* blocked the down-regulation of mitochondrial chaperones, therefore improving mitochondrial proteostasis and neuronal health. This observation therefore explains why the mitochondrial hyperpolarisation associated with *dPGC-1* activation resulted in overall beneficial effects in Aβ-over-expressing flies. Indeed it has been shown in fly muscle that over-expression of *dPGC-1* increases the levels of the mitochondrial chaperone HSP60 and mitochondrial function (Rera et al., 2011). My work therefore supports the idea that neuronal up-regulation of *dPGC-1* leads to an improved mitochondrial matrix environment, which can reverse the negative effects of Aβ toxicity. A previous study demonstrated that over-expression of *dPGC-1* in the fly gut increased the basal levels of HSP60 (Rera et al., 2011). Conversely, I observed a reduction in the basal levels in HSP60 in young adult brains expressing *dPGC-1* in the absence of Aβ, while the mechanisms are not fully understood. It would be interesting to know whether *dPGC-1* modulates the basal levels of mitochondrial chaperones in fly brains during ageing. My work demonstrated that over-expression of *dPGC-1* in neurons up-regulated mitochondrial chaperones in response to Aβ-induced mitochondrial stress, re-establishing homeostasis and protecting against mitochondrial stress.

Ageing-dependent failure in ER-related proteostasis also contributes to disease progression in AD (Taylor and Dillin, 2011, Hipp et al., 2014). The UPR^{ER} is activated early in AD disease pathogenesis (van der Harg et al., 2014), and both AD patients and animal model studies have shown increased UPR^{ER} components, including Grp78 and Xbp1 (Niccoli et al., 2016, Kondo et al., 2013). Interestingly, I demonstrated that the rescue of Aβ toxicity by *dPGC-1* was associated with a reduction in Grp78 protein levels, leading to a further increase in UPR^{ER} and activation of the IRE1 and ATF6a branches. Indeed, it has been shown that down-regulation of Grp78, the master negative regulator of the UPR^{ER}, leads to activation of the downstream cascades of the UPR^{ER}, to ameliorate Aβ toxicity (Niccoli et al., 2016). Grp78 protein levels are tightly controlled at the levels of translation (Gulow et al., 2002), suggesting that *dPGC-1* reduced either Grp78 translation or stability.

Moreover, over-expression of *Xbp1* alone can ameliorate Aβ toxicity (Casas-Tinto et al., 2011), supporting the idea that up-regulation of UPR^{ER} components is beneficial in AD models. Grp78 is becoming an increasingly important therapeutic target for AD (Niccoli et al., 2016) and cancer, where its inhibition increases the cell's susceptibility to stress (Lee et al., 2014). Although up-regulation of *Grp78* showed detrimental effects in an animal model of Parkinson's disease (Gorbatyuk et al., 2012), its function in other neurodegenerative disorders may depend on the precise experimental conditions. For example, a mild up-regulation of the UPR^{ER} in neurons may increase ER proteostasis in response to the increased burden of mis-folded proteins, whereas, a strong induction of the UPR^{ER} may lead to apoptosis and be detrimental to neurons (Hetz and Mollereau, 2014).

Studies have shown that PGC-1α can modulate Grp78 levels. In skeletal muscle, in response to exercise, PGC-1α can increase the transcription of *Grp78* and *Xbp1* by co-activating ATF6a (Wu et al., 2011). Already it has been shown that ablation of PGC-1β, the homologue of PGC-1α, increases basal Grp78 levels and modulates the neuronal ER response in the mouse brain (Camacho et al., 2012), suggesting that PGC-1 might directly regulate Grp78 levels. I showed that activation of *dPGC-1* in adult neurons does not change basal levels of Grp78 in young flies, but reduces Grp78 levels and activates UPR^{ER} in the presence of Aβ. Since it has been shown that the UPR^{ER} and proteostasis decline with age in *C. elegans* (Ben-Zvi et al., 2009, Taylor and Dillin, 2013, Taylor and Dillin, 2011), it would therefore be interesting to know whether *dPGC-1* affects the basal level of Grp78 levels to maintain proteostasis in old age.

My work suggests a model where Aβ accumulation in the brain induces the UPR^{ER}, and activation of *dPGC-1* in neurons blocks the negative feedback loop linked to Grp78 up-regulation, resulting in even further increased UPR^{ER} activity. In turn this allows neurons to re-establish the protein-folding environment and to restore protein homeostasis. This mechanism of action may be responsible for the benefits of PGC-1α observed in models of other neurodegenerative disorders. PGC-1α displayed neuroprotective effects in a mouse model of HD with mechanisms including

attenuation of oxidative stress, activation of the lysosomal autophagy pathway and proteostasis (Tsunemi et al., 2012).

Rifampicin, a well-known antibiotic widely in the treatment of tuberculosis and leprosy, has been proposed to be neuro-protective in PD and AD animal models (Jing et al., 2014, Umeda et al., 2016). Here I showed that treatment with rifampicin increased lifespan and improved locomotor ability in Aβ-expressing flies, in agreement with a previous APP mice model (Umeda et al., 2016). In accordance with previous observations in humans that rifampicin treatment reduced the risk of developing AD (Mcgeer et al., 1992), I also found that rifampicin treatment increased lifespan in wild type *Drosophila,* suggesting broad spectrum anti-ageing effects. A recent study suggested that rifampicin could reduce Aß oligomerization and improve the memory defects in an APP mouse model via improved autophagy-lysosomal function (Umeda et al., 2016). Here I confirmed that the amelioration of Aß-induced neurotoxic phenotypes by rifampicin are not due to a reduction in the level of Aß peptides, and therefore exclude an effect of rifampicin on APP processing. I found that rifampicin reduced Grp78 levels, suggesting that the rescue of Aβ toxicity is likely due to an increase in the UPR^{ER}. Our study points to a novel and unexplored role of rifampicin as a modulator of the UPR^{ER} in neurodegeneration downstream of Aβ accumulation. This may provide a useful therapeutic avenue in AD patients already displaying accumulation of Aβ peptides in the brain.

Metabolic defects and disturbances in redox state can lead to alterations in circadian rhythm. In agreement with previous human and animal studies, I showed that Aβ disrupted the circadian rhythm (Harper et al., 2005, Niccoli et al., 2016, Blake et al., 2015), leading to an increase in the period tau. *dPGC-1* activation has been shown to restore the period change in Aβ –expressing flies, which likely protects neurons from further deterioration (Kang et al., 2009). Moreover, a previous study found that knockout of the clock gene *period* did not further affect lifespan, climbing ability or neurodegeneration in an Aβ-expressing fly model that already exhibited circadian rhythm disruption (Long et al., 2014). Therefore, it would be interesting to know whether directly targeting the other clock gene could ameliorate Aβ neurotoxicity. Mammalian PGC-1α regulates the clock gene CLOCK expression by coactivating the

transcription factor RORα and is therefore involved in the second feedback loop (Liu et al., 2007). In the *Drosophila* second feedback loop, the transcription factor that induces the expression of clock gene dCLOCK is PDP1ϵ (Cyran et al., 2003). I first assessed the interplay between *dPGC-1* and PDP1ϵ by FRET, and found these two molecules might physically interact in the fly brain. This suggests that the amelioration of circadian rhythm disruption by *dPGC-1* over-expression in Aβ flies may be due to its direct interaction and co-activation with the transcription factor PDP1ϵ in the circadian clock. To evaluate this hypothesis, I over-expressed *Pdp1ϵ* in the neurons of Aβ-expressing flies, and found that this lead to a small but significant extension in lifespan without affecting Aβ levels. Over-expression of *Pdp1ϵ* did not rescue the climbing defects and therefore did not prevent Aβ-induced neurodegeneration. Similar to *dPGC-1* gain-of-function, over-expression of *Pdp1ϵ* lead to a further increase in Grp78 transcription, and therefore activation of the UPR^{ER}. In keeping with this previous work has shown that flies lacking *Pdp1ϵ* are sensitive to oxidative damage, confirming its role in the maintenance of the redox state (Beaver et al., 2010). Here I also demonstrated that over-expression of *Pdp1ϵ* in neurons leads to increased expression of *DHR96*, suggesting a role in the detoxification pathway. Taken together, my results demonstrate that either genetic activation of *dPGC-1* or *Pdp1ϵ,* or pharmacological treatment with rifampicin may provide novel therapeutic strategies in the prevention of AD.

3.5 Materials and Methods

3.5.1 Fly Husbandry and stocks

All flies were reared at 25ºC on a 12:12 light: dark cycle at constant humidity and on standard sugar-yeast medium (15g/L agar, 50 g/L sugar, 100 g/L autolysed yeast). Adult-onset, neuron–specific expression of UAS constructs was achieved as previously described (Sofola et al., 2010). Briefly, 24-28 hours after eclosion female flies carrying a heterozygous copy of *elavGS* and at least one UAS-construct were fed SY medium supplemented with 200μM mifepristone (RU486) to induce transgene expression. Rifampicin was added to the SY medium food at a concentration of 200μM or 500μM. The *elavGS* driver line was derived from the original *elavGS* 301.2 line (Osterwalder et al., 2001) and obtained as generous gift from Dr H. Tricoire

(CNRS, France). The *UAS-Aβ42Arc* stock was a gift from Dr D. Crowther (University of Cambridge, UK). The *UAS-spargel* (*UAS-dPGC-1*) line was a gift from Dr. Christian Frei, and the *UAS-Pdp1ϵ* was obtained from FlyORF. All the lines were backcrossed 6 generations into the w^{1118} background. The *UAS- Pdp1ϵ* lines were backcrossed over 6 generations into the w^{Dah} background. All experiments were carried out on mated females, unless otherwise stated.

3.5.2 Lifespan analyses

Flies were raised at a standard density in 200mL bottles. After eclosion, flies were allowed to mate for 24-48 hours in the bottles. Mated females were then split into vials containing SYA medium with or without drugs, with 15 flies in each vial. Approximately 150 females flies were used for each condition in the lifespan experiments. Deaths were scored throughout the lifespan and flies tipped onto fresh food 3 times a week. Data were presented as cumulative survival curves, and survival rates were compared using log-rank tests. All procedures for lifespan experiments were performed at 25ºC unless otherwise stated.

3.5.3 Climbing assays

The climbing assay was performed as previously described (Kinghorn et al., 2015). Briefly, 15 flies were placed in a 25cm pipette, tapped to the bottom and allowed to climb for 45 seconds. The number of flies in the top 5cm, middle, and bottom 3cm was scored. A performance index was calculated for each time-point and plotted. Statistical analysis was performed in R using ordinal logistics regression, using the individual heights for each fly as data points.

3.5.4 Circadian rhythm

Individual, 21-day-old male flies were placed in 65 x 5 mm glass tubes containing standard 1xSYA, and their activity was recorded using the DAM system (*Drosophila* Activity Monitoring System, TriKinetics, Waltham, MA) as described previously (Veleri et al., 2007). Flies were entrained to a 12:12 hour LD cycle at 25°C and 65% humidity 24-36 hours before recording. 5 days of 12:12 hours LD were recorded followed by 5 days of 12:12 hours DD. Analysis of locomotor activity was performed using the fly toolbox and MATLAB software (MathWorks, Natick, MA) as described

previously (Levine et al., 2002). The circadian period was calculated using autocorrelation as described previously (Levine et al., 2002), and was presented by the mean values with their SEM.

3.5.5 The DR protocol

The specific preparation of the DR media has been described in Chapter 2. Work in this chapter used a DR-tent with 0.1SY, 1.0SY, and 2.0SY. RU486 was supplemented into the food to give a final concentration of 200μM.

3.5.6 Paraquat injection

Paraquat (Sigma 856177) was delivered at a dose of 50ng/mg as previously described (Bjedov et al., 2010). To deliver the compound, injection pipettes were prepared from 10mm glass capillaries using the Flaming-Brown micropipette puller (Programme 2). A home-built microinjection machine was used for injections. In parallel flies were also injected with control Ringer's solution. Both injected solutions contained blue dye for visualization of the injection (FD&C Blue No.1).

3.5.7 Rifampicin treatment

After eclosion flies were split into vials containing standard SY food supplemented with and without 200μM mifepristone (RU486), and with and without 200μM or 500μM Rifampicin (Sigma R3501). Deaths were scored throughout the lifespan and flies tipped onto fresh food 3 times a week. Data were presented as the cumulative survival curves, and survival rates were compared using log-rank tests.

3.5.8 Fly brain imaging using FRET acceptor photobleaching

The following primary antibodies were used: the anti-HA (Abcam, #ab18181, 1:1000) and the anti-GFP (Invitrogen, A21311, 1μg/mL) antibodies. The goat anti-mouse IgG antibody (H+L) (Life technologies, A11019, 1μg/mL) was used as the secondary antibody. Brains were dissected in ice cold PBS and immediately fixed in 4% formaldehyde for 20 mins. Brains were then washed in 0.2% Triton-X/PBS, blocked in 5% bovine serum albumin/PBS, incubated in primary antibody overnight at 4°C and in secondary for 2 hours at RT. Brains were mounted in mounting medium containing DAPI (Vectastain). The method for FRET photobleaching was as

described previously (Broussard et al., 2013). Briefly, the system was set up to use the 488 nm and the 555 nm lines of the laser as an excitation source for the GFP-based donor and RFP acceptor flurophores. 10% of the laser power was sufficient for the 488 nm and 3% for the 555 nm. The image size was set to 512*512 pixel, with a line averaging of 2. GFP emission was measured from 454 to 505 nm, and the RFP emission from 530 to 590 nm. Photobleaching of the RFP was achieved within the ROI using the 555nm laser line. 100% power was sufficient. Images were captured with a Zeiss (UK) LSM 700 confocal laser-scanning microscope using a 60x oil-immersion objective.

3.5.9 Live cell imaging of the mitochondrial membrane potential

For measurements of mitochondrial membrane potential, the dissected brains were loaded for 40 mins at room temperature with 25 nM tetramethylrhodamine methylester (TMRM) in HBSS (156 mM NaCl, 3 mM KCl, 2 mM MgSO4, 1.25 mM KH2PO4, 2 mM CaCl2 10 mM glucose and 10 mM HEPES at pH 7.35). TMRM was present in the imaging media throughout the experiment and was used in the quench mode to assess $\Delta\psi m$. Hence a reduction in TMRM intensity represents mitochondrial depolarization. Confocal images were obtained using a Zeiss 710 CLSM equipped with a ×40 oil immersion objective. Illumination intensity was kept to a minimum (at 0.1–0.2% of laser output) to avoid phototoxicity. Fluorescence was quantified in individual mitochondria by exciting TMRM using the 561 nm laser line of a confocal microscope. Excitation and emission were measured above 580 nm. 4–5 fields per brain were acquired, and the mean maximal fluorescence intensity was measured for each group. The differences in $\Delta\psi m$ were expressed as intensity units, arb.U, of TMRM.

3.5.10 mtDNA measurement

Genomic DNA and mitochondrial DNA from 20 fly heads were isolated using the Qiagen blood and tissue kit according to the manufacturer's instruction. Quantitative PCR was performed suing the PRISM 7000 sequence-detection system (Applied Biosystem) and SYBR® Green (Molecular Probes) by following the manufacturer's instructions. mtDNA in each sample were presented as a ratio of mitochondrial DNA/genomic DNA. Each sample was analysed in duplicate and values were

expressed as the mean of the 4 independent biological repeats +/- SEM. Primers used for genomic DNA were as follows:

GAPDH:

For: GACGAAATCAAGGCTAAGGTCG

Rev: AATGGGTGTCGCTGAAGAAGTC

For mitochondrial DNA the primers were as follows:

COX I:

For: GAATTAGGACATCCTGGAGC

Rev: GCACTAATCAATTTCCAAATCC

3.5.11 Quantitative PCR

Total RNA was extracted from 20-25 fly heads per sample using TRIzol® (GIBCO) according to the manufacturer's instructions. The concentration of total RNA purified for each sample was measured using the Nano Drop. 5µg of total RNA was then subjected to DNA digestion using DNase I (Ambion), immediately followed by reverse transcription using the SuperScript® II system (Invitrogen) with oligo(dT) primers. Quantitative PCR was performed suing the PRISM 7000 sequence-detection system (Applied Biosystem) and SYBR® Green (Molecular Probes) as per the manufacturer's instructions. Each sample was analysed in duplicate and the values were presented as the means of 3-4 independent biological repeats +/- SEM. The primers used were:

dPGC-1

For; TCGGCGAGGATTTTTTGATC

Rev: CGATTCGCCGCTCTTCA

Aß42

For: CGATCCTTCTCCTGCTAACC

Rev: CACCATCAAGCCAATAATCG

Grp78

For: TCTTGTACACACCAACGCAGG

Rev: CAAGGAGCTGGGCACAGTGA

Spliced Xbp1

For: CCGAACTGAAGCAGCAACAGC

Rev: GTATACCCTGCGGCAGATCC

RP49

For: ATCGGTTACGGATCGAACAA

Rev: GACAATCTCCTTGCGCTTCT

Cyt-c-p

For: TAACGCGCGCTCGTCAT

Rev: TTAACACGGACTCGAATTGAACAC

DHR96

For: CAAAGAGAGCATATTTAGGATACCAAG

Rev: CACAGAACCCACGCTTCCAAG

Cyp6a2

For: GCGCAACGAGATCCAAAC

Rev: TGTAGAGCCTCAGGGTTTCTG

3.5.12 ATP assay

ATP concentrations were determined using Roche ATP Bioluminesence Assay Kit HS II (Roche, West Sussex, UK). Briefly, 2 whole flies or 8 fly heads were decapitated and homogenized in 100 µl ice-cold lysis buffer using a Kontes pellet pestle. The lysate was then boiled for 5 min and centrifuged at 20,000g for 1 min. Cleared lysate was then diluted 1 in 200 in dilution buffer and ready to load with 10 µL luciferase. The luminescence was immediately measured using a Tecan Infinite M2000 microplate reader and Magellan V6.5 software. Total proteins were measured using the Thermo Scientific BCA assay. ATP levels in each sample were expressed as a ratio of the total protein content. Data were expressed as the mean+/-SEM and obtained from 5-6 biological repeats for each genotype.

3.5.13 Western blot analysis

15 fly heads in each sample were prepared by homogenising in 2xSDS Laemmli sample buffer (4% SDS, 20% glycerol, 120 mM Tris-HCl pH6.8, 200 mM DTT with bromophenol blue) and boiled at 95ºC for 5 minutes. Samples were separated on pre-cast 4-12% Invitrogen Bis-Tris gels (NP0322) and blotted onto nitrocellulose paper in Tris-glycine buffer supplemented with 10% ethanol. Membranes were blocked in 5% milk in TBST (TBS with 0.05% Tween-20) for 1 hour at RT and then incubated with the primary antibody in blocking solution. The primary antibody dilutions used were

anti-Grp78 (novusbio NBP1-06274, 1:1000) in 1% milk, 5% BSA in TBST for 1 hour at RT, anti-β actin (Abcam, #ab8224, 1:5000), anti-HSP60 (Cayman chemical, 10011429, 1:1000) and anti-Grp75 (Abcam, #ab82591, 1:1000). The membranes were incubated in primary antibody in 5% BSA in TBS-T at 4ºC overnight unless otherwise stated. Secondary antibodies used were anti-rabbit and anti-mouse (Abcam #ab6721 and Abcam #ab6789 respectively) at 1:5000 dilutions for 1 hour at RT. Bands were visualized with Luminata Forte (Millipore) and imaged with ImageQuant LAS4000 (GE Healthcare Life Science). Quantification was carried out with ImageJ.

3.5.14 Quantification of Aß42

Five fly heads were homogenized in 50 ml GnHCl extraction buffer (5 M Guanidinium HCl, 50 mM Hepes pH 7.3, protease inhibitor cocktail (Sigma, P8340) and 5mM EDTA), centrifuged at 21,000g for 5 min at 4^{o}C, and cleared supernatant was retained. Aß42 was measured with an ELISA kit (Millipore, EZHS42), according to the manufacturer's instructions. The protein concentrations of the samples were measured using a Bradford assay (Bio-Rad protein assay reagent; Bio-Rad laboratories Ltd (UK) and the amount of Aß42 in each sample expressed as a ratio of the total protein content (pg/µg total protein). Data are expressed as the means +/- SEM and were obtained from three biological repeats for each genotype.

3.5.15 Statistics

Survival experiments were analyzed using a log rank test. The interactions between interventions in lifespan were analyzed using the Cox Proportional Hazard in a survival package developed from Terry M Therneau and Thomas Lumley (https://cran.r-project.org/web/packages/survival/survival.pdf) in R. Climbing assays were analyzed using ordinal logistics regression in R. Circadian rhythm data were analyzed using METLAB. Other data are presented as the means ± SEM obtained from at least 3 independent experiments, and single comparisons were analysed using the Student's t-test. Other data were tested by either one-way analyses of variance (Casali et al.) for three conditions or two-way ANOVA for four conditions with induction and genotype as main effects, and planned comparisons of means were made using Newman-Keuls test. Statistical analyses were performed using GraphPad Prism.

Chapter 4 The role of PGC-1α in a *Drosophila* model of Parkinson's disease

4.1 Summary

Mitochondrial dysfunction has been implicated in the pathogenesis of PD. PGC-1α is the key regulator of mitochondrial biogenesis, and the possible link to PD arose from studies demonstrating decreased PGC-1α levels in human postmortem brain tissue, as well as in PD mouse models. Moreover, a genome-wide expression meta-analysis demonstrated that a number of genes downstream of PGC-1α are down-regulated in sporadic PD, suggesting that elevation of PGC-1α may offer a potential therapeutic strategy in PD. Here I found that over-expression of *dPGC-1* did not rescue the toxic phenotypes of flies lacking *PINK1* or *parkin*. Moreover, activation of *dPGC-1* further increased the sensitivity to oxidative stress in *PINK1* and *parkin* null mutants. This work demonstrates that the neuroprotective effects of *dPGC-1* seen in the AD fly model are just not effective in these PD models. Further studies using different PD fly models and alternative organisms will be required to fully assess the role of *dPGC-1* in PD.

4.2 Introduction

Parkinson's disease (PD) is the most common movement disorder. Studies on PD related genes have demonstrated that mitochondrial dysfunction plays a central role in the pathogenesis of PD. One of the most significant contributions of *Drosophila* models to the understanding of PD came from the elegant experiments in which the biology of PINK1 and parkin were elucidated (Greene et al., 2003, Whitworth and Pallanck, 2009, Whitworth et al., 2005, Park et al., 2009, Clark et al., 2006, Yang et al., 2006). Two genes related to autosomal recessive parkinsonism are *PINK1* and *PARK2*. The *Drosophila* homologue of the *PINK1* gene (also called CG4523) encodes a polypeptide of 721 amino acids with a molecular mass of about 80kDa. Similar to human PINK1, the structural analysis of the *Drosophila* PINK1 (*dPINK1*) protein also revealed 2 characteristic motifs: a mitochondrial targeting motif and a

serine/threonine kinase domain, which exhibited 60% similarity (42% identity) to that of human PINK1. Consistent with the localization of human PINK1, *Drosophila* PINK1 was also found localized to mitochondria (Park et al., 2006). Loss of *dPINK1* leads to a number of toxic phenotypes, including reduced longevity, indirect flight muscle and dopaminergic neuronal degeneration, accompanied by locomotor defects, increased sensitivity to oxidative stress, wing and thorax abnormalities and defective mitochondrial morphology and function (Park et al., 2006).

Parkin functions as an E3 ligase in the ubiquitin protein degradation pathway. The *Drosophila* homologue of *parkin* (CG10523) encodes a polypeptide of 482 amino acid exhibiting 42% identity and 59% similarity overall with that of human *parkin*. Loss of the *Drosophila* homologue of *parkin* led to similar phenotypes to those of *PINK1* knockdown, including reduced lifespan, locomotor defects and male sterility (Greene et al 2003). The locomotor defects derive from apoptotic cell death of muscle fibres, whereas the male sterile phenotype derives from a spermatid individualization defect at a late stage of spermatogenesis. Mitochondrial pathology is the earliest manifestation of muscle degeneration and a prominent characteristic of individualizing spermatids in *parkin* mutants (Greene et al., 2003). This study supported the concept that the tissue-specific phenotypes observed in *Drosophila parkin* mutants result from mitochondrial impairment, which is likely a main trigger to neurodegeneration in autosomal recessive juvenile Parkinsonism (ARJP). Further studies have shown that *Drosophila parkin* mutants display degeneration of a subset of dopaminergic neurons in the brain, mimicking the dopaminergic neuronal loss observed in sporadic PD (Whitworth et al., 2005). Moreover, these *parkin* mutant flies have increased oxidative stress and an impaired immune response, suggesting that these processes play a role in the pathogenesis of ARJP.

Interestingly, it has also been demonstrated that over-expression of parkin ameliorates the loss-of-function phenotypes of PINK1, suggesting that parkin acts downstream of PINK1 (Park et al., 2006, Clark et al., 2006). Moreover, PINK1 kinase activity is required for its function in mitochondria, where PINK1 recruits parkin to localize to the mitochondria in a kinase-activity-dependent manner. This work in *Drosophila* has provided significant insights into the essential role of the PINK1-parkin pathway in regulating mitochondrial function, and highlights the importance of mitochondrial

dysfunction in the pathogenesis of PD. Furthermore, it has stimulated considerable research into the precise mechanisms linking loss-of-function of these two genes with mitochondrial dysfunction and neurotoxicity (Whitworth and Pallanck, 2009). In the normal state, PINK1 recruits parkin to translocate from the cytosol to the mitochondria in response to a fall in mitochondrial membrane potential, when mitochondria are under stress or become damaged (Zhang and Ney, 2010, Poole et al., 2008, Narendra et al., 2008, Vives-Bauza et al., 2010, Kim et al., 2008). This physiological process terminates with a specialized form of autophagy, known as mitophagy, in which damaged mitochondria are engulfed in a double membrane and targeted to the lysosome for degradation (Deas et al., 2011, Youle and Narendra, 2011). When either PINK1 or parkin function is lost (i.e. if the *PINK1* or *PARK2* genes are mutated), this process cannot proceed and damaged mitochondria are retained within the cytoplasm. In turn, damaged mitochondria act as a source of oxidative stress that leads to DNA and cellular damage, ultimately causing neuronal death or muscle degeneration (Deas et al., 2011, Youle and Narendra, 2011, Green et al., 2011).

As previously described, most of the physiological functions of PGC-1α have been studies in more details in metabolic tissues such as adipose tissue, liver and muscle. However, there have been only a few studies on the importance of PGC-1α in the brain. PGC-1α null mice show hyperactivity and other movement disorders that represent ganglia pathology, such as stimulus-induced myoclonus, dystonic posturing and frequent limb clasping. They also develop spongiform lesions in the striatum with axonal loss (Lin et al., 2004). In addition, PGC-1α has been demonstrated to play a role in the stress defense system. PGC-1α null mice display a severe loss of dopaminergic neurons compared to controls when challenged with MPTP (1- methyl-4-phenyl-1, 2, 3, 6-tetrahydropyridine), an oxidative stressor that induces PD in human and animal models (St-Pierre et al., 2006). Flies over-expressing *dPGC-1* show increased resistance to paraquat, a potent oxidizer, highlighting its protective role in response to oxidative stress. In the previous Chapter, I demonstrated the neuroprotective effects of *dPGC-1* in a *Drosophila* model of Aβ toxicity. Over-expression of *dPGC-1* ameliorated the shortened lifespan and neuronal phenotypes, including climbing defects and circadian rhythm disruption. This amelioration was associated with improved mitochondrial function and up-regulation of the UPR.

As described above, mitochondrial dysfunction is a predominant pathogenic feature in both familial and sporadic PD. A recent study demonstrated that parkin plays an important role in regulating mitochondrial biogenesis (Shin et al., 2011). It was shown that parkin physiologically ubiquitinates and thus regulates the proteasomal degradation of the genetic repressor PARIS. In turn, PARIS functions as a major genetic repressor of PGC-1α expression. Therefore, parkin loss-of-function leads to increased PARIS and reduced PGC-1α levels. The conditional knockout of parkin in adult mice leads to the progressive loss of dopaminergic neurons in a PARIS-dependent manner, and this is reversed by over-expression of PGC-1α. This work therefore highlights the importance of PGC-1α in PD, and the potential therapeutic benefits of augmenting PGC-1α, especially in parkin-associated familial PD (Figure 4.1).

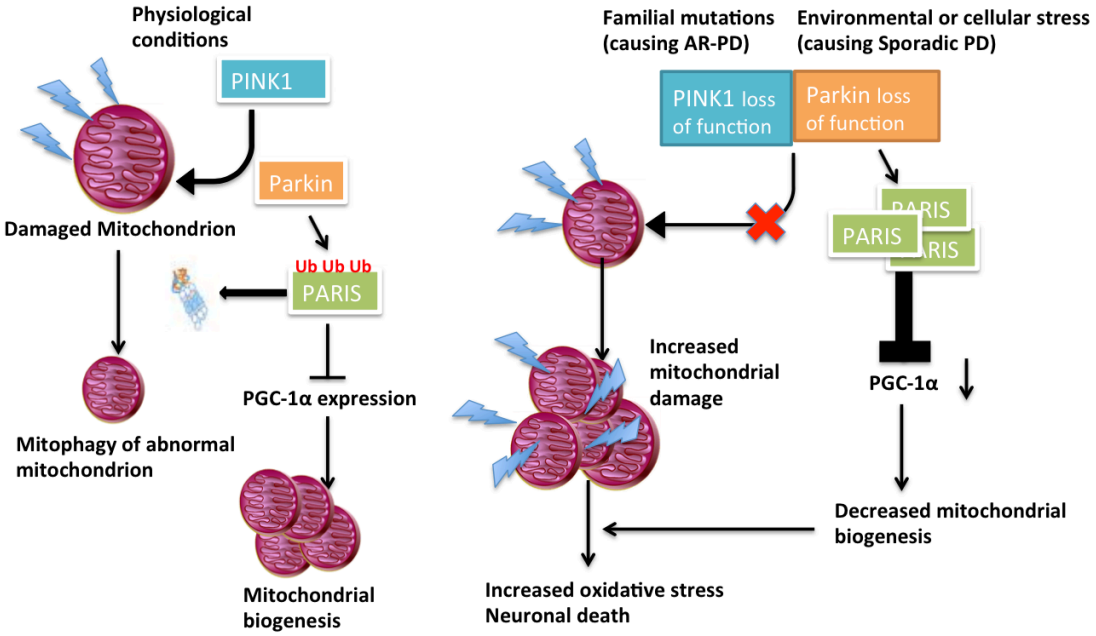

Figure 4.1 The PINK1-parkin pathway regulates mitochondrial function via PARIS and PGC-1α.

Under physiological conditions PINK1 recruits parkin to damaged mitochondria to induce mitophagy Parkin ubiquitinates PARIS, targeting it to degradation by the ubiquitin proteasome system. Reduced levels of PARIS lead to accumulation of PGC-1α, which in turn leads to increased mitochondrial biogenesis. If the *parkin* gene is mutated and there is loss-of-function of parkin, then it cannot be recruited to the damaged mitochondria to promote mitophagy. This therefore leads to increased production of ROS and mitochondrial damage. As a result of parkin loss-of-function PARIS accumulates and suppresses PGC-1α activity, leading to a reduction in mitochondrial biogenesis. As a result there is an increase in the number of damaged mitochondria and reduced mitochondrial biogenesis, leading to increased oxidative stress and neuronal death.

Moreover, the role of PGC-1α is not confined to patients with parkin mutations, but is also implicated in those with sporadic PD. Human postmortem brain tissue analysis revealed that sporadic PD patients displayed increased levels of PARIS and reduced expression of PGC-1α (Shin et al., 2011). In addition, a genome-wide expression meta-analysis independently demonstrated that 10 genes, which are known downstream targets of PGC-1α, were down-regulated in the SN of PD patients (Zheng et al., 2010). These genes mostly function in mitochondrial the ETC activity, glucose utilization, and glucose sensing, indicating that defects in energy metabolism mediated by PGC-1α occur early in the disease pathogenesis. PD pathology thus causes a reduction in PGC-1α and its downstream factors, leading to worsening of the disease pathology. Interestingly, over-expression of PGC-1α rescues dopaminergic neuronal loss in primary neuronal cultures expressing mutant α-synuclein, in association with up-regulation of genes in the mitochondrial ETC (Zheng et al., 2010). Taken together, this work suggests that elevating PGC-1α may be a useful therapeutic target for treating PD.

The question of whether reduced PGC-1α is a causal factor in the pathogenesis of PD is yet to be resolved. The reduction in PGC-1α seen in PD brains may contribute to the disease progression. Indeed it has been shown that a reduction in PGC-1α leads to increased sensitivity to stressors by elevating ROS, thereby impairing mitochondrial proteostasis, eventually leading to neuronal death (St-Pierre et al., 2006, Lu et al., 2014, Haynes and Ron, 2010). I therefore studied the role of PGC-1α in PD pathogenesis, using a model of PINK1 and parkin loss-of-function in *Drosophila melanogaster*, which display shortened lifespans, behavioural defects and neurodegeneration (Clark et al., 2006, Greene et al., 2003).

In order to determine whether PGC-1α contributes to the pathogenic cascades downstream of PINK1 and parkin loss-of-function, I genetically over-expressed *dPGC-1* in *PINK1* and *parkin* null mutant flies. I first demonstrated that the transcript levels of *dPGC-1* were up-regulated in both *PINK1* null mutants and *parkin* null mutants. *dPGC-1* over-expression did not rescue the toxic phenotypes in either *parkin* or *PINK1* null mutants in either males or females. Interestingly, *PINK1* or *parkin* null mutants over-expressing of *dPGC-1* were more sensitive to H_2O_2 or paraquat-induced

oxidative stress. Taken together, our results showed that elevation of *dPGC-1* does not provide a beneficial effect in PD fly models lacking *PINK1* and *parkin*.

4.3 Results:

4.3.1 Over-expression of *dPGC-1* did not rescue the toxic phenotypes of *PINK1* null mutants

To investigate the role of *dPGC-1* in PINK1 loss-of-function, I over-expressed *dPGC-1* in $PINK1^{B9}$ null mutants, which have been previously characterized (Clark et al., 2006). *PINK1* is on the X chromosome and null mutant *PINK1* males are sterile. I therefore only used male progeny for experiments. qRT-PCR analysis demonstrated that the transcript levels of *dPGC-1* were increased in response to PINK1 loss-of-function (Figure 4.2). I then assessed whether over-expression of *dPGC-1* can ameliorate the neurotoxic phenotypes induced by PINK1 loss-of-function. I confirmed the over-expression of *dPGC-1* using the *UAS-dPGC-1* construct driven ubiquitously by the *ActGS* driver using qRT-PCR (Figure 4.3). Ubiquitous over-expression of *dPGC-1* throughout development using the *DaGAL4* driver neither extended lifespan nor improved the climbing defects in $PINK1^{B9}$ null mutants (Figure 4.4 and 4.5), suggesting that elevation of *dPGC-1* does not rescue the toxic phenotypes induced by *PINK1* loss-of-function.

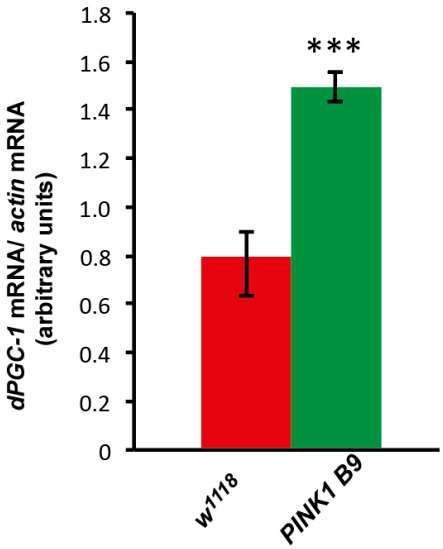

Figure 4.2 The mRNA expression levels of *dPGC-1* were increased in PINK1 loss-of-function flies

The *dPGC-1* mRNA levels (relative to *actin*) in male *PINK1*^{B9} null mutant flies at 15-day-old were increased compared to control flies. This was measured using qRT-PCR and the bars represent the means ± SEM (n=4, ***p<0.001 by t test). The genotypes used were: *w*^{1118} and *PINK* ^{B9}.

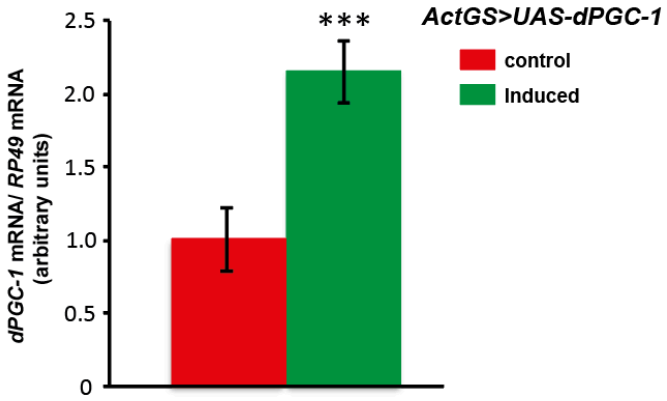

Figure 4.3 The mRNA expression levels of *dPGC-1* were raised in *dPGC-1*-over-expressing flies

The *dPGC-1* mRNA levels (relative to *RP49*) were increased in 15-day-old flies ubiquitously over-expressing *dPGC-1*, as measured by qRT-PCR. The bars represent the means ± SEM (n=4, ***p<0.001 by t test). The genotypes used were: *ActGS> UAS-dPGC-1*.

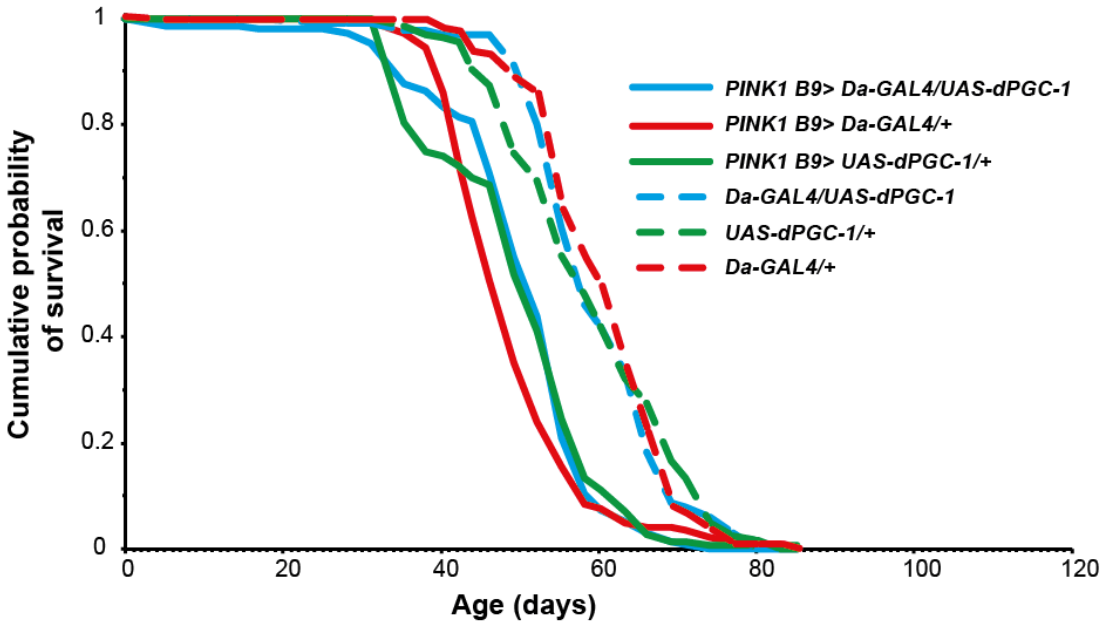

Figure 4.4 Ubiquitous over-expression of *dPGC-1* did not extend the lifespan of *PINK1* null mutant male flies

Male flies lacking *PINK1* show reduced survival compared to wild type flies (p=4.5 x 10^{-19} when comparing *DaGAL4/+* with *PINK1*^{B9}*>DaGAL4/+*). The survival curves demonstrated that ubiquitous over-expression of *dPGC-1* did not rescue the shortened lifespan of *PINK1*^{B9} males. P=0.04 when comparing *PINK1*^{B9}*> Da-GAL4/+* with *PINK1*^{B9}*> Da-GAL4/UAS-dPGC-1*. P=0.93 when comparing

PINK1^{B9}> UAS-dPGC-1/+ with *PINK1^{B9}> Da-GAL4/UAS-dPGC-1* by log-rank test. The genotypes used were: *Da-GAL4/+; UAS-dPGC-1/+; Da-GAL4/UAS-dPGC-1*; *PINK1^{B9}> Da-GAL4/+; PINK1^{B9}> UAS-dPGC-1/+; PINK1^{B9}> Da-GAL4/UAS-dPGC-1*.

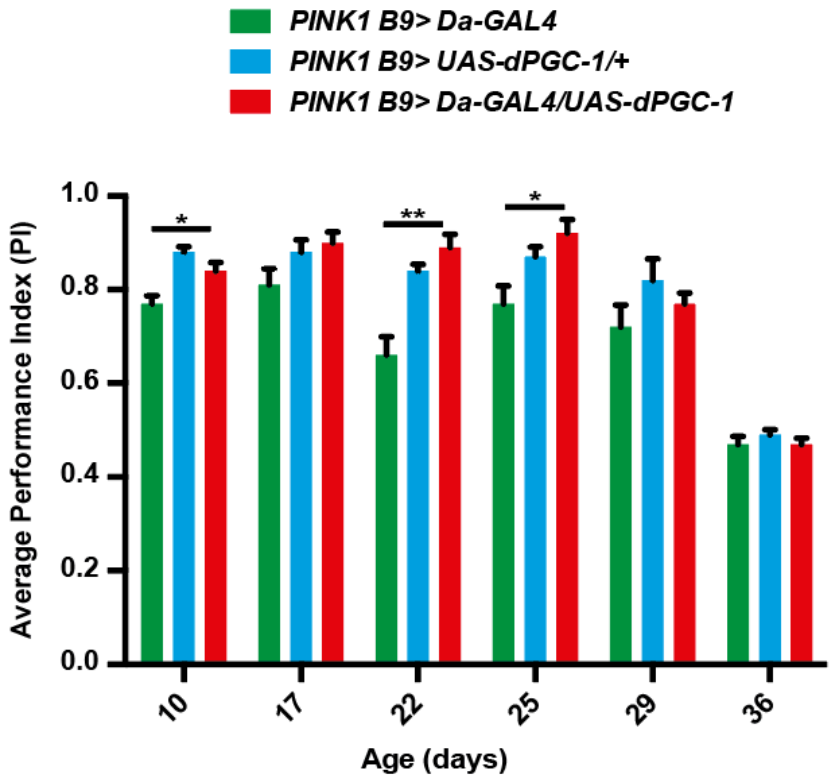

Figure 4.5 The over-expression of *dPGC-1* in *PINK1^{B9}* null mutant male flies did not rescue the climbing defects

The ubiquitous over-expression of *dPGC-1* using the *Da-GAL4* driver did not rescue the locomotor ability of *PINK1^{B9}* null mutant male flies using the negative geotaxis climbing assay. The bars are plotted as the means ± SEM, n=3, 15 flies per condition. **P<0.01, *p<0.05 by ANOVA analysis.

4.3.2 Over-expression of *dPGC-1* did not rescue the toxic phenotypes of *parkin* null mutants

To investigate the role of *dPGC-1* in neurotoxicity mediated by the loss of *parkin*, I first measured the levels of *dPGC-1* in *park^{25}* null mutants, which have been previously characterized (Greene et al., 2003). qRT-PCR showed that the mRNA levels of *dPGC-1* were increased in response to loss of parkin (Figure 4.6). I then assessed whether over-expression of *dPGC-1* could ameliorate the neurotoxic phenotypes induced by parkin loss-of-function. Ubiquitous over-expression of *dPGC-1* throughout development using the *ActGAL4* driver extended lifespan in both male

and female *parkin* null mutants (Figure 4.7 and 4.8), and improved the climbing defects in female *parkin* null mutants (Figure 4.9). However, the lifespan extension was not consistent and repeatable (Figure 4.10 and 4.11). These results therefore suggest that over-expression of *dPGC-1* does not rescue the toxic phenotypes induced by *parkin* loss-of-function.

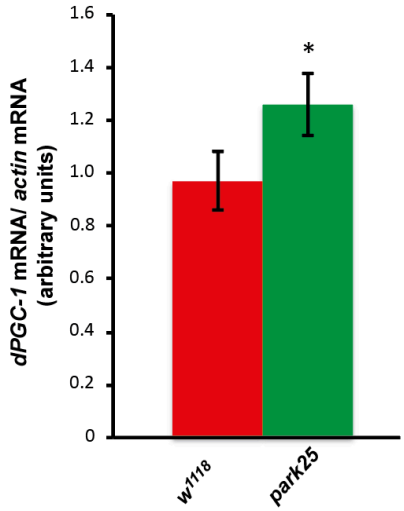

Figure 4.6 The expression of *dPGC-1* was increased in *park*^{25} null mutant flies

dPGC-1 mRNA levels (relative to *actin*) in female *park*^{25} null flies at 15-day-old, measured by qRT-PCR. The bars were plotted as the means ± SEM (n=4, *p<0.05 by t test). The genotypes used were: *w*^{1118} and *park*^{25}.

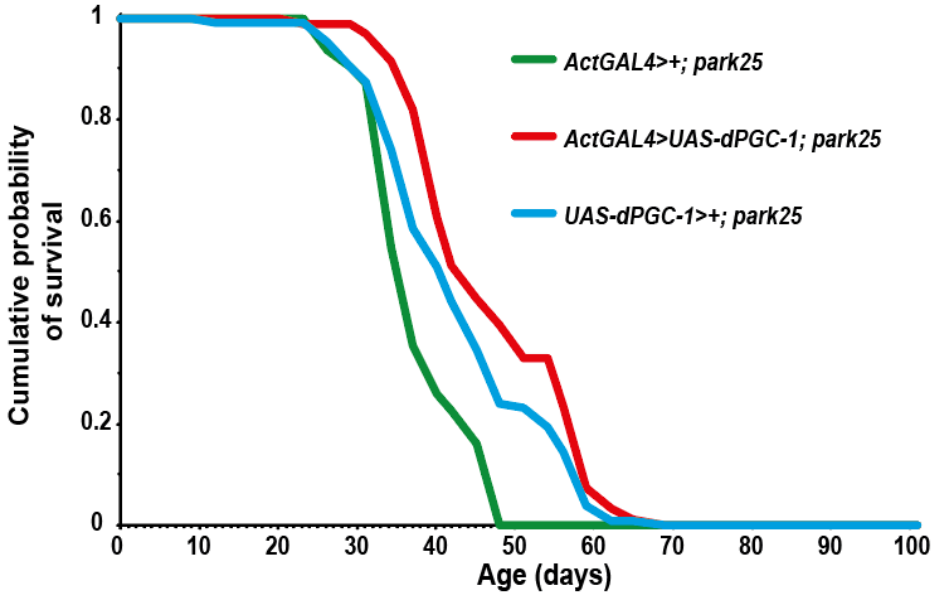

Figure 4.7 Ubiquitous over-expression of *dPGC-1* extended the lifespan of *park*^{25} null mutant female flies

The survival curves of *park*^{25} female flies ubiquitously over-expressing *dPGC-1*. P=3.3 x 10^{-8} when comparing *ActGAL4>+; park*^{25} with *ActGAL4>UAS-dPGC-1*; *park*^{25}. P=0.01 when comparing *UAS-dPGC-1>+; park*^{25} with *ActGAL4>UAS-dPGC-1; park*^{25} by log-rank test. The genotypes used were: *ActGAL4>+; park*^{25}, *ActGAL4>UAS-dPGC-1*; *park*^{25}, *UAS-dPGC-1>+; park*^{25}.

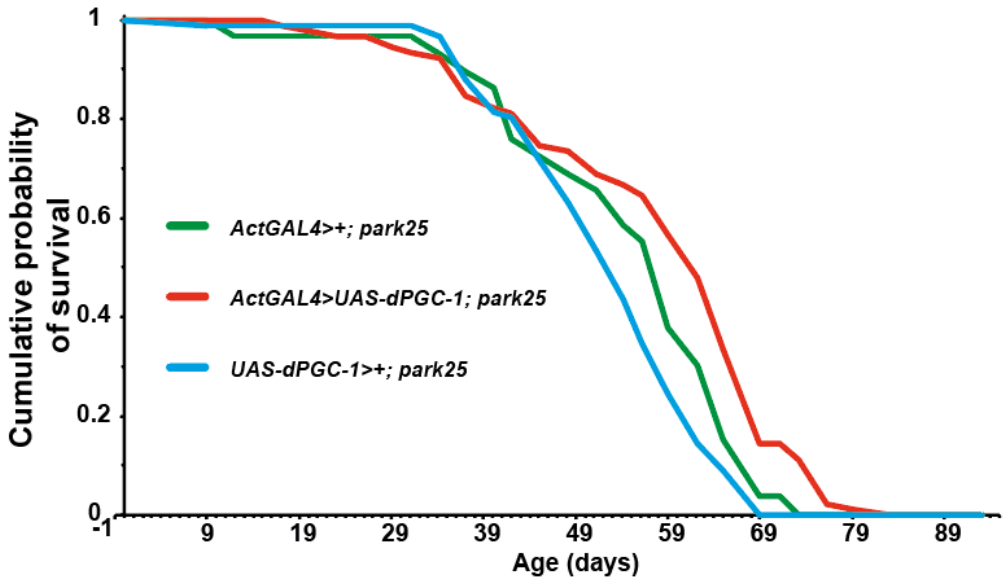

Figure 4.8 Ubiquitous over-expression of *dPGC-1* extended the lifespan of *park*^{25} null mutant male flies

Ubiquitous over-expression of *dPGC-1* in *park*^{25} null mutant male flies *(ActGAL4>UAS-dPGC-1;park*^{25} (red line)) extended lifespan. P=0.03 when comparing *ActGAL4>+; park*^{25} with *ActGAL4>UAS-dPGC-1*; *park*^{25}, P=1.7 x 10^{-6} when comparing *UAS-dPGC-1>+; park*^{25} with *ActGAL4>UAS-dPGC-1; park*^{25} by log-rank test. The genotypes used were: *ActGAL4>+; park*^{25}, UAS-*dPGC-1*>+; *park*^{25}, *ActGAL4>UAS-dPGC-1; park*^{25}.

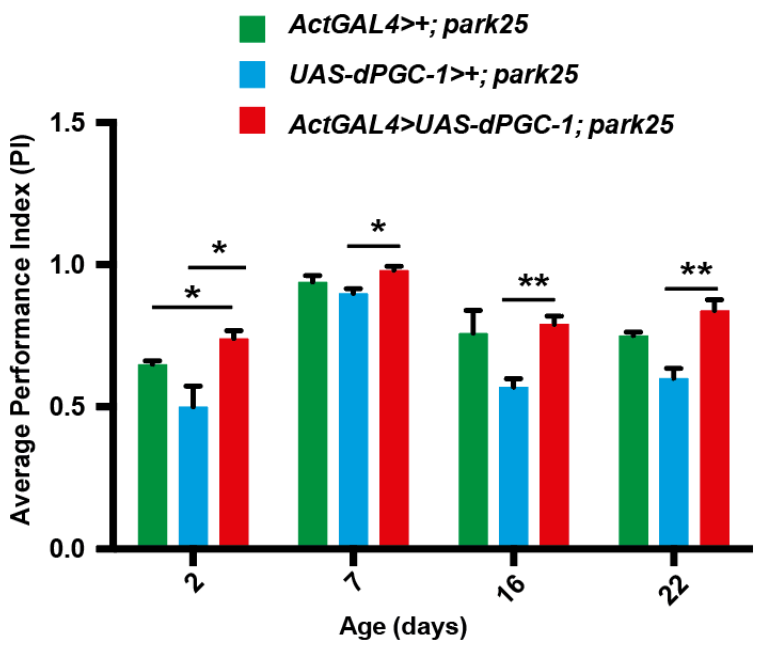

Figure 4.9 Ubiquitous over-expression of *dPGC-1* in *park*^{25} null mutant female flies partially ameliorated the climbing defects

Ubiquitous over-expression of *dPGC-1* using the *ActGAL4* driver rescued the climbing ability of *park*^{25} null mutant female flies. The bars represent the means ± SEM, n=3, 15 flies per condition. **P<0.01, *p<0.05 by ANOVA.

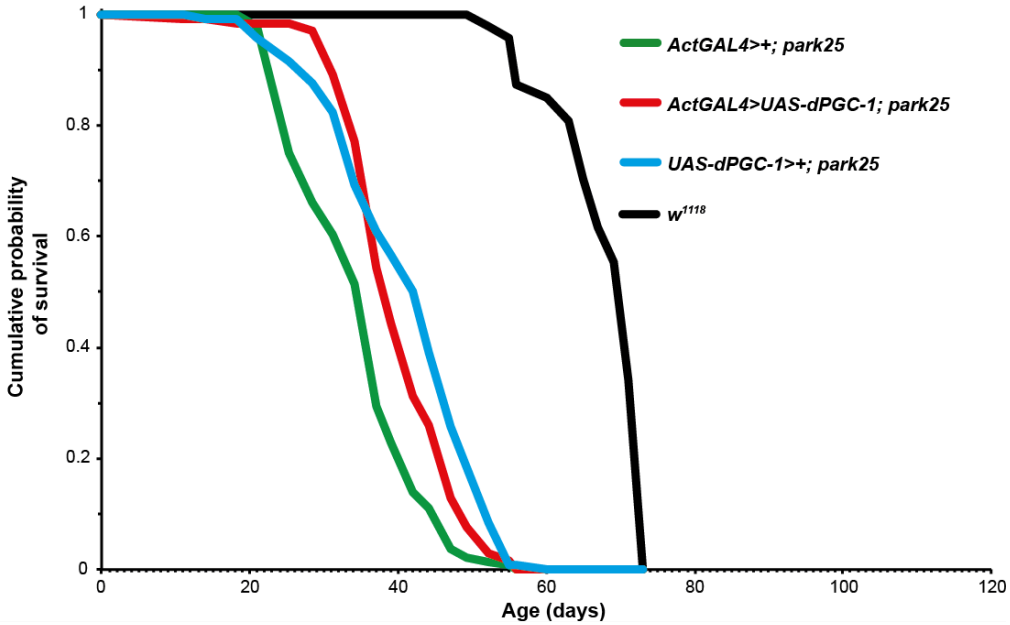

Figure 4.10 Ubiquitous over-expression of *dPGC-1* did not extend the lifespan of *park*^{25} null mutant female flies

Female flies lacking *parkin* show reduced survival compared to wild type flies ($p=4.3 \times 10^{-42}$ when comparing *DaGAL4/+* with *PINK1*^{B9}*>DaGAL4/+*). Ubiquitous over-expression of *dPGC-1* in *park*^{25}

null mutant female flies did not recue the lifespan phenotype. P=1.6 x 10^{-6} when comparing *ActGAL4>+; park^{25}* with *ActGAL4>UAS-dPGC-1; park^{25}*. P=0.03 when comparing *UAS-dPGC-1>+; park^{25}* with *ActGAL4>UAS-dPGC-1; park^{25}* by log-rank test. The genotypes used were: *w^{1118}*, *ActGAL4>+; park^{25}*, *UAS-dPGC-1>+; park^{25}*, *ActGAL4>UAS-dPGC-1; park^{25}*.

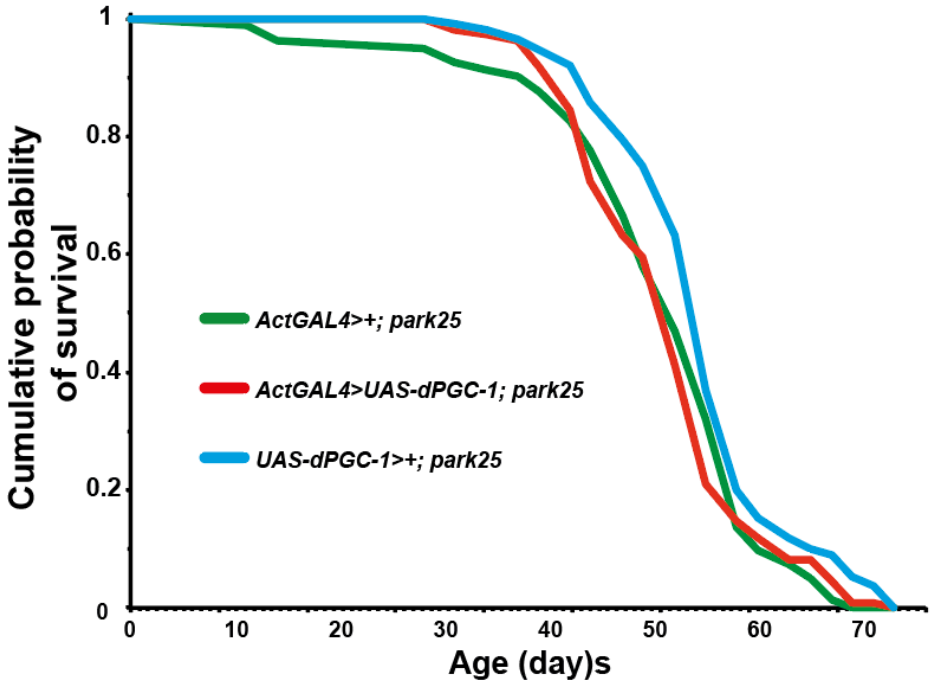

Figure 4.11 Ubiquitous over-expression of *dPGC-1* did not extend the lifespan of *park^{25}* null mutant male flies

The survival curves of *park^{25}* male flies ubiquitously over-expresses *dPGC-1*. P=0.97 when comparing *ActGAL4>+; park^{25} with ActGAL4>UAS-dPGC-1; park^{25}*, P=0.005 when comparing *UAS-dPGC-1>+; park^{25}* with *ActGAL4>UAS-dPGC-1; park^{25}* by log-rank test. The genotypes used were: *ActGAL4>+; park^{25}*, *UAS-dPGC-1>+; park^{25}*, *ActGAL4>UAS-dPGC-1; park^{25}*.

4.3.3 Over-expression of *dPGC-1* increased the sensitivity to oxidative stress of *park^{25}* null mutant male flies

To assess whether flies over-expressing *dPGC-1* are resistant to oxidative stress I assessed the survival of *park^{25}* null mutant flies treated with H_2O_2, a potent oxidizer, and with paraquat, a redox cycler. I demonstrated that both male and female flies lacking *parkin* had significantly reduced survival upon exposure to H_2O_2 (Figures 4.12 and 4.13) and paraquat (Figures 4.14 and 4.15). Surprisingly ubiquitous over-expression of *dPGC-1* (*ActGAL4>dPGC-1; park^{25}*) even further increased the

sensitivity of *park*^{25} null mutant male flies to oxidative stress, while further increased the sensitivity of *park*^{25} null mutant female flies to oxidative stress compared to one the control lines (*UAS-dPGC-1>+; park*^{25}) but not the others (*ActGAL4>+; park*^{25}).

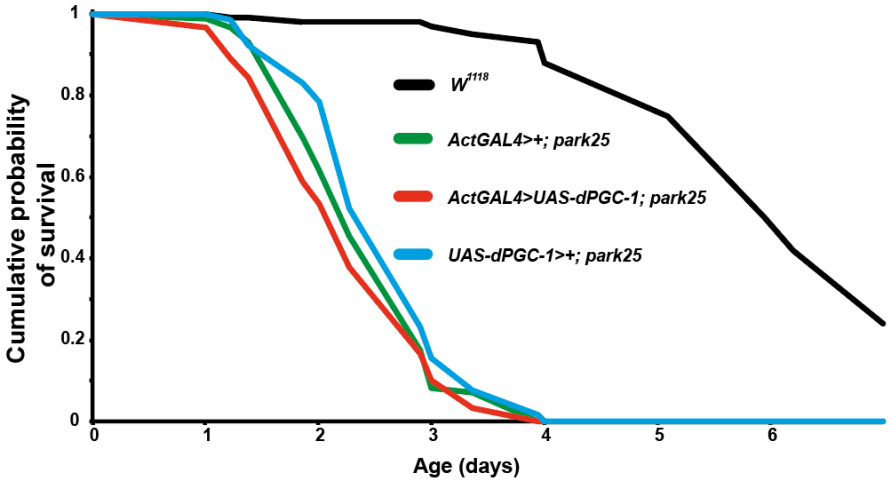

Figure 4.12 Ubiquitous over-expression of *dPGC-1* did not alter the sensitivity to H_2O_2 of *park*^{25} null mutant female flies

Female flies lacking *parkin (ActGAL4>+; park*^{25}*)* show increased sensitivity to 2.5% H_2O_2 compared to wild type flies ($p=3.1 \times 10^{-41}$). Ubiquitous over-expression of *dPGC-1* using the *ActGAL4* driver did not alter the sensitivity of *park*^{25} null mutant female flies on exposure to 2.5% H_2O_2 at 15-days of age. P=0.24 when comparing *ActGAL4>+; park*^{25} *with ActGAL4>UAS-dPGC-1; park*^{25}. P=0.01 when comparing *UAS-dPGC-1>+; park*^{25} with *ActGAL4>UAS-dPGC-1; park*^{25} by log-rank test. The genotypes used were: *w*^{1118}, *ActGAL4>+; park*^{25}, *UAS-dPGC-1>+; park*^{25}, *ActGAL4>UAS-dPGC-1; park*^{25}.

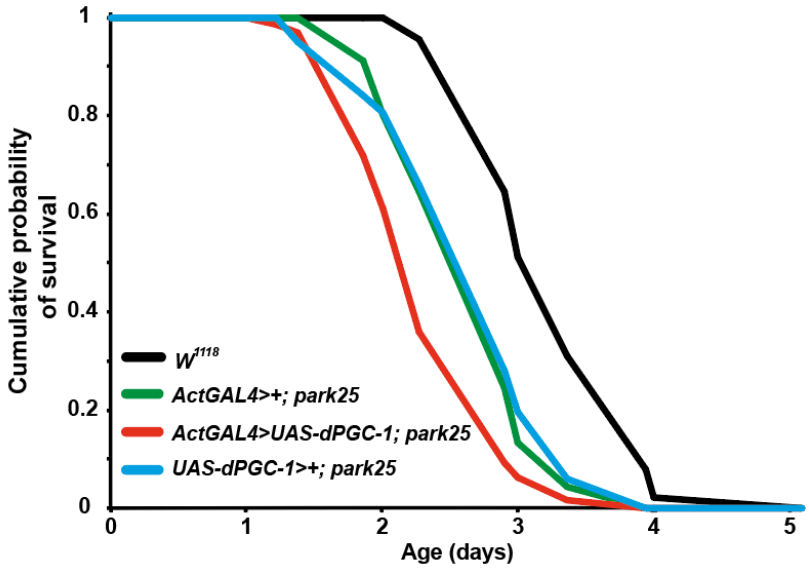

Figure 4.13 Ubiquitous over-expression of *dPGC-1* increased the sensitivity of *park*^{25} null mutant male flies to oxidative stress with H_2O_2

Male flies lacking *parkin (ActGAL4>+; park*^{25}*)* show increased sensitivity to 2.5% H_2O_2 compared to wild type flies (p=7.1 x 10^{-9}). Ubiquitous over-expression of *dPGC-1* in *park*^{25} null mutant flies (*ActGAL4>UAS-dPGC-1;park*^{25}) reduced the survival on exposure to 2.5% H_2O_2 at 15-days of age. P=0.005 when comparing *ActGAL4>+; park*^{25} *with ActGAL4>UAS-dPGC-1; park*^{25}, P=0.0003 when comparing *UAS-dPGC-1>+; park*^{25} with *ActGAL4>UAS-dPGC-1; park*^{25} by log-rank test. The genotype used were: *w*^{1118}, *ActGAL4>+; park*^{25}, *UAS-dPGC-1>+; park*^{25}, *ActGAL4>UAS-dPGC-1; park*^{25}.

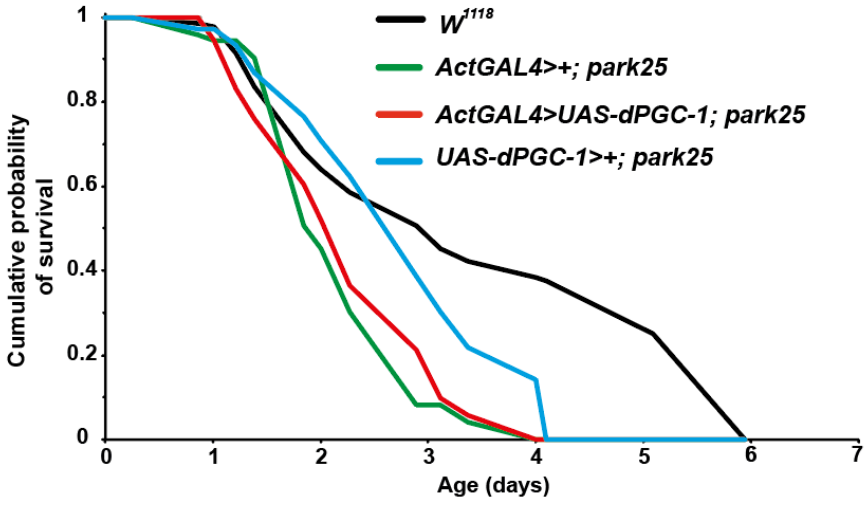

Figure 4.14 Ubiquitous over-expression of *dPGC-1* did not alter the sensitivity of *park*^{25} female flies to paraquat

Female flies lacking *parkin* (*UAS-dPGC-1>+; park*^{25}*)* show increased sensitivity to 2.5% H_2O_2 compared to wild type flies (p=5.5 x 10^{-6}). Ubiquitous over-expression of *dPGC-1* in *park*^{25} null mutant flies did not alter the sensitivity to treatment with 10mM paraquat at 15-days of age. P=0.5 when comparing *ActGAL4>+; park*^{25} with *ActGAL4>UAS-dPGC-1; park*^{25}. P=3.2 x 10^{-5} when

comparing *UAS-dPGC-1>+; park*^{25} with *ActGAL4>UAS-dPGC-1; park*^{25} by log-rank test. The genotypes used were: *w*^{1118}, *ActGAL4>+; park*^{25}, *UAS-dPGC-1>+; park*^{25}, *ActGAL4>UAS-dPGC-1; park*^{25}.

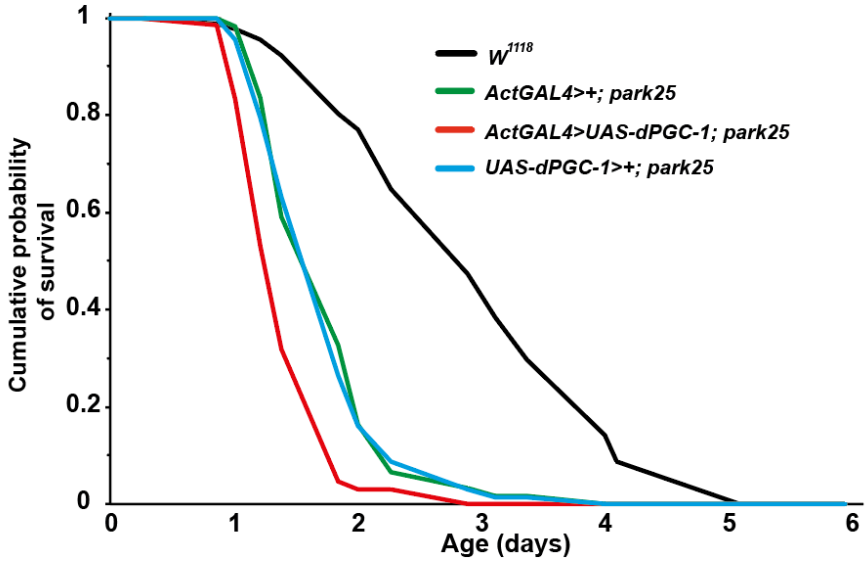

Figure 4.15 Ubiquitous over-expression of *dPGC-1* increased the sensitivity to oxidative stress on exposure to paraquat in *park*^{25} null mutant male flies

Male flies lacking *parkin* (*UAS-dPGC-1>+; park*^{25}*)* show increased sensitivity to 2.5% H_2O_2 compared to wild type flies (p=3.0 x 10^{-17}). The survival curves of *park*^{25} null mutant male flies over-expressing *dPGC-1* (*ActGAL4>UAS-dPGC-1; park*^{25}) compared to flies lacking *parkin* only (*ActGAL4>+; park*^{25} and *UAS-dPGC-1>+; park*^{25}) on exposure to 10mM paraquat at 15-days of age. P=2.2 x 10^{-5} when comparing *ActGAL4>+; park*^{25} with *ActGAL4>UAS-dPGC-1; park*^{25}. P=3.1 x 10^{-5} when comparing *UAS-dPGC-1>+; park*^{25} with *ActGAL4>UAS-dPGC-1; park*^{25} by log-rank test. The genotypes used were: *w*^{1118}, *ActGAL4>+; park*^{25}, *UAS-dPGC-1>+; park*^{25}, *ActGAL4>UAS-dPGC-1; park*^{25}.

4.4 Discussion

I demonstrated that the gene expression levels of *dPGC-1* were up-regulated in *PINK1* or *parkin* null mutant flies. This is opposite to what has been shown in human and mouse models, displaying reduced levels of PGC-1α in familial and sporadic PD (Shin et al., 2011, Zheng et al., 2010). The up-regulation of *dPGC-1* that I see in the fly models of familial PD may represent a compensatory response to the mitochondrial dysfunction induced by *PINK1* and *parkin* loss-of-function. Since flies do not have a homologue of PARIS, the transcriptional repressor of PGC-1α, this transcriptional regulation may not be conserved in *Drosophila*. To dissect the role of *dPGC-1* in *PINK1* and *parkin* loss-of-function, I further assessed the lifespan and

behavioral phenotypes in the corresponding null mutants over-expressing *dPGC-1*. I found that over-expression of *dPGC-1* did not extend the lifespan of either *PINK1* or *parkin* null mutant flies. Moreover, *dPGC-1* over-expression did not improve the climbing phenotypes of *PINK1* or *parkin* null mutants. These results suggest that elevation of *dPGC-1* is not neuroprotective in PD fly models.

4.5 Experimental procedures

4.5.1 Fly strains and backcrossing

The $PINK1^{B9}$ line (*w* $PINK1^{B9}$/FM7i*) was obtained from the Bloomington *Drosophila* Stock Centre (Park et al., 2006, Park et al., 2009) and contains a deletion of *PINK1* on chromosome X. The $park^{25}$ line (*w; $park^{25}$/TM6B. GFP*) and the *PINK1* genomic rescue line were kind gifts from Dr. Alex Whitworth (University of Cambridge). All of the lines were backcrossed into the w^{1118} strain for at least 6 generations before they were used in experiments. The $PINK^{B9}$ and $park^{25}$ lines have no visible phenotypes to follow for backcrossing. Therefore, the progeny from every generation of backcrossing were identified by PCR analysis with primers designed to detect the presence of the transgenic construct. This was performed as follows: a single cross was set up in an individual vial (one virgin female was crossed with one wild type male). They were then left for several days to mate and lay eggs. Female flies were then individually taken from each vial and used for PCR analysis. Only the progeny from female flies that were PCR-positive were selected for the next backcrossing. The PCR primers were designed using the Primer3 software. The PCR primers for $PINK1^{B9}$ were: FOR: CCAAATGATTCGAGTCCACA+ REV: TCCAGTTCATCCTCCTTGCT. The size of the PCR product for $PINK1^{B9}$ null flies was 721bp, while the size of the full *PINK1* construct was 1291bp. For $park^{25}$ the primers used were: FOR: CAGGAGTTTGTTTGTGGCACTGG+ REV: GCCATTACCTACCGAAACTTTACA. The PCR product size of the mutant flies was 500bp, while wild type flies had a 1.8kb PCR product size. The $PINK1^{B9}$ null males are sterile, and females are balanced with *FM7* on chromosome X. In order to pass the cytoplasmic content from w^{1118} virgin females to the progeny, I made double transgenic lines carrying both $PINK1^{B9}$ and the *PINK1* genomic rescue construct, so

that males were fertile and able to mate with w^{1118} virgin females. Once the initial cross was complete, the *PINK1* genomic construct was removed by excluding orange eye color in the following generation. After 6 back-crosses the $park^{25}$ null mutant lines were balanced twice with w^{1118}; *Cyo/Sp; TM6B/MKRS* to create a stable stock. The $PINK1^{B9}$ lines were balanced with *FM6* to create a stable stock.

4.5.2 qRT-PCR

RNA extraction and cDNA synthesis have been previously described. The primers for qRT-PCR were:

Actin: For: TTGTCTGGGCAAGAGGATCAG

REV: ACCACTCGCACTTGCACTTTC

Chapter 5 PGC-1α-GABPα modulates ageing in *Drosophila*

5.1 Summary

Dietary restriction is an evolutionarily conserved intervention that extends healthy lifespan across different species. Our understanding of the molecular mechanisms downstream of the nutrient-sensing network has improved significantly over the last 30 years, but is still not fully understood. PGC-1α is a key transcriptional co-activator in energy metabolism, and has recently been identified as a novel modulator of fly ageing, however the mechanism is not completely understood. Here I identified the transcription factor GA-binding protein (*dGABPα*), downstream of PGC-1α, as a key modulator of fly ageing. *dGABPα* gain-of-function extended female lifespan beyond dietary restriction (DR), with an associated reduction in IIS/mTOR signalling. Over-expression of *dGABPα* improved gut homeostasis by delaying age-related over-proliferation in intestinal stem cells. Additionally, *dGABPα* gain-of-function flies displayed resistance to xenobiotic stress. Finally, I demonstrated that *dGABPα* up-regulates *ImpL2*, encoding the insulin ligand binding protein, which down-regulates IIS and extends lifespan. Given the evolutionarily conserved effects of reduced IIS/mTOR, the findings suggest that GABPα may be an effective modulator of mammalian ageing.

5.2 Introduction

An increasing ageing population coupled with the rising prevalence of age-related diseases, highlights the need for effective strategies to improve healthy ageing. Ageing is a complex process that includes genetic and environmental factors. The most successful insights into ageing came from the discovery that ageing could be ameliorated by dietary, genetic, or pharmacological interventions. DR, an intervention that chronically reduces food intake without malnourishment, is the most robust environmental method to extend longevity in a wide range of evolutionarily diverse organisms, from yeast to mammals (Fontana et al., 2010, Colman et al., 2009, Katewa and Kapahi, 2010). DR can also improve healthy lifespan and reduce the prevalence

of age-related diseases in humans and mammalian models (Colman et al., 2014, Mattison et al., 2012, Ikeno et al., 2006, Maeda et al., 1985, Cava and Fontana, 2013, Heilbronn et al., 2006, Masoro, 2003). The mechanisms by which DR improves healthy lifespan have not been fully elucidated. However, the wide use of shorter-lived organisms including, *C. elegans* and *Drosophila,* has facilitated the experimental discovery of genetic and pharmacological interventions that extend healthy lifespan. The molecular mediators of the effects of DR on longevity include the mTOR (Kaeberlein et al., 2005, Chen et al., 2009b, Honjoh et al., 2009, Jia et al., 2004, Hansen et al., 2008), insulin/IGF-1-like signalling (IIS) (Broughton et al., 2010, Laplante and Sabatini, 2012, Takano et al., 2001), the energy sensor 5' adenosine monophosphate-activated protein kinase (AMPK) (Burkewitz et al., 2014, Greer et al., 2007, Slack et al., 2012), sirtuins (Guarente, 2013), NF-E2-related factor (NRF2) (Castillo-Quan et al., 2016) and heat shock factors (HSFs) (Heydari et al., 1996).

In addition to reducing food intake, the timing of the meal has also emerged as an important determinant of ageing. Intermittent fasting (IF) or chronic starvation extends lifespan in *C. elegans* through mechanisms that include reduced IIS/mTOR signalling (Honjoh et al., 2009, Kaeberlein et al., 2006, Lee et al., 2006, Uno et al., 2013). Moreover, short term fasting in human or mammalian models results in an improved healthy lifespan and the reduced prevalence of age-related chronic disorders. This involves mechanisms such as induction of the chaperone HSP70 and inhibition of the IIS/mTOR signalling network (Brown-Borg and Rakoczy, 2013, Mattson et al., 2014, Cheng et al., 2014). However, the effect of fasting or starvation on cachexia, such as in cancer, may be detrimental, leading to organ wasting and loss of body mass. Fasting in rats increased the production of TGF-beta1, leading to the initiation and promotion of liver carcinogenesis (Tessitore and Bollito, 2006). In a *Drosophila* tumour model, resulting from activation of the oncogene *Yorkie* in intestinal stem cells, there was organ-wasting associated with a sustained and dramatic reduction in systemic IIS signalling, via increased levels of the secreted insulin antagonist ImpL2 (Kwon et al., 2015, Figueroa-Clarevega and Bilder, 2015). Interestingly, over-expression of *ImpL2* extends lifespan in *Drosophila* via mechanisms consistent with reduced IIS signalling, suggesting a possible involvement in mammalian ageing (Alic et al., 2011b). Therefore, wasting, starvation, IF, and DR

might share similar molecular mechanisms, including reduced IIS signalling, in response to nutritional limitation. However, the outcomes are varied depending on multiple factors, including the levels of signalling reduction, nutrient availability and the sensitivity of the host.

The functions of the insulin/IGF-1-like signalling (IIS) pathway include regulation of growth, development, reproduction, stress resistance and metabolic homeostasis. Insulin-like ligands mediate cell-to-cell signalling by activating an insulin-like receptor, leading to the activation of PI3K (Phosphatidylinositide 3-kinase), AKT, mTOR, and ERK (extracellular signal-regulated kinases) intracellular signalling pathways (Tatar et al., 2003, Piper et al., 2008, Slack et al., 2015). Reduced IIS increases longevity in nematodes, fruit flies and mice (Fontana et al., 2010, Kenyon, 2010), highlighting the relevance of IIS in human ageing. Lifespan extension and stress resistance resulting from down-regulation of IIS are mediated by the FOXO family of transcription factors through PI3K and AKT kinase signalling (Laplante and Sabatini, 2012). Inhibition of AKT activates FOXO, which in turn up-regulates several “longevity genes” controlling DNA repair, autophagy, antioxidant activity, stress resistance, as well as cell proliferation (Wang et al., 2014, Webb and Brunet, 2014).

The evolutionarily conserved mTOR signalling pathway responds to growth factors and amino acids to regulate the growth and metabolism of all eukaryotic cells. mTOR functions via two distinct multiprotein complexes: mTOR complex 1 (mTORC1) and mTOR complex 2 (mTORC2) (Johnson et al., 2013). mTORC1 regulates growth through phosphorylation of the downstream effectors ribosomal protein S6 kinases (S6Ks). Under favourable conditions, such as an amino acid-rich diet, phosphorylated S6K promotes cellular growth and alters metabolism (Um et al., 2006). mTORC1-dependent phosphorylation of the eukaryotic translation initiation factor 4E-binding protein 1 (4E-BP1) disrupts its association with the translation initiation factor 4E (elF4E), allowing the latter to promote cap-dependent translation (Sonenberg and Hinnebusch, 2009). Rapamycin, a natural macrolide compound isolated from bacteria, inhibits mTORC1 activity, extending the lifespan across species from yeast to mammals. Rapamycin acts by reducing mRNA translation and by inducing autophagy

through at least two mTORC1 substrates, S6K and 4E-BP1 (Bjedov et al., 2010, Powers et al., 2006, Robida-Stubbs et al., 2012, Harrison et al., 2009, Medvedik et al., 2007, Miller et al., 2011). Moreover, inhibition of mTORC1 also improves proteostasis and enhances stem cell function (Kapahi et al., 2010, Johnson et al., 2013). mTORC2 is not sensitive to inhibition by rapamycin, and is usually considered not relevant to nutrient sensing. However it can positively regulate the IIS pathway by activating phosphorylation of AKT, the main kinase in the IIS pathway (Guertin and Sabatini, 2009). In addition, AKT kinase can then phosphorylate and inactivate mTORC1, while S6K negatively regulates the insulin receptor substrate 1 (Laplante and Sabatini, 2012, Takano et al., 2001, Um et al., 2006). It has also been shown that the mTORC1 substrate 4E-BP is a transcriptional target of FOXO in fruit flies (Tettweiler et al., 2005).

PGC-1α is the master regulator of many biological processes, including adaptive thermogenesis (Puigserver et al., 1998), mitochondrial biogenesis (Wu et al., 1999), glucose metabolism (Miura et al., 2003), hepatic gluconeogenesis, fatty acid oxidation (Li et al., 2007b, Puigserver et al., 2003), circadian rhythmicity (Liu et al., 2007) as well as stress response systems (St-Pierre et al., 2006). PGC-1α is directly regulated by insulin-stimulated AKT phosphorylation in hepatic metabolism (Li et al., 2007b). Phosphorylation and inhibition prevent the recruitment of PGC-1α to its cognate promoters, impairing its ability to bind and co-activate FOXO1 or HNF4 (hepatocyte nuclear factor) to promote gluconeogenesis and fatty acid oxidation (Puigserver et al., 2003, Li et al., 2007b). Moreover, PGC-1α can also be regulated by FOXO1 in the control of mitochondrial biogenesis in response to insulin signalling (Cheng et al., 2009). *Drosophila* PGC-1 (*dPGC-1*), the only homologue of the mammalian PGC-1 family, regulates mitochondrial activity, cellular growth and metabolism in response to insulin signalling in parallel with FOXO, the main IIS downstream effector responsible for cellular growth (Mukherjee and Duttaroy, 2013, Tiefenböck et al., 2010). Interestingly, *dPGC-1* can also negatively regulate insulin signalling, although the precise mechanisms involved are not known (Tiefenböck et al., 2010).

dPGC-1 is also a terminal target of the mTOR signalling pathway in regulating cellular growth and metabolism (Mukherjee and Duttaroy, 2013, Tiefenböck et al.,

2010). It may be regulated in a number of different ways. Inhibition of mTOR1 by rapamycin reduces the transcript levels of PGC-1α (Cunningham et al., 2007), and inhibition of mTORC1 induces Mitf, the *Drosophila* homologue of the transcription factor EB (TFEB). This translocates to the nucleus and directly up-regulates the transcript levels of *dPGC-1* (Bouche et al., 2016). Moreover, the mTOR signalling pathway is associated with human longevity (Passtoors et al., 2013), and over-expressing *dPGC-1* in the intestinal system of the fruit fly extends lifespan with improved gut homeostasis and increased mitochondrial biogenesis, suggesting PGC-1a might be a modulator for mammalian ageing. However, the direct contribution of mitochondrial function in regulating longevity has not been investigated (Rera et al., 2011). Therefore, whether mitochondrial function is the major determinant of PGC-1α-mediated lifespan extension in response to reduced mTOR signalling is yet to be proven. Some studies have however demonstrated that inhibition of mTORC1, or up-regulation of 4E-BP, results in a metabolic shift towards greater mitochondrial respiration and increased lifespan across species from yeast to mice (Bonawitz et al., 2007, Polak et al., 2008, Morita et al., 2013, Zid et al., 2009). In addition, mild inhibition of mitochondrial respiration extends lifespan of many organisms including worms, flies and mice (Feng et al., 2001, Dillin et al., 2002, Lee et al., 2003, Lee et al., 2010, Liu et al., 2005, Dell'agnello et al., 2007, Copeland et al., 2009). I therefore hypothesised that PGC-1α, being-downstream of IIS/mTOR signalling, may regulate longevity partially through a mitochondrial-independent manner.

In order to address this hypothesis, I first investigated whether genetic activation of the transcription factors required by PGC-1α in regulating mitochondrial biogenesis and respiration can affect lifespan. PGC-1α co-activates a number of different transcription factors, including NRF1, GABPα, YY1 and ERRα (Puigserver and Spiegelman, 2003, Scarpulla, 2008, Cunningham et al., 2007). GABPα is the alpha subunit of the GA binding protein complex, which is a mammalian E26 transformation-specific (ETS) transcription factor required for mitochondrial biogenesis (Yang et al., 2014). In addition, GABPα can be induced and co-activated by PGC-1α in skeletal muscle, forming a double-positive-feedback loop that drives the expression of many genes in OXPHOS and during neuromuscular junction (NMJ) programming (Handschin et al., 2007, Mootha et al., 2004, Wu et al., 1999). In

Drosophila, PGC-1α and GABPα work by overlapping mechanisms required for mitochondrial abundance and gene expression for OXPHOS (Baltzer et al., 2009), suggesting a conserved function with their mammalian counterparts (Mootha et al., 2004, Yang et al., 2014). I hypothesised that if PGC-1α extends lifespan partially through GABPα, then over-expression of GABPα might be enough to extend lifespan.

As described in this Chapter, I first re-examined the effect of *dPGC-1* over-expression on the lifespan of *Drosophila*, and found that both ubiquitous and CNS specific over-expression of *dPGC-1* extends lifespan. In keeping with its human counterpart, *dPGC-1* over-expression also up-regulated the transcription of *dGABPα*. Either ubiquitous or tissue-specific (brain or gut and fat body) over-expression of *dGABPα* was sufficient to extend lifespan via mechanisms beyond DR. It also improved measures of health, including increased resistance to xenobiotic stress and improved gut homeostasis. Surprisingly I found that *dGABPα* up-regulated the levels of *ImpL2*, the secreted insulin antagonist and an important negative regulator of IIS. This suggests that up-regulation of *dGABPα* may therefore modulate insulin sensitivity. To assess this further I performed both lifespan and bioinformatics analyses, and confirmed that over-expression of *dGABPα* extends lifespan through overlapping mechanisms with reduced IIS. In addition, over-expression of *dGABPα* also reduced mTORC1 activity, therefore extending lifespan in a similar manner to rapamycin. My results point to the possibility that GABPα, or a related protein, may be an effective modulator of mammalian ageing and age-related diseases. Further work is now required to study the effects of up-regulating GABPα in specific disease models, such as the AD and PD fly models.

5.3 Results

5.3.1 Over-expression of *dPGC-1* extended the lifespan of female *Drosophila*

Previous studies demonstrated that over-expression of *dPGC-1* specifically in the intestine extends lifespan (Rera et al., 2011). I then asked whether over-expression of *dPGC-1* throughout the fly is also sufficient to extend lifespan. Ubiquitous over-expression of *dPGC-1,* either throughout development using the *ActGAL4* driver, or

in adulthood using the *Actin-GeneSwitch* (*ActGS*) driver, significantly increased the median lifespan of female flies by 9% (Figure 5.1, p=3.28 x 10^{-18}; Figure 5.3, p=3.54 x 10^{-6}) but not in males (Figure 5.2, p=0.1). Additionally, over-expression of *dPGC-1* delayed the age-related decline in climbing ability (Figure 5.4), a behavioural measurement of neuromuscular health. My results therefore confirm that *dPGC-1* is indeed a modulator for healthy ageing.

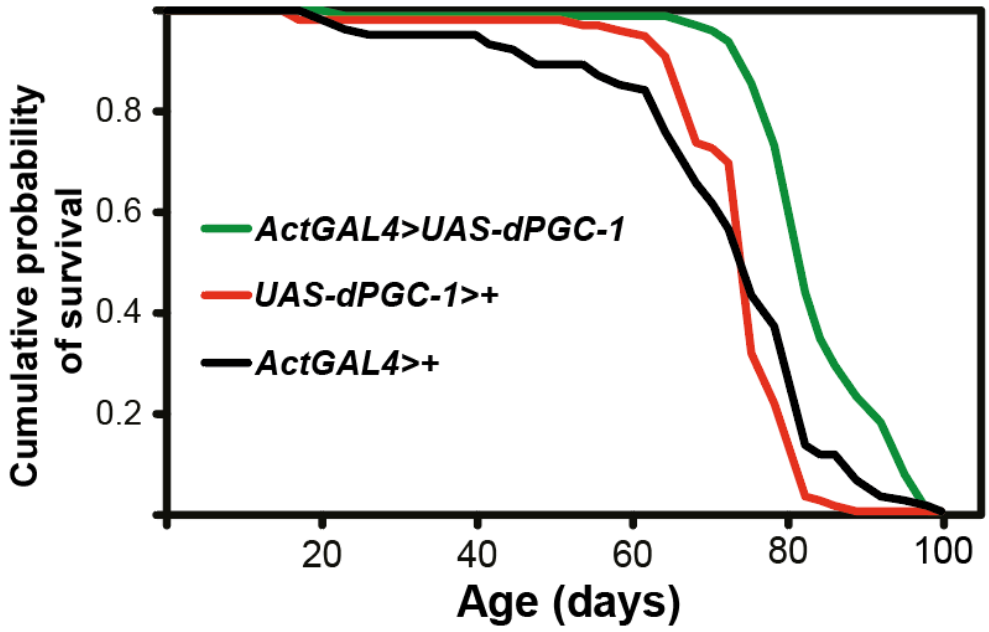

Figure 5.1 Ubiquitous over-expression of *dPGC-1* extended the lifespan of female flies

Ubiquitous over-expression of *dPGC-1* throughout development and adulthood using the *ActGAL4* driver (*ActGAL>UAS-dPGC-1*, green line) extended the lifespan of female flies (the median lifespan was extended by 9%, p=3.28 x 10^{-18} when comparing *ActGAL4>UAS-dPGC-1* and *+>UAS-dPGC-1*; p=2.2 x 10^{-8} when comparing *ActGAL4/UAS-dPGC-1* and *ActGAL4/+* by log-rank test). The genotypes used were: *ActGAL4/UAS-dPGC-1, ActGAL4>+, +>UAS-dPGC-1.*

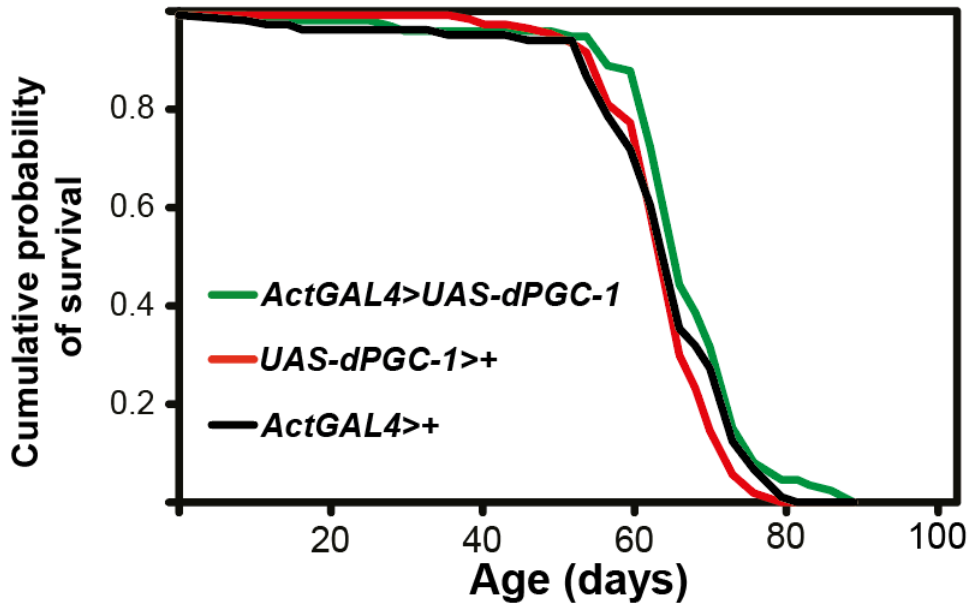

Figure 5.2 Ubiquitous over-expression of *dPGC-1* during development and in adulthood did not extend the lifespan of male flies

Ubiquitous expression of *dPGC-1* throughout development and in adulthood using the *ActGAL4* driver (*ActGAL4>UAS-dPGC-1*, green line) did not extend the lifespan of male flies. P=0.1 when comparing *ActGAL4>UAS-dPGC-1* and *ActGAL4>+* by log-rank test. The genotypes used were: *ActGAL4>UAS-dPGC-1, ActGAL4>+, +>UAS-dPGC-1*.

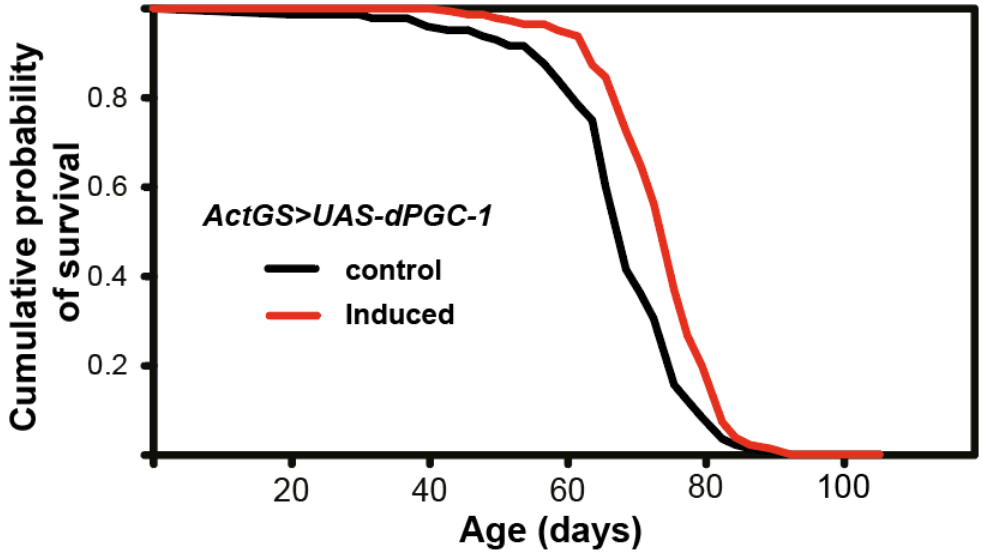

Figure 5.3 Ubiquitous over-expression of *dPGC-1* only in adulthood extended the lifespan of female flies

Ubiquitous over-expression of *dPGC-1* in adulthood only using the *ActGS* driver in the presence of RU (*ActGS>UAS-dPGC-1*, RU+, red line) extended the lifespan of flies compared to un-induced (RU-) controls (the median lifespan was extended by 8.7%, $p=3.54 \times 10^{-6}$ by log-rank test). The genotypes used were: *ActGS>UAS-dPGC-1*.

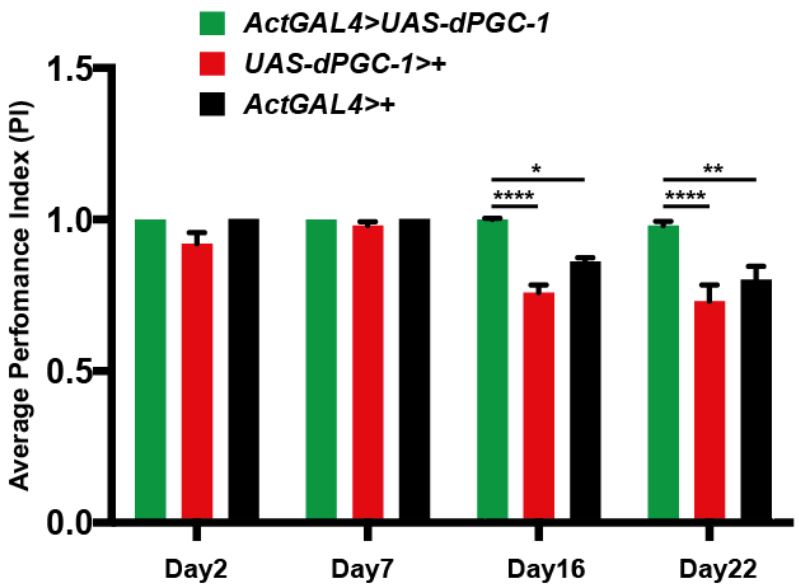

Figure 5.4 Ubiquitous over-expression of *dPGC-1* partially ameliorated the locomotor abnormalities of flies

Ubiquitous over-expression of *dPGC-1* using the *ActGAL4* driver (*ActGAL4>UAS-dPGC-1*, black bars) partially rescued the age-dependent climbing defects of control flies. ***P<0.001 when comparing the *dPGC-1* over-expressing flies to age-matched control flies response by two-way ANOVA analysis. For example, ****p<0.0001 when comparing *ActGAL4>UAS-dPGC-1* over-expressing flies and *+>UAS-dPGC-1* flies at day 22 by Tukey's multiple comparisons test. The genotypes used were: *ActGAL4>UAS-dPGC-1, ActGAL4>+, +>UAS-dPGC-1*.

I previously demonstrated that over-expression of *dPGC-1* extends lifespan in AD flies expressing Aβ (Chapter 3). I hence asked whether longevity would be affected if *dPGC-1* is over-expressed in neurons in the absence of Aβ. Interestingly, over-expression of *dPGC-1* in adult neurons using the *elavGS* driver was sufficient to extend lifespan (Figure 5.5, the median lifespan was extended by 6%, p<0.0001), suggesting a broad-spectrum effect of neuronal *dPGC-1* on lifespan regulation.

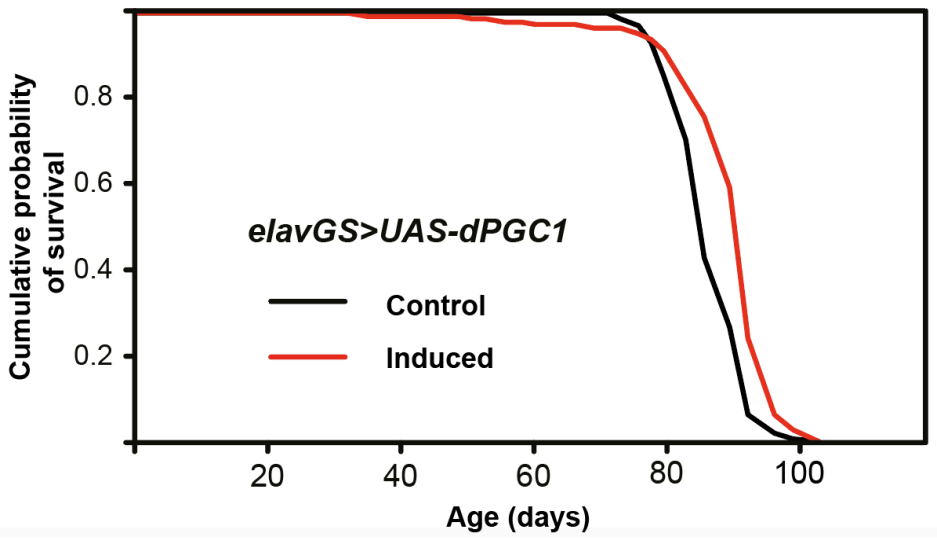

Figure 5.5 Over-expression of *dPGC-1* in adult neurons extended lifespan

Over-expression of *dPGC-1* in adult neurons using the *elavGS* driver induced in the presence of RU (*elavGS>UAS-dPGC-1*, RU+, red line) extended the lifespan of flies compared to the un-induced control (RU-, black line). The median lifespan was increased by 6%, $P<7 \times 10^{-5}$ by log-rank test. The genotypes used were: *elavGS>UAS-dPGC-1*.

Interventions that extend the lifespan of flies are often associated with resistance to various stressors (Castillo-Quan et al., 2016, Broughton et al., 2005, Afschar et al., 2016). Ablation of PGC-1α in cultured cells down-regulates antioxidants including SOD1 and 2, resulting in hypersensitivity to hydrogen peroxide (H_2O_2)-induced oxidative stress. Conversely, over-expression of PGC-1α in muscles up-regulates the same genes, suggesting that PGC-1α regulates the antioxidant defence system as well as mitochondrial ROS (St-Pierre et al., 2006). Tissue-specific over-expression of *dPGC-1* has been reported to suppress ROS in the gut of flies (Rera et al., 2011), and even when *dPGC-1* is ubiquitously over-expressed there is resistance to paraquat-induced oxidative stress. However the levels of SOD1 and SOD2 are not changed in response to *dPGC-1* (Mukherjee et al., 2014). I therefore investigated the survival of flies over-expressing *dPGC-1* under exposure to H_2O_2, a potent oxidizer, or paraquat, a redox cycler, which produces superoxide in part through the mitochondria (Cocheme and Murphy, 2008). I found that ubiquitous over-expression of *dPGC-1* increased the sensitivity of flies to H_2O_2-induced oxidative stress (Figure 5.6, $p=3 \times 10^{-21}$). Moreover, *dPGC-1* activation did not change the survival of flies exposed to paraquat (Figure 5.7, p=8.5). These results therefore do not support previous findings

(Mukherjee et al., 2014), and suggest an increased sensitivity to oxidative stress in response to *dPGC-1* over-expression.

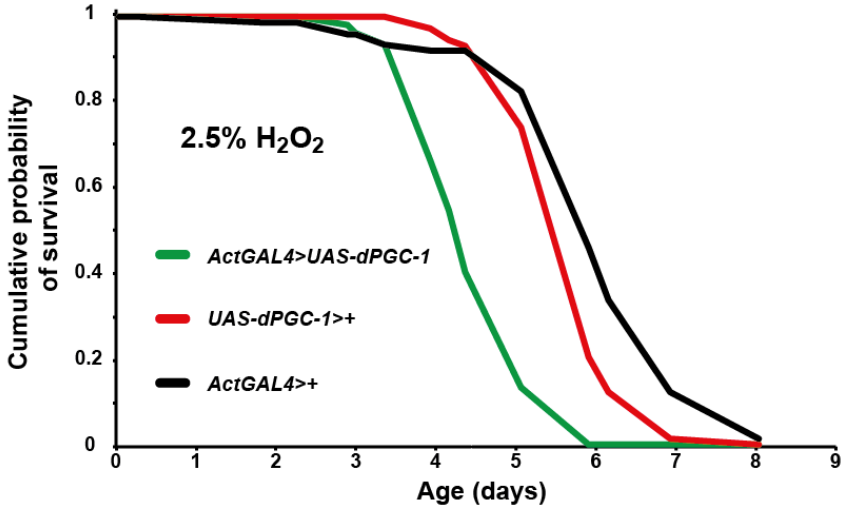

Figure 5.6 Ubiquitous over-expression of *dPGC-1* increased the sensitivity of female flies to H_2O_2

Ubiquitous over-expression of *dPGC-1* throughout development and in adulthood using the *ActGAL4* driver (*ActGAL4>UAS-dPGC-1*, red line) decreased the survival of females flies on food containing 2.5% H_2O_2. P=1.61x 10^{-18} when comparing *ActGAL4>UAS-dPGC-1* and *+>UAS-dPGC-1*. P=3 x 10^{-21} when comparing *ActGAL4>UAS-dPGC-1* and *ActGAL4>+* by log-rank test. The genotypes used were: *ActGAL4>UAS-dPGC-1, ActGAL4>+, +>UAS-dPGC-1*.

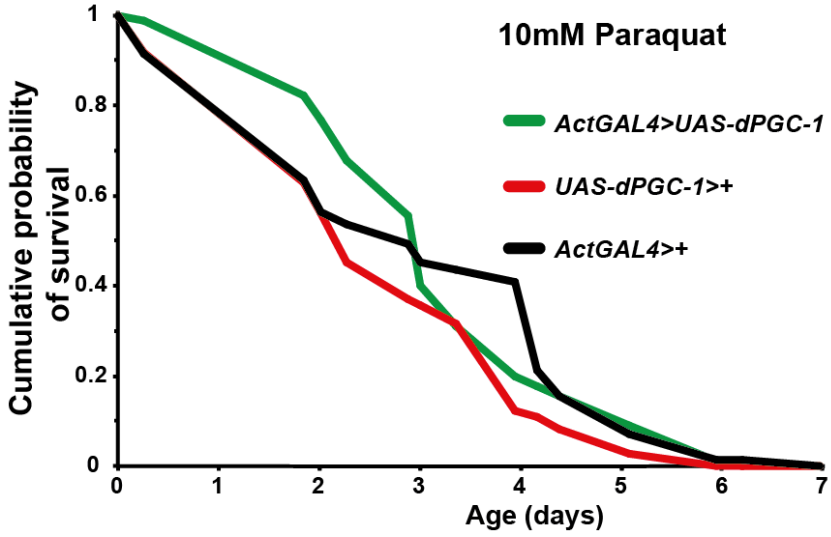

Figure 5.7 Ubiquitous over-expression of dPGC-*1* did not significantly affect the lifespan of flies exposed to paraquat.

Ubiquitous over-expression of *dPGC-1* using the *ActGAL4* driver (*ActGAL4>UAS-dPGC-1*; red line, RU+) did not significantly alter the survival of female flies exposed to 10mM paraquat. P=0.85 when comparing *ActGAL4>UAS-dPGC-1* and *ActGAL4>+*. P=0.04 when comparing *ActGAL4>UAS-dPGC-1* and *+>UAS-dPGC-1* by log-rank test). The genotypes used were: *ActGAL4>UAS-dPGC-1*, *ActGAL4>+*, *+>UAS-dPGC-1*.

5.3.2 Over-expression of *dYY1* extended lifespan in female flies

To investigate whether downstream TFs mediate the lifespan extension of *dPGC-1* over-expression, the effects of YY1 (Cunningham et al., 2007), PDP1ε (Cyran et al., 2003), and GABPα (Mootha et al., 2004, Baltzer et al., 2009) on survival were tested. Mammalian YY1 regulates mitochondrial biogenesis by co-activation with PGC-1α in response to mTOR signalling. However the effect of the *Drosophila* homologue of YY1 (*pho*, CG17743) on mitochondrial function and lifespan is not yet known. Here I show that ubiquitous over-expression of *dYY1* extended the median lifespan by 6% and maximum lifespan by 12% in female flies (Figure 5.8).

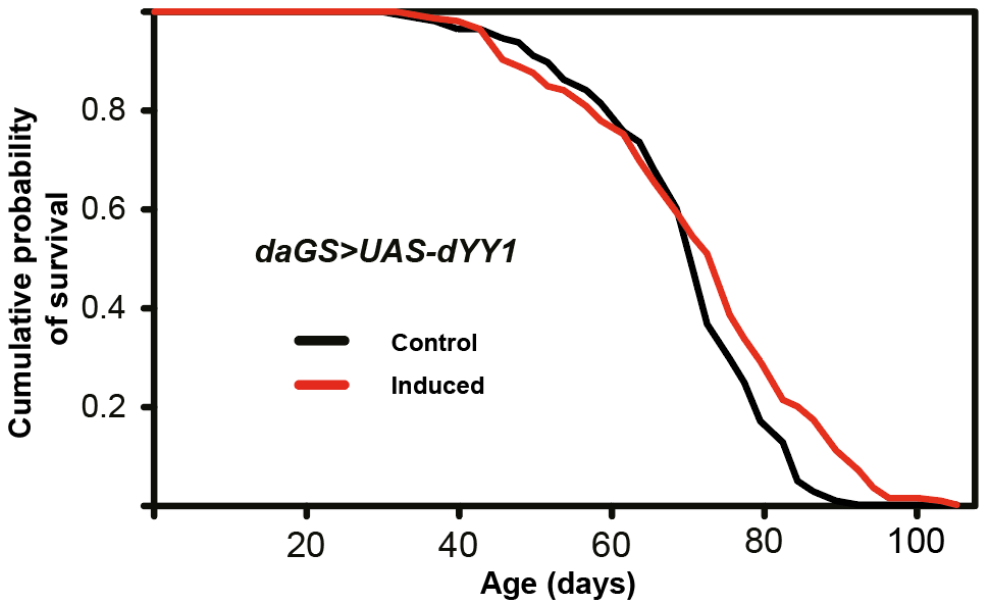

Figure 5.8 Ubiquitous over-expression of *dYY1* in adulthood extended the lifespan of female flies

Ubiquitous over-expression of *dYY1* in adulthood using the *daGS* driver and inducing expression with RU (*daGS>UAS-dYY1*, red line, RU+) increased the lifespan of female flies compared with un-induced controls (black line, RU-). The median lifespan extension was 6%, the maximum lifespan extension was 12%, p=0.003 by log-rank test. The genotypes used were: *daGS>UAS-dYY1*.

PDP1ε is a transcription factor involved in the second feedback loop of the circadian clock and positively regulates the transcription levels of *dCLOCK*. Conversely VRI is the transcription factor that negatively regulate*s dCLOCK* (Cyran et al., 2003). Flies lacking *Pdp1ε* display hypersensitivity to oxidative stress (Beaver et al., 2010), whereas over-expression of *Pdp1ε* increases the transcription levels of genes involved in the stress-response pathway such as *DHR96, Xbp1 and Grp78* (Figure 3.34, 3.36, and 3.37). Disturbances in circadian rhythm and the stress response pathway contribute to ageing (Harper et al., 2005, Taylor and Dillin, 2013, Hipp et al., 2014, Musiek et al., 2013), suggesting that PDP1ε and VRI may be significant modulators of fly ageing. I previously showed that *dPGC-1* and PDP1ε may physically interact in the fly brain. I therefore investigated whether over-expression of *Pdp1ε* modulates longevity. I found that ubiquitous over-expression of *Pdp1ε* did not extend the lifespan of flies (Figure 5.9, p=0.9). Similarly, ubiquitous over-expression of *vri* shortened the lifespan of flies (Figure 5.10, p=0.008). These results therefore suggest that activation of the circadian genes involved in the second feedback loop in *Drosophila* does not extend lifespan.

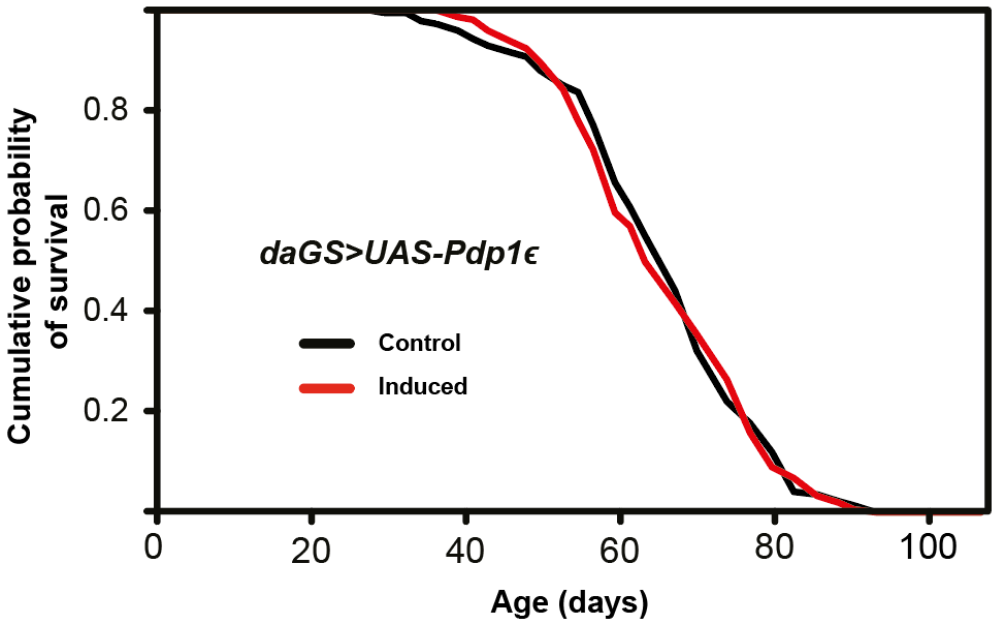

Figure 5.9 Ubiquitous over-expression of *Pdp1ε* in adulthood does not extend lifespan in female flies

Ubiquitous over-expression of *Pdp1ε* in adulthood using the *daGS* driver induced by the presence of RU (*daGS>UAS-Pdp1 ε* , red line, RU+) did not affect the lifespan compared to non-induced controls (black line, RU-). P=0.9 by log-rank test. The genotypes used were: *daGS>UAS- Pdp1ε.*

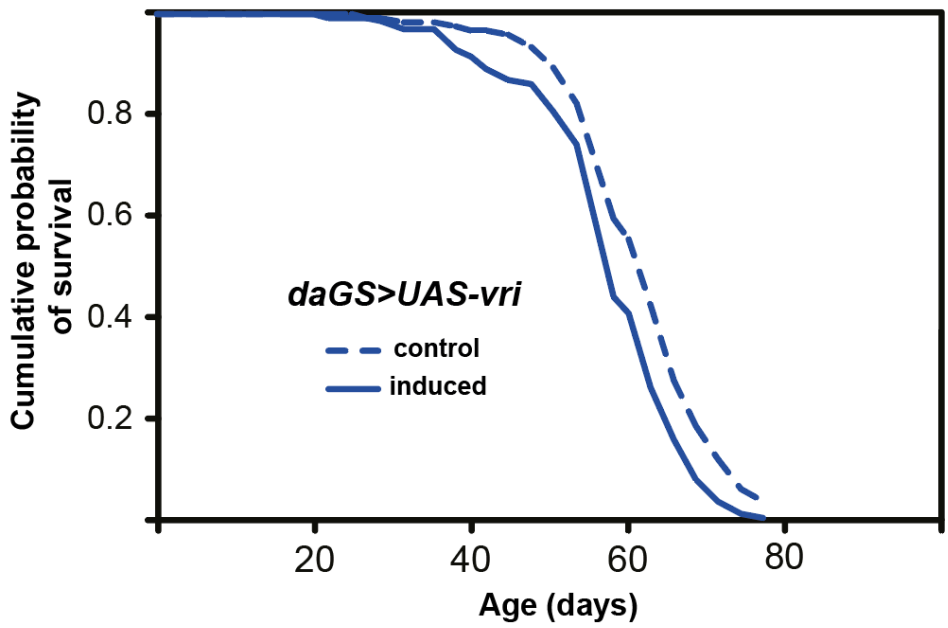

Figure 5.10 Ubiquitous over-expression of *vri* shortened the lifespan of female flies

Ubiquitous over-expression of *vri* in adulthood using the *daGS* driver induced by RU (*daGS>UAS-vri*, blue unbroken line, RU+) shortened the lifespan compared to un-induced female flies (blue broken line, RU-). P=0.008 by log-rank test. The genotypes used were: *daGS>UAS-vri.*

5.3.3 Adult-onset over-expression of *dGABPα* extended lifespan.

I then assessed whether direct activation of *dGABPα* was sufficient to extend lifespan. Adult ubiquitous over-expression of *dGABPα* resulted in a modest but significant lifespan extension in female flies (Figure 5.11), with an increase in median survival of 8.9% ($p=1.93 \times 10^{-8}$). qRT-PCR confirmed the increase in transcript level of *dGABPα* following induction with RU486 administration (Figure 5.13). In addition, ubiquitous knockdown of *dGABPα* using RNAi significantly shortened lifespan in female flies (Figure 5.12, $p=3.6 \times 10^{-20}$), and qRT-PCR confirmed the reduced transcript levels of *dGABPα* by ~20% in these flies (Figure 5.13). Interventions that extend fly lifespan are often associated with reduced fecundity (Bjedov et al., 2010, Alic et al., 2011b, Broughton et al., 2010, Slack et al., 2015). I therefore assessed whether *dGABPα* over-expression affects reproductive ability. Although there was a trend towards a reduction in egg laying in response to *dGABPα* over-expression, this did not reach statistical significance (Figure 5.14). Therefore, our results show that *dGABPα* is a modulator of longevity.

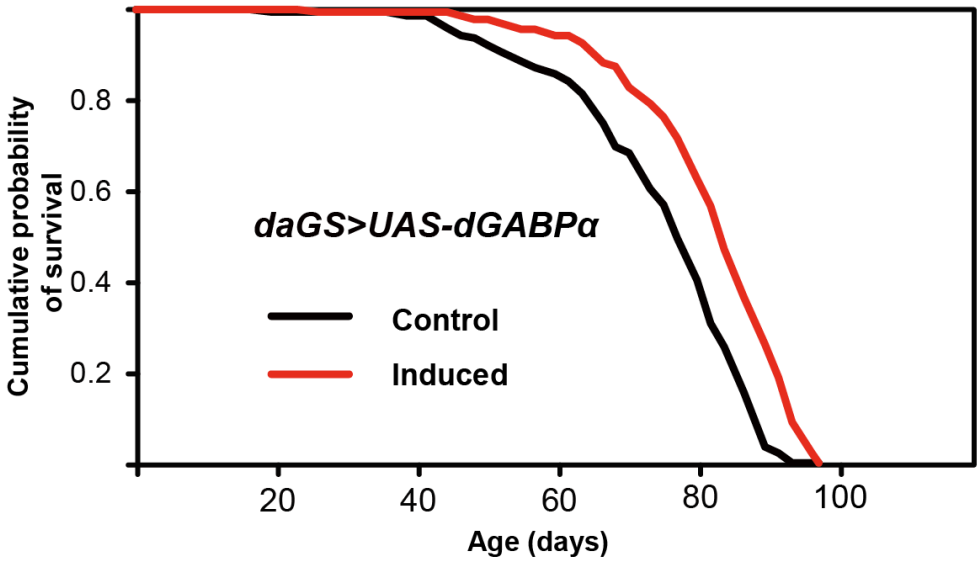

Figure 5.11 Over-expression of *dGABPα* in adulthood extended the lifespan in female flies.

Ubiquitous over-expression of *dGABPα* in adulthood using the *daGS* driver induced by RU (*daGS>UAS-dGABPa*, red line, RU+) extended lifespan compared with non-induced controls (black line, RU-). The median lifespan was extended by 9 % $p=1.93 \times 10^{-8}$ by log-rank test. The genotypes used were: *daGS>UAS-dGABPa*.

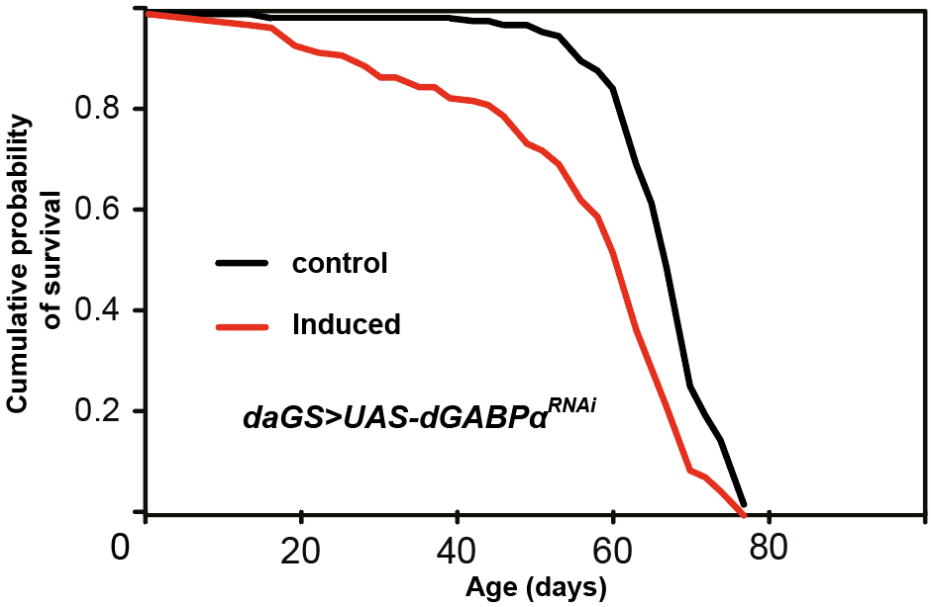

Figure 5.12 Knockdown of *dGABPα* in adulthood using RNAi shortened the lifespan of female flies

Knockdown of *dGABPα* in adulthood using RNAi (*daGS>UAS-dGABPα*^{RNAi}, red line, RU+) resulted in a decrease in lifespan compared with the un-induced control flies (black line, RU-). The median

lifespan was shortened by 13% p=3.6 x 10^{-20} by log-rank test. The genotypes used were: *daGS>UAS-dGABPα^{RNAi}*.

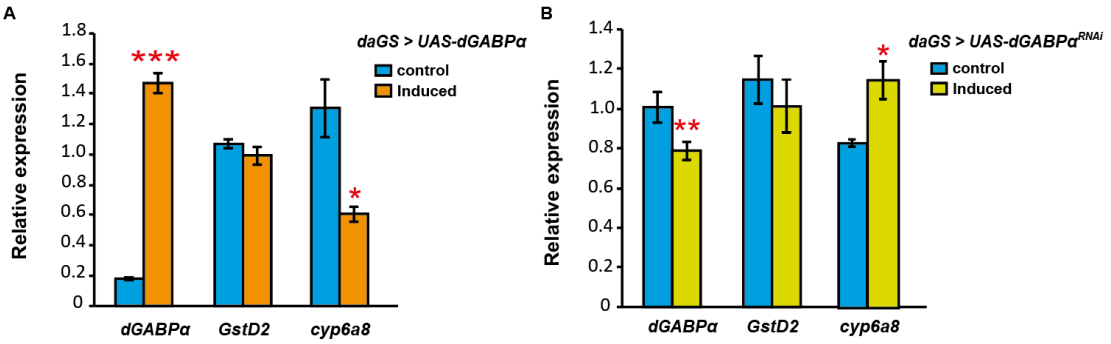

Figure 5.13 *dGABPα* expression levels in flies either over-expressing *dGABPα* or expressing the RNAi construct against *dGABPα*

(A, B) The mRNA levels of *dGABPα*, *GstD2*, and *cyp6a8* were determined by qRT-PCR and normalized to a control gene (*RP49*). The bars are plotted as the means ± SEM, n=4. ***P<0.001, **p<0.01, *p<0.05 by t-test. The genotypes used were: (A*) daGS>UAS-dGABPα* and (B*) daGS>UAS-dGABPα^{RNAi}*.

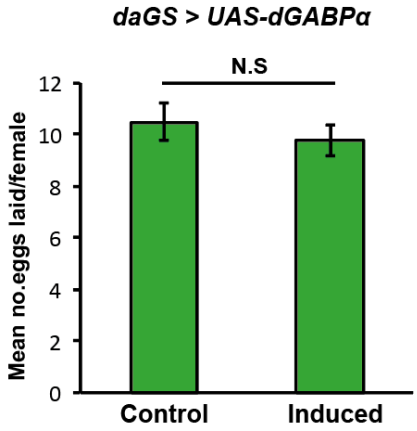

Figure 5.14 Ubiquitous over-expression of *dGABPα* did not affect fecundity

Ubiquitous over-expression of *dGABPα* in adulthood using the *daGS* driver (*daGS>UAS-dGABPα,* RU+) did not alter the average number of eggs laid per female over 24 hours compared to that of un-induced control flies (-RU) at 12-days of age. The bars represent the means ± SEM, p>0.05 by t-test. The genotypes used were: *daGS>UAS-dGABPα*.

I then asked whether *dGABPα*, similar to its mammalian counterpart, is itself downstream of *dPGC-1* (Mootha et al., 2004). Indeed I showed that over-expression of *dPGC-1* significantly increased the transcript levels of *dGABPa* (Figure 5.15, p<0.01), suggesting that *dGABPa* is activated downstream of *dPGC-1*.

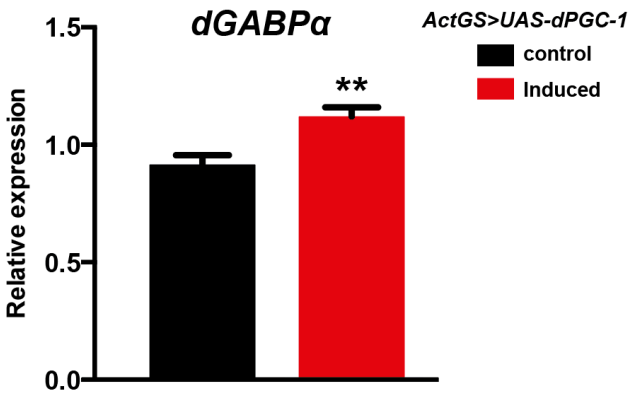

Figure 5.15 Over-expression of *dPGC-1* up-regulated *dGABPα*

Ubiquitous over-expression of *dPGC-1* in adulthood using the *ActGS* driver by induction with RU (*ActGS>UAS-dPGC-1,* red bar, RU+) resulted in an up-regulation of *dGABPa* gene expression. The mRNA levels of *dGABPα* were determined by qRT-PCR and normalized to the control gene (*RP49*). The bars are representative of the means ± SEM, n=4. **P<0.01, by t-test. The genotypes used were: *ActGS>UAS-dPGC-1*.

5.3.4 The tissue-specific over-expression of *dGABPα* extended lifespan

The *Drosophila* brain, gut, and fat body, the latter functionally being equivalent to the mammalian liver and adipose tissue, have an evolutionarily conserved function in ageing (Fontana et al., 2010). I therefore examined whether confining *dGABPα* over-expression to these organs is sufficient to extend lifespan. Using the inducible, pan-neuronal *elavGS* driver or the gut- and fat body-specific *S$_1$106* driver, I over-expressed *dGABPα* specifically within these tissues. In each case, induction of expression with RU486 resulted in a significant extension of lifespan (Figures 5.16 and 5.17, median lifespan extensions were 6% and 3%, p=4.8 x 10^{-8}, p=0.002, respectively). Taken together, these data clearly show that over-expression of *dGABPα* in the brain as well as in the gut and fat body is sufficient to extend lifespan.

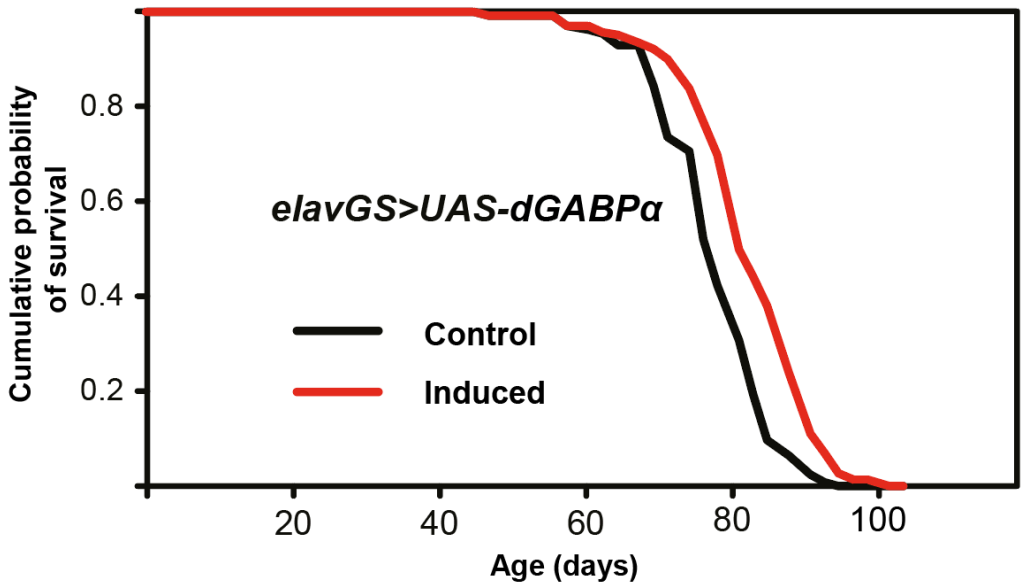

Figure 5.16 Over-expression of *dGABPα* in adult neurons extended the lifespan in female flies

Neuronal expression of *dGABPa* in adulthood using the *elavGS* driver induced by RU (*elavGS>UAS-dGABPa*, red line, RU+) extended the lifespan compared to non-induced control flies (black line, RU-). The median lifespan was extended by 6%, p=4.8 x 10^{-8} by log-rank test. The genotypes used were: *elavGS>UAS-dGABPα*.

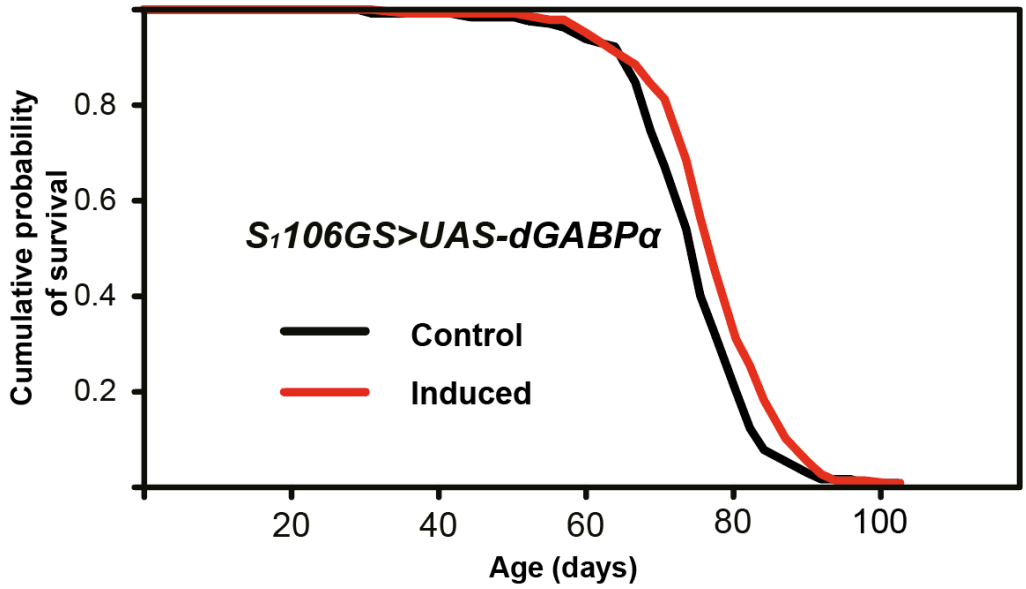

Figure 5.17 Over-expression of *dGABPα* in the adult gut and fat body extended the lifespan in female flies

Over-expression of *dGABPα* in the adult gut and fat body using the *S1106GS* driver induced by RU (*S1106GS>UAS-dGABPα*, red line, RU+) extended the lifespan compared with un-induced female flies (black line, RU-). The median lifespan was extended by 3% p=0.003 by log-rank test. The genotype used was: *S1106GS>UAS-dGABPα*.

5.3.5 Energy production was uncoupled from energy consumption in *dGABPα*-over-expressing flies

Long-lived invertebrate mutants often display a reduction in the rate of cellular functions, with a slowing in energy metabolism, and a lower accumulation of age-related stress. This manifests in resistance to various stressors, including oxidative stress and xenobiotic stress (Castillo-Quan et al., 2016, Broughton et al., 2005, Afschar et al., 2016, Braeckman et al., 1999, Lakowski and Hekimi, 1996). Animal models lacking *dGABPα* exhibit mitochondrial dysfunction (Baltzer et al., 2009, Yang et al., 2014). It is therefore interesting to assess whether *dGABPα* gain-of-function leads to an improvement in mitochondrial function. To test this hypothesis, I determined whether up-regulation of *dGABPα* increased mitochondrial activity by measuring four independent mitochondrial markers: ATP production, mitochondrial mass, mitochondrial protein synthesis and oxygen consumption. Firstly, I found that over-expression of *dGABPα* significantly increased ATP production by approximately 50% (Figure 5.18), suggesting an increased steady state of mitochondrial homeostasis. I then measured the amount of mtDNA, relative to the amount of the nuclear DNA (nDNA) amplicon, in heads and thoraxes of young and old flies expressing *dGABPα*. Interestingly, there was no significant difference in mitochondrial mass between *dGABPα*-over-expressing flies and wild type controls at either young or old age. There was however a significant increase in aged *dGABPα*-over-expressing flies compared to their younger counterparts (Figure 5.19). In addition, immunoblots with antibodies against NDUFS3, one of the complex I subunits of the ETC, did not show any significant difference between flies over-expressing *dGABPα* and un-induced controls (Figure 5.20).

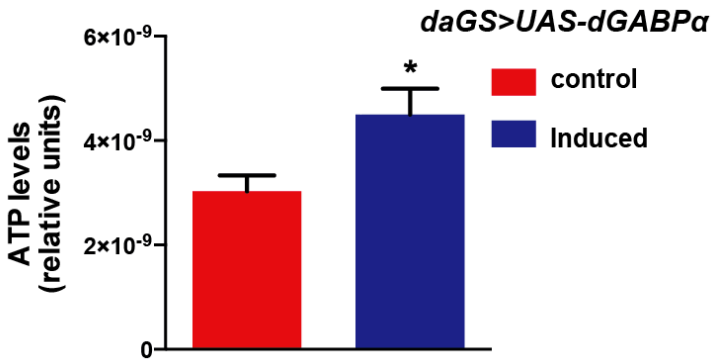

Figure 5.18 ATP levels were increased in *dGABPα*-over-expressing flies.

Ubiquitous over-expression of *dGABPα* using the *daGS* driver induced with RU (*daGS>UAS-dGABPα*, blue bar, RU+) resulted in increased ATP levels compared to un-induced control female flies (red bar, RU-). ATP levels were measured in 40-day-old whole fly lysates with the ovaries removed. The bars represent the means ± SEM (n=6), *p<0.05 by t-test. The genotype used was: *daGS>UAS-dGABPα*.

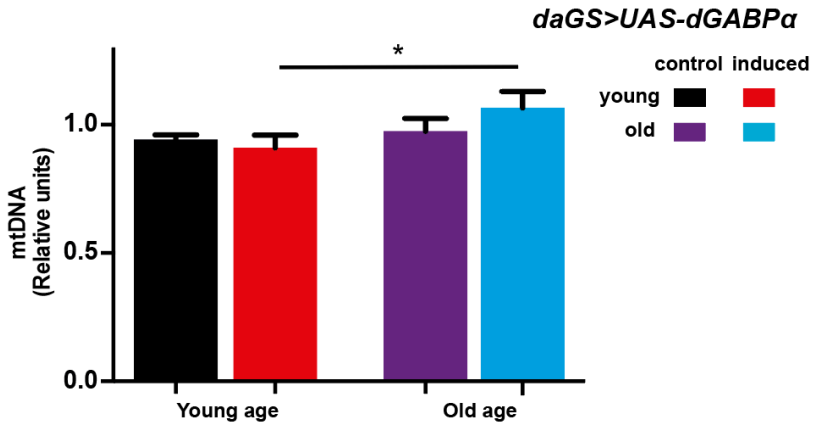

Figure 5.19 Over-expression of *dGABPα* did not alter the mitochondrial mass in young or older flies

Mitochondrial DNA (mtDNA), relative to the nuclear DNA (nDNA) amplicon, was measured by qRT-PCR in the heads and thoraxes of flies over-expressing *dGABPα* (+RU) and un-induced controls (-RU) at 12 or 40 days of age. A significant increase was observed in old flies over-expressing *dGABPα* (*daGS>UAS-dGABPα,* blue bar, RU+) compared to young flies over-expressing *dGABPα* (red bar). The bars represent the means ± SEM (n=4, *p<0.05 by ANOVA). The genotype used was: *daGS>UAS-dGABPα*.

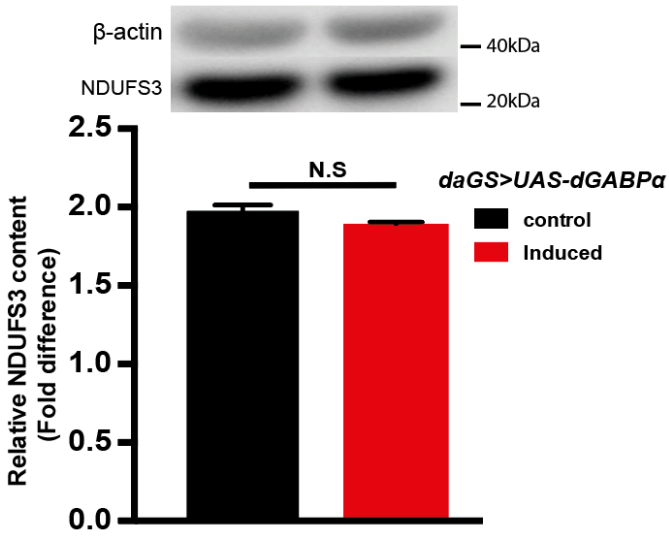

Figure 5.20 Over-expression of *dGABPα* did not alter NDUFS3 protein levels

Western blot analysis of NDUFS3 in 14-day-old flies demonstrated that ubiquitous over-expression of *dGABPα* using the *daGS* driver induced by RU486 (*daGS>UAS-dGABPα*, red bar, RU+) did not alter the protein levels of NDUFS3 compared to un-induced controls (black bar RU-). The protein levels were normalized to β-actin. The bars represent the means ± SEM (n=3). The image is a representative gel from one biological repeat. The genotype used was: *daGS>UAS-dGABPα*.

Finally, I sought to analyse the effect of elevated *dGABPα* expression on mitochondrial respiratory chain activity. The rate of oxygen consumption was measured using the Oroboros Oxygraph-2k on fly heads rather than whole fly lysates, enabling a more defined and tissue-specific signal. The steps in respiration were compared in mitochondria separated from *dGABPα*-over-expressing fly head homogenates and controls by using substrates, uncouplers, and inhibitors specific to individual respiratory complexes. In doing so, I observed there was no significant difference in the oxygen consumption rate (OCR) for Complex I-, and II-dependent respiration (Figure 5.21). Moreover, there was no significant difference in OCR in state 2, state 3, or in the maximum uncoupled state between flies over-expressing *dGABPα* and controls (Figure 5.21). This is consistent with the observations of mitochondrial mass and mitochondrial-related protein levels, suggesting that over-expression of *dGABPα* does not change energy consumption. Taken together, these data suggest that over-expression of *dGABPα* increases ATP production, but this is uncoupled from mitochondrial respiration rates.

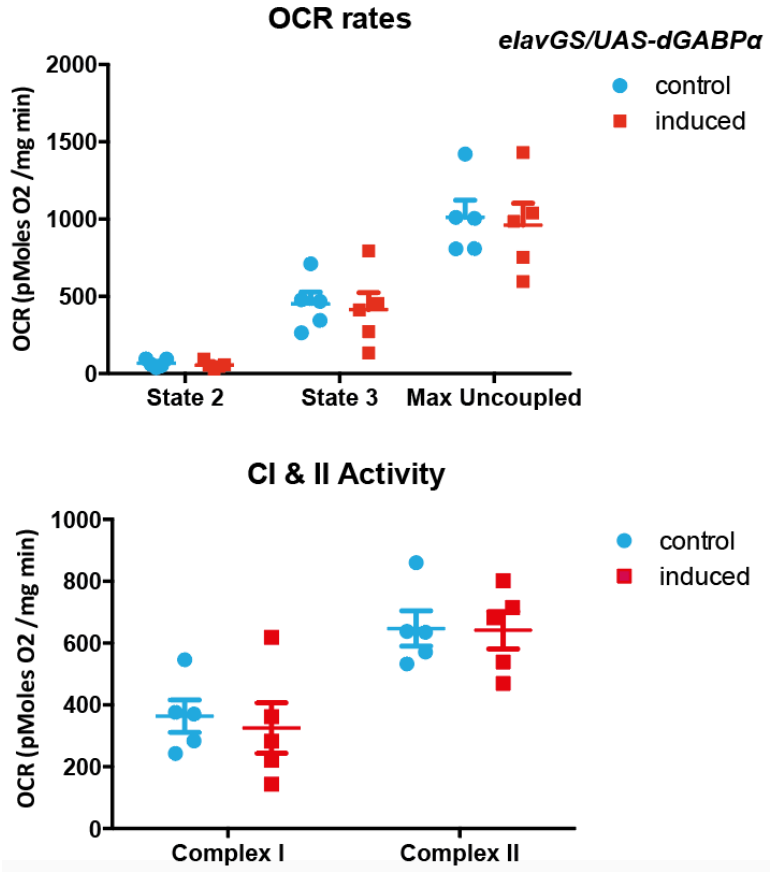

Figure 5.21 Oxygen consumption rates were not altered in *dGABPα*-over-expressing fly heads

Oxygen consumption rate (OCR) were measured in the heads of flies over-expressing *dGABPα* (RU+) and un-induced controls (RU-) at day 14. There was no significant difference in OCR in state 2, state 3, and in the maximum uncoupled state, or for Complex I- and II-dependent respiration. The values are plotted as the means ± SEM, n=5, p>0.05 by t-test. The genotype used was: *elavGS>UAS-dGABPα.* These experiments were performed in collaboration with Dr.Vassilios N Kotiadis.

5.3.6 Over-expression of *dGABPα* increased the resistance to phenobarbital stress

I then assessed whether the long-lived flies over-expressing *dGABPα* were resistant to different stressors. I tested the survival of *dGABPα*-over-expressing flies under starvation conditions and on exposure to oxidative stress with H_2O_2 and paraquat, and phenobarbital. Here we show that *dGABPα* over-expression did not significantly affect survival compared to controls under starvation conditions or when challenged with H_2O_2 (Figure 5.22, p=0.3, p=0.7 respectively). However, flies over-expressing *dGABPα* exhibited a small but significant increase in sensitivity to paraquat (Figure 5.22, p<0.05). In addition, flies over-expressing *dGABPα* were significantly resistant

to phenobarbital stress (Figure 5.22, p=1.75 x 10^{-11}). Taken together these results suggest that *dGABPα* may extend lifespan through increased detoxification of endobiotic and xenobiotic compounds.

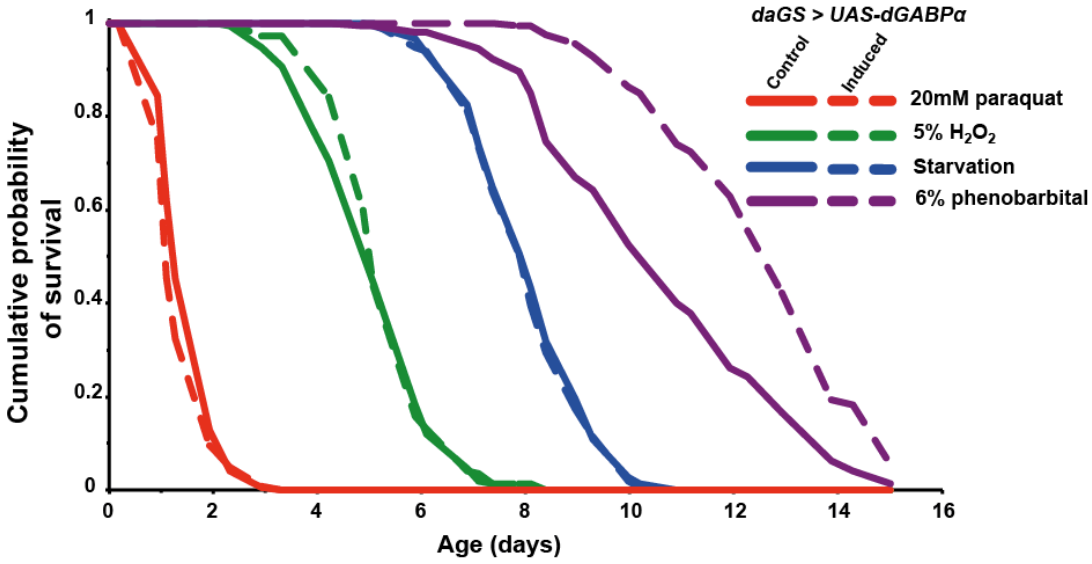

Figure 5.22 The effect of ubiquitous over-expression of *dGABPα* in adulthood on exposure to various stressors in female flies

The survival curves of flies over-expressing *dGABPα* in adulthood (RU+) or un-induced control flies (RU-) using the inducible *daGS* driver. Flies were pre-treated with RU for 14 days and then transferred to either agar-only food for starvation assays (p=0.7), or to sugar/agar food supplemented with paraquat (p=0.04), H_2O_2 (p=0.33) or phenobarbital (p=1.75 x 10^{-11} by log-rank test). The genotype was: *daGS>UAS-dGABPα.*

Increased resistance to phenobarbital stress in *dGABPα* over-expressing flies may rely on the UPS (Ubiquitin-Proteasome System), the lysosomal-autophagy pathway, and the chaperone network, acting to maintain cellular protein homeostasis by removing unwanted or damaged proteins that could become toxic to cells (Jung et al., 2009, Glickman and Ciechanover, 2002, Ross et al., 2015, Lopez-Otin et al., 2013). I therefore investigated whether over-expression of *dGABPα* affects proteasomal activity and autophagy. Here I show that the 26S proteasomal activity was significantly increased in flies over-expressing *dGABPα* compared to controls (Figure 5.23). Immunoblots with antibodies against the alpha subunit of the 26S proteasome complexes demonstrated that levels of the 26S were not altered in flies over-expressing *dGABPα* compared to controls (Figure 5.24). This suggests that over-

expression of *dGABPα* may increase the assembly of the proteasome and therefore its activity, rather than the total load of the proteasomal machinery. In addition, western blot analysis with an antibody against the fly LC-3 orthologue, Atg8, demonstrated no significant change in Atg8-I levels or Atg8-II levels in response to *dGABPα* over-expression (Figure 5.25). Even the ratio of Atg8-II/Atg8-I was not changed, indicating no change in autophagasome formation (Figure 5.25). Taken together, over-expression of *dGABPα* increased proteasome activity but not autophagy.

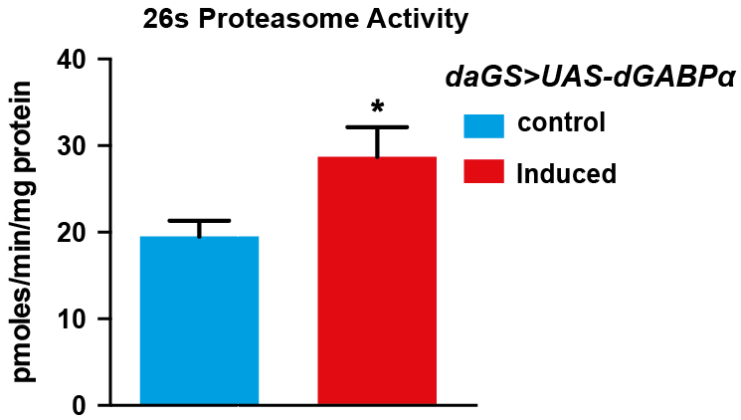

Figure 5.23 Over-expression of *dGABPα* increased proteasome activity

Proteasome activity, as measured using the fluorogenic peptide substrate LLVY-AMC, was increased in flies over-expressing *dGABPα* (*daGS>UAS-dGABPα*, red bar, +RU) compared to non-RU induced controls (blue bar, RU-). The bars are plotted as the means of activity (pmol/min/mg protein) ± SEM. *p<0.05, n=6 by t-test. The genotype used was: *daGS>UAS-dGABPα*.

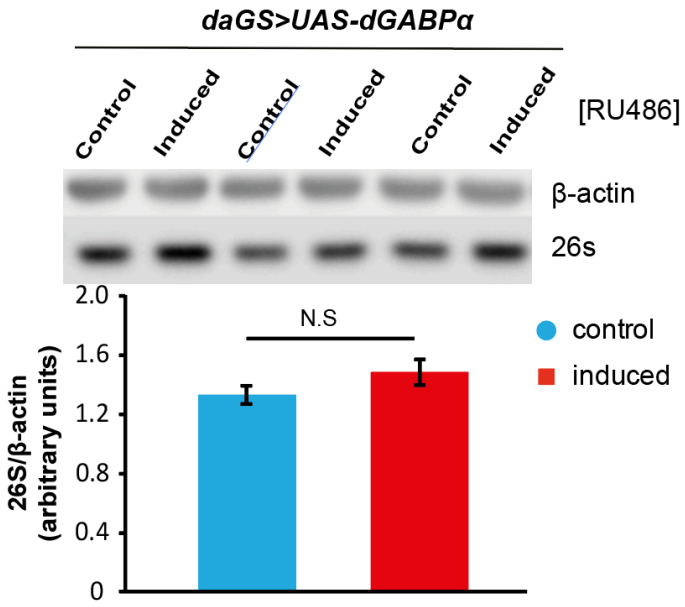

Figure 5.24 Ubiquitous over-expression of *dGABPα* in adulthood did not alter the protein levels of the 26S proteasome

Western blot analysis with an antibody against the alpha subunit of the 26S proteasome demonstrated no significant change in the amount of the alpha subunit protein in *dGABPα*-over-expressing flies (*daGS>UAS-dGABPα,* red bar, +RU) compared with age-matched non-RU induced control flies (blue bar, RU-). The bars represent the means ± SEM, n=3 by t-test. The genotype used was: *daGS>UAS-dGABPα*.

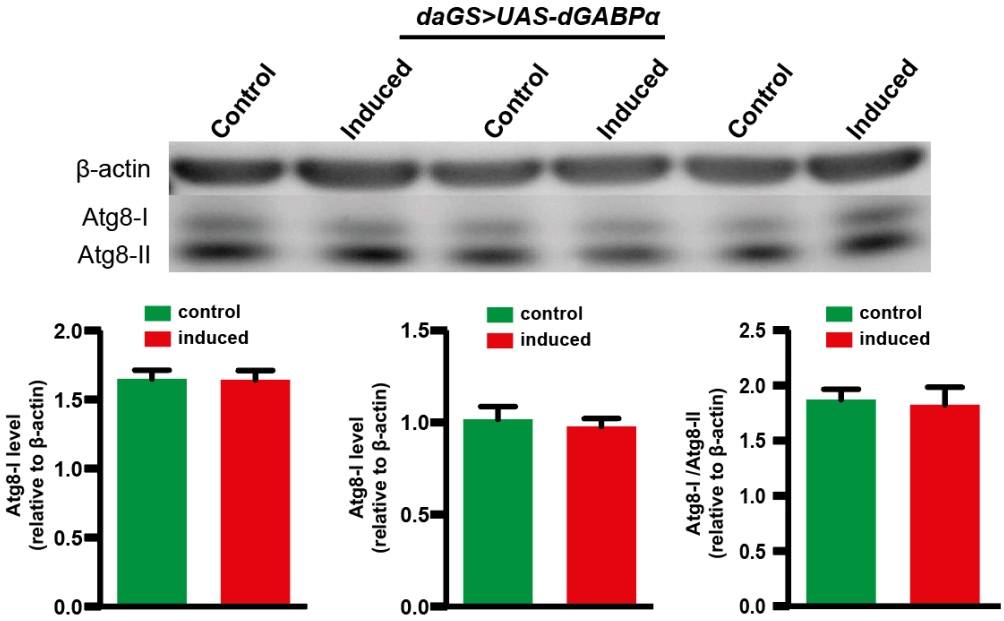

Figure 5.25 Flies over-expressing *dGABPα* did not show any change in autophagy

Western blot analysis with an antibody against the fly LC-3 orthologue, Atg8, demonstrated no significant change in Atg8-I levels (normalized to β-actin levels), Atg8-II levels or the Atg8-II/Atg8-I

ratio in flies over-expressing *dGABPα* (*daGS>UAS-dGABPα*, red bars, RU+) compared with age-matched non-RU induced control flies (green bars, RU-) at day 14. The bars represent the means ± SEM, n=3 by t-test. The genotype used was: *daGS>UAS-dGABPα.*

5.3.7 Over-expression of *dGABPα* extended the lifespan via mechanisms beyond those of DR

To explore the mechanisms of lifespan extension by *dGABPα* activation, I first investigated whether over-expression of *dGABPα* was acting as a DR mimetic. DR is a well-established anti-ageing intervention that extends healthy lifespan in diverse species (Fontana and Partridge, 2015, de Cabo et al., 2014), and some genetic interventions that extend lifespan have features of DR mimetics (Ingram and Roth, 2015, de Cabo et al., 2014). To determine whether *dGABPα* and DR extend lifespan by similar mechanisms, I assessed whether *dGABPα* can extend lifespan beyond the maximum achievable by DR. To maximize lifespan under DR, the yeast concentrations were varied in the food, while maintaining a constant concentration of sucrose (Bass et al., 2007), resulting in a typical tent-shaped response, with a peak median lifespan with food containing a 1.0 yeast concentration (Figure 5.26 A and B). If *dGABPα* activation and DR share overlapping pathways, then activation of *dGABPα* would not be able to further extend lifespan already maximized by DR (Castillo-Quan et al., 2016, Gems et al., 2002, Broughton et al., 2010, Bjedov et al., 2010). Activation of *dGABPα* significantly extended median lifespan in the yeast condition that maximized lifespan (1.0 yeast; $p=1.93 \times 10^{-8}$), in full feeding (2.0 yeast; $p=3.9 \times 10^{-5}$), and under reduced yeast concentrations (0.5 yeast; $p=2.94 \times 10^{-7}$), with the greatest extension of median lifespan seen using 2.0 SY food (Figures 5.26 A and B). Cox proportional hazards (CPH) analysis confirmed that the response to RU was not significantly different across the different yeast concentrations on the right side of the DR-tent (Table 3, p=0.11), suggesting that over-expression of *dGABPα* extended the lifespan via mechanisms independent to those of DR and beyond DR. Interestingly, *dGABPα* over-expression significantly reduced lifespan (Figure 5.26 A and B, $p=3.27 \times 10^{-14}$) on the 'starvation-inducing' yeast concentration of 0.1 SY food. CPH analysis confirmed that the response to RU was modulated by food on the 'starvation side' of the DR tent (Table 2, p=0.02), suggesting that the effect of over-expression of *dGABPα* on lifespan is dependent on nutrient-availability.

A

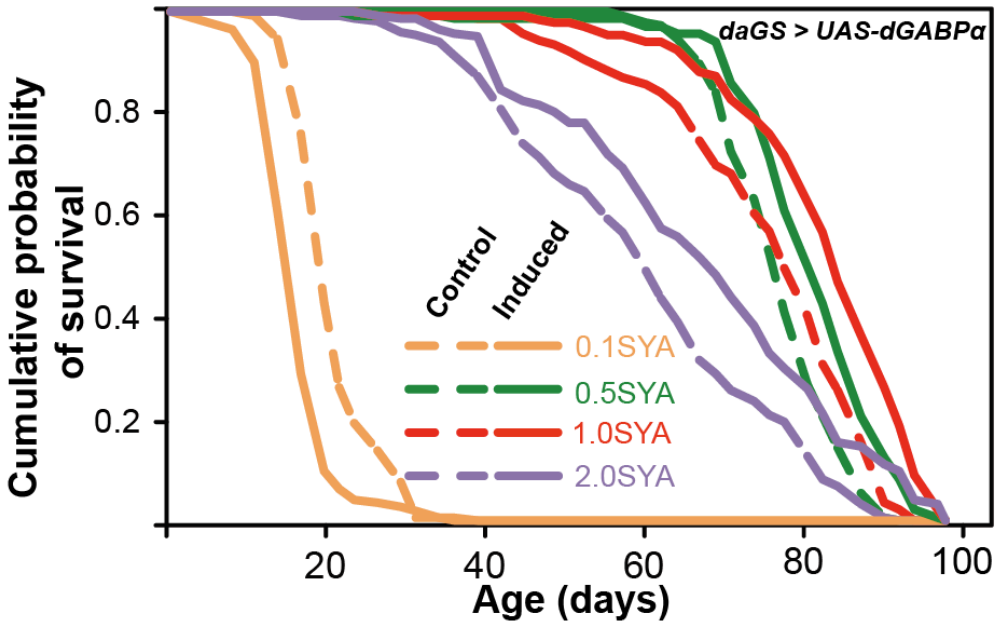

B

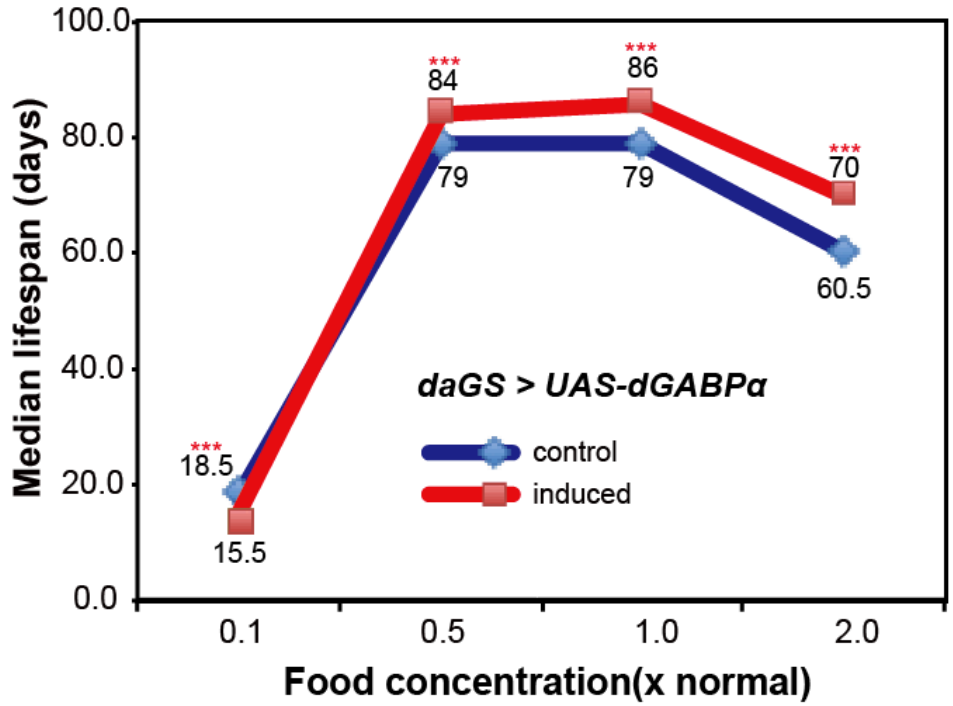

Figure 5.26 Ubiquitous over-expression of *dGABPα* extended the lifespan via mechanisms independent of those of DR

(A) The survival curves of female flies ubiquitously over-expressing *dGABPα* in adulthood using the *daGS* driver induced by RU (*daGS>UAS-dGABPα*, RU+, full lines) compared to non-induced controls (RU-, dash lines). The RU was supplemented into food containing different yeast concentrations (0.1x, 0.5x, 1.0x, and 2.0x yeast concentrations). (B) The median lifespans are plotted at four different yeast concentrations: over-expression of *dGABPα* extended lifespan under the 0.5x, 1.0x, and 2.0x dietary

conditions tested. Over-expression of *dGABPα* significantly shortened the lifespan on the 0.1x yeast containing diet. ***P<0.001 by log-rank test; n=145 flies per condition. The genotype used was: *daGS>UAS-dGABPα*.

```
coxph(formula = S ~ a$RU * a$diet)

  n= 1149, number of events= 1136

                  coef  exp(coef)   se(coef)      z Pr(>|z|)
a$RU        -0.0008422  0.9991582  0.0005882 -1.432   0.1522
a$diet      -0.2919340  0.7468178  0.0746905 -3.909 9.28e-05 ***
a$RU:a$diet -0.0012515  0.9987493  0.0005597 -2.236   0.0254 *
---
Signif. codes:  0 ‘***’ 0.001 ‘**’ 0.01 ‘*’ 0.05 ‘.’ 0.1 ‘ ’ 1
```

Table 2 CPH analysis of the survival of flies over-expressing *dGABPα* on different yeast concentrations of food

CPH analysis showed that there is an interaction between the response to different diets and the response to over-expression of *dGABPα* (p=0.02). This means that the response to RU (absence or presence of *dGABPα* over-expression) is modulated by diet. Flies fed with ‘starvation-inducing’ low yeast food (0.1SY) were shorter lived in response to *dGABPα* over-expression, while flies fed with any other diets were longer lived in response to *dGABPα* over-expression. Therefore the responses to RU across all the diets are not in same direction (p=0.15).

```
coxph(formula = Surv(b$day, b$event) ~ b$RU * b$diet)

  n= 856, number of events= 845

                  coef  exp(coef)   se(coef)      z Pr(>|z|)
b$RU        -0.0020446  0.9979575  0.0007711 -2.652  0.00801 **
b$diet       0.5423485  1.7200417  0.0812000  6.679  2.4e-11 ***
b$RU:b$diet -0.0009132  0.9990872  0.0005841 -1.563  0.11798
---
Signif. codes:  0 ‘***’ 0.001 ‘**’ 0.01 ‘*’ 0.05 ‘.’ 0.1 ‘ ’ 1
```

Table 3 CPH analysis of the survival of flies over-expressing *dGABPα* on DR and full-feeding food

CPH analysis showed that there is no interaction between the response to different diets (DR food and full-feeding food) and the response to over-expression of *dGABPα* (p=0.11). This means that the response to RU is not modulated by food. Therefore over-expression of *dGABPα* extends lifespan independently of DR and beyond DR.

5.3.8 Next-generation Transcriptome profiling

In order to determine the molecular mechanisms by which *dGABPα* over-expression mediates its pro-longevity effects, I undertook next generation sequencing to analyse the transcript profile in flies over-expressing *dGABPα*. RNAseq analysis was

performed at the Glasgow Polyomics Unit, and the bioinformatics analysis was performed in collaboration with Dr. Dobril Ivanov. Given that the brain specific over-expression of *dGABPα* using the inducible *elavGS* driver significantly extended lifespan (Figure 5.16), I sought to investigate the brain specific transcriptional response to *dGABPα* over-expression. Fly heads over-expressing *dGABPα* for 10 days were subjected to RNAseq analysis and compared to non-RU induced controls, and 4 replicates each condition were used. According to FDR correction for multiple hypothesis testing, which is an acronym for adjusted p-value, there is around 50 differentially expressed genes in response to *dGABPα* over-expression, including genes involved in memory, learning, synaptic formation and in the perception of sound and pain (Figure 5.27). For example, *SIFaR* (SIFamide receptor) was up-regulated in response to *dGABPα* over-expression. This is a G-protein coupled peptide receptor involved in both neuropeptide and the G-protein coupled receptor signalling pathways. It is required for the sensory perception of pain and is involved in sexual behaviour and the determination of lifespan (Figueroa-Clarevega and Bilder, 2015, Paik et al., 2012). In addition, *dGABPα* regulated several genes involved in insulin signalling pathway, including up-regulated *nord*, *daw*, *ImpL2*, and down-regulated *Glt*, *tobi*, and *Gnmt*, suggesting that over-expression of *dGABPα* might regulate IIS.

Figure 5.27 Heat-map of the genes differentially expressed in fly heads over-expressing dGABPα

Heat-map showing genes that were significantly up-regulated (red colour) or down-regulated (blue colour) in fly heads over-expressing *dGABPα* (RU+) compared to non-induced controls (RU-). The intensity of the color represents the statistical significance. N=4 per condition, P<0.05 for statistically

significant changes according to multiple hypothesis testing. Genotypes used were: *elavGS>UAS-dGABPα.*

I then sought to look at the gene ontology (GO) annotations using Catmap analysis (Breslin et al., 2004). GO categories include three classes: Biological Process ontology, Cellular Component ontology and Molecular Function ontology. The Biological Process ontology includes terms that represent collections of processes as well as terms that represent a specific, entire process that the gene product is involved in. The Cellular Component ontology describes locations, at the levels of subcellular structures and macromolecular complexes. The Molecular Functions of a gene product are the functions that it performs or the "properties" that it has. These may include transporting molecules around, binding to molecules, holding molecules together and changing one molecule into another. This is different from the Biological Processes, which involve more than one activity. Down-regulated GOs mean that the results represent GO categories are significantly enriched in genes that are mainly down-regulated, while up-regulated GO categories are enriched in genes that are predominantly up-regulated. For GO analysis, all genes were used along with p-values (not-adjusted for multiple hypothesis testing), and the statistical significance of the GO categories is calculated using p-value-adjusted FDR correction for multiple hypothesis testing. Here I have listed the top 10 GO categories in each class (Figure 5.28). For example, over-expression of *dGAPBα* up-regulated biological processes including 'development', 'regulation of signalling pathway', and 'regulation of response to stimulus'， while down-regulated biological processes including 'nitrogen compound metabolic process (cellular amino acid metabolic process)', 'translation', and 'oxidation-reduction process'. In terms of molecular function, over-expression of *dGAPBα* up-regulated 'transcription factor activity' and 'protein kinase activity', while down-regulated 'ribosome', 'translation activity', and 'electron carrier activity'. In addition, over-expression of *dGAPBα* up-regulated cellular components mainly involved in membrane, neurons, synapses and axon, while down-regulated GO terms involved in mitochondrion, respiratory chain complex, lipid particle and ribosome.

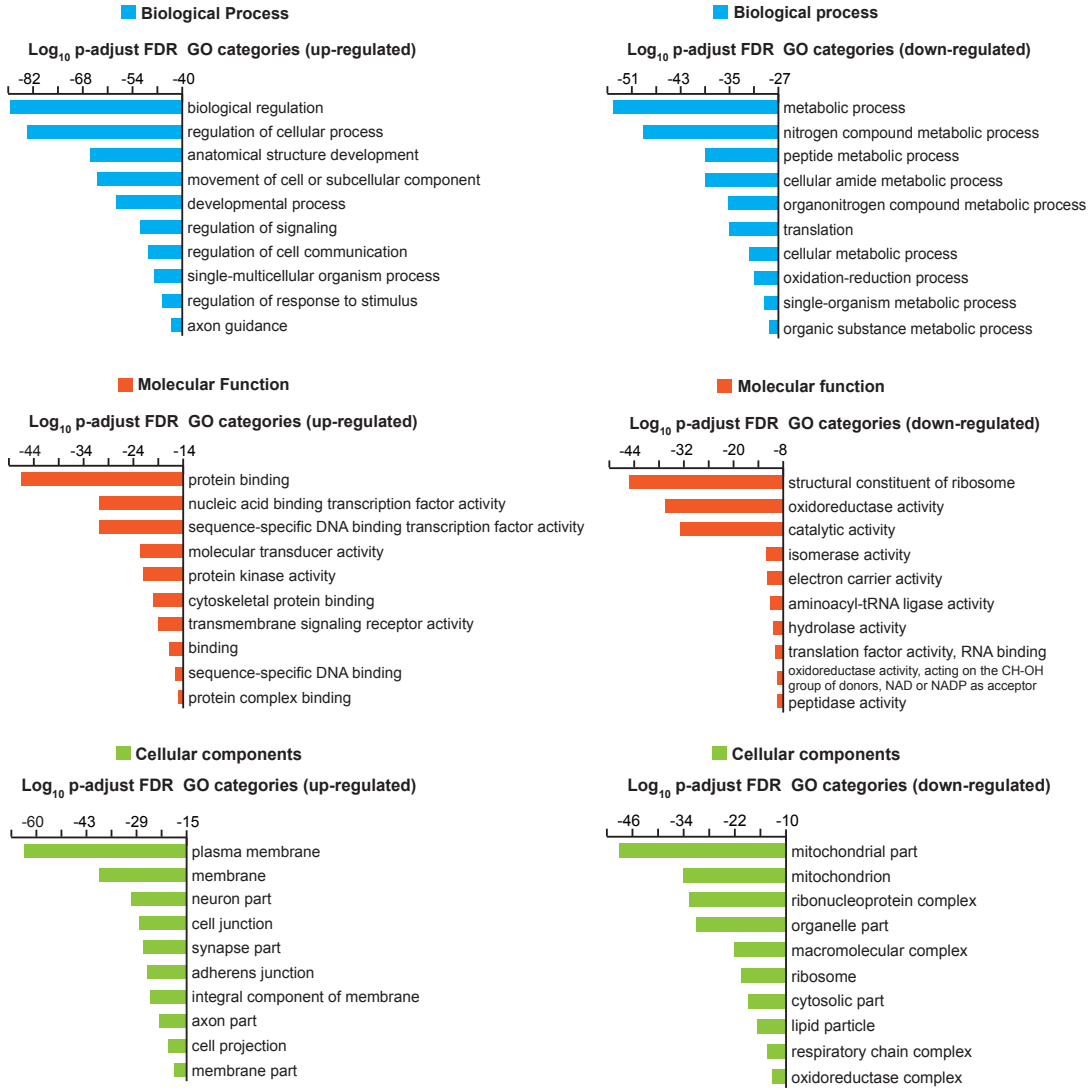

Figure 5.28 GO categories of fly heads over-expressing *dGAPBα*

The graphs showthe top 10 GO categories that significantly enriched in genes that are mainly up-regulated (left side) or down-regulated (righ side) in response to *dGAPBα* over-expression in fly heads using inducible *elavGS* driver (RU+) compared to non-induced control (RU-). GO terms are classified into 3 different groups, including Biological Process (blue colour), Molecular Function (orange colour) and Cellular Components (green colour). GO annotations have been analyzed using Catmap, and calculated using p-value-adjusted FDR correction for multiple hypothesis testing. N=4 per condition, $p<0.05$ for statistically significance. Genotypes used were: *elavGS>UAS-dGABPα.*

5.3.9 Over-expression of *dGABPα* extended lifespan in overlapped mechanisms with reduced IIS likely through up-regulation of *ImpL2*

As described above, overexpression of *dGAPBα* regulates several genes involved in insulin signalling pathway. Among those differentially expressed genes that were up-

regulated in response to *dGABPα* over-expression, ImpL2 is particularly interesting. ImpL2 (Imaginal morphogenesis Protein-late 2), the ortholog of the mammalian insulin-like growth factor-binding protein 7 (IFGBP7), resembles IGFBP7 in sequence and acts as a negative regulator of IIS during development, regulating growth cell-non-autonomously (Sloth Andersen et al., 2000, Alic and Partridge, 2008, Honegger et al., 2008). ImpL2 is a secreted protein belonging to the immunoglobulin superfamily that forms a protein complex with the circulating dilps, and inhibits their ability to bind the insulin receptor, thus reducing IIS (Sloth Andersen et al., 2000, Alic et al., 2011b). In addition, a modest over-expression of *ImpL2* extends lifespan in association with reduced IIS (Alic et al., 2011b, Paik et al., 2012). Therefore, I hypothesised that over-expression of *dGABPα* may mediate lifespan extension through mechanisms that up-regulate *ImpL2* to down-regulate IIS. Although the direct evidence showing that ImpL2 mediates the lifespan extension of *dGABPα* over-expression is still lacking, it is possible that activation of *dGABPα* may reduce insulin signalling and therefore affect IIS-related traits.

It is known that down-regulation of IIS extends lifespan in diverse organisms (Piper et al., 2008). To further assess whether *dGABPα* activation extends lifespan through reduced IIS, I investigated whether *dGABPα* over-expression can further extend the lifespan of flies that already have reduced IIS. To do this I tested the lifespan effect of *dGABPα* over-expression on flies co-expressing the INR^{DN} (Slack et al., 2011). Adult-onset, ubiquitous over-expression of either *dGABPα* or the INR^{DN} significantly extended lifespan (Figure 5.29, the median lifespans were increased by 7% and 9.8%, $p=3.04 \times 10^{-7}$ and p=0.0001, respectively). In addition, co-expressing *dGABPα* and INR^{DN} also extended lifespan (Figure 5.29, the median lifespan extension was 9.7%, $p= 3 \times 10^{-8}$). To compare the extent of lifespan extension between the two interventions, CPH analysis was used. The lifespan extension observed in the INR^{DN} flies was not significantly different to that in the *dGABPα* over-expressing flies in the response to RU486 (Table 4, RU486 by genotype interaction, p=0.76). CPH analysis also confirmed that there was no significant difference between the lifespan extension in INR^{DN} expressing flies and *dGABPα*-INR^{DN} co-expressing flies (Table 4, RU486 by genotype interaction, p=0.43), suggesting that *dGABPα* over-expression and reduced IIS signalling may mediate lifespan extension via overlapping mechanisms.

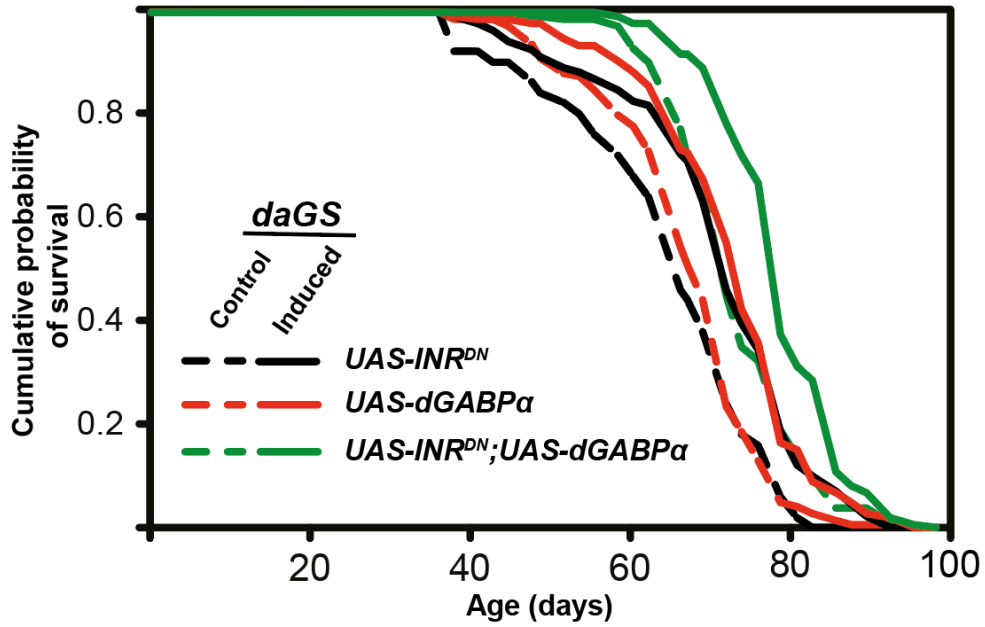

Figure 5.29 Female flies over-expressing *INR^{DN}* and *dGABPα* mediated lifespan extension

The survival curves of flies over-expressing either the dominant negative form of the insulin receptor (*INR^{DN}*, black line), or *dGABPα* (red line), or both INR^{DN} and *dGABPα* (green line, +RU) and non-RU induced controls (broken lines, -RU) are shown. Ubiquitous over-expression of *dGABPα* extended lifespan (p=3.04 x10^{-7}). Ubiquitous over-expression of a dominant negative form of INR also extended lifespan (p=0.0001), and co-expression of both *dGABPα* and the *INR^{DN}* also extended lifespan (p= 3 x 10^{-8}). The lifespans were analyzed by the log-rank test. N=130 flies per condition. The genotypes used were: *daGS>UAS-INR^{DN}, daGS>UAS-dGABPα, daGS> UAS-INR^{DN}; UAS-dGABPα.*

```
  n= 773, number of events= 755

                                    coef exp(coef) se(coef)      z Pr(>|z|)
dataC$RU                         -0.70476   0.49423  0.16625 -4.239 2.24e-05 ***
dataC$genotypedaDELG             -0.13434   0.87429  0.16429 -0.818    0.414
dataC$genotypedaInRDNDELG        -0.71837   0.48755  0.16581 -4.333 1.47e-05 ***
dataC$RU:dataC$genotypedaDELG     0.06181   1.06376  0.20392  0.303    0.762
dataC$RU:dataC$genotypedaInRDNDELG 0.16112   1.17483  0.20340  0.792    0.428
---
Signif. codes:  0 '***' 0.001 '**' 0.01 '*' 0.05 '.' 0.1 ' ' 1
```

Table 4 CPH analysis of the survival of flies co-expressing *dGABPα* and *INR^{DN}*

CPH analysis demonstrated that three genotypes (*daGS>UAS-INR^{DN}, daGS>UAS-dGABPα, daGS> UAS-INR^{DN}; UAS-dGABPα)* responded to RU in the same way (p=2.24 x 10^{-5}). There was no significant difference between the genotypes *daGS>UAS-INR^{DN}* and *daGS>UAS-dGABPα* (p=0.414). There was a significant difference between the genotypes *daGS>UAS-INR^{DN}* and *daGS> UAS-INR^{DN}; UAS-dGABPα* (p=1.47 x 10^{-5}). There was no significant difference between the genotypes *daGS>UAS-INR^{DN}* and *daGS>UAS-dGABPα* in response to RU (P=0.762). There was also no significant difference between *daGS>UAS-INR^{DN}* and *daGS> UAS-INR^{DN}; UAS-dGABPα* in response to RU (P=0.428). This

means that the three genotypes are responsive to RU in a similar way, suggesting that over-expression of *dGABPα* and over-expression of INR^{DN} extended lifespan via similar mechanisms.

5.3.10 *dGABPα* over-expression and reduced IIS in flies shared overlapping transcriptional responses

I next investigated whether the transcriptional response to *dGABPα* over-expression is similar to that observed when IIS is genetically down-regulated. I used a recently published microarray analysis performed on whole flies over-expressing the dominant negative form of the insulin receptor, INR^{DN}, as a means of reducing IIS (Alic et al., 2011a). I compared the overlap of genes elicited by both interventions, and detected statistical significance for down-regulated genes (Figure 5.30 A, p=0.004). By comparing the overlap of GO categories elicited by both interventions, I found the two most significant overlapping enriched GO terms in both interventions are either up-regulated or down-regulated (Figure 5.30 B, $p=6.5 \times 10^{-87}$ and $p=1.5 \times 10^{-12}$ respectively), suggesting that these two interventions share highly overlapped transcriptional response in same direction. There was also a significant overlap between GOs down-regulated by lowering IIS and those up-regulated by over-expressing *dGABPα* (Figure 5.30 B, $p=8.54 \times 10^{-11}$), suggesting that they may regulate some of the transcriptional responses in opposite ways.

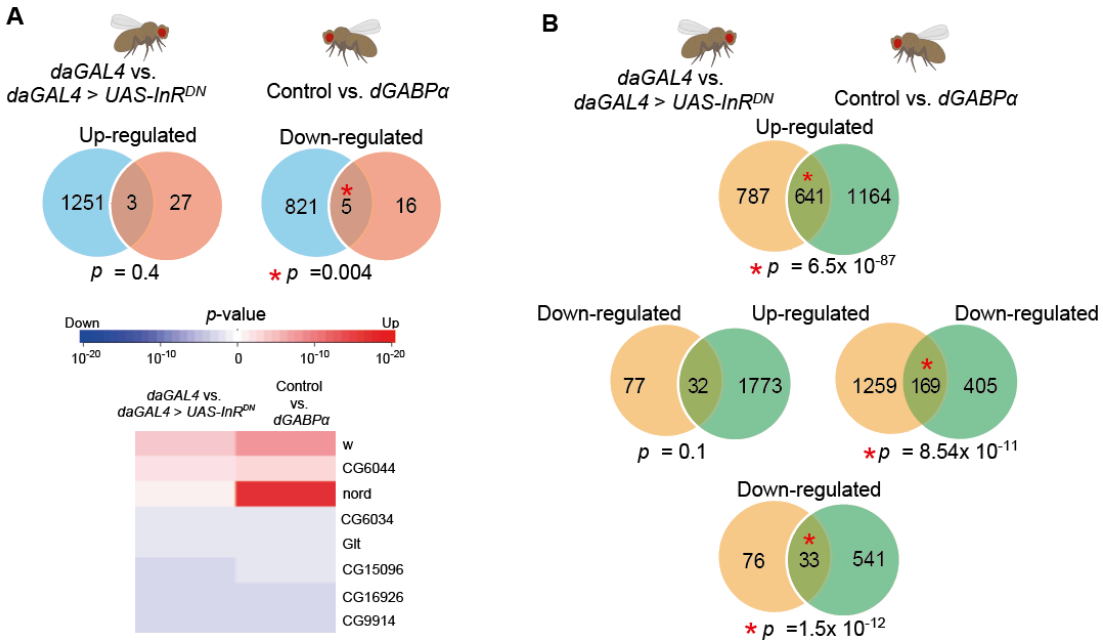

Figure 5.30 Comparative analyses of the transcriptional response of IIS down-regulation and *dGABPα* over-expression.

(A) Venn diagrams showing overlap between genes regulated by IIS down-regulation via the over-expression of a dominant negative version of *InR* (Blue color), and the transcriptional response to *dGABPα* over-expression (red color). P<0.05. The heat map shows genes that were overlapped between the two interventions.

(B) Venn diagrams demonstrating overlapping enriched GO categories regulated by IIS down-regulation (yellow color) and *dGABPα* over-expression (green color). P<0.05. The bioinformatics analysis was performed by Dr. Dobril Ivanov.

5.3.11 *dGABPα* over-expression mediated the lifespan extension of reduced IIS signalling in flies

The long-term beneficial effect of modest reductions in IIS on lifespan is largely dependent on the fine-tuning of the IIS down-regulation and the potential tissue and systemic adaptation. However, when *dGABPα* is genetically knocked-down, *ImpL2* maybe down-regulated, which would reduce binding to the circulating dilps, leading to increased binding to the insulin receptor. Continuous ligand stimulation of the insulin receptor and the resulting increase in IIS activity can be harmful, because it eventually leads to tissue insensitivity to the ligand, which is referred to insulin resistance. I previous showed that down-regulation of *dGABPα* increased the early mortality, which mechanisms might be associated with a constant insulin receptor stimulation and resulting "insulin resistance". Down-regulation of IIS through the co-expression of a dominant negative form of the insulin receptor may further exacerbate

the *dGABPα*-mediated insulin resistance, accelerating mortality. In keeping with this, I showed that adult-onset ubiquitous over-expression of the INR^{DN} significantly extended lifespan (Figure 5.31, p=0.002), and RNAi-mediated ubiquitous knockdown of *dGABPα* shortened lifespan (Figure 5.31, p=0.005). Co-expression of $dGABP\alpha^{RNAi}$ in flies expressing INR^{DN} shortened lifespan (Figure 5.31, p=4.8 x 10^{-7}) even further than flies expressing $dGABP\alpha^{RNAi}$ alone (p=0.01). This result suggested that *dGABPα* is at least partially required for the lifespan extension of reduced IIS, and that reduction of the insulin receptor, and hence IIS signalling, further exacerbates the negative effect of knocking down of *dGABPα*.

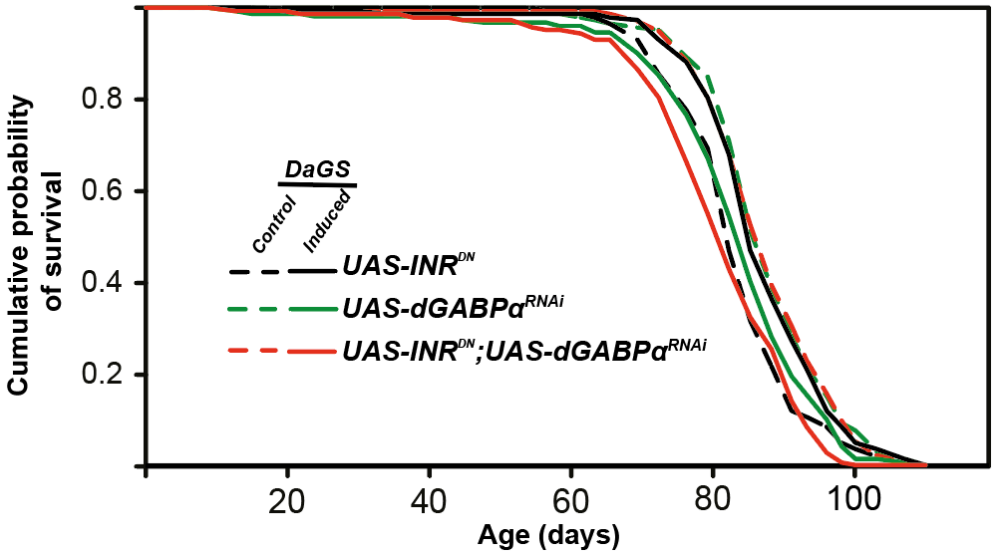

Figure 5.31 *dGABPα* mediated the lifespan extension of reduced IIS

The survival curves of flies over-expressing either INR^{DN} (black line, RU+) or $dGABP\alpha^{RNAi}$ (green line, RU+), or both INR^{DN} and $dGABP\alpha^{RNAi}$ (red line, +RU) and non-RU induced controls (broken lines, RU-). Ubiquitous RNAi-mediated down-regulation of *dGABPα* using the *daGS* driver shortened the lifespan (p=0.005), and abolished the lifespan extension mediated by over-expression of a dominant negative form of *INR* (p=4.8 x 10^{-7}). Over-expression of the dominant negative form of the *INR* extended lifespan (p=0.002), but further shortened the lifespan when *dGABPα* was knocked-down using RNAi (p=0.01). The lifespans were analyzed by using the log-rank test. N=150 flies per condition. The genotypes used were: $daGS>UAS\text{-}INR^{DN}$, $daGS>UAS\text{-}dGABP\alpha^{RNAi}$, $daGS>UAS\text{-}INR^{DN;}$ $UAS\text{-}dGABP\alpha^{RNAi}$.

5.3.12 Over-expression of *dGABPα* reduced AKT signalling

Reducing IIS inhibits the PI3K-PDK1-AKT signalling pathway and activates FOXO, a transcription factor that up-regulates several "longevity pathways" (Webb and

Brunet, 2014, Wang et al., 2014). To examine whether over-expression of *dGABPα* reduces systemic insulin signalling, I firstly measured the levels of phosphorylated AKT (p-AKT), a downstream target of the insulin receptor, by western blot analysis. Given the lack of an antibody recognizing the PDK1 phospho-site on AKT, I evaluated the phosphorylation status at the S505 site, which is phosphorylated by mTORC2 (Guertin and Sabatini, 2009). Previous studies have used this antibodies as a readout of insulin activity (Palu and Thummel, 2016). This analysis demonstrated that over-expression of *dGABPα* caused a modest but significant reduction in the levels of phosphorylated AKT normalized to total AKT (Figure 5.32, p=0.03), suggesting reduced activity of the IIS pathway.

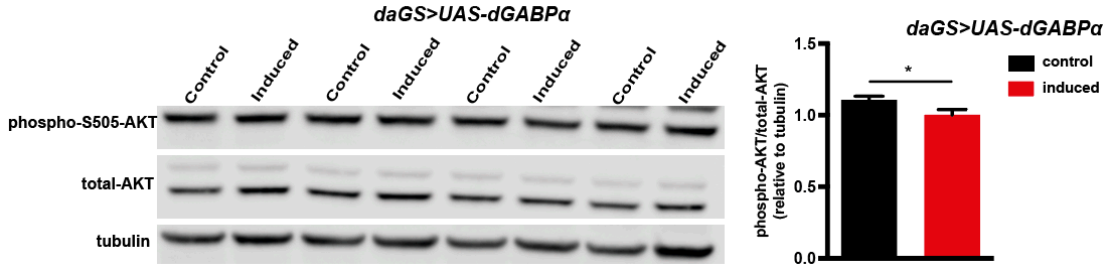

Figure 5.32 Over-expression of *dGABPα* reduced systemic insulin signalling

Whole fly lysates from flies over-expressing *dGABPα* (red bar, +RU), and non-induced controls (black bar, RU-) were analysed by western blot analysis using antibodies directed against phosphorylated AKT (p-AKT), total AKT, and tubulin as a loading control. Flies were 2-weeks old. The same samples were loaded onto separate gels for blotting either p-AKT or total AKT. The levels of p-AKT and t-AKT were measured using ImageJ, and normalized to same-gel loading control. The ratio of p-AKT levels to total AKT levels were then calculated, and plotted as the means ± SEM, n=4. *P=0.03 using the t-test. A representative gel is shown for the loading control, tubulin, and was derived from the p-AKT gel. The genotype was used: *daGS>UAS-dGABPα.*

5.3.13 *dGABPα* over-expression inhibited mTORC1 and mimicked the effect of rapamycin on lifespan

The transcriptional profiling showed that over-expression of *dGABPα* significantly down-regulated the biological functions including amino acid metabolism and translation, which both are tightly linked with reduced mTOR signalling pathway.

The mTOR signalling pathway regulates ageing by mechanisms that overlap with IIS (Johnson et al., 2013). mTORC1 is activated by insulin through PI(Powers et al.)K and AKT kinase signalling (Laplante and Sabatini, 2012). I demonstrated above that over-expression of *dGABPα* inhibited AKT kinase activity. I therefore assessed whether mTORC1 activity is altered by *dGABPα* activation. To do this I measured the phosphorylation levels of S6K, a well-described downstream target of TORC1, using western blot analysis with the phospho-Thr398-dependent S6K antibody. I observed a significant reduction in phospho-T398-S6K levels in response to *dGABPα* over-expression (Figure 5.33), confirming that *dGABPα* inhibits mTORC1 activity *in vivo*.

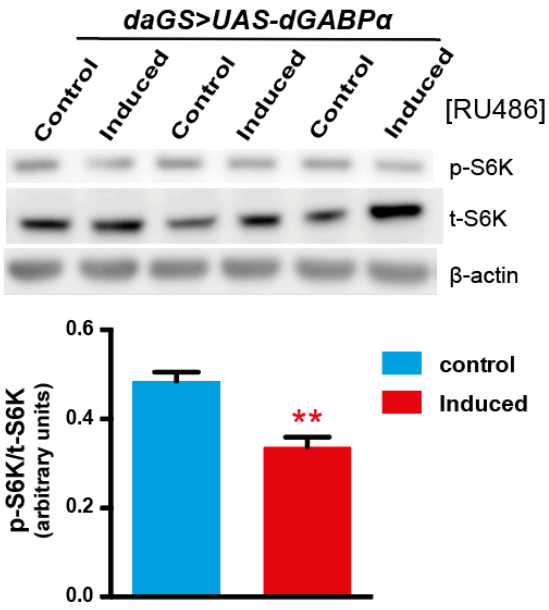

Figure 5.33 The ubiquitous over-expression of *dGABPα* reduced the phosphorylation levels of S6K

Whole fly lysates from flies over-expressing *dGABPα* ubiquitously in adulthood (*daGS>UAS-dGABPα*, red bar, +RU) demonstrated reduced levels of S6K phosphorylation compared to non-induced controls (blue bar, RU-). Western blots were performed using antibodies directed against phosphorylated S6K (p-S6K), total S6K and β-actin as a loading control. Animals were collected at two weeks of age. The same samples were loaded onto separate gels for blotting either p-S6K or total S6K. The levels of p-S6K and t-S6K were measured using ImageJ and normalized to same-gel loading control. The ratio of p-S6K levels to total S6K levels was then calculated. Bars represent the means ± SEM, n=3. **P=0.004 using the t-test. A representative gel is shown for the loading control β-actin, which was derived from the p-S6K gel. The genotype used was: *daGS>UAS-dGABPα*.

I next investigated whether the lifespan extension of *dGABPα* is mediated by mTORC1 signalling. Rapamycin inhibits mTORC1 activity and extends lifespan by mechanisms that include reduced mRNA translation and autophagy induction (Bjedov et al., 2010). I therefore assessed whether the lifespan extension mediated by *dGABPα* over-expression mimics the effects of reduced mTOC1 activity. To do this I observed whether *dGABPα* over-expression can further extend the lifespan extension mediated by rapamycin treatment. I first confirmed that induction of *dGABPα* with RU extended the lifespan compared to un-induced controls (Figure 5.34, the median lifespan was extended by 6%, p=0.03). I then used two concentrations of rapamycin, 50 and 200μM, both of which have been shown to mediate lifespan extension through a dose-dependent reduction of S6K activity, the most effective dose being 200μM (Bjedov et al., 2010). I showed that both 50 and 200μM of rapamycin extended lifespan in a dose-dependent manner (Figure 5.34, the median lifespan was extended by 16%, and 25%, p= 2.29 x 10^{-14}, p= 1.52 x 10^{-28} respectively by log-rank test). However no further extension occurred when the rapamycin-flies over-expressed *dGABPα* (for rapamycin 50μM: p=0.24 and for rapamycin 200μM: p=0.67 by log-rank test), suggesting that *dGABPα* acts in a similar manner to rapamycin. Indeed, 200μM rapamycin-treated flies over-expresssing *dGABPα* showed reduced survival compared to 200μM rapamycin-treated controls (the median lifespan was shortened by 5%, p=0.046 by Wilcoxon test), suggesting a toxic effect likely due to the excessive inhibition of mTOR that is detrimental to the lifespan of the flies. Surprisingly, the CPH analysis failed to detect any significant interaction between the response to RU and the response to rapamycin 50μM (Table 5, p=0.47), likely due to the limitation of the test. Taken together, these results demonstrated that over-expression of *dGABPα* may act via similar mechanisms of action with rapamycin/mTORC1 in regulating of lifespan, likely through inhibition of S6K.

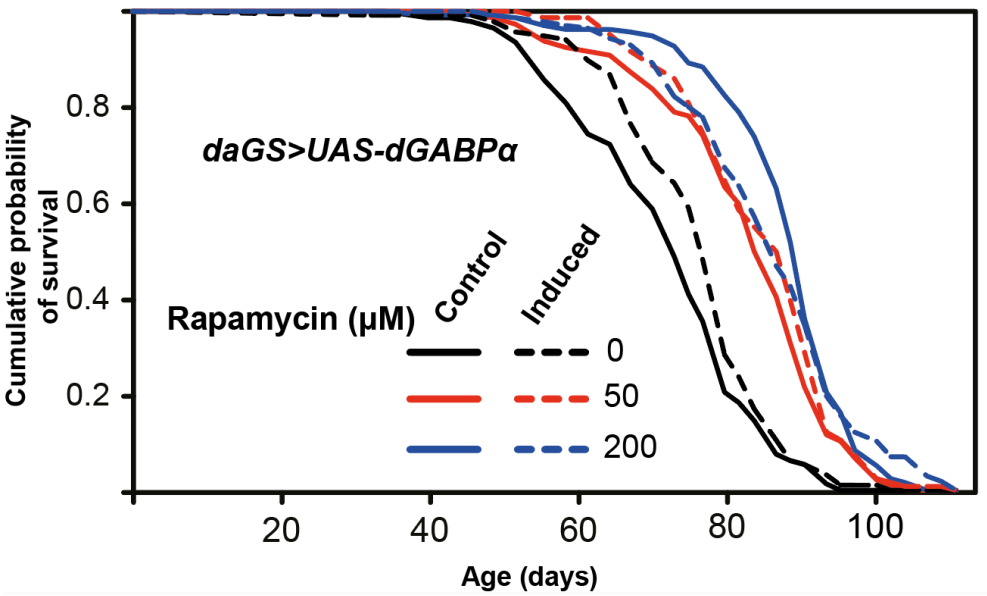

Figure 5.34 The survival of flies over-expressing *dGABPα* in response to rapamycin treatment

Ubiquitous over-expression of *dGABPα* extended lifespan (p=0.03 by log-rank test). Rapamycin treatment (50μM**)** also extended lifespan compared to non-treated controls (p=2.29 x 10^{-14}), and no further extension occurred with the over-expression of *dGABPα* (p=0.24 by log-rank test). Treatment with a higher dose of rapamycin (200μM) extended lifespan, to a greater extent than 50μM**,** compared to non-treated controls (p= 1.52 x 10^{-28}), but the lifespan was shortened when *dGABPα* was over-expressed in the rapamycin-treated flies (p=0.67 by log-rank test and p=0.046 by Wilcoxon test). N=140 flies per condition. The lifespans were analyzed using the log-rank test or Wilcoxon test. The genotype used was: *daGS>UAS-dGABPα*.

```
  n= 571, number of events= 534

                      coef exp(coef) se(coef)      z Pr(>|z|)
dataC$RU           -0.2410    0.7859   0.1226 -1.966   0.0493 *
dataC$RAPA         -0.9878    0.3724   0.1249 -7.910 2.55e-15 ***
dataC$RU:dataC$RAPA  0.1234    1.1314   0.1737  0.711   0.4773
---
Signif. codes:  0 '***' 0.001 '**' 0.01 '*' 0.05 '.' 0.1 ' ' 1
```

Table 5 The CPH analysis of the survival of rapamycin-treated flies co-expressing *dGABPα*

CPH analysis showed that there was no significant interaction between the response to *dGABPα* over-expression and the response to 50μM rapamycin treatment, p=0.4773.

5.3.14 *dGABPα* modulated intestinal homeostasis

The *Drosophila* intestine is an accessible model system to study tissue homeostasis in ageing (Biteau et al., 2010). Intestinal stem cells (ISCs) in the gut drive cell division

in response to environmental stress (Choi et al., 2008, Biteau et al., 2008, Jiang et al., 2009, Cronin et al., 2009, Buchon et al., 2009, Amcheslavsky et al., 2009). However, age-related over-proliferation of ISCs has deleterious consequences with accumulation of mis-differentiated cells ultimately contributing to the disruption of epithelial integrity and to the increased mortality of ageing flies (Choi et al., 2008, Biteau et al., 2008). Previous studies have shown that limiting cell proliferation rates by moderately reducing IIS/mTOR signalling in stem cells, is sufficient to delay intestinal dysplasia, improving metabolic health and extending lifespan (Biteau et al., 2010, Regan et al., 2016). Since over-expression of *dGABPα* extends female lifespan in the mechanisms associated with a reduction in IIS/mTOR signalling, I hypothesised that improvements in gut homeostasis may be responsible for some of the beneficial effects of *dGABPα* over-expression. Therefore, I assessed whether over-expression of *dGABPα* improves the proliferative homeostasis in the ageing fly gut. I therefore over-expressed *dGABPα* using the gut-specific driver *TIGs-Geneswitch-GAL4* (*TIGs-GS*), to direct intestinal-specific expression in adulthood. Female flies over-expressing *dGABPα* showed a moderate, but significant, reduction in the number of actively dividing (pH3+) cells at 45-days of age (Figure 5.35, p=0.02). This suggests that over-expression of *dGABPα* modulates intestinal homeostasis by preventing over-proliferation of stem cells with age, likely through a reduction in IIS/mTOR signalling.

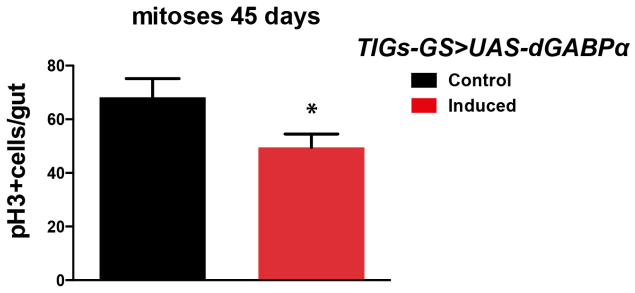

Figure 5.35 Over-expression of *dGABPα* in gut prevented the over-proliferation of stem cells

Quantification of pH3+ cells per gut demonstrated that over-expression of *dGABPα* specifically in the fly gut, using the *TIGs-GS* driver (*TIGs-GS>UAS-dGABPα,* red bar, RU+) showed a reduced number of mitoses compared with non-induced controls (black bar, RU-) at 45 days. N>16 per condition; p=0.02 using the t-test. The genotype used was: *TIGs-GS>UAS-dGABPα.* The gut dissection was performed in collaboration with Dr. Mobina Khericha and Dr. Jennifer C Regan.

5.3.15 Over-expression of *dGABPα* extended lifespan via mechanisms independent of those of lithium treatment

Over-expression of *dGABPα* increases resistance to phenobarbital stress (Figure 5.22). The responses to xenobiotics in *Drosophila* are not only regulated by the transcription factors *dFOXO* and DHR96 (Salih and Brunet, 2008, Sykiotis and Bohmann, 2010, Hoffmann and Partridge, 2015), which mediate the xenobiotic stress response in insulin mutants (Afschar et al., 2016), but also by the transcription factor CncC (Sykiotis and Bohmann, 2010). We recently showed that CncC-induced xenobiotic resistance and longevity can be achieved through the administration of lithium (Castillo-Quan et al., 2016). I therefore assessed whether the lifespan extension mediated by *dGABPα* over-expression mimics the effect of lithium treatment. To test this, I investigated whether *dGABPα* over-expression could further extend the lifespan of lithium-treated flies. Flies treated with 10mM lithium displayed a significant lifespan extension (Figure 5.36, $p= 5.3 \times 10^{-5}$), consistent with previously reported observations (Castillo-Quan et al., 2016), and further extension occurred when the lithium-flies over-expressed *dGABPα* (p=0.001). Induction of *dGABPα* by RU486 extended the lifespan of wild type flies (Figure 5.36, p=0.007), and further extension occurred when *dGABPα*-over-expressing flies were treated with 10mM lithium (p=0.01). CPH analysis also confirmed that there was no significant interaction between the response to RU and the response to lithium treatment (Table 6, p=0.7), suggesting that over-expression of *dGABPα* extends lifespan via mechanisms independent of those of lithium treatment.

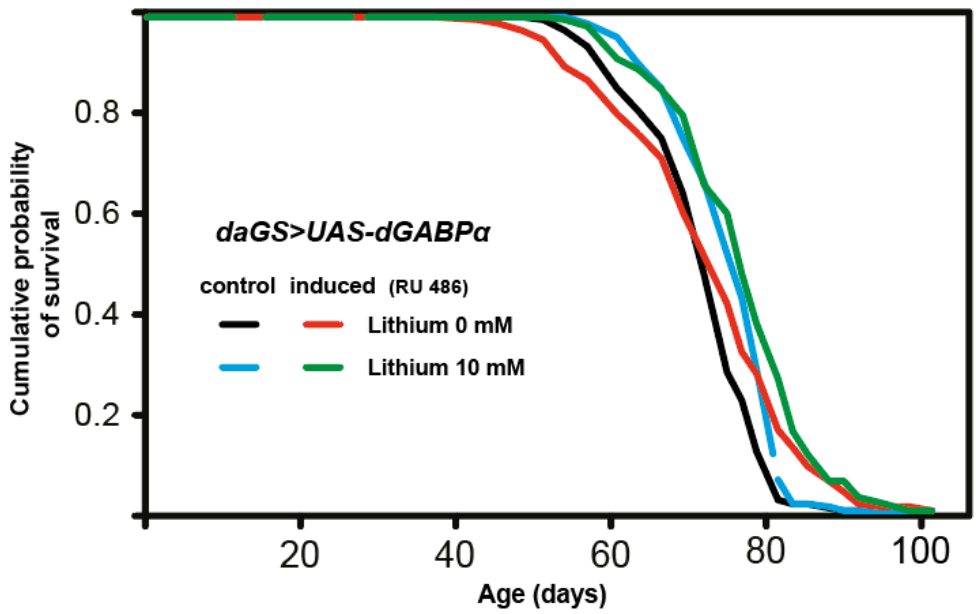

Figure 5.36 Ubiquitous over-expression of *dGABPα* extended the lifespan of lithium-treated flies

The survival curves of flies over-expressing *dGABPα* with the *daGS* driver (RU+) and non-RU induced controls (RU+) with and without lithium treatment. Ubiquitous over-expression of *dGABPα* extended lifespan in wild types flies (p=0.007), and a further extension occurred in *dGABPα*-over-expressing flies treated with 10mM lithium (p=0.01). 10mM lithium extended lifespan in wild type flies (p= 5.3 x 10^{-5}), and a further extension occurred when the lithium-flies over-expressed *dGABPα* (p=0.001). The lifespans were analyzed using the log-rank test. N=150 flies per condition. The genotype used was: *daGS>UAS-dGABPα.*

	coef	exp(coef)	se(coef)	z	Pr(>|z|)	
dataC$RU	-0.44048	0.64373	0.12159	-3.623	0.000292	***
dataC$LITHIUM	-0.38898	0.67775	0.11853	-3.282	0.001032	**
dataC$RU:dataC$LITHIUM	0.06301	1.06503	0.16914	0.373	0.709511	

Signif. codes: 0 '***' 0.001 '**' 0.01 '*' 0.05 '.' 0.1 ' ' 1

Table 6 CPH analysis of the survival of flies over-expressing *dGABPα* with and without lithium treatment

The CPH showed that there is no significant interaction between the response to RU and the response to lithium treatment (p=0.7). This means that lithium extended lifespan regardless of whether *dGABPα* is over-expressed. This suggests that over-expression of *dGABPα* extends lifespan via mechanisms independent of those of lithium treatment.

I then assessed whether the transcriptional response mediated by *dGABPα* over-expression was similar to that observed in lithium treatment. I used our recently published microarray data for whole flies treated with 10mM lithium (Castillo-Quan et al., 2016). By comparing the overlap of GO categories elicited by both

interventions, I detected statistical significance in GO terms of those that are up-regulated or down-regulated in both interventions (Figure 5.37), suggesting that the transcriptional response changed in the same directions.

Lithium protects flies from xenobiotic stress by up-regulating the genes involved in the detoxification pathway (Castillo-Quan et al., 2016). The RNAseq data suggested that over-expression of *dGABPα* does not change the transcript levels of *GstD2*, and down-regulates the levels of *cyp6a8*, two genes involved in the detoxification pathway. I further confirmed these findings by qRT-PCR analysis of whole flies over-expressing or lacking *dGABPα* (Figure 5.13). Since the direct contribution of individual detoxification proteins to the xenobiotic stress and lifespan regulation is as yet unexplored, it will be interesting to further study whether any of these proteins mediate the effects of *dGABPα* on xenobiotic stress resistance and lifespan extension.

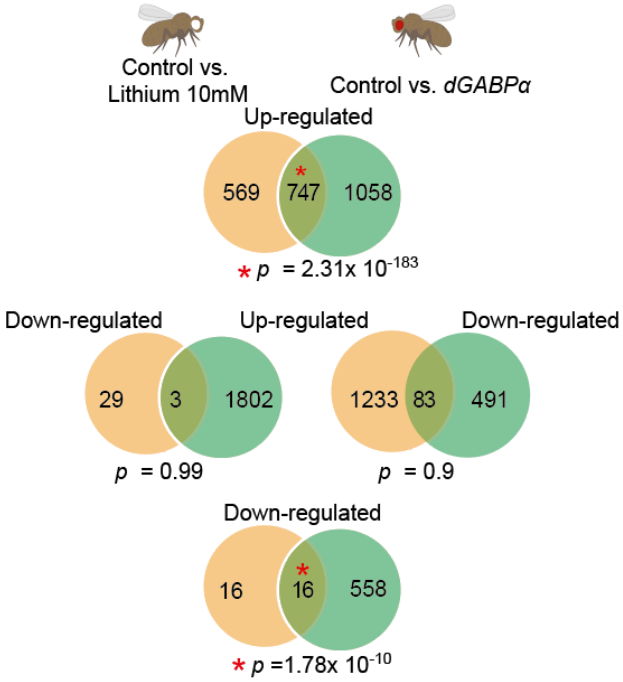

Figure 5.37 Comparative analyses of the transcriptional response of lithium and *dGABPα* over-expression

Venn diagrams showing the overlap between the GO terms enriched by 10mM lithium treatment (yellow color) and those enriched by *dGABPα* over-expression (green color). P<0.05. Bioinformatics analysis was performed by Dr.Dobril Ivanov.

5.3.16 Ubiquitous knockdown of AKT increased ER stress resistance

We previously demonstrated the importance of nutrient sensing pathway in regulation of the lifespan, although the molecular mechanisms of the improvement of healthy ageing are not fully elucidated. Age-related proteostatic failure contributes to ageing and age-related diseases (Taylor and Dillin, 2011, Hetz, 2012). Direct up-regulation of the components of the UPR^{ER} delays ageing in *C. elegans* (Taylor and Dillin, 2013). Whether the UPR^{ER} plays an important role in fly ageing has not yet been determined. I therefore asked whether long-lived mutants mediate their effects via modulation of the UPR^{ER}. To test this, I genetically knocked down AKT, the main kinase in the nutrient-sensing pathway that has been previously reported to extend lifespan (Biteau et al., 2010). RNAi knockdown of AKT in flies dramatically increased the resistance to tunicamycin, a well-known ER stress inducer (Figure 5.38), suggesting up-regulation of the UPR^{ER}. Given the central position of AKT in the nutrient-sensing pathway, this result suggests that the UPR^{ER}, being downstream of the nutrient-sensing pathway, may play an important role in lifespan regulation.

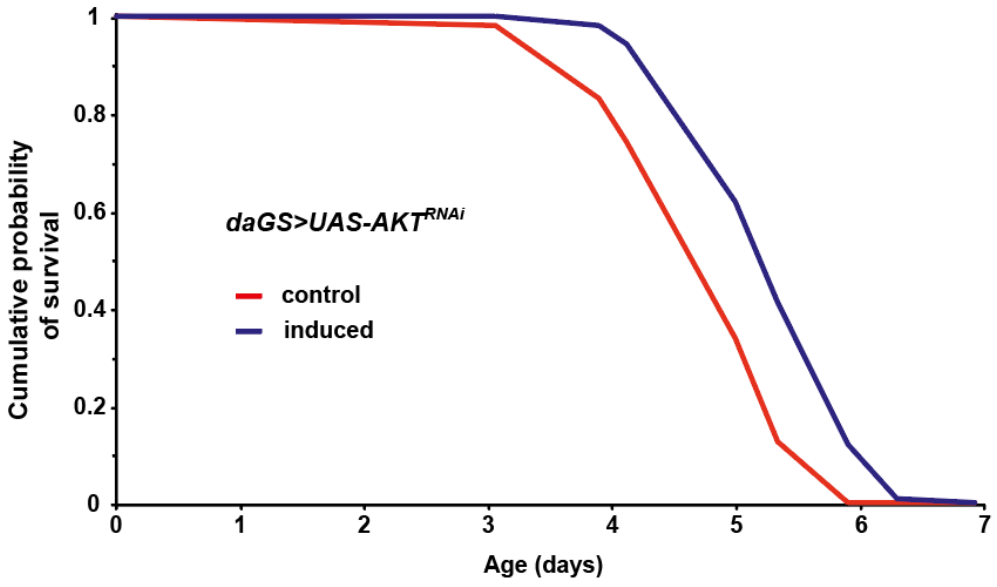

Figure 5.38 Flies lacking AKT are more resistant to the ER stressor tunicamycin

The survival curves of flies over-expressing AKT^{RNAi} in adulthood using the inducible *daGS* driver (*daGS>UAS-*AKT^{RNAi}, dark blue line, RU+) and un-induced controls (red line, RU-). Flies were pre-treated with RU486 for 14 days and then transferred to sugar/agar food supplemented with tunicamycin. $P=1.52 \times 10^{-11}$ using the log-rank test. The genotype used was: *daGS>UAS-*AKT^{RNAi}.

5.4 Discussion

PGC-1α is a key transcriptional co-activator in energy metabolism, regulating growth and mitochondrial biogenesis in response to IIS/mTOR signalling (Mukherjee and Duttaroy, 2013, Tiefenböck et al., 2010). Recent studies highlight its importance for longevity in *Drosophila melanogaster* (Rera et al., 2011), suggesting an evolutionary conserved function in lifespan regulation. Here I showed that ubiquitous over-expression of *dPGC-1* extends lifespan and improves behavioural phenotypes in *Drosophila*, confirming it is indeed a modulator for healthy longevity. Interestingly, over-expression of *dPGC-1* only extended female lifespan, and not the lifespan of males, suggesting that sex difference may mediate the effects of *dPGC-1* on lifespan regulation. Indeed, interventions that down-regulate the nutrient-sensing pathway extend fly lifespan mostly in female flies, and furthermore the sex differences in the ageing-gut have been identified as mediators of this response (Regan et al., 2016). This highlights the intricate link between gut homeostasis, the nutrient sensing pathway and female lifespan. *dPGC-1* has been shown to improve gut homeostasis (Rera et al., 2011) and therefore improving gut health and homeostasis during the ageing process may be an important determinant of healthy ageing. The link between *dPGC-1* and reduced nutrient-sensing pathway signalling in ageing has been highlighted in a developmental study, showing that *dPGC-1* forms a negative feedback loop to fine-tune the insulin signalling. However the mechanisms mediating this are yet to be fully elucidated (Mukherjee and Duttaroy, 2013, Tiefenböck et al., 2010).

To identify the mechanisms involved in the regulation of lifespan by *dPGC-1*, I assessed the effect of downstream TFs on longevity. I identified that ubiquitous over-expression of the *Drosophila* homologue of human GA-binding protein α subunit (also known as nuclear respiratory factor 2α) extended lifespan. Moreover, tissue specific *dGABPα* gain-of-function in the central nervous system or in the gut and fat body was sufficient to extend lifespan, suggesting its broad beneficial effects in different tissues. In addition, *dGABPα* was up-regulated followed by *dPGC-1* over-expression, consistent with human data suggesting that GABPα is induced by PGC-1α (Mootha et al., 2004).

Consistent with their mammalian counterparts, *dPGC-1* and *dGABPα* are required for the appropriate expression of genes in mitochondrial OXPHOS (Tiefenböck et al., 2010, Mootha et al., 2004). Previous work has already shown that *dPGC-1* gain-of-function correlates with increased mitochondrial oxygen consumption, mitochondrial mass, and ATP production (Rera et al., 2011). However, the transcriptional profiling suggested that over-expression of *dGABPα* in CNS down-regulated the cellular components involved in respiratory chain complex and mitochondrial part, suggesting mitochondrial-related functions might be repressed in response to *dGABPα* over-expression. I found that over-expression of *dGABPα* increased ATP production, but not oxygen consumption and mitochondrial mass, suggesting that energy production and consumption are uncoupled. Indeed this has been observed in long-lived worms showing elevated ATP but not respiration rate (Braeckman et al., 1999). In addition, the contribution of mitochondrial function to longevity is controversial, and whether direct up-regulation of mitochondrial components extend lifespan is yet to be unequivocally answered. It is already known that mild inhibition of mitochondrial respiration extends lifespan in diverse organisms, including worms, flies and mice (Feng et al., 2001, Dillin et al., 2002, Lee et al., 2003, Lee et al., 2010, Liu et al., 2005, Dell'agnello et al., 2007, Copeland et al., 2009). The role of mitochondrial function in the coordination of the ageing process is therefore very complex and yet to be fully elucidated.

The ETC is the major site of ROS production. PGC-1α, the "captain" of the mitochondrion, has dual effects, not only regulating mitochondrial biogenesis, but also controlling mitochondrial ROS, by regulating the antioxidant defence system (St-Pierre et al., 2006). Although *Drosophila* PGC-1 gain-of-function results in resistance to paraquat-induced oxidative stress, the studies have failed to detect any changes in the main antioxidant enzymes, including SOD1, and SOD2 (Mukherjee et al., 2014). Here I demonstrated that the long-lived flies over-expressing *dPGC-1* does not show increased resistance to paraquat-induced oxidative stress, and shows hypersensitivity to H_2O_2-induced oxidative stress. The difference in the two studies may be attributable to the background strains used to over-express *dPGC-1*, possibly with different expression levels of *dPGC-1*. In addition, the contribution of ROS to the ageing process is still a controversial area, since ROS production and lifespan can be

uncoupled (Copeland et al., 2009). Increasing ROS and oxidative damage in mice does not lead to increased ageing (Zhang et al., 2009), and reducing ROS via activation of the antioxidant defence system in mice does not extend lifespan (Van Raamsdonk and Hekimi, 2009). There is increasing evidence that a moderately inducing ROS may be beneficial and leads to lifespan extension in yeast and worms (Doonan et al., 2008, Mesquita et al., 2010, Van Raamsdonk and Hekimi, 2009). Here I demonstrated that *dGABPα* gain-of-function does not change sensitivity to either H_2O_2- or paraquat-induced oxidative stress, therefore excluding the possibility that oxidative stress is the driving force behind the lifespan prolonging effects of *dGABPα.*

To investigate the mechanisms by which *dGABPα* over-expression extends lifespan, I first assessed whether *dGABPα* acts like a DR-mimetic. DR is the most established anti-ageing intervention that extends lifespan in diverse species, by shifting metabolism from reproduction and growth to somatic maintenance (Fontana and Partridge, 2015, de Cabo et al., 2014, Holliday, 1989). By comparing the effects of *dGABPα* gain-of-function and DR on lifespan, I found that *dGABPα* gain of function: 1) further extended lifespan beyond that already maximized by DR; 2) extended lifespan via mechanisms independent of DR; and 3) shortened lifespan in starvation-like low yeast food.

To further explore the molecular mechanisms involved in these effects, I performed transcript profiling to assess the transcriptional response to *dGABPα* gain-of-function. This also enabled me to compare the data with the available sequencing data from previous studies. I showed that *dGABPα* regulates several genes involved in insulin signalling, in which over-expression of *dGABPα* up-regulates *ImpL2*, the secreted antagonist of insulin signalling (Sloth Andersen et al., 2000, Alic and Partridge, 2008, Honegger et al., 2008), thereby reducing insulin signalling. I showed that *dGABPα* gain-of-function shares similar transcriptional response with reduced IIS. In addition, over-expression of *dGABPα* extends lifespan via overlapping mechanism with reduced IIS. This finding supports the negative feedback loop of *dPGC-1* on IIS that has been proposed (Tiefenböck et al., 2010), involving up-regulation of *dGABPα* and *ImpL2*. It will be interesting to determine whether the *dGABPα*-IIS link is conserved across species.

It is known that a modest reduction in insulin signalling extends lifespan in diverse species (Piper et al., 2008), likely due to a beneficial effect of increased insulin sensation in later life. Here I showed that down-regulation of *dGABPα* increased the early mortality, which is likely an outcome secondary of reduced *ImpL2*, leading to increased binding of dilps to the insulin receptor, with a reduction in the insulin sensitivity. Insulin resistance in type-2 diabetes and leptin resistance in obesity are common clinical examples (Chiu et al., 2007, Pan et al., 2014). In both of these conditions, cells fail to respond normally to the hormone. Type-2 diabetes is a chronic metabolic disease that normally develops over several years. Under physiological conditions, insulin is secreted from the pancreas in response to increased blood glucose levels after a meal, and binds to the insulin receptor on the cell surface of tissue-sensitive organs, triggering a series of downstream cascades including glucose uptake and metabolism. However, a long-term high-fat diet/high-calorie diet causes a constant stimulus to the insulin-insulin receptor interaction, which in turn leads to a reduction in sensitivity of the insulin receptor to insulin. This is referred to as insulin resistance. Patients with insulin resistance, or leptin resistance in obesity, normally show increased levels of circulating insulin or leptin, with a lower tissue sensitivity to these hormones. In keeping with this, I demonstrated that down-regulation of *dGABPα* shortens lifespan and knockdown of the insulin receptor further accelerates ageing, resulting in down-regulation of IIS beyond beneficial levels. Thus *dGABPα* is required for reduced IIS, in order to maintain the insulin sensitivity necessary for lifespan extension.

I further showed that flies over-expressing *dGABPα* displayed reduced phosphorylation of AKT, the main enzyme in the IIS/mTOR signalling pathway, suggesting a reduction in IIS/mTOR signalling activity (Webb and Brunet, 2014, Wang et al., 2014, Guertin and Sabatini, 2009, Palu and Thummel, 2016, Laplante and Sabatini, 2012). Interestingly, the transcriptional profiling showed that over-expression of *dGABPα* significantly down-regulated the biological functions including amino acid metabolism and translation, which both are tightly linked with reduced mTOR signalling pathway. Indeed, *dGABPα* gain-of-function inhibited mTORC1 activity, as evident from the reduction in S6K phosphorylation levels (Um

et al., 2006). In addition, *dGABPα* gain-of-function extended the lifespan via overlapping mechanisms with rapamycin, the mTORC1 inhibitor, likely through inhibition of S6K (Bjedov et al., 2010). Taken together, *dGABPα* gain-of-function extends lifespan via overlapping mechanisms with that of reduced IIS/mTOR signalling. *dFOXO* is one of the main transcription factors responsible for many metabolic traits of reduced IIS/mTOR signalling (Alic et al., 2011a, Slack et al., 2011).

I then looked at whether *dGABPα* gain of function improved healthy lifespan. Here I found that over-expression of *dGABPα* reduced the age-related over-proliferation of intestinal stem cells, preventing the disruption of epithelial integrity, and reducing the mortality of ageing flies (Choi et al., 2008, Biteau et al., 2008). Our results are consistence with previous findings showing that *dPGC-1* gain-of-function and reduced IIS/mTOR signalling, all contribute to improved gut homeostasis via similar mechanisms (Rera et al., 2011). Since all of the above effectors extend only female lifespan, this indicates that the gut differences between the sexes may mediate the lifespan extension from reduced nutrient sensing pathway.

Interestingly, I observed that, unlike many other genetic and pharmacological interventions (eg. DR, reduced IIS, rapamycin, or trametinib treatment), *dGABPα* gain-of-function did not reduce fecundity (Slack et al., 2011, Slack et al., 2015, Bjedov et al., 2010). It therefore promotes healthy lifespan in adult *Drosophila* with limited side effects. Indeed, extended longevity is not consistently correlated with reduced fertility (Copeland et al., 2009) and in our recently published work, we pointed out that flies treated with lithium show extended lifespan without a reduction in fecundity (Castillo-Quan et al., 2016). Lithium induces lifespan-extension and protection against xenobiotic via GSK3/NRF2-dependent mechanisms. Here I show that *dGABPα* gain-of-function shares overlapped transcriptional responses with those of lithium, suggesting they might share similar mechanisms in meditating lifespan regulation. However, over-expression of *dGABPα* does further extend lifespan in flies treated with lithium, suggesting that over-expression of *dGABPα* also extends lifespan via mechanisms independent of lithium treatment. In addition, flies over-expressing *dGABPα* show increased resistance to phenobarbital stress, indicating that it improves

healthy lifespan through up-regulation of the detoxification pathway. Since both lithium and NRF-2 and reduced IIS are involved in the detoxification pathway (Salih and Brunet, 2008, Sykiotis and Bohmann, 2010, Hoffmann and Partridge, 2015, Afschar et al., 2016, Castillo-Quan et al., 2016), it will be interesting to know which mediator is particularly responsible for this effect of *dGABPα* over-expression in flies.

My work has thus shown that *dGABPα* gain-of-function extends lifespan via similar mechanisms to those of reduced IIS and rapamycin treatment, all of which further extend lifespan beyond the maximum achieved by DR in *Drosophila* (Bjedov et al., 2010, Broughton et al., 2010). This suggests that *dGABPα* may be one of the main molecular modulators of lifespan extension beyond DR. In addition, *dGAPBa* gain-of-function up-regulates the chaperones HSP70, together with inhibition of IIS/mTOR signalling pathway, which both mediate the beneficial effects in short-term fasting in humans or mammalian models (Brown-Borg and Rakoczy, 2013, Mattson et al., 2014, Cheng et al., 2014, Hine et al., 2015). This therefore highly suggests that GABPα may be the central mediator of the benefits of short term fasting in mammalian ageing and chronic diseases. Moreover, *dGABPα* up-regulates HSP70, which is known to improve proteostasis in IF and short-term fasting (Brown-Borg and Rakoczy, 2013). Whether direct over-expression of *dGABPα* improves protesostasis is yet to be determined. Furthermore I demonstrated here that down-regulation of AKT, the key enzyme in the nutrient-sensing pathway, increased the resistance to ER stress in flies, suggesting activation of the UPR^{ER}. These results therefore indicate that up-regulation of UPR^{ER} may be beneficial for fly ageing.

Finally, the effects of both genetic interventions that down-regulate the IIS/mTOR signalling pathway, and the environmental interventions that alter meal timing, are dependent on the levels of the signal reduction and nutrient availability. Under normal conditions, GABPα activation may be beneficial for mammalian ageing through the use of mechanisms that mimic IF. However, in cachexic states, such as in cancer and type-2 diabetes, activation of GABPα maybe harmful. A previous study suggested that under adverse nutritional conditions, *ImpL2* is up-regulated in the fat body and represses systemic IIS activity (Honegger et al., 2008). Indeed, starvation or fasting in cachexic states, as seen in *Drosophila* tumour models (Kwon et al., 2015, Figueroa-

Clarevega and Bilder, 2015), lead to organ wasting and loss of body mass (Tessitore and Bollito, 2006). This is associated with a sustained and dramatic reduction in systemic IIS signalling via increased levels of secreted ImpL2, suggesting that sustained activation of the ImpL2/IIS pathway under malnutrition accelerates ageing. Here I show that under low-yeast food conditions, flies over-expressing *dGABPα* are more sensitive than non-induced controls to malnutrition, through activation of *ImpL2* and repression of IIS. In type-2 diabetes (high-insulin but profound insulin resistance), hepatic gluconeogenesis is highly induced, through both up-regulation of PGC-1α mRNA levels via either the cAMP-CREB pathway (Herzig et al., 2001), or through co-activation with the transcription factor HNF4 (Rhee et al., 2003). This leads to increased blood glucose levels and exacerbates insulin resistance. Therefore in conclusion up-regulation of PGC-1α or GABPα activity may prove to be a useful therapeutic strategy in modulating human ageing and age-related diseases. However, activation of these genes will require careful optimisation, especially in the established disease state.

5.5Experimental procedures

5.5.1 Fly strains

The UAS-*dPGC-1* and UAS-*dGABPα* lines were gifts from Dr. Christian Frei and Dr. Hugo Stocker (Tiefenböck et al., 2010, Baltzer et al., 2009). The AKT^{RNAi} and $dGABP\alpha^{RNAi}$ lines were obtained from the VDRC. *Actin-GAL4 (ActGal4) and UAS-*INR^{DN} *(K1409A)* stocks were obtained from the Bloomington *Drosophila* Stock Centre. The *$S_1$106-GeneSwitch ($S_1$106GS)* driver was a kind gift from the R**.** Davis lab (Roman et al., 2001). The *Daughterless-GeneSwitch (daGS)* driver line was kindly provided by Dr. Veronique Monnier (Tricoire et al., 2009). The *ActGS* driver line was kindly provided by Dr. Laurent Seroude (Poirier et al., 2008). All of the lines were backcrossed over 6 generations into the $white^{Dahomey}$ *(*w^{Dah}*)* stock, which was maintained in population cages. w^{Dah} was derived by backcrossing the w^{1118} into the outbred wild-type *Dahomey* background. Flies were raised and maintained on standard sugar/yeast medium (Bass et al., 2007). Experiments were conducted at 25°C in a 12:12 hours light/dark cycle at constant humidity.

5.5.2 Dietary restriction protocol

The specific preparation of the DR media has been described in Chapter 2. In this chapter, I used 0.1SY, 0.5SY, 1.0SY and 2.0SY. RU486 was supplemented into the SY food to give a final concentration of 200 μM.

5.5.3 Rapamycin preparation and delivery

Rapamycin (LC Laboratories #R-500) was dissolved in 100% ethanol at a concentration of 50mM and then added to the fly medium to give the final concentration.

5.5.4 Lithium preparation and delivery

Lithium chloride (LiCl; Sigma L0505) was dissolved in ddH_2O to give a stock concentration of 5M and then supplemented into 1.0 SY medium to give the final concentration. Food was then dispensed into plastic vials and stored at 4 °C. Cold refrigerated vials were placed at 25 °C for a minimum of 2 hours before use.

5.5.5 Stress experiments

Flies were reared and housed as for lifespan experiments until 14 days of age, and then flies were transferred onto the specific foods containing the various stress reagents. The preparation and delivery of the various stress assay foods has been described in Chapter 2.

5.5.6 Fecundity assays

For fecundity measurement, eggs were collected over a 24-hour period and counted. Data was reported as the mean number of eggs laid per female ± SEM over this 24-hour period.

5.5.7 Oxygen consumption

The mitochondrial Oxygen Consumption Rate (OCR) was analyzed using an Oroboros Oxygraph-2k (O2k). *Drosophila* heads (30-40 heads per run) were collected and placed in ice-cold homogenization buffer (pH 7.4, Sucrose 320 mM, Tris-HCl 10

mM, K+EDTA 1 mM, BSA essentially fatty acid free 2.5 g/L), homogenized with a Teflon homogenizer over ice, spun down and re-suspended in ice-cold homogenization buffer without BSA. The homogenate was added to the MiR05 buffer (pH 7.1, EGTA 0.5 mM, MgCl2.6H2O 3 mM, Lactobionic Acid 60 mM, Taurine 20 mM, KH2PO4 10 mM, HEPES 20 mM, D-Sucrose 110 mM, BSA essentially fatty acid free 1 g/L) for OCR recordings. The experimental temperature of the O2k was set at 30°C and electrodes were calibrated according to the manufacturer's protocol. Acquisition and analysis of the OCR was done through the Oroboros Datlab software. Substrates, uncouplers and inhibitors were added in the following order and final concentrations: 2 mM malate, 10 mM glutamate, 2.5 mM ADP, 10 µM cytochrome c, 10 mM succinate, 0.25 µM titrations with the protonophore uncoupler Carbonyl cyanide 4-(trifluoromethoxy) phenylhydrazone (FCCP) until maximal uncoupled respiration was reached, 0.5 µM rotenone, and finally 2.5 µM antimycin A. State 2 respiration was obtained after the additions of malate and glutamate, State 3 after ADP, and maximal uncoupling after FCCP. The OCR was normalized to total protein levels obtained from the homogenate and units of activity are presented as pmol O2/mg*s. All reagents were from Sigma, unless stated otherwise

5.5.8 Immunohistochemistry

The following antibodies were used for cell division analyses: the primary antibody rabbit anti-PH3 (Cell Signaling (Danvers, MA) 9701) 1:500, and the secondary antibody Alexa Fluor 594 donkey anti-rabbit (A21207) Thermo Fisher Scientific, Waltham, MA) 1:1000. Guts were dissected in ice cold PBS and immediately fixed in 4% formaldehyde for 15 mins. They were then serially dehydrated in MeOH, stored at -20°C and subsequently stained. For staining guts were defrosted and washed in 0.2% Triton-X/PBS, blocked in 5% bovine serum albumin/PBS, incubated in primary antibody overnight at 4°C and in secondary for 2 hour at RT. At least 16 guts per condition were mounted in mounting medium containing DAPI (Vectastain). Scoring was performed under the Zeiss (UK) fluorescence microscope using a 40X oil-immersion objective.

5.5.9 Quantitative RT-PCR

Total RNA was isolated from 10 whole adult flies using standard TRIZOL (Invitrogen) protocols and converted to cDNA using oligo d(T)s, primers and Superscript II reverse transcriptase (Invitrogen). Quantitative RT-PCR was performed using the Power SYBR Green PCR Master Mix (ABI), and relative quantities of transcripts were determined using the relative standard curve method normalized to the internal control gene *RP49*.

The following primers sequences were used for the qRT-PCR:

dGABPα:

FOR: GCAACATCTTCTGGACCCAC

REV: CCGCATAATCCGCTGTTCAA

Cyp6a8:

FOR: CAAGATAAGGTTCGGGCTGA

REV: TGGTGTACAGTCGCAGAGTTTC

GstD2:

FOR: CGGACATTGCCATCCTGT

REV: TGCTGAAGTCGAACTCACTAACTT

4EBP:

FOR: CACTCCTGGAGGCACCA

REV: GAGTTCCCCTCAGCAAGCAA

RP49:

FOR: ATCGGTTACGGATCGAACAA

REV: GACGGTCTCCTTGCGCTTCT

ImpL2:

FOR: CCTCATTAAGTACGGGATAC

REV: CTTCTGATCTCCGAGATCAAG

5.5.10 Immunoblot analyses

Protein extraction and western blot techniques were described in Chapter 2. Primary antibodies used in this work were: pSer505-AKT (Cell Signalling Technologies #4054, 1:1000), total-AKT (Cell Signalling Technologies #9272, 1:1000), pThr398-S6K (Cell Signalling Technologies #9209, 1:1000), custom made total-S6K (kindly provided by Dr. Cathy Slack, 1:1000), β-actin (Abcam #ab8224, 1:5000), tubulin

(Sigma-aldrich T6199, 1:5000), NDUFS3 (Abcam #ab14711, 1:1000), and custom made Atg8 (kindly provided by Dr. Ivana Bjedov, 1:1000). Secondary antibodies used in this work were: anti-rabbit and anti-mouse (Abcam #ab6721 and Abcam #ab6789) at 1:5000 dilutions.

5.5.11 Proteasome activity

Two whole flies were homogenized in 25mM Tris, pH 7.5 and the protein content was determined using a BCA assay. Chymotrypsin-like peptidase activity of the proteasome was assayed by using the fluorogenic peptide substrate Succinyl-Leu-Leu-Val-Tyr-amidomethylcoumarin (LLVY-AMC), based on a previously published protocol (Bulteau et al., 2002, Rogers et al., 2012). 20 μg of crude fly homogenate total protein was incubated at 37°C with 25uM LLVY-AMC in a final volume of 200 μLs. Enzymatic kinetics were measured in a temperature-controlled microplate fluorimeter (Tecan Infinite M200), at excitation/emission wavelengths of 360/460 nm, measuring fluorescence every 2 min for 1 h. Proteasome activity was determined as the slope of AMC accumulation over time per mg of total protein (pmoles/min/mg).

5.5.12 RNA sequencing

RNA was extracted using Trizol (Invitrogen) from four biological repeats of 25 heads of 10-day-old flies of the following genotypes: *elavGS>UAS-dGABPα* (+RU) and non-RU treated controls. The RNA was purified with the RNeasy columns (Qiagen) and its quality and concentration were determined using a NanoDrop. The RNA was further processed for RNAseq analysis at the Glasgow Polyomics Unit, University of Glasgow. The differentially expressed genes were measured for multiple hypothesis testing. The raw data were analysed by Dr. Dobril Ivanov, University of Cambridge.

5.5.13 Gene-Ontology (Catmap analysis)

For the functional analysis of all the expressed genes, I used the Wilcoxon rank sum test available in Catmap (Breslin et al., 2004). Ranks of genes were based on the Bayes t-statistic for differential expression and for a given functional category. The significance of the rank sum for all genes in the category was calculated analytically based on a random gene-rank distribution. Catmap analysis was performed by Dr. Dobril Ivanov.

5.5.14 Statistical analysis

Survival experiments were analysed using log-rank test or wilcoxon test. Cox Proportional Hazards analysis was performed in R to compare interactions for survivals. Other statistical analyses were performed using Excel and Prism (GraphPad, La Jolla, CA), have been indicated in the figure legends.

Chapter 6 General Discussion and future plan

PGC-1α is the key transcriptional co-activator in energy metabolism, regulating many biological processes, including growth, mitochondrial biogenesis, stress defence system, circadian rhythm and proteostasis. In my thesis, I focused on dissecting the role of PGC-1α in ageing and age-related neurodegeneration. I have found that genetic activation of PGC-1α in the central nervous system could ameliorate the neurotoxic phenotypes in a *Drosophila* model of Aβ toxicity. The improvements were associated with an improved mitochondrial homeostasis and the activation of UPR^{ER}. In keeping with this, I found that both rifampicin, the antibiotic used in the treatment of tuberculosis and leprosy, and metformin, the drug used in the treatment of type-2 diabetes, activated the UPR^{ER} and rescued the neurotoxicity in Aβ-expressing flies. These findings suggested that the pharmacological interventions that activating UPR^{ER}, or elevating PGC-1α may offer significant therapeutic benefits in AD. My findings are significant in the field. Although both mitochondrial dysfunction and ER-related proteostastic failure have been implicated in the disease progression in AD, *in-vivo* studies using animal models targeting above effectors are still limited. It would be interesting to investigate in future studies whether directly targeting components of UPR^{mt} or UPR^{ER} could provide beneficial effects in animal models. This knowledge could eventually be translated into drug discovery for human use.

There is urgent need for effective strategies to improve healthy ageing, with facts that the increasing ageing population coupled with the rising prevalence of age-related neurodegeneration. PGC-1α has also been implicated in fly ageing, however the mechanisms are not fully elucidated. Previous studies suggested that over-expression of PGC-1α in intestine extends lifespan associated with improved stress-defence system. However, I found that the long-lived flies were not resistant to different oxidative stressors, therefore excluding the possibility that oxidative stress is the driving force behind the lifespan prolonging effects of PGC-1α. There are three clues as to the mechanisms underlying the anti-ageing effects of PGC-1α over-expression. Over-expression of PGC-1α: 1) extended lifespan only in females but not males; 2)

formed an un-defined negative feedback loop on IIS/mTOR signalling pathway; 3) improved gut homeostasis. The sex difference in gut pathology in modulating lifespan prolonging effects has previously been observed in interventions involving down-regulation of nutrient-sensing pathways. To investigate the link between PGC-1α and nutrient-sensing pathways, I identified that transcription factor GABPα being downstream of PGC-1α, extended fly lifespan, through mechanisms associated with reduced IIS/mTOR signalling pathway. This finding supports the negative feedback loop of *dPGC-1* on IIS that has been proposed (Tiefenböck et al., 2010), involving up-regulation of *dGABPα* and *ImpL2*. It will be interesting to determine whether the *dGABPα*-IIS link is conserved in mammalian systems. Moreover, over-expression of GABPα improved gut homeostasis by delaying age-related over-proliferation in intestinal stem cells. My findings are novel and important in the ageing field. Given the evolutionarily conserved effects of reduced IIS/mTOR, the findings suggest that GABPα may be an effective modulator of mammalian ageing.

Moreover, I have demonstrated that lifespan could be uncoupled from oxidative stress, mitochondrial function, and fecundity. Xenobiotic stress seems to play an important role in the lifespan pro-longing effects of GABPα over-expression. It would be interesting in future studies to target this pathway genetically or pharmacologically for healthy ageing.

References:

ABRAMOV, A. Y., CANEVARI, L. & DUCHEN, M. R. 2004. Beta-amyloid peptides induce mitochondrial dysfunction and oxidative stress in astrocytes and death of neurons through activation of NADPH oxidase. *J Neurosci,* 24**,** 565-75.

ABRAMOV, A. Y., GEGG, M., GRUNEWALD, A., WOOD, N. W., KLEIN, C. & SCHAPIRA, A. H. 2011. Bioenergetic consequences of PINK1 mutations in Parkinson disease. *PLoS One,* 6**,** e25622.

ABRAMOV, A. Y., SMULDERS-SRINIVASAN, T. K., KIRBY, D. M., ACIN-PEREZ, R., ENRIQUEZ, J. A., LIGHTOWLERS, R. N., DUCHEN, M. R. & TURNBULL, D. M. 2010. Mechanism of neurodegeneration of neurons with mitochondrial DNA mutations. *Brain,* 133**,** 797-807.

AFSCHAR, S., TOIVONEN, J. M., HOFFMANN, J. M., TAIN, L. S., WIESER, D., FINLAYSON, A. J., DRIEGE, Y., ALIC, N., EMRAN, S., STINN, J., FROEHLICH, J., PIPER, M. D. & PARTRIDGE, L. 2016. Nuclear hormone receptor DHR96 mediates the resistance to xenobiotics but not the increased lifespan of insulin-mutant Drosophila. *Proc Natl Acad Sci U S A,* 113**,** 1321-6.

AKERFELT, M., MORIMOTO, R. I. & SISTONEN, L. 2010. Heat shock factors: integrators of cell stress, development and lifespan. *Nat Rev Mol Cell Biol,* 11**,** 545-55.

ALDRIDGE, J. E., HORIBE, T. & HOOGENRAAD, N. J. 2007. Discovery of genes activated by the mitochondrial unfolded protein response (mtUPR) and cognate promoter elements. *PLoS One,* 2**,** e874.

ALERS, S., LOFFLER, A. S., WESSELBORG, S. & STORK, B. 2012. Role of AMPK-mTOR-Ulk1/2 in the regulation of autophagy: cross talk, shortcuts, and feedbacks. *Mol Cell Biol,* 32**,** 2-11.

ALIC, N., ANDREWS, T. D., GIANNAKOU, M. E., PAPATHEODOROU, I., SLACK, C., HODDINOTT, M. P., COCHEME, H. M., SCHUSTER, E. F., THORNTON, J. M. & PARTRIDGE, L. 2011a. Genome-wide dFOXO targets and topology of the transcriptomic response to stress and insulin signalling. *Mol Syst Biol,* 7**,** 502.

ALIC, N., HODDINOTT, M. P., VINTI, G. & PARTRIDGE, L. 2011b. Lifespan extension by increased expression of the Drosophila homologue of the IGFBP7 tumour suppressor. *Aging Cell,* 10**,** 137-47.

ALIC, N. & PARTRIDGE, L. 2008. Stage debut for the elusive Drosophila insulin-like growth factor binding protein. *J Biol,* 7**,** 18.

ALZHEIMER, A. 1907. Ubereine eigenartige Erkrankung der Hirnrinde. *Allg Z Psychiatr-Gerichtl Med***,** 146-148.

AMCHESLAVSKY, A., JIANG, J. & IP, Y. T. 2009. Tissue damage-induced intestinal stem cell division in Drosophila. *Cell Stem Cell,* 4**,** 49-61.

AMEUR, A., STEWART, J. B., FREYER, C., HAGSTROM, E., INGMAN, M., LARSSON, N. G. & GYLLENSTEN, U. 2011. Ultra-deep sequencing of mouse mitochondrial DNA: mutational patterns and their origins. *PLoS Genet,* 7**,** e1002028.

ANANDATHEERTHAVARADA, H. K., BISWAS, G., ROBIN, M. A. & AVADHANI, N. G. 2003. Mitochondrial targeting and a novel transmembrane arrest of Alzheimer's amyloid precursor protein impairs mitochondrial function in neuronal cells. *J Cell Biol,* 161**,** 41-54.

ANDERSSON, U. & SCARPULLA, R. C. 2001. Pgc-1-related coactivator, a novel, serum-inducible coactivator of nuclear respiratory factor 1-dependent transcription in mammalian cells. *Mol Cell Biol,* 21**,** 3738-49.

ANDORFER, C., KRESS, Y., ESPINOZA, M., DE SILVA, R., TUCKER, K. L., BARDE, Y. A., DUFF, K. & DAVIES, P. 2003. Hyperphosphorylation and aggregation of tau in mice expressing normal human tau isoforms. *J Neurochem,* 86**,** 582-90.

ANISIMOV, V. N., BERSTEIN, L. M., POPOVICH, I. G., ZABEZHINSKI, M. A., EGORMIN, P. A., PISKUNOVA, T. S., SEMENCHENKO, A. V., TYNDYK, M. L., YUROVA, M. N., KOVALENKO, I. G. & POROSHINA, T. E. 2011. If started early in life, metformin treatment increases life span and postpones tumors in female SHR mice. *Aging (Albany NY),* 3**,** 148-57.

BALCH, W. E., MORIMOTO, R. I., DILLIN, A. & KELLY, J. W. 2008. Adapting proteostasis for disease intervention. *Science,* 319**,** 916-9.

BALTZER, C., TIEFENBÖCK, S. K., MARTI, M. & FREI, C. 2009. Nutrition controls mitochondrial biogenesis in the Drosophila adipose tissue through Delg and cyclin D/Cdk4. *PLoS One,* 4**,** e6935.

BANERJEE, K., SINHA, M., PHAM CLE, L., JANA, S., CHANDA, D., CAPPAI, R. & CHAKRABARTI, S. 2010. Alpha-synuclein induced membrane depolarization and loss of phosphorylation capacity of isolated rat brain mitochondria: implications in Parkinson's disease. *FEBS Lett,* 584**,** 1571-6.

BARNES, A. I., WIGBY, S., BOONE, J. M., PARTRIDGE, L. & CHAPMAN, T. 2008. Feeding, fecundity and lifespan in female Drosophila melanogaster. *Proc Biol Sci,* 275**,** 1675-83.

BARTKE, A. & BROWN-BORG, H. 2004. Life extension in the dwarf mouse. *Curr Top Dev Biol,* 63**,** 189-225.

BASS, T. M., GRANDISON, R. C., WONG, R., MARTINEZ, P., PARTRIDGE, L. & PIPER, M. D. 2007. Optimization of dietary restriction protocols in Drosophila. *J Gerontol A Biol Sci Med Sci,* 62**,** 1071-81.

BATEMAN, R. J., SIEMERS, E. R., MAWUENYEGA, K. G., WEN, G., BROWNING, K. R., SIGURDSON, W. C., YARASHESKI, K. E., FRIEDRICH, S. W., DEMATTOS, R. B., MAY, P. C., PAUL, S. M. & HOLTZMAN, D. M. 2009. A gamma-secretase inhibitor decreases amyloid-beta production in the central nervous system. *Ann Neurol,* 66**,** 48-54.

BEAVER, L. M., HOOVEN, L. A., BUTCHER, S. M., KRISHNAN, N., SHERMAN, K. A., CHOW, E. S. & GIEBULTOWICZ, J. M. 2010. Circadian clock regulates response to pesticides in Drosophila via conserved Pdp1 pathway. *Toxicol Sci,* 115**,** 513-20.

BECK, G., SUGIURA, Y., SHINZAWA, K., KATO, S., SETOU, M., TSUJIMOTO, Y., SAKODA, S. & SUMI-AKAMARU, H. 2011. Neuroaxonal dystrophy in calcium-independent phospholipase A2beta deficiency results from insufficient remodeling and degeneration of mitochondrial and presynaptic membranes. *J Neurosci,* 31**,** 11411-20.

BEN-ZVI, A., MILLER, E. A. & MORIMOTO, R. I. 2009. Collapse of proteostasis represents an early molecular event in Caenorhabditis elegans aging. *Proc Natl Acad Sci U S A,* 106**,** 14914-9.

BENDER, A., SCHWARZKOPF, R. M., MCMILLAN, A., KRISHNAN, K. J., RIEDER, G., NEUMANN, M., ELSTNER, M., TURNBULL, D. M. & KLOPSTOCK, T. 2008.

Dopaminergic midbrain neurons are the prime target for mitochondrial DNA deletions. *J Neurol,* 255**,** 1231-5.

BENILOVA, I., KARRAN, E. & DE STROOPER, B. 2012. The toxic Abeta oligomer and Alzheimer's disease: an emperor in need of clothes. *Nat Neurosci,* 15**,** 349-57.

BENZING, W. C., WUJEK, J. R., WARD, E. K., SHAFFER, D., ASHE, K. H., YOUNKIN, S. G. & BRUNDEN, K. R. 1999. Evidence for glial-mediated inflammation in aged APP(SW) transgenic mice. *Neurobiol Aging,* 20**,** 581-9.

BERTOLOTTI, A., ZHANG, Y., HENDERSHOT, L. M., HARDING, H. P. & RON, D. 2000. Dynamic interaction of BiP and ER stress transducers in the unfolded-protein response. *Nat Cell Biol,* 2**,** 326-32.

BITEAU, B., HOCHMUTH, C. E. & JASPER, H. 2008. JNK activity in somatic stem cells causes loss of tissue homeostasis in the aging Drosophila gut. *Cell Stem Cell,* 3**,** 442-55.

BITEAU, B., KARPAC, J., SUPOYO, S., DEGENNARO, M., LEHMANN, R. & JASPER, H. 2010. Lifespan extension by preserving proliferative homeostasis in Drosophila. *PLoS Genet,* 6**,** e1001159.

BJEDOV, I., TOIVONEN, J. M., KERR, F., SLACK, C., JACOBSON, J., FOLEY, A. & PARTRIDGE, L. 2010. Mechanisms of life span extension by rapamycin in the fruit fly Drosophila melanogaster. *Cell Metab,* 11**,** 35-46.

BLAKE, M. R., HOLBROOK, S. D., KOTWICA-ROLINSKA, J., CHOW, E. S., KRETZSCHMAR, D. & GIEBULTOWICZ, J. M. 2015. Manipulations of amyloid precursor protein cleavage disrupt the circadian clock in aging Drosophila. *Neurobiol Dis,* 77**,** 117-26.

BLENNOW, K., DE LEON, M. J. & ZETTERBERG, H. 2006. Alzheimer's disease. *Lancet,* 368**,** 387-403.

BONAWITZ, N. D., CHATENAY-LAPOINTE, M., PAN, Y. & SHADEL, G. S. 2007. Reduced TOR signaling extends chronological life span via increased respiration and upregulation of mitochondrial gene expression. *Cell Metab,* 5**,** 265-77.

BONIFATI, V., RIZZU, P., SQUITIERI, F., KRIEGER, E., VANACORE, N., VAN SWIETEN, J. C., BRICE, A., VAN DUIJN, C. M., OOSTRA, B., MECO, G. & HEUTINK, P. 2003. DJ-1(PARK7), a novel gene for autosomal recessive, early onset parkinsonism. *Neurol Sci,* 24**,** 159-60.

BOUCHE, V., ESPINOSA, A. P., LEONE, L., SARDIELLO, M., BALLABIO, A. & BOTAS, J. 2016. Drosophila Mitf regulates the V-ATPase and the lysosomal-autophagic pathway. *Autophagy,* 12**,** 484-98.

BOYCE, M., BRYANT, K. F., JOUSSE, C., LONG, K., HARDING, H. P., SCHEUNER, D., KAUFMAN, R. J., MA, D., COEN, D. M., RON, D. & YUAN, J. 2005. A selective inhibitor of eIF2alpha dephosphorylation protects cells from ER stress. *Science,* 307**,** 935-9.

BRAAK, H. & BRAAK, E. 1991. Neuropathological stageing of Alzheimer-related changes. *Acta Neuropathol,* 82**,** 239-59.

BRAECKMAN, B. P., HOUTHOOFD, K., DE VREESE, A. & VANFLETEREN, J. R. 1999. Apparent uncoupling of energy production and consumption in long-lived Clk mutants of Caenorhabditis elegans. *Curr Biol,* 9**,** 493-6.

BRAND, A. H. & PERRIMON, N. 1993. Targeted gene expression as a means of altering cell fates and generating dominant phenotypes. *Development,* 118**,** 401-15.

BRESLIN, T., EDEN, P. & KROGH, M. 2004. Comparing functional annotation analyses with Catmap. *BMC Bioinformatics,* 5**,** 193.

BRION, J. P., COUCK, A. M., PASSAREIRO, E. & FLAMENT-DURAND, J. 1985. Neurofibrillary tangles of Alzheimer's disease: an immunohistochemical study. *J Submicrosc Cytol,* 17**,** 89-96.

BROUGHTON, S. J., PIPER, M. D., IKEYA, T., BASS, T. M., JACOBSON, J., DRIEGE, Y., MARTINEZ, P., HAFEN, E., WITHERS, D. J., LEEVERS, S. J. & PARTRIDGE, L. 2005. Longer lifespan, altered metabolism, and stress resistance in Drosophila from ablation of cells making insulin-like ligands. *Proc Natl Acad Sci U S A,* 102**,** 3105-10.

BROUGHTON, S. J., SLACK, C., ALIC, N., METAXAKIS, A., BASS, T. M., DRIEGE, Y. & PARTRIDGE, L. 2010. DILP-producing median neurosecretory cells in the Drosophila brain mediate the response of lifespan to nutrition. *Aging Cell,* 9**,** 336-46.

BROUSSARD, J. A., RAPPAZ, B., WEBB, D. J. & BROWN, C. M. 2013. Fluorescence resonance energy transfer microscopy as demonstrated by measuring the activation of the serine/threonine kinase Akt. *Nat Protoc,* 8**,** 265-81.

BROWN-BORG, H. M. & RAKOCZY, S. 2013. Metabolic adaptations to short-term every-other-day feeding in long-living Ames dwarf mice. *Exp Gerontol,* 48**,** 905-19.

BUCHON, N., BRODERICK, N. A., POIDEVIN, M., PRADERVAND, S. & LEMAITRE, B. 2009. Drosophila intestinal response to bacterial infection: activation of host defense and stem cell proliferation. *Cell Host Microbe,* 5**,** 200-11.

BULTEAU, A. L., MOREAU, M., NIZARD, C. & FRIGUET, B. 2002. Impairment of proteasome function upon UVA- and UVB-irradiation of human keratinocytes. *Free Radic Biol Med,* 32**,** 1157-70.

BURKEWITZ, K., ZHANG, Y. & MAIR, W. B. 2014. AMPK at the nexus of energetics and aging. *Cell Metab,* 20**,** 10-25.

BURNETT, C., VALENTINI, S., CABREIRO, F., GOSS, M., SOMOGYVARI, M., PIPER, M. D., HODDINOTT, M., SUTPHIN, G. L., LEKO, V., MCELWEE, J. J., VAZQUEZ-MANRIQUE, R. P., ORFILA, A. M., ACKERMAN, D., AU, C., VINTI, G., RIESEN, M., HOWARD, K., NERI, C., BEDALOV, A., KAEBERLEIN, M., SOTI, C., PARTRIDGE, L. & GEMS, D. 2011. Absence of effects of Sir2 overexpression on lifespan in C. elegans and Drosophila. *Nature,* 477**,** 482-5.

BUSCIGLIO, J., PELSMAN, A., WONG, C., PIGINO, G., YUAN, M., MORI, H. & YANKNER, B. A. 2002. Altered metabolism of the amyloid beta precursor protein is associated with mitochondrial dysfunction in Down's syndrome. *Neuron,* 33**,** 677-88.

CABREJO, L., GUYANT-MARECHAL, L., LAQUERRIERE, A., VERCELLETTO, M., DE LA FOURNIERE, F., THOMAS-ANTERION, C., VERNY, C., LETOURNEL, F., PASQUIER, F., VITAL, A., CHECLER, F., FREBOURG, T., CAMPION, D. & HANNEQUIN, D. 2006. Phenotype associated with APP duplication in five families. *Brain,* 129**,** 2966-76.

CALKINS, M. J., MANCZAK, M., MAO, P., SHIRENDEB, U. & REDDY, P. H. 2011. Impaired mitochondrial biogenesis, defective axonal transport of mitochondria, abnormal mitochondrial dynamics and synaptic degeneration in a mouse model of Alzheimer's disease. *Hum Mol Genet,* 20**,** 4515-29.

CAMACHO, A., RODRIGUEZ-CUENCA, S., BLOUNT, M., PRIEUR, X., BARBARROJA, N., FULLER, M., HARDINGHAM, G. E. & VIDAL-PUIG, A. 2012. Ablation of PGC1 beta prevents mTOR dependent endoplasmic reticulum stress response. *Exp Neurol,* 237**,** 396-406.

CANNON, B., HOUSTEK, J. & NEDERGAARD, J. 1998. Brown adipose tissue. More than an effector of thermogenesis? *Ann N Y Acad Sci,* 856**,** 171-87.

CARRARA, M., PRISCHI, F. & ALI, M. M. 2013. UPR Signal Activation by Luminal Sensor Domains. *Int J Mol Sci,* 14**,** 6454-66.

CASALI, C., VALENTE, E. M., BERTINI, E., MONTAGNA, G., CRISCUOLO, C., DE MICHELE, G., VILLANOVA, M., DAMIANO, M., PIERALLINI, A., BRANCATI, F., SCARANO, V., TESSA, A., CRICCHI, F., GRIECO, G. S., MUGLIA, M., CARELLA, M., MARTINI, B., ROSSI, A., AMABILE, G. A., NAPPI, G., FILLA, A., DALLAPICCOLA, B. & SANTORELLI, F. M. 2004. Clinical and genetic studies in hereditary spastic paraplegia with thin corpus callosum. *Neurology,* 62**,** 262-8.

CASAS-TINTO, S., ZHANG, Y., SANCHEZ-GARCIA, J., GOMEZ-VELAZQUEZ, M., RINCON-LIMAS, D. E. & FERNANDEZ-FUNEZ, P. 2011. The ER stress factor XBP1s prevents amyloid-beta neurotoxicity. *Hum Mol Genet,* 20**,** 2144-60.

CASLEY, C. S., CANEVARI, L., LAND, J. M., CLARK, J. B. & SHARPE, M. A. 2002. Beta-amyloid inhibits integrated mitochondrial respiration and key enzyme activities. *J Neurochem,* 80**,** 91-100.

CASSARD-DOULCIER, A. M., LAROSE, M., MATAMALA, J. C., CHAMPIGNY, O., BOUILLAUD, F. & RICQUIER, D. 1994. In vitro interactions between nuclear proteins and uncoupling protein gene promoter reveal several putative transactivating factors including Ets1, retinoid X receptor, thyroid hormone receptor, and a CACCC box-binding protein. *J Biol Chem,* 269**,** 24335-42.

CASTILLO-QUAN, J. I., KINGHORN, K. J. & BJEDOV, I. 2015. Genetics and pharmacology of longevity: the road to therapeutics for healthy aging. *Adv Genet,* 90**,** 1-101.

CASTILLO-QUAN, J. I., LI, L., KINGHORN, K. J., IVANOV, D. K., TAIN, L. S., SLACK, C., KERR, F., NESPITAL, T., THORNTON, J., HARDY, J., BJEDOV, I. & PARTRIDGE, L. 2016. Lithium Promotes Longevity through GSK3/NRF2-Dependent Hormesis. *Cell Rep,* 15**,** 638-50.

CAVA, E. & FONTANA, L. 2013. Will calorie restriction work in humans? *Aging-Us,* 5**,** 507-514.

CHA, G. H., KIM, S., PARK, J., LEE, E., KIM, M., LEE, S. B., KIM, J. M., CHUNG, J. & CHO, K. S. 2005. Parkin negatively regulates JNK pathway in the dopaminergic neurons of Drosophila. *Proc Natl Acad Sci U S A,* 102**,** 10345-50.

CHAPMAN, T. & PARTRIDGE, L. 1996. Female fitness in Drosophila melanogaster: an interaction between the effect of nutrition and of encounter rate with males. *Proc Biol Sci,* 263**,** 755-9.

CHARIER-HARLIN, M. 1991. Early-onset Alzheimer's disease caused by mutations at codon 717 of the beta-amyloid precursor protein gene. *Nature*, 844-846.

CHEN, C., LIU, Y., LIU, Y. & ZHENG, P. 2009a. mTOR regulation and therapeutic rejuvenation of aging hematopoietic stem cells. *Sci Signal,* 2**,** ra75.

CHEN, D., THOMAS, E. L. & KAPAHI, P. 2009b. HIF-1 modulates dietary restriction-mediated lifespan extension via IRE-1 in Caenorhabditis elegans. *PLoS Genet,* 5**,** e1000486.

CHEN, L. & FEANY, M. B. 2005. Alpha-synuclein phosphorylation controls neurotoxicity and inclusion formation in a Drosophila model of Parkinson disease. *Nat Neurosci,* 8**,** 657-63.

CHENG, C. W., ADAMS, G. B., PERIN, L., WEI, M., ZHOU, X., LAM, B. S., DA SACCO, S., MIRISOLA, M., QUINN, D. I., DORFF, T. B., KOPCHICK, J. J. & LONGO, V. D. 2014. Prolonged fasting reduces IGF-1/PKA to promote hematopoietic-stem-cell-based regeneration and reverse immunosuppression. *Cell Stem Cell,* 14**,** 810-23.

CHENG, I. H., PALOP, J. J., ESPOSITO, L. A., BIEN-LY, N., YAN, F. & MUCKE, L. 2004. Aggressive amyloidosis in mice expressing human amyloid peptides with the Arctic mutation. *Nat Med,* 10**,** 1190-2.

CHENG, Z., GUO, S., COPPS, K., DONG, X., KOLLIPARA, R., RODGERS, J. T., DEPINHO, R. A., PUIGSERVER, P. & WHITE, M. F. 2009. Foxo1 integrates insulin signaling with mitochondrial function in the liver. *Nat Med,* 15**,** 1307-11.

CHIN, L. S., OLZMANN, J. A. & LI, L. 2010. Parkin-mediated ubiquitin signalling in aggresome formation and autophagy. *Biochem Soc Trans,* 38**,** 144-9.

CHIU, H. K., TSAI, E. C., JUNEJA, R., STOEVER, J., BROOKS-WORRELL, B., GOEL, A. & PALMER, J. P. 2007. Equivalent insulin resistance in latent autoimmune diabetes in adults (LADA) and type 2 diabetic patients. *Diabetes Res Clin Pract,* 77**,** 237-44.

CHOI, N. H., KIM, J. G., YANG, D. J., KIM, Y. S. & YOO, M. A. 2008. Age-related changes in Drosophila midgut are associated with PVF2, a PDGF/VEGF-like growth factor. *Aging Cell,* 7**,** 318-34.

CHUI, D. H., TABIRA, T., IZUMI, S., KOYA, G. & OGATA, J. 1994. Decreased Beta-Amyloid and Increased Abnormal Tau-Deposition in the Brain of Aged Patients with Leprosy. *American Journal of Pathology,* 145**,** 771-775.

CHUNG, H. Y., CESARI, M., ANTON, S., MARZETTI, E., GIOVANNINI, S., SEO, A. Y., CARTER, C., YU, B. P. & LEEUWENBURGH, C. 2009. Molecular inflammation: underpinnings of aging and age-related diseases. *Ageing Res Rev,* 8**,** 18-30.

CITRON, M., OLTERSDORF, T., HAASS, C., MCCONLOGUE, L., HUNG, A. Y., SEUBERT, P., VIGO-PELFREY, C., LIEBERBURG, I. & SELKOE, D. J. 1992. Mutation of the beta-amyloid precursor protein in familial Alzheimer's disease increases beta-protein production. *Nature,* 360**,** 672-4.

CLANCY, D. J., GEMS, D., HAFEN, E., LEEVERS, S. J. & PARTRIDGE, L. 2002. Dietary restriction in long-lived dwarf flies. *Science,* 296**,** 319.

CLANCY, D. J., GEMS, D., HARSHMAN, L. G., OLDHAM, S., STOCKER, H., HAFEN, E., LEEVERS, S. J. & PARTRIDGE, L. 2001. Extension of life-span by loss of CHICO, a Drosophila insulin receptor substrate protein. *Science,* 292**,** 104-6.

CLARK, I. E., DODSON, M. W., JIANG, C., CAO, J. H., HUH, J. R., SEOL, J. H., YOO, S. J., HAY, B. A. & GUO, M. 2006. Drosophila pink1 is required for mitochondrial function and interacts genetically with parkin. *Nature,* 441**,** 1162-6.

CLARK, J., REDDY, S., ZHENG, K., BETENSKY, R. A. & SIMON, D. K. 2011. Association of PGC-1alpha polymorphisms with age of onset and risk of Parkinson's disease. *BMC Med Genet,* 12**,** 69.

COCHEME, H. M. & MURPHY, M. P. 2008. Complex I is the major site of mitochondrial superoxide production by paraquat. *J Biol Chem,* 283**,** 1786-98.

COLMAN, R. J., ANDERSON, R. M., JOHNSON, S. C., KASTMAN, E. K., KOSMATKA, K. J., BEASLEY, T. M., ALLISON, D. B., CRUZEN, C., SIMMONS, H. A., KEMNITZ, J. W. & WEINDRUCH, R. 2009. Caloric restriction delays disease onset and mortality in rhesus monkeys. *Science,* 325**,** 201-4.

COLMAN, R. J., BEASLEY, T. M., KEMNITZ, J. W., JOHNSON, S. C., WEINDRUCH, R. & ANDERSON, R. M. 2014. Caloric restriction reduces age-related and all-cause mortality in rhesus monkeys. *Nat Commun,* 5**,** 3557.

CONWAY, K. A., LEE, S. J., ROCHET, J. C., DING, T. T., WILLIAMSON, R. E. & LANSBURY, P. T., JR. 2000. Acceleration of oligomerization, not fibrillization, is a shared property of both alpha-synuclein mutations linked to early-onset Parkinson's disease: implications for pathogenesis and therapy. *Proc Natl Acad Sci U S A,* 97**,** 571-6.

COOKSON, M. R. & VAN DER BRUG, M. 2008. Cell systems and the toxic mechanism(s) of alpha-synuclein. *Exp Neurol,* 209**,** 5-11.

COPELAND, J. M., CHO, J., LO, T., JR., HUR, J. H., BAHADORANI, S., ARABYAN, T., RABIE, J., SOH, J. & WALKER, D. W. 2009. Extension of Drosophila life span by RNAi of the mitochondrial respiratory chain. *Curr Biol,* 19**,** 1591-8.

COSKUN, P. E., BEAL, M. F. & WALLACE, D. C. 2004. Alzheimer's brains harbor somatic mtDNA control-region mutations that suppress mitochondrial transcription and replication. *Proc Natl Acad Sci U S A,* 101**,** 10726-31.

CREWS, L. & MASLIAH, E. 2010. Molecular mechanisms of neurodegeneration in Alzheimer's disease. *Hum Mol Genet,* 19**,** R12-20.

CRONIN, S. J., NEHME, N. T., LIMMER, S., LIEGEOIS, S., POSPISILIK, J. A., SCHRAMEK, D., LEIBBRANDT, A., SIMOES RDE, M., GRUBER, S., PUC, U., EBERSBERGER, I., ZORANOVIC, T., NEELY, G. G., VON HAESELER, A., FERRANDON, D. & PENNINGER, J. M. 2009. Genome-wide RNAi screen identifies genes involved in intestinal pathogenic bacterial infection. *Science,* 325**,** 340-3.

CROUCH, P. J., BLAKE, R., DUCE, J. A., CICCOTOSTO, G. D., LI, Q. X., BARNHAM, K. J., CURTAIN, C. C., CHERNY, R. A., CAPPAI, R., DYRKS, T., MASTERS, C. L. & TROUNCE, I. A. 2005. Copper-dependent inhibition of human cytochrome c oxidase by a dimeric conformer of amyloid-beta1-42. *J Neurosci,* 25**,** 672-9.

CROWTHER, D. C., KINGHORN, K. J., MIRANDA, E., PAGE, R., CURRY, J. A., DUTHIE, F. A., GUBB, D. C. & LOMAS, D. A. 2005. Intraneuronal Abeta, non-amyloid aggregates and neurodegeneration in a Drosophila model of Alzheimer's disease. *Neuroscience,* 132**,** 123-35.

CUI, L., JEONG, H., BOROVECKI, F., PARKHURST, C. N., TANESE, N. & KRAINC, D. 2006. Transcriptional repression of PGC-1alpha by mutant huntingtin leads to mitochondrial dysfunction and neurodegeneration. *Cell,* 127**,** 59-69.

CUNNINGHAM, J. T., RODGERS, J. T., ARLOW, D. H., VAZQUEZ, F., MOOTHA, V. K. & PUIGSERVER, P. 2007. mTOR controls mitochondrial oxidative function through a YY1-PGC-1alpha transcriptional complex. *Nature,* 450**,** 736-40.

CYRAN, S. A., BUCHSBAUM, A. M., REDDY, K. L., LIN, M. C., GLOSSOP, N. R., HARDIN, P. E., YOUNG, M. W., STORTI, R. V. & BLAU, J. 2003. vrille, Pdp1, and dClock form a second feedback loop in the Drosophila circadian clock. *Cell,* 112**,** 329-41.

DA CRUZ, S., PARONE, P. A., LOPES, V. S., LILLO, C., MCALONIS-DOWNES, M., LEE, S. K., VETTO, A. P., PETROSYAN, S., MARSALA, M., MURPHY, A. N., WILLIAMS, D. S., SPIEGELMAN, B. M. & CLEVELAND, D. W. 2012. Elevated PGC-1alpha activity sustains mitochondrial biogenesis and muscle function without extending survival in a mouse model of inherited ALS. *Cell Metab,* 15**,** 778-86.

DARIOS, F., CORTI, O., LUCKING, C. B., HAMPE, C., MURIEL, M. P., ABBAS, N., GU, W. J., HIRSCH, E. C., ROONEY, T., RUBERG, M. & BRICE, A. 2003. Parkin prevents mitochondrial swelling and cytochrome c release in mitochondria-dependent cell death. *Hum Mol Genet,* 12**,** 517-26.

DASURI, K., ZHANG, L. & KELLER, J. N. 2013. Oxidative stress, neurodegeneration, and the balance of protein degradation and protein synthesis. *Free Radic Biol Med,* 62**,** 170-85.

DE CABO, R., CARMONA-GUTIERREZ, D., BERNIER, M., HALL, M. N. & MADEO, F. 2014. The search for antiaging interventions: from elixirs to fasting regimens. *Cell,* 157**,** 1515-26.

DE STROOPER, B., SAFTIG, P., CRAESSAERTS, K., VANDERSTICHELE, H., GUHDE, G., ANNAERT, W., VON FIGURA, K. & VAN LEUVEN, F. 1998. Deficiency of presenilin-1 inhibits the normal cleavage of amyloid precursor protein. *Nature,* 391**,** 387-90.

DEAS, E., WOOD, N. W. & PLUN-FAVREAU, H. 2011. Mitophagy and Parkinson's disease: the PINK1-parkin link. *Biochim Biophys Acta,* 1813**,** 623-33.

DELL'AGNELLO, C., LEO, S., AGOSTINO, A., SZABADKAI, G., TIVERON, C., ZULIAN, A., PRELLE, A., ROUBERTOUX, P., RIZZUTO, R. & ZEVIANI, M. 2007. Increased longevity and refractoriness to Ca(2+)-dependent neurodegeneration in Surf1 knockout mice. *Hum Mol Genet,* 16**,** 431-44.

DEVI, L., RAGHAVENDRAN, V., PRABHU, B. M., AVADHANI, N. G. & ANANDATHEERTHAVARADA, H. K. 2008. Mitochondrial import and accumulation of alpha-synuclein impair complex I in human dopaminergic neuronal cultures and Parkinson disease brain. *J Biol Chem,* 283**,** 9089-100.

DEWACHTER, I., RIS, L., CROES, S., BORGHGRAEF, P., DEVIJVER, H., VOETS, T., NILIUS, B., GODAUX, E. & VAN LEUVEN, F. 2008. Modulation of synaptic plasticity and Tau phosphorylation by wild-type and mutant presenilin1. *Neurobiol Aging,* 29**,** 639-52.

DICKSON, D. W., BRAAK, H., DUDA, J. E., DUYCKAERTS, C., GASSER, T., HALLIDAY, G. M., HARDY, J., LEVERENZ, J. B., DEL TREDICI, K., WSZOLEK, Z. K. & LITVAN, I. 2009. Neuropathological assessment of Parkinson's disease: refining the diagnostic criteria. *Lancet Neurol,* 8**,** 1150-7.

DILLIN, A., HSU, A. L., ARANTES-OLIVEIRA, N., LEHRER-GRAIWER, J., HSIN, H., FRASER, A. G., KAMATH, R. S., AHRINGER, J. & KENYON, C. 2002. Rates of

behavior and aging specified by mitochondrial function during development. *Science,* 298**,** 2398-401.

DIVRY, P. & FLORKIN, M. 1927. Sur les proprietes optiques de l'amyloid. Societe de Biologie. 180-181.

DOONAN, R., MCELWEE, J. J., MATTHIJSSENS, F., WALKER, G. A., HOUTHOOFD, K., BACK, P., MATSCHESKI, A., VANFLETEREN, J. R. & GEMS, D. 2008. Against the oxidative damage theory of aging: superoxide dismutases protect against oxidative stress but have little or no effect on life span in Caenorhabditis elegans. *Genes Dev,* 22**,** 3236-41.

DU, H., GUO, L., YAN, S., SOSUNOV, A. A., MCKHANN, G. M. & YAN, S. S. 2010. Early deficits in synaptic mitochondria in an Alzheimer's disease mouse model. *Proc Natl Acad Sci U S A,* 107**,** 18670-5.

DUFF, K. 1997. Alzheimer transgenic mouse models come of age. *Trends Neurosci,* 20**,** 279-80.

DUMONT, M., STACK, C., ELIPENAHLI, C., JAINUDDIN, S., LAUNAY, N., GERGES, M., STARKOVA, N., STARKOV, A. A., CALINGASAN, N. Y., TAMPELLINI, D., PUJOL, A. & BEAL, M. F. 2014. PGC-1alpha overexpression exacerbates beta-amyloid and tau deposition in a transgenic mouse model of Alzheimer's disease. *FASEB J,* 28**,** 1745-55.

EDBAUER, D., WINKLER, E., REGULA, J. T., PESOLD, B., STEINER, H. & HAASS, C. 2003. Reconstitution of gamma-secretase activity. *Nat Cell Biol,* 5**,** 486-8.

EGAWA, N., YAMAMOTO, K., INOUE, H., HIKAWA, R., NISHI, K., MORI, K. & TAKAHASHI, R. 2011. The endoplasmic reticulum stress sensor, ATF6alpha, protects against neurotoxin-induced dopaminergic neuronal death. *J Biol Chem,* 286**,** 7947-57.

ENERBACK, S., JACOBSSON, A., SIMPSON, E. M., GUERRA, C., YAMASHITA, H., HARPER, M. E. & KOZAK, L. P. 1997. Mice lacking mitochondrial uncoupling protein are cold-sensitive but not obese. *Nature,* 387**,** 90-4.

EVANS, M. J. & SCARPULLA, R. C. 1990. NRF-1: a trans-activator of nuclear-encoded respiratory genes in animal cells. *Genes Dev,* 4**,** 1023-34.

FABER-LANGENDOEN, K., MORRIS, J. C., KNESEVICH, J. W., LABARGE, E., MILLER, J. P. & BERG, L. 1988. Aphasia in senile dementia of the Alzheimer type. *Ann Neurol,* 23**,** 365-70.

FARRER, M., CHAN, P., CHEN, R., TAN, L., LINCOLN, S., HERNANDEZ, D., FORNO, L., GWINN-HARDY, K., PETRUCELLI, L., HUSSEY, J., SINGLETON, A., TANNER, C., HARDY, J. & LANGSTON, J. W. 2001. Lewy bodies and parkinsonism in families with parkin mutations. *Ann Neurol,* 50**,** 293-300.

FARRER, M., KACHERGUS, J., FORNO, L., LINCOLN, S., WANG, D. S., HULIHAN, M., MARAGANORE, D., GWINN-HARDY, K., WSZOLEK, Z., DICKSON, D. & LANGSTON, J. W. 2004. Comparison of kindreds with parkinsonism and alpha-synuclein genomic multiplications. *Ann Neurol,* 55**,** 174-9.

FEANY, M. B. & BENDER, W. W. 2000. A Drosophila model of Parkinson's disease. *Nature,* 404**,** 394-8.

FENG, J., BUSSIERE, F. & HEKIMI, S. 2001. Mitochondrial electron transport is a key determinant of life span in Caenorhabditis elegans. *Dev Cell,* 1**,** 633-44.

FERNANDEZ-FUNEZ, P., DE MENA, L. & RINCON-LIMAS, D. E. 2015. Modeling the complex pathology of Alzheimer's disease in Drosophila. *Exp Neurol,* 274**,** 58-71.

FIGUEROA-CLAREVEGA, A. & BILDER, D. 2015. Malignant Drosophila tumors interrupt insulin signaling to induce cachexia-like wasting. *Dev Cell,* 33**,** 47-55.

FINELLI, A., KELKAR, A., SONG, H. J., YANG, H. & KONSOLAKI, M. 2004. A model for studying Alzheimer's Abeta42-induced toxicity in Drosophila melanogaster. *Mol Cell Neurosci,* 26**,** 365-75.

FONTANA, L., KENNEDY, B. K., LONGO, V. D., SEALS, D. & MELOV, S. 2014. Medical research: treat ageing. *Nature,* 511**,** 405-7.

FONTANA, L. & PARTRIDGE, L. 2015. Promoting health and longevity through diet: from model organisms to humans. *Cell,* 161**,** 106-18.

FONTANA, L., PARTRIDGE, L. & LONGO, V. D. 2010. Extending healthy life span--from yeast to humans. *Science,* 328**,** 321-6.

FORD, D., HOE, N., LANDIS, G. N., TOZER, K., LUU, A., BHOLE, D., BADRINATH, A. & TOWER, J. 2007. Alteration of Drosophila life span using conditional, tissue-specific expression of transgenes triggered by doxycyline or RU486/Mifepristone. *Exp Gerontol,* 42**,** 483-97.

GADD, M. E., BROEKEMEIER, K. M., CROUSER, E. D., KUMAR, J., GRAFF, G. & PFEIFFER, D. R. 2006. Mitochondrial iPLA2 activity modulates the release of cytochrome c from mitochondria and influences the permeability transition. *J Biol Chem,* 281**,** 6931-9.

GALINDO, M. F., IKUTA, I., ZHU, X., CASADESUS, G. & JORDAN, J. 2010. Mitochondrial biology in Alzheimer's disease pathogenesis. *J Neurochem,* 114**,** 933-45.

GAMES, D., ADAMS, D., ALESSANDRINI, R., BARBOUR, R., BERTHELETTE, P., BLACKWELL, C., CARR, T., CLEMENS, J., DONALDSON, T., GILLESPIE, F. & ET AL. 1995. Alzheimer-type neuropathology in transgenic mice overexpressing V717F beta-amyloid precursor protein. *Nature,* 373**,** 523-7.

GANDHI, S., WOOD-KACZMAR, A., YAO, Z., PLUN-FAVREAU, H., DEAS, E., KLUPSCH, K., DOWNWARD, J., LATCHMAN, D. S., TABRIZI, S. J., WOOD, N. W., DUCHEN, M. R. & ABRAMOV, A. Y. 2009. PINK1-associated Parkinson's disease is caused by neuronal vulnerability to calcium-induced cell death. *Mol Cell,* 33**,** 627-38.

GARCIA-ESCUDERO, V., MARTIN-MAESTRO, P., PERRY, G. & AVILA, J. 2013. Deconstructing mitochondrial dysfunction in Alzheimer disease. *Oxid Med Cell Longev,* 2013**,** 162152.

GARGANO, J. W., MARTIN, I., BHANDARI, P. & GROTEWIEL, M. S. 2005. Rapid iterative negative geotaxis (RING): a new method for assessing age-related locomotor decline in Drosophila. *Exp Gerontol,* 40**,** 386-95.

GAUTIER, C. A., KITADA, T. & SHEN, J. 2008. Loss of PINK1 causes mitochondrial functional defects and increased sensitivity to oxidative stress. *Proc Natl Acad Sci U S A,* 105**,** 11364-9.

GEGG, M. E., COOPER, J. M., SCHAPIRA, A. H. & TAANMAN, J. W. 2009. Silencing of PINK1 expression affects mitochondrial DNA and oxidative phosphorylation in dopaminergic cells. *PLoS One,* 4**,** e4756.

GEMS, D., PLETCHER, S. & PARTRIDGE, L. 2002. Interpreting interactions between treatments that slow aging. *Aging Cell,* 1**,** 1-9.

GERSHMAN, B., PUIG, O., HANG, L., PEITZSCH, R. M., TATAR, M. & GAROFALO, R. S. 2007. High-resolution dynamics of the transcriptional response to nutrition in Drosophila: a key role for dFOXO. *Physiol Genomics,* 29**,** 24-34.

GIBSON, G. E., SHEU, K. F., BLASS, J. P., BAKER, A., CARLSON, K. C., HARDING, B. & PERRINO, P. 1988. Reduced activities of thiamine-dependent enzymes in the brains and peripheral tissues of patients with Alzheimer's disease. *Arch Neurol,* 45**,** 836-40.

GLICKMAN, M. H. & CIECHANOVER, A. 2002. The ubiquitin-proteasome proteolytic pathway: destruction for the sake of construction. *Physiol Rev,* 82**,** 373-428.

GOATE, A., CHARTIER-HARLIN, M. C., MULLAN, M., BROWN, J., CRAWFORD, F., FIDANI, L., GIUFFRA, L., HAYNES, A., IRVING, N., JAMES, L. & ET AL. 1991. Segregation of a missense mutation in the amyloid precursor protein gene with familial Alzheimer's disease. *Nature,* 349**,** 704-6.

GOMEZ-ISLA, T., HOLLISTER, R., WEST, H., MUI, S., GROWDON, J. H., PETERSEN, R. C., PARISI, J. E. & HYMAN, B. T. 1997. Neuronal loss correlates with but exceeds neurofibrillary tangles in Alzheimer's disease. *Ann Neurol,* 41**,** 17-24.

GOODRICK, C. L., INGRAM, D. K., REYNOLDS, M. A., FREEMAN, J. R. & CIDER, N. 1990. Effects of intermittent feeding upon body weight and lifespan in inbred mice: interaction of genotype and age. *Mech Ageing Dev,* 55**,** 69-87.

GORBATYUK, M. S., SHABASHVILI, A., CHEN, W., MEYERS, C., SULLIVAN, L. F., SALGANIK, M., LIN, J. H., LEWIN, A. S., MUZYCZKA, N. & GORBATYUK, O. S. 2012. Glucose regulated protein 78 diminishes alpha-synuclein neurotoxicity in a rat model of Parkinson disease. *Mol Ther,* 20**,** 1327-37.

GRANDISON, R. C., WONG, R., BASS, T. M., PARTRIDGE, L. & PIPER, M. D. 2009. Effect of a standardised dietary restriction protocol on multiple laboratory strains of Drosophila melanogaster. *PLoS One,* 4**,** e4067.

GREEN, D. R., GALLUZZI, L. & KROEMER, G. 2011. Mitochondria and the autophagy-inflammation-cell death axis in organismal aging. *Science,* 333**,** 1109-12.

GREENBAUM, E. A., GRAVES, C. L., MISHIZEN-EBERZ, A. J., LUPOLI, M. A., LYNCH, D. R., ENGLANDER, S. W., AXELSEN, P. H. & GIASSON, B. I. 2005. The E46K mutation in alpha-synuclein increases amyloid fibril formation. *J Biol Chem,* 280**,** 7800-7.

GREENE, J. C., WHITWORTH, A. J., KUO, I., ANDREWS, L. A., FEANY, M. B. & PALLANCK, L. J. 2003. Mitochondrial pathology and apoptotic muscle degeneration in Drosophila parkin mutants. *Proc Natl Acad Sci U S A,* 100**,** 4078-83.

GREENSPAN, R. J. 2004. Fly pushing: the theory and practice of Drosophila genetics. *(Cold Spring Harbor, New York: Cold Spring Harbor Laboratory Press)*.

GREER, E. L., DOWLATSHAHI, D., BANKO, M. R., VILLEN, J., HOANG, K., BLANCHARD, D., GYGI, S. P. & BRUNET, A. 2007. An AMPK-FOXO pathway mediates longevity induced by a novel method of dietary restriction in C. elegans. *Curr Biol,* 17**,** 1646-56.

GRONKE, S., CLARKE, D. F., BROUGHTON, S., ANDREWS, T. D. & PARTRIDGE, L. 2010. Molecular evolution and functional characterization of Drosophila insulin-like peptides. *PLoS Genet,* 6**,** e1000857.

GRUNEWALD, A., VOGES, L., RAKOVIC, A., KASTEN, M., VANDEBONA, H., HEMMELMANN, C., LOHMANN, K., OROLICKI, S., RAMIREZ, A., SCHAPIRA, A. H., PRAMSTALLER, P. P., SUE, C. M. & KLEIN, C. 2010. Mutant Parkin impairs mitochondrial function and morphology in human fibroblasts. *PLoS One,* 5**,** e12962.

GUARENTE, L. 2013. Calorie restriction and sirtuins revisited. *Genes Dev,* 27**,** 2072-85.

GUARENTE, L. & KENYON, C. 2000. Genetic pathways that regulate ageing in model organisms. *Nature,* 408**,** 255-62.

GUERTIN, D. A. & SABATINI, D. M. 2009. The pharmacology of mTOR inhibition. *Sci Signal,* 2**,** pe24.

GUIX, F. X., WAHLE, T., VENNEKENS, K., SNELLINX, A., CHAVEZ-GUTIERREZ, L., ILL-RAGA, G., RAMOS-FERNANDEZ, E., GUARDIA-LAGUARTA, C., LLEO, A., ARIMON, M., BEREZOVSKA, O., MUNOZ, F. J., DOTTI, C. G. & DE STROOPER, B. 2012. Modification of gamma-secretase by nitrosative stress links neuronal ageing to sporadic Alzheimer's disease. *EMBO Mol Med,* 4**,** 660-73.

GULOW, K., BIENERT, D. & HAAS, I. G. 2002. BiP is feed-back regulated by control of protein translation efficiency. *J Cell Sci,* 115**,** 2443-52.

GUNAWARDENA, S. & GOLDSTEIN, L. S. 2001. Disruption of axonal transport and neuronal viability by amyloid precursor protein mutations in Drosophila. *Neuron,* 32**,** 389-401.

GUO, L., KARPAC, J., TRAN, S. L. & JASPER, H. 2014. PGRP-SC2 promotes gut immune homeostasis to limit commensal dysbiosis and extend lifespan. *Cell,* 156**,** 109-22.

HALDANE, J. 1941. The relative importance of principal and modifying genes in determining some

human diseases. *J. Genet***,** 149-1257.

HANDSCHIN, C., KOBAYASHI, Y. M., CHIN, S., SEALE, P., CAMPBELL, K. P. & SPIEGELMAN, B. M. 2007. PGC-1alpha regulates the neuromuscular junction program and ameliorates Duchenne muscular dystrophy. *Genes Dev,* 21**,** 770-83.

HANSEN, M., CHANDRA, A., MITIC, L. L., ONKEN, B., DRISCOLL, M. & KENYON, C. 2008. A role for autophagy in the extension of lifespan by dietary restriction in C. elegans. *PLoS Genet,* 4**,** e24.

HARDY, J. A. & HIGGINS, G. A. 1992. Alzheimer's disease: the amyloid cascade hypothesis. *Science,* 256**,** 184-5.

HARMAN, D. 1965. The Free Radical Theory of Aging: Effect of Age on Serum Copper Levels. *J Gerontol,* 20**,** 151-3.

HARPER, D. G., VOLICER, L., STOPA, E. G., MCKEE, A. C., NITTA, M. & SATLIN, A. 2005. Disturbance of endogenous circadian rhythm in aging and Alzheimer disease. *Am J Geriatr Psychiatry,* 13**,** 359-68.

HARRISON, D. E., STRONG, R., SHARP, Z. D., NELSON, J. F., ASTLE, C. M., FLURKEY, K., NADON, N. L., WILKINSON, J. E., FRENKEL, K., CARTER, C. S., PAHOR, M., JAVORS, M. A., FERNANDEZ, E. & MILLER, R. A. 2009. Rapamycin fed late in life extends lifespan in genetically heterogeneous mice. *Nature,* 460**,** 392-5.

HARTWELL, L. H., HOOD, L., GOLDBERG, M. L., REYNOLDS, A. E. & SILVER, L. M. 2011. Drosophila

melanogaster: Genetic Portrait of the Fruit Fly. *In Genetics: From Genes to Genomes, (New*
York, USA: McGraw-Hill), 75-107.
HARVEY, R. J., SKELTON-ROBINSON, M. & ROSSOR, M. N. 2003. The prevalence and causes of dementia in people under the age of 65 years. *J Neurol Neurosurg Psychiatry,* 74**,** 1206-9.
HARVIE, M. N., PEGINGTON, M., MATTSON, M. P., FRYSTYK, J., DILLON, B., EVANS, G., CUZICK, J., JEBB, S. A., MARTIN, B., CUTLER, R. G., SON, T. G., MAUDSLEY, S., CARLSON, O. D., EGAN, J. M., FLYVBJERG, A. & HOWELL, A. 2011. The effects of intermittent or continuous energy restriction on weight loss and metabolic disease risk markers: a randomized trial in young overweight women. *Int J Obes (Lond),* 35**,** 714-27.
HAYNES, C. M., PETROVA, K., BENEDETTI, C., YANG, Y. & RON, D. 2007. ClpP mediates activation of a mitochondrial unfolded protein response in C. elegans. *Dev Cell,* 13**,** 467-80.
HAYNES, C. M. & RON, D. 2010. The mitochondrial UPR - protecting organelle protein homeostasis. *J Cell Sci,* 123**,** 3849-55.
HEAD, E., GARZON-RODRIGUEZ, W., JOHNSON, J. K., LOTT, I. T., COTMAN, C. W. & GLABE, C. 2001. Oxidation of Abeta and plaque biogenesis in Alzheimer's disease and Down syndrome. *Neurobiol Dis,* 8**,** 792-806.
HEILBRONN, L. K., DE JONGE, L., FRISARD, M. I., DELANY, J. P., LARSON-MEYER, D. E., ROOD, J., NGUYEN, T., MARTIN, C. K., VOLAUFOVA, J., MOST, M. M., GREENWAY, F. L., SMITH, S. R., DEUTSCH, W. A., WILLIAMSON, D. A., RAVUSSIN, E. & PENNINGTON, C. T. 2006. Effect of 6-month calorie restriction on biomarkers of longevity, metabolic adaptation, and oxidative stress in overweight individuals: a randomized controlled trial. *JAMA,* 295**,** 1539-48.
HELISALMI, S., VEPSALAINEN, S., HILTUNEN, M., KOIVISTO, A. M., SALMINEN, A., LAAKSO, M. & SOININEN, H. 2008. Genetic study between SIRT1, PPARD, PGC-1alpha genes and Alzheimer's disease. *J Neurol,* 255**,** 668-73.
HERZIG, S., LONG, F., JHALA, U. S., HEDRICK, S., QUINN, R., BAUER, A., RUDOLPH, D., SCHUTZ, G., YOON, C., PUIGSERVER, P., SPIEGELMAN, B. & MONTMINY, M. 2001. CREB regulates hepatic gluconeogenesis through the coactivator PGC-1. *Nature,* 413**,** 179-83.
HETZ, C. 2012. The unfolded protein response: controlling cell fate decisions under ER stress and beyond. *Nat Rev Mol Cell Biol,* 13**,** 89-102.
HETZ, C., MARTINON, F., RODRIGUEZ, D. & GLIMCHER, L. H. 2011. The unfolded protein response: integrating stress signals through the stress sensor IRE1alpha. *Physiol Rev,* 91**,** 1219-43.
HETZ, C. & MOLLEREAU, B. 2014. Disturbance of endoplasmic reticulum proteostasis in neurodegenerative diseases. *Nat Rev Neurosci,* 15**,** 233-49.
HEYDARI, A. R., YOU, S., TAKAHASHI, R., GUTSMANN, A., SARGE, K. D. & RICHARDSON, A. 1996. Effect of caloric restriction on the expression of heat shock protein 70 and the activation of heat shock transcription factor 1. *Dev Genet,* 18**,** 114-24.
HINE, C., HARPUTLUGIL, E., ZHANG, Y., RUCKENSTUHL, C., LEE, B. C., BRACE, L., LONGCHAMP, A., TREVINO-VILLARREAL, J. H., MEJIA, P., OZAKI, C. K., WANG, R., GLADYSHEV, V. N., MADEO, F., MAIR, W. B. & MITCHELL, J. R.

2015. Endogenous hydrogen sulfide production is essential for dietary restriction benefits. *Cell,* 160**,** 132-44.

HIPP, M. S., PARK, S. H. & HARTL, F. U. 2014. Proteostasis impairment in protein-misfolding and -aggregation diseases. *Trends in Cell Biology,* 24**,** 506-514.

HOEPKEN, H. H., GISPERT, S., MORALES, B., WINGERTER, O., DEL TURCO, D., MULSCH, A., NUSSBAUM, R. L., MULLER, K., DROSE, S., BRANDT, U., DELLER, T., WIRTH, B., KUDIN, A. P., KUNZ, W. S. & AUBURGER, G. 2007. Mitochondrial dysfunction, peroxidation damage and changes in glutathione metabolism in PARK6. *Neurobiol Dis,* 25**,** 401-11.

HOFFMANN, J. M. & PARTRIDGE, L. 2015. Nuclear hormone receptors: Roles of xenobiotic detoxification and sterol homeostasis in healthy aging. *Crit Rev Biochem Mol Biol,* 50**,** 380-92.

HOLCOMB, L. A., GORDON, M. N., JANTZEN, P., HSIAO, K., DUFF, K. & MORGAN, D. 1999. Behavioral changes in transgenic mice expressing both amyloid precursor protein and presenilin-1 mutations: lack of association with amyloid deposits. *Behav Genet,* 29**,** 177-85.

HOLLIDAY, R. 1989. Food, reproduction and longevity: is the extended lifespan of calorie-restricted animals an evolutionary adaptation? *Bioessays,* 10**,** 125-7.

HONEGGER, B., GALIC, M., KOHLER, K., WITTWER, F., BROGIOLO, W., HAFEN, E. & STOCKER, H. 2008. Imp-L2, a putative homolog of vertebrate IGF-binding protein 7, counteracts insulin signaling in Drosophila and is essential for starvation resistance. *J Biol,* 7**,** 10.

HONJOH, S., YAMAMOTO, T., UNO, M. & NISHIDA, E. 2009. Signalling through RHEB-1 mediates intermittent fasting-induced longevity in C. elegans. *Nature,* 457**,** 726-30.

HOOZEMANS, J. J. & SCHEPER, W. 2012. Endoplasmic reticulum: the unfolded protein response is tangled in neurodegeneration. *Int J Biochem Cell Biol,* 44**,** 1295-8.

HOOZEMANS, J. J., VAN HAASTERT, E. S., EIKELENBOOM, P., DE VOS, R. A., ROZEMULLER, J. M. & SCHEPER, W. 2007. Activation of the unfolded protein response in Parkinson's disease. *Biochem Biophys Res Commun,* 354**,** 707-11.

HOYER, S. 1996. Oxidative metabolism deficiencies in brains of patients with Alzheimer's disease. *Acta Neurol Scand Suppl,* 165**,** 18-24.

HSU, A. L., MURPHY, C. T. & KENYON, C. 2003. Regulation of aging and age-related disease by DAF-16 and heat-shock factor. *Science,* 300**,** 1142-5.

HUNG, W. W., ROSS, J. S., BOOCKVAR, K. S. & SIU, A. L. 2011. Recent trends in chronic disease, impairment and disability among older adults in the United States. *BMC Geriatr,* 11**,** 47.

HYMAN, B. T., VAN HOESEN, G. W., DAMASIO, A. R. & BARNES, C. L. 1984. Alzheimer's disease: cell-specific pathology isolates the hippocampal formation. *Science,* 225**,** 1168-70.

IIJIMA, K., LIU, H. P., CHIANG, A. S., HEARN, S. A., KONSOLAKI, M. & ZHONG, Y. 2004. Dissecting the pathological effects of human Abeta40 and Abeta42 in Drosophila: a potential model for Alzheimer's disease. *Proc Natl Acad Sci U S A,* 101**,** 6623-8.

IKENO, Y., LEW, C. M., CORTEZ, L. A., WEBB, C. R., LEE, S. & HUBBARD, G. B. 2006. Do long-lived mutant and calorie-restricted mice share common anti-aging mechanisms?--a pathological point of view. *Age (Dordr),* 28**,** 163-71.

IKEYA, T., BROUGHTON, S., ALIC, N., GRANDISON, R. & PARTRIDGE, L. 2009. The endosymbiont Wolbachia increases insulin/IGF-like signalling in Drosophila. *Proc Biol Sci,* 276**,** 3799-807.

INGRAM, D. K. & ROTH, G. S. 2015. Calorie restriction mimetics: can you have your cake and eat it, too? *Ageing Res Rev,* 20**,** 46-62.

INTERNATIONAL PARKINSON DISEASE GENOMICS, C., NALLS, M. A., PLAGNOL, V., HERNANDEZ, D. G., SHARMA, M., SHEERIN, U. M., SAAD, M., SIMON-SANCHEZ, J., SCHULTE, C., LESAGE, S., SVEINBJORNSDOTTIR, S., STEFANSSON, K., MARTINEZ, M., HARDY, J., HEUTINK, P., BRICE, A., GASSER, T., SINGLETON, A. B. & WOOD, N. W. 2011. Imputation of sequence variants for identification of genetic risks for Parkinson's disease: a meta-analysis of genome-wide association studies. *Lancet,* 377**,** 641-9.

JIA, K., CHEN, D. & RIDDLE, D. L. 2004. The TOR pathway interacts with the insulin signaling pathway to regulate C. elegans larval development, metabolism and life span. *Development,* 131**,** 3897-906.

JIANG, H., PATEL, P. H., KOHLMAIER, A., GRENLEY, M. O., MCEWEN, D. G. & EDGAR, B. A. 2009. Cytokine/Jak/Stat signaling mediates regeneration and homeostasis in the Drosophila midgut. *Cell,* 137**,** 1343-55.

JIN, M., SHEPARDSON, N., YANG, T., CHEN, G., WALSH, D. & SELKOE, D. J. 2011. Soluble amyloid beta-protein dimers isolated from Alzheimer cortex directly induce Tau hyperphosphorylation and neuritic degeneration. *Proc Natl Acad Sci U S A,* 108**,** 5819-24.

JING, X. N., SHI, Q. Y., BI, W., ZENG, Z. F., LIANG, Y. R., WU, X., XIAO, S. H., LIU, J., YANG, L. H. & TAO, E. X. 2014. Rifampicin Protects PC12 Cells from Rotenone-Induced Cytotoxicity by Activating GRP78 via PERK-eIF2 alpha-ATF4 Pathway. *Plos One,* 9.

JOHNSON, S. C., RABINOVITCH, P. S. & KAEBERLEIN, M. 2013. mTOR is a key modulator of ageing and age-related disease. *Nature,* 493**,** 338-45.

JONES, M. A., GARGANO, J. W., RHODENIZER, D., MARTIN, I., BHANDARI, P. & GROTEWIEL, M. 2009. A forward genetic screen in Drosophila implicates insulin signaling in age-related locomotor impairment. *Exp Gerontol,* 44**,** 532-40.

JUNG, T., CATALGOL, B. & GRUNE, T. 2009. The proteasomal system. *Mol Aspects Med,* 30**,** 191-296.

KAEBERLEIN, M., POWERS, R. W., 3RD, STEFFEN, K. K., WESTMAN, E. A., HU, D., DANG, N., KERR, E. O., KIRKLAND, K. T., FIELDS, S. & KENNEDY, B. K. 2005. Regulation of yeast replicative life span by TOR and Sch9 in response to nutrients. *Science,* 310**,** 1193-6.

KAEBERLEIN, T. L., SMITH, E. D., TSUCHIYA, M., WELTON, K. L., THOMAS, J. H., FIELDS, S., KENNEDY, B. K. & KAEBERLEIN, M. 2006. Lifespan extension in Caenorhabditis elegans by complete removal of food. *Aging Cell,* 5**,** 487-94.

KALIA, L. V. & LANG, A. E. 2015. Parkinson's disease. *Lancet,* 386**,** 896-912.

KAMP, F., EXNER, N., LUTZ, A. K., WENDER, N., HEGERMANN, J., BRUNNER, B., NUSCHER, B., BARTELS, T., GIESE, A., BEYER, K., EIMER, S., WINKLHOFER,

K. F. & HAASS, C. 2010. Inhibition of mitochondrial fusion by alpha-synuclein is rescued by PINK1, Parkin and DJ-1. *EMBO J,* 29**,** 3571-89.

KANG, J., LEMAIRE, H. G., UNTERBECK, A., SALBAUM, J. M., MASTERS, C. L., GRZESCHIK, K. H., MULTHAUP, G., BEYREUTHER, K. & MULLER-HILL, B. 1987. The precursor of Alzheimer's disease amyloid A4 protein resembles a cell-surface receptor. *Nature,* 325**,** 733-6.

KANG, J. E., LIM, M. M., BATEMAN, R. J., LEE, J. J., SMYTH, L. P., CIRRITO, J. R., FUJIKI, N., NISHINO, S. & HOLTZMAN, D. M. 2009. Amyloid-beta dynamics are regulated by orexin and the sleep-wake cycle. *Science,* 326**,** 1005-7.

KAPAHI, P., CHEN, D., ROGERS, A. N., KATEWA, S. D., LI, P. W., THOMAS, E. L. & KOCKEL, L. 2010. With TOR, less is more: a key role for the conserved nutrient-sensing TOR pathway in aging. *Cell Metab,* 11**,** 453-65.

KAPAHI, P., ZID, B. M., HARPER, T., KOSLOVER, D., SAPIN, V. & BENZER, S. 2004. Regulation of lifespan in Drosophila by modulation of genes in the TOR signaling pathway. *Curr Biol,* 14**,** 885-90.

KAPOGIANNIS, D. & MATTSON, M. P. 2011. Disrupted energy metabolism and neuronal circuit dysfunction in cognitive impairment and Alzheimer's disease. *Lancet Neurol,* 10**,** 187-98.

KARPINAR, D. P., BALIJA, M. B., KUGLER, S., OPAZO, F., REZAEI-GHALEH, N., WENDER, N., KIM, H. Y., TASCHENBERGER, G., FALKENBURGER, B. H., HEISE, H., KUMAR, A., RIEDEL, D., FICHTNER, L., VOIGT, A., BRAUS, G. H., GILLER, K., BECKER, S., HERZIG, A., BALDUS, M., JACKLE, H., EIMER, S., SCHULZ, J. B., GRIESINGER, C. & ZWECKSTETTER, M. 2009. Pre-fibrillar alpha-synuclein variants with impaired beta-structure increase neurotoxicity in Parkinson's disease models. *EMBO J,* 28**,** 3256-68.

KATEWA, S. D. & KAPAHI, P. 2010. Dietary restriction and aging, 2009. *Aging Cell,* 9**,** 105-12.

KATSOURI, L., PARR, C., BOGDANOVIC, N., WILLEM, M. & SASTRE, M. 2011. PPARgamma co-activator-1alpha (PGC-1alpha) reduces amyloid-beta generation through a PPARgamma-dependent mechanism. *J Alzheimers Dis,* 25**,** 151-62.

KENYON, C. J. 2010. The genetics of ageing. *Nature,* 464**,** 504-12.

KILIC, U., KILIC, E., LINGOR, P., YULUG, B. & BAHR, M. 2004. Rifampicin inhibits neurodegeneration in the optic nerve transection model in vivo and after 1-methyl-4-phenylpyridinium intoxication in vitro. *Acta Neuropathol,* 108**,** 65-8.

KIM, J., BASAK, J. M. & HOLTZMAN, D. M. 2009. The role of apolipoprotein E in Alzheimer's disease. *Neuron,* 63**,** 287-303.

KIM, Y., PARK, J., KIM, S., SONG, S., KWON, S. K., LEE, S. H., KITADA, T., KIM, J. M. & CHUNG, J. 2008. PINK1 controls mitochondrial localization of Parkin through direct phosphorylation. *Biochem Biophys Res Commun,* 377**,** 975-80.

KINGHORN, K. J., CASTILLO-QUAN, J. I., BARTOLOME, F., ANGELOVA, P. R., LI, L., POPE, S., COCHEME, H. M., KHAN, S., ASGHARI, S., BHATIA, K. P., HARDY, J., ABRAMOV, A. Y. & PARTRIDGE, L. 2015. Loss of PLA2G6 leads to elevated mitochondrial lipid peroxidation and mitochondrial dysfunction. *Brain,* 138**,** 1801-16.

KINGHORN, K. J., CASTILLO-QUAN, J. I., LI, L., BHATIA, K. P., ABRAMOV, A. Y., HARDY, J. & PARTRIDGE, L. 2016. Reply: Glial mitochondropathy in

infantile neuroaxonal dystrophy: pathophysiological and therapeutic implications. *Brain*.

KIRKWOOD, T. B. & AUSTAD, S. N. 2000. Why do we age? *Nature,* 408**,** 233-8.

KITADA, T., ASAKAWA, S., HATTORI, N., MATSUMINE, H., YAMAMURA, Y., MINOSHIMA, S., YOKOCHI, M., MIZUNO, Y. & SHIMIZU, N. 1998. Mutations in the parkin gene cause autosomal recessive juvenile parkinsonism. *Nature,* 392**,** 605-8.

KONDO, T., ASAI, M., TSUKITA, K., KUTOKU, Y., OHSAWA, Y., SUNADA, Y., IMAMURA, K., EGAWA, N., YAHATA, N., OKITA, K., TAKAHASHI, K., ASAKA, I., AOI, T., WATANABE, A., WATANABE, K., KADOYA, C., NAKANO, R., WATANABE, D., MARUYAMA, K., HORI, O., HIBINO, S., CHOSHI, T., NAKAHATA, T., HIOKI, H., KANEKO, T., NAITOH, M., YOSHIKAWA, K., YAMAWAKI, S., SUZUKI, S., HATA, R., UENO, S., SEKI, T., KOBAYASHI, K., TODA, T., MURAKAMI, K., IRIE, K., KLEIN, W. L., MORI, H., ASADA, T., TAKAHASHI, R., IWATA, N., YAMANAKA, S. & INOUE, H. 2013. Modeling Alzheimer's disease with iPSCs reveals stress phenotypes associated with intracellular Abeta and differential drug responsiveness. *Cell Stem Cell,* 12**,** 487-96.

KOO, S. H., SATOH, H., HERZIG, S., LEE, C. H., HEDRICK, S., KULKARNI, R., EVANS, R. M., OLEFSKY, J. & MONTMINY, M. 2004. PGC-1 promotes insulin resistance in liver through PPAR-alpha-dependent induction of TRB-3. *Nat Med,* 10**,** 530-4.

KOZAK, U. C., KOPECKY, J., TEISINGER, J., ENERBACK, S., BOYER, B. & KOZAK, L. P. 1994. An upstream enhancer regulating brown-fat-specific expression of the mitochondrial uncoupling protein gene. *Mol Cell Biol,* 14**,** 59-67.

KRUGER, R., KUHN, W., MULLER, T., WOITALLA, D., GRAEBER, M., KOSEL, S., PRZUNTEK, H., EPPLEN, J. T., SCHOLS, L. & RIESS, O. 1998. Ala30Pro mutation in the gene encoding alpha-synuclein in Parkinson's disease. *Nat Genet,* 18**,** 106-8.

KUJOTH, G. C., HIONA, A., PUGH, T. D., SOMEYA, S., PANZER, K., WOHLGEMUTH, S. E., HOFER, T., SEO, A. Y., SULLIVAN, R., JOBLING, W. A., MORROW, J. D., VAN REMMEN, H., SEDIVY, J. M., YAMASOBA, T., TANOKURA, M., WEINDRUCH, R., LEEUWENBURGH, C. & PROLLA, T. A. 2005. Mitochondrial DNA mutations, oxidative stress, and apoptosis in mammalian aging. *Science,* 309**,** 481-4.

KUKREJA, L., KUJOTH, G. C., PROLLA, T. A., VAN LEUVEN, F. & VASSAR, R. 2014. Increased mtDNA mutations with aging promotes amyloid accumulation and brain atrophy in the APP/Ld transgenic mouse model of Alzheimer's disease. *Mol Neurodegener,* 9**,** 16.

KWON, Y., SONG, W., DROUJININE, I. A., HU, Y., ASARA, J. M. & PERRIMON, N. 2015. Systemic organ wasting induced by localized expression of the secreted insulin/IGF antagonist ImpL2. *Dev Cell,* 33**,** 36-46.

LAKOWSKI, B. & HEKIMI, S. 1996. Determination of life-span in Caenorhabditis elegans by four clock genes. *Science,* 272**,** 1010-3.

LAKOWSKI, B. & HEKIMI, S. 1998. The genetics of caloric restriction in Caenorhabditis elegans. *Proc Natl Acad Sci U S A,* 95**,** 13091-6.

LANGSTON, J. W., BALLARD, P., TETRUD, J. W. & IRWIN, I. 1983. Chronic Parkinsonism in humans due to a product of meperidine-analog synthesis. *Science,* 219**,** 979-80.

LAPLANTE, M. & SABATINI, D. M. 2012. mTOR signaling in growth control and disease. *Cell,* 149**,** 274-93.

LEE, G. D., WILSON, M. A., ZHU, M., WOLKOW, C. A., DE CABO, R., INGRAM, D. K. & ZOU, S. 2006. Dietary deprivation extends lifespan in Caenorhabditis elegans. *Aging Cell,* 5**,** 515-24.

LEE, S. J., HWANG, A. B. & KENYON, C. 2010. Inhibition of respiration extends C. elegans life span via reactive oxygen species that increase HIF-1 activity. *Curr Biol,* 20**,** 2131-6.

LEE, S. J., LEE, I., LEE, J., PARK, C. & KANG, W. K. 2014. Statins, 3-hydroxy-3-methylglutaryl coenzyme A reductase inhibitors, potentiate the anti-angiogenic effects of bevacizumab by suppressing angiopoietin2, BiP, and Hsp90alpha in human colorectal cancer. *Br J Cancer,* 111**,** 497-505.

LEE, S. S., LEE, R. Y., FRASER, A. G., KAMATH, R. S., AHRINGER, J. & RUVKUN, G. 2003. A systematic RNAi screen identifies a critical role for mitochondria in C. elegans longevity. *Nat Genet,* 33**,** 40-8.

LEES, A. J., HARDY, J. & REVESZ, T. 2009. Parkinson's disease. *Lancet,* 373**,** 2055-66.

LEONE, T. C., LEHMAN, J. J., FINCK, B. N., SCHAEFFER, P. J., WENDE, A. R., BOUDINA, S., COURTOIS, M., WOZNIAK, D. F., SAMBANDAM, N., BERNAL-MIZRACHI, C., CHEN, Z., HOLLOSZY, J. O., MEDEIROS, D. M., SCHMIDT, R. E., SAFFITZ, J. E., ABEL, E. D., SEMENKOVICH, C. F. & KELLY, D. P. 2005. PGC-1alpha deficiency causes multi-system energy metabolic derangements: muscle dysfunction, abnormal weight control and hepatic steatosis. *PLoS Biol,* 3**,** e101.

LEVINE, J. D., FUNES, P., DOWSE, H. B. & HALL, J. C. 2002. Signal analysis of behavioral and molecular cycles. *BMC Neurosci,* 3**,** 1.

LEVY-LAHAD, E., WASCO, W., POORKAJ, P., ROMANO, D. M., OSHIMA, J., PETTINGELL, W. H., YU, C. E., JONDRO, P. D., SCHMIDT, S. D., WANG, K. & ET AL. 1995. Candidate gene for the chromosome 1 familial Alzheimer's disease locus. *Science,* 269**,** 973-7.

LEWIS, J., MCGOWAN, E., ROCKWOOD, J., MELROSE, H., NACHARAJU, P., VAN SLEGTENHORST, M., GWINN-HARDY, K., PAUL MURPHY, M., BAKER, M., YU, X., DUFF, K., HARDY, J., CORRAL, A., LIN, W. L., YEN, S. H., DICKSON, D. W., DAVIES, P. & HUTTON, M. 2000. Neurofibrillary tangles, amyotrophy and progressive motor disturbance in mice expressing mutant (P301L) tau protein. *Nat Genet,* 25**,** 402-5.

LI, F., CALINGASAN, N. Y., YU, F., MAUCK, W. M., TOIDZE, M., ALMEIDA, C. G., TAKAHASHI, R. H., CARLSON, G. A., FLINT BEAL, M., LIN, M. T. & GOURAS, G. K. 2004. Increased plaque burden in brains of APP mutant MnSOD heterozygous knockout mice. *J Neurochem,* 89**,** 1308-12.

LI, J., NI, M., LEE, B., BARRON, E., HINTON, D. R. & LEE, A. S. 2008. The unfolded protein response regulator GRP78/BiP is required for endoplasmic reticulum integrity and stress-induced autophagy in mammalian cells. *Cell Death Differ,* 15**,** 1460-71.

LI, W. W., YANG, R., GUO, J. C., REN, H. M., ZHA, X. L., CHENG, J. S. & CAI, D. F. 2007a. Localization of alpha-synuclein to mitochondria within midbrain of mice. *Neuroreport,* 18**,** 1543-6.

LI, X., MONKS, B., GE, Q. & BIRNBAUM, M. J. 2007b. Akt/PKB regulates hepatic metabolism by directly inhibiting PGC-1alpha transcription coactivator. *Nature,* 447**,** 1012-6.

LIANG, H., WARD, W. F., JANG, Y. C., BHATTACHARYA, A., BOKOV, A. F., LI, Y., JERNIGAN, A., RICHARDSON, A. & VAN REMMEN, H. 2011. PGC-1alpha protects neurons and alters disease progression in an amyotrophic lateral sclerosis mouse model. *Muscle Nerve,* 44**,** 947-56.

LIBERT, S., CHAO, Y., CHU, X. & PLETCHER, S. D. 2006. Trade-offs between longevity and pathogen resistance in Drosophila melanogaster are mediated by NFkappaB signaling. *Aging Cell,* 5**,** 533-43.

LIN, J., PUIGSERVER, P., DONOVAN, J., TARR, P. & SPIEGELMAN, B. M. 2002. Peroxisome proliferator-activated receptor gamma coactivator 1beta (PGC-1beta), a novel PGC-1-related transcription coactivator associated with host cell factor. *J Biol Chem,* 277**,** 1645-8.

LIN, J., WU, P. H., TARR, P. T., LINDENBERG, K. S., ST-PIERRE, J., ZHANG, C. Y., MOOTHA, V. K., JAGER, S., VIANNA, C. R., REZNICK, R. M., CUI, L., MANIERI, M., DONOVAN, M. X., WU, Z., COOPER, M. P., FAN, M. C., ROHAS, L. M., ZAVACKI, A. M., CINTI, S., SHULMAN, G. I., LOWELL, B. B., KRAINC, D. & SPIEGELMAN, B. M. 2004. Defects in adaptive energy metabolism with CNS-linked hyperactivity in PGC-1alpha null mice. *Cell,* 119**,** 121-35.

LIN, J., YANG, R., TARR, P. T., WU, P. H., HANDSCHIN, C., LI, S., YANG, W., PEI, L., ULDRY, M., TONTONOZ, P., NEWGARD, C. B. & SPIEGELMAN, B. M. 2005. Hyperlipidemic effects of dietary saturated fats mediated through PGC-1beta coactivation of SREBP. *Cell,* 120**,** 261-73.

LINNANE, A. W., MARZUKI, S., OZAWA, T. & TANAKA, M. 1989. Mitochondrial DNA mutations as an important contributor to ageing and degenerative diseases. *Lancet,* 1**,** 642-5.

LIU, C., LI, S., LIU, T., BORJIGIN, J. & LIN, J. D. 2007. Transcriptional coactivator PGC-1alpha integrates the mammalian clock and energy metabolism. *Nature,* 447**,** 477-81.

LIU, G., ZHANG, C., YIN, J., LI, X., CHENG, F., LI, Y., YANG, H., UEDA, K., CHAN, P. & YU, S. 2009. alpha-Synuclein is differentially expressed in mitochondria from different rat brain regions and dose-dependently down-regulates complex I activity. *Neurosci Lett,* 454**,** 187-92.

LIU, S. Y., WANG, W., CAI, Z. Y., YAO, L. F., CHEN, Z. W., WANG, C. Y., ZHAO, B. & LI, K. S. 2013. Polymorphism -116C/G of human X-box-binding protein 1 promoter is associated with risk of Alzheimer's disease. *CNS Neurosci Ther,* 19**,** 229-34.

LIU, X., JIANG, N., HUGHES, B., BIGRAS, E., SHOUBRIDGE, E. & HEKIMI, S. 2005. Evolutionary conservation of the clk-1-dependent mechanism of longevity: loss of mclk1 increases cellular fitness and lifespan in mice. *Genes Dev,* 19**,** 2424-34.

LIU, Y. 2006. Rapamycin and chronic kidney disease: beyond the inhibition of inflammation. *Kidney Int,* 69**,** 1925-7.

LIU, Y., LIU, X., HAO, W., DECKER, Y., SCHOMBURG, R., FULOP, L., PASPARAKIS, M., MENGER, M. D. & FASSBENDER, K. 2014. IKKbeta deficiency in myeloid cells ameliorates Alzheimer's disease-related symptoms and pathology. *J Neurosci,* 34**,** 12982-99.

LONG, D. M., BLAKE, M. R., DUTTA, S., HOLBROOK, S. D., KOTWICA-ROLINSKA, J., KRETZSCHMAR, D. & GIEBULTOWICZ, J. M. 2014. Relationships between the circadian system and Alzheimer's disease-like symptoms in Drosophila. *PLoS One,* 9**,** e106068.

LOPEZ-OTIN, C., BLASCO, M. A., PARTRIDGE, L., SERRANO, M. & KROEMER, G. 2013. The hallmarks of aging. *Cell,* 153**,** 1194-217.

LOVELL, M. A., XIONG, S., XIE, C., DAVIES, P. & MARKESBERY, W. R. 2004. Induction of hyperphosphorylated tau in primary rat cortical neuron cultures mediated by oxidative stress and glycogen synthase kinase-3. *J Alzheimers Dis,* 6**,** 659-71; discussion 673-81.

LU, T., ARON, L., ZULLO, J., PAN, Y., KIM, H., CHEN, Y. W., YANG, T. H., KIM, H. M., DRAKE, D., LIU, X. S., BENNETT, D. A., COLAIACOVO, M. P. & YANKNER, B. A. 2014. REST and stress resistance in ageing and Alzheimer's disease. *Nature,* 507**,** 448-+.

LUCAS, E. K., REID, C. S., MCMEEKIN, L. J., DOUGHERTY, S. E., FLOYD, C. L. & COWELL, R. M. 2014. Cerebellar transcriptional alterations with Purkinje cell dysfunction and loss in mice lacking PGC-1alpha. *Front Cell Neurosci,* 8**,** 441.

LUSTBADER, J. W., CIRILLI, M., LIN, C., XU, H. W., TAKUMA, K., WANG, N., CASPERSEN, C., CHEN, X., POLLAK, S., CHANEY, M., TRINCHESE, F., LIU, S., GUNN-MOORE, F., LUE, L. F., WALKER, D. G., KUPPUSAMY, P., ZEWIER, Z. L., ARANCIO, O., STERN, D., YAN, S. S. & WU, H. 2004. ABAD directly links Abeta to mitochondrial toxicity in Alzheimer's disease. *Science,* 304**,** 448-52.

MA, T., TRINH, M. A., WEXLER, A. J., BOURBON, C., GATTI, E., PIERRE, P., CAVENER, D. R. & KLANN, E. 2013. Suppression of eIF2alpha kinases alleviates Alzheimer's disease-related plasticity and memory deficits. *Nat Neurosci,* 16**,** 1299-305.

MAEDA, H., GLEISER, C. A., MASORO, E. J., MURATA, I., MCMAHAN, C. A. & YU, B. P. 1985. Nutritional influences on aging of Fischer 344 rats: II. Pathology. *J Gerontol,* 40**,** 671-88.

MAHLEY, R. W., WEISGRABER, K. H. & HUANG, Y. 2006. Apolipoprotein E4: a causative factor and therapeutic target in neuropathology, including Alzheimer's disease. *Proc Natl Acad Sci U S A,* 103**,** 5644-51.

MAIR, W., GOYMER, P., PLETCHER, S. D. & PARTRIDGE, L. 2003. Demography of dietary restriction and death in Drosophila. *Science,* 301**,** 1731-3.

MAIR, W., MORANTTE, I., RODRIGUES, A. P., MANNING, G., MONTMINY, M., SHAW, R. J. & DILLIN, A. 2011. Lifespan extension induced by AMPK and calcineurin is mediated by CRTC-1 and CREB. *Nature,* 470**,** 404-8.

MAIR, W., PIPER, M. D. & PARTRIDGE, L. 2005. Calories do not explain extension of life span by dietary restriction in Drosophila. *PLoS Biol,* 3**,** e223.

MANCZAK, M., ANEKONDA, T. S., HENSON, E., PARK, B. S., QUINN, J. & REDDY, P. H. 2006. Mitochondria are a direct site of A beta accumulation in Alzheimer's disease neurons: implications for free radical generation and oxidative damage in disease progression. *Hum Mol Genet,* 15**,** 1437-49.

MAOR, G., RENCUS-LAZAR, S., FILOCAMO, M., STELLER, H., SEGAL, D. & HOROWITZ, M. 2013. Unfolded protein response in Gaucher disease: from human to Drosophila. *Orphanet J Rare Dis,* 8**,** 140.

MARTIN, I., DAWSON, V. L. & DAWSON, T. M. 2011. Recent advances in the genetics of Parkinson's disease. *Annu Rev Genomics Hum Genet,* 12**,** 301-25.

MARTIN, L. J., PAN, Y., PRICE, A. C., STERLING, W., COPELAND, N. G., JENKINS, N. A., PRICE, D. L. & LEE, M. K. 2006. Parkinson's disease alpha-synuclein transgenic mice develop neuronal mitochondrial degeneration and cell death. *J Neurosci,* 26**,** 41-50.

MARTIN-MONTALVO, A., VILLALBA, J. M., NAVAS, P. & DE CABO, R. 2011. NRF2, cancer and calorie restriction. *Oncogene,* 30**,** 505-20.

MASLIAH, E., ROCKENSTEIN, E., VEINBERGS, I., MALLORY, M., HASHIMOTO, M., TAKEDA, A., SAGARA, Y., SISK, A. & MUCKE, L. 2000. Dopaminergic loss and inclusion body formation in alpha-synuclein mice: implications for neurodegenerative disorders. *Science,* 287**,** 1265-9.

MASORO, E. J. 2003. Subfield history: caloric restriction, slowing aging, and extending life. *Sci Aging Knowledge Environ,* 2003**,** RE2.

MASSI, F., KLIMOV, D., THIRUMALAI, D. & STRAUB, J. E. 2002. Charge states rather than propensity for beta-structure determine enhanced fibrillogenesis in wild-type Alzheimer's beta-amyloid peptide compared to E22Q Dutch mutant. *Protein Sci,* 11**,** 1639-47.

MATTISON, J. A., ROTH, G. S., BEASLEY, T. M., TILMONT, E. M., HANDY, A. M., HERBERT, R. L., LONGO, D. L., ALLISON, D. B., YOUNG, J. E., BRYANT, M., BARNARD, D., WARD, W. F., QI, W., INGRAM, D. K. & DE CABO, R. 2012. Impact of caloric restriction on health and survival in rhesus monkeys from the NIA study. *Nature,* 489**,** 318-21.

MATTSON, M. P., ALLISON, D. B., FONTANA, L., HARVIE, M., LONGO, V. D., MALAISSE, W. J., MOSLEY, M., NOTTERPEK, L., RAVUSSIN, E., SCHEER, F. A., SEYFRIED, T. N., VARADY, K. A. & PANDA, S. 2014. Meal frequency and timing in health and disease. *Proc Natl Acad Sci U S A,* 111**,** 16647-53.

MCGEER, P. L., HARADA, N., KIMURA, H., MCGEER, E. G. & SCHULZER, M. 1992. Prevalence of Dementia Amongst Elderly Japanese with Leprosy - Apparent Effect of Chronic Drug-Therapy. *Dementia,* 3**,** 146-149.

MCGOWAN, E., PICKFORD, F., KIM, J., ONSTEAD, L., ERIKSEN, J., YU, C., SKIPPER, L., MURPHY, M. P., BEARD, J., DAS, P., JANSEN, K., DELUCIA, M., LIN, W. L., DOLIOS, G., WANG, R., ECKMAN, C. B., DICKSON, D. W., HUTTON, M., HARDY, J. & GOLDE, T. 2005. Abeta42 is essential for parenchymal and vascular amyloid deposition in mice. *Neuron,* 47**,** 191-9.

MCGURK, L., BERSON, A. & BONINI, N. M. 2015. Drosophila as an In Vivo Model for Human Neurodegenerative Disease. *Genetics,* 201**,** 377-402.

MEDAWAR, P. B. 1957. The Uniqness of the Individual. *(Basic Books, Inc.)*.

MEDVEDIK, O., LAMMING, D. W., KIM, K. D. & SINCLAIR, D. A. 2007. MSN2 and MSN4 link calorie restriction and TOR to sirtuin-mediated lifespan extension in Saccharomyces cerevisiae. *PLoS Biol,* 5**,** e261.

MENZIES, F. M., YENISETTI, S. C. & MIN, K. T. 2005. Roles of Drosophila DJ-1 in survival of dopaminergic neurons and oxidative stress. *Curr Biol,* 15**,** 1578-82.

MERKWIRTH, C., JOVAISAITE, V., DURIEUX, J., MATILAINEN, O., JORDAN, S. D., QUIROS, P. M., STEFFEN, K. K., WILLIAMS, E. G., MOUCHIROUD, L., TRONNES, S. U., MURILLO, V., WOLFF, S. C., SHAW, R. J., AUWERX, J. &

DILLIN, A. 2016. Two Conserved Histone Demethylases Regulate Mitochondrial Stress-Induced Longevity. *Cell,* 165**,** 1209-23.

MERSHIN, A., PAVLOPOULOS, E., FITCH, O., BRADEN, B. C., NANOPOULOS, D. V. & SKOULAKIS, E. M. 2004. Learning and memory deficits upon TAU accumulation in Drosophila mushroom body neurons. *Learn Mem,* 11**,** 277-87.

MERZETTI, E. M. & STAVELEY, B. E. 2015. spargel, the PGC-1alpha homologue, in models of Parkinson disease in Drosophila melanogaster. *BMC Neurosci,* 16**,** 70.

MESQUITA, A., WEINBERGER, M., SILVA, A., SAMPAIO-MARQUES, B., ALMEIDA, B., LEAO, C., COSTA, V., RODRIGUES, F., BURHANS, W. C. & LUDOVICO, P. 2010. Caloric restriction or catalase inactivation extends yeast chronological lifespan by inducing H2O2 and superoxide dismutase activity. *Proc Natl Acad Sci U S A,* 107**,** 15123-8.

METAXAKIS, A. & PARTRIDGE, L. 2013. Dietary restriction extends lifespan in wild-derived populations of Drosophila melanogaster. *PLoS One,* 8**,** e74681.

MEULENER, M., WHITWORTH, A. J., ARMSTRONG-GOLD, C. E., RIZZU, P., HEUTINK, P., WES, P. D., PALLANCK, L. J. & BONINI, N. M. 2005. Drosophila DJ-1 mutants are selectively sensitive to environmental toxins associated with Parkinson's disease. *Curr Biol,* 15**,** 1572-7.

MICHAEL, L. F., WU, Z., CHEATHAM, R. B., PUIGSERVER, P., ADELMANT, G., LEHMAN, J. J., KELLY, D. P. & SPIEGELMAN, B. M. 2001. Restoration of insulin-sensitive glucose transporter (GLUT4) gene expression in muscle cells by the transcriptional coactivator PGC-1. *Proc Natl Acad Sci U S A,* 98**,** 3820-5.

MILLER, R. A., HARRISON, D. E., ASTLE, C. M., BAUR, J. A., BOYD, A. R., DE CABO, R., FERNANDEZ, E., FLURKEY, K., JAVORS, M. A., NELSON, J. F., ORIHUELA, C. J., PLETCHER, S., SHARP, Z. D., SINCLAIR, D., STARNES, J. W., WILKINSON, J. E., NADON, N. L. & STRONG, R. 2011. Rapamycin, but not resveratrol or simvastatin, extends life span of genetically heterogeneous mice. *J Gerontol A Biol Sci Med Sci,* 66**,** 191-201.

MILLER, R. A., HARRISON, D. E., ASTLE, C. M., FERNANDEZ, E., FLURKEY, K., HAN, M., JAVORS, M. A., LI, X., NADON, N. L., NELSON, J. F., PLETCHER, S., SALMON, A. B., SHARP, Z. D., VAN ROEKEL, S., WINKLEMAN, L. & STRONG, R. 2014. Rapamycin-mediated lifespan increase in mice is dose and sex dependent and metabolically distinct from dietary restriction. *Aging Cell,* 13**,** 468-77.

MIURA, S., KAI, Y., ONO, M. & EZAKI, O. 2003. Overexpression of peroxisome proliferator-activated receptor gamma coactivator-1alpha down-regulates GLUT4 mRNA in skeletal muscles. *J Biol Chem,* 278**,** 31385-90.

MOOTHA, V. K., HANDSCHIN, C., ARLOW, D., XIE, X., ST PIERRE, J., SIHAG, S., YANG, W., ALTSHULER, D., PUIGSERVER, P., PATTERSON, N., WILLY, P. J., SCHULMAN, I. G., HEYMAN, R. A., LANDER, E. S. & SPIEGELMAN, B. M. 2004. Erralpha and Gabpa/b specify PGC-1alpha-dependent oxidative phosphorylation gene expression that is altered in diabetic muscle. *Proc Natl Acad Sci U S A,* 101**,** 6570-5.

MOOTHA, V. K., LINDGREN, C. M., ERIKSSON, K. F., SUBRAMANIAN, A., SIHAG, S., LEHAR, J., PUIGSERVER, P., CARLSSON, E., RIDDERSTRALE, M., LAURILA,

E., HOUSTIS, N., DALY, M. J., PATTERSON, N., MESIROV, J. P., GOLUB, T. R., TAMAYO, P., SPIEGELMAN, B., LANDER, E. S., HIRSCHHORN, J. N., ALTSHULER, D. & GROOP, L. C. 2003. PGC-1alpha-responsive genes involved in oxidative phosphorylation are coordinately downregulated in human diabetes. *Nat Genet,* 34**,** 267-73.

MORETTO, A. & COLOSIO, C. 2013. The role of pesticide exposure in the genesis of Parkinson's disease: epidemiological studies and experimental data. *Toxicology,* 307**,** 24-34.

MORIMOTO, R. I. 2008. Proteotoxic stress and inducible chaperone networks in neurodegenerative disease and aging. *Genes Dev,* 22**,** 1427-38.

MORITA, M., GRAVEL, S. P., CHENARD, V., SIKSTROM, K., ZHENG, L., ALAIN, T., GANDIN, V., AVIZONIS, D., ARGUELLO, M., ZAKARIA, C., MCLAUGHLAN, S., NOUET, Y., PAUSE, A., POLLAK, M., GOTTLIEB, E., LARSSON, O., ST-PIERRE, J., TOPISIROVIC, I. & SONENBERG, N. 2013. mTORC1 controls mitochondrial activity and biogenesis through 4E-BP-dependent translational regulation. *Cell Metab,* 18**,** 698-711.

MORLEY, J. F. & MORIMOTO, R. I. 2004. Regulation of longevity in Caenorhabditis elegans by heat shock factor and molecular chaperones. *Mol Biol Cell,* 15**,** 657-64.

MORTIBOYS, H., THOMAS, K. J., KOOPMAN, W. J., KLAFFKE, S., ABOU-SLEIMAN, P., OLPIN, S., WOOD, N. W., WILLEMS, P. H., SMEITINK, J. A., COOKSON, M. R. & BANDMANN, O. 2008. Mitochondrial function and morphology are impaired in parkin-mutant fibroblasts. *Ann Neurol,* 64**,** 555-65.

MOSCONI, L., PUPI, A. & DE LEON, M. J. 2008. Brain glucose hypometabolism and oxidative stress in preclinical Alzheimer's disease. *Ann N Y Acad Sci,* 1147**,** 180-95.

MOUCHIROUD, L., HOUTKOOPER, R. H. & AUWERX, J. 2013. NAD(+) metabolism: a therapeutic target for age-related metabolic disease. *Crit Rev Biochem Mol Biol,* 48**,** 397-408.

MUCKE, L., MASLIAH, E., YU, G. Q., MALLORY, M., ROCKENSTEIN, E. M., TATSUNO, G., HU, K., KHOLODENKO, D., JOHNSON-WOOD, K. & MCCONLOGUE, L. 2000. High-level neuronal expression of abeta 1-42 in wild-type human amyloid protein precursor transgenic mice: synaptotoxicity without plaque formation. *J Neurosci,* 20**,** 4050-8.

MUCKE, L. & SELKOE, D. J. 2012. Neurotoxicity of amyloid beta-protein: synaptic and network dysfunction. *Cold Spring Harb Perspect Med,* 2**,** a006338.

MUFTUOGLU, M., ELIBOL, B., DALMIZRAK, O., ERCAN, A., KULAKSIZ, G., OGUS, H., DALKARA, T. & OZER, N. 2004. Mitochondrial complex I and IV activities in leukocytes from patients with parkin mutations. *Mov Disord,* 19**,** 544-8.

MUKHERJEE, S., BASAR, M. A., DAVIS, C. & DUTTAROY, A. 2014. Emerging functional similarities and divergences between Drosophila Spargel/dPGC-1 and mammalian PGC-1 protein. *Front Genet,* 5**,** 216.

MUKHERJEE, S. & DUTTAROY, A. 2013. Spargel/dPGC-1 is a new downstream effector in the insulin-TOR signaling pathway in Drosophila. *Genetics,* 195**,** 433-41.

MUSIEK, E. S. & HOLTZMAN, D. M. 2015. Three dimensions of the amyloid hypothesis: time, space and 'wingmen'. *Nat Neurosci,* 18**,** 800-6.

MUSIEK, E. S., LIM, M. M., YANG, G., BAUER, A. Q., QI, L., LEE, Y., ROH, J. H., ORTIZ-GONZALEZ, X., DEARBORN, J. T., CULVER, J. P., HERZOG, E. D.,

HOGENESCH, J. B., WOZNIAK, D. F., DIKRANIAN, K., GIASSON, B. I., WEAVER, D. R., HOLTZMAN, D. M. & FITZGERALD, G. A. 2013. Circadian clock proteins regulate neuronal redox homeostasis and neurodegeneration. *J Clin Invest,* 123**,** 5389-400.

NAKAMURA, K., NEMANI, V. M., WALLENDER, E. K., KAEHLCKE, K., OTT, M. & EDWARDS, R. H. 2008. Optical reporters for the conformation of alpha-synuclein reveal a specific interaction with mitochondria. *J Neurosci,* 28**,** 12305-17.

NAMBA, Y., KAWATSU, K., IZUMI, S., UEKI, A. & IKEDA, K. 1992. Neurofibrillary Tangles and Senile Plaques in Brain of Elderly Leprosy Patients. *Lancet,* 340**,** 978-978.

NARENDRA, D., TANAKA, A., SUEN, D. F. & YOULE, R. J. 2008. Parkin is recruited selectively to impaired mitochondria and promotes their autophagy. *J Cell Biol,* 183**,** 795-803.

NEGRI, I. 2011. Wolbachia as an "infectious" extrinsic factor manipulating host signaling pathways. *Front Endocrinol (Lausanne),* 2**,** 115.

NESS, D. K., BOGGS, L. N., HEPBURN, D. L., GITTER, B., LONG, G. G., MAY, P. C., PIROOZI, K. S., SCHAFER, K. A. & YANG, Z. X. 2004. Reduced beta-amyloid burden, increased C-99 concentrations and evaluation of neuropathology in the brains of PDAPP mice given LY450139 dihydrate daily by gavage for 5 months. *Neurobiology of Aging,* 25**,** S238-S239.

NEUPERT, W. & HERRMANN, J. M. 2007. Translocation of proteins into mitochondria. *Annu Rev Biochem,* 76**,** 723-49.

NICCOLI, T., CABECINHA, M., TILLMANN, A., KERR, F., WONG, C. T., CARDENES, D., VINCENT, A. J., BETTEDI, L., LI, L., GRONKE, S., DOLS, J. & PARTRIDGE, L. 2016. Increased Glucose Transport into Neurons Rescues Abeta Toxicity in Drosophila. *Curr Biol*.

NICCOLI, T. & PARTRIDGE, L. 2012. Ageing as a risk factor for disease. *Curr Biol,* 22**,** R741-52.

NILSBERTH, C., WESTLIND-DANIELSSON, A., ECKMAN, C. B., CONDRON, M. M., AXELMAN, K., FORSELL, C., STENH, C., LUTHMAN, J., TEPLOW, D. B., YOUNKIN, S. G., NASLUND, J. & LANNFELT, L. 2001. The 'Arctic' APP mutation (E693G) causes Alzheimer's disease by enhanced Abeta protofibril formation. *Nat Neurosci,* 4**,** 887-93.

NIXON, R. A. & YANG, D. S. 2011. Autophagy failure in Alzheimer's disease--locating the primary defect. *Neurobiol Dis,* 43**,** 38-45.

NUHRENBERG, T. G., VOISARD, R., FAHLISCH, F., RUDELIUS, M., BRAUN, J., GSCHWEND, J., KOUNTIDES, M., HERTER, T., BAUR, R., HOMBACH, V., BAEUERLE, P. A. & ZOHLNHOFER, D. 2005. Rapamycin attenuates vascular wall inflammation and progenitor cell promoters after angioplasty. *FASEB J,* 19**,** 246-8.

NUNOMURA, A., PERRY, G., ALIEV, G., HIRAI, K., TAKEDA, A., BALRAJ, E. K., JONES, P. K., GHANBARI, H., WATAYA, T., SHIMOHAMA, S., CHIBA, S., ATWOOD, C. S., PETERSEN, R. B. & SMITH, M. A. 2001. Oxidative damage is the earliest event in Alzheimer disease. *J Neuropathol Exp Neurol,* 60**,** 759-67.

OHYAGI, Y., YAMADA, T., NISHIOKA, K., CLARKE, N. J., TOMLINSON, A. J., NAYLOR, S., NAKABEPPU, Y., KIRA, J. & YOUNKIN, S. G. 2000. Selective increase in cellular A beta 42 is related to apoptosis but not necrosis. *Neuroreport,* 11**,** 167-71.

OIDA, Y., KITAICHI, K., NAKAYAMA, H., ITO, Y., FUJIMOTO, Y., SHIMAZAWA, M., NAGAI, H. & HARA, H. 2006. Rifampicin attenuates the MPTP-induced neurotoxicity in mouse brain. *Brain Res,* 1082**,** 196-204.

ONKEN, B. & DRISCOLL, M. 2010. Metformin induces a dietary restriction-like state and the oxidative stress response to extend C. elegans Healthspan via AMPK, LKB1, and SKN-1. *PLoS One,* 5**,** e8758.

OSTERWALDER, T., YOON, K. S., WHITE, B. H. & KESHISHIAN, H. 2001. A conditional tissue-specific transgene expression system using inducible GAL4. *Proc Natl Acad Sci U S A,* 98**,** 12596-601.

OYAMA, F., SAWAMURA, N., KOBAYASHI, K., MORISHIMA-KAWASHIMA, M., KURAMOCHI, T., ITO, M., TOMITA, T., MARUYAMA, K., SAIDO, T. C., IWATSUBO, T., CAPELL, A., WALTER, J., GRUNBERG, J., UEYAMA, Y., HAASS, C. & IHARA, Y. 1998. Mutant presenilin 2 transgenic mouse: effect on an age-dependent increase of amyloid beta-protein 42 in the brain. *J Neurochem,* 71**,** 313-22.

PAIK, D., JANG, Y. G., LEE, Y. E., LEE, Y. N., YAMAMOTO, R., GEE, H. Y., YOO, S., BAE, E., MIN, K. J., TATAR, M. & PARK, J. J. 2012. Misexpression screen delineates novel genes controlling Drosophila lifespan. *Mech Ageing Dev,* 133**,** 234-45.

PAISAN-RUIZ, C., BHATIA, K. P., LI, A., HERNANDEZ, D., DAVIS, M., WOOD, N. W., HARDY, J., HOULDEN, H., SINGLETON, A. & SCHNEIDER, S. A. 2009. Characterization of PLA2G6 as a locus for dystonia-parkinsonism. *Ann Neurol,* 65**,** 19-23.

PAISAN-RUIZ, C., JAIN, S., EVANS, E. W., GILKS, W. P., SIMON, J., VAN DER BRUG, M., LOPEZ DE MUNAIN, A., APARICIO, S., GIL, A. M., KHAN, N., JOHNSON, J., MARTINEZ, J. R., NICHOLL, D., CARRERA, I. M., PENA, A. S., DE SILVA, R., LEES, A., MARTI-MASSO, J. F., PEREZ-TUR, J., WOOD, N. W. & SINGLETON, A. B. 2004. Cloning of the gene containing mutations that cause PARK8-linked Parkinson's disease. *Neuron,* 44**,** 595-600.

PAISAN-RUIZ, C., LI, A., SCHNEIDER, S. A., HOLTON, J. L., JOHNSON, R., KIDD, D., CHATAWAY, J., BHATIA, K. P., LEES, A. J., HARDY, J., REVESZ, T. & HOULDEN, H. 2012. Widespread Lewy body and tau accumulation in childhood and adult onset dystonia-parkinsonism cases with PLA2G6 mutations. *Neurobiol Aging,* 33**,** 814-23.

PALU, R. A. & THUMMEL, C. S. 2016. Sir2 Acts through Hepatocyte Nuclear Factor 4 to maintain insulin Signaling and Metabolic Homeostasis in Drosophila. *PLoS Genet,* 12**,** e1005978.

PAN, H., GUO, J. & SU, Z. 2014. Advances in understanding the interrelations between leptin resistance and obesity. *Physiol Behav,* 130**,** 157-69.

PARK, C. B. & LARSSON, N. G. 2011. Mitochondrial DNA mutations in disease and aging. *J Cell Biol,* 193**,** 809-18.

PARK, J., KIM, Y. & CHUNG, J. 2009. Mitochondrial dysfunction and Parkinson's disease genes: insights from Drosophila. *Dis Model Mech,* 2**,** 336-40.

PARK, J., LEE, S. B., LEE, S., KIM, Y., SONG, S., KIM, S., BAE, E., KIM, J., SHONG, M., KIM, J. M. & CHUNG, J. 2006. Mitochondrial dysfunction in Drosophila PINK1 mutants is complemented by parkin. *Nature,* 441**,** 1157-61.

PARKER, W. D., JR., FILLEY, C. M. & PARKS, J. K. 1990. Cytochrome oxidase deficiency in Alzheimer's disease. *Neurology,* 40**,** 1302-3.

PARTRIDGE, L. 2001. Evolutionary theories of ageing applied to long-lived organisms. *Exp Gerontol,* 36**,** 641-50.

PARTRIDGE, L. & GEMS, D. 2007. Benchmarks for ageing studies. *Nature,* 450**,** 165-7.

PARTRIDGE, L., GEMS, D. & WITHERS, D. J. 2005. Sex and death: what is the connection? *Cell,* 120**,** 461-72.

PASSTOORS, W. M., BEEKMAN, M., DEELEN, J., VAN DER BREGGEN, R., MAIER, A. B., GUIGAS, B., DERHOVANESSIAN, E., VAN HEEMST, D., DE CRAEN, A. J., GUNN, D. A., PAWELEC, G. & SLAGBOOM, P. E. 2013. Gene expression analysis of mTOR pathway: association with human longevity. *Aging Cell,* 12**,** 24-31.

PATTI, M. E., BUTTE, A. J., CRUNKHORN, S., CUSI, K., BERRIA, R., KASHYAP, S., MIYAZAKI, Y., KOHANE, I., COSTELLO, M., SACCONE, R., LANDAKER, E. J., GOLDFINE, A. B., MUN, E., DEFRONZO, R., FINLAYSON, J., KAHN, C. R. & MANDARINO, L. J. 2003. Coordinated reduction of genes of oxidative metabolism in humans with insulin resistance and diabetes: Potential role of PGC1 and NRF1. *Proc Natl Acad Sci U S A,* 100**,** 8466-71.

PAYNE, B. A., WILSON, I. J., HATELEY, C. A., HORVATH, R., SANTIBANEZ-KOREF, M., SAMUELS, D. C., PRICE, D. A. & CHINNERY, P. F. 2011. Mitochondrial aging is accelerated by anti-retroviral therapy through the clonal expansion of mtDNA mutations. *Nat Genet,* 43**,** 806-10.

PERIQUET, M., FULGA, T., MYLLYKANGAS, L., SCHLOSSMACHER, M. G. & FEANY, M. B. 2007. Aggregated alpha-synuclein mediates dopaminergic neurotoxicity in vivo. *J Neurosci,* 27**,** 3338-46.

PICCOLI, C., SARDANELLI, A., SCRIMA, R., RIPOLI, M., QUARATO, G., D'APRILE, A., BELLOMO, F., SCACCO, S., DE MICHELE, G., FILLA, A., IUSO, A., BOFFOLI, D., CAPITANIO, N. & PAPA, S. 2008. Mitochondrial respiratory dysfunction in familiar parkinsonism associated with PINK1 mutation. *Neurochem Res,* 33**,** 2565-74.

PIPER, M. D., SELMAN, C., MCELWEE, J. J. & PARTRIDGE, L. 2008. Separating cause from effect: how does insulin/IGF signalling control lifespan in worms, flies and mice? *J Intern Med,* 263**,** 179-91.

POIRIER, L., SHANE, A., ZHENG, J. & SEROUDE, L. 2008. Characterization of the Drosophila gene-switch system in aging studies: a cautionary tale. *Aging Cell,* 7**,** 758-70.

POLAK, P., CYBULSKI, N., FEIGE, J. N., AUWERX, J., RUEGG, M. A. & HALL, M. N. 2008. Adipose-specific knockout of raptor results in lean mice with enhanced mitochondrial respiration. *Cell Metab,* 8**,** 399-410.

POLYMEROPOULOS, M. H., LAVEDAN, C., LEROY, E., IDE, S. E., DEHEJIA, A., DUTRA, A., PIKE, B., ROOT, H., RUBENSTEIN, J., BOYER, R., STENROOS, E. S., CHANDRASEKHARAPPA, S., ATHANASSIADOU, A., PAPAPETROPOULOS, T., JOHNSON, W. G., LAZZARINI, A. M., DUVOISIN, R. C., DI IORIO, G., GOLBE, L. I. & NUSSBAUM, R. L. 1997. Mutation in the alpha-synuclein gene identified in families with Parkinson's disease. *Science,* 276**,** 2045-7.

POOLE, A. C., THOMAS, R. E., ANDREWS, L. A., MCBRIDE, H. M., WHITWORTH, A. J. & PALLANCK, L. J. 2008. The PINK1/Parkin pathway regulates mitochondrial morphology. *Proc Natl Acad Sci U S A,* 105**,** 1638-43.

POWERS, E. T., MORIMOTO, R. I., DILLIN, A., KELLY, J. W. & BALCH, W. E. 2009. Biological and chemical approaches to diseases of proteostasis deficiency. *Annu Rev Biochem,* 78**,** 959-91.

POWERS, R. W., 3RD, KAEBERLEIN, M., CALDWELL, S. D., KENNEDY, B. K. & FIELDS, S. 2006. Extension of chronological life span in yeast by decreased TOR pathway signaling. *Genes Dev,* 20**,** 174-84.

PRAMSTALLER, P. P., SCHLOSSMACHER, M. G., JACQUES, T. S., SCARAVILLI, F., ESKELSON, C., PEPIVANI, I., HEDRICH, K., ADEL, S., GONZALES-MCNEAL, M., HILKER, R., KRAMER, P. L. & KLEIN, C. 2005. Lewy body Parkinson's disease in a large pedigree with 77 Parkin mutation carriers. *Ann Neurol,* 58**,** 411-22.

PRATICO, D., URYU, K., LEIGHT, S., TROJANOSWKI, J. Q. & LEE, V. M. 2001. Increased lipid peroxidation precedes amyloid plaque formation in an animal model of Alzheimer amyloidosis. *J Neurosci,* 21**,** 4183-7.

PRICE, D. L. & SISODIA, S. S. 1998. Mutant genes in familial Alzheimer's disease and transgenic models. *Annu Rev Neurosci,* 21**,** 479-505.

PRICE, J. L., MCKEEL, D. W., JR., BUCKLES, V. D., ROE, C. M., XIONG, C., GRUNDMAN, M., HANSEN, L. A., PETERSEN, R. C., PARISI, J. E., DICKSON, D. W., SMITH, C. D., DAVIS, D. G., SCHMITT, F. A., MARKESBERY, W. R., KAYE, J., KURLAN, R., HULETTE, C., KURLAND, B. F., HIGDON, R., KUKULL, W. & MORRIS, J. C. 2009. Neuropathology of nondemented aging: presumptive evidence for preclinical Alzheimer disease. *Neurobiol Aging,* 30**,** 1026-36.

PRIEST, N. K., MACKOWIAK, B. & PROMISLOW, D. E. 2002. The role of parental age effects on the evolution of aging. *Evolution,* 56**,** 927-35.

PUIGSERVER, P., RHEE, J., DONOVAN, J., WALKEY, C. J., YOON, J. C., ORIENTE, F., KITAMURA, Y., ALTOMONTE, J., DONG, H., ACCILI, D. & SPIEGELMAN, B. M. 2003. Insulin-regulated hepatic gluconeogenesis through FOXO1-PGC-1alpha interaction. *Nature,* 423**,** 550-5.

PUIGSERVER, P., RHEE, J., LIN, J., WU, Z., YOON, J. C., ZHANG, C. Y., KRAUSS, S., MOOTHA, V. K., LOWELL, B. B. & SPIEGELMAN, B. M. 2001. Cytokine stimulation of energy expenditure through p38 MAP kinase activation of PPARgamma coactivator-1. *Mol Cell,* 8**,** 971-82.

PUIGSERVER, P. & SPIEGELMAN, B. M. 2003. Peroxisome proliferator-activated receptor-gamma coactivator 1 alpha (PGC-1 alpha): transcriptional coactivator and metabolic regulator. *Endocr Rev,* 24**,** 78-90.

PUIGSERVER, P., WU, Z., PARK, C. W., GRAVES, R., WRIGHT, M. & SPIEGELMAN, B. M. 1998. A cold-inducible coactivator of nuclear receptors linked to adaptive thermogenesis. *Cell,* 92**,** 829-39.

QIN, W., HAROUTUNIAN, V., KATSEL, P., CARDOZO, C. P., HO, L., BUXBAUM, J. D. & PASINETTI, G. M. 2009. PGC-1alpha expression decreases in the Alzheimer disease brain as a function of dementia. *Arch Neurol,* 66**,** 352-61.

RAMIREZ, A., HEIMBACH, A., GRUNDEMANN, J., STILLER, B., HAMPSHIRE, D., CID, L. P., GOEBEL, I., MUBAIDIN, A. F., WRIEKAT, A. L., ROEPER, J., AL-DIN, A., HILLMER, A. M., KARSAK, M., LISS, B., WOODS, C. G., BEHRENS, M. I. & KUBISCH, C. 2006. Hereditary parkinsonism with dementia is caused by mutations in ATP13A2, encoding a lysosomal type 5 P-type ATPase. *Nat Genet,* 38**,** 1184-91.

REDDY, P. H., MCWEENEY, S., PARK, B. S., MANCZAK, M., GUTALA, R. V., PARTOVI, D., JUNG, Y., YAU, V., SEARLES, R., MORI, M. & QUINN, J. 2004. Gene expression profiles of transcripts in amyloid precursor protein transgenic mice: up-regulation of mitochondrial metabolism and apoptotic genes is an early cellular change in Alzheimer's disease. *Hum Mol Genet,* 13**,** 1225-40.

REGAN, J. C., KHERICHA, M., DOBSON, A. J., BOLUKBASI, E., RATTANAVIROTKUL, N. & PARTRIDGE, L. 2016. Sex difference in pathology of the ageing gut mediates the greater response of female lifespan to dietary restriction. *Elife,* 5.

REINHARDT, S., SCHUCK, F., GROSGEN, S., RIEMENSCHNEIDER, M., HARTMANN, T., POSTINA, R., GRIMM, M. & ENDRES, K. 2014. Unfolded protein response signaling by transcription factor XBP-1 regulates ADAM10 and is affected in Alzheimer's disease. *FASEB J,* 28**,** 978-97.

REN, C., WEBSTER, P., FINKEL, S. E. & TOWER, J. 2007. Increased internal and external bacterial load during Drosophila aging without life-span trade-off. *Cell Metab,* 6**,** 144-52.

RERA, M., BAHADORANI, S., CHO, J., KOEHLER, C. L., ULGHERAIT, M., HUR, J. H., ANSARI, W. S., LO, T., JR., JONES, D. L. & WALKER, D. W. 2011. Modulation of longevity and tissue homeostasis by the Drosophila PGC-1 homolog. *Cell Metab,* 14**,** 623-34.

RHEE, J., INOUE, Y., YOON, J. C., PUIGSERVER, P., FAN, M., GONZALEZ, F. J. & SPIEGELMAN, B. M. 2003. Regulation of hepatic fasting response by PPARgamma coactivator-1alpha (PGC-1): requirement for hepatocyte nuclear factor 4alpha in gluconeogenesis. *Proc Natl Acad Sci U S A,* 100**,** 4012-7.

ROBIDA-STUBBS, S., GLOVER-CUTTER, K., LAMMING, D. W., MIZUNUMA, M., NARASIMHAN, S. D., NEUMANN-HAEFELIN, E., SABATINI, D. M. & BLACKWELL, T. K. 2012. TOR signaling and rapamycin influence longevity by regulating SKN-1/Nrf and DAF-16/FoxO. *Cell Metab,* 15**,** 713-24.

RODGERS, J. T., LERIN, C., HAAS, W., GYGI, S. P., SPIEGELMAN, B. M. & PUIGSERVER, P. 2005. Nutrient control of glucose homeostasis through a complex of PGC-1alpha and SIRT1. *Nature,* 434**,** 113-8.

ROGAEV, E. I., SHERRINGTON, R., ROGAEVA, E. A., LEVESQUE, G., IKEDA, M., LIANG, Y., CHI, H., LIN, C., HOLMAN, K., TSUDA, T. & ET AL. 1995. Familial Alzheimer's disease in kindreds with missense mutations in a gene on chromosome 1 related to the Alzheimer's disease type 3 gene. *Nature,* 376**,** 775-8.

ROGERS, I., KERR, F., MARTINEZ, P., HARDY, J., LOVESTONE, S. & PARTRIDGE, L. 2012. Ageing increases vulnerability to aβ42 toxicity in Drosophila. *PLoS One,* 7**,** e40569.

ROGINA, B., HELFAND, S. L. & FRANKEL, S. 2002. Longevity regulation by Drosophila Rpd3 deacetylase and caloric restriction. *Science,* 298**,** 1745.

ROMAN, G., ENDO, K., ZONG, L. & DAVIS, R. L. 2001. P[Switch], a system for spatial and temporal control of gene expression in Drosophila melanogaster. *Proc Natl Acad Sci U S A,* 98**,** 12602-7.

RON, D. & WALTER, P. 2007. Signal integration in the endoplasmic reticulum unfolded protein response. *Nat Rev Mol Cell Biol,* 8**,** 519-29.

ROSE, M. R. 1999. Can human aging be postponed? *Sci Am,* 281**,** 106-11.

ROSEN, D. R., MARTIN-MORRIS, L., LUO, L. Q. & WHITE, K. 1989. A Drosophila gene encoding a protein resembling the human beta-amyloid protein precursor. *Proc Natl Acad Sci U S A,* 86**,** 2478-82.

ROSS, J. M., OLSON, L. & COPPOTELLI, G. 2015. Mitochondrial and Ubiquitin Proteasome System Dysfunction in Ageing and Disease: Two Sides of the Same Coin? *Int J Mol Sci,* 16**,** 19458-76.

ROTHWELL, N. J. & STOCK, M. J. 1979. A role for brown adipose tissue in diet-induced thermogenesis. *Nature,* 281**,** 31-5.

SAFRA, M., BEN-HAMO, S., KENYON, C. & HENIS-KORENBLIT, S. 2013. The ire-1 ER stress-response pathway is required for normal secretory-protein metabolism in C. elegans. *J Cell Sci,* 126**,** 4136-46.

SALIH, D. A. & BRUNET, A. 2008. FoxO transcription factors in the maintenance of cellular homeostasis during aging. *Curr Opin Cell Biol,* 20**,** 126-36.

SATAKE, W., NAKABAYASHI, Y., MIZUTA, I., HIROTA, Y., ITO, C., KUBO, M., KAWAGUCHI, T., TSUNODA, T., WATANABE, M., TAKEDA, A., TOMIYAMA, H., NAKASHIMA, K., HASEGAWA, K., OBATA, F., YOSHIKAWA, T., KAWAKAMI, H., SAKODA, S., YAMAMOTO, M., HATTORI, N., MURATA, M., NAKAMURA, Y. & TODA, T. 2009. Genome-wide association study identifies common variants at four loci as genetic risk factors for Parkinson's disease. *Nat Genet,* 41**,** 1303-7.

SCARPULLA, R. C. 2008. Transcriptional paradigms in mammalian mitochondrial biogenesis and function. *Physiol Rev,* 88**,** 611-38.

SCHAPIRA, A. H., COOPER, J. M., DEXTER, D., JENNER, P., CLARK, J. B. & MARSDEN, C. D. 1989. Mitochondrial complex I deficiency in Parkinson's disease. *Lancet,* 1**,** 1269.

SCHAPIRA, A. H. & GEGG, M. 2011. Mitochondrial contribution to Parkinson's disease pathogenesis. *Parkinsons Dis,* 2011**,** 159160.

SEARS, I. B., MACGINNITIE, M. A., KOVACS, L. G. & GRAVES, R. A. 1996. Differentiation-dependent expression of the brown adipocyte uncoupling protein gene: regulation by peroxisome proliferator-activated receptor gamma. *Mol Cell Biol,* 16**,** 3410-9.

SELMAN, C., TULLET, J. M., WIESER, D., IRVINE, E., LINGARD, S. J., CHOUDHURY, A. I., CLARET, M., AL-QASSAB, H., CARMIGNAC, D., RAMADANI, F., WOODS, A., ROBINSON, I. C., SCHUSTER, E., BATTERHAM, R. L., KOZMA, S. C., THOMAS, G., CARLING, D., OKKENHAUG, K., THORNTON, J. M., PARTRIDGE, L., GEMS, D. & WITHERS, D. J. 2009. Ribosomal protein S6 kinase 1 signaling regulates mammalian life span. *Science,* 326**,** 140-4.

SENA, L. A. & CHANDEL, N. S. 2012. Physiological roles of mitochondrial reactive oxygen species. *Mol Cell,* 48**,** 158-67.

SEVIGNY, J., CHIAO, P., BUSSIERE, T., WEINREB, P. H., WILLIAMS, L., MAIER, M., DUNSTAN, R., SALLOWAY, S., CHEN, T., LING, Y., O'GORMAN, J., QIAN, F., ARASTU, M., LI, M., CHOLLATE, S., BRENNAN, M. S., QUINTERO-MONZON, O., SCANNEVIN, R. H., ARNOLD, H. M., ENGBER, T., RHODES, K., FERRERO, J., HANG, Y., MIKULSKIS, A., GRIMM, J., HOCK, C., NITSCH, R. M. & SANDROCK, A. 2016. The antibody aducanumab reduces Abeta plaques in Alzheimer's disease. *Nature,* 537**,** 50-6.

SHANKAR, G. M., LI, S., MEHTA, T. H., GARCIA-MUNOZ, A., SHEPARDSON, N. E., SMITH, I., BRETT, F. M., FARRELL, M. A., ROWAN, M. J., LEMERE, C. A., REGAN, C. M., WALSH, D. M., SABATINI, B. L. & SELKOE, D. J. 2008.

Amyloid-beta protein dimers isolated directly from Alzheimer's brains impair synaptic plasticity and memory. *Nat Med,* 14**,** 837-42.

SHARP, Z. D. & BARTKE, A. 2005. Evidence for down-regulation of phosphoinositide 3-kinase/Akt/mammalian target of rapamycin (PI3K/Akt/mTOR)-dependent translation regulatory signaling pathways in Ames dwarf mice. *J Gerontol A Biol Sci Med Sci,* 60**,** 293-300.

SHENG, B., WANG, X., SU, B., LEE, H. G., CASADESUS, G., PERRY, G. & ZHU, X. 2012. Impaired mitochondrial biogenesis contributes to mitochondrial dysfunction in Alzheimer's disease. *J Neurochem,* 120**,** 419-29.

SHIMURA, H., HATTORI, N., KUBO, S., MIZUNO, Y., ASAKAWA, S., MINOSHIMA, S., SHIMIZU, N., IWAI, K., CHIBA, T., TANAKA, K. & SUZUKI, T. 2000. Familial Parkinson disease gene product, parkin, is a ubiquitin-protein ligase. *Nat Genet,* 25**,** 302-5.

SHIN, J. H., KO, H. S., KANG, H., LEE, Y., LEE, Y. I., PLETINKOVA, O., TROCONSO, J. C., DAWSON, V. L. & DAWSON, T. M. 2011. PARIS (ZNF746) repression of PGC-1alpha contributes to neurodegeneration in Parkinson's disease. *Cell,* 144**,** 689-702.

SHORE, G. C., PAPA, F. R. & OAKES, S. A. 2011. Signaling cell death from the endoplasmic reticulum stress response. *Curr Opin Cell Biol,* 23**,** 143-9.

SIEGEL, S. J., BIESCHKE, J., POWERS, E. T. & KELLY, J. W. 2007. The oxidative stress metabolite 4-hydroxynonenal promotes Alzheimer protofibril formation. *Biochemistry,* 46**,** 1503-10.

SIMON-SANCHEZ, J., SCHULTE, C., BRAS, J. M., SHARMA, M., GIBBS, J. R., BERG, D., PAISAN-RUIZ, C., LICHTNER, P., SCHOLZ, S. W., HERNANDEZ, D. G., KRUGER, R., FEDEROFF, M., KLEIN, C., GOATE, A., PERLMUTTER, J., BONIN, M., NALLS, M. A., ILLIG, T., GIEGER, C., HOULDEN, H., STEFFENS, M., OKUN, M. S., RACETTE, B. A., COOKSON, M. R., FOOTE, K. D., FERNANDEZ, H. H., TRAYNOR, B. J., SCHREIBER, S., AREPALLI, S., ZONOZI, R., GWINN, K., VAN DER BRUG, M., LOPEZ, G., CHANOCK, S. J., SCHATZKIN, A., PARK, Y., HOLLENBECK, A., GAO, J., HUANG, X., WOOD, N. W., LORENZ, D., DEUSCHL, G., CHEN, H., RIESS, O., HARDY, J. A., SINGLETON, A. B. & GASSER, T. 2009. Genome-wide association study reveals genetic risk underlying Parkinson's disease. *Nat Genet,* 41**,** 1308-12.

SINGLETON, A. B., FARRER, M., JOHNSON, J., SINGLETON, A., HAGUE, S., KACHERGUS, J., HULIHAN, M., PEURALINNA, T., DUTRA, A., NUSSBAUM, R., LINCOLN, S., CRAWLEY, A., HANSON, M., MARAGANORE, D., ADLER, C., COOKSON, M. R., MUENTER, M., BAPTISTA, M., MILLER, D., BLANCATO, J., HARDY, J. & GWINN-HARDY, K. 2003. alpha-Synuclein locus triplication causes Parkinson's disease. *Science,* 302**,** 841.

SLACK, C., ALIC, N., FOLEY, A., CABECINHA, M., HODDINOTT, M. P. & PARTRIDGE, L. 2015. The Ras-Erk-ETS-Signaling Pathway Is a Drug Target for Longevity. *Cell,* 162**,** 72-83.

SLACK, C., FOLEY, A. & PARTRIDGE, L. 2012. Activation of AMPK by the putative dietary restriction mimetic metformin is insufficient to extend lifespan in Drosophila. *PLoS One,* 7**,** e47699.

SLACK, C., GIANNAKOU, M. E., FOLEY, A., GOSS, M. & PARTRIDGE, L. 2011. dFOXO-independent effects of reduced insulin-like signaling in Drosophila. *Aging Cell,* 10**,** 735-48.

SLOTH ANDERSEN, A., HERTZ HANSEN, P., SCHAFFER, L. & KRISTENSEN, C. 2000. A new secreted insect protein belonging to the immunoglobulin superfamily binds insulin and related peptides and inhibits their activities. *J Biol Chem,* 275**,** 16948-53.

SOFOLA, O., KERR, F., ROGERS, I., KILLICK, R., AUGUSTIN, H., GANDY, C., ALLEN, M. J., HARDY, J., LOVESTONE, S. & PARTRIDGE, L. 2010. Inhibition of GSK-3 ameliorates Abeta pathology in an adult-onset Drosophila model of Alzheimer's disease. *PLoS Genet,* 6**,** e1001087.

SOFOLA-ADESAKIN, O., CASTILLO-QUAN, J. I., RALLIS, C., TAIN, L. S., BJEDOV, I., ROGERS, I., LI, L., MARTINEZ, P., KHERICHA, M., CABECINHA, M., BAHLER, J. & PARTRIDGE, L. 2014. Lithium suppresses Abeta pathology by inhibiting translation in an adult Drosophila model of Alzheimer's disease. *Front Aging Neurosci,* 6**,** 190.

SONENBERG, N. & HINNEBUSCH, A. G. 2009. Regulation of translation initiation in eukaryotes: mechanisms and biological targets. *Cell,* 136**,** 731-45.

SPILLANTINI, M. G., SCHMIDT, M. L., LEE, V. M., TROJANOWSKI, J. Q., JAKES, R. & GOEDERT, M. 1997. Alpha-synuclein in Lewy bodies. *Nature,* 388**,** 839-40.

ST-PIERRE, J., DRORI, S., ULDRY, M., SILVAGGI, J. M., RHEE, J., JAGER, S., HANDSCHIN, C., ZHENG, K., LIN, J., YANG, W., SIMON, D. K., BACHOO, R. & SPIEGELMAN, B. M. 2006. Suppression of reactive oxygen species and neurodegeneration by the PGC-1 transcriptional coactivators. *Cell,* 127**,** 397-408.

STRITTMATTER, W. J., SAUNDERS, A. M., SCHMECHEL, D., PERICAK-VANCE, M., ENGHILD, J., SALVESEN, G. S. & ROSES, A. D. 1993. Apolipoprotein E: high-avidity binding to beta-amyloid and increased frequency of type 4 allele in late-onset familial Alzheimer disease. *Proc Natl Acad Sci U S A,* 90**,** 1977-81.

SUZUKI, N., CHEUNG, T. T., CAI, X. D., ODAKA, A., OTVOS, L., JR., ECKMAN, C., GOLDE, T. E. & YOUNKIN, S. G. 1994. An increased percentage of long amyloid beta protein secreted by familial amyloid beta protein precursor (beta APP717) mutants. *Science,* 264**,** 1336-40.

SWINDELL, W. R. 2012. Dietary restriction in rats and mice: a meta-analysis and review of the evidence for genotype-dependent effects on lifespan. *Ageing Res Rev,* 11**,** 254-70.

SYKIOTIS, G. P. & BOHMANN, D. 2010. Stress-activated cap'n'collar transcription factors in aging and human disease. *Sci Signal,* 3**,** re3.

TABAS, I. & RON, D. 2011. Integrating the mechanisms of apoptosis induced by endoplasmic reticulum stress. *Nat Cell Biol,* 13**,** 184-90.

TAKANO, A., USUI, I., HARUTA, T., KAWAHARA, J., UNO, T., IWATA, M. & KOBAYASHI, M. 2001. Mammalian target of rapamycin pathway regulates insulin signaling via subcellular redistribution of insulin receptor substrate 1 and integrates nutritional signals and metabolic signals of insulin. *Mol Cell Biol,* 21**,** 5050-62.

TAMAGNO, E., PAROLA, M., BARDINI, P., PICCINI, A., BORGHI, R., GUGLIELMOTTO, M., SANTORO, G., DAVIT, A., DANNI, O., SMITH, M. A., PERRY, G. & TABATON, M. 2005. Beta-site APP cleaving enzyme up-regulation induced by 4-hydroxynonenal is mediated by stress-activated protein kinases pathways. *J Neurochem,* 92**,** 628-36.

TANNER, C. M., KAMEL, F., ROSS, G. W., HOPPIN, J. A., GOLDMAN, S. M., KORELL, M., MARRAS, C., BHUDHIKANOK, G. S., KASTEN, M., CHADE, A. R., COMYNS, K., RICHARDS, M. B., MENG, C., PRIESTLEY, B., FERNANDEZ, H. H., CAMBI, F., UMBACH, D. M., BLAIR, A., SANDLER, D. P. & LANGSTON, J. W. 2011. Rotenone, paraquat, and Parkinson's disease. *Environ Health Perspect,* 119**,** 866-72.

TATAR, M., BARTKE, A. & ANTEBI, A. 2003. The endocrine regulation of aging by insulin-like signals. *Science,* 299**,** 1346-51.

TATSUTA, T. & LANGER, T. 2008. Quality control of mitochondria: protection against neurodegeneration and ageing. *EMBO J,* 27**,** 306-14.

TAYLOR, R. C. & DILLIN, A. 2011. Aging as an Event of Proteostasis Collapse. *Cold Spring Harbor Perspectives in Biology,* 3.

TAYLOR, R. C. & DILLIN, A. 2013. XBP-1 Is a Cell-Nonautonomous Regulator of Stress Resistance and Longevity. *Cell,* 153**,** 1435-1447.

TESSITORE, L. & BOLLITO, E. 2006. Early induction of TGF-beta1 through a fasting-re-feeding regimen promotes liver carcinogenesis by a sub-initiating dose of diethylnitrosamine. *Cell Prolif,* 39**,** 105-16.

TETTWEILER, G., MIRON, M., JENKINS, M., SONENBERG, N. & LASKO, P. F. 2005. Starvation and oxidative stress resistance in Drosophila are mediated through the eIF4E-binding protein, d4E-BP. *Genes Dev,* 19**,** 1840-3.

TIAN, Y., GARCIA, G., BIAN, Q., STEFFEN, K. K., JOE, L., WOLFF, S., MEYER, B. J. & DILLIN, A. 2016. Mitochondrial Stress Induces Chromatin Reorganization to Promote Longevity and UPR(mt). *Cell,* 165**,** 1197-208.

TIEFENBÖCK, S. K., BALTZER, C., EGLI, N. A. & FREI, C. 2010. The Drosophila PGC-1 homologue Spargel coordinates mitochondrial activity to insulin signalling. *EMBO J,* 29**,** 171-83.

TINKERHESS, M. J., HEALY, L., MORGAN, M., SUJKOWSKI, A., MATTHYS, E., ZHENG, L. & WESSELLS, R. J. 2012. The Drosophila PGC-1alpha homolog spargel modulates the physiological effects of endurance exercise. *PLoS One,* 7**,** e31633.

TOIVONEN, J. M., WALKER, G. A., MARTINEZ-DIAZ, P., BJEDOV, I., DRIEGE, Y., JACOBS, H. T., GEMS, D. & PARTRIDGE, L. 2007. No influence of Indy on lifespan in Drosophila after correction for genetic and cytoplasmic background effects. *PLoS Genet,* 3**,** e95.

TOMIYAMA, T., ASANO, S., SUWA, Y., MORITA, T., KATAOKA, K., MORI, H. & ENDO, N. 1994. Rifampicin prevents the aggregation and neurotoxicity of amyloid beta protein in vitro. *Biochem Biophys Res Commun,* 204**,** 76-83.

TOMIYAMA, T., MATSUYAMA, S., ISO, H., UMEDA, T., TAKUMA, H., OHNISHI, K., ISHIBASHI, K., TERAOKA, R., SAKAMA, N., YAMASHITA, T., NISHITSUJI, K., ITO, K., SHIMADA, H., LAMBERT, M. P., KLEIN, W. L. & MORI, H. 2010. A mouse model of amyloid beta oligomers: their contribution to synaptic alteration, abnormal tau phosphorylation, glial activation, and neuronal loss in vivo. *J Neurosci,* 30**,** 4845-56.

TRICOIRE, H., BATTISTI, V., TRANNOY, S., LASBLEIZ, C., PRET, A. M. & MONNIER, V. 2009. The steroid hormone receptor EcR finely modulates Drosophila lifespan during adulthood in a sex-specific manner. *Mech Ageing Dev,* 130**,** 547-52.

TRIFUNOVIC, A., WREDENBERG, A., FALKENBERG, M., SPELBRINK, J. N., ROVIO, A. T., BRUDER, C. E., BOHLOOLY, Y. M., GIDLOF, S., OLDFORS, A., WIBOM,

R., TORNELL, J., JACOBS, H. T. & LARSSON, N. G. 2004. Premature ageing in mice expressing defective mitochondrial DNA polymerase. *Nature,* 429**,** 417-23.

TSUNEMI, T., ASHE, T. D., MORRISON, B. E., SORIANO, K. R., AU, J., ROQUE, R. A., LAZAROWSKI, E. R., DAMIAN, V. A., MASLIAH, E. & LA SPADA, A. R. 2012. PGC-1alpha rescues Huntington's disease proteotoxicity by preventing oxidative stress and promoting TFEB function. *Sci Transl Med,* 4**,** 142ra97.

TULLET, J. M., HERTWECK, M., AN, J. H., BAKER, J., HWANG, J. Y., LIU, S., OLIVEIRA, R. P., BAUMEISTER, R. & BLACKWELL, T. K. 2008. Direct inhibition of the longevity-promoting factor SKN-1 by insulin-like signaling in C. elegans. *Cell,* 132**,** 1025-38.

UBHI, K. K., SHAIBAH, H., NEWMAN, T. A., SHEPHERD, D. & MUDHER, A. 2007. A comparison of the neuronal dysfunction caused by Drosophila tau and human tau in a Drosophila model of tauopathies. *Invert Neurosci,* 7**,** 165-71.

UM, S. H., D'ALESSIO, D. & THOMAS, G. 2006. Nutrient overload, insulin resistance, and ribosomal protein S6 kinase 1, S6K1. *Cell Metab,* 3**,** 393-402.

UMEDA, T., ONO, K., SAKAI, A., YAMASHITA, M., MIZUGUCHI, M., KLEIN, W. L., YAMADA, M., MORI, H. & TOMIYAMA, T. 2016. Rifampicin is a candidate preventive medicine against amyloid-beta and tau oligomers. *Brain,* 139**,** 1568-86.

UNO, M., HONJOH, S., MATSUDA, M., HOSHIKAWA, H., KISHIMOTO, S., YAMAMOTO, T., EBISUYA, M., YAMAMOTO, T., MATSUMOTO, K. & NISHIDA, E. 2013. A fasting-responsive signaling pathway that extends life span in C. elegans. *Cell Rep,* 3**,** 79-91.

URANO, F., WANG, X., BERTOLOTTI, A., ZHANG, Y., CHUNG, P., HARDING, H. P. & RON, D. 2000. Coupling of stress in the ER to activation of JNK protein kinases by transmembrane protein kinase IRE1. *Science,* 287**,** 664-6.

URRA, H., DUFEY, E., LISBONA, F., ROJAS-RIVERA, D. & HETZ, C. 2013. When ER stress reaches a dead end. *Biochim Biophys Acta,* 1833**,** 3507-17.

VALENTE, E. M., ABOU-SLEIMAN, P. M., CAPUTO, V., MUQIT, M. M., HARVEY, K., GISPERT, S., ALI, Z., DEL TURCO, D., BENTIVOGLIO, A. R., HEALY, D. G., ALBANESE, A., NUSSBAUM, R., GONZALEZ-MALDONADO, R., DELLER, T., SALVI, S., CORTELLI, P., GILKS, W. P., LATCHMAN, D. S., HARVEY, R. J., DALLAPICCOLA, B., AUBURGER, G. & WOOD, N. W. 2004. Hereditary early-onset Parkinson's disease caused by mutations in PINK1. *Science,* 304**,** 1158-60.

VALLE, I., ALVAREZ-BARRIENTOS, A., ARZA, E., LAMAS, S. & MONSALVE, M. 2005. PGC-1alpha regulates the mitochondrial antioxidant defense system in vascular endothelial cells. *Cardiovasc Res,* 66**,** 562-73.

VAN DER HARG, J. M., NOLLE, A., ZWART, R., BOEREMA, A. S., VAN HAASTERT, E. S., STRIJKSTRA, A. M., HOOZEMANS, J. J. & SCHEPER, W. 2014. The unfolded protein response mediates reversible tau phosphorylation induced by metabolic stress. *Cell Death Dis,* 5**,** e1393.

VAN RAAMSDONK, J. M. & HEKIMI, S. 2009. Deletion of the mitochondrial superoxide dismutase sod-2 extends lifespan in Caenorhabditis elegans. *PLoS Genet,* 5**,** e1000361.

VELERI, S., RIEGER, D., HELFRICH-FORSTER, C. & STANEWSKY, R. 2007. Hofbauer-Buchner eyelet affects circadian photosensitivity and coordinates TIM and PER expression in Drosophila clock neurons. *J Biol Rhythms,* 22**,** 29-42.

VELLAI, T., TAKACS-VELLAI, K., ZHANG, Y., KOVACS, A. L., OROSZ, L. & MULLER, F. 2003. Genetics: influence of TOR kinase on lifespan in C. elegans. *Nature,* 426**,** 620.

VELLIQUETTE, R. A., O'CONNOR, T. & VASSAR, R. 2005. Energy inhibition elevates beta-secretase levels and activity and is potentially amyloidogenic in APP transgenic mice: possible early events in Alzheimer's disease pathogenesis. *J Neurosci,* 25**,** 10874-83.

VERMULST, M., WANAGAT, J., KUJOTH, G. C., BIELAS, J. H., RABINOVITCH, P. S., PROLLA, T. A. & LOEB, L. A. 2008. DNA deletions and clonal mutations drive premature aging in mitochondrial mutator mice. *Nat Genet,* 40**,** 392-4.

VIRBASIUS, J. V., VIRBASIUS, C. A. & SCARPULLA, R. C. 1993. Identity of GABP with NRF-2, a multisubunit activator of cytochrome oxidase expression, reveals a cellular role for an ETS domain activator of viral promoters. *Genes Dev,* 7**,** 380-92.

VIVES-BAUZA, C., ZHOU, C., HUANG, Y., CUI, M., DE VRIES, R. L., KIM, J., MAY, J., TOCILESCU, M. A., LIU, W., KO, H. S., MAGRANE, J., MOORE, D. J., DAWSON, V. L., GRAILHE, R., DAWSON, T. M., LI, C., TIEU, K. & PRZEDBORSKI, S. 2010. PINK1-dependent recruitment of Parkin to mitochondria in mitophagy. *Proc Natl Acad Sci U S A,* 107**,** 378-83.

WALSH, D. M., KLYUBIN, I., FADEEVA, J. V., CULLEN, W. K., ANWYL, R., WOLFE, M. S., ROWAN, M. J. & SELKOE, D. J. 2002. Naturally secreted oligomers of amyloid beta protein potently inhibit hippocampal long-term potentiation in vivo. *Nature,* 416**,** 535-9.

WALTER, P. & RON, D. 2011. The unfolded protein response: from stress pathway to homeostatic regulation. *Science,* 334**,** 1081-6.

WANG, L., KARPAC, J. & JASPER, H. 2014. Promoting longevity by maintaining metabolic and proliferative homeostasis. *J Exp Biol,* 217**,** 109-18.

WANG, S. & KAUFMAN, R. J. 2012. The impact of the unfolded protein response on human disease. *J Cell Biol,* 197**,** 857-67.

WARESKI, P., VAARMANN, A., CHOUBEY, V., SAFIULINA, D., LIIV, J., KUUM, M. & KAASIK, A. 2009. PGC-1{alpha} and PGC-1{beta} regulate mitochondrial density in neurons. *J Biol Chem,* 284**,** 21379-85.

WAXMAN, E. A. & GIASSON, B. I. 2009. Molecular mechanisms of alpha-synuclein neurodegeneration. *Biochim Biophys Acta,* 1792**,** 616-24.

WEBB, A. E. & BRUNET, A. 2014. FOXO transcription factors: key regulators of cellular quality control. *Trends Biochem Sci,* 39**,** 159-69.

WESTERHEIDE, S. D., ANCKAR, J., STEVENS, S. M., JR., SISTONEN, L. & MORIMOTO, R. I. 2009. Stress-inducible regulation of heat shock factor 1 by the deacetylase SIRT1. *Science,* 323**,** 1063-6.

WEYDT, P., PINEDA, V. V., TORRENCE, A. E., LIBBY, R. T., SATTERFIELD, T. F., LAZAROWSKI, E. R., GILBERT, M. L., MORTON, G. J., BAMMLER, T. K., STRAND, A. D., CUI, L., BEYER, R. P., EASLEY, C. N., SMITH, A. C., KRAINC, D., LUQUET, S., SWEET, I. R., SCHWARTZ, M. W. & LA SPADA, A. R. 2006. Thermoregulatory and metabolic defects in Huntington's disease

transgenic mice implicate PGC-1alpha in Huntington's disease neurodegeneration. *Cell Metab,* 4**,** 349-62.

WHITWORTH, A. J. & PALLANCK, L. J. 2009. The PINK1/Parkin pathway: a mitochondrial quality control system? *J Bioenerg Biomembr,* 41**,** 499-503.

WHITWORTH, A. J., THEODORE, D. A., GREENE, J. C., BENES, H., WES, P. D. & PALLANCK, L. J. 2005. Increased glutathione S-transferase activity rescues dopaminergic neuron loss in a Drosophila model of Parkinson's disease. *Proc Natl Acad Sci U S A,* 102**,** 8024-9.

WILLETTE, A. A., BENDLIN, B. B., STARKS, E. J., BIRDSILL, A. C., JOHNSON, S. C., CHRISTIAN, B. T., OKONKWO, O. C., LA RUE, A., HERMANN, B. P., KOSCIK, R. L., JONAITIS, E. M., SAGER, M. A. & ASTHANA, S. 2015. Association of Insulin Resistance With Cerebral Glucose Uptake in Late Middle-Aged Adults at Risk for Alzheimer Disease. *JAMA Neurol,* 72**,** 1013-20.

WILLIAMS, G. C. 1957. Pleiotropy, natural selection, and the evolution of senescence. *Evolution(N.Y)***,** 398-411.

WINKLER, E. A., NISHIDA, Y., SAGARE, A. P., REGE, S. V., BELL, R. D., PERLMUTTER, D., SENGILLO, J. D., HILLMAN, S., KONG, P., NELSON, A. R., SULLIVAN, J. S., ZHAO, Z., MEISELMAN, H. J., WENBY, R. B., SOTO, J., ABEL, E. D., MAKSHANOFF, J., ZUNIGA, E., DE VIVO, D. C. & ZLOKOVIC, B. V. 2015. GLUT1 reductions exacerbate Alzheimer's disease vasculo-neuronal dysfunction and degeneration. *Nat Neurosci,* 18**,** 521-30.

WITTMANN, C. W., WSZOLEK, M. F., SHULMAN, J. M., SALVATERRA, P. M., LEWIS, J., HUTTON, M. & FEANY, M. B. 2001. Tauopathy in Drosophila: neurodegeneration without neurofibrillary tangles. *Science,* 293**,** 711-4.

WU, J. & KAUFMAN, R. J. 2006. From acute ER stress to physiological roles of the Unfolded Protein Response. *Cell Death Differ,* 13**,** 374-84.

WU, J., RUAS, J. L., ESTALL, J. L., RASBACH, K. A., CHOI, J. H., YE, L., BOSTROM, P., TYRA, H. M., CRAWFORD, R. W., CAMPBELL, K. P., RUTKOWSKI, D. T., KAUFMAN, R. J. & SPIEGELMAN, B. M. 2011. The unfolded protein response mediates adaptation to exercise in skeletal muscle through a PGC-1alpha/ATF6alpha complex. *Cell Metab,* 13**,** 160-9.

WU, Z., PUIGSERVER, P., ANDERSSON, U., ZHANG, C., ADELMANT, G., MOOTHA, V., TROY, A., CINTI, S., LOWELL, B., SCARPULLA, R. C. & SPIEGELMAN, B. M. 1999. Mechanisms controlling mitochondrial biogenesis and respiration through the thermogenic coactivator PGC-1. *Cell,* 98**,** 115-24.

XIE, L., KANG, H., XU, Q., CHEN, M. J., LIAO, Y., THIYAGARAJAN, M., O'DONNELL, J., CHRISTENSEN, D. J., NICHOLSON, C., ILIFF, J. J., TAKANO, T., DEANE, R. & NEDERGAARD, M. 2013. Sleep drives metabolite clearance from the adult brain. *Science,* 342**,** 373-7.

YANG, Y., GEHRKE, S., IMAI, Y., HUANG, Z., OUYANG, Y., WANG, J. W., YANG, L., BEAL, M. F., VOGEL, H. & LU, B. 2006. Mitochondrial pathology and muscle and dopaminergic neuron degeneration caused by inactivation of Drosophila Pink1 is rescued by Parkin. *Proc Natl Acad Sci U S A,* 103**,** 10793-8.

YANG, Z. F., DRUMEA, K., MOTT, S., WANG, J. & ROSMARIN, A. G. 2014. GABP transcription factor (nuclear respiratory factor 2) is required for mitochondrial biogenesis. *Mol Cell Biol,* 34**,** 3194-201.

YONEDA, T., BENEDETTI, C., URANO, F., CLARK, S. G., HARDING, H. P. & RON, D. 2004. Compartment-specific perturbation of protein handling activates genes encoding mitochondrial chaperones. *J Cell Sci,* 117**,** 4055-66.

YOON, J. C., PUIGSERVER, P., CHEN, G., DONOVAN, J., WU, Z., RHEE, J., ADELMANT, G., STAFFORD, J., KAHN, C. R., GRANNER, D. K., NEWGARD, C. B. & SPIEGELMAN, B. M. 2001. Control of hepatic gluconeogenesis through the transcriptional coactivator PGC-1. *Nature,* 413**,** 131-8.

YOON, S. O., PARK, D. J., RYU, J. C., OZER, H. G., TEP, C., SHIN, Y. J., LIM, T. H., PASTORINO, L., KUNWAR, A. J., WALTON, J. C., NAGAHARA, A. H., LU, K. P., NELSON, R. J., TUSZYNSKI, M. H. & HUANG, K. 2012. JNK3 perpetuates metabolic stress induced by Abeta peptides. *Neuron,* 75**,** 824-37.

YOULE, R. J. & NARENDRA, D. P. 2011. Mechanisms of mitophagy. *Nat Rev Mol Cell Biol,* 12**,** 9-14.

ZARRANZ, J. J., ALEGRE, J., GOMEZ-ESTEBAN, J. C., LEZCANO, E., ROS, R., AMPUERO, I., VIDAL, L., HOENICKA, J., RODRIGUEZ, O., ATARES, B., LLORENS, V., GOMEZ TORTOSA, E., DEL SER, T., MUNOZ, D. G. & DE YEBENES, J. G. 2004. The new mutation, E46K, of alpha-synuclein causes Parkinson and Lewy body dementia. *Ann Neurol,* 55**,** 164-73.

ZECHNER, C., LAI, L., ZECHNER, J. F., GENG, T., YAN, Z., RUMSEY, J. W., COLLIA, D., CHEN, Z., WOZNIAK, D. F., LEONE, T. C. & KELLY, D. P. 2010. Total skeletal muscle PGC-1 deficiency uncouples mitochondrial derangements from fiber type determination and insulin sensitivity. *Cell Metab,* 12**,** 633-42.

ZHANG, J. & NEY, P. A. 2010. Reticulocyte mitophagy: monitoring mitochondrial clearance in a mammalian model. *Autophagy,* 6**,** 405-8.

ZHANG, Y., GAO, J., CHUNG, K. K., HUANG, H., DAWSON, V. L. & DAWSON, T. M. 2000. Parkin functions as an E2-dependent ubiquitin- protein ligase and promotes the degradation of the synaptic vesicle-associated protein, CDCrel-1. *Proc Natl Acad Sci U S A,* 97**,** 13354-9.

ZHANG, Y., IKENO, Y., QI, W., CHAUDHURI, A., LI, Y., BOKOV, A., THORPE, S. R., BAYNES, J. W., EPSTEIN, C., RICHARDSON, A. & VAN REMMEN, H. 2009. Mice deficient in both Mn superoxide dismutase and glutathione peroxidase-1 have increased oxidative damage and a greater incidence of pathology but no reduction in longevity. *J Gerontol A Biol Sci Med Sci,* 64**,** 1212-20.

ZHANG, Y., LU, L., JIA, J., JIA, L., GEULA, C., PEI, J., XU, Z., QIN, W., LIU, R., LI, D. & PAN, N. 2014. A lifespan observation of a novel mouse model: in vivo evidence supports abeta oligomer hypothesis. *PLoS One,* 9**,** e85885.

ZHAO, Q., WANG, J., LEVICHKIN, I. V., STASINOPOULOS, S., RYAN, M. T. & HOOGENRAAD, N. J. 2002. A mitochondrial specific stress response in mammalian cells. *EMBO J,* 21**,** 4411-9.

ZHAO, W., VARGHESE, M., YEMUL, S., PAN, Y., CHENG, A., MARANO, P., HASSAN, S., VEMPATI, P., CHEN, F., QIAN, X. & PASINETTI, G. M. 2011. Peroxisome proliferator activator receptor gamma coactivator-1alpha (PGC-1alpha) improves motor performance and survival in a mouse model of amyotrophic lateral sclerosis. *Mol Neurodegener,* 6**,** 51.

ZHENG, B., LIAO, Z., LOCASCIO, J. J., LESNIAK, K. A., RODERICK, S. S., WATT, M. L., EKLUND, A. C., ZHANG-JAMES, Y., KIM, P. D., HAUSER, M. A., GRUNBLATT, E., MORAN, L. B., MANDEL, S. A., RIEDERER, P., MILLER, R. M., FEDEROFF, H. J., WULLNER, U., PAPAPETROPOULOS, S., YOUDIM, M. B., CANTUTI-

CASTELVETRI, I., YOUNG, A. B., VANCE, J. M., DAVIS, R. L., HEDREEN, J. C., ADLER, C. H., BEACH, T. G., GRAEBER, M. B., MIDDLETON, F. A., ROCHET, J. C., SCHERZER, C. R. & GLOBAL, P. D. G. E. C. 2010. PGC-1alpha, a potential therapeutic target for early intervention in Parkinson's disease. *Sci Transl Med,* 2**,** 52ra73.

ZID, B. M., ROGERS, A. N., KATEWA, S. D., VARGAS, M. A., KOLIPINSKI, M. C., LU, T. A., BENZER, S. & KAPAHI, P. 2009. 4E-BP extends lifespan upon dietary restriction by enhancing mitochondrial activity in Drosophila. *Cell,* 139**,** 149-60.

Appendix

Appendix 1

Sofola-Adesakin, O., Castillo-Quan, J.I., Rallis, C., Tain, L.S., Bjedov, I., Rogers, I., **Li, L.**, Martinez, P., Khericha, M., Cabecinha, M., et al. (2014). Lithium suppresses Abeta pathology by inhibiting translation in an adult Drosophila model of Alzheimer's disease. Front Aging Neurosci *6*, 190.

frontiers in
AGING NEUROSCIENCE

ORIGINAL RESEARCH ARTICLE
published: 30 July 2014
doi: 10.3389/fnagi.2014.00190

Lithium suppresses Aβ pathology by inhibiting translation in an adult *Drosophila* model of Alzheimer's disease

Oyinkan Sofola-Adesakin[1,2], Jorge I. Castillo-Quan[1,2†], Charalampos Rallis[1†], Luke S. Tain[2†], Ivana Bjedov[1,3], Iain Rogers[1], Li Li[1], Pedro Martinez[1,2], Mobina Khericha[1,2], Melissa Cabecinha[1], Jürg Bähler[1] and Linda Partridge[1,2]*

[1] *Department of Genetics, Evolution and Environment, Institute of Healthy Ageing, University College London, London, UK*
[2] *Max Planck Institute for Biology of Ageing, Cologne, Germany*
[3] *Laboratory of Molecular Biology of Cancer, UCL Cancer Institute, London, UK*

Edited by:
Fernanda Laezza, University of Texas Medical Branch, USA

Reviewed by:
Ricardo Maccioni, University of Chile, Chile
Francisco G. Wandosell, Centro de Biologia Molecular "Seveo Ochoa" CSIC-UAM & CIBERNED, Spain
Jian Luo, Stanford Univesity, USA
Yogesh P. Wairkar, University of Texas Medical Branch, USA

***Correspondence:**
Linda Partridge, Department of Genetics, Evolution and Environment, Institute of Healthy Ageing, University College London, Darwin Building, Gower Street, London, WC1E 6BT, UK
e-mail: l.partridge@ucl.ac.uk

† *These authors contributed equally to this work.*

The greatest risk factor for Alzheimer's disease (AD) is age, and changes in the ageing nervous system are likely contributors to AD pathology. Amyloid beta (Aβ) accumulation, which occurs as a result of the amyloidogenic processing of amyloid precursor protein (APP), is thought to initiate the pathogenesis of AD, eventually leading to neuronal cell death. Previously, we developed an adult-onset *Drosophila* model of AD. Mutant Aβ42 accumulation led to increased mortality and neuronal dysfunction in the adult flies. Furthermore, we showed that lithium reduced Aβ42 protein, but not mRNA, and was able to rescue Aβ42-induced toxicity. In the current study, we investigated the mechanism/s by which lithium modulates Aβ42 protein levels and Aβ42 induced toxicity in the fly model. We found that lithium caused a reduction in protein synthesis in *Drosophila* and hence the level of Aβ42. At both the low and high doses tested, lithium rescued the locomotory defects induced by Aβ42, but it rescued lifespan only at lower doses, suggesting that long-term, high-dose lithium treatment may have induced toxicity. Lithium also down-regulated translation in the fission yeast *Schizosaccharomyces pombe* associated with increased chronological lifespan. Our data highlight a role for lithium and reduced protein synthesis as potential therapeutic targets for AD pathogenesis.

Keywords: lithium, Drosophila, Alzheimer's disease, translation, lifespan

INTRODUCTION

Alzheimer's disease (AD) is the most common form of dementia in the ageing population. The proportion of deaths due to heart disease and stroke decreased by 13 and 20% respectively between 2000 and 2008, while those due to AD increased by a staggering 66% (Alzheimer's Association, 2012). AD is a neurodegenerative disorder characterized by the presence of amyloid beta (Aβ) deposits and neurofibrillary, hyperphosphorylated tau tangles in the brain (Spires and Hyman, 2005). Age is the major risk factor for AD, and the fruit fly *Drosophila* has been used to demonstrate experimentally that the neurons of older adult flies are intrinsically more susceptible to Aβ toxicity (Rogers et al., 2012). The ageing process could contribute to increased vulnerability to protein toxicity through several routes, including reduced protein turnover through inefficient proteasome- and autophagy-mediated clearance mechanisms (Rubinsztein et al., 2011; Rogers et al., 2012). Interestingly, Aβ accumulation has been linked to several processes affected by ageing. For instance, in a *Drosophila* model of AD, Aβ increased the appearance of abnormal autophagic vesicles, which lost their structural integrity and function with age, and thus influenced neuronal integrity (Ling et al., 2009).

In a previous study, we developed an adult-onset *Drosophila* model of AD, using an inducible gene expression system to express Arctic mutant Aβ42 specifically in adult neurons (Sofola et al., 2010). Aβ42 accumulated in these flies and they displayed increased mortality together with progressive neuronal dysfunction. We also demonstrated that, if we treated the adult flies expressing Aβ chronically with lithium, we rescued toxicity caused by Aβ. Furthermore, we found that Aβ protein, but not mRNA levels were reduced upon lithium treatment (Sofola et al., 2010).

Lithium has been used to treat psychiatric conditions such as bipolar disorder, and it also has interesting neuroprotective effects (Rybakowski, 2011). Lithium is able to promote neurogenesis, and increase the levels of neurotrophins such as brain-derived neurotrophic factor (BDNF), and to inhibit glycogen synthase kinase-3 (GSK-3), which is involved in AD (Machado-Vieira et al., 2009; Rybakowski, 2011). Lithium also reduces amyloid production by affecting APP processing/cleavage in cells and mice, presumably by down regulating the levels of phosphorylated APP (Phiel et al., 2003; Rockenstein et al., 2007).

Lithium can also influence various ageing-regulated processes that could interfere with protein turnover and consequently affect neurological function. For instance, lithium has

been shown to induce autophagy (Sarkar et al., 2005), promote proteasome-mediated degradation (Jing et al., 2013), and influence components of the translational machinery (Bosetti et al., 2002; Karyo et al., 2010). Also, inhibiting GSK-3 in HCC1806 cells by a GSK-3 inhibitor or knockdown of GSK-3β has been reported to significantly decrease polysome assembly, and thus affect translation (Shin et al., 2014). GSK-3 was shown in these cells to partially exert its effects on translation via eIF4E-binding protein 1 (4E-BP1). Knocking down 4E-BP1 only partially restored the cap-dependent translation suppressed by GSK-3 inhibition, suggesting that GSK-3β may regulate other components involved in protein synthesis (Shin et al., 2014).

In this study, we investigated underlying mechanism/s by which lithium can reduce Aβ protein levels and thus pathology in the adult-onset, *Drosophila* model of AD. Aβ peptide is directly expressed in this model, and therefore, any effect of lithium on Aβ levels is not due to its ability to alter APP processing, but rather a consequence of its role in protein synthesis or degradation.

MATERIALS AND METHODS

FLY STOCKS AND MAINTENANCE

All fly stocks were maintained at 25°C on a 12:12-h light:dark cycle at constant humidity on a standard sugar-yeast (SY) medium (15 gl^{-1} agar, 50 gl^{-1} sugar, 100 gl^{-1} autolyzed yeast, 100 gl^{-1} nipagin and 3 ml l^{-1} propionic acid). Adult-onset, neuronal-specific expression of Arctic mutant Aβ42 peptide was achieved by using the elav GeneSwitch (elavGS)-UAS system [GAL4-dependent upstream activator sequence; (Osterwalder et al., 2001)]. ElavGS was derived from the original elavGS 301.2 line (Osterwalder et al., 2001) and obtained as a generous gift from Dr H. Tricoire (CNRS, France). UAS-ArcAβ42 were obtained from Crowther et al. (2005). elavGS and UAS-lines used in all experiments were backcrossed six times into the w^{1118} genetic background. For the fly AD model, flies carrying homozygous UAS-ArcAβ42;elavGS constructs were out-crossed to either w1118 flies, or flies expressing EGFP in a w1118 background; and adult-onset neuronal expression was induced in the female progeny by treatment with mifepristone (RU486; 200 μM) added to the standard SY medium.

LITHIUM TREATMENT PROTOCOL

Lithium chloride solution was made at 10 M concentration and added to 200 μM RU486 standard SY medium for final concentrations of lithium.

LIFESPAN ANALYSES

For all experiments, flies were raised at a standard density on standard SY medium in 200 mL bottles. Two days after eclosion once-mated females were transferred to experimental vials containing SY medium with or without RU486 (200 μM) at a density of 15 flies per vial. Deaths were scored almost every other day and flies were transferred to fresh food. Data are presented as survival curves and statistical analysis was performed using log-rank tests to compare survival of groups.

NEGATIVE GEOTAXIS ASSAYS

Climbing assays were performed at 25°C according to previously published methods (Sofola et al., 2010). Climbing was analyzed every 2–3 days post-RU486 treatment. Fifteen adult flies were placed in a vertical column (25 cm long, 1.5 cm diameter) with a conic bottom end, tapped to the bottom of the column, then their climb to the top of the column was analyzed. Flies reaching the top and flies remaining at the bottom of the column after a 45 s period were counted separately, and three trials were performed at 1 min intervals for each experiment. Scores recorded were the mean number of flies at the top (n_{top}), the mean number of flies at the bottom (n_{bottom}) and the total number of flies assessed (n_{tot}). A performance index (PI) defined as $½(n_{tot} + n_{top} - n_{bottom})/ n_{tot}$) was calculated. Data are presented as the mean PI ± s.e.m. obtained in three independent experiments for each group, and analyses of variances (ANOVA) were performed using JMP 10.0 software.

QUANTIFICATION OF Aβ42 PEPTIDE

To extract total Aβ42, five *Drosophila* heads were homogenized in 50 μl GnHCl extraction buffer (5 M Guanidine HCl, 50 mM Hepes pH 7.3, protease inhibitor cocktail (Sigma, P8340) and 5 mM EDTA), centrifuged at 21,000 g for 5 min at 4°C, and cleared supernatant retained as the total fly Aβ42 sample. Aβ42 content was measured in Arctic mutant Aβ42 flies and controls using the hAmyloid β42 ELISA kit (HS) (Millipore). Samples were diluted in sample/standard dilution buffer and the ELISA performed according to the manufacturers' instructions. Protein extracts were quantified using the Bradford protein assay (Bio-Rad protein assay reagent; Bio-Rad laboratories (UK) Ltd) and the amount of Aβ42 in each sample expressed as a ratio of the total protein content (pmol/g total protein). Data are expressed as the mean ± s.e.m. obtained in three independent experiments for each genotype. ANOVAs and Tukey's-HSD *post-hoc* analyses were performed using JMP 7.0 software.

WESTERN BLOTTING

The same number *of Drosophila* heads for each sample were homogenized in Laemmli sample buffer containing β-mercaptoethanol and boiled for 10 min. Proteins were separated on SDS polyacrylamide gels and blotted onto nitrocellulose membranes. Membranes were incubated in a blocking solution containing 5% milk proteins in TBST for 1 hr at room temperature, then probed with primary antibodies diluted in TBST + 5% BSA overnight at 4°C. Antibodies were from Cell Signaling unless specified. GFP antibody was used at 1 in 1000 dilution (2955), phospho eIF2B and total eIF2B at 1 in 1000 (Ab4775 and Ab32713), phospho and total eEF2 at 1 in 500 (2331 and 2332), and phospho S6K (9206), total S6K at 1 in 1000 [made from previously published sequence (Pearson et al., 1995)]. Appropriate secondary antibodies were used at a dilution of 1 in 10,000.

PROTEASOME ACTIVITY

Fly heads were homogenized in 25 mM Tris, pH 7.5 and protein content determined by Bradford assay. Chymotrypsin-like peptidase activity of the proteasome was assayed the

using fluorogenic peptide substrate Succinyl-Leu-Leu-Val-Tyr-amidomethylcoumarin (LLVY-AMC), based on a previously published protocol (Bulteau et al., 2002; Rogers et al., 2012). 20 μg of crude fly head homogenate total protein was incubated at 37°C with 25 μM LLVY-AMC in a final volume of 200 μLs. Enzymatic kinetics were measured in a temperature-controlled microplate fluorimeter (Tecan Infinite M200), at excitation/emission wavelengths of 360/460 nm, measuring fluorescence every 2 min for 1 h. Proteasome activity was determined as the slope of AMC accumulation over time per mg of total protein (pmoles/min/mg).

^{35}S-METHIONINE INCORPORATION

Protein translation was measured in fly heads using a method adapted from Bjedov et al. (2010). Standard SY medium was first supplemented with 100 μCi ^{35}S methionine/mL of food (American Radiolabeled Chemicals 1mCi/37MBq ARS0104A). 15 flies were transferred to each vial containing 1 mL radioactive SY medium. After three-hours of feeding, flies were transferred to non-radioactive SY for 30 min in order to purge any undigested radioactive food from the intestines. Flies that were in contact with the radioactive food for 1 min were used as a background control. Flies were then decapitated using liquid nitrogen and the heads and bodies homogenized in 1% SDS and heated for 5 min at 95°C. Samples were centrifuged twice for 5 min at 16,000 g. Proteins were precipitated by the addition of the same volume of 20% cold TCA (10% TCA final concentration) and incubated for 15 min on ice. Samples were then centrifuged at 16,000 g for 15 min, the pellet washed twice with acetone and re-suspended in 200 μl of 4 M guanidine-HCl.

Samples (100 μl) were mixed with 3 mL of Fluoran-Safe 2, BDH and radioactivity counted in a liquid scintillation analyzer (TriCarb 2800TR, Perkin Elmer), with appropriate quench corrections. SDS-homogenates, prior to TCA precipitation, were also sampled and analyzed as a measure of the total radioactivity (incorporated and un-incorporated) present. Total protein for each sample was determined by Bradford assay and a translation index was calculated as follows: (TCA protein cpm/total cpm)/μg protein per sample.

CHRONOLOGICAL LIFESPAN ASSAYS IN FISSION YEAST

Standard *S. pombe* laboratory strain *972 h*$^{-}$ cells were grown in EMM2 as previously described (Rallis et al., 2013). When cultures reached a stable maximal density, cells were harvested, serially diluted and plated on YES plates. The measurement of Colony Forming Units (CFUs) was taken as time-point 0 at the beginning of CLS curve (i.e., 100% cell survival). Measurements of CFUs were conducted on the following days. Error bars represent standard deviation calculated from three independent cultures, with each culture measured three times at each time-point. Statistical significance (*t*-test) was determined at the time-point when medial lifespan (50% cells dead) was reached for the untreated cells.

POLYSOME PROFILING IN FISSION YEAST

Translational profiles were acquired as previously described (Rallis et al., 2013). Briefly, *S. pombe* cells were treated with 100 μM Cycloheximide for 5 min. Cells were then collected by centrifugation at 3500 rpm for 5 min and diluted in 20 mM Tris-HCl pH 7.5, 50 mM KCL, 10 mM MgCl supplemented with protease (PMSF), 100 μM cycloheximide, 1 mM DTT and 200 ng/mL Heparin. Cells were lysed in a Fastprep-24 machine using glass beads. Sucrose gradients (10–50%) were generated using a Biocomp Gradient Master, and protein preparations were loaded and centrifuged at 35,000 rpm for 2 h 40 min. Polysome gradients were then loaded to the fractionator to obtain the translational profiles.

POLYSOME PROFILING IN *DROSOPHILA*

Polysome profiles were generated as previously described with minor modifications (Dinkova et al., 2005). Heads (300) were homogenized on ice in 1200 μl polysome extraction buffer (300 mM NaCl, 50 mM Tris-HCL (pH 8.0), 10 mM $MgCl_2$, 1 mM EGTA, 200 mg heparin/ml, 400 U RNAsin/ml, 1.0 mM phenylmethylsulfonyl fluoride, 0.2 mg cycloheximide/ml, 1% Triton X-100, 0.1% Sodium Deoxycholate). Lysates were mixed gently and placed on ice for 10 min. Debris was the removed by spinning at 20,000 g (4°C) for 10 min and the supernatant was layered onto a 10–50% sucrose gradient in high salt resolving buffer (140 mM NaCl, 25 mM Tris-HCL (pH 8.0), 10 mM $MgCl_2$). Using a Beckman SW41Ti rotor (38,000 rpm at 90 min, 4°C) polysomes and ribosomal subunits were separated before the gradients were fractionated. Profiles were continuously monitored (Ab 252 nm) using a Teledyne density gradient fractionator.

STATISTICAL ANALYSES

Data are presented as means ± s.e.m. obtained in at least three independent experiments. JMP (version 10.0) software (SAS Institute, Cary, NC, USA) was used for data analyses.

RESULTS

LITHIUM REDUCED Aβ LOAD IN ARCTIC Aβ42 EXPRESSING FLIES THROUGH PROTEIN CLEARANCE/DEGRADATION-INDEPENDENT MECHANISMS

To understand the mechanism/s by which lithium reduces Aβ42 protein level, we first investigated the speed of Aβ42 accumulation after induction of expression, in the presence and absence of lithium. We measured total Aβ protein in the flies expressing Arctic mutant Aβ42 specifically in adult neurons (elav gene switch system was used to induce Aβ expression with the activator mifepistrone, RU486/RU) (Sofola et al., 2010) at a very early time-point, 2 days post Aβ induction. We found by ELISA analysis that even at this early time point, UAS-ArcAβ42/UAS-gfp;elavGS/+ +RU +Li flies that were fed either 25 or 100 mM lithium showed a major reduction in total Aβ burden in comparison to UAS-ArcAβ42/UAS-gfp;elavGS/+ +RU controls, $P < 0.01$ and $P < 0.001$ respectively (**Figure 1A**). These data suggest that lithium may affect synthesis rather than degradation of Aβ, because a reduction in Aβ levels was already present at such an early time point.

Next, we directly assessed the effects of lithium on degradation of Aβ42. We induced Aβ expression for 6 days in the presence of lithium (UAS-ArcAβ42/UAS-gfp;elavGS/+ +RU +Li), then stopped Aβ induction and divided the flies randomly into two

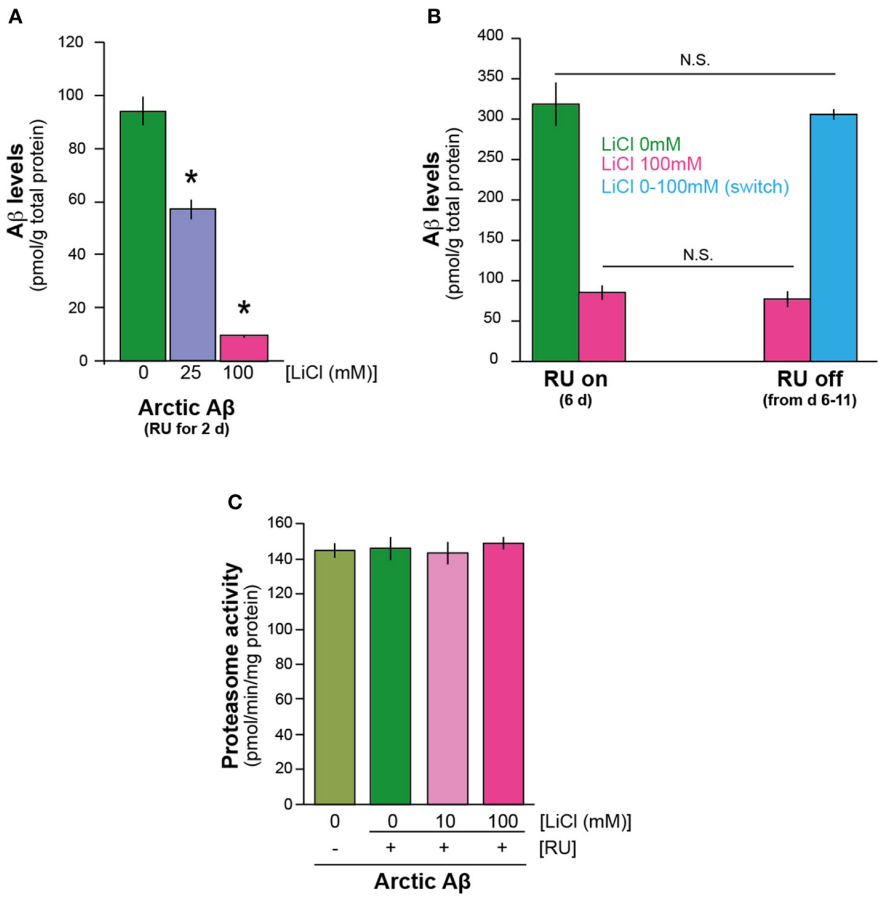

FIGURE 1 | Lithium reduced the level of Aβ42 peptide in the adult *Drosophila* nervous system. (A) Lithium reduced amyloid levels of Arctic Aβ42 flies at a very early time-point. Protein levels of UAS-ArcAβ42/UAS-gfp;elavGS/+ flies on +RU486 SY medium, and UAS-ArcAβ42/UAS-gfp;elavGS/+ flies on +RU +lithium (LiCl), were measured by ELISA at 2 days post-induction (see Materials and Methods). Data were compared using One-Way ANOVA, number of independent tests (n) = 4. $^*P < 0.01$ and $^*P < 0.001$ when comparing UAS-ArcAβ42/UAS-gfp;elavGS/+ +RU to UAS-ArcAβ42/UAS-gfp;elavGS/+ +RU +LiCl 25 or 100 mM respectively. **(B)** Protein levels of UAS-ArcAβ42/UAS-gfp;elavGS/+ flies on RU + 100 mM LiCl medium at 6 days post induction, and then switched to –RU LiCl for 5 days were not significantly different from ArcAβ42/UAS-gfp;elavGS/+ flies on RU + 100 mM LiCl medium for 6 days, $P = 0.6$, nor were UAS-ArcAβ42/UAS-gfp;elavGS/+ flies on +RU 6 days post induction different in comparison to UAS-ArcAβ42/UAS-gfp;elavGS/+ flies on +RU –LiCl for 6 days switched on to –RU + LiCl for 5 days, $P = 0.7$. Data were compared using One-Way ANOVA, number of independent tests (n) = 4. **(C)** Proteasome activity, as measured using the fluorogenic peptide substrate LLVY-AMC, was not changed in flies over-expressing Arctic Aβ42 with or without LiCl treatment. Data are presented as mean activities (pmol/min/mg protein) ± s.e.m., $P = 0.72$ and 0.82 for 10 and 100 mM Li ($n = 5$).

groups, in one of which lithium treatment was continued for a further 5 days (UAS-ArcAβ42/UAS-gfp;elavGS/+ -RU+Li), while no lithium was added to the food of the control group (UAS-ArcAβ42/UAS-gfp;elavGS/+ -RU -Li). Thus, if lithium promoted degradation of Aβ, then the level of Aβ at the end of the treatment period should have been lower in the flies with continued lithium treatment. Aβ levels at the end of the 11-day period did not differ significantly between the two groups (**Figure 1B**), indicating that lithium treatment did not enhance degradation of Aβ. To confirm this finding, we again induced Aβ expression for 6 days, but in the absence of lithium (UAS-ArcAβ42/UAS-gfp;elavGS/+ +RU -Li), then stopped Aβ induction and divided the flies randomly into two groups, one of which was frozen immediately, while in the other, lithium treatment was administered for 5 days (UAS-ArcAβ42/UAS-gfp;elavGS/+ -RU +Li). Aβ levels at the end of the 5-day lithium treatment period did not differ significantly from levels in the untreated, 6-day old flies (**Figure 1B**). These data suggest that lithium does not promote Aβ degradation or clearance, and point instead to a role in Aβ protein synthesis. We also tested if lithium modulated proteasome activity in Aβ expressing flies (2 days post Aβ induction) and found that at 10 and 100 mM doses it did not (**Figure 1C**), consistent with our finding that lithium does not appear to affect Aβ protein degradation.

LITHIUM DOWN-REGULATED TRANSLATION

To determine whether the effect of lithium on Aβ protein level was specific to Aβ, we investigated whether it affected

the level of green fluorescent protein (GFP), a protein that is irrelevant to AD pathology. Surprisingly, we found that 100 mM lithium significantly reduced levels of GFP in the neurons of adult flies (UAS-egfp/+;elavGS/+ +RU), $P = 0.01$ (**Figure 2A**). These data suggest that lithium affects protein synthesis through a mechanism that is not specific to Aβ. To determine whether overall level of translation was reduced by lithium, we carried out S-methionine radioactive tracer experiments in UAS-egfp/+;elavGS/+ flies. Interestingly, we found lower ^{35}S-methionine incorporation into protein in the bodies of flies treated with lithium (pooled data of 10 and 100 mM lithium) in comparison to untreated control flies (**Figure 2B**), $P < 0.05$. Based on this finding, we measured the effect of lithium on polysome profiles of Aβ flies, as an indication of activity of the translation machinery. There was a significant reduction in the ratio of high (polysomes >4) to low (monosome/polysome 1-2-3) fraction in flies treated with lithium (10 mM) (UAS-ArcAβ42/+;elavGS/+ +RU +Li) in comparison to untreated controls (UAS-ArcAβ42/+;elavGS/+ +RU flies), 0.34 vs. 0.40, $P < 0.001$ (**Figure 2C**), again demonstrating that lithium reduced activity of the translation machinery, possibly through a stall in translation initiation.

We next determined whether lithium exerted its effect on translation through an effect on the activity of the mechanistic target of rapamyicin (mTOR) pathway, which is involved in control of translation. S6K is a phosphorylation target of mTOR kinase in the mTORC1 complex (Bjedov and Partridge, 2011); interestingly, both phosphorylated S6K and total S6K were reduced in Aβ flies treated with lithium (UAS-ArcAβ42/+;elavGS/+ +RU +Li) in comparison to untreated flies (UAS-ArcAβ42/+;elavGS/+ +RU) (**Figure 3A**). However, the ratio of phosphorylated S6K to total S6K was not significantly

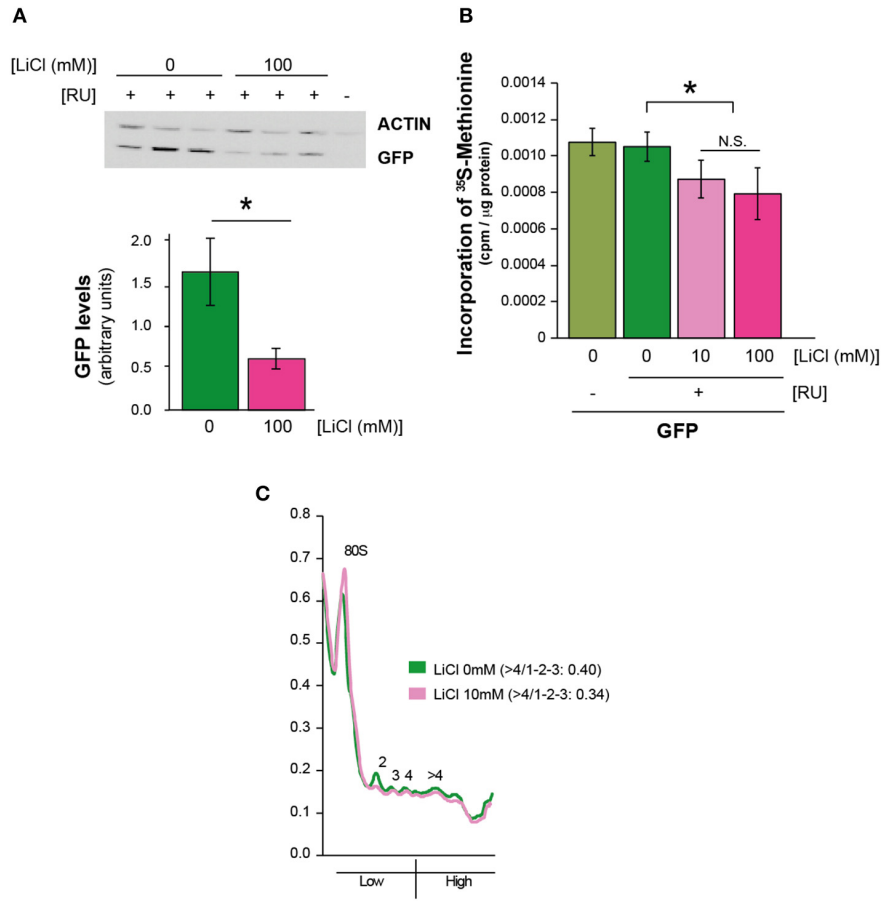

FIGURE 2 | Lithium reduced overall protein synthesis/translation. (A) Protein levels of UAS-egfp/+;elavGS/+ flies on +RU486 SY medium, and UAS-egfp/+;elavGS/+ flies on +RU +100 mM LiCl were measured by Western blot analyses at 7 days post-induction (see Materials and Methods). GFP levels were significantly reduced when comparing UAS-egfp/+;elavGS/+ +RU to UAS-egfp/+;elavGS/+ +RU +LiCl 100 mM, $^*P < 0.001$. Data were compared using One-Way ANOVA, number of independent tests (n) = 6. **(B)** Protein synthesis was reduced in pooled UAS-egfp/+;elavGS/+ +RU +LiCl 10 mM and Li 100 mM treated flies in comparison to UAS-egfp/+;elavGS/+ +RU flies measured by ^{35}S-methionine incorporation, $^*P < 0.05$. Data were analyzed by One-Way ANOVA ($n = 7$ for +RU and $n = 13$ for +RU +LiCl treated flies). **(C)** Polysome profiles showed a reduction in translation in lithium treated Aβ expressing flies, measured by calculating the area under the different fractions, and their ratios (area under the first 3 peaks for low fraction, and >4 for high, ratio >4/1-2-3) $P < 0.001$. Data were analyzed by paired t-test ($n = 5$). One representative figure is shown.

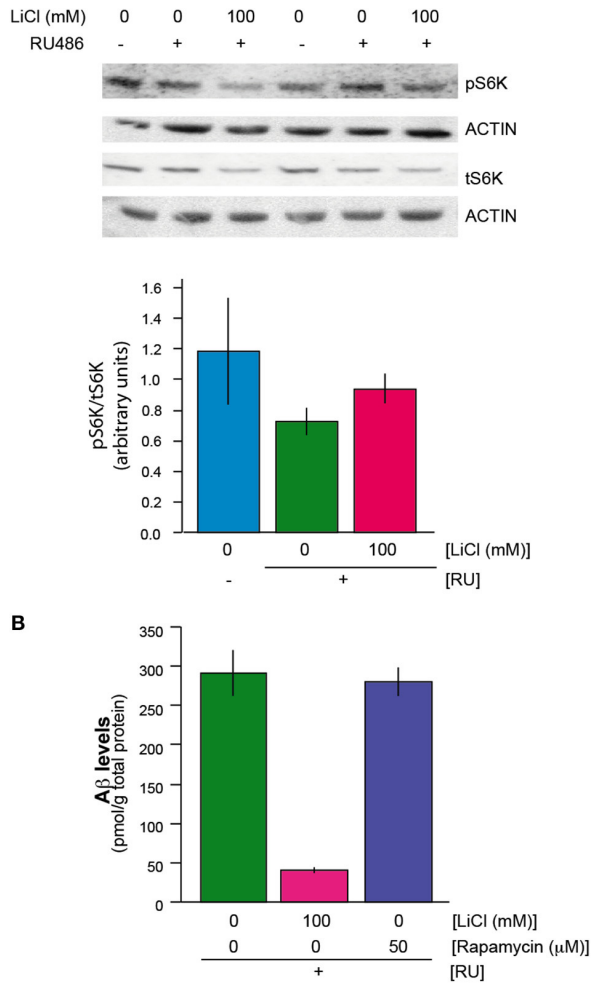

FIGURE 3 | (A) Lithium reduced protein levels of phosphorylated and total S6K. There was no change in the ratio of phosphorylated S6K to total S6K protein levels when UAS-ArcAβ42/+;elavGS/+ +RU +LiCl 100 mM flies are compared to UAS-ArcAβ42/+;elavGS/+ +RU controls, $P = 0.2$ ($n = 3$) **(B)** Rapamycin did not reduce Aβ levels in UAS-ArcAβ42/+;elavGS/+ +RU +50 μM flies in comparison to UAS-ArcAβ42/+;elavGS/+ +RU untreated flies, $P = 0.8$ ($n = 3$).

different between the two groups (**Figure 3A**). In these blots, because of the possibility that total protein content of the flies could have been altered by lithium, samples derived from a fixed number of fly heads were used. Interestingly, actin levels did not seem to be affected by lithium and were used as an additional loading control. This finding suggests that either the turnover rate of actin is very low, or there is a subset of proteins that is not down-regulated by lithium. Treatment of Aβ expressing flies (UAS-ArcAβ42/+;elavGS/+ +RU) with rapamycin, an inhibitor of mTOR that inhibits translation and extends lifespan in *Drosophila* (Bjedov et al., 2010) also did not reduce the levels of Aβ in the Aβ-expressing flies (**Figure 3B**), and nor did it ameliorate the Aβ-induced toxicity (**Supplemental Figure 1A**). These data suggest that lithium did not act through the mTOR pathway to reduce translation in the Aβ-expressing flies, and that the reduced levels of total and phosphorylated S6K were instead a consequence of a general reduction in translation.

Lithium has been shown to regulate the translation initiation factor eIF2B in rats (Bosetti et al., 2002) and the elongation factor, eEF-2 in SH-SY5Y cells and mice (Karyo et al., 2010). We investigated whether lithium reduced protein synthesis by regulating one or both of these factors. Again, we observed a reduction in both the phosphorylated and total forms of eIF2B-epsilon and eEF-2 in Aβ expressing flies treated with 100 mM lithium (UAS-ArcAβ42/+;elavGS/+ +RU +Li) in comparison to untreated flies (UAS-ArcAβ42/+;elavGS/+ +RU), but the ratio of phosphorylated to total eIF2B-epsilon or eEF-2 was not significantly affected (**Figures 4A,B**). These data again demonstrate that lithium down-regulated protein levels, but they do not point to a specific role for eIF2B-epsilon or eEF-2.

Indeed, a clear-cut explanation of the effects of lithium may be elusive, since translation of many proteins involved in the protein synthesis machinery is presumably inhibited by lithium. Furthermore, we used a high dose of lithium (100 mM) to maximize our chances of identifying these downstream factors that are responsible for the effect of lithium on translation, and were unable to identify a specific role for the proteins we tested; and thus did not test lower concentrations of lithium. Overall, the data suggest that the reduction in Aβ levels we observe upon lithium treatment is as a consequence of reduction in protein synthesis, probably because of reduced expression of multiple proteins involved in initiation of translation, but do not identify the specific targets responsible.

LITHIUM ALSO INHIBITS PROTEIN SYNTHESIS IN FISSION YEAST

Reduction in protein synthesis has been frequently linked to increased lifespan, possibly attributable to both a reduction in energy consumption, because translation requires a significant amount of the energy budget, and a reduction in mis-translated polypeptides (Browne and Proud, 2002; Proud, 2002; Hansen et al., 2007; Hipkiss, 2007). Additionally, lithium has been shown to cause significant lifespan-extension in the nematode worm *C. elegans* and in *Drosophila* (McColl et al., 2008; Kasuya et al., 2009; Zarse et al., 2011). Therefore, we decided to turn into a simpler system to determine whether lithium has an evolutionarily conserved effect on translation, and whether it has an associated effect on lifespan. Unicellular yeasts have been pivotal in the advancement of understanding of mechanisms of ageing (Kaeberlein et al., 2005; Rallis et al., 2013). Fast-growing fission yeast cells in mid-log phase were treated with 0.1 mM lithium chloride for 1 h and their translational profiles were compared to those of untreated (control) cells. Following lithium treatment, translation was reduced: high (polysomes >4) to low (monosome/polysome 1-2-3) ratios were lower (0.51) in lithium treated yeast cells in comparison to control cells (0.63), $P < 0.001$ (**Figure 5A**). Interestingly, the same dose of lithium extended the chronological lifespan of fission yeast, $P = 0.001$ (**Figure 5B**). Yeast is hence an ideal model organism in which to perform a genetic screen to identify the relevant targets of lithium for reduced protein synthesis and increased lifespan.

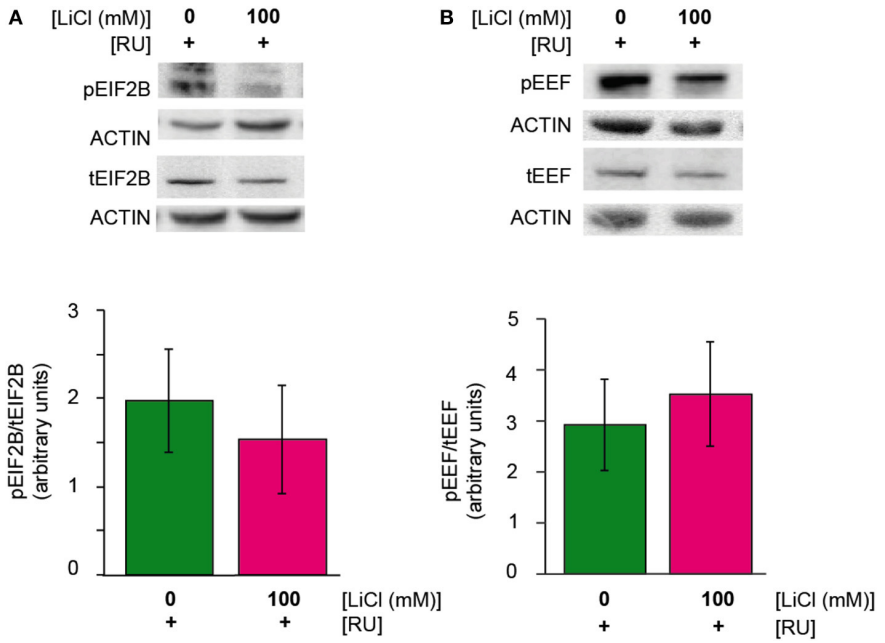

FIGURE 4 | (A,B) Lithium reduced protein levels of phosphorylated and total eIF2Be and eEF-2. There was no change in the ratio of phosphorylated eIF2Be or eEF-2 to total protein levels of eIF2Be or eEF-2 in UAS-ArcAβ42/+;elavGS/+ +RU +LiCl 100 mM flies in comparison to UAS-ArcAβ42/+;elavGS/+ +RU controls, $P = 0.6$ and 0.7 respectively ($n = 3$).

LITHIUM EXTENDED LIFESPAN OF FLIES EXPRESSING Aβ

Since we observed an association between reduced global protein synthesis and increased longevity in fission yeast, we determined whether lithium could also extend the survival of Aβ expressing flies. We measured lifespan of flies expressing Arctic Aβ42 (UAS-ArcAβ42/+;elavGS/+ +RU) and treated chronically with different concentrations of lithium from two days post-eclosion. Flies expressing Arctic Aβ42 in adult neurons had a shortened median and maximum lifespan as previously reported (Sofola et al., 2010), which could be extended with 10, 25, and 50 mM ($P < 0.001$ for all doses), but not with 1 or 100 mM lithium (**Figure 5C**). The data suggest that above a certain a threshold, somewhere between 50 and 100 mM, lithium no longer rescued the shortened lifespan of flies expressing Aβ, possibly because it became toxic. However, this toxicity with a high lithium dose was only evident when taken long term and/or in older flies, since both 10 mM (**Supplemental Figure 1B**) and 100 mM lithium previously published (Sofola et al., 2010) were able to protect against the Aβ-induced locomotor dysfunction measured after shorter term treatment and earlier in life.

DISCUSSION

Human life expectancy continues to increase at a steady rate in most countries worldwide, and has done so by almost 3 months per year in the last 160 years (Oeppen and Vaupel, 2002). Therefore, it is of great importance to tackle ageing-related diseases such as AD, because they are becoming increasingly prevalent. Because age is the biggest risk factor for AD, interventions that promote general increases in health during ageing could also be important and beneficial in AD.

Lithium is becoming increasingly implicated as a drug that can ameliorate ageing and neurodegenerative diseases. Several groups have shown that it extends lifespan in model organisms such as the nematode worm *C. elegans* and *Drosophila* (McColl et al., 2008; Kasuya et al., 2009; Zarse et al., 2011). Here, we showed that it also extends lifespan in fission yeast *Schizosaccharomyces pombe*, highlighting that this effect is conserved over large evolutionary distances. Fission yeast is an ideal organism for genetic screens, and future work should identify the molecular targets of lithium both for control of protein synthesis and of lifespan. Furthermore, slightly higher levels of lithium present in the drinking water have been reported as associated with reduced mortality in a Japanese human population (Zarse et al., 2011).

A substantial body of work has demonstrated that several neurodegenerative diseases and neurological disorders, including but not confined to stroke, schizophrenia, Fragile X syndrome, Huntington's disease and Parkinson's disease, benefit from the therapeutic properties of lithium (Chiu et al., 2011). In addition, several studies have investigated whether lithium has a beneficial effect in AD pathogenesis. Clinical trials conducted with lithium have yielded conflicting results; some have found benefits, whilst others have not (Nunes et al., 2007; Macdonald and Briggs, 2008; Hampel et al., 2009). Interestingly, a correlative study conducted in patients with bipolar disorder, suggested that patients that had been on chronic lithium treatment showed a reduced incidence of AD in comparison to patients that had not been on treatment (Nunes et al., 2007). And a more recent small-scale clinical trial on

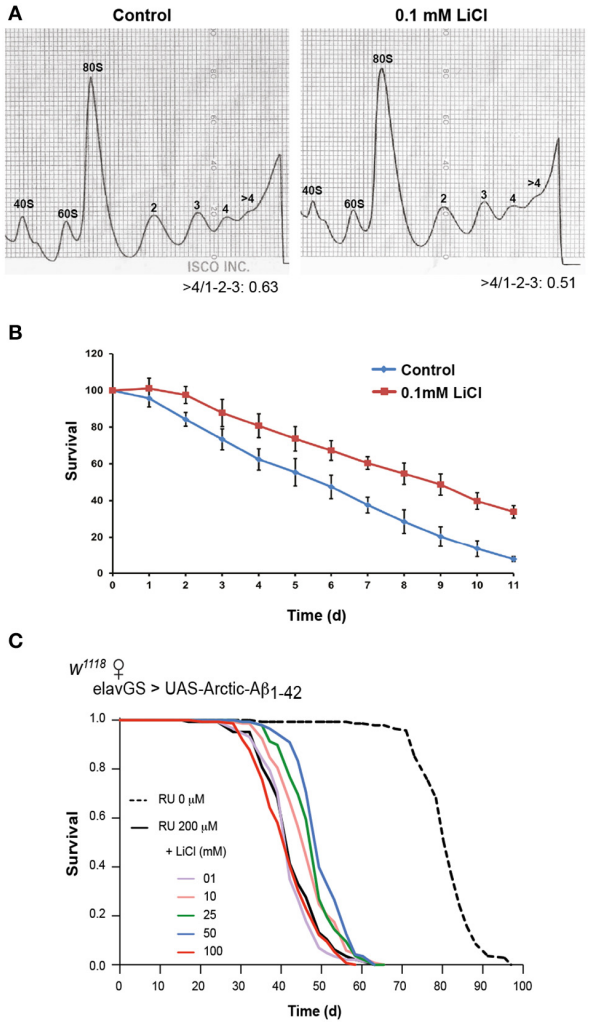

FIGURE 5 | Lithium reduced overall protein synthesis/translation and extended lifespan in fission yeast. (A) Polysome profiles showed a reduction in translation in lithium treated fission yeast cells. The area under the different fractions and their ratios were calculated (area under the first 3 peaks for low fraction, and >4 for high, fraction, ratio >4/1-2-3). Data were analyzed by paired *t*-test ($n = 3$), $P < 0.001$. **(B)** 0.1 mM LiCl increased the chronological median lifespan of fission yeast (paired *t*-test comparing triplicates of lifespan values at 50% survival/medial lifespan, $P = 0.001$). **(C)** Survival curves of flies expressing Arctic Aβ42 with or without lithium treatment are depicted, data were compared using the log-rank test, comparing UAS-ArcAβ42/+;elavGS/+ +RU +LiCl 1, 10, 25, 50 or 100 mM flies to UAS-ArcAβ42/+;elavGS/+ +RU controls. No significant difference was seen between UAS-ArcAβ42/+;elavGS/+ +RU controls and UAS-ArcAβ42/+;elavGS/+ +RU +LiCl 1 or 100 mM, $P = 0.24$ and 0.17 respectively, a significant difference was observed with 10, 25, and 50 mM LiCl, $P < 0.001$.

mild cognitive impaired (MCI) patients found that low doses of lithium slowed cognitive decline (Forlenza et al., 2011). The investigators suggested that a reason for the previous conflicting data on the efficacy of lithium was probably attributable to the pathological states/stages at which the patients were given lithium. It is becoming increasingly evident that drug trials are most likely to yield positive effects when initiated early, at the MCI stage.

Our results add to existing data suggesting that lithium could be beneficial in ameliorating Aβ toxicity, and should be considered for a potential large-scale trial on MCI patients. It has the added advantage of being an already approved drug, used to treat bipolar patients. It does have side-effects, but these are minimal at the low doses used in the recent small-scale clinical study (Forlenza et al., 2011). We also found that there are limits to the beneficial/therapeutic benefits of lithium in fission yeast in chronological lifespan—lithium was unable to increase chronological lifespan at higher doses (data not shown) as well as in the *Drosophila* AD model. Previously, we showed in Sofola et al. (2010) that administering both 30 and 100 mM lithium into the fly food are effective in modulating Aβ neuronal toxicity as evidenced by the improved locomotor function in young flies (Sofola et al., 2010). These lithium concentrations were initially chosen based on the paper by Dokucu et al. (2005)—they showed that lithium concentrations ranging from 10 to 100 mM lithium in the fly food translates to roughly 0.05–0.4 mM in the fly tissue (Dokucu et al., 2005), so well below the toxic levels in patients and mice (Wood et al., 1986; Schou, 2001; Can et al., 2011). In this paper, we show that both 25 and 100 mM lithium reduce Aβ levels in a dose dependent manner at an early time point. We also find that lower doses of Lithium (10 and 25 mM) rescue the shortened longevity of the Aβ flies, but 100 mM lithium was unable to extend lifespan when given to the flies throughout adulthood. It will be important to determine the therapeutic thresholds for lithium in patients that could offer therapeutic benefits without overt side effects.

Similar to the published data on the role of GSK-3 inhibition in down-regulating translation in HCC1806 cells (Shin et al., 2014), we find that lithium is able to reduce translation in fission yeast and flies, suggesting that perhaps some of the effect of lithium on translation down-regulation is via GSK-3 inhibition. However, this is correlative and future work will involve carrying out epistasis interactions between lithium and GSK-3, and identifying molecular targets of GSK-3 and lithium for control of protein synthesis.

Nonetheless, our study highlights the potential benefits of lithium through down-regulation of translation, associated with extension of lifespan in very distantly related organisms. By reducing protein synthesis, lithium may reduce the increased proteostatic burden in ageing, a recognized hallmark of ageing (López-Otín et al., 2013). Lithium is also of specific benefit in AD, because of its ability to down-regulate translation, and hence levels of proteins involved in promoting the presence of toxic Aβ.

The mutant Arctic Aβ42 protein present in the transgenic flies used in this study has a propensity to aggregate faster than wild type Aβ (Spires and Hyman, 2005). However, we have observed both soluble and insoluble Aβ in the Arctic Aβ42 flies [(Rogers et al., 2012), and data not shown]; and the ability of lithium to reduce translation of the Aβ peptide without affecting its clearance may lower the level of soluble Aβ. In a wider context, lithium might be beneficial in ameliorating toxicity of AD by lowering expression of APP and of proteins that are involved in the generation of Aβ from APP. Our model does not express full length APP,

and may therefore not include other potential/additional benefits of lithium on Aβ toxicity. As well as the increased ratio of Aβ42 to Aβ40 peptide observed in familial AD cases with APP mutations (De Jonghe et al., 2001), increased levels of APP could also contribute to AD pathogenesis. Indeed, patients with Down syndrome have a high risk of developing AD possibly due to trisomy of the APP gene which leads to increased APP expression (Wiseman et al., 2009). Also, several mutations in the APP promoter region were found to significantly increase APP expression in SH-SY5Y cells, and were associated with risk for AD (Theuns et al., 2006).

The ability of lithium to down-regulate translation could therefore be beneficial at several stages in AD pathogenesis. Lithium might also have therapeutic benefits for other neurodegenerative disorders that are caused by over-expression of wild type or mutant forms of proteins such as α-synuclein in Parkinson's disease. Lithium could also reduce the production of mis-translated polypeptides, and free proteases or/and chaperones that can then participate in cellular proteostasis (Proud, 2002; Singleton et al., 2003). Furthermore, diseases where protein turnover is compromised by loss of function of the degradation machinery could also benefit from lowering the burden of protein production hence reducing cellular stress. This could be particularly important in lysosomal storage diseases, where the intrinsic function of the degradative machinery is compromised (Kinghorn, 2011; Sarkar et al., 2013). Moreover, induction of autophagy in some cases increases the load of an already dysfunctional lysosome, worsening the cellular proteostatic stress (Wong and Cuervo, 2010; Nixon and Yang, 2011). Hence lowering the production of proteins could again be a viable mechanism to restore proteostasis. Other neurodegenerative models where the role of lithium in lowering protein translation could be beneficial are, for example, the *Drosophila* models of Pink1 and Parkin, which do not include the over-expression of toxic proteins (Whitworth et al., 2006; Castillo-Quan, 2011). Flies lacking either of these proteins accumulate unfolded proteins in mitochondria, resulting in mitochondria impairment (Pimenta de Castro et al., 2012). It would be interesting to study whether lithium could ameliorate mitochondrial stress by reducing the production of the proteins accumulating in the mitochondria of the Pink1 or parkin null flies. Lithium could hence be a useful drug with an overall benefit for health during ageing and protection against AD and other neurodegenerative diseases.

ACKNOWLEDGMENTS

We thank Dr. D. Crowther (University of Cambridge) and Dr. H. Tricoire (CNRS, France) for their kind donation of UAS-Aβ42 and elavGS fly stocks, and Dr. Cathy Slack for total S6K antibody. This work was supported by grants from the Max Plank Institute for the Biology of Ageing (Oyinkan Sofola-Adesakin, Jorge I. Castillo-Quan, Luke S. Tain, Iain Rogers, Ivana Bjedov, Mobina Khericha, Linda Partridge), Alzheimer's Society (Oyinkan Sofola-Adesakin), Eisai London Research Laboratories (UK) (Iain Rogers), Alzheimer's Research UK (Pedro Martinez), a BBSRC Research Grant (Charalampos Rallis, Jürg Bähler), and the Wellcome Trust (Linda Partridge). This work is dedicated to Pedro Martinez—your legacy lives on.

SUPPLEMENTARY MATERIAL

The Supplementary Material for this article can be found online at: http://www.frontiersin.org/journal/10.3389/fnagi.2014.00190/abstract

Supplemental Figure 1 | (A) Rapamycin did not rescue the climbing phenotype of UAS-ArcAβ42/+;elavGS/+ flies on +RU486 +200 μM rapamycin, $P = 0.83$ **(B)** Lithium suppressed the locomotor dysfunction phenotype, $P < 0.05$. Climbing ability of UAS-ArcAβ42/UAS-gfp;elavGS/+ +RU486 and UAS-ArcAβ42/+;elavGS/+ flies on +RU486 +LiCl 10 mM SY medium or +Rapamycin 200 μM was assessed at the indicated time-points (see Materials and Methods). Data are presented as the percentage climbing performance of flies ± s.e.m. [Two-Way ANOVA, number of independent tests (n) = 3].

REFERENCES

Alzheimer's Association. (2012). 2012 Alzheimer's disease facts and figures. *Alzheimer's Dement.* 8, 131–168. doi: 10.1016/j.jalz.2012.02.001

Bjedov, I., and Partridge, L. (2011). A longer and healthier life with TOR down-regulation: genetics and drugs. *Biochem. Soc. Trans.* 39, 460–465. doi: 10.1042/BST0390460

Bjedov, I., Toivonen, J. M., Kerr, F., Slack, C., Jacobson, J., Foley, A., et al. (2010). Mechanisms of life span extension by rapamycin in the fruit fly *Drosophila melanogaster*. *Cell Metab.* 11, 35–46. doi: 10.1016/j.cmet.2009.11.010

Bosetti, F., Seemann, R., and Rapoport, S. I. (2002). Chronic lithium chloride administration to rats decreases brain protein level of epsilon (epsilon) subunit of eukaryotic initiation factor-2B. *Neurosci. Lett.* 327, 71–73. doi: 10.1016/S0304-3940(02)00354-3

Browne, G. J., and Proud, C. G. (2002). Regulation of peptide-chain elongation in mammalian cells. *Eur. J. Biochem.* 269, 5360–5368. doi: 10.1046/j.1432-1033.2002.03290.x

Bulteau, A., Moreau, M., Nizard, C., and Friguet, B. (2002). Imapairment of Proteasome function upon UVA- and UVB- irradiation of human keratinocytes. *Free Radic. Biol. Med.* 32, 1157–1170. doi: 10.1016/S0891-5849(02)00816-X

Can, A., Blackwell, R. A., Piantadosi, S. C., Dao, D. T., O'Donnell, K. C., and Gould, T. D. (2011). Antidepressant-like responses to lithium in genetically diverse mouse strains. *Genes. Brain. Behav.* 10, 434–443. doi: 10.1111/j.1601-183X.2011.00682.x

Castillo-Quan, J. I. (2011). Parkin' control: regulation of PGC-1α through PARIS in Parkinson's disease. *Dis. Model. Mech.* 4, 427–429. doi: 10.1242/dmm.008227

Chiu, C.-T., Liu, G., Leeds, P., and Chuang, D.-M. (2011). Combined treatment with the mood stabilizers lithium and valproate produces multiple beneficial effects in transgenic mouse models of Huntington's disease. *Neuropsychopharmacology* 36, 2406–2421. doi: 10.1038/npp.2011.128

Crowther, D. C., Kinghorn, K. J., Miranda, E., Page, R., Curry, J. A., Duthie, F. A. I., et al. (2005). Intraneuronal Abeta, non-amyloid aggregates and neurodegeneration in a Drosophila model of Alzheimer's disease. *Neuroscience* 132, 123–135. doi: 10.1016/j.neuroscience.2004.12.025

De Jonghe, C., Esselens, C., Kumar-Singh, S., Craessaerts, K., Serneels, S., Checler, F., et al. (2001). Pathogenic APP mutations near the gamma-secretase cleavage site differentially affect Abeta secretion and APP C-terminal fragment stability. *Hum. Mol. Genet.* 10, 1665–1671. doi: 10.1093/hmg/10.16.1665

Dinkova, T. D., Keiper, B. D., Korneeva, N. L., Aamodt, E. J., and Rhoads, R. E. (2005). Translation of a small subset of caenorhabditis elegans mRNAs is dependent on a specific eukaryotic translation initiation factor 4E isoform. *Mol. Cell. Biol.* 1, 100–113. doi: 10.1128/MCB.25.1.100-113.2005

Dokucu, M. E., Yu, L., and Taghert, P. H. (2005). Lithium- and valproate-induced alterations in circadian locomotor behavior in Drosophila. *Neuropsychopharmacology* 30, 2216–2224. doi: 10.1038/sj.npp.1300764

Forlenza, O. V., Torres, C. A., Talib, L. L., de Paula, V. J., Joaquim, H. P. G., Diniz, B. S., et al. (2011). Increased platelet GSK3B activity in patients with mild cognitive impairment and Alzheimer's disease. *J. Psychiatr. Res.* 45, 220–224. doi: 10.1016/j.jpsychires.2010.06.002

Hampel, H., Ewers, M., Bürger, K., Annas, P., Mörtberg, A., Bogstedt, A., et al. (2009). Lithium trial in Alzheimer's disease: a randomized, single-blind, placebo-controlled, multicenter 10-week study. *J. Clin. Psychiatry* 70, 922–931. doi: 10.4088/JCP.08m04606

Appendix 2

Kinghorn, K.J., Castillo-Quan, J.I., Bartolome, F., Angelova, P.R., **Li, L.**, Pope, S., Cocheme, H.M., Khan, S., Asghari, S., Bhatia, K.P., et al. (2015). Loss of PLA2G6 leads to elevated mitochondrial lipid peroxidation and mitochondrial dysfunction. Brain *138*, 1801-1816.

doi:10.1093/brain/awv132 BRAIN 2015: 138; 1801–1816 | 1801

BRAIN
A JOURNAL OF NEUROLOGY

Loss of *PLA2G6* leads to elevated mitochondrial lipid peroxidation and mitochondrial dysfunction

Kerri J. Kinghorn,[1,2] Jorge Iván Castillo-Quan,[1,2,3] Fernando Bartolome,[2] Plamena R. Angelova,[2] Li Li,[1,2] Simon Pope,[4] Helena M. Cochemé,[1,3] Shabana Khan,[1] Shabnam Asghari,[5] Kailash P. Bhatia,[2] John Hardy,[2] Andrey Y. Abramov[2] and Linda Partridge[1,3]

The *PLA2G6* gene encodes a group VIA calcium-independent phospholipase A2 beta enzyme that selectively hydrolyses glycerophospholipids to release free fatty acids. Mutations in *PLA2G6* have been associated with disorders such as infantile neuroaxonal dystrophy, neurodegeneration with brain iron accumulation type II and Karak syndrome. More recently, *PLA2G6* was identified as the causative gene in a subgroup of patients with autosomal recessive early-onset dystonia-parkinsonism. Neuropathological examination revealed widespread Lewy body pathology and the accumulation of hyperphosphorylated tau, supporting a link between *PLA2G6* mutations and parkinsonian disorders. Here we show that knockout of the *Drosophila* homologue of the *PLA2G6* gene, *iPLA2-VIA*, results in reduced survival, locomotor deficits and organismal hypersensitivity to oxidative stress. Furthermore, we demonstrate that loss of *iPLA2-VIA* function leads to a number of mitochondrial abnormalities, including mitochondrial respiratory chain dysfunction, reduced ATP synthesis and abnormal mitochondrial morphology. Moreover, we show that loss of *iPLA2-VIA* is strongly associated with increased lipid peroxidation levels. We confirmed our findings using cultured fibroblasts taken from two patients with mutations in the *PLA2G6* gene. Similar abnormalities were seen including elevated mitochondrial lipid peroxidation and mitochondrial membrane defects, as well as raised levels of cytoplasmic and mitochondrial reactive oxygen species. Finally, we demonstrated that deuterated polyunsaturated fatty acids, which inhibit lipid peroxidation, were able to partially rescue the locomotor abnormalities seen in aged flies lacking *iPLA2-VIA* gene function, and restore mitochondrial membrane potential in fibroblasts from patients with *PLA2G6* mutations. Taken together, our findings demonstrate that loss of normal *PLA2G6* gene activity leads to lipid peroxidation, mitochondrial dysfunction and subsequent mitochondrial membrane abnormalities. Furthermore we show that the *iPLA2-VIA* knockout fly model provides a useful platform for the further study of *PLA2G6*-associated neurodegeneration.

1 Institute of Healthy Ageing and Department of Genetics, Evolution and Environment, University College London, London WC1E 6BT, UK
2 Institute of Neurology, University College London, Queen Square, London WC1N 3BG, UK
3 Max Planck Institute for Biology of Ageing, Joseph-Stelzmann Str. 9b, D-50931, Cologne, Germany
4 Neurometabolic Unit, National Hospital for Neurology and Neurosurgery, London WC1N 3BG, UK
5 Department of Family Medicine, Memorial University, St. John's, NL, Canada

Correspondence to: Kerri Kinghorn,
Institute of Healthy Ageing and Department of Genetics, Evolution and Environment,
University College London,

Received November 9, 2014. Revised March 9, 2015. Accepted March 17, 2015. Advance Access publication May 23, 2015

London, WC1E 6BT, UK
E-mail: k.kinghorn@ucl.ac.uk

Keywords: PLA2G6; infantile neuroaxonal dystrophy; neurodegeneration with brain iron accumulation; *Drosophila*

Abbreviations: D/H-PUFA = deuterated/hydrogenated polyunsaturated fatty acids; D_2-linoleic acid = 11-11-D_2-linoleic acid; D_4-linoleic acid = 11,11,14,14-D4-α-linolenic acid; TMRM = tetramethylrhodamine methylester

Introduction

The *PLA2G6* gene encodes an 85-kDa group VI calcium-independent phospholipase A_2 beta (PLA2G6). This enzyme hydrolyses the sn-2 acyl chain of glycerophospholipids to release free fatty acids and lysophospholipids (Wolf and Gross, 1996; Ma and Turk, 2001). PLA2G6 localizes to the mitochondria, and has proposed roles in the remodelling of membrane phospholipids, signal transduction and calcium signalling, cell proliferation and apoptosis (Gadd *et al.*, 2006; Seleznev *et al.*, 2006; Strokin *et al.*, 2012).

Humans with *PLA2G6* mutations can show progressive cognitive and motor skill regression, as displayed in disorders such as infantile neuroaxonal dystrophy, neurodegeneration with brain iron accumulation type II and Karak syndrome (Khateeb *et al.*, 2006; Morgan *et al.*, 2006). Infantile neuroaxonal dystrophy is a neurodegenerative disease with onset in infancy and fatality in the teenage years or in early adulthood. It is characterized neuropathologically by axonal swelling and the presence of spheroid bodies in the central and peripheral nervous systems in addition to hallmark cerebellar atrophy. Neurodegeneration with brain iron accumulation comprises a clinically and genetically heterogeneous group of disorders with a progressive extrapyramidal syndrome and high basal ganglia iron, and includes pantothenate kinase-associated neurodegeneration caused by mutations in *PANK2* (neurodegeneration with brain iron accumulation type I). Post-mortem examination of the brain of a patient with neurodegeneration with brain iron accumulation associated with homozygous *PLA2G6* mutations demonstrated both Parkinson's and Alzheimer's disease pathology with widespread Lewy bodies, dystrophic neurites and cortical neuronal neurofibrillary tangles (Gregory *et al.*, 2008).

Furthermore, PLA2G6 has also been implicated in a number of other brain diseases including Alzheimer's disease (Schaeffer and Gattaz, 2008) and bipolar disorder (Xu *et al.*, 2013). More recently, *PLA2G6*, at the PARK14 locus, has also been characterized as the causative gene in a subgroup of patients with autosomal recessive early-onset dystonia-parkinsonism. Interestingly these patients did not display cerebellar atrophy or basal ganglia iron on MRI (Paisan-Ruiz *et al.*, 2009), and neuropathological examination revealed widespread Lewy body pathology and the accumulation of hyperphosphorylated tau (Paisan-Ruiz *et al.*, 2012). These clinical and neuropathological features further support a link between *PLA2G6* mutations and parkinsonian disorders, and demonstrate the clinical heterogeneity in *PLA2G6*-associated neurodegeneration.

It is not known how mutations in *PLA2G6* cause neuropathology. However, it has been suggested that the loss of normal PLA2G6 activity in neurodegenerative disease involves structural abnormalities of cell or mitochondrial membranes and disturbances in lipid homeostasis and lipid metabolism. Indeed, a study in a mouse *Pla2g6* knockout model demonstrated ultrastructural abnormalities in mitochondrial and synaptic membranes (Beck *et al.*, 2011). As well as possible mitochondrial defects, it is thought that changes in the composition of the plasma membrane and other intracellular membranes may in turn affect the normal processes responsible for the movement of membranes within axons and dendrites, subsequently leading to accumulation of membranes as so-called spheroids.

Support for a loss-of-function of PLA2G6 enzyme activity in causing disease comes from a recent study on recombinant wild-type and mutant human PLA2G6 proteins. This demonstrated that mutations in *PLA2G6* associated with infantile neuroaxonal dystrophy or neurodegeneration with brain iron accumulation resulted in encoded proteins that exhibited $<20\%$ of control levels of phospholipase and lysophospholipase activities. Conversely, mutations associated with dystonia-parkinsonism did not impair catalytic activity. The differential enzymatic activities associated with *PLA2G6* mutations in infantile neuroaxonal dystrophy/neurodegeneration with brain iron accumulation and dystonia-parkinsonism may explain the relatively later onset and milder phenotype seen in the latter. Furthermore, the preserved enzymatic function of dystonia-parkinsonism causing mutations must be interpreted with caution as there may be differences in PLA2G6 activity *in vivo* that are not detected by these *in vitro* assays. For example, there may be alternative mechanisms that alter the regulation of PLA2G6 activity, such as changes in the binding to calmodulin or other proteins (Engel *et al.*, 2010). Further support for the loss of enzymatic function hypothesis comes from a recent study of a Chinese population with Parkinson's disease, which identified novel *PLA2G6* mutations occurring in the heterozygous state, associated with an inhibition in the phospholipid-hydrolysing functions of PLA2G6 (Gui *et al.*, 2013). Moreover Gregory *et al.* (2008) found a genotype–phenotype correlation in patients with infantile neuroaxonal dystrophy and neurodegeneration with brain iron accumulation: mutations that are predicted to lead to an absence of protein were associated with more severe

infantile neuroaxonal dystrophy-type clinical phenotypes, while those with compound heterozygous missense mutations correlated with the less severe phenotype of neurodegeneration with brain iron accumulation and are predicted to result in protein with some residual enzyme function.

Genetic ablation of *Pla2g6* in mice is associated with an *in vivo* disturbance of brain phospholipid metabolism (Cheon *et al.*, 2012), mitochondrial membrane degeneration (Beck *et al.*, 2011) and marked cerebellar atrophy (Zhao *et al.*, 2011). Furthermore, *in vitro* experiments demonstrated a disturbance in calcium signalling in astrocytes from PLA2G6-deficient mice (Strokin *et al.*, 2012). However, despite these studies, the precise molecular mechanisms linking loss of PLA2G6 activity to mitochondrial morphological abnormalities and neurodegeneration remain unclear and further studies are required.

The fruit fly *Drosophila melanogaster* has proven to be an excellent model system for studying neurodegenerative diseases, especially the role of mitochondrial activity in Parkinson's disease (Clark *et al.*, 2006; Park *et al.*, 2006). Once a faithful model is established, the fly has the advantage over mouse models in that it can be used to perform high-throughput screening to identify genetic modifiers and novel therapeutic targets. Here we show that *iPLA2-VIA*, the *Drosophila* homologue of *PLA2G6*, plays an essential role in maintaining normal mitochondrial function. We demonstrate that knockout of the *iPLA2-VIA* gene activity in the fly results in reduced survival, locomotor deficits and organismal hypersensitivity to oxidative stress. Furthermore, loss of *iPLA2-VIA* function leads to a number of mitochondrial abnormalities, including reduced mitochondrial membrane potential, mitochondrial respiratory chain dysfunction and reduced ATP synthesis. We also show that levels of lipid peroxidation are significantly elevated in the brains of flies lacking *iPLA2-VIA*. In addition, we examined cultured fibroblasts taken from two patients with known *PLA2G6* mutations and found similar abnormalities to those seen in the fly, including mitochondrial membrane abnormalities and raised levels of cytoplasmic and mitochondrial reactive oxygen species. Moreover, lipid peroxidation levels, especially in the mitochondria, were elevated in the *PLA2G6* mutant human fibroblasts compared to controls. Taken together, our findings suggest that loss of normal *PLA2G6* gene activity leads to mitochondrial lipid peroxidation, mitochondrial dysfunction and mitochondrial membrane abnormalities. Finally we demonstrate that reduction of lipid peroxidation, by treatment with deuterated polyunsaturated fatty acids (D-PUFAs), is able to recover the mitochondrial membrane potential of *PLA2G6* mutant human fibroblasts and partially rescue the locomotor deficits in *iPLA2-VIA* knockout flies. We have therefore shown that the *iPLA2-VIA* knockout fly appears to be a useful model organism for studying PLA2G6-associated neurodegeneration.

Materials and methods

Fly stocks and husbandry

The fly stocks y[1] w[67c23]; P{w[+mC] y[+mDint2]=EPgy2}iPLA2-VIA[EY05103], *actin-5C-GAL4*, *elav-GAL4*^{c155} were obtained from the Bloomington *Drosophila* Stock Centre. The *iPLA2-VIA* RNAi (HMS01544) line was provided by the TRiP at Harvard Medical School. All fly strains used were backcrossed at least six generations into the w^{1118} background to obtain isogenic lines. All fly stocks were maintained at 25°C on a 12:12 hour light: dark cycle at constant humidity on a standard sugar-yeast (SY) medium (15 g/l agar, 50 g/l sugar, 100 g/l autolysed yeast, 100 g/l nipagin and 3 ml l/ propionic acid). For all experiments, flies were raised at a standard density on standard SY medium in 200 ml bottles unless otherwise stated. Tissue-specific expression of *iPLA2-VIA* RNAi constructs was achieved by using the *GAL4-UAS* system [GAL4-dependant upstream activator sequence (Brand and Perrimon, 1993)].

Lifespan analyses

The survival assays were performed using newly eclosed flies that were allowed to mature and mate for 24 h before the females and males were separated and collected. One hundred and fifty flies were housed in groups of 15 and the flies were transferred every 2 to 3 days onto fresh food and the number of dead flies recorded. Data are presented as cumulative survival curves, and survival rates were compared using log-rank tests.

Climbing assays

The climbing assay was performed using a negative geotaxis assay according to previously published methods (Rival *et al.*, 2004). Briefly, 15 adult flies were placed in a vertical column (25 ml tissue culture pipette), and allowed to climb for 45 s before the number of flies at the top and bottom was determined. A performance index (PI) defined as $0.5(n(\text{total}) + n(\text{top}) - n(\text{bottom})/\ n(\text{total}))$ was calculated. The experiment was repeated three times for each time point.

Fertility tests

For female fecundity tests, female flies were housed with males for 48 h post-eclosion and then separated into vials at a density of 10 females per vial. Eggs were collected over a 24-h period at different time points. The number of eggs laid per vial at each time point was counted.

Quantitative RT-PCR

Total RNA was extracted from 15 flies per sample using TRIzol® (GIBCO) according to the manufacturer's instructions. The concentration of total RNA purified for each sample was measured using an Eppendorf biophotometer. One microgram of total RNA was then subjected to DNA digestion using DNase I (Ambion), immediately followed by reverse transcription using the SuperScript® II system

(Invitrogen) with oligo(dT) primers. Quantitative PCR was performed using the PRISM 7000 sequence-detection system (Applied Biosystems), SYBR® Green (Molecular Probes), ROX Reference Dye (Invitrogen), and HotStarTaq (Qiagen) by following the manufacturer's instructions. Each sample was analysed in triplicate with both target gene (*iPLA2-VIA*) and reference gene (*RP49*) primers in parallel. The end products of the RT-PCR reactions were also visualized by staining with ethidium bromide following separation with agarose-gel electrophoresis. The primers for the *Drosophila iPLA2-VIA* used in the RT-PCR of the EY05103 fly line were as follows: forward 5'-TACTGGAATTGTGCGATAA GG-'3 and reverse 5'-GATGTGGTATTGGAATCCGAG-'3. The primers used for the RT-PCR performed on the *iPLA2-VIA* RNAi (HMS01544) fly line were as follows: forward 5'- AACtriacylglycerolTAGTGCCGATCGTCCAA-'3 and reverse 5'-GAACCAGTATCCTTGCAGCG-'3. The reference gene primers were as follows: forward 5'-ATGACCAT CCGCCCAGCATCAGG-'3 and reverse 5'-ATCTCGCCGCAGTAAACG-'3.

Stress experiments

For all stress assays, flies were reared and housed as for lifespan experiments. For oxidative stress assays, 7-day or 15-day old flies were transferred onto 5% sucrose/agar containing 5% hydrogen peroxide (Sigma) or 20 mM paraquat (Sigma). For starvation and osmotic stress experiments, 7-day or 15-day old flies were transferred to 1% agar or 500 mM NaCl respectively. For hypoxia experiments 15-day old flies were transferred to a hypoxia chamber with oxygen levels of 7%. After 15 h the flies were removed from the chamber and the number of dead flies was counted.

Triacylglyceride and ATP assays

Levels of triacylglyceride in adult females were measured using the Triglyceride Infinity Reagent (ThermoScientific) and normalized to total body protein using a BCA assay (Sigma). The ATP concentration of whole female flies was determined using the Roche ATP Bioluminescence Assay Kit HS II (Roche). Briefly, two live whole flies or eight fly heads were homogenized in 100 µl ice-cold lysis buffer (provided in the kit) for 1 min using a Kontes pellet pestle. The lysate was then boiled for 5 min and centrifuged at 20 000*g* for 1 min. 2.5 µl of cleared lysate was added to 187.5 µl dilution buffer and 10 µl luciferase and the luminescence was immediately measured using a Tecan Infinite M2000 microplate reader and Magellan V6.5 software. Each reading was converted to the amount of ATP per fly based on the standard curve generated with ATP standards. At least three measurements were made for each genotype and the experiment was repeated three times.

Isolation of *Drosophila* mitochondria

Fly mitochondria were isolated by differential centrifugation, essentially as described in Miwa *et al.* (2003). Briefly, adult flies ($n = 500$ for each time point) were chilled on ice and gently pressed using a pre-chilled pestle and mortar. Importantly, the pestle was moved in a vertical motion (with no horizontal motion) until the shape of the flies was no longer visible. The flies were then washed in STE + BSA buffer [250 mM sucrose, 5 mM Tris, 2 mM EGTA, pH 7.4 (4°C), 1% bovine serum albumin]. The flies were then pressed further in 5 ml of STE + BSA buffer. The squashed flies were then passed through double-layered muslin cloth. The collected pulp was then spun for 3 min at 4°C at 1500 rpm to remove debris. The supernatant was then passed through a single layer of muslin into a clean centrifuge tube and spun for 10 min at 4°C and 10 000 rpm to collect the mitochondria. The mitochondrial pellet was then suspended in 250 µl STE + BSA buffer and stored on ice. A BCA assay (Sigma) was used to determine the protein concentration of the mitochondrial preparations. The isolated mitochondria were kept on ice and used immediately for experiments.

Drosophila mitochondrial respiration measurement

Oxygen consumption was measured using a Clark-type oxygen electrode thermostatically maintained at 25°C. Glutamate (5 mM) and malate (5 mM) or pyruvate (5 mM) were added to measure Complex I-linked respiration, and succinate (5 mM) with rotenone (5 µM) were added to measure Complex II-linked respiration. All data were obtained using an Oxygraph Plus system with Chart recording software.

Light and electron microscopy of fly brains

Flies were decapitated and the proboscis was removed to allow penetration of the fixative. The heads were perfused with 3% glutaraldehyde in phosphate buffer overnight. Brains were then treated with 1% osmium tetroxide for 3 h at 4°C and embedded in Araldite® CY212 resin. Thin sections were stained with toluidine blue and the brain visualized with the light microscope. Ultrathin sections (70 µm) were stained with lead citrate and uranyl acetate and digital images taken on a Phillips CM10 electron microscope with a Megaview III digital camera (Olympus).

Human fibroblast collection and culture

The p.R747W *PLA2G6* fibroblasts were generated from a 4 mm skin punch biopsy taken under local anaesthetic. Biopsies were dissected into ~1 mm pieces and cultured in 5 cm petri dishes in Dulbecco's modified Eagle's medium (DMEM), 10% foetal bovine serum, 1% L-glutamine until fibroblasts were seen to grow out from the explants. When fibroblasts reached confluency, they were detached from culture dishes using TrypleE™ (Invitrogen) and transferred to larger culture vessels for further expansion and cryopreservation. This sample was collected with the written consent of the participant and formal ethical approval from the National Hospital for Neurology and Neurosurgery–Institute of Neurology Joint Research Ethics Committee (London, UK). The GM11529 mutant PLA2G6 human fibroblast cell cultures were obtained from the Coriell Cell Repositories. This line was sampled from a patient with infantile neuroaxonal dystrophy.

Fibroblasts were seeded at a density of 4×10^4 cells/cm^2, grown to 75–80% confluence and maintained at 37°C and 5% CO_2 in DMEM supplemented with 10% (v/v) foetal bovine serum, 2 mM L-glutamine and 1% (v/v) penicillin/streptomycin.

Measurement of mitochondrial membrane potential and cytosolic and mitochondrial reactive oxygen species

For measurements of mitochondrial membrane potential ($\Delta\Psi_m$), dissected fly brains or cells were loaded with 25 nM tetramethylrhodamine methylester (TMRM) for 30 min at room temperature and the dye was present for the duration of the experiment. TMRM is used in the redistribution mode to assess $\Delta\Psi_m$, and therefore a reduction in TMRM fluorescence represents depolarization.

Confocal microscopy of mitochondrial membranes in fly brains and human fibroblasts

Confocal images were obtained using a Zeiss 710 VIS CLSM equipped with a META detection system and a ×40 oil immersion objective. Illumination intensity was kept to a minimum (at 0.1–0.2% of laser output) to avoid phototoxicity and the pinhole set to give an optical slice of ~2 µm. TMRM was excited using the 560 nm laser line and fluorescence measured above 580 nm. All data presented were obtained from at least five coverslips and two to three different cell preparations for cell experiments, and six coverslips and at least six counts for fly brain experiments. The same anatomical area of the fly brain was used each time.

Measurement of reactive oxygen species levels in human fibroblasts

For measurement of mitochondrial reactive oxygen species production, cells were preincubated with 5 µM MitoSOX™ (Molecular Probes) for 10 min at room temperature. Cytosolic reactive oxygen species generation was measured with 2 µM dihydroethidium with the dye present in all solutions throughout the duration of the experiment.

Fluorescence images were obtained on an epifluoresence inverted microscope equipped with a ×20 fluorite objective (Cairn Research). Ratiometric dihydroethidium and MitoSOX fluorescence was recorded with an excitation light at 380 and 530 nm and emission at 440 and 630 nm, respectively.

Measurement of lipid peroxidation in fly brains and human fibroblasts

C11-BODIPY581/591 (Molecular Probes) is a sensitive fluorescent probe for indexing lipid peroxidation in model membrane systems and living cells undergoing a shift from red to green fluorescence emission upon oxidation, even under physiological oxidation (Vaarmann *et al.*, 2010). Fly brains were dissected in phosphate-buffered saline and placed into Hank's balanced salt solution (HBSS). C11-BODIPY581/591 (5 µM) was loaded for 15 min at 20°C. Coverslips were washed once and resuspended in 1 ml of HBSS. Ratiometric measurements of probe oxidation were taken over a 12 min time course. Fluorescence excitation was at 488 nm, green fluorescence was detected at 530 nm and red fluorescence at 670 nm.

Cardiolipin analysis by mass spectrometry

Cardiolipin and oxidized cardiolipin were measured by mass spectrometry essentially as described previously (Pope *et al.*, 2008; Heather *et al.*, 2010; Rodriguez-Cuenca *et al.*, 2010) with some minor modifications to make the analysis specific for *Drosophila* cardiolipin species. In brief, 500 flies of each genotype were homogenized in NaPi buffer (50 mM NaPi, 1 mM EDTA, 100 µM DTPA, pH 7.5) using a Kontes pellet pestle. The homogenates were then spun for 2 min at 13 000 rpm to remove fly debris. Lipids were extracted using a modified Folch extraction and the combined organic layers were evaporated to dryness under nitrogen. Before analysis, samples were resuspended in 1 ml of a 1:1 mix of buffers A and B (buffer A, 15% water, 85% methanol containing 1 ml of 250 ml/l aqueous ammonia per litre; buffer B, 97% chloroform, 3% methanol containing 0.1 ml of 250 ml/l aqueous ammonia per litre). 1 nmol of $(C14:0)_4$-cardiolipin (Avanti Polar Lipids) was used as an internal standard and was added to *Drosophila* head homogenates.

The LC/MS/MS system (Waters 2795 separation unit and a Quattro Micro API triple quadrupole mass spectrometer) and parameters were as described previously (Heather *et al.*, 2010; Rodriguez-Cuenca *et al.*, 2010) except that the multiple reaction monitoring (MRM) transitions were specific for *Drosophila* cardiolipin. Mass spectra from retention times 5.5–6.0 min were combined to generate cardiolipin spectra. Cardiolipin species were identified in MRM mode with the collision gas at 0.25 Pa and collision energy at 35 eV. Cardiolipin species were analysed as their dianions $[CL–2H]^{2-}$. In these samples, the dominant form of cardiolipin was $(C16:1)_4$-cardiolipin (m/z 671), which was therefore selected for analysis based on its fragmentation to a C16:1 fatty acid (m/z 253) by monitoring the $671 > 253$ transition. Similarly, other cardiolpin species $(C18:2)_1(C16:1)_3$-cardiolipin (m/z 684) and $(C18:2)_2(C16:1)_2$-cardiolipin (m/z 697) were analysed by assessing transitions of $684 > 253$ and $697 > 253$, respectively. Oxidized cardiolipin was analysed by the transitions $678 > 253$ and $691 > 253$ transition. The internal standard $(C14:0)_4$-cardiolipin (m/z 619) was analysed by its fragmentation to a C14:0 fatty acid (m/z 227) using the transition $619 > 227$. Data were analysed with QuanLynx software (Waters). Total cardiolipin content was expressed as peak area relative to that of the internal standard. The amounts of each cardiolipin and oxidized cardiolipin were expressed relative to the total amount of cardiolipin in the sample, giving dimensionless ratios.

Deuterated polyunsaturated fatty acids

Deuterated polyunsaturated fatty acids (D-PUFAs) 11,11-D_2-linoleic acid (D_2-linoleic acid) and 11,11,14, 14-D_4-α-linolenic acid (D_4-linoleic acid) were kindly provided by Dr Mikhail S. Shchepinov (Retrotope, Inc), and their synthesis has been previously described (Hill *et al.*, 2012). Hydrogenated polyunsaturated fatty acids (H-PUFAs) were obtained from Sigma–Aldrich (99%). Cells were preincubated with 10 µM H- or D-PUFA (D_4-linoleic acid) in the culture media for 24 h and then washed with HBSS before experiments. For the fly experiments, D_2-linoleic acid was diluted in water and added to the standard fly medium to give a final concentration of 10 or 100 µM.

Statistics

Data were expressed as means ± standard error of the mean (SEM). Significant differences were evaluated by unpaired two-tailed Student's *t*-test and significance levels are described in individual figure legends. Climbing assays were analysed using a two-way ANOVA or a one-way ANOVA with Bonferroni correction.

Results

Drosophila lacking *iPLA2-VIA* activity display age-dependent locomotor deficits and reduced lifespan

A null mutant fly stock completely lacking the *Drosophila* orthologue of the *PLA2G6* gene, *iPLA2-VIA*, was obtained from the Bloomington *Drosophila* Stock Centre. We will refer to null mutant flies lacking both *iPLA2-VIA* genes as *iPLA2-VIA*$^{-/-}$ henceforth. This fly strain carries a P-element insertion (EY05103) in the *iPLA2-VIA* gene (Fig. 1A). As previously shown, RT-PCR analysis confirmed that there was complete knockout of *iPLA2-VIA* gene expression in this strain with no detectable SYBR green signal produced. The end products of the RT-PCR reactions were also visualized on agarose gel electrophoresis, which confirmed the complete absence of *iPLA2-VIA* gene expression in the *iPLA2-VIA*$^{-/-}$ flies (Fig. 1B) (Malhotra *et al.*, 2009). Knockout of *iPLA2-VIA* activity in the fly did not produce any gross changes in body size or obvious differences in morphology (data not shown). *iPLA2-VIA* is expressed throughout the adult fly body, including the brain and eye. The *iPLA2-VIA* gene displays good homology with the human *PLA2G6* gene, with a 51% identity and 67% positivity (FlyBase).

The *iPLA2-VIA*$^{-/-}$ flies displayed progressive locomotor deficits, with the climbing ability of *iPLA2-VIA*$^{-/-}$ flies in response to light tapping progressively falling below that of w^{1118} controls from ~20 days of age (Fig. 1C). Accompanying this climbing defect the *iPLA2-VIA*$^{-/-}$ flies also showed an ~50% reduction in lifespan, in both females (Fig. 1D) and males (Supplementary Fig. 1A). Furthermore, flies heterozygous for the EY05103 P-element insertion (*iPLA2-VIA*), with presumed 50% gene activity only, did not display reduced survival (Fig. 1D and Supplementary Fig. 1A). To ensure that the reduced lifespan was, indeed, due to the EY05103 P-element insertion, we generated flies with precise excisions of the P-element, by introducing a transposase in an appropriate cross, and found that this restored a normal lifespan (Supplementary Fig. 1B).

To confirm the effect of *iPLA2-VIA* deficiency in the fly, we also inhibited *iPLA2-VIA* gene expression by transgenic RNA interference (RNAi) technology, using the *GAL4/UAS* system (Brand and Perrimon, 1993). Ubiquitous expression of *iPLA2-VIA* dsRNAi (*UAS-iPLA2-VIA-RNAi*) with the *actin-GAL4* driver resulted in a ~40% reduction in whole body *iPLA2-VIA* gene expression using RT-PCR analysis (Supplementary Fig. 1C). This reduction was associated with an age-dependent decrease in climbing ability (Fig. 1E) and a shortened lifespan (Fig. 1F). It can therefore be robustly concluded that genetic inactivation of *iPLA2-VIA* activity results in progressive locomotor deficits and a reduction in lifespan in *Drosophila*. To determine whether these phenotypes were specific to loss of *iPLA2-VIA* activity in the brain, we knocked down *iPLA2-VIA* in fly neural tissue using *UAS-iPLA2-VIA-RNAi* driven by the *elav*^{c155}*-Gal4* driver. We observed a significant reduction in lifespan in these flies (Fig. 1G), confirming the brain-specific effects of *iPLA2-VIA* deficiency.

We also assessed the fecundity of *iPLA2-VIA*$^{-/-}$ female flies. The number of eggs laid per female significantly declined with age compared with age-matched w^{1118} control flies, and by Day 25 the null mutant flies were almost completely infertile (Supplementary Fig. 1D).

Brains lacking *iPLA2-VIA* display severe, widespread neurodegeneration and mitochondrial degeneration

Light microscopic examination of thin paraffin sections of *iPLA2-VIA*$^{-/-}$ fly brain revealed normal brain architecture in young Day 2 flies that was indistinguishable from w^{1118} controls (Fig. 2A and B). However, by Day 32 there was significant widespread vacuolation in the *iPLA2-VIA*$^{-/-}$ fly brains that was not present in w^{1118} control flies (Fig. 2C and D). Ultrastructural examination using electron microscopy revealed that the mitochondria were grossly abnormal and swollen with fragmented cristae in aged Day 32 *iPLA2-VIA*$^{-/-}$ fly brains as compared to the mitochondria in age-matched w^{1118} control brains (Fig. 2E–H) or younger Day 2 *iPLA2-VIA*$^{-/-}$ flies (data not shown), which were both filled with densely packed cristae. Furthermore, examination of the fly eye using electron microscopy revealed abnormal retinal structure in the aged Day 32 *iPLA2-VIA*$^{-/-}$ flies compared with age-matched

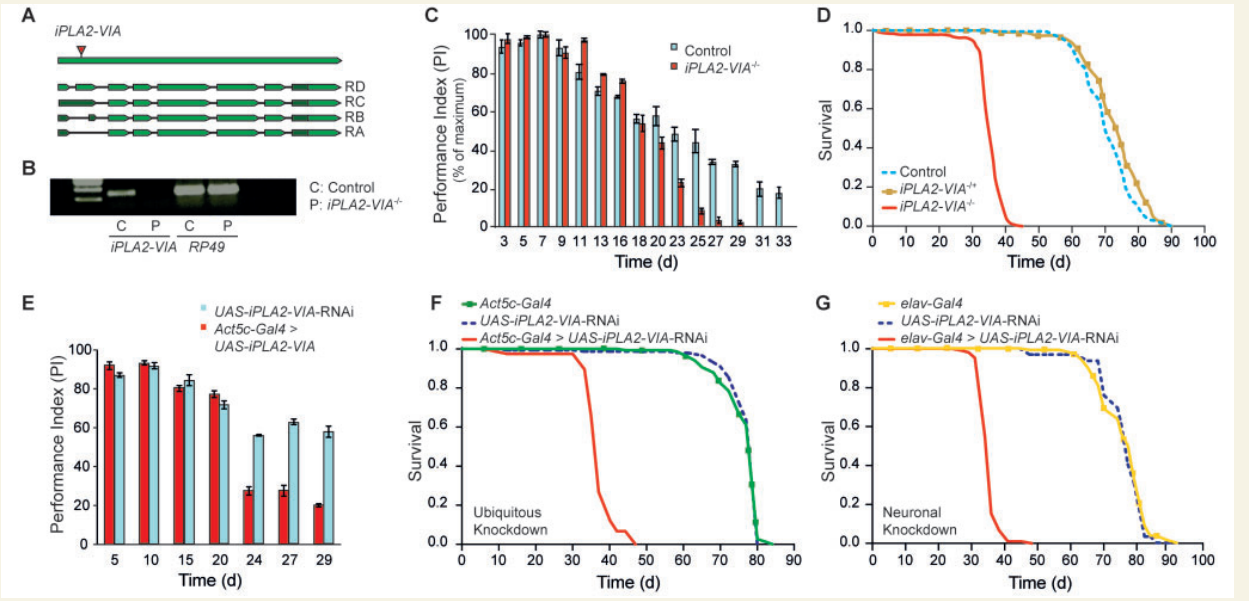

Figure 1 Lack of *iPLA2-VIA* gene activity leads to reduced survival and locomotor deficits. (**A**) Schematic of the *Drosophila iPLA2-VIA* gene, showing the position of the P-element insertion (arrowhead). The *iPLA2-VIA* gene has four main transcripts: *iPLA2-VIA-RB*, *iPLA2-VIA-RC*, *iPLA2-VIA-RD* and *iPLA2-VIA-RA* (FlyBase). The position of the primers has been previously shown (Malhotra *et al.*, 2009). (**B**) RT-PCR analysis of *iPLA2-VIA*$^{-/-}$ flies shows that there is no mRNA expression of the *iPLA2-VIA* gene compared with w^{1118} control flies. The end products of the RT-PCR reaction were run on an agarose gel. *RP49* is an internal control gene and is expressed in both the *iPLA2-VIA*$^{-/-}$ and control w^{1118} flies. (**C**) *iPLA2-VIA*$^{-/-}$ flies display an age-dependent reduction in climbing ability compared with w^{1118} controls ($n = 45$ flies per genotype, three repeats per genotype, $P < 0.05$). Climbing ability is expressed as a perfomance index (PI) over time in days (d). (**D**) Female flies lacking both *iPLA2-VIA* genes (*iPLA2-VIA*$^{-/-}$) have a significantly reduced lifespan compared with w^{1118} control flies ($P < 0.0001$). Furthermore female flies lacking only one *iPLA2-VIA* gene (*iPLA2-VIA*$^{+/-}$; $n = 150$ flies per genotype) do not display a reduction in lifespan. (**E**) Ubiquitous downregulation of iPLA2-VIA activity using sRNAi (*UAS-iPLA2-VIA-RNAi*) driven by *Act5c-Gal4* (Act5c-Gal4 > *UAS-iPLA2-VIA*-RNAi) results in an age-dependent reduction in climbing ability compared with control *UAS-iPLA2-VIA-RNAi* flies ($P < 0.05$; $n = 45$ flies per genotype, three repeats each). (**F**) Knockdown of iPLA2-VIA activity using *iPLA2-VIA* sRNAi (*UAS-iPLA2-VIA-RNAi*) driven ubiquitously by *Act5c-Gal4* (*Act5c-Gal4 > UAS-iPLA2-VIA-RNAi*) results in a decrease in lifespan compared with control non-expressing *UAS-iPLA2-VIA-RNAi* flies ($P < 0.0001$) or driver *Act5c-Gal4* flies ($P < 0.0001$), similar to that seen with the null mutant flies (*iPLA2-VIA*$^{-/-}$; $n = 150$ flies per genotype). (**G**) Knockdown of *iPLA2-VIA* activity using sRNAi (*UAS-iPLA2-VIA-RNAi*) driven in the fly nervous system using the *elav-Gal4* driver results in a decrease in lifespan compared with control non-expressing *UAS-iPLA2-VIA-RNAi* flies ($P < 0.0001$), or driver *elav-Gal4* ($P < 0.0001$; $n = 150$ flies per genotype), similar to that seen with the null mutant flies (*iPLA2-VIA*$^{-/-}$).

control flies, with grossly abnormal ommatidial structure (Supplementary Fig. 2A and B).

Loss of *iPLA2-VIA* resulted in reduced mitochondrial membrane potential and abnormal mitochondrial respiratory chain activity

Given the abnormal mitochondrial membrane morphology in older *iPLA2-VIA*$^{-/-}$ flies, we investigated whether loss of *iPLA2-VIA* affected mitochondrial membrane potential ($\Delta\Psi$m), an indicator of mitochondrial health and function. Mitochondrial membrane potential was assessed in the brains of 25-day-old flies using TMRM fluorescence and imaging with confocal microscopy. This revealed a significant reduction in mitochondrial membrane potential in *iPLA2-VIA*$^{-/-}$ fly brains compared to controls (Fig. 3A). We next isolated mitochondria from *iPLA2-VIA*$^{-/-}$ flies and assessed respiratory chain activity by measuring oxygen consumption using a Clark-type oxygen electrode. The steps in respiration were compared in mitochondria isolated from *iPLA2-VIA*$^{-/-}$ flies and control w^{1118} flies with substrates and inhibitors specific to individual respiratory complexes. We found that knockout of *iPLA2-VIA* activity conferred a decrease in complex I and II-dependent respiration (Fig. 3B), manifested as significantly decreased oxygen consumption in state 3 respiration, whether using substrates for complex I (5 mM glutamate and 5 mM malate) or for complex II (5 mM succinate in the presence of rotenone) (Fig. 3B). The respiratory control ratio is the ratio of state 3 respiration (ADP stimulated) to state 4 respiration (no ADP present), and is considered an indication of the degree of coupling of mitochondrial respiratory chain activity to oxidative phosphorylation (Chance and Williams, 1955). The respiratory control ratio was significantly lower in *iPLA2-VIA*$^{-/-}$ mitochondria compared with age-matched control w^{1118} flies (Fig. 3C), because of

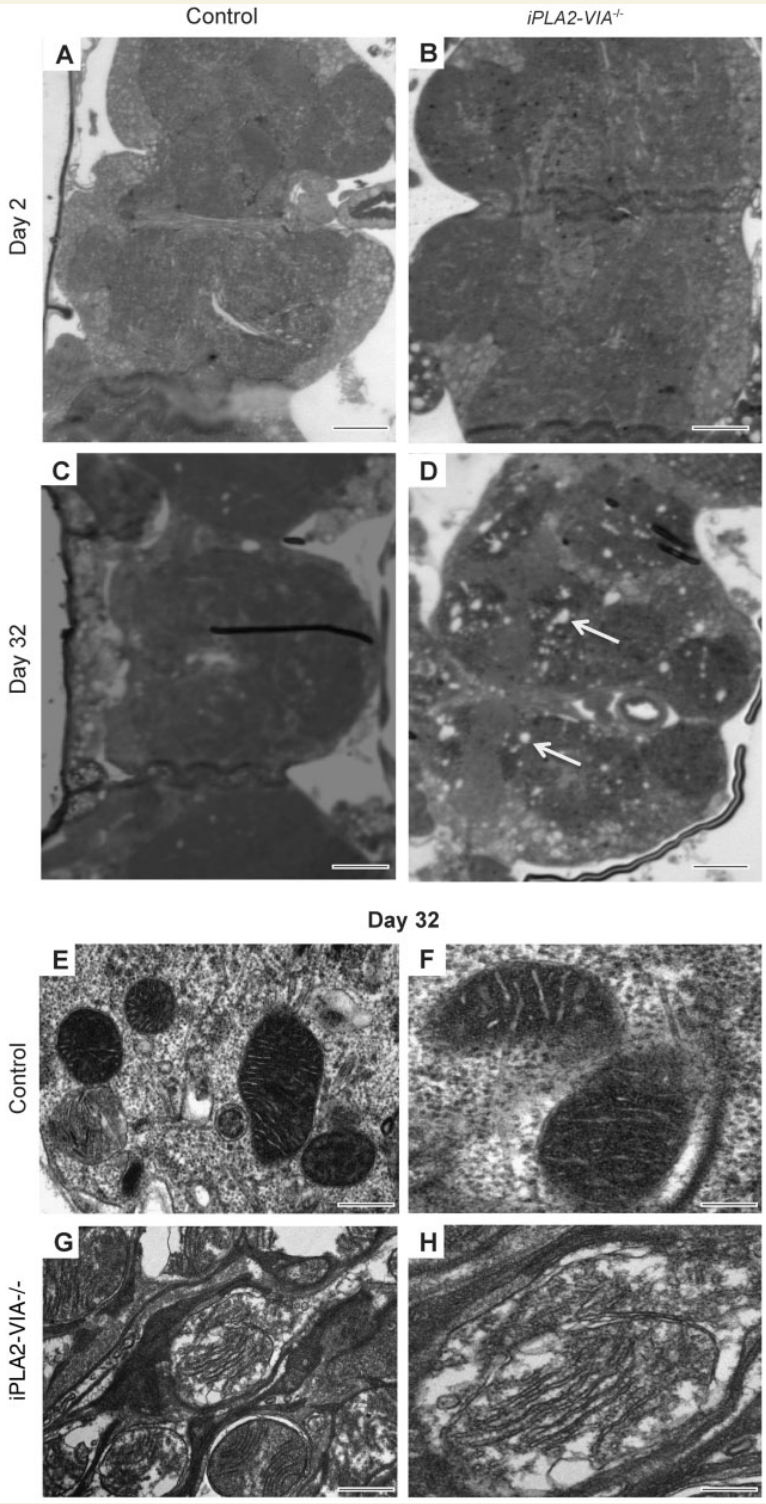

Figure 2 Fly brains lacking *iPLA2-VIA* display severe mitochondrial degeneration at the ultrastructural level. (**A**) Light microsopic examination of Day 2 w^{1118} control (scale bar = 20 μm) and (**B**) *iPLA2-VIA*$^{-/-}$ fly brains (scale bar = 30 μm). (**C**) At Day 32 w^{1118} control fly brains display healthy brain tissue compared with (**D**) *iPLA2-VIA*$^{-/-}$ flies brains, which display widespread vacuolation (arrows) (× 60 magnification; scale bars 20 = μm). (**E** and **F**) Ultrastructural examination of aged Day 32 w^{1118} control fly brains (× 2500; scale bar = 0.6 μm and × 5300; scale bar = 0.2 μm) revealed normal mitochondrial morphology, which is in contrast to (**G** and **H**) Day 32 *iPLA2-VIA*$^{-/-}$ fly brains, which display significant degeneration of the mitochondrial cristae (× 3100; scale bar = 0.5 μm and × 5300; scale bar = 0.2 μm). Images representative of six fly brains examined for each genotype. No abnormal mitochondria were seen in the w^{1118} control fly brains.

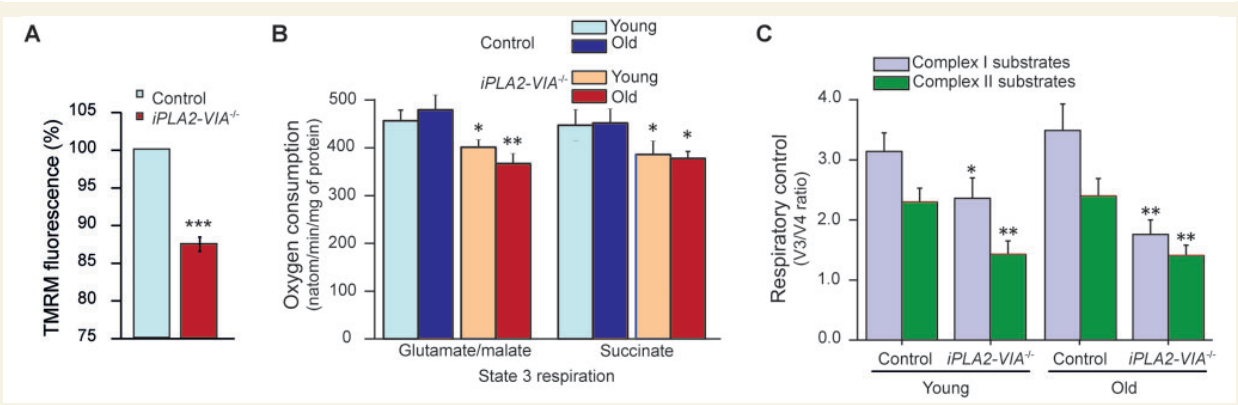

Figure 3 Flies lacking *iPLA2-VIA* have reduced mitochondrial membrane potential and decreased mitochondrial respiratory chain activity. (**A**) The mitochondrial membrane potential measured using TMRM fluorescence in the brains of 25-day-old flies was significantly decreased in *iPLA2-VIA*$^{-/-}$ brains compared to w^{1118} controls (***$P < 0.001$; $n = 6$ brains for each genotype). (**B**) The respiratory chain activity was measured by assessing oxygen consumption and demonstrated that mitochondria from young Day 2 and old Day 32 *iPLA2-VIA*$^{-/-}$ flies have reduced complex I and II–dependent respiration compared with w^{1118} control flies, manifested as significantly decreased oxygen consumption in state 3 respiration (*$P < 0.05$, **$P < 0.001$). (**C**) The respiratory control ratio was significantly lower in *iPLA2-VIA*$^{-/-}$ mitochondria compared with age-matched control w^{1118} mitochondria. Furthermore, the respiratory control ratio of *iPLA2-VIA*$^{-/-}$ flies in the presence of glutamate/malate was dependent on the age of the flies: older flies having lower respiratory control ratio values (*$P < 0.05$, **$P < 0.001$).

the inhibition of state 3 respiration. Furthermore, the respiratory control ratio of *iPLA2-VIA*$^{-/-}$ flies in the presence of glutamate/malate was dependent on the age of the flies: older flies having lower respiratory control ratio values (Fig. 3C). Thus, loss of *iPLA2-VIA* activity reduces mitochondrial membrane potential as a result of mitochondrial uncoupling, which increases with age in the *iPLA2-VIA*$^{-/-}$ flies.

Loss of *iPLA2-VIA* activity results in reduced ATP levels and increased sensitivity to oxidative stress

In keeping with the mitochondrial dysfunction caused by loss of *iPLA2-VIA* activity, we also demonstrated that ATP levels in aged, Day 25, *iPLA2-VIA*$^{-/-}$ fly heads were reduced by 40% compared with control flies (Fig. 4A). Levels were also reduced in whole *iPLA2-VIA*$^{-/-}$ flies compared with controls (Supplementary Fig. 3A).

Mitochondrial dysfunction can lead to decreased resistance to reactive oxygen species, which has been implicated in many neurodegenerative diseases. To explore the role of *iPLA2-VIA* in resistance to oxidative stress, we examined the survival of *iPLA2-VIA*$^{-/-}$ flies after exposure to the potent oxidizer hydrogen peroxide and paraquat, a free radical generator. Consistent with the structural mitochondrial abnormalities in aged flies, *iPLA2-VIA*$^{-/-}$ flies showed an age-dependent, mild sensitivity at Day 15 to hydrogen peroxide and, more so, to paraquat (Fig. 4B and C) that was not consistently present in younger 7-day-old flies (data not shown). Both young Day 7 and older Day 15 *iPLA2-VIA*$^{-/-}$ flies were also sensitive to osmotic stress and showed reduced survival compared to w^{1118} control flies when fed 500 mM NaCl (Supplementary Fig. 3B). Day 15 *iPLA2-VIA*$^{-/-}$ flies also displayed increased sensitivity to hypoxic and xenobiotic (dichlorodiphenyltrichloroethane, DDT) stresses (Supplementary Fig. 3C and D).

Loss of *iPLA2-VIA* was not associated with changes in cardiolipin composition

Given that mitochondrial membrane morphology appeared to be abnormal in the *iPLA2-VIA*$^{-/-}$ flies, we performed mass spectroscopic analysis of cardiolipin, one of the major phospholipids in mitochondrial membranes. It has been hypothesized that PLA2G6 is critical for the normal repair and remodelling of damage to cardiolipin caused by mitochondrial reactive oxygen species, and that loss of PLA2G6 activity may lead to cardiolipin oxidation and pathogenic downstream events such as induction of apoptosis. To test this hypothesis, we performed mass spectroscopic analysis on *iPLA2-VIA*$^{-/-}$ fly heads to compare the cardiolipin composition with that in w^{1118} control flies. We found no significant differences in the cardiolipin content, monolysocardiolipin content or fatty acid composition between *iPLA2-VIA*$^{-/-}$ and control w^{1118} fly brains (Supplementary Fig. 4). Similar results have previously been reported in whole flies lacking *iPLA2-VIA* (Malhotra *et al.*, 2009). Furthermore, we found that oxidized cardiolipin was not detected in significant amounts in either the *iPLA2-VIA*$^{-/-}$ or control w^{1118} fly head homogenates (Supplementary Fig. 4). Oxidized cardiolipin

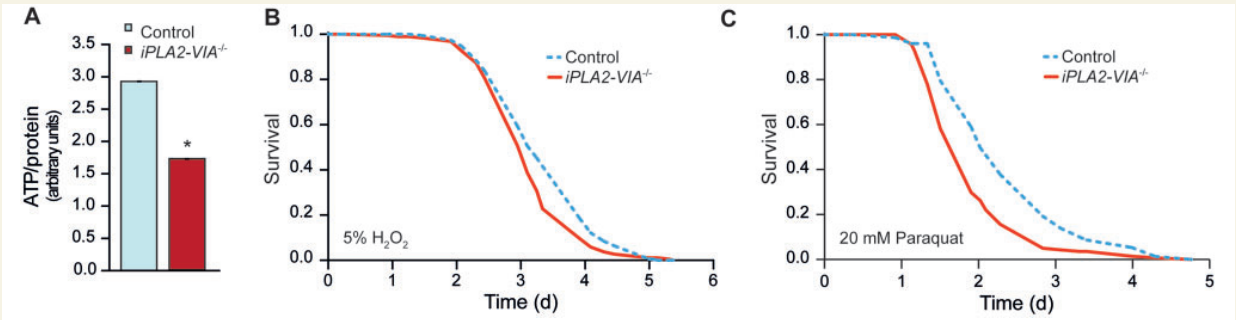

Figure 4 *iPLA2-VIA*$^{-/-}$ flies have reduced ATP levels and are more sensitive to oxidative stress. (**A**) ATP levels are reduced in the heads of Day 25 *iPLA2-VIA*$^{-/-}$ flies compared with age-matched w^{1118} control flies (*$P < 0.05$). (**B**) Aged Day 15 *iPLA2-VIA*$^{-/-}$ flies show reduced survival when treated with 5% hydrogen peroxide (H_2O_2) ($P = 5.6 \times 10^{-7}$) and (**C**) 20 mM paraquat ($P = 4.6 \times 10^{-7}$) compared with w^{1118} control flies (n = 150 flies per genotype).

species would be expected to be present as additions of +7/8 m/z on the scan spectra. Our results therefore do not support a role for oxidized cardiolipin in causing mitochondrial dysfunction and neurodegeneration in flies lacking *iPLA2-VIA* activity.

Loss of *iPLA2-VIA* promotes brain lipid peroxidation and reduces whole body triacylglycerol levels

Despite the absence of changes in oxidized cardiolipin, we hypothesized that loss of *PLA2G6* may lead to abnormal and excessive oxidation of other mitochondrial membrane lipids, which in turn would lead to the observed mitochondrial dysfunction. We therefore studied the effect of knocking out *iPLA2-VIA* on lipid peroxidation in *Drosophila*. Rates of lipid peroxidation were measured by live imaging of Day 25 *iPLA2-VIA*$^{-/-}$ and w^{1118} control dissected fly brains, using the fluorescent ratiometric oxidation-sensitive dye C11 BODIPY581/591, which shifts its fluorescence from red to green in a time-dependent manner, the rate being proportional to levels of lipid peroxidation. The changes in colour shift were detected by confocal microscopy. This demonstrated that levels of lipid peroxidation in flies lacking the *iPLA2-VIA* gene were 3.5-fold higher than in age-matched control fly brains (Fig. 5A).

There is evidence that PLA2G6 may play a role in the regulation of triacylglycerol synthesis by providing endogenous fatty acids (Gubern *et al.*, 2009). Triacylglycerol is the main form of lipid storage in the fly and therefore reflects the ability of flies to respond to starvation conditions (Ballard *et al.*, 2008). Measurement of whole-body triacylglycerol levels in female flies revealed a significant age-dependent reduction in both control w^{1118} and *iPLA2-VIA*$^{-/-}$ flies. However, the reduction was significantly greater by Day 20 in the flies lacking *iPLA2-VIA* activity (Fig. 5B). In keeping with an age-dependent decrease in triacylglycerol levels, *iPLA2-VIA*$^{-/-}$ flies were not sensitive to starvation conditions at Day 7 but became sensitive at Day 15 compared with control w^{1118} flies (Fig. 5C).

Human mutant PLA2G6 fibroblasts display abnormal mitochondrial physiology

Given that loss of *iPLA2-VIA* led to increased lipid peroxidation and mitochondrial dysfunction in *Drosophila*, we examined fibroblasts taken from a patient with a known homozygous p.R747W mutation in *PLA2G6* causing dystonia-parkinsonism (Paisan-Ruiz *et al.*, 2009). Using TMRM fluorescence to probe for mitochondrial membrane potential, we found that there was a significant decrease in basal mitochondrial membrane potential in the mutant human fibroblasts (Fig. 6A and B), similar to that seen in fly brains lacking *iPLA2-VIA*.

Abnormal respiration and low mitochondrial membrane potential can induce excessive reactive oxygen species production in the matrix of mitochondria. Indeed the rate of mitochondrial reactive oxygen species production, as assessed using MitoSOX fluorescence, was increased by 28% relative to control human fibroblasts (Fig. 6C and E). Cytosolic reactive oxygen species were also significantly higher in the fibroblasts with a *PLA2G6* mutation (Fig. 6D and E).

Mutations in *PLA2G6* are associated with elevated mitochondrial lipid peroxidation levels in human fibroblasts and are reversed by treatment with deuterated polyunsaturated fatty acids

Following the demonstration that there is an increase in lipid peroxidation in the brains of flies lacking *iPLA2-VIA* compared with controls, we also assessed lipid peroxidation in two human PLA2G6 fibroblast lines; one taken

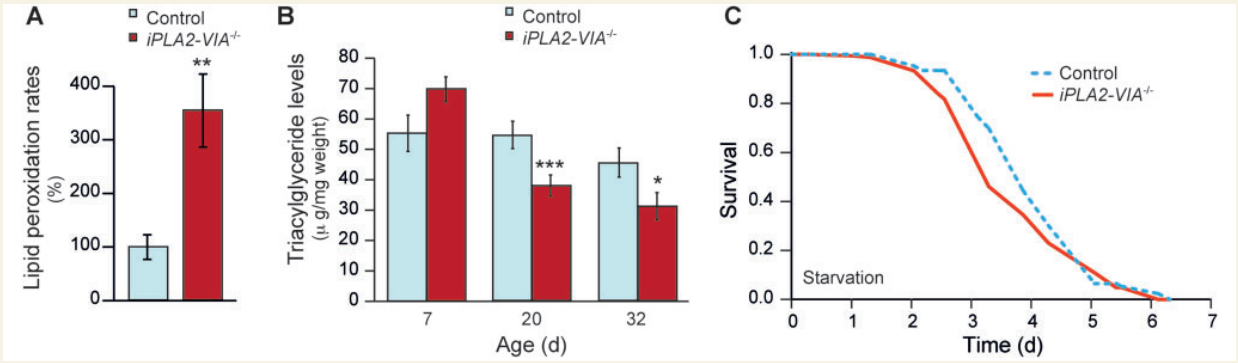

Figure 5 Flies lacking *iPLA2-VIA* have increased lipid peroxidation in their brains and reduced triacylglycerol (TAG) levels. (**A**) Lipid peroxidation was measured using C11-BODIPY581/591 and demonstrated that Day 25 *iPLA2-VIA*$^{-/-}$ fly brains have elevated levels of lipid peroxidation compared with age-matched w^{1118} controls ($n = 6$ fly brains per experiment; $^{**}P < 0.01$). (**B**) Whole-body triacylglycerol levels are decreased in *iPLA2-VIA*$^{-/-}$ flies in an age-dependent manner compared with w^{1118} control flies. ($^{***}P = 0.005$ Day 20 and $^{*}P = 0.01$ Day 32). (**C**) Day 15 *iPLA2-VIA*$^{-/-}$ flies are more sensitive to starvation conditions than age-matched w^{1118} control flies ($P = 0.001$; $n = 150$ flies per genotype).

from a patient with dystonia-parkinsonism with a p.R747W mutation (Paisan-Ruiz *et al.*, 2009) and the other from a child with infantile neuroaxonal dystrophy. We assessed lipid peroxidation levels using the fluorescent ratiometric oxidation-sensitive C11 BODIPY581/591 dye. This demonstrated that *PLA2G6* mutant fibroblasts had an increased level of lipid peroxidation compared to controls (Fig. 7A), suggesting therefore that lipid peroxides may be a potential therapeutic target.

Natural polyunsaturated fatty acids (PUFAs) such as linoleic acid undergo autoxidation by reactive oxygen species, resulting in the production of toxic reactive carbonyl compounds that can mediate DNA damage, carcinogenesis and inflammation. However, replacement of the bis-allylic hydrogen atoms with deuterium atoms (termed site-specific isotope-reinforcement) arrests PUFA autoxidation due to the isotope effect. Indeed, even small amounts of isotope-reinforced D-PUFA are able to protect yeast from lipid autoxidation-mediated cell killing (Hill *et al.*, 2011, 2012). These benefits have also been confirmed *in vivo* with the demonstration that D-PUFAs reduce nigrostriatal degeneration in a mouse model of Parkinson's disease (Shchepinov *et al.*, 2011). We therefore pretreated human *PLA2G6* mutant fibroblasts for 24 h with D-PUFA (D_4-linoleic acid) and found that this decreased lipid peroxidation in the cells to below control levels (Fig. 7A). This was also associated with a rescue in the reduced mitochondrial membrane potential (Fig 7B). Moreover, assessment specifically of lipid peroxidation levels in digitonin-permeabilized cells, which destroys all cell membranes except mitochondrial ones, also demonstrated that lipid peroxidation was substantially increased. In addition, when rotenone was added to the fibroblasts there was no further significant increase in the lipid peroxidation level, indicating that the lipid peroxidation was predominantly produced by mitochondria in the cell (Fig. 7C).

Deuterated linoleic acid partially rescued the locomotor abnormalities of flies lacking *iPLA2-VIA*

Finally, we tested the effect of inhibiting lipid peroxidation with D-PUFAs on the neurodegenerative locomotor phenotype seen in flies lacking *iPLA2-VIA*. Crosses for *iPLA2-VIA*$^{-/-}$ and w^{1118} control flies were set up on food containing vehicle (H_20), 10 or 100 µM D_2-linoleic acid. Eclosed offspring were also kept on standard food containing either vehicle or D_2-linoleic acid and aged while their climbing ability was assessed. *iPLA2-VIA*$^{-/-}$ flies treated with 10 µM D_2-linoleic acid had significantly improved motor performance in old age compared to flies treated with control food (Fig. 7D). There was a trend towards improved climbing ability at older ages when *iPLA2-VIA*$^{-/-}$ flies were treated with 100 µM D_2-linoleic acid, but this was not statistically significant. The rescuing effect of D_2-linoleic acid on climbing ability was specific to *iPLA2-VIA*$^{-/-}$ flies, as the climbing ability of control w^{1118} flies treated with 10 µM D_2-linoleic acid was indistinguishable from controls (Supplementary Fig. 5B). The effect of D_2-linoleic acid on the survival of *iPLA2-VIA*$^{-/-}$ flies was also assessed. There was no significant effect of 10 µM D_2-linoleic acid on the lifespan of flies lacking *iPLA2-VIA*. Indeed, at the higher concentration of 100 µM D_2-linoleic, the lifespan of the *iPLA2-VIA*$^{-/-}$ flies was reduced compared to control w^{1118} flies demonstrating that D_2-linoleic acid is toxic to flies at higher concentrations (Supplementary Fig. 5B). Despite the lack of lifespan-prolonging effects, the fact that deuterated linoleic acid significantly improved the locomotor abnormalities of *iPLA2-VIA* flies suggests that low concentrations of D-PUFAs, or similar compounds, may act as potential therapeutic compounds for the treatment of PLA2G6-associated neurodegeneration.

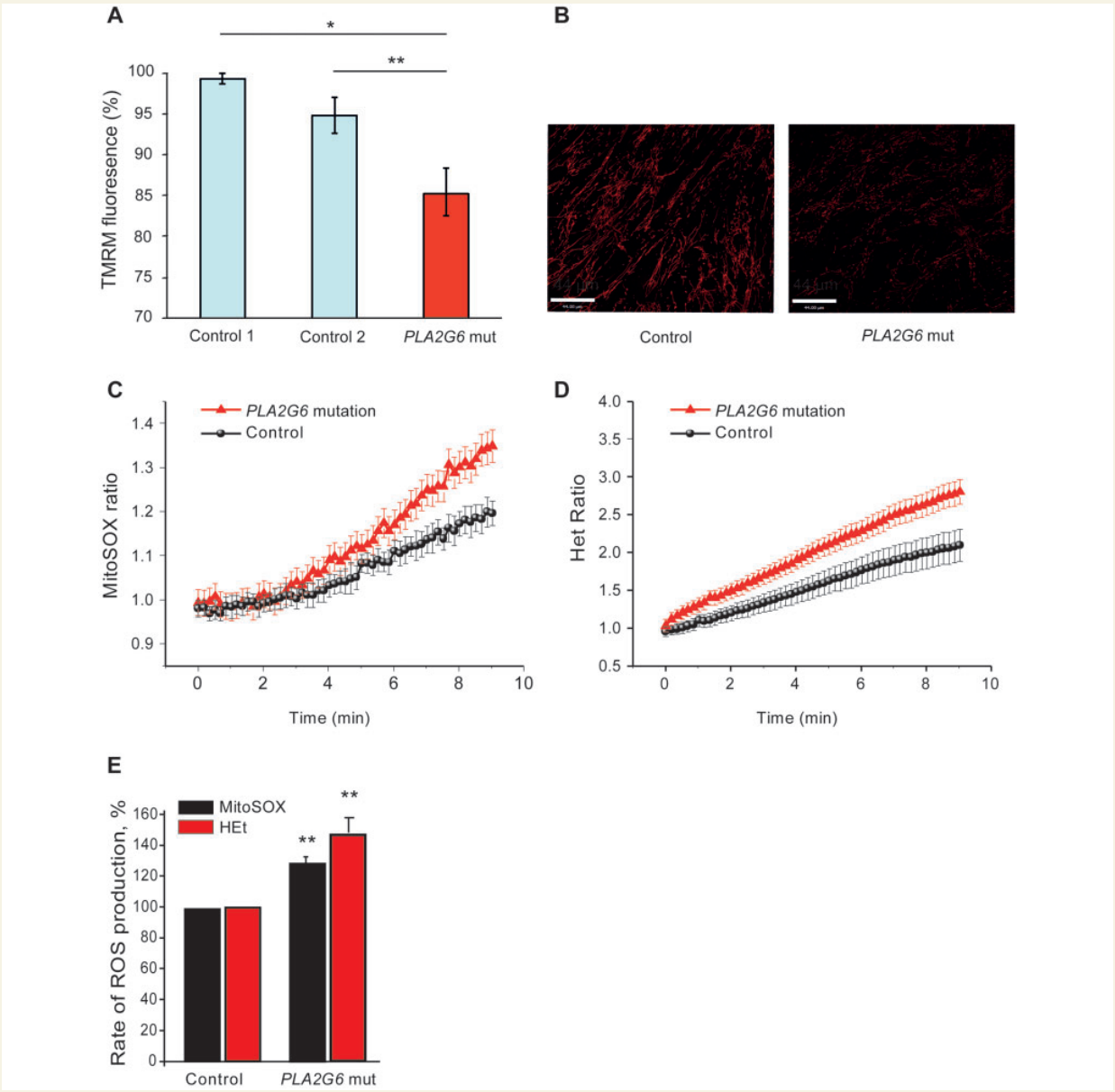

Figure 6 Human mutant *PLA2G6* fibroblasts have reduced mitochondrial membrane potential and increased levels of mitochondrial and cytosolic reactive oxygen species levels. (**A**) The mitochondrial membrane potential of human p.R747W mutant *PLA2G6* fibroblasts is reduced compared with control human fibroblasts (*$P < 0.05$ control 1 and **$P < 0.002$ control 2) as measured by TMRM fluorescence. (**B**) This is clearly seen as a reduction in red TMRM staining in the p.R747W mutant *PLA2G6* human fibroblasts compared with control fibroblasts (Scale bars = 44 μm). (**C**) Mitochondrial reactive oxygen species production is increased 28% in human p.R747W mutant *PLA2G6* fibroblasts compared to control fibroblasts ($P < 0.001$; $n = 6$). (**D**) Cytosolic reactive oxygen species production is also increased in human p.R747W mutant *PLA2G6* fibroblasts compared with control fibroblasts (1.47-fold increase; $P < 0.001$; $n = 6$). (**E**) Rates of reactive oxygen species production in **C** and **D** are shown as a percentage. Het = dihydroethidium.

Discussion

As the energy factories of cells, mitochondria play an essential role in neurons, in which oxidative phosphorylation is the main source of ATP. A previous study in a mouse model demonstrated that knockout of *Pla2g6* results in abnormal mitochondrial membrane morphology (Beck *et al.*, 2011). These findings lead to the question as to how loss of normal *PLA2G6* gene function leads to abnormal mitochondrial morphology, and whether mitochondrial dysfunction is an early feature of PLA2G6-associated neurodegeneration.

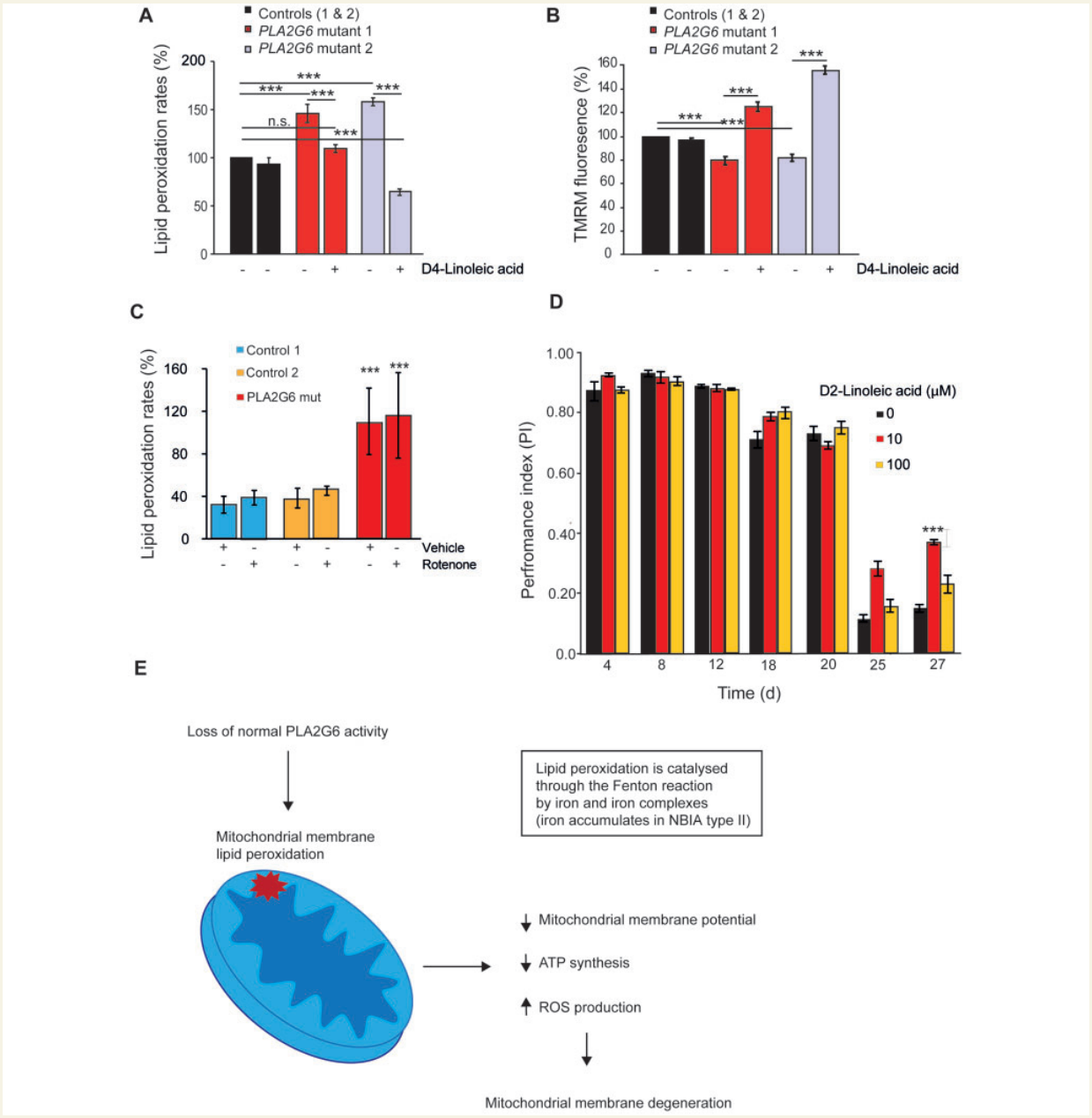

Figure 7 Elevated lipid peroxidation is a possible therapeutic target in *PLA2G6*-associated disease. (**A**) Lipid peroxidation levels in intact human fibroblasts taken from two patients with *PLA2G6* mutations (mutant 1 fibroblasts were taken from a patient with a p.R747W *PLA2G6* mutation and mutant 2 fibroblasts were from a patient with a *PLA2G6* mutation and infantile neuroaxonal dystrophy) are increased compared with fibroblasts from healthy controls. In addition, pretreatment with D-PUFAs (D_4-linoleic acid) for 24 h significantly rescues the elevated lipid peroxidation rates in the human *PLA2G6* mutant fibroblasts (***$P < 0.0001$; n.s = non-significant). (**B**) The mitochondrial membrane potential of human mutant *PLA2G6* fibroblasts is considerably reduced compared with control fibroblasts and is significantly recovered below control levels following 24 h pre-treatment with D_4-linoleic acid (***$P < 0.0001$). (**C**) Lipid peroxidation levels are also increased in permeabilized mutant p.R747W *PLA2G6* fibroblasts compared with controls in the absence (***$P < 0.05$ for control 1 and control 2) and presence of rotenone (***$P < 0.05$ for controls 1 and 2), suggesting that it is generated from a mitochondrial source. (**D**) Treatment of *iPLA2-VIA*$^{-/-}$ flies with 10 μM D_2-linoleic acid partially rescues the climbing deficits in an age-dependent manner compared with untreated controls ($n = 45$ flies per group, three repeats per group; one-way ANOVA with Bonferroni correction ***$P < 0.003$). There is a trend for 100 μM D_2-linoleic acid to rescue the climbing deficits of *iPLA2-VIA*$^{-/-}$ flies but this is not statistically significant. (**E**) Schematic diagram showing how loss of normal PLA2G6 activity might lead to mitochondrial dysfunction. A mutation in *PLA2G6* results in loss of PLA2G6 activity. In turn this results in elevated lipid peroxidation of mitochondria, with the resultant decrease in mitochondrial membrane potential, decrease in ATP synthesis and mitochondrial reactive oxygen species production. The mitochondria eventually degenerate and become swollen in appearance. All of these abnormalities result in mitochondrial dysfunction and subsequent cellular dysfunction with consequent neuronal death. NBIA = neurodegeneration with brain iron accumulation; ROS = reactive oxygen species.

Loss of normal phospholipase A2 activity leads to mitochondrial dysfunction, which precedes mitochondrial membrane defects

In this study, we demonstrated that loss of normal phospholipase A_2 activity in the fruit fly and in fibroblasts taken from patients harbouring mutations in *PLA2G6*, results in striking abnormalities in both mitochondrial function and morphology. Furthermore, we demonstrate that mitochondrial dysfunction precedes the mitochondrial morphological abnormalities that are seen at the ultrastructural level. Deficits in mitochondrial oxidative respiration are seen in *iPLA2-VIA* knockout flies as young as 2 days of age, when there are no associated mitochondrial membrane abnormalities present on electron microscopy.

Moreover, our findings that mitochondrial dysfunction occurs early in PLA2G6-associated neurodegeneration, is consistent with the clinical features seen in infantile neuroaxonal dystrophy, neurodegeneration with brain iron accumulation and dystonia-parkinsonism, all of which display clear early-onset phenotypes, that have previously been associated with mitochondrial disease.

Loss of normal PLA2G6 activity leads to reactive oxygen species production

In addition to mitochondrial dysfunction, we also demonstrate that loss of PLA2G6 activity is associated with raised levels of reactive oxygen species. These species play important roles in cell signalling, but at abnormally high levels are detrimental to cells, ultimately leading to cell death (Martindale and Holbrook, 2002). Lipids are important targets of reactive oxygen species and therefore elevated reactive oxygen species levels will lead to increases in mitochondrial lipid peroxidation. Furthermore, it may also be that elevated lipid peroxidation arises in the absence of phospholipase A_2 activity because some phospholipases preferentially cleave oxidized lipids to maintain redox homeostasis (Domijan *et al.*, 2014). In turn, lipid peroxides are known to trigger a cascade of events that include a fall in mitochondrial membrane potential, mitochondrial swelling and loss of mitochondrial matrix components (Castilho *et al.*, 1994). Furthermore, it has been shown that complex I, the largest complex of the respiratory chain, is susceptible to oxidative stress (Lin and Beal, 2006). Indeed we saw a decrease in oxidative respiration in flies lacking *iPLA2-VIA* when we used substrates specific for complex I of the respiratory chain. Furthermore, Lewy body disease has been shown to be associated with reduced levels of complex I activity (Gu *et al.*, 1998), further implicating mitochondrial dysfunction in neurodegeneration, and more specifically in PLA2G6-associated neurodegeneration, which has been linked to parkinsonism and Lewy body pathology.

In addition, lipid peroxidation is strongly catalysed through the Fenton reaction by iron and iron complexes (Koster *et al.*, 1980) and it is iron that is often deposited in the basal ganglia of the brains of patients affected with *PLA2G6* mutations (Morgan *et al.*, 2006). Thus, iron-mediated oxidative insults seem to have a crucial role in the function of *PLA2G6* and in the progression of diseases associated with mutations in this gene.

PLA2G6-associated neurodegeneration is not likely mediated by oxidization of mitochondrial cardiolipin

Given the increase in levels of lipid peroxidation in flies lacking *iPLA2-VIA*, we looked for elevated levels of oxidized cardiolipin, one of the most common lipids in the inner mitochondrial membrane. It has previously been hypothesized that PLA2G6 is involved in the remodelling of cardiolipin's fatty acid side chains (Malhotra *et al.*, 2009) and in removing oxidized fatty acid side chains. Oxidation of mitochondrial phospholipids such as cardiolipin leads to cytochrome *c* release and apoptosis (Kagan *et al.*, 2005). To determine whether cardiolipin is oxidized in PLA2G6 loss-of-function, we analysed the cardiolipin composition of *iPLA2-VIA*$^{-/-}$ fly heads using mass spectrometry. We demonstrated that mitochondrial membrane disintegration and mitochondrial dysfunction occur in the absence of any significant differences in cardiolipin amount or side chain composition in fly brains lacking *iPLA2-VIA*. Furthermore, oxidized cardiolipin was not detected in significant amounts. This may be related to the types of fatty acids present in *Drosophila* cardiolipin. Palmitic acid is the major component of cardiolipin side chains in *Drosophila* and is more resistant to oxidation than linoleic acid, the main cardiolipin side chain in most mammalian tissues. However, it could also point towards redundancy in the cardiolipin remodelling enzymes. There are a number of enzymes involved in cardiolipin remodelling and it may be the case that fatty acid remodelling of the side chains, in particular removal of oxidized fatty acids, can be performed by other enzymes involved in cardiolipin remodelling such as tafazzin (Schlame, 2013).

The abnormal lipid peroxidation seen in *PLA2G6* knockout leads to a toxic cascade of downstream events

In this work we report that loss of normal PLA2G6 function is strongly associated with elevated mitochondrial lipid peroxidation. Furthermore lipid peroxidation is known to induce mitochondrial injury, leading to a decrease in oxidative respiratory chain function, reduced mitochondrial

membrane potential, reduced cellular ATP levels and raised reactive oxygen species levels, all features we have demonstrated in flies and human fibroblasts lacking normal *PLA2G6* gene activity (Fig. 7D). This in turn would be predicted to lead to cell death and neurodegeneration. As lipid peroxides are harmful mediators of oxidative stress, strategies focused on quenching, recycling or protecting such products could be highly effective in the treatment of the disease.

This work suggests that lipid peroxidation-lowering strategies may be beneficial in PLA2G6-associated neurodegeneration

In addition to showing that lipid peroxidation is increased in both fly brains lacking *iPLA2-VIA* and human *PLA2G6* mutant fibroblasts, we have demonstrated that D-PUFAs reduce the rates of lipid peroxidation in two lines of *PLA2G6* mutant fibroblasts and restore mitochondrial membrane potential. This suggests that D-PUFAs may have potential therapeutic roles in PLA2G6-associated neurodegeneration and its associated mitochondrial dysfunction.

Our data promote *Drosophila* as a useful model for studying PLA2G6-associated neurodegeneration, and for manipulating pathways and therapeutic targets in order to reverse or prevent the deleterious effects of lipid peroxides. Loss of *iPLA2-VIA* gene function results in reduced lifespan and locomotor ability, increased sensitivity to oxidative insults as well as hypoxia, osmotic and starvation stressors. Thus flies lacking *iPLA2-VIA* display phenotypes that can be used as markers in genetic modifying screens or in the screening of potential therapeutic compounds. To test the validity of the fly model for drug screening and to confirm the benefits of D-PUFAs *in vivo* in an organism lacking *iPLA2-VIA*, we examined the effects of D-PUFAs on the locomotor deficits of *iPLA2-VIA*$^{-/-}$ flies. This demonstrated that treatment with D_2-linoleic acid partially rescues the climbing abnormalities in aged *iPLA2-VIA* knockout flies. Therefore this approach of using compounds, which act to reduce the autoxidation of lipids, may represent a future therapeutic strategy for patients with PLA2G6-associated neurodegeneration and warrants further investigation.

Acknowledgements

We would like to thank Drs Fiona Kerr, Teresa Niccoli, Nazif Alic and Ekin Bolukbasi for technical advice and useful discussions, and Filiz Senbabaoglu and Helena Cantwell for technical assistance. We also thank Kerrie Venner for help with electron microscopy and Dr Una Sheerin for help with patient fibroblast sample collection. We also thank the TRiP at Harvard Medical School (NIH/NIGMS R01-GM084947) for providing a transgenic RNAi fly stock used in this study, and Dr Mikhail S. Shchepinov (Retrotope, Inc) for providing D-PUFAs.

Funding

K.J.K, L.P. and J.H. are funded by the Wellcome Trust. F.B. is supported by a fellowship from the Spanish Ministerio de Educacion through the FECYT and partially supported by an ALS Association Initiated award (ID 2109) and Motor Neuron Disease Association Small Grants (Hardy/Oct12/6603). L.P. is also supported by the Max Planck Society. This work was also supported by the Welcome Trust MRC strategic neurodegenerative disease initiative award (Ref. number WT089698). K.J.K. was the recipient of a post-doctoral Wellcome Trust fellowship (Ref. number 090541/Z/09/Z). Part of this work was undertaken at the University College of London Hospitals who received a proportion of their funding from the Department of Health's NIHR Biomedical Research Centres funding scheme. K.B.B. was also funded by a Parkinson's UK Grant (Ref. number G-1009). L.L. is also the recipient of a Parkinson's UK PhD studentship (Ref. number H-1105).

Supplementary material

Supplementary material is available at *Brain* online.

References

Ballard JW, Melvin RG, Simpson SJ. Starvation resistance is positively correlated with body lipid proportion in five wild caught Drosophila simulans populations. J Insect Physiol 2008; 54: 1371–6.

Brand AH, Perrimon N. Targeted gene expression as a means of altering cell fates and generating dominant phenotypes. Development 1993; 118: 401–15.

Beck G, Sugiura Y, Shinzawa K, Kato S, Setou M, Tsujimoto Y, et al. Neuroaxonal dystrophy in calcium-independent phospholipase A2β deficiency results from insufficient remodeling and degeneration of mitochondrial and presynaptic membranes. J Neurosci 2011; 31: 11411–20.

Castilho RF, Meinicke AR, Almeida AM, Hermes-Lima M, Vercesi AE. Oxidative damage of mitochondria induced by Fe (II) citrate is potentiated by Ca2 + and includes lipid peroxidation and alterations in membrane proteins. Arch Biochem Biophys 1994; 308: 158–63.

Chance B, Williams GR. A simple and rapid assay of oxidative phosphorylation. Nature 1955; 175: 1120–1.

Cheon Y, Kim HW, Igarashi M, Modi HR, Chang L, Ma K, et al. Disturbed brain phospholipid and docosahexaenoic acid metabolism in calcium-independent phospholipase A(2)-VIA (iPLA(2)β)-knockout mice. Biochim Biophys Acta 2012; 1821: 1278–86.

Clark IE, Dodson MW, Jiang C, Cao JH, Huh JR, Seol JH, et al. *Drosophila* pink1 is required for mitochondrial function and interacts genetically with parkin. Nature 2006; 441: 1162–6.

Appendix 3

Castillo-Quan, J.I., **Li, L.**, Kinghorn, K.J., Ivanov, D.K., Tain, L.S., Slack, C., Kerr, F., Nespital, T., Thornton, J., Hardy, J., et al. (2016). Lithium Promotes Longevity through GSK3/NRF2-Dependent Hormesis. Cell Rep *15*, 638-650.

OPEN ACCESS
CellPress

Cell Reports
Article

Lithium Promotes Longevity through GSK3/NRF2-Dependent Hormesis

Jorge Iván Castillo-Quan,[1,2,3] Li Li,[1,3] Kerri J. Kinghorn,[1,3] Dobril K. Ivanov,[4] Luke S. Tain,[2] Cathy Slack,[1,2] Fiona Kerr,[1] Tobias Nespital,[2] Janet Thornton,[4] John Hardy,[3] Ivana Bjedov,[1,5] and Linda Partridge[1,2,*]

[1]Institute of Healthy Ageing and Department of Genetics, Evolution and Environment, University College London, Darwin Building, Gower Street, London WC1E 6BT, UK

[2]Max Planck Institute for Biology of Ageing, Joseph-Stelzmann Strasse 9-b, 50931 Köln, Germany

[3]Department of Molecular Neuroscience, Institute of Neurology, University College London, Queen Square, London WC1N 3BG, UK

[4]European Molecular Biology Laboratory, European Bioinformatics Institute (EMBL-EBI), Wellcome Trust Genome Campus, Hinxton, Cambridge CB10 1SD, UK

[5]UCL Cancer Institute, Paul O'Gorman Building, 72 Huntley Street, London WC1E 6BT, UK

*Correspondence: l.partridge@ucl.ac.uk

http://dx.doi.org/10.1016/j.celrep.2016.03.041

SUMMARY

The quest to extend healthspan via pharmacological means is becoming increasingly urgent, both from a health and economic perspective. Here we show that lithium, a drug approved for human use, promotes longevity and healthspan. We demonstrate that lithium extends lifespan in female and male *Drosophila*, when administered throughout adulthood or only later in life. The life-extending mechanism involves the inhibition of glycogen synthase kinase-3 (GSK-3) and activation of the transcription factor nuclear factor erythroid 2-related factor (NRF-2). Combining genetic loss of the NRF-2 repressor Kelch-like ECH-associated protein 1 (Keap1) with lithium treatment revealed that high levels of NRF-2 activation conferred stress resistance, while low levels additionally promoted longevity. The discovery of GSK-3 as a therapeutic target for aging will likely lead to more effective treatments that can modulate mammalian aging and further improve health in later life.

INTRODUCTION

Lithium is the most commonly prescribed drug for the treatment of bipolar disorder. It also improves disease phenotypes in animal models of many clinical conditions including Alzheimer disease, depression, and stroke (Chiu and Chuang, 2010). The effects of lithium on aging have been documented in yeast and *Caenorhabditis elegans*, with lithium extending lifespan (McColl et al., 2008; Zarse et al., 2011; Tam et al., 2014; Sofola-Adesakin et al., 2014). The effects of lithium on *Drosophila* aging have previously been inconclusive, with demonstration of both positive and negative effects on survival (Matsagas et al., 2009; Zhu et al., 2015). Moreover, lithium concentration in the drinking water of a large Japanese population has been associated with reduced all-cause mortality (Zarse et al., 2011), suggesting that lithium may be a bona fide anti-aging drug. However, the mechanisms by which lithium acts in humans remain poorly understood.

In vitro studies have reported that lithium can protect against several forms of oxidative and xenobiotic stressors (Lai et al., 2006; Schäfer et al., 2004), but in vivo evidence for such protective effects of lithium is lacking. Longevity has been extensively correlated with resistance to stress (Minois, 2000; Rattan, 2008; Calabrese et al., 2011; Epel and Lithgow, 2014). Transcriptomic analysis of interventions known to extend lifespan have identified particular genes likely to be involved in stress resistance (McElwee et al., 2007; Steinbaugh et al., 2012). Up-regulation of the transcription factor cap'n'collar C (CncC, an NRF-2 homolog) has been shown not only to confer resistance to toxic compounds, but also to promote longevity in *C. elegans* and flies (Tullet et al., 2008; Sykiotis and Bohmann, 2008; Ewald et al., 2015). In flies and mammals, NRF-2/CncC is negatively inhibited through cytosolic sequestration and proteasomal degradation by the canonical Keap1 (Hayes and Dinkova-Kostova, 2014; Pitoniak and Bohmann, 2015). However, a second emerging upstream regulator of NRF-2/CncC is GSK-3, a well-documented target of lithium (Jope, 2003; Hayes and Dinkova-Kostova, 2014; Cuadrado, 2015; Hayes et al., 2015; Blackwell et al., 2015). GSK-3 regulates NRF-2 by phosphorylation and nuclear exclusion, an effect that is evolutionarily conserved from invertebrates to mammals (Salazar et al., 2006; An et al., 2005). Interestingly, GSK-3 inhibition has been shown to phenocopy the effects of lithium for protection against xenobiotic stress in vitro (Lai et al., 2006; Schäfer et al., 2004).

Activation of NRF-2/CncC produces hormetic effects on lifespan, such that at low level NRF-2/CncC activity extends lifespan while higher levels of activation limit it (Mattson, 2008; Maher and Yamamoto, 2010). Interestingly a hormetic signature was recently reported for the survival of a mammalian cell line treated with lithium (Suganthi et al., 2012), suggesting that lithium and GSK-3 inhibition could influence

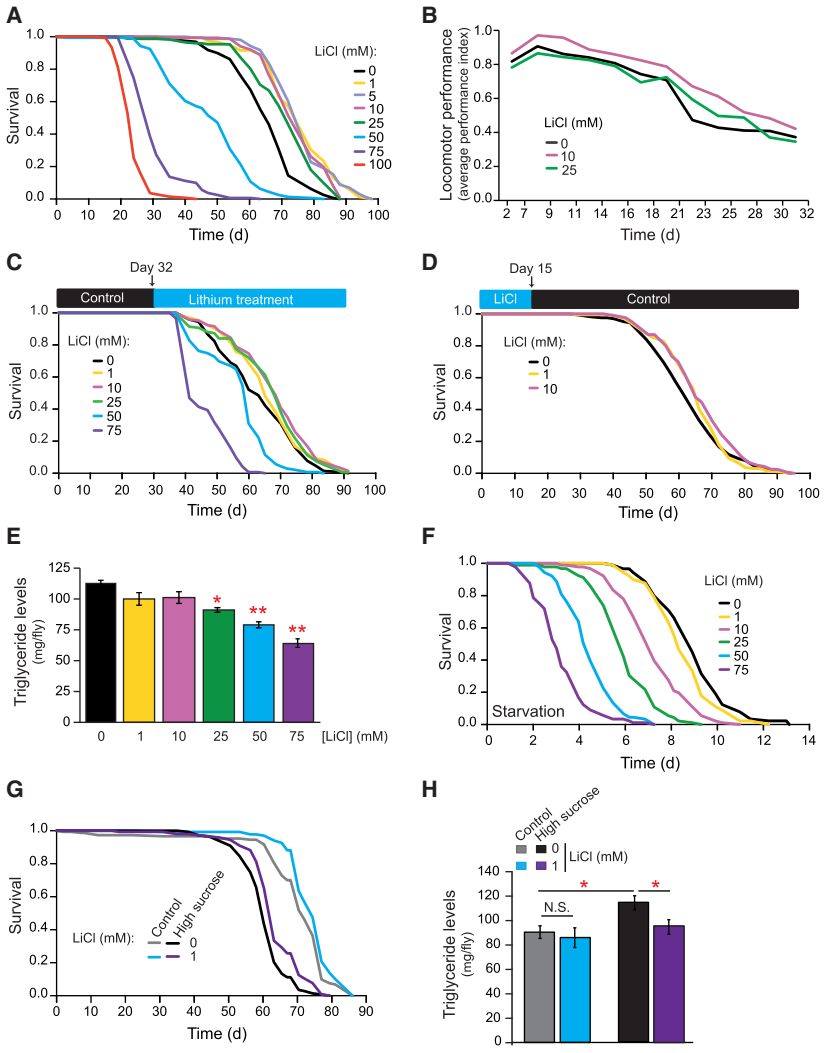

Figure 1. Lithium Regulated Longevity and Metabolism in *Drosophila*

(A) Lithium extended lifespan of w^{Dah} *Drosophila* females (n = 160 flies per condition) at concentrations between 1 and 25 mM (+16% and +18% median and maximum lifespan extension; $p < 0.001$), but resulted in a dose-dependent reduction in lifespan at concentrations between 50 and 100 mM ($p < 0.001$).

(B) Lithium treated female w^{1118} flies showed a significant improvement and protection against age-related locomotor decline ($p < 0.01$, two-way ANOVA for 10 mM).

(C) Lithium extended lifespan of aged, 32-day-old female w^{Dah} flies at concentrations from 1 to 25 mM (30 days later than in Figure 1A): 1 mM extended median lifespan by 5% (4 days) and maximum lifespan by 13% (8 days; $p < 0.05$); 10 and 25 mM lithium increased median lifespan by 9% (6 days); 10 mM increased maximum lifespan by 4.5% (3.5 days); whereas 25 mM lengthened it by 8% or 6 days ($p < 0.01$); and 50 and 75 mM significantly shortened lifespan ($p < 0.01$). n = 150 flies per condition.

(D) Brief treatment with lithium for 15 days early in adulthood extended lifespan of female w^{Dah} flies ($p < 0.05$ for 1 mM and $p < 0.01$ for 10 mM; n = 150 flies per condition).

(E) Lithium induced a dose-dependent reduction in triglyceride levels. Bars represent means of six replicas of five flies per condition ± SEM. *$p < 0.01$, **$p < 0.001$.

(F) Female w^{Dah} flies pre-treated with lithium for 15 days were subsequently sensitive to starvation in a dose-dependent manner (n = 90 flies per condition).

(G) Lithium treatment significantly extended the lifespan of w^{1118} female flies exposed to a four times higher sucrose concentration (2g/L; $p < 0.001$; n = 120 flies per condition).

(H) The increase of triglycerides observed on a high-sucrose diet was completely blocked after 15 days of treatment with 1 mM lithium. Bars represent means of six replicas of five w^{1118} female flies per condition ± SEM. *$p < 0.01$.

animal lifespan and stress resistance through activation of NRF-2.

Here we show that lithium supplementation in the diet can modulate longevity, stress resistance, and metabolism in *Drosophila* through the inhibition of GSK-3. Correspondingly, genetic downregulation of GSK-3 and lithium treatment are epistatic, suggesting a common molecular pathway. We also show that lithium and the genetic inhibition of GSK-3 promote xenobiotic stress resistance and lifespan extension through the activation of a transcriptional response mediated by CncC/NRF-2. Furthermore, lithium protects against a high-sucrose diet and acts through mechanisms that only partially overlap with those mediating lifespan extension by dietary restriction (DR). These findings demonstrate an alternative genetic and pharmacological target for the promotion of longevity and stress resistance, and emphasize the potential of pharmacological inhibitors of GSK-3 as viable anti-aging treatments.

RESULTS

Lithium Extends Healthy Lifespan in *Drosophila*

To assess the role of lithium in *Drosophila* aging, we treated adult female flies with lithium chloride (LiCl) by supplementation in their food. Lithium treatment in the range of 1 to 25 mM resulted in lifespan extension, whereas higher doses (50–100 mM) shortened lifespan (Figure 1A). These effects of lithium treatment on lifespan extension were also observed in an independent genetic background (Figure S1A) and in males (Figure S1B). Thus, lithium treatment extended *Drosophila* lifespan independently of genetic background and sex.

To ensure that the increased lifespan observed with lithium supplementation was dependent on the addition of lithium itself, we treated flies with equivalent molar concentrations of sodium chloride (NaCl) and found no lifespan extension (Figures S1C and S1D). Thus, the pro-longevity effect of LiCl is specific to lithium and not its chloride counterion.

Interestingly, we observed that, unlike with many other genetic and pharmacological interventions (e.g., DR, insulin/IGF down-regulation, rapamycin, or trametinib treatment), lithium did not reduce fecundity at life-extending doses or compromise feeding behavior (Figures S1E and S1F). Moreover, it delayed locomotor decline at two concentrations that extend lifespan (Figure 1B). Thus, lithium promotes healthspan in adult *Drosophila* with limited side effects.

Lithium Extends Lifespan in Mid-life or with Short-Term Treatment in Young Flies

To limit the side effects of long-term use, a drug that improves lifespan and healthspan will ideally do so with late-onset administration (Castillo-Quan et al., 2015; Longo et al., 2015). We therefore assessed the effect of commencing lithium treatment at older ages. Flies were switched onto food containing a range of lithium concentrations (1–75 mM) at 32 days of age (Figure 1C). Lower doses (1–25 mM) of lithium extended lifespan, whereas higher doses (50 and 75 mM) significantly reduced lifespan, similar to the dose-dependent effects we observed in younger flies.

We also tested whether transient lithium treatment early in life could increase lifespan. We therefore exposed young flies to 1 or 10 mM lithium for 15 days and then switched them to control food for the remainder of their lifespans. Early treatment with these doses of lithium extended lifespan (Figure 1D). Lithium treatment early in life, and for a transient period, can therefore increase survival later in life.

Lithium Alters Lipid Metabolism and Promotes Survival under a High-Sugar Diet

Genetic and environmental interventions that extend lifespan often induce abnormalities in carbohydrate and lipid metabolism (Barzilai et al., 2012; Wang et al., 2014; Lamming et al., 2013). We therefore examined the effects of lithium on whole body trehalose, glycogen, and triglyceride levels. Following 15 days of lithium treatment, and over a wide range of lithium concentrations, we were unable to detect a significant change in the levels of either trehalose or glycogen (Figures S1G and S1H). However, we observed a dose-dependent reduction in whole body triglycerides, the main lipid storage in flies (Ballard et al., 2008; Skorupa et al., 2008) (Figures 1E and S1I). In keeping with the lowered triglyceride levels (Ballard et al., 2008; Ulgherait et al., 2014), lithium treatment reduced survival under starvation conditions in a dose-dependent manner (Figures 1F and S1J). Moreover, lithium also extended lifespan under dietary conditions that promote triglyceride accumulation (Skorupa et al., 2008). Flies fed a high-sucrose diet were short lived and lithium was able to partially rescue this defect (Figure 1G) while completely blocking the increase in triglycerides observed with a sucrose-rich diet (Figure 1H). Therefore, lithium can extend lifespan under obesogenic dietary conditions.

Lithium and DR Extend Lifespan via Partially Overlapping Mechanisms

We next investigated whether lithium treatment was acting as a DR mimetic. DR is a well-established anti-aging intervention that extends healthy lifespan in diverse species (de Cabo et al., 2014; Fontana and Partridge, 2015), and some pharmacological and genetic interventions that extend lifespan have features of DR mimetics (Ingram and Roth, 2015; de Cabo et al., 2014). To determine whether lithium and DR extend lifespan by similar mechanisms, we assessed whether lithium could extend lifespan beyond the maximum achievable by DR. To maximize lifespan under DR, we varied the yeast concentration in the food while maintaining a constant concentration of sucrose (Bass et al., 2007), resulting in a typical tent-shaped response, with peak lifespan at food containing a 1.0 yeast concentration (Figures 2A and S2A–S2D). If lithium treatment and DR share overlapping pathways, then lithium would not be able to further extend lifespan already maximized by DR (Gems et al., 2002; Castillo-Quan et al., 2015). All lithium doses tested significantly extended median lifespan in both the yeast condition that maximized lifespan (1.0 yeast; Figures 2A and S2C) and under full feeding (2.0 yeast; Figures 2A and S2D), with greatest extension of median lifespan with 10 mM lithium under full feeding. However, under reduced yeast concentrations that shorten lifespan (0.2 and 0.5 yeast), 10 mM lithium either significantly reduced lifespan (Figure S2B) or did not confer a significant lifespan benefit (Figure S2A). Cox proportional hazards analysis showed a significant interaction between lithium and yeast concentrations for lifespan (interaction term $p < 0.0001$). The extension of lifespan from lithium increased with the level of yeast in the fly diet, suggesting partially overlapping mechanisms to those of DR.

Lithium Extends Lifespan through Inhibition of GSK-3

A well-known target of lithium is GSK-3 (Phiel and Klein, 2001; Jope, 2003; Eldar-Finkelman and Martinez, 2011). We therefore evaluated the phosphorylation status of the fly ortholog of GSK-3, Shaggy (Sgg), in response to lithium treatment. Lithium addition to the fly medium resulted in a dose-dependent increase in the inhibitory phosphorylation (Serine 9 or S9) of Sgg (Figure 2B). To evaluate the role of Sgg in lithium-mediated lifespan extension, we directly manipulated its activity in adult flies. Ubiquitous overexpression of wild-type or constitutively active Sgg (SggS9A) significantly reduced lifespan by ~30% and 50%, respectively (Figures 2C and S2E). This reduction in lifespan was almost completely reversed by lithium treatment. Furthermore, RNAi-mediated reduction in *sgg* expression using two independent dsRNA-expressing transgenes significantly increased lifespan (Figures 2D and S2F). Importantly, lithium was unable to further increase the lifespan of these *sgg* RNAi knockdown mutants flies (Figure 2D). Taken together, these findings suggest that Sgg/GSK-3 inhibition and lithium treatment increase lifespan by acting on the same downstream targets.

Lithium Activates the Cap'n'Collar C/NRF-2 Transcription Factor

To identify downstream mediators of lifespan extension by lithium and of GSK-3 inhibition, we analyzed the genome-wide transcript profiles of lithium-treated flies using microarrays. Genes encoding ribosomal proteins were among the most upregulated (Figure 3A) and downregulated (Figure S3A) gene ontology (GO) categories in lithium-treated flies. This transcriptional response could underlie the translational repression following lithium treatment that has been previously observed

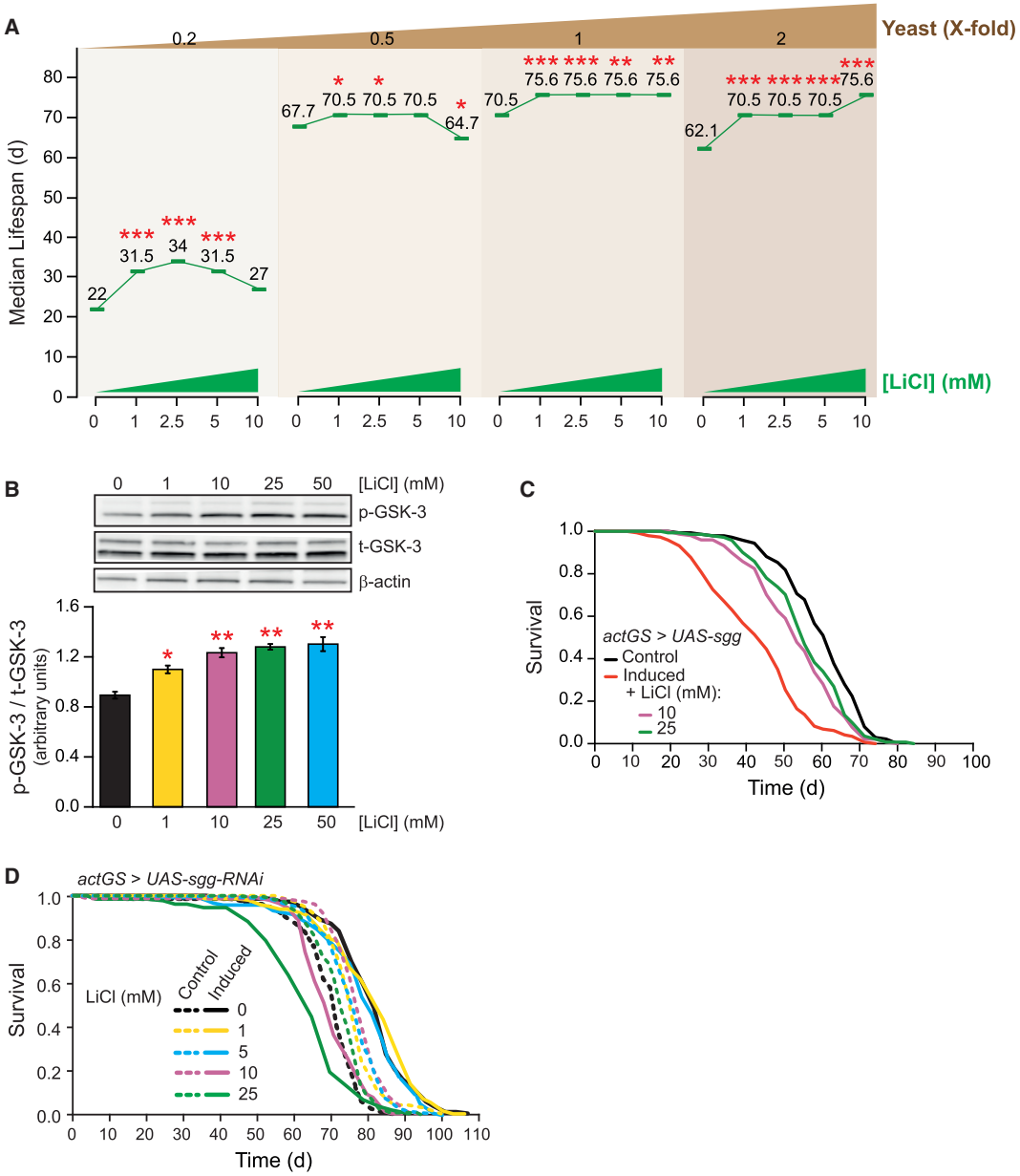

Figure 2. Lithium Extended Lifespan beyond Dietary Restriction by Inhibiting Sgg/GSK-3

(A) Median lifespans at different lithium concentrations (0, 1, 2.5, 5, or 10 mM) are plotted for four different yeast concentrations (0.2×, 0.5×, 1.0×, and 2.0× yeast): 1–5 mM lithium extended lifespan under all dietary conditions tested. Although 10 mM lithium prolonged life at 1.0× and 2.0×, it showed no effect at 0.2× and significantly shortened lifespan at 0.5× yeast. *$p < 0.05$, **$p < 0.01$, ***$p < 0.001$, from 0 lithium; n = 160 flies per condition. Complete survival curves are shown in Figures S2A–S2D.

(B) Lithium treatment for 15 days significantly increased the inhibitory phosphorylation of Sgg/GSK-3 in a dose-dependent manner. Bars represent means of triplicates of ten flies per biological repeat ± SEM, *$p < 0.05$, **$p < 0.01$.

(C) Ubiquitous overexpression of wild-type *sgg* significantly shortened lifespan ($p < 0.001$) and this was partially rescued by lithium treatment at two concentrations (10 and 25 mM; $p < 0.001$). See Figure S2E for the interaction of *sgg(S9A)* and lithium treatment on lifespan.

(D) Ubiquitous RNAi-mediated downregulation of *sgg* extended lifespan ($p < 0.001$) and no further extension occurred when the flies were treated with 1 or 5 mM lithium ($p > 0.05$), whereas 10 mM lithium treatment restored the lifespan to control levels ($p > 0.05$), and 25 mM was significantly toxic ($p > 0.05$). See Figure S2F for lifespan extension obtained with an independent RNAi line.

in fission yeast and *Drosophila* heads (Sofola-Adesakin et al., 2014). In addition, five GO terms for genes encoding enzymes in the detoxification pathway were also in the ten most upregulated categories (Figure 3A).

The responses to xenobiotics and oxidative stress in *Drosophila* are regulated by the transcription factors dFOXO, CncC, and DHR96 (Salih and Brunet, 2008; Sykiotis and Bohmann, 2010; Tullet, 2015; Hoffmann and Partridge, 2015; Blackwell et al., 2015). We therefore assessed whether the transcriptional responses to activation of these transcription factors overlapped with that of lithium treatment. The transcriptomic response to lithium did not overlap with that of dFOXO-dependent or -independent transcriptional regulation downstream of IIS (Figures S3B and S3C) (Alic et al., 2011). Furthermore, although we detected a significant overlap in the transcriptional signatures of lithium and DHR96 (King-Jones et al., 2006), they did not share the same directionality (Figure S4). However, we found a significant overlap (Figure 3B) between the genes that were upregulated by lithium and *cncC* overexpression (Misra et al., 2011), but not between genes downregulated by both treatments (Figure S5A), suggesting that lithium might activate a CncC transcriptional response downstream of GSK-3. The barbiturate phenobarbital activates CncC and induces a similar transcriptional response to that of *cncC* overexpression (Misra et al., 2011). We therefore analyzed the overlap between the transcriptional profiles induced by lithium and phenobarbital treatment, and again found a significant overlap (Figure 3B) between upregulated, but not downregulated, genes (Figure S5B). The genes upregulated in common between lithium treatment, phenobarbital treatment and *cncC* overexpression (Figures 3B and S5C) encoded enzymes that participate in all three phases of xenobiotic metabolism (Figure 3C). To further confirm the activation of CncC by lithium, we used a previously generated CncC reporter that responds to both chemical and genetic inducers of CncC (Sykiotis and Bohmann, 2008). Flies carrying the GstD-eGFP CncC reporter showed a dose-dependent increase in GFP expression with increasing concentrations of lithium (Figure 3D). Taken together, our results suggest that lithium activates CncC to upregulate the expression of genes in the detoxification pathway.

Lithium Induces Lifespan-Extension, Hormesis, and Protection against Xenobiotics via CncC-Dependent Mechanisms

We next assessed whether CncC activity is required for the pro-longevity effects of lithium. Ubiquitous, RNAi-mediated knockdown of *cncC* expression blocked the lifespan extension of 1 to 10 mM lithium, but was detrimental to survival in flies treated with 25 mM lithium, the highest dose that extends lifespan under basal conditions, albeit to a lesser extent (Figure 4A). Thus, lithium treatment requires CncC activity to confer its longevity benefits.

Because CncC/NRF-2 can induce hormesis (Mattson, 2008; Maher and Yamamoto, 2010), we assessed whether lithium can also do this. To test for a hormetic effect of lithium at low doses, we pre-treated flies with a range of concentrations of lithium and then challenged them with a toxic dose of 500 mM. Most pre-treatment doses of lithium induced subsequent resistance to the toxic dose (Figure 4B). To assess whether the hormetic response of lithium was mediated by CncC, we knocked down expression of *cncC* using RNAi, and treated the flies with 1–25 mM lithium. Reduction in *cncC* expression completely blocked the hormetic response induced by 10 mM lithium pre-treatment, and significantly reduced the effect of 25 mM lithium (Figure 4C).

We next assessed the ability of lithium pre-treatment to protect against other xenobiotics. Flies pre-treated with increasing concentrations of lithium ranging from 1 to 100 mM were significantly resistant to a toxic concentration of phenobarbital, with lithium doses between 1 and 75 mM almost doubling survival (Figure 4D). Lower doses of lithium also protected against a toxic dose of the anti-malarial drug, chloroquine (Figure S5D; 1–10 mM), and the pesticide paraquat (Figure 4E). Thus, low to intermediate concentrations of lithium protect against xenobiotic toxicity. To determine the role of CncC activity in lithium-mediated protection against phenobarbital, we used RNAi to knock down expression of *cncC*, which sensitized the flies to phenobarbital and completely abrogated the protection against phenobarbital afforded by lithium supplementation (Figure 4F). Thus, CncC is at least partly responsible for the hormetic effect induced by low-level treatment with lithium.

To confirm that Sgg, upstream of CncC, is also necessary for the resistance to xenobiotic stress (Blackwell et al., 2015; Cuadrado, 2015; Hayes et al., 2015), we assessed the effect of ubiquitous overexpression of wild-type *sgg* or the constitutively active Sgg(S9A) on xenobiotic resistance. Both significantly sensitized flies to phenobarbital (Figures 5A and S5E). We confirmed that *sgg* or *sgg(S9A)* overexpression regulated CncC by showing significantly lower levels of *MRP* and *keap1* (Figures 5B and S5F), both CncC target genes. Correspondingly, RNAi-mediated knockdown of *sgg* resulted in resistance to phenobarbital (Figure 5C), and paraquat (Figure S5G). An increase of mRNA levels of *cncC*, *keap1*, and *gstD2* confirmed that CncC was active in *sgg* knockdown flies (Figure 5D). Thus, increased Sgg activity sensitizes against xenobiotic stressors, whereas its inhibition protects against them.

Lifespan and Stress Resistance Depend on the Degree of Activation of CncC by Keap1 and Lithium Treatment

In addition to activating CncC by repressing Sgg/GSK-3, lithium could potentially increase CncC activity by inhibiting its canonical repressor Keap1 (Cuadrado, 2015; Pitoniak and Bohmann, 2015). Hence, we analyzed the interaction between lithium treatment and Keap1. Overexpression of Keap1, which inhibits CncC activity in vivo (Sykiotis and Bohmann, 2008), was unable to prevent the lifespan-extending properties of lithium (Figure 6A), suggesting that the longevity effect of lithium treatment is independent of Keap1. Next, we analyzed the interaction of loss of Keap1 and lithium treatment. We generated a deletion of the *keap1* coding sequence by P-element-mediated male recombination using a previously described P-element insertion line (Sykiotis and Bohmann, 2008) (Figure 6B). The *keap1* deletion ($keap1^{Del}$) was homozygous lethal, but activated CncC 4-fold in the heterozygous state, as measured by the CncC reporter (Figure 6C). Lithium treatment of the $keap1^{Del}$ flies further activated CncC (Figure 6C). We next tested whether this effect on CncC

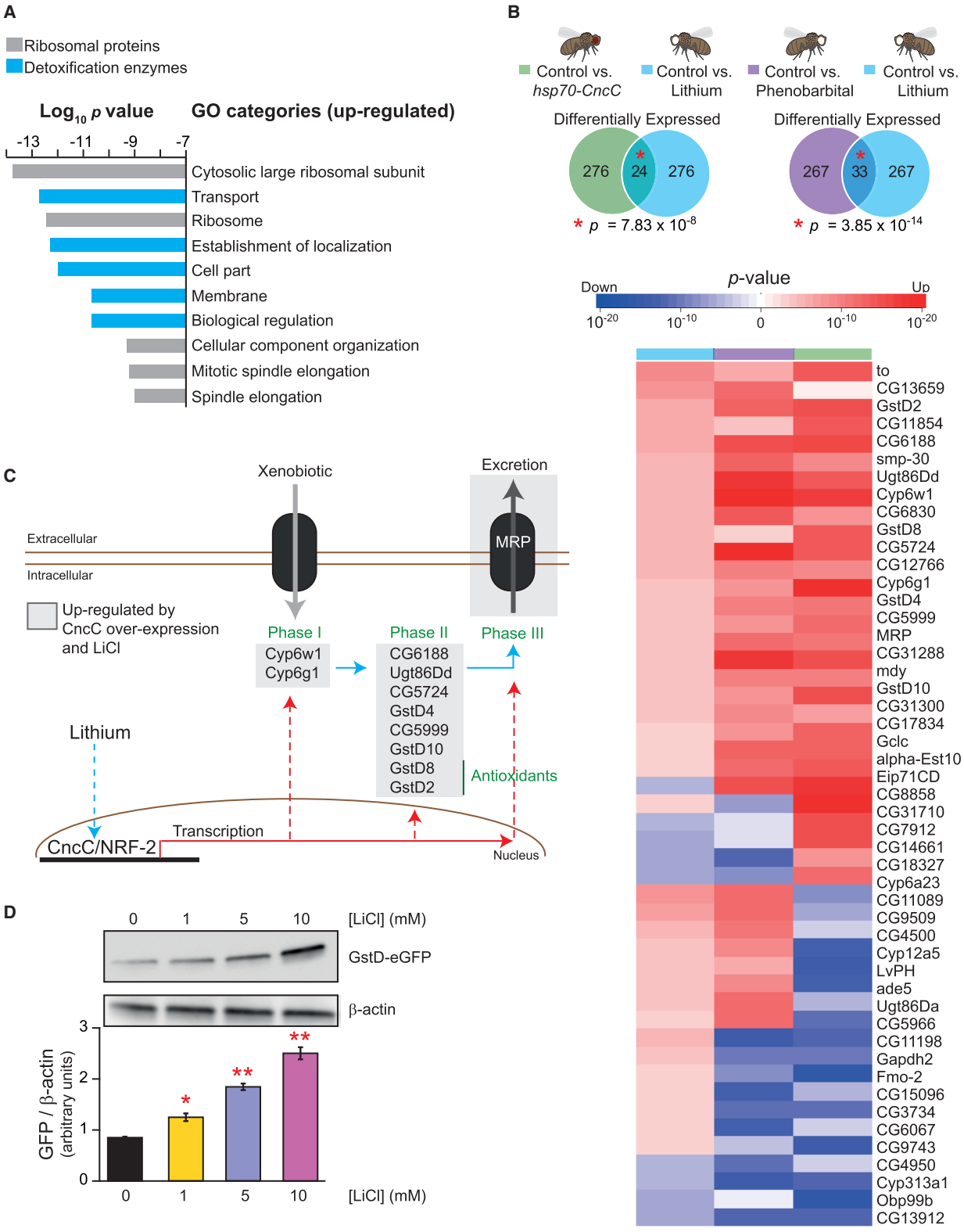

(legend on next page)

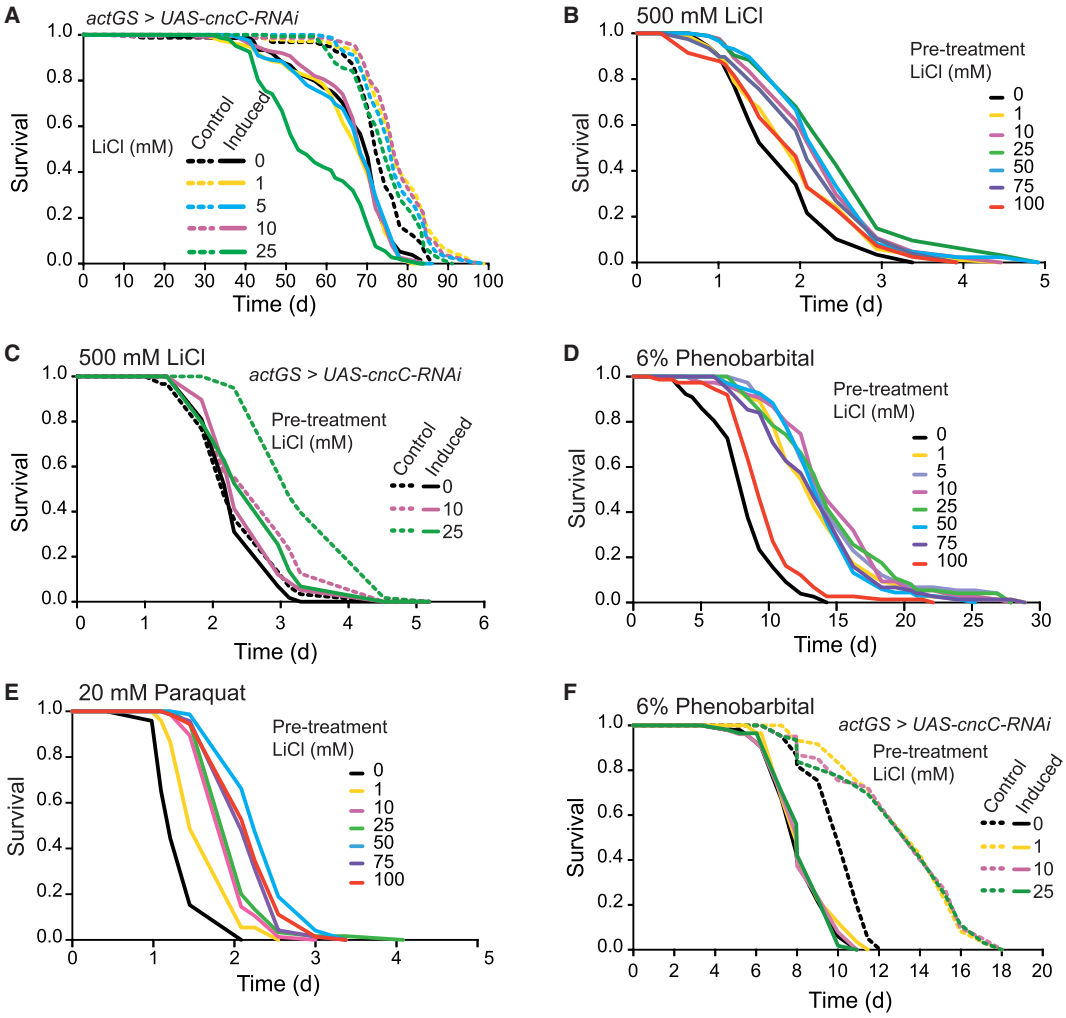

Figure 4. Lithium-Induced Xenobiotic Resistance and Longevity Were Mediated by CncC

(A) Ubiquitous knockdown of *cncC* blocked lifespan extension by lithium.

(B) Pre-treatment with increasing concentrations of lithium protected against a subsequent toxic dose of lithium (500 mM; $p < 0.01$ for doses from 10 to 100 mM; $p < 0.05$ for 1 mM).

(C) Ubiquitous downregulation of *cncC* blocked the protective effect of 10 mM lithium pre-treatment against a subsequent toxic dose and partially blocked the protective effect of 25 mM lithium pre-treatment.

(D) 1 to 100 mM lithium pre-treatment protected against a 6% phenobarbital ($p < 0.001$ for all doses).

(E) Lithium pre-treatment (for 15 days) protected against the herbicide paraquat in a dose-dependent manner ($p < 0.001$ for all doses, with maximal protection at 50 mM).

(F) RNAi-mediated downregulation of *cncC* completely blocked the protective effect of lithium against phenobarbital.

activation protected against paraquat and lithium toxicity. *keap1*^{Del} flies were significantly resistant to both paraquat and lithium (Figures 6D and 6E), and pre-treatment with lithium further protected them. We confirmed these findings using a previously described heterozygous loss-of-function mutation in the *keap1* gene (*keap1*^{EY5}) (Sykiotis and Bohmann, 2008) (Figures

Figure 3. Lithium Activated a Transcriptional Response Similar to that of CncC/NRF-2

(A) Ten most significantly upregulated GO categories induced by lithium treatment of w^{1118} female flies. See Figure S3A for downregulated GO categories.

(B) Lithium treatment of w^{1118} females flies induced a transcriptional response that significantly overlapped with that induced by *cncC* overexpression ($p = 7.83 \times 10^{-8}$) or phenobarbital treatment ($p = 3.85 \times 10^{-14}$) (Misra et al., 2011). Heatmap showing the 57 genes most significantly changed by lithium or phenobarbital treatment and overexpression of *cncC*.

(C) Genes upregulated by lithium treatment mapped to the three phases of the xenobiotic detoxification pathway in flies.

(D) Lithium treatment of w^{Dah} female flies upregulated Gst-D protein levels. Bars represent means of triplicates of ten flies per condition ± SEM. *$p < 0.05$, **$p < 0.01$.

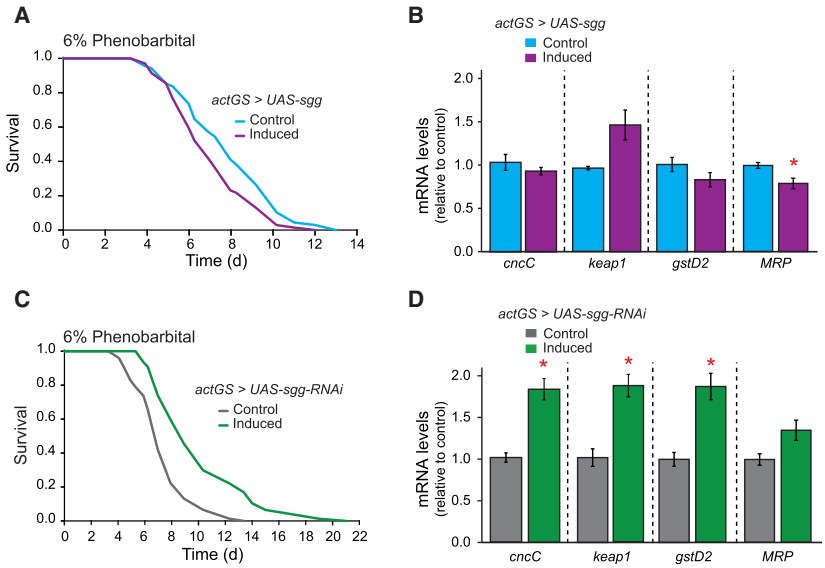

Figure 5. Reduced Activity of GSK-3 Increased Resistance to Xenobiotics

(A) Ubiquitous overexpression of wild-type *sgg* significantly ($p < 0.05$) reduced survival under xenobiotic stress with phenobarbital. n = 75 flies per condition.

(B) Overexpression of wild-type *sgg* significantly reduced multidrug-resistance like protein 1 (*MRP*) mRNA levels ($p < 0.05$, paired t test), whereas non-significant trends were detected for glutathione S transferase D2 (*gstD2*) and *cncC* mRNA levels ($p > 0.05$). A non-significant increase of *keap1* mRNA levels was observed.

(C) RNAi-mediated knockdown of *sgg* protected against phenobarbital stress ($p < 0.001$). n = 75 flies per condition.

(D) Knockdown of *sgg* increased mRNA levels of *cncC*, *keap1* and *gstD2* ($p < 0.05$), while a non-significant increase was observed for *MRP* mRNA levels.

S6A and S6B). Thus, the combination of loss of *keap1* and lithium treatment further protected against paraquat and lithium-induced toxicity, suggesting that stronger CncC activation results in greater protection against these xenobiotics.

We subsequently evaluated the interaction between loss of *keap1* and lithium treatment for longevity. Survival analysis showed that the lifespan of $keap1^{Del}$ mutant flies was indistinguishable from controls, but that addition of 1 mM lithium marginally, yet significantly, extended lifespan (Figure 6F). Increasing the dose of lithium to 10 mM restored longevity to control levels. The $keap1^{EY5}$ mutant flies showed a significant lifespan extension (Figure 6G). However, supplementation of either 1 or 10 mM lithium to the $keap1^{EY5}$ mutant shortened lifespan in a dose-dependent manner. These results suggest that the level of activation of CncC that maximizes extension of lifespan is considerably lower than that which maximizes protection against toxic doses of lithium and paraquat.

Lithium Does Not Induce or Require Autophagy to Promote Longevity

Activation of autophagy has been proposed as a mechanism for the beneficial effects of lithium (Sarkar et al., 2005). We therefore analyzed the induction of autophagy by LC3-I/LC3-II (Atg8 in *Drosophila*) levels without detecting statistically significant changes. Indeed, there was a tendency for lower LC3-I that did not reach statistical significance (Figure S7A). Moreover, lithium treatment was able to extend the lifespan of flies with autophagy defects due to heterozygous loss of *atg1* (Figure S7B) (Lee et al., 2007). Thus, taken together our results do not immediately support a role for autophagy in the pro-longevity effects of lithium treatment, and strengthen our conclusion that they are mediated through the inhibition of GSK-3 and the subsequent activation of CncC/NRF-2 (Figure 7). However, it remains possible that induction of autophagy occurs in *atg1*-deficient flies, or that lithium induces autophagy in a tissue-specific manner.

DISCUSSION

Lithium Acts as a Pro-longevity Drug

Drug repurposing is the most promising approach for developing pharmacological agents to improve healthy aging. So far, two medically approved drugs, metformin and rapamycin, have been reported to promote longevity and provide health benefits across species from invertebrates to mammals (de Cabo et al., 2014; Madeo et al., 2014; Riera and Dillin, 2015). We and others have shown that lithium can extend lifespan in fission yeast, *C. elegans*, and *Drosophila* (McColl et al., 2008; Matsagas et al., 2009; Sofola-Adesakin et al., 2014). We also showed that this effect was common between two different laboratory strains and, unlike other interventions that seem to be more effective in females (Austad and Bartke, 2015), lithium similarly extended lifespan in both sexes.

Lifespan-extending drugs can often act like DR mimetics (Madeo et al., 2014; Ingram and Roth, 2015); hence, it was important to determine whether lithium was acting in a similar manner. While low doses of lithium were able to extend lifespan at all dietary levels tested, median lifespan extension was greatest under full feeding conditions. Our data thus suggest that lithium and DR act via partially overlapping mechanisms and confirms the observation made in *C. elegans* that lithium extends lifespan of *eat-2* mutants (McColl et al., 2008), a genetic model of DR in worms. Lithium also extended the lifespan of flies fed a diet enriched with sucrose, possibly by modulating lipid metabolism (Sykiotis et al., 2011; Pang et al., 2014; Karim et al., 2015; Steinbaugh et al., 2015). However, the role of CncC in modulating the triglyceride phenotype of lithium remains to be explored. Overall, our observations strongly suggest that lithium is a pro-longevity drug capable of extending lifespan at low doses independent of sex and genetic background, and under a variety of dietary conditions.

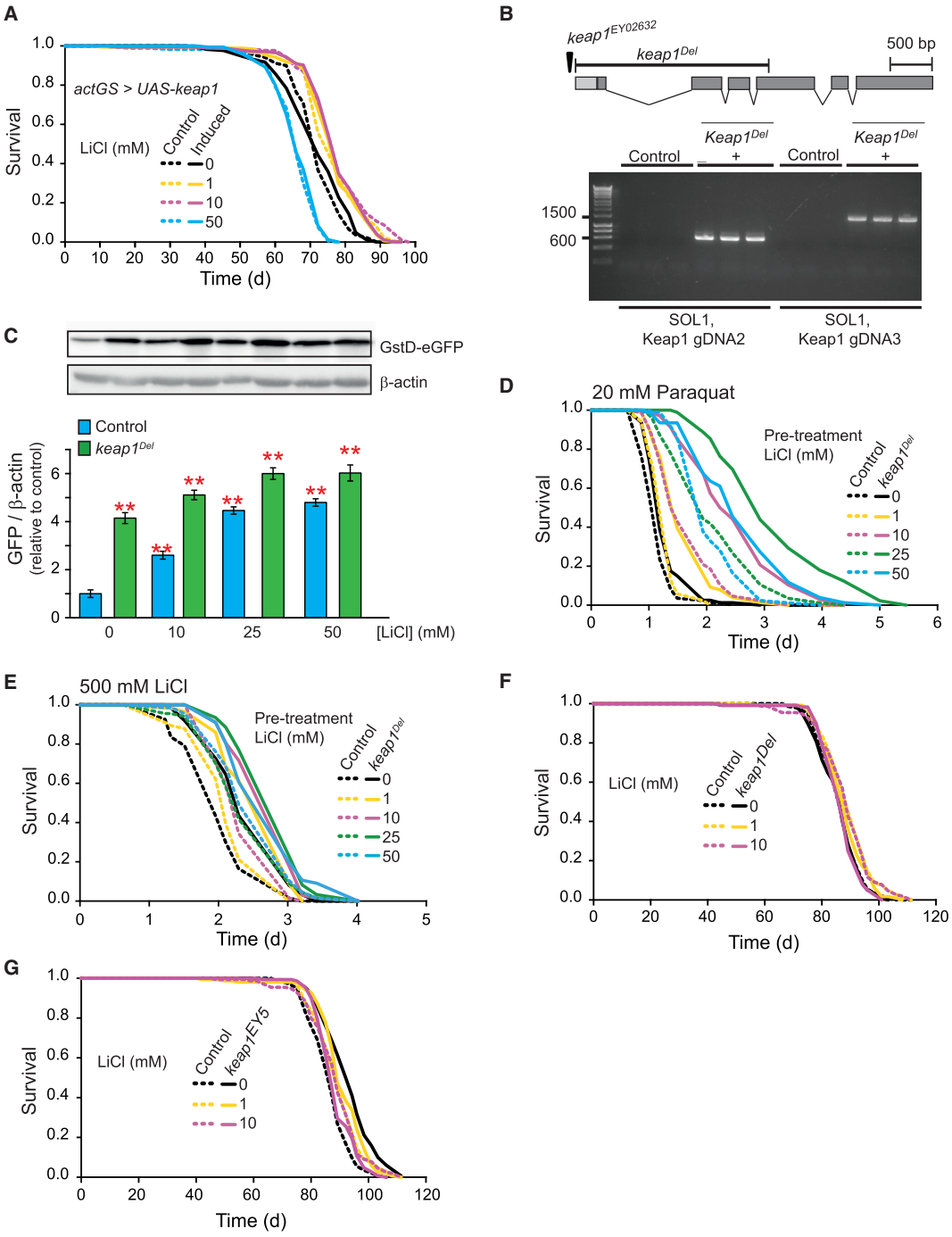

Figure 6. Higher Activation Levels of CncC Promote Xenobiotic Resistance but Not Lifespan

(A) Overexpression of *keap1* did not prevent the lifespan-modulatory effects of lithium treatment. n = 150 flies per condition.

(B) Schematic of the *keap1* gene showing the portion deleted in the $keap1^{Del}$ mutant (top) and agarose gel showing start and end of P-element disrupting *keap1* coding sequence in the $keap1^{Del}$ mutant (bottom).

(C) Combination of heterozygous deletion of *keap1* and lithium treatment showed a greater activation of CncC than on their own. Bars represent means of four replicas of five flies per repeat ± SEM. **p < 0.01.

(legend continued on next page)

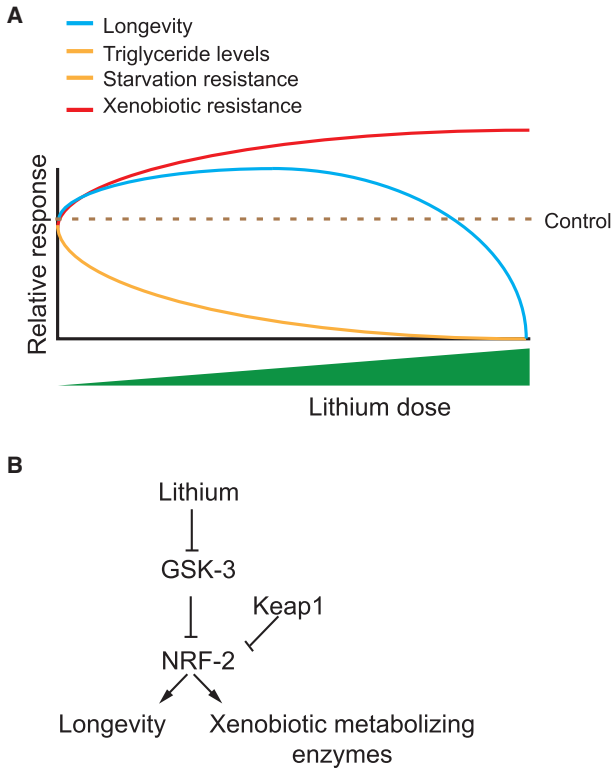

Figure 7. Lithium Regulates Longevity, Metabolism, and Stress Resistance by Inhibiting GSK-3 and Activating NRF-2

(A) Summary of findings with lithium for longevity, stress resistance, starvation, and triglyceride levels.

(B) Proposed model showing the mechanism by which lithium, Sgg/GSK-3, and CncC/NRF-2 act in the same pathway to modulate longevity and xenobiotic resistance.

Lithium Toxicity, Hormesis, and Stress Resistance

In humans, the therapeutic window for lithium treatment of bipolar disorder lies between 0.5 and 1 mM in serum, whereas concentrations of 1.5 mM and above severely increase the risk of tissue damage (Malhi and Tanious, 2011). Previous work in *Drosophila* suggests that the dose range at which we observed lifespan extension (0.5–25 mM) translates to *Drosophila* tissue concentrations below 0.5 mM (Dokucu et al., 2005). As previously reported for *C. elegans* and *Drosophila* (McColl et al., 2008; Zhu et al., 2015), concentrations above 50 mM were highly toxic.

Drug interventions to promote healthy lifespan are less likely to have side effects if started late in life (Castillo-Quan et al., 2015). Only a handful of drugs approved by the US Food and Drug Administration , namely rapamycin, metformin, and the Ras inhibitor trametinib, induce lifespan extension when commenced at later ages in model organisms (Harrison et al., 2009; Cabreiro et al., 2013; Martin-Montalvo et al., 2013; Slack et al., 2015). We found that lithium extends lifespan when first administered in mid-late life. In humans, long-term treatment with lithium for psychiatric disorders is associated with progressive and permanent renal damage (Malhi and Tanious, 2011). We showed that short treatment periods in *Drosophila*, 15 days during early adulthood, are sufficient to prolong life. Taken together, our data suggest that when testing lithium as a pro-longevity drug in mammals, lower doses than those used in psychiatric disorders are likely to be sufficient, and other strategies such as alternate-day dosing or transient treatment periods (either early or late in life), may be sufficient to reduce undesirable side effects and maximize the potential health benefits.

Interestingly, doses of lithium that shortened lifespan were protective against certain forms of xenobiotic stress. In vitro studies in mammalian cells have shown that lithium, and other GSK-3 inhibitors, protect against cell death caused by rotenone-induced oxidative stress (Lai et al., 2006), glutamate excitotoxicity, and H_2O_2 (Schäfer et al., 2004). This is likely mediated through a hormetic response (Suganthi et al., 2012), in this case orchestrated by NRF-2 activation. We observed that while simultaneous activation of CncC by loss of Keap1 and lithium treatment is additive and confers greater stress resistance to xenobiotics, the threshold for lifespan extension is perhaps considerably lower. A similar situation has been observed in *C. elegans* in which strong activation of the endoplasmic reticulum unfolded protein response conferred stress resistance benefits, while shortening lifespan (Taylor and Dillin, 2013). Our findings thus suggest that while NRF-2 activation either by loss of Keap1 or inhibition of GSK-3 is beneficial for longevity and stress resistance, at low levels of activation, stronger induction is detrimental for lifespan. This suggests that the hormetic benefits of lithium are more likely to occur at low levels under basal non-stress conditions (Calabrese, 2013). Hence, when testing for GSK-3 inhibitors or NRF-2 activators in modulating animal (and especially mammalian) aging, the degree of NRF-2 activation within the hormetic curve will determine positive or negative longevity outcomes. Future work studying the convergence of the salutary and damaging effects of lithium will aid in understanding to what extent the molecular mechanisms are shared (Calabrese and Mattson, 2011; Calabrese et al., 2013; Epel and Lithgow, 2014). Additionally, our microarray analysis was performed in heads and thoraces; therefore, it remains to be explored to what extent systemic or localized activation of NRF-2 modulates longevity, stress resistance, and lipid metabolism at the tissue level (Douglas et al., 2015).

(D) Deletion of *keap1* in flies treated with lithium showed greater protection against paraquat than either treatment on its own, with maximal effects observed at 25 mM ($p < 0.001$).

(E) The *keap1* deletion protected against toxic concentrations of lithium (500 mM), and this protection was augmented with lithium pre-treatment ($p < 0.01$).

(F) Deletion of *keap1* did not extend lifespan: 1 mM lithium ($p < 0.05$), but not 10 mM ($p > 0.05$), treatment of *keap1* flies resulted in a small but significant extension. n = 150 flies per condition.

(G) $keap1^{EY5}$ mutant flies showed significant lifespan extension ($p < 0.001$), that was dose-dependently abolished ($p > 0.05$) by lithium, likely as a result of overactivation of CncC. n = 150 flies per condition.

GSK-3 and NRF-2 as Drug Targets for Aging

Complete absence of GSK-3 in *C. elegans*, *Drosophila*, and mice shortens lifespan or prevents development (Hoeflich et al., 2000; McColl et al., 2008; Bourouis, 2002), while moderate inhibition has been associated with most of its positive effects (Avrahami et al., 2013). GSK-3 is upregulated in many disease states, including neurodegeneration, diabetes, inflammatory conditions, and some cancers (Takahashi-Yanaga, 2013). We have shown that adult-specific genetic manipulation of the fly ortholog of GSK-3, Sgg, affects longevity. Downregulation of Sgg prolonged lifespan and lithium was unable to further extend the lifespan, suggesting that lithium and inhibition of Sgg act through a common molecular pathway to extend lifespan.

In *C. elegans* and mammalian cells, GSK-3 directly interacts with NRF-2 to repress its activity, independently of Keap1 (An et al., 2005; Salazar et al., 2006; Rojo et al., 2008; Rada et al., 2012). Therefore, we hypothesized that lithium might act via Sgg/GSK-3, to de-repress CncC, the fly ortholog of NRF-2 and activate the oxidative and xenobiotic stress transcriptional signature (An et al., 2005; Hayes et al., 2015), which in turn would induce a CncC/NRF-2-dependent protective response (Jones et al., 2015; Blackwell et al., 2015). GO enrichment analysis identified a transcriptional signature that indeed suggested that lithium acts via CncC/NRF-2. CncC activity was indispensable for the lifespan extension conferred by lithium. In keeping with our results, work in rodents and mammalian cell lines has shown that lithium treatment and GSK-3 inhibition activate NRF-2 (Lee et al., 2014; Rizak et al., 2014). Because activation of CncC/NRF-2 modulates longevity in *C. elegans* and *Drosophila* (Tullet et al., 2008; Sykiotis and Bohmann, 2008; Ewald et al., 2015), our results provide evidence that GSK-3 is a viable therapeutic target to promote longevity via activation of NRF-2.

To date, the only GSK-3 inhibitor approved for human use is lithium (Williams and Harwood, 2000; Meijer et al., 2004; Martinez et al., 2011). However, researchers and pharmaceutical companies have developed more selective GSK-3 inhibitors, some of which have already entered the early stages of clinical trials for obesity, Alzheimer disease, and progressive supranuclear palsy (Eldar-Finkelman and Martinez, 2011). Our results call for a reassessment of the potential use of GSK-3 inhibitors and NRF-2 activators as potential anti-aging compounds.

EXPERIMENTAL PROCEDURES

Fly Stocks and Husbandry

The w^{1118} stock was obtained from Bloomington *Drosophila* Stock Center. The control white *Dahomey* (w^{Dah}) stock has been maintained in large population cages with overlapping generations since 1970. The w^{Dah} stock was initially derived by incorporation of the w^{1118} mutation into the outbred *Dahomey* background by backcrossing (Bass et al., 2007). Further details concerning fly mutants can be found in the Supplemental Experimental Procedures.

Lithium Treatment

LiCl (Sigma) or NaCl (Sigma) were dissolved in ddH_2O at a concentration of 5 M before supplementing to the medium. Equivalent volumes of vehicle were supplemented to the medium to compensate for dilution.

Dietary Restriction Protocol

The DR protocol was performed as described previously (Bass et al., 2007).

Statistical Analyses

Statistical analyses were performed using Excel, GraphPad Prism, or JMP software version 9 (SAS Institute). Survival experiments were analyzed using log rank test. Other data were tested by one-way analyses of variance (ANOVA) and planned comparisons of means were made using Tukey-Kramer HSD test. Cox proportional hazards analysis was performed to compare interactions for survival.

ACCESSION NUMBERS

The accession number reported for the microarray data in this paper is ArrayExpress: E-MTAB-3809.

SUPPLEMENTAL INFORMATION

Supplemental Information includes Supplemental Experimental Procedures and seven figures and can be found with this article online at http://dx.doi.org/10.1016/j.celrep.2016.03.041.

AUTHOR CONTRIBUTIONS

J.I.C.-Q. and I.B. conceived the experiments. J.I.C.-Q., I.B., L.L., K.J.K., L.S.T., T.N., and F.K. performed the experiments. D.K.I. analyzed the microarray data. C.S. and I.B. contributed reagents. J.I.C.-Q., I.B., J.T., J.H., and L.P. supervised experiments/project. J.I.C.-Q. and L.P. wrote the manuscript. All authors approved the final submission.

ACKNOWLEDGMENTS

We thank Profs. D. Gems, M. Murphy, and D. Rubinsztein, and Drs. H. Cochemé, F. Cabreiro, S. Emran, Y. de la Guardia, M. Piper, N. Woodling, A. Gilliat, and O. Sofola-Adesakin for insightful advice and comments; Dr. N. Alic for advice and assistance with statistical testing; and Dr. D. Wieser for initial analysis of microarray data. We thank the Max Planck-Genome-centre Cologne (http://mpgc.mpipz.mpg.de/home/) for microarray analysis. We acknowledge funding from UCL Scholarships (to J.I.C.-Q.), the Max Planck Society (to J.I.C.-Q., L.S.T., C.S., T.N., and L.P.), European Research Council (to I.B. and L.P.), Research Into Ageing (to I.B. and L.P.), Wellcome Trust (to D.K.I., K.J.K., J.T., J.H., and L.P.), Parkinson's UK (to L.L. and L.P.), and Alzheimer's Research UK (to F.K. and L.P.).

Received: November 9, 2015
Revised: January 31, 2016
Accepted: March 10, 2016
Published: April 7, 2016

REFERENCES

Alic, N., Andrews, T.D., Giannakou, M.E., Papatheodorou, I., Slack, C., Hoddinott, M.P., Cochemé, H.M., Schuster, E.F., Thornton, J.M., and Partridge, L. (2011). Genome-wide dFOXO targets and topology of the transcriptomic response to stress and insulin signalling. Mol. Syst. Biol. *7*, 502.

An, J.H., Vranas, K., Lucke, M., Inoue, H., Hisamoto, N., Matsumoto, K., and Blackwell, T.K. (2005). Regulation of the Caenorhabditis elegans oxidative stress defense protein SKN-1 by glycogen synthase kinase-3. Proc. Natl. Acad. Sci. USA *102*, 16275–16280.

Austad, S.N., and Bartke, A. (2015). Sex Differences in Longevity and in Responses to Anti-Aging Interventions: A Mini-Review. Gerontology *62*, 40–46.

Avrahami, L., Licht-Murava, A., Eisenstein, M., and Eldar-Finkelman, H. (2013). GSK-3 inhibition: achieving moderate efficacy with high selectivity. Biochim. Biophys. Acta *1834*, 1410–1414.

Ballard, J.W.O., Melvin, R.G., and Simpson, S.J. (2008). Starvation resistance is positively correlated with body lipid proportion in five wild caught Drosophila simulans populations. J. Insect Physiol. *54*, 1371–1376.

Appendix 4

Kinghorn, K.J., Castillo-Quan, J.I., **Li, L.**, Bhatia, K.P., Abramov, A.Y., Hardy, J., and Partridge, L. (2016). Reply: Glial mitochondropathy in infantile neuroaxonal dystrophy: pathophysiological and therapeutic implications. Brain.

Appendix 5

Niccoli, T., Cabecinha, M., Tillmann, A., Kerr, F., Wong, C.T., Cardenes, D., Vincent, A.J., Bettedi, L., **Li, L.**, Gronke, S., et al. (2016). Increased Glucose Transport into Neurons Rescues Abeta Toxicity in *Drosophila*. Curr Biol.

Current Biology
Article

Increased Glucose Transport into Neurons Rescues Aβ Toxicity in *Drosophila*

Teresa Niccoli,[1] Melissa Cabecinha,[1] Anna Tillmann,[1] Fiona Kerr,[1] Chi T. Wong,[1] Dalia Cardenes,[1] Alec J. Vincent,[1] Lucia Bettedi,[1] Li Li,[1] Sebastian Grönke,[2] Jacqueline Dols,[2] and Linda Partridge[1,2,*]
[1]Institute of Healthy Ageing, Department of Genetics, Evolution and Environment (GEE), University College London, Darwin Building, Gower Street, London WC1E 6BT, UK
[2]Max Planck Institute for Biology of Ageing, Joseph-Stelzmann-Strasse 9b, 50931 Cologne, Germany
*Correspondence: partridge@age.mpg.de
http://dx.doi.org/10.1016/j.cub.2016.07.017

SUMMARY

Glucose hypometabolism is a prominent feature of the brains of patients with Alzheimer's disease (AD). Disease progression is associated with a reduction in glucose transporters in both neurons and endothelial cells of the blood-brain barrier. However, whether increasing glucose transport into either of these cell types offers therapeutic potential remains unknown. Using an adult-onset *Drosophila* model of Aβ (amyloid beta) toxicity, we show that genetic overexpression of a glucose transporter, specifically in neurons, rescues lifespan, behavioral phenotypes, and neuronal morphology. This amelioration of Aβ toxicity is associated with a reduction in the protein levels of the unfolded protein response (UPR) negative master regulator Grp78 and an increase in the UPR. We further demonstrate that genetic downregulation of Grp78 activity also protects against Aβ toxicity, confirming a causal effect of its alteration on AD-related pathology. Metformin, a drug that stimulates glucose uptake in cells, mimicked these effects, with a concomitant reduction in Grp78 levels and rescue of the shortened lifespan and climbing defects of Aβ-expressing flies. Our findings demonstrate a protective effect of increased neuronal uptake of glucose against Aβ toxicity and highlight Grp78 as a novel therapeutic target for the treatment of AD.

INTRODUCTION

46.8 million people live with dementia worldwide [1], with Alzheimer's disease (AD) being the most common type. Prevalence continues to rise with increasing life expectancy. Currently there are no cures, and there is an urgent need to identify ways of preventing or modifying disease progression. AD is thought to be triggered by the accumulation of extracellular Aβ (amyloid beta) peptides, derived from the misprocessing of amyloid precursor protein (APP) [2], leading to cellular stress, accumulation of toxic intracellular Tau, and eventual neuronal cell death [2]. However, recent evidence suggests that Aβ might also potentially play a protective, antimicrobial role [3].

A prominent feature of AD progression is a substantial reduction in glucose metabolism [4]. This drop precedes the onset of clinical symptoms [4], worsens with disease progression [4], and is a more accurate marker of neuronal atrophy than is Aβ accumulation itself [5]. Patients with type 2 diabetes, who are at higher risk of AD, display increased insulin resistance, which has been linked both to reduced glucose uptake in the brain and to memory impairments [6]. Mouse models of AD also show a decrease in glucose metabolism, suggesting that it may be part of the disease process [7]. However, the exact role of lowered glucose metabolism in disease progression is unknown.

Glucose does not freely cross cell membranes and is, instead, actively shuttled by transporters. In humans, there are 12 glucose transporters, with different expression patterns and affinities. In the brain, Glut1 is expressed mainly in glia and endothelial cells, whereas Glut3 is expressed in neurons [7]. A reduction in expression of a number of glucose transporters has been observed in the brains of mouse AD models [8] and of human patients [7]. The timing of this decrease correlates with increases in Tau phosphorylation and neurofibrillary tangles (NFTs) [7]. In a mouse model of AD pathogenesis, a reduction in neuronal Glut3 expression coincided with a reduction in glucose metabolism [8], while a drop in Glut1 in endothelial cells exacerbated pathology in another mouse AD model [9].

Whether impaired neuronal glucose metabolism plays a causal role in neurodegeneration in AD awaits investigation. The drop in glucose metabolism could contribute to disease progression in several ways. It could lead to a reduction in ATP in neurons, since glucose is the main source of energy. Downregulation of the hexosamine pathway, which relies on glucose for GlcNAc production, would lead to a reduction in Tau GlcNAcylation, which, in turn, could drive up toxic Tau phosphorylation, since the two are negatively correlated [10]. Hypometabolism and glucose deprivation have been shown to induce the unfolded protein response (UPR) [11]; this, too, could drive Tau phosphorylation [11]. Any or all of these mechanisms could contribute to neurodegeneration.

To begin to experimentally test the role of glucose transport and metabolism in AD pathogenesis, we used a model of Aβ toxicity in the fruit fly *Drosophila melanogaster* [12]. *Drosophila* has proved to be an excellent model system in which to study neurodegenerative diseases. The fly has a distinct brain structure with cell types analogous to the human brain, as well as a blood-brain barrier (BBB), and is, therefore, ideal for studying

the neurodegenerative process in a complex tissue. The metabolic coupling between glia and neurons observed in mammalian brains is also conserved in flies [13]. The fly AD model that we used expresses pathogenic Arctic Aβ42 tagged with an endoplasmic reticulum (ER) export signal peptide [14] exclusively in the neurons of the adult fly, thereby removing any confounding developmental effects. These flies have shortened lifespans, behavioral defects, and neurodegeneration [12].

If lowered glucose metabolism in neurons is part of the pathogenic cascade from toxic Aβ, then experimentally increasing glucose metabolism in neurons should ameliorate the pathogenesis in the AD model. Therefore, we assessed the effect of overexpressing a glucose transporter, Glut1, in the neurons of the AD flies. We found that this partially rescued the Aβ phenotypes, without affecting the expression level of the toxic Aβ peptide. Glut1 overexpression led to downregulation of the expression of Grp78 (glucose-regulated protein 78/BiP), the negative master regulator of the UPR. This, in turn, increased the UPR, in association with an improvement in protein homeostasis. Interestingly, feeding the flies the drug metformin, which increases glucose transport, also caused a drop in Grp78 levels and an increase in lifespan, suggesting a possible pharmacological therapeutic avenue.

RESULTS

Drosophila melanogaster has two glucose transporters: Glut1 and Glut3. Glut3 is expressed only in testes, while Glut1 is expressed ubiquitously [15]. In order to increase glucose metabolism, we cloned Glut1 under the control of the UAS (upstream activating sequence) promoter and drove its expression with a constitutive and ubiquitous daGal4 driver. This led to increased uptake of a glucose analog (Figure S1A), demonstrating that increased Glut1 expression can, indeed, increase transport of glucose into cells.

Next, we overexpressed Glut1 in the neurons of adult flies, using an inducible elavGS (elav-GeneSwitch-Gal4) driver and confirmed the overexpression by qPCR in fly heads (Figure S1B). Overexpression of Glut1 had no effect on the lifespan of wild-type flies (Figure S1C), but it increased lifespan in Arctic-Aβ42(Aβ)-expressing flies (Figure 1A) and slowed their decline in climbing ability, a behavioral measure of neuronal health (Figure 1B). Interestingly, the climbing ability of flies expressing Aβ and Glut1 was worse than that of flies expressing Aβ alone at early time points, possibly suggesting that Glut1 expression could impair climbing ability in early life, before its beneficial effect on disease development takes effect (Figure 1B). Sleep pattern, too, is directly controlled by neuronal activity. Flies are diurnal, sleeping mainly at night. Expression of Aβ rendered the flies more arrhythmic, with fewer flies showing a clear change in sleep pattern between day and night, largely as a consequence of a substantial increase in day sleep (Figure 1C). The Aβ flies also spent more total time sleeping than did non-induced controls (Figure 1C). Overexpression of Glut rescued this pattern, with the flies partially recovering their diurnal sleep pattern and spending less total time sleeping (Figure 1C). To confirm that the phenotypic rescue of the Aβ toxicity was, indeed, due to increased glucose uptake and not some other activity of Glut1, we checked whether altering sugar concentration in the food could modulate the Glut1 rescue of lifespan in Aβ-expressing flies (Figure S1D). We found that reducing dietary sugar intake differentially affected the lifespans of flies expressing Aβ alone, relative to the flies expressing Aβ and Glut1, with no rescue of lifespan by Glut 1 at the lowest sugar concentration of 2.5%. As the sugar in the food was reduced, so did the lifespan extension afforded by Glut1. This suggests that the phenotypic rescue is linked to an increased uptake of sugar.

To determine whether Glut1 could rescue neurodegeneration after adult induction of Aβ, we marked a sub-population of neurons with GFP driven by the Q system [16], using nSyb-QF2 > GFP [17], which marks a set of neurons in the central portion of the *Drosophila* brain (Figure 1D) while, at the same time, driving Aβ pan-neuronally with the UAS system. The two misexpression systems are independent of each other, and we could thus monitor the morphology of a sub-population of neurons in the presence of Aβ and of overexpression of Glut1. When Aβ was expressed, a number of filamentous structures clearly visible in the wild-type brain were lost, reflecting the degeneration of axons or dendrites. Strikingly, when Glut1 was overexpressed, the neuronal morphology was completely restored (Figure 1D).

Surprisingly, Glut1 overexpression did not affect Aβ protein or mRNA levels in heads (Figures 1E and 1F), suggesting that Glut1 reduced the toxicity, rather than the total load, of Aβ.

In humans and mouse models of AD, disease progression has been linked to a decrease in glucose transporters [8], and in mouse AD models, a reduction of glucose transporters in endothelial cells exacerbates disease development. Similarly, in our *Drosophila* model, RNAi of Glut1 in neurons (Figure S1E) reduced the lifespan of Aβ-expressing flies, indicating that reduction of glucose import into neurons worsens Aβ toxicity, similar to the mechanism suggested in humans.

In both mammalian and fly brains under normal physiological conditions, glycolysis occurs primarily in glia [13]. Therefore, we assessed whether increasing glucose uptake in glia could also affect pathology. For this, we generated a fly model concomitantly expressing Aβ in neurons and Glut1 in glia. Aβ was driven in neurons by the nSyb-QF2 driver [17], which was induced starting from eclosion, whereas Glut1 was induced by the constitutive glial driver repo-Gal4. Overexpression of Glut1 in glia did not rescue the toxicity of neuronal Aβ, as assessed by lifespan (Figure S1F). Hence, either the Aβ toxicity in neurons was too great for the induction of Glut1 that we achieved to rescue it, or Glut1 in glia cannot rescue Aβ toxicity.

Glucose uptake can influence many cellular processes and could, therefore, rescue Aβ toxicity in several ways. The most obvious candidate is energy metabolism, since glucose is the source of most cellular energy. However, we did not observe an obvious energy deficit in the brains of our Aβ-expressing flies, and the ADP/ATP ratio in brains was unchanged when Glut1 was overexpressed (Figure S1G).

Next, we considered whether Glut1 overexpression reduced Aβ toxicity by acting through the hexosamine biosynthetic pathway, by increasing protein GlcNAcylation. However, upregulation in neurons of GFAT2, the first and rate-limiting enzyme in the hexosamine biosynthetic pathway, shortened the lifespan of the Aβ-expressing flies (Figure S1H), contrary to what would be predicted from this hypothesis.

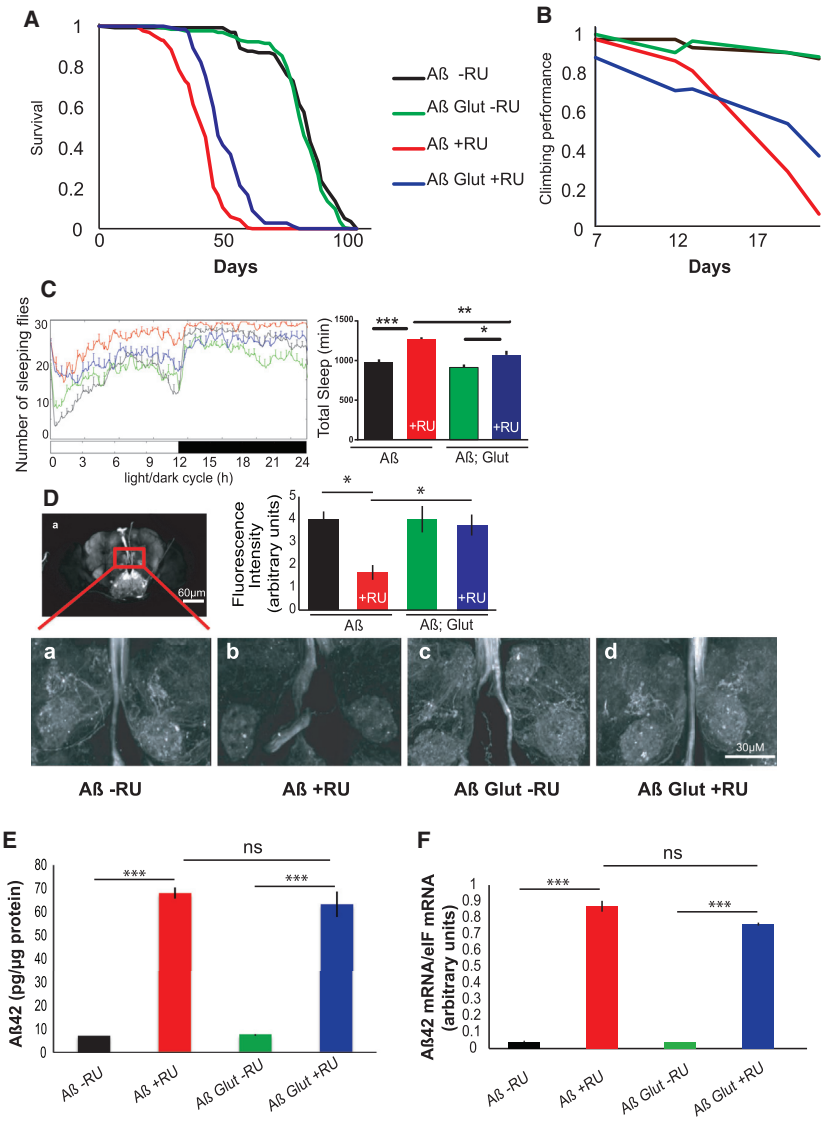

Figure 1. Glut1 Overexpression Rescues Aβ Toxicity

(A) Survival curves of flies expressing Aβ or Aβ Glut1 in adult neurons (+RU) and uninduced controls (-RU). $p < 0.01$, when comparing Aβ +RU and Aβ Glut1 +RU by log-rank test.

(B) Climbing assay performance index of flies of the same genotypes. $p < 1E\text{-}10$ when comparing Aβ response to RU relative to Aβ Glut response by ordinal logistics regression.

(C). 24-hr sleep profile of 21-day-old flies expressing Aβ or Aβ Glut1 in neurons (+RU) and uninduced controls (-RU) on day 3 in the LD cycle. At the right, total sleep amount for females of each genotype are shown (plotted as means ± SEM). *$p < 0.01$; **$p < 0.001$; and ***$p < 0.0001$, by two-way ANOVA. Genotypes: *UAS Aβ/UAS Glut1; elavGS*, *UAS Aβ; elavGS*.

(D) Confocal images of brains of 21-day-old control flies (-RU) and flies expressing Aβ or Aβ Glut1 driven by elavGS (+RU). The nSyb-QF2 driver, kept in an inactive state by the tub-QS repressor, drives GFP. Once flies eclosed, they were fed QA, which binds QS to induce expression of GFP, thus labeling a subset of neurons. Fluorescence intensity scores are plotted as means ± SEM. *$p < 0.05$, by ANOVA ($n = 3$–4). Genotypes: *UAS cd8GFP; nSyb2QF2 tubQS/elavGS*, *UAS cd8GFP/UAS Aβ; elavGS/nSyb2QF2 tubQS*, *UAS cd8GFP/UAS Aβ UAS Glut1; elavGS/nSyb2QF2 tubQS*.

(E) Aβ42 protein levels, measured by ELISA, in the heads of 9-day-old flies expressing Aβ or Aβ Glut1 in neurons (+RU) and uninduced controls (-RU), plotted as means ± SEM ($n = 3$). ***$p < 0.0001$, by ANOVA; ns, not significant.

(F) Aβ42 mRNA levels (relative to eIF1A) in the heads of similar 14-day-old flies, measured by qPCR, plotted as means ± SEM ($n = 4$). ***$p < 0.0001$, by ANOVA; ns, not significant. Genotypes: *UAS Aβ; elavGS*, *UAS Aβ/UAS Glut1; elavGS*.

See also Figure S1.

Glucose uptake can affect the UPR [18], which is becoming increasingly recognized as important in neurodegenerative diseases, including AD [19], although whether it plays a protective or detrimental role remains unclear [19]. The UPR signaling cascade is activated in response to ER stress, allowing the cell either to restore protein homeostasis or to enter apoptosis [19], and is mediated by three trans-membrane proteins: pancreatic ER kinase (PERK), inositol-requiring enzyme 1 (IRE1), and activating transcription factor 6 (ATF6). Grp78, also known as BiP, binds and keeps these three proteins in an inactive state. Upon ER stress, Grp78 targets misfolded proteins to act as a chaperone, and thus releases PERK, IRE1, and ATF6 to activate a series of downstream cascades, leading to the phosphorylation of eIF2alpha and reduction of protein translation, activation of downstream transcription factors such as ATF4 and Xbp1, and increases in chaperones such as Grp78 itself (Figure S2A) [19].

The main marker of PERK activation, eIF2alpha phosphorylation, was not affected by either Aβ or Glut1 expression in neurons (Figure 2A); however, we did confirm that the antibody we used was able to detect eIF2alpha phosphorylation in response to a strong UPR inducer (Figure S2B). However, *Grp78* mRNA expression, a marker of ATF6 activation, was increased in flies expressing Aβ (Figure 2B). *Xbp1* splicing, a marker of IRE1 activation, increases in response to Aβ in flies [20]. In our model, we noticed a trend toward an increase in the fluorescence of a GFP reporter for *Xbp1* splicing, but this did not reach significance (Figure 2C). However, when we measured the spliced *Xbp1* isoform by qPCR, it was significantly increased in response to Aβ (Figure 2D), in agreement to what has previously been described [20]. Aβ thus induces the ATF6 and IRE1, but not the PERK, branches of the UPR. Unexpectedly, co-expression of Glut1 increased *Grp78* mRNA (Figure 2B) and *Xbp1* splicing (Figure 2C) even further, suggesting an additional increase of the UPR in

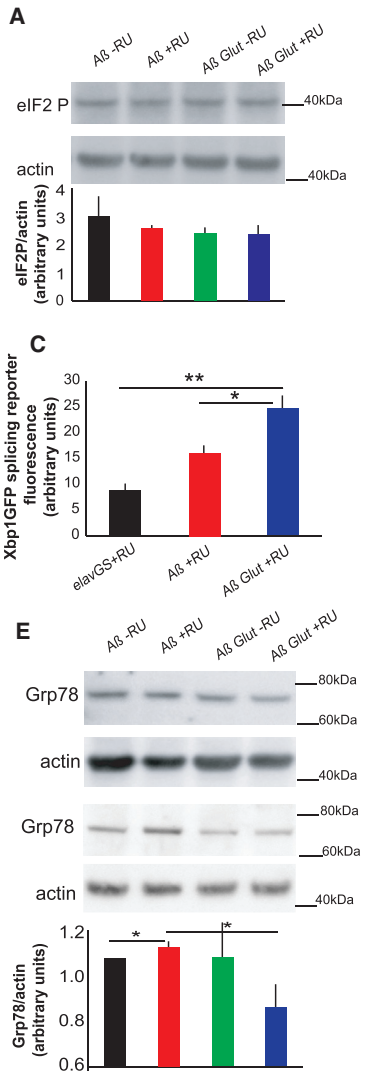

Figure 2. UPR Components Activated in Aβ-Expressing Flies Are Induced Even Further by Glut1 Overexpression

(A) Western blot of eIF2 phosphorylation levels in heads of Aβ- and AβGlut1-expressing flies (+RU) and in controls (-RU), showing no significant difference. Bottom: plotted as means ± SEM (n = 3). Top: a representative gel from the same samples.

(B) Grp78 mRNA levels in heads of 18-day-old flies expressing Aβ or Aβ Glut1 in neurons (+RU) and uninduced controls (-RU), measured by qPCR (relative to eIF1A), plotted as means ± SEM. Genotypes: *UAS Aβ; elavGS*, *UAS Aβ/UAS Glut1; elavGS*.

(C) Quantification of GFP fluorescence in fly brains expressing an Xbp1GFP splicing reporter, plotted as means ± SEM (n = 6–13). Genotypes: *elavGS/UAS-Xbp1GFP*, *UAS Aβ; elavGS/UAS-Xbp1GFP*, *UAS Aβ/UAS Glut1; elavGS/UAS-Xbp1GFP*.

(D) Spliced Xbp1 mRNA levels in heads of 18-day-old flies expressing Aβ or Aβ Glut1 in neurons (+RU) and uninduced controls (-RU), measured by qPCR (relative to eIF1A), plotted as means ± SEM

(E) Western blot of Grp78 in 14-day-old flies of the same genotypes, plotted below as means ± SEM (n = 6–16). The image is a representative gel of the same samples. Genotypes: *UAS Aβ; elavGS*, *UAS Aβ/UAS Glut1; elavGS*.

*p ≤ 0.05; **p ≤ 0.01, by ANOVA. See also Figure S2.

response to glucose uptake. Grp78 protein levels are tightly controlled at the level of translation [21], and an increase in the mRNA, therefore, does not necessarily indicate higher protein levels. Therefore, we measured Grp78 protein and found that it also increased in the presence of Aβ, albeit to a smaller extent (Figure 2E). However, surprisingly, overexpression of Glut1 resulted in reduced expression of Grp78 protein (Figure 2E), suggesting that Glut1 and the increased glucose uptake that it produced reduced either Grp78 translation or stability.

Grp78 is broadly considered a negative regulator of the UPR, since it binds and maintains ATF6 and IRE1 in an inactive state. Overexpression of Grp78 can attenuate UPR signaling both in non-neuronal cells [22] and in neurons [19], and its knockdown can lead to increased activation of the UPR upon ER stress [23]. Our results point to a similar mechanism, with a drop in Grp78 protein levels upon Glut1 expression leading to an increase in ATF6 and IRE1 activity. Aβ induced only the IRE1 and ATF6 branches of the UPR, similar to tunicamycin treatment [24]. Therefore, we determined whether Glut1 overexpression could also increase resistance to tunicamycin. Indeed, Glut1 overexpression protected flies from tunicamycin stress (Figure 3A), accompanied by a block in Grp78 induction (Figure 3B) and a trend toward a further increase in UPR markers upon Glut1 expression (Figures 3C and 3D), similar to what was observed in the Aβ expressing brains. Glut1 could, therefore, protect against UPR stress, attributable to a reduction in Grp78 levels.

If Glut1 overexpression protects against Aβ-induced UPR stress by reducing Grp78 levels, then a reduction in Grp78 activity should also rescue Aβ toxicity. We tested this by overexpressing a dominant-negative version of Grp78, Grp78K97S, which carries a point mutation affecting the coupling of ATP binding to substrate release [25]. Expression of Grp78K97S in neurons increased both the lifespan and the climbing ability of Aβ-expressing flies (Figures 4A and 4B), suggesting that, indeed, reduced Grp78 activity is causal in the amelioration of Aβ toxicity by Glut1.

AD is characterized by a deregulation of protein homeostasis [26], which could contribute to disease. Therefore, we hypothesized that increased glucose metabolism in neurons allows the UPR to increase even further and, thus, to restore protein homeostasis. To test this idea, we measured insoluble ubiquitinated protein levels in heads and found that Aβ expression led to the accumulation of insoluble ubiquitinated proteins, which was abrogated by Glut1 overexpression (Figure 5), Glut1 overexpression, therefore, allowed neurons to

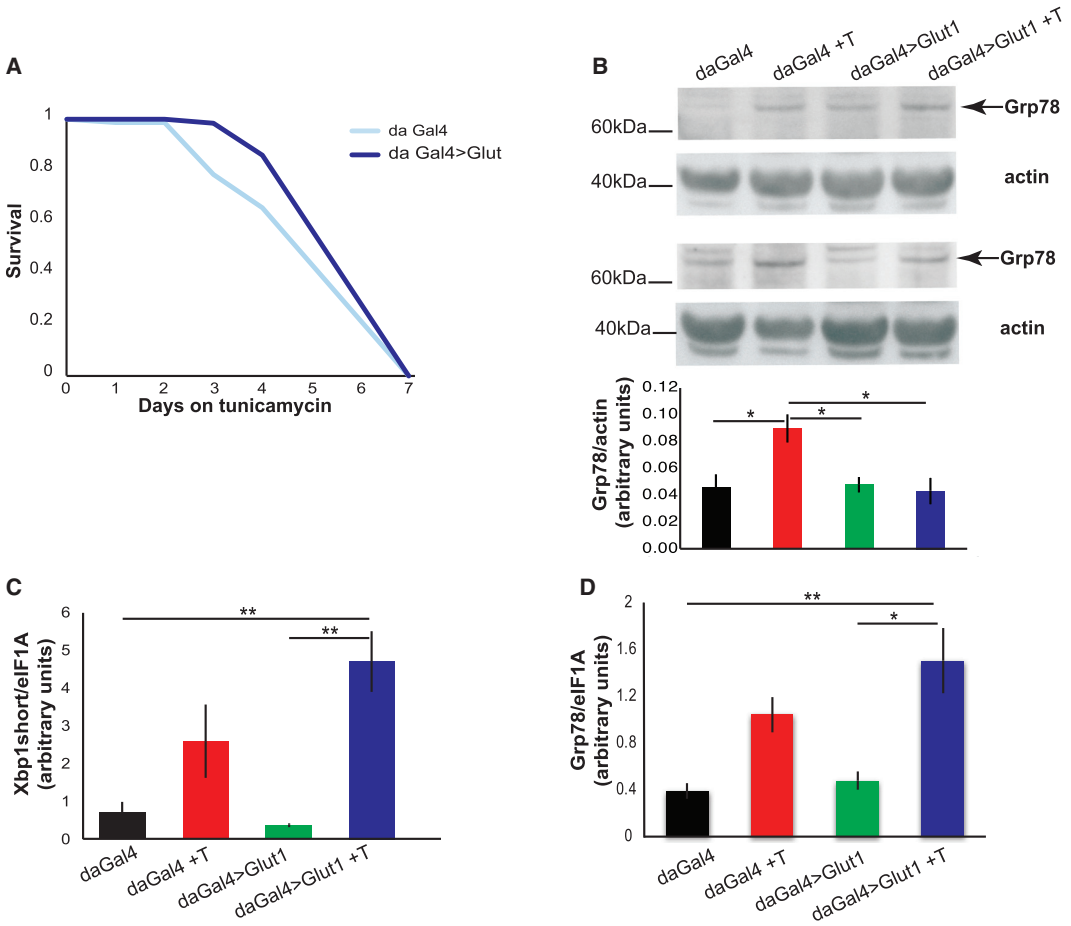

Figure 3. Glut1 Protects Flies from Tunicamycin-Induced ER Stress

(A) Survival of Glut1-overexpressing flies on food containing tunicamycin ($p < 0.05$ for effect of Glut1 relative to driver-alone control by log-rank test).

(B) Western blot of Grp78 in whole flies after 48 hr on tunicamycin, plotted below as means ± SEM (n = 5–8); the image shows representative gels of similar samples. *$p \leq 0.05$ by ANOVA.

(C) qPCR of Xbp1-spliced isoform levels (normalized to eIF1A), in flies treated for 48 hr with tunicamycin, plotted as means ± SEM (n = 3–4). **$p \leq 0.01$ by ANOVA.

(D) qPCR of Grp78 (normalized to eIF1A), in flies treated for 48 hr with tunicamycin, plotted as means ± SEM (n = 3–4). *$p \leq 0.05$; **$p \leq 0.01$, by ANOVA.

Genotypes: *daGal4*, *UASGlut1; daGal4*.

re-establish protein homeostasis, presumably via upregulation of the UPR.

Metformin is a drug used to treat type 2 diabetes, and it increases glucose uptake in several tissues [27, 28] by increasing the translocation of glucose transporters to the plasma membrane [27]. Therefore, we treated our Aβ-overexpressing flies with metformin to determine whether we could recapitulate the rescue observed by overexpressing Glut1. Indeed, feeding Aβ-overexpressing flies with a range of metformin concentrations resulted in a significant lifespan extension (Figure 6A) and increase in climbing ability (Figure 6B) without altering Aβ levels (Figure 6C). Interestingly, 80 mM metformin reduced the lifespan of flies that did not express Aβ and was also less effective than lower doses at extending the lifespan of Aβ-expressing flies, but it gave the strongest rescue of climbing ability. These results suggest that this high concentration of metformin shows a beneficial effect on neuronal-related health before 25 days but that continuous exposure to a high dose of metformin leads, at later ages, to systemic toxicity and reduced lifespan. The rescue was dependent on Glut1 expression, since RNAi of Glut1 blocked the lifespan extension from metformin treatment (Figure 6D). Metformin treatment, like Glut1 overexpression, also blocked the increase in Grp78 levels associated with Aβ expression (Figure 6E). Metformin could, therefore, be a potential therapeutic modulator of Aβ pathology by blocking toxic Grp78 induction.

DISCUSSION

Glucose metabolism has been strongly implicated the pathogenesis of AD [5, 7]. Patients display a marked reduction in glucose metabolism in brain areas vulnerable to degeneration, and this precedes the onset of clinical symptoms and mirrors disease progression more closely than does Aβ deposition [4]. Expression of neuronal glucose transporters also drops in AD patients

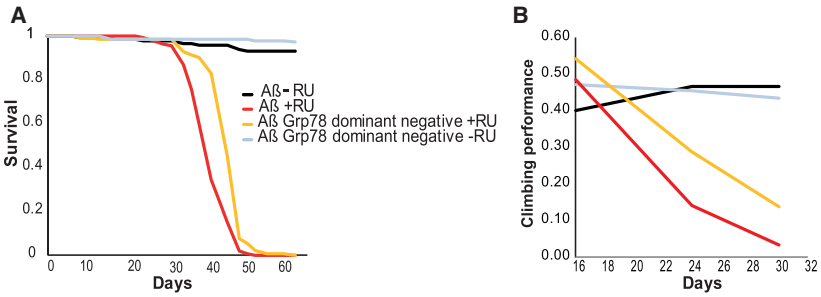

Figure 4. Grp78 Dominant-Negative Version Rescues Aβ Toxicity

(A) Lifespan survival curves of flies expressing Aβ or the Aβ Grp78 dominant-negative version in neurons (+RU) and uninduced controls (-RU). (Aβ +RU and Aβ Grp78 dominant-negative +RU are different. $p < 1E\text{-}13$ by log rank).

(B) Climbing assay performance index for the same flies plotted over time ($p < 0.005$ when comparing Aβ response to RU relative to Aβ Grp78.K97S response by ordinal logistics regression). Genotypes: *UAS Aβ; elavGS*, *UAS Aβ/UAS Grp78.K97S; elavGS*.

and in AD mouse models [7]. Recently, it was shown that reduction of glucose transport across the BBB in mouse AD models exacerbates Aβ toxicity [9]. However, whether impaired glucose metabolism in neurons plays a causal role in AD pathogenesis has not been addressed directly.

Our study has shown that experimentally increasing glucose uptake in neurons can protect against Aβ toxicity. In our *Drosophila* AD model, Glut1 overexpression led to a lifespan increase, an amelioration of phenotypes linked to neuronal health—namely, climbing and sleep—and a restoration of normal neuronal morphology. This improvement was associated with a reduction in Grp78 protein levels and an upregulation of the UPR.

In AD patients, the UPR is activated early in disease pathogenesis [11]. Similarly, Aβ expression in the neurons of adult flies led to the induction of the UPR. Grp78 levels were increased, similarly to those of mice models of AD [29], of AD patients early in disease development [30], and in neuronal cells derived from AD patients' induced pluripotent stem cells (iPSCs) [31].

Intriguingly, the rescue of Aβ toxicity by Glut1 was associated with a reduction in Grp78 expression. Grp78 is becoming an increasingly important therapeutic target, especially in cancer biology, where its inhibition increases cells' susceptibility to chemotherapy agents [32]. Its role in neurodegeneration is less well defined. In rat models of Parkinson's disease, activation of Grp78 is protective [33], and its downregulation is detrimental [34]. However, its role in AD models has not been tested. Our studies suggest that Grp78 downregulation can ameliorate Aβ toxicity by allowing upregulation of the UPR. Already, it has been shown in flies that overexpression of Xbp1 can ameliorate Aβ42 toxicity [20], supporting the idea that upregulation of UPR components could be beneficial in AD models. The role of Grp78 has not been tested in other models of neurodegeneration, and a complex picture is emerging regarding the role of downstream UPR effectors, where, depending on the precise experimental conditions, upregulation of the UPR appears to be protective or detrimental [19]. For example, downregulation of PERK is protective in some ALS (amyotrophic lateral sclerosis) or prion disease models, whereas increased Xbp1 can be protective in Parkinson's and Huntington's disease models [19]. This could be because the UPR is a complex pathway with extensive crosstalk between the different signaling cascades, so it would be difficult to predict reliably the outcome of an intervention. Alternatively, a mild upregulation of the UPR could allow the induction of an ER-hormetic response, increasing ER proteostasis to allow a neuron to deal with an increase in misfolded proteins, whereas, in other conditions, a strong induction of the UPR could lead to apoptosis, and, therefore, blocking this response could also increase neuronal survival [19].

How glucose regulates Grp78 expression is unclear. It is well established that glucose starvation induces expression of Grp78 [35], and, in one study, increased glucose reduced Grp78 expression in cultured neurons [36]. However, little is known about how physiological changes in glucose metabolism modulate Grp78, and it will be important to identify the mechanisms at work.

Our study suggests a model where Aβ accumulation in the brain induces the UPR, and increased glucose uptake in neurons blocks the negative feedback loop linked to Grp78 upregulation, resulting in even further increased UPR, which allows neurons to clear insoluble ubiquitinated proteins and restore protein homeostasis, resulting in the rescue of neurodegeneration and increased lifespan. This mechanism of action could be relevant to the benefits observed by administration of insulin nasal spray in AD patients [37]. Insulin is thought to act via PI3K/MAPK (phosphatidylinositol 3-kinase/mitogen-activated protein kinase) to influence Aβ trafficking and decrease Tau phosphorylation by inhibiting Gsk3 [38]. However, insulin can upregulate glucose transporters in neurons [39] and increase glucose metabolism [39]. It would be interesting to determine whether insulin administration also upregulates the UPR.

Glucose metabolism has also been implicated in the increased risk of AD associated with type 2 diabetes. The link is well established, but the mechanism is less so [40]; possibilities include increased vascular risk factors associated with metabolic syndrome in type 2 diabetes, as well as hyperglycemia-linked dysregulation of cellular signaling pathways, leading to advanced glycation products and increased reactive oxygen species. Also, the rise in brain insulin resistance, which could, in part, lead to increased production of Aβ [40], could also result in decreased glucose transporters and glucose metabolism within neurons, leading to an upregulation of Grp78.

Metformin, a type 2 diabetes therapy, is a drug that has been shown to increase glucose uptake in cells. Interestingly, treatment with a metformin dose known not to affect lifespan in wild-type *Drosophila* [41] increased the lifespan of Aβ-expressing flies. In accordance with previous studies [42], we also found that metformin decreased expression of Grp78, suggesting that the rescue of Aβ toxicity could be due to increased UPR. Metformin's effect in AD is controversial, with some studies reporting patient benefits [43] but others finding that it worsened cognitive performance [44], possibly related to metformin's ability to

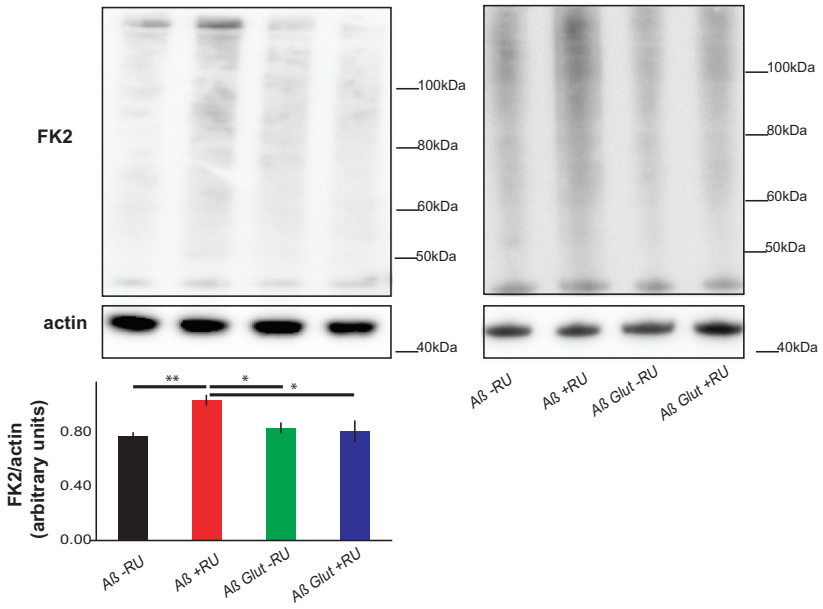

Figure 5. Glut1 Reduces Accumulation of Insoluble Ubiquitinated Proteins

Western blots of SDS-soluble protein fraction from the heads of day-17 flies expressing Aβ or Aβ Glut1 in neurons (+RU) and uninduced controls (-RU), probed for ubiquitinated proteins (FK2) and for actin, plotted below as means ± SEM (n = 4). The two blots shown are from different experiments. *p < 0.05; **p < 0.01, by ANOVA. Genotypes: *UAS Aβ; elavGS*, *UAS Aβ/UAS Glut1; elavGS*.

increase APP levels and processing to increase Aβ production [45]. Our study points to a novel and unexplored role of metformin as a modulator of the UPR in neurodegeneration downstream of Aβ accumulation, which could provide a useful therapeutic avenue in a clinical context where AD patients present quite late in disease development and have already accumulated Aβ peptide in their brain.

EXPERIMENTAL PROCEDURES

Fly Husbandry and Stocks

All flies were reared at 25°C on a 12-hr:12-hr light:dark (LD) cycle at constant humidity and on standard sugar-yeast-agar (SYA) medium (agar, 15 g/l; sugar, 50 g/l; autolyzed yeast, 100 g/l; nipagin, 100 g/l; and propionic acid, 2 ml/l). Adult-onset, neuron-specific expression of UAS constructs was achieved as described elsewhere [12]. Briefly, 24–48 hr after eclosion, female flies carrying a heterozygous copy of elavGS and at least one UAS construct were fed SYA medium supplemented with 200 μM mifepristone (RU486) to induce transgene expression. For induction with quinic acid (QA), flies were put on food containing 7.5 g of QA per liter. Metformin was added to the food at the stated concentrations. ElavGS was derived from the original elavGS 301.2 line [46] and obtained as a generous gift from Dr. H. Tricoire (CNRS); the UAS-Aβ42Arc (UAS Aβ) stock was a gift from Dr. D. Crowther (University of Cambridge). The nSyb-QF2 stock was a gift from Dr. C. Potter (Johns Hopkins School of Medicine) [17]. W1118, tubulin-QS (tub-QS), UAS-Grp78.K97S, UAS-Xbp1GFP, daughterless-Gal4 (daGal4), Glut1 RNAi line (TRiP.HMS02152) and Repo-Gal4 were obtained from the Bloomington Drosophila Stock Center.

All transgenes were backcrossed into the w1118 background to ensure a homogeneous genetic background between transgenic lines. All experiments were carried out on mated females, unless otherwise stated.

Lifespan Analysis

Flies were raised at standard density in 200-ml bottles. After eclosion, flies were allowed to mate for 24–48 hr. At least 110–150 females of the appropriate genotype were split into groups of 15 and housed in vials containing SYA medium with or without drugs. Deaths were scored, and flies tipped onto fresh food three times a week. Data are presented as cumulative survival curves, and survival rates were compared using log-rank tests or Cox proportional hazards performed in JMP (version 9.0) software (SAS Institute). All lifespans were performed at 25°C unless otherwise stated.

Climbing Assay

The climbing assay in Figure 1 was performed as previously described [47]. Briefly, 15 flies were placed in a 25-cm pipette, tapped to the bottom, and allowed to climb for 45 s. The number of flies in the top 5 cm, center, and bottom 3 cm was scored. A performance index was calculated for each time point and plotted. Statistical analysis was performed in R using ordinal logistics regression, using the individual heights for each fly as data points. For the climbing assay in Figures 4 and 6, the assay was performed with the following modifications: 45 flies were housed in a glass-walled chamber 25 cm tall, and flies were tapped to the bottom as described earlier and allowed to climb for 20 s before scoring. The analysis was the same as described earlier.

Western Blotting

Protein samples were prepared by homogenizing in 2× SDS Laemmli sample (4% SDS, 20% glycerol, 120 mM Tris-HCl [pH 6.8], 200 mM DTT with bromophenol blue) and boiled at 95°C for 5 min. Samples were separated on pre-cast 4%–12% Invitrogen Bis-Tris gels (NP0322) and blotted onto PVDF (polyvinylidene fluoride) or nitrocellulose membrane (for Grp78) in Tris-glycine buffer supplemented with 10% ethanol. Membranes were blocked in 5% milk and 1% BSA in TBS-T (Tris-buffered saline with 0.05% Tween-20) for 1 hr at room temperature (RT) and then incubated with primary antibodies in block. Ubiquitin westerns were blocked in 1% BSA. Primary antibody dilutions used were as follows: anti-Grp78, 1:1,000 (Novus Biologicals, NBP1-06274); anti-actin, 1:10,000 (Abcam, ab1801); anti-Ubiquitin, 1:1,000 (Millipore, FK2); and anti-eIF2A-phospho, 1:1,000 (Cell Signaling, 3597). Secondaries used were anti-rabbit and anti-mouse (Abcam, ab6789 and ab6721) at 1:10,000 dilutions for 1 hr at RT. Bands were visualized with Luminata Forte (Millipore) and imaged with ImageQuant LAS4000 (GE Healthcare Life Sciences). Quantification was carried out with ImageQuant software or ImageJ.

Preparation of Detergent-Soluble Fractions for Insoluble Ubiquitinated Protein Gels

The method was adapted from [48]. Briefly, 10–20 heads were extracted in 75 μl Triton X extraction buffer and spun at 13,000 × *g* for 10 min at 4°C, and the supernatant was collected as the Triton X soluble fraction. The pellet was re-suspended in 50 μl SDS extraction buffer and spun again, and the supernatant was collected as the SDS soluble fraction. Samples were stored at −80°C and run as described earlier.

qPCR

Total RNA was extracted from heads or whole flies (for Figure 3) and converted to cDNA (see Supplemental Experimental Procedures for details). qPCR was performed using the PRISM 7000 sequence detection system (Applied Biosystems). Each sample was analyzed in duplicate, and values are the mean of three or four independent biological repeats ±SEM.

Quantification of Aβ42

Five fly heads were homogenized in 50 ml GnHCl extraction buffer (5 M guanidinium HCl, 50 mM HEPES [pH 7.3], 1:10 dilution of protease inhibitor cocktail

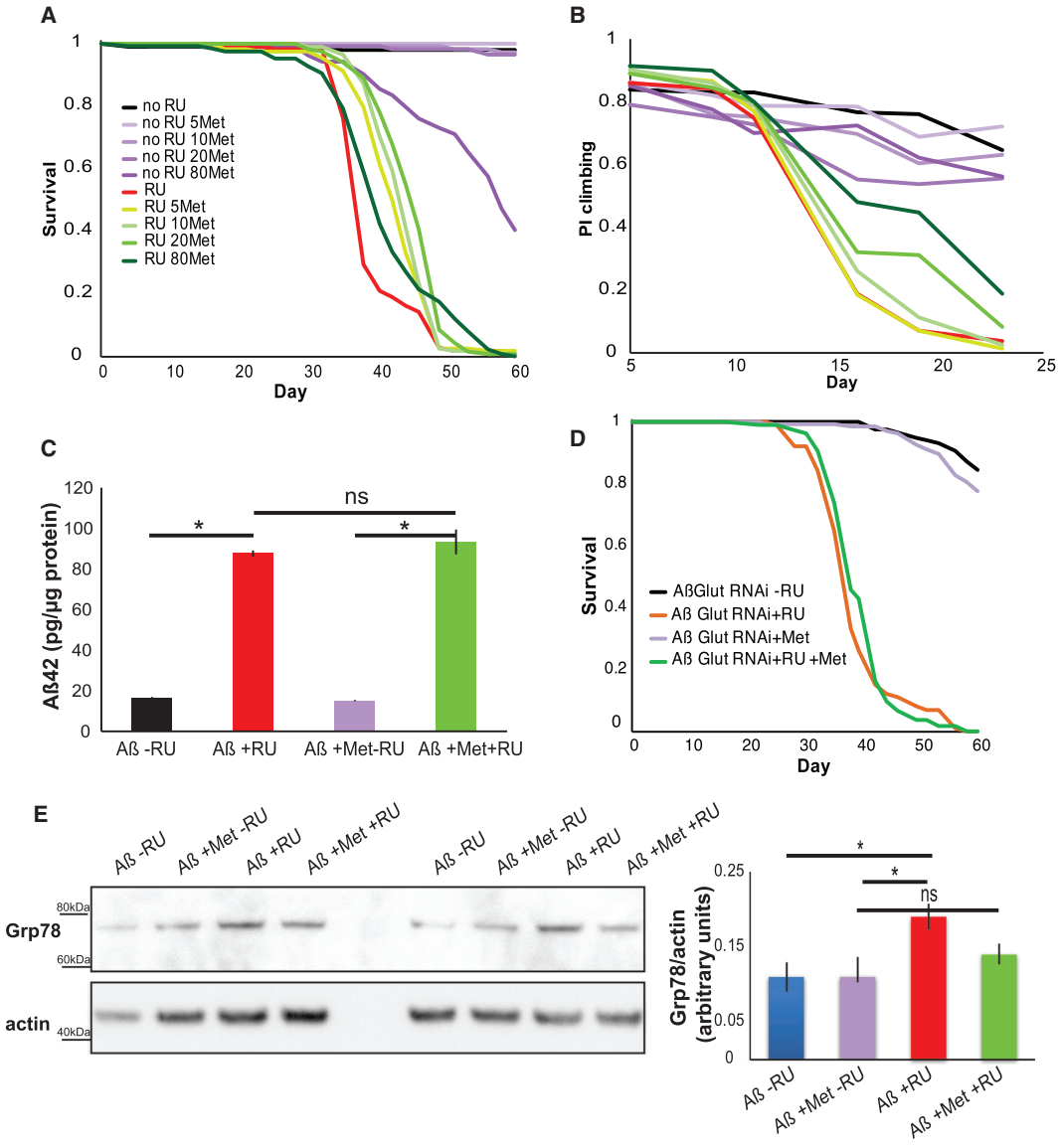

Figure 6. Metformin Extends the Lifespan of Aβ-Expressing Flies

(A) Lifespan survival curves of flies expressing Aβ (+RU) and controls (-RU) in the presence of different metformin (Met) concentrations (all the metformin-treated +RU flies were significantly longer lived than the +RU-alone control: p < E-4 for 5 mM, p < E-6 for 10 mM, p < E-8 for 20 mM, and p < 0.01 for 80 mM by log-rank test).

(B) Climbing assay performance index (PI) for the same flies (p < 1E-5 when comparing the +RU control relative to the +RU flies treated with 20 mM or 80 mM metformin by ordinal logistics regression).

(C) Aβ42 protein levels, measured by ELISA, in the heads of 15-day-old flies expressing Aβ (+RU) and controls (-RU) in the presence or absence of 10 mM metformin, plotted as means ± SEM (n = 3). *p < 0.0001, by ANOVA; ns, not significant.

(D) Lifespan survival curves of flies expressing Aβ Glut1 RNAi (+RU) and controls (-RU) in the presence or absence of 10 mM metformin (no difference between +RU-treated flies by log-rank test). Genotype: *wv; UAS Aβ; elavGS/Glut1RNAi*. (C).

(E) Western blots for Grp78 and actin control in the heads of flies treated with 10 mM meformin, plotted as means ± SEM (n = 4). *p < 0.01, by ANOVA; ns, not significant.

Genotype for (A)–(C) and (E): *UAS Aβ; elavGS*.

[Sigma, P8340], and 5 mM EDTA) and centrifuged at 21,000 × *g* for 5 min at 4°C, and cleared supernatant was retained as the total fly Aβ42 sample. Aβ42 was measured with an ELISA kit (Millipore, EZHS42), according to the manufacturer's instructions, and protein was measured with a Bradford assay (Bio-Rad protein assay reagent), and the amount of Aβ42 in each sample was expressed as a ratio of the total protein content (picograms per microgram of total protein). Data are expressed as the mean ± SEM obtained from three biological repeats for each genotype.

Microscopy

Brains were dissected in 4% paraformaldehyde in PBS with Tween 20 (PBST), incubated for 20 min, rinsed in PBST, mounted in Vectashield with DAPI, and imaged on a Zeiss LSM510 inverted confocal microscope. Images were taken on the 20× or 40× objective as stacks and are shown as maximum intensity projections of the complete stack. The same size stacks were taken for experimental and control samples. All images for one experiment were taken at the same settings. For Xbp1 fluorescence (in Figure 2C), total fluorescence intensity of a given area of the brain was measured with ImageJ. Values shown are the averages for 6–13 brains ± SEM. Samples were compared by ANOVA. For neuronal GFP, images were blind scored and given a score from 1 to 5 based on fluorescent intensity; average scores are presented with their SEM (n = 3–5).

Analysis of Activity and Sleep

Individual, 21-day-old, mated female flies were placed in glass tubes (65 mm × 5 mm) containing standard 1× SYA, and activity was recorded using the DAM System (*Drosophila* Activity Monitoring System; TriKinetics) as described previously [49]. Flies were entrained to a 12-hr:12-hr light:dark (LD) cycle at 25°C and 65% humidity 24–36 hr before recording. 5 days of the 12:12 hr LD cycle were recorded, followed by 5 days of a 12-hr:12-hr dark:dark (DD) cycle. Analysis of locomotor activity was performed using the fly toolbox and MATLAB software (MathWorks), as described previously [50]. Sleep was defined as a bout of inactivity lasting 5 min or more, and sleep analysis was performed with pySOLO [51]. All behavioral data (activity and sleep duration) are represented by mean values with their SEM.

Tunicamycin Stress Assay

Flies were tipped into vials containing 1% agar, 1.5% sucrose, and 10 mg/l of tunicamycin. Dead flies were scored at regular intervals, and lifespan curves were compared with log-rank test.

SUPPLEMENTAL INFORMATION

Supplemental Information includes two figures and Supplemental Experimental Procedures and can be found with this article online at http://dx.doi.org/10.1016/j.cub.2016.07.017.

AUTHOR CONTRIBUTIONS

Conceptualization, T.N. and L.P.; Methodology, T.N., A.T., F.K., and L.P.; Investigation, T.N., M.C., A.T., F.K., L.L., C.T.W., D.C., L.B., and A.J.V.; Writing – Original Draft, T.N.; Writing – Review & Editing, T.N. and L.P.; Funding Acquisition, L.P.; Resources, S.G. and J.D.; Supervision, T.N. and L.P.

ACKNOWLEDGMENTS

We thank Nazif Alic for help with statistical analysis and Nathan Woodling for comments on the manuscript. We also thank the neuro group for helpful discussion and Alexander Hassabis for help with scoring. This work was supported by the Wellcome Trust (grant number WT098565/Z/12/Z to L.P.), the ARUK (grant number ART/PG2009/4 to L.P.), and the Max Planck Society (to L.P.).

Received: November 29, 2015
Revised: June 9, 2016
Accepted: July 11, 2016
Published: August 11, 2016

REFERENCES

1. Prince, M., Wimo, A., Guerchet, M., Ali, G.-C., Wu, Y.-T., and Prina, M.; Alzheimer's Disease International (2015). World Alzheimer Report 2015: The Global Impact of Dementia: An Analysis of Prevalence, Incidence, Cost and Trends. http://www.alz.co.uk/research/WorldAlzheimerReport2015.pdf.
2. Hardy, J.A., and Higgins, G.A. (1992). Alzheimer's disease: the amyloid cascade hypothesis. Science *256*, 184–185.
3. Kumar, D.K., Choi, S.H., Washicosky, K.J., Eimer, W.A., Tucker, S., Ghofrani, J., Lefkowitz, A., McColl, G., Goldstein, L.E., Tanzi, R.E., and Moir, R.D. (2016). Amyloid-β peptide protects against microbial infection in mouse and worm models of Alzheimer's disease. Sci. Transl. Med. *8*, 340ra72.
4. Dukart, J., Kherif, F., Mueller, K., Adaszewski, S., Schroeter, M.L., Frackowiak, R.S., and Draganski, B.; Alzheimer's Disease Neuroimaging Initiative (2013). Generative FDG-PET and MRI model of aging and disease progression in Alzheimer's disease. PLoS Comput. Biol. *9*, e1002987.
5. La Joie, R., Perrotin, A., Barré, L., Hommet, C., Mézenge, F., Ibazizene, M., Camus, V., Abbas, A., Landeau, B., Guilloteau, D., et al. (2012). Region-specific hierarchy between atrophy, hypometabolism, and β-amyloid (Aβ) load in Alzheimer's disease dementia. J. Neurosci. *32*, 16265–16273.
6. Willette, A.A., Bendlin, B.B., Starks, E.J., Birdsill, A.C., Johnson, S.C., Christian, B.T., Okonkwo, O.C., La Rue, A., Hermann, B.P., Koscik, R.L., et al. (2015). Association of insulin resistance with cerebral glucose uptake in late middle-aged adults at risk for Alzheimer disease. JAMA Neurology *72*, 1013–1020.
7. Shah, K., Desilva, S., and Abbruscato, T. (2012). The role of glucose transporters in brain disease: diabetes and Alzheimer's disease. Int. J. Mol. Sci. *13*, 12629–12655.
8. Ding, F., Yao, J., Rettberg, J.R., Chen, S., and Brinton, R.D. (2013). Early decline in glucose transport and metabolism precedes shift to ketogenic system in female aging and Alzheimer's mouse brain: implication for bioenergetic intervention. PLoS ONE *8*, e79977.
9. Winkler, E.A., Nishida, Y., Sagare, A.P., Rege, S.V., Bell, R.D., Perlmutter, D., Sengillo, J.D., Hillman, S., Kong, P., Nelson, A.R., et al. (2015). GLUT1 reductions exacerbate Alzheimer's disease vasculo-neuronal dysfunction and degeneration. Nat. Neurosci. *18*, 521–530.
10. Liu, F., Shi, J., Tanimukai, H., Gu, J., Gu, J., Grundke-Iqbal, I., Iqbal, K., and Gong, C.X. (2009). Reduced O-GlcNAcylation links lower brain glucose metabolism and tau pathology in Alzheimer's disease. Brain *132*, 1820–1832.
11. van der Harg, J.M., Nölle, A., Zwart, R., Boerema, A.S., van Haastert, E.S., Strijkstra, A.M., Hoozemans, J.J., and Scheper, W. (2014). The unfolded protein response mediates reversible tau phosphorylation induced by metabolic stress. Cell Death Dis. *5*, e1393.
12. Sofola, O., Kerr, F., Rogers, I., Killick, R., Augustin, H., Gandy, C., Allen, M.J., Hardy, J., Lovestone, S., and Partridge, L. (2010). Inhibition of GSK-3 ameliorates Abeta pathology in an adult-onset *Drosophila* model of Alzheimer's disease. PLoS Genet. *6*, e1001087.
13. Volkenhoff, A., Weiler, A., Letzel, M., Stehling, M., Klämbt, C., and Schirmeier, S. (2015). Glial glycolysis is essential for neuronal survival in *Drosophila*. Cell Metab. *22*, 437–447.
14. Crowther, D.C., Kinghorn, K.J., Miranda, E., Page, R., Curry, J.A., Duthie, F.A., Gubb, D.C., and Lomas, D.A. (2005). Intraneuronal Abeta, non-amyloid aggregates and neurodegeneration in a *Drosophila* model of Alzheimer's disease. Neuroscience *132*, 123–135.
15. Chintapalli, V.R., Wang, J., and Dow, J.A. (2007). Using FlyAtlas to identify better *Drosophila melanogaster* models of human disease. Nat. Genet. *39*, 715–720.
16. Potter, C.J., and Luo, L. (2011). Using the Q system in *Drosophila melanogaster*. Nat. Protoc. *6*, 1105–1120.
17. Riabinina, O., Luginbuhl, D., Marr, E., Liu, S., Wu, M.N., Luo, L., and Potter, C.J. (2015). Improved and expanded Q-system reagents for genetic manipulations. Nat. Methods *12*, 219–222.
18. Kaufman, R.J. (2002). Orchestrating the unfolded protein response in health and disease. J. Clin. Invest. *110*, 1389–1398.
19. Hetz, C., and Mollereau, B. (2014). Disturbance of endoplasmic reticulum proteostasis in neurodegenerative diseases. Nat. Rev. Neurosci. *15*, 233–249.
20. Casas-Tinto, S., Zhang, Y., Sanchez-Garcia, J., Gomez-Velazquez, M., Rincon-Limas, D.E., and Fernandez-Funez, P. (2011). The ER stress factor

Appendix 6

Kinghorn, K.J., Gronke, S., Castillo-Quan, J.I., Woodling, N.S., **Li, L.**, Sirka, E., Gegg, M., Mills, K., Hardy, J., Bjedov, I., et al. (2016). A Drosophila Model of Neuronopathic Gaucher Disease Demonstrates Lysosomal-Autophagic Defects and Altered mTOR Signalling and Is Functionally Rescued by Rapamycin. J Neurosci *36*, 11654-11670.

Neurobiology of Disease

A *Drosophila* Model of Neuronopathic Gaucher Disease Demonstrates Lysosomal-Autophagic Defects and Altered mTOR Signalling and Is Functionally Rescued by Rapamycin

Kerri J. Kinghorn,[1,2] Sebastian Grönke,[3] Jorge Iván Castillo-Quan,[1,2,3] Nathaniel S. Woodling,[1] Li Li,[1,2] Ernestas Sirka,[4] Matthew Gegg,[5] Kevin Mills,[4] John Hardy,[2] Ivana Bjedov,[6] and Linda Partridge[1,3]

[1]Institute of Healthy Ageing and Department of Genetics, Evolution and Environment, University College London, London WC1E 6BT, United Kingdom, [2]Institute of Neurology, University College London, London WC1N 3BG, United Kingdom, [3]Max Planck Institute for Biology of Ageing, D-50931 Köln, Germany, [4]Centre for Translational Omics, Institute of Child Health, University College London, London WC1N 1EH, United Kingdom, [5]Clinical Neuroscience, Institute of Neurology, University College London, London NW3 2PF, United Kingdom, and [6]University College London Cancer Institute, London WC1E 6DD, United Kingdom

Glucocerebrosidase (*GBA1*) mutations are associated with Gaucher disease (GD), an autosomal recessive disorder caused by functional deficiency of glucocerebrosidase (GBA), a lysosomal enzyme that hydrolyzes glucosylceramide to ceramide and glucose. Neuronopathic forms of GD can be associated with rapid neurological decline (Type II) or manifest as a chronic form (Type III) with a wide spectrum of neurological signs. Furthermore, there is now a well-established link between *GBA1* mutations and Parkinson's disease (PD), with heterozygote mutations in *GBA1* considered the commonest genetic defect in PD. Here we describe a novel *Drosophila* model of GD that lacks the two fly *GBA1* orthologs. This knock-out model recapitulates the main features of GD at the cellular level with severe lysosomal defects and accumulation of glucosylceramide in the fly brain. We also demonstrate a block in autophagy flux in association with reduced lifespan, age-dependent locomotor deficits and accumulation of autophagy substrates in dGBA-deficient fly brains. Furthermore, mechanistic target of rapamycin (mTOR) signaling is downregulated in dGBA knock-out flies, with a concomitant upregulation of *Mitf* gene expression, the fly ortholog of mammalian *TFEB*, likely as a compensatory response to the autophagy block. Moreover, the mTOR inhibitor rapamycin is able to partially ameliorate the lifespan, locomotor, and oxidative stress phenotypes. Together, our results demonstrate that this *dGBA1*-deficient fly model is a useful platform for the further study of the role of lysosomal-autophagic impairment and the potential therapeutic benefits of rapamycin in neuronopathic GD. These results also have important implications for the role of autophagy and mTOR signaling in GBA1-associated *PD*.

Key words: autophagy; *Drosophila*; Gaucher disease; glucocerebrosidase; mTOR; rapamycin

Significance Statement

We developed a *Drosophila* model of neuronopathic GD by knocking-out the fly orthologs of the *GBA1* gene, demonstrating abnormal lysosomal pathology in the fly brain. Functioning lysosomes are required for autophagosome-lysosomal fusion in the autophagy pathway. We show *in vivo* that autophagy is impaired in dGBA-deficient fly brains. In response, mechanistic target of rapamycin (mTOR) activity is downregulated in dGBA-deficient flies and rapamycin ameliorates the lifespan, locomotor, and oxidative stress phenotypes. *dGBA* knock-out flies also display an upregulation of the *Drosophila* ortholog of mammalian *TFEB*, *Mitf,* a response that is unable to overcome the autophagy block. Together, our results suggest that rapamycin may have potential benefits in the treatment of GD, as well as PD linked to *GBA1* mutations.

Introduction

Homozygous mutations in the glucocerebrosidase gene (*GBA1*) can cause Gaucher disease (GD), the commonest lysosomal storage disorder. *GBA1* encodes glucocerebrosidase (GBA, also known as glucosylceramidase [GCase]), which mediates the lysosomal hydrolysis of glucosylceramide to form ceramide and glucose. Loss of GBA activity leads to lysosomal accumulation of glucosylceramide and its nonacylated analog glucosylsphingosine in a number of cell types,

Received Dec. 18, 2015; revised Aug. 17, 2016; accepted Sept. 6, 2016.

Author contributions: K.J.K., S.G., J.I.C.-Q., N.S.W., J.H., I.B., and L.P. designed research; K.J.K., S.G., J.I.C.-Q., N.S.W., E.S., L.L., M.G., and K.M. performed research; K.J.K., S.G., J.I.C.-Q., N.S.W., L.L., E.S., and M.G. analyzed data; K.J.K., J.H., and L.P. wrote the paper.

K.J.K., L.P., and J.H. were supported by the Wellcome Trust. This work was supported by Wellcome Trust MRC strategic neurodegenerative disease initiative award WT089698. K.J.K. received a postdoctoral Wellcome Trust fellowship 090541/Z/09/Z. L.P., S.G., L.L., and J.I.C.-Q. were supported by the Max Planck Society. L.L. received a Parkinson's UK PhD studentship H-1105. J.I.C.-Q. was supported by UCL Scholarships. I.B. was supported by an ERC

including macrophages and neurons, giving rise to the visceral and neurological manifestations of GD, respectively (Cox, 2010). GD is classified into three clinical subtypes based on the absence (Type I) or presence (Types II and III) of neurological involvement. Type II, or acute neuronopathic GD, is rare but results in rapidly progressive neurological decline, with a wide spectrum of clinical signs and death in infancy or early childhood. Type III, or chronic neuronopathic GD, is a more slowly progressive disorder with neurological features, including eye movement abnormalities, myoclonic epilepsy, ataxia, and dementia (Sidransky, 2004). There are currently no therapies available that target the neuronal pathology associated with GD because existing treatments, such as recombinant enzyme replacement therapy, fail to permeate the blood–brain barrier (Cox, 2010).

As well as causing GD, heterozygous *GBA1* mutations are now well-established genetic risk factors for PD and other synucleinopathies, characterized by the presence of intraneuronal aggregates called Lewy bodies (LBs), predominantly containing α-synuclein as well as ubiquitin (Shults, 2006). Both loss-of-function and gain-of-function hypotheses have been put forward to explain how mutations in *GBA1* lead to lysosomal dysfunction and neurodegeneration, and there is mounting evidence in support of the loss of GBA function hypothesis (Kinghorn, 2011). Lysosomal dysfunction in GD has far-reaching implications, not only for the degradation of α-synuclein, but also for the autophagic degradation of other superfluous or damaged cellular material and organelles, as the fusion of lysosomes with autophagosomes is a critical step in the autophagic pathway (Ravikumar et al., 2010). The process of macroautophagy can be divided into key stages, including initiation, elongation, and maturation of autophagosomes, followed by the fusion with lysosomes.

In keeping with the importance of lysosomes in the autophagy pathway, it was recently shown in macrophages and induced pluripotent stem cell (iPSC)-derived neuronal cells from GD patients that autophagy is impaired (Awad et al., 2015; Aflaki et al., 2016). Furthermore, this defect in autophagy was shown to trigger inflammasome activation and the production of inflammatory cytokines (Aflaki et al., 2016). Moreover, Osellame et al. (2013) demonstrated that there is accumulation of dysfunctional and fragmented mitochondria in a neuronopathic mouse model of GD, thought to be secondary to autophagic and proteasomal defects.

To further understand the mechanisms linking loss of GBA activity to neurodegeneration in neuronopathic GD, and also to determine whether autophagy plays a role in neurons *in vivo*, we developed a novel *Drosophila* model that lacks the two *GBA1* orthologs, *dGBA1a* and *dGBA1b*. The fruit fly has proven to be a useful model system for studying neurodegenerative diseases (Kinghorn et al., 2015) and lysosomal storage disorders, including those affecting the nervous system, such as neuronal ceroid lipofuscionoses (Myllykangas et al., 2005; Hindle et al., 2011). It is therefore a useful model for studying the mechanisms of pathogenesis of GD as well as the role of *GBA1* in neurodegeneration.

The dGBA knock-out flies proved to be faithful models of GD, with significant lysosomal dysfunction and buildup of the dGBA substrate, glucosylceramide, in the fly brain. Furthermore, there was significant neuronal autophagy impairment, which was associated with reduced survival and age-dependent locomotor abnormalities. At the cellular level, we demonstrated accumulation of p62 and polyubiquitinated proteins, both of which accumulate to form LBs in PD (Zatloukal et al., 2002), in addition to mitochondrial abnormalities. Moreover, dGBA-deficient flies displayed decreased mechanistic target of rapamycin (mTOR) signaling with a reduction in p70 S6 kinase (S6K) phosphorylation, and the mTOR inhibitor rapamycin was able to partially ameliorate the neurodegenerative phenotypes. Our results thus show an important role of autophagy and mTOR signaling in GD, and provide a useful model for the further study of pathogenic mechanisms downstream of lysosomal dysfunction.

Materials and Methods

Fly stocks and husbandry. All fly strains used were backcrossed at least 6 generations into the w^{1118} background to obtain isogenic lines. All fly stocks were maintained at 25°C on a 12:12 h light: dark cycle at constant humidity on a standard sugar-yeast medium (15 g/L-1 agar, 50 g/L-1 sugar, 100 gl-1 autolyzed yeast, 3g/L nipagin, and 3 ml/L propionic acid). For all experiments, flies were raised at a controlled density on standard sugar-yeast medium in 200 ml bottles.

Generation of dGBA1a *and* dGBA1b *mutants by ends-out homologous recombination.* The genes encoding *dGBA1a* (CG31148) and *dGBA1b* (CG31414) are located in close proximity on *Drosophila* chromosome 3, separated by the *CG31413* gene (see Fig. 1*A*). We generated specific mutants for *dGBA1a, dGBA1b* and a *dGBA1a* and *dGBA1b* double-mutant, without affecting the coding sequence of CG31413 by ends-out homologous recombination (Gong and Golic, 2004). *dGBA1a* was mutated by replacing the whole ORF with a $white^{hs}$ marker gene. *dGBA1b* was mutated by introducing a stop codon and a subsequent frame shift mutation 12 bp downstream of the predicted ATG start codon. In addition, an EcoRV restriction site was introduced to allow PCR screening of the introduced mutations. To clone the donor construct for homologous recombination, ~4 kb of 5′ and 3′ flanking sequences of the *dGBA1a* gene were cloned into the pBluescript II SK+ vector (Stratagene) by ET recombination using BAC clone CH321–50J5 (BACPAC Resource Center, Oakland, California) as template and primers SOL474/475 and SOL476/477 for the 5′ and 3′ arms, respectively. Mutations in the 3′ arm were introduced using the QuikChange site-directed mutagenesis kit (Agilent Technologies) and primers SOL482/483. Both 5′ and 3′ homologous arms were subcloned into the pW25 vector (Gong and Golic, 2004) and full-length sequenced. pW25 was obtained from the *Drosophila* Genomics Resource Centre. The dGBA donor construct was transformed into the germline of *Drosophila melanogaster* by P-element-mediated germ line transformation using the Best Gene *Drosophila* Embryo Injection Service. Crosses for ends-out homologous recombination were performed according to the rapid targeting scheme (Gong and Golic, 2004). Subsequently, the $white^{hs}$ marker gene was genetically mapped and homologous recombination events were identified by PCR. Point mutations introduced into *dGBA1b* were identified by PCR with primers SOL484 and SOL485 and subsequent digestion with EcoRV, which results in two specific DNA fragments of 120 and 193 bp from the uncut 313 bp wild-type DNA fragment. Oligonucleotide primers used for cloning and genotyping are listed in Table 1.

qRT-PCR. Total RNA was extracted from 25 heads or 25 thoraces and abdomens of 6-d-old adult flies per sample using Trizol (Invitrogen) and further purified over an RNeasy Mini column (QIAGEN) with on-column DNase digestion. cDNA was prepared from 2.5 μg RNA using the SuperScript Vil cDNA synthesis kit (Invitrogen). qRT-PCR data were performed with TaqMan primers (Applied Biosystems) in a 7900HT

Starting Grant 311331. We thank all members of the L.P. laboratory for helpful discussions and advice (especially Drs Fiona Kerr and Teresa Nicoli); Dr. Manolis Fanto (Kings College London) for help with interpretation of the electron micrographs; and Dr Kerrie Venner (Institute of Neurology Electron Microscopy Unit) for technical help with electron microscopy. We also thank Dr. Alex Whitworth, University of Cambridge, for useful discussions.

The authors declare no competing financial interests.

This article is freely available online through the *J Neurosci* Author Open Choice option.

Correspondence should be addressed to either Dr. Kerri J. Kinghorn or Professor Dame Linda Partridge, Institute of Healthy Ageing and Department of Genetics, Environment and Evolution, University College London, London WC1E 6BT, United Kingdom. E-mail: k.kinghorn@ucl.ac.uk and l.partridge@ucl.ac.uk.

DOI:10.1523/JNEUROSCI.4527-15.2016

Table 1. The oligonucleotide primers used for cloning and genotyping in the generation of the dGBA knockout flies

Name	Gene	Sequence	RS	Comment
SOL474	*GBA1a*	TTCGTAAACAATTTATTTTTCCGATAAAATTCGAATCTCCTATTATTAAACGTACGcacaacatacgagccggaagcata	BsiWI	ET Rec
SOL475	*GBA1a*	CTCCAGTTGCGTTTTGCCAAAAGAACCAGGTGTCAATCAGGTGGCAGCGTGGCGCGCCatgtgcgcggaacccctatttg	AscI	ET Rec
SOL476	*GBA1a*	AACATGTCTTTATTTAATTTTTTGTTTTGTTTAGAAAAAATAAGTTTTCAGCATGCcacaacatacgagccggaagcata	SphI	ET Rec
SOL477	*GBA1a*	CGCTCCTCCCGCAACAATTCGCTGAACTACTTGGATGGCCTAGCTGTTCAGCGGCCGCatgtgcgcggaacccctatttg	NotI	ET Rec
SOL482	*GBA1b*	ATGCCAGATATCTAGTACACCACTGCTTGG		
SOL483	*GBA1b*	CCAAGCAGTGGTGTACTAGATATCTGGCAT		
SOL484	*GBA1b*	ATTCGCCGGTCCGGCTGCTT		
SOL485	*GBA1b*	CTGCAATGCGTTTCATTTGAGG		
SOL804	*CG31468*	TAATCTACGCCCAGCCCACTTG		
SOL846	*CG31468*	ACGCTGCCACCTGATTGACA		
SOL847	*GBA1a*	ATGGGAAAAATGTTCGCCAGC		
SOL848	*GBA1a*	CTGTACAGCAGAGTGTGAATGG		
SOL850	*CG31413*	CATCAGTGGCAGTTTACCAGTC		
SOL851	*CG31413*	AAGCAGCCGGACCGGCGAAT		

real-time PCR system (Applied Biosystems). The TaqMan primers used were as follows: Dm02150554_m1 for *dGBA1b*, Dm02143806_g1 for *dGBA1a*, Dm02150538_s1 for CG31413, and a custom-made probe against Rpl32. For each sample, 4 biological replicates and 4 technical replicates were used. Relative expression was calculated using the ΔΔCT method and Rpl32 as normalization control.

For assessment of *Mitf* and *Atg8a* gene expression levels, total RNA was extracted from 20–25 fly heads per sample using TRIzol (Invitrogen) according to the manufacturer's instructions. Then 5 μg of total RNA was subjected to DNA digestion using DNase I (Ambion), immediately followed by reverse transcription using the SuperScript II system (Invitrogen) with oligo(dT) primers. qPCR was performed using the PRISM 7000 sequence-detection system (Applied Biosystems) and SYBR Green (Invitrogen) by following the manufacturer's instructions. Each sample was analyzed in duplicate, and values are the mean of the 3 or 4 independent biological repeats. The primers used were as follows: *atg8*, ATTCC ACCAACATCGGCTAC and GCCATGCCGTAAACATTCTC; *Mitf*, GC GTTCTTCTTCAGGGATTG and ACTTACGCTCGGCGAAATAG; and RP49, ATCGGTTACGGATCGAACAA and GACAATCTCCTTGCG CTTCT.

Lifespan, climbing, and fecundity analyses. The survival, climbing, and fecundity assays were performed as previously described (Kinghorn et al., 2015). For the lifespan experiments, 150 female flies (unless otherwise stated) were housed in groups of 15 and the flies were transferred every 2–3 d onto fresh food and the number of dead flies recorded.

Feeding assay (proboscis extension). Feeding rates of flies were measured using a proboscis-extension assay in undisturbed conditions as previously described (Wong et al., 2009). Briefly, flies were housed in groups of 5 per vial and kept undisturbed for 24 h before recording observation. Feeding rate was scored by a brief but continuous observation for at least 1 h of the number of flies actively extending their proboscis on the fly medium. Observation recordings were made blindly. Feeding ability was calculated by the number of feeding events divided by the number of flies in the vial over the time period measured and then by averaging this for all of the vials per genotype.

Stress experiments and rapamycin treatment. For all stress assays, flies were reared and housed as for lifespan experiments, and oxidative stress and starvation assays were performed as previously described (Kinghorn et al., 2015). Rapamycin (LC Laboratories) was dissolved in 100% ethanol to give a 50 mM stock concentration. It was then added to the standard fly medium to give the desired final concentration. Equivalent volumes of vehicle were supplemented to the medium to compensate for dilution.

Measurement of dGBA activity. dGBA activity was measured using a similar method to that previously described (Davis et al., 2016). Briefly, 20 fly heads of each genotype were homogenized and debris cleared by centrifugation. Lysates (7.5 μg protein) were mixed with 0.1 M sodium acetate, pH 4.5, and 5 mM 4-methyllumbelliferyl-β-D-glucopyranoside and incubated at 37°C. The reaction was stopped with 0.25 M glycine buffer, pH 10.4, and fluorescence measured on fluorescent plate reader (excitation, 360 nm; emission, 460 nm). dGBA activity was also measured in the presence of the inhibitor conduritol-β-epoxide (100 μM) and dGBA activity calculated as total GBA activity minus CBE-sensitive GBA activity and expressed as pmol/h/mg protein. Approximately 50% of the total dGBA activity was abolished by incubation with conduritol-β-epoxide in w^{1118} control flies.

Measurement of glucosylceramide levels. Fly heads ($n = 70$) were analyzed for glucosylceramide accumulation. The substrate was extracted in 500 μl of chloroform/methanol (2:1 v/v) containing 80 μg/ml of d4-C16:0-glucosylceramide internal standard, which was synthesized in house (Mills et al., 2005). The samples were shaken for 30 min at room temperature before the addition of 100 μl of PBS for phase separation. After a 10 min centrifugation at 16,000 × *g*, upper and lower phases were collected and 5 μl of each was injected into the ultra-performance liquid chromatography-tandem mass spectrometry system. Synthetic glucosylceramide standard (Matreya) was also analyzed to confirm analyte identity.

The samples were injected onto Waters ACQUITY UPLC system operated in partial loop mode and separated on Waters ACQUITY UPLC BEH C18 column (130Å, 1.7 μm, 2.1 mm × 50 mm) under the following gradient conditions: 0.00–0.20 → 80% A; 0.20–5.00 → 0.1% A; 5.00–9.00 → 0.1% A; 9.01–11.00 → 80% A, where mobile Phase A was ddH_2O [0.1% FA] and Phase B was methanol. Column and sample temperatures were kept at 40°C and 10°C, respectively. Weak wash solvent was ddH_2O (0.1% FA), and strong wash solvent was acetonitrile: methanol:isopropanol:ddH_2O (1:1:1:1 v/v). The eluting analytes were detected on a Waters XEVO TQ-S triple quadrupole mass spectrometer, which was equipped with the electrospray ion source and operated in MRM and positive ion mode with the tune page parameters set to achieve the maximum sensitivity for glycosphingolipids as described previously (Auray-Blais et al., 2015). The data were processed with MassLynx version 4.1.

Measurement of lysosomal enzymes. Twenty flies were homogenized in RIPA buffer (150 mM NaCl, 50 mM Tris, pH 8.0, 1% (v/v) NP-40, 1% (w/v) sodium deoxycholate, 0.1% (w/v) SDS, protease inhibitor mixture) with a micro-pestle. Debris was pelleted at 17, 000 × *g* and protein concentration of the supernatant was determined using the protein BCA kit (Pierce). β-Hexosaminidase activity (10 μg protein) was measured in McIlvaine citrate buffer, pH 4.2, with 2 mM 4-methylumbelliferyl-*N*-acetyl-glucosamide substrate. β-Galactosidase activity (10 μg protein) was measured in McIlvaine citrate buffer, pH 4.1, with 0.25 mM 4-methylumbelliferyl-β-D-galactopyransoside substrate. Both enzyme assays were incubated at 37°C for 30 min and the reaction stopped by addition of 0.25 M glycine, pH 10.4. Fluorescent product was measured using a plate reader (excitation, 340 nm; emission, 460 nm) and compared against 1 nmol 4-methyllumbelliferone standard.

Triacylglyceride and ATP assays. Levels of triacylglyceride (TAG) in adult females were measured using the Triglyceride Infinity Reagent (Thermo Scientific) and normalized to total body protein using a BCA assay (Sigma). The ATP concentration of whole female flies was determined using the ATP Bioluminescence Assay Kit HS II (Roche) as previously described (Kinghorn et al., 2015).

Antibodies and Western blotting. For Atg8 Western blotting, 10 to 15 fly heads or 5 headless bodies were homogenized in 2 × Laemmli loading buffer (100 mM Tris 6.8, 20% glycerol, 4% SDS) containing 5% β-mercaptoethanol and then boiled for 5 min. Approximately 40 μg of protein extract was loaded per lane. Proteins were separated on SDS polyacrylamide gels and transferred to a nitrocellulose membrane. For ubiquitin Western blots, 12 fly heads per sample were homogenized in Triton-X buffer (1% Triton-X, 10 mM NEM, 50 μm MG132, Complete Mini protease inhibitors, Roche, in PBS). After centrifugation, the insoluble pellet was resuspended in SDS buffer (2% SDS, 10 mM NEM, 50 μm MG132, complete mini protease inhibitors, Roche, 50 mM Tris, pH 7.4), centrifuged, and the supernatant collected as the insoluble sample for Western blot. Proteins were separated on 4%–12% NuPage Bis-Tris gels (Invitrogen) and transferred to a PVDF membrane. The membranes were then blocked in 5% BSA in TBST (TBS with 0.05% Tween 20) for 1 h at room temperature, after which they were probed with primary antibodies diluted in 5% BSA in TBST overnight at 4°C. Blots were developed using the ECL detection system. The following primary antibodies were used: β-actin (Abcam, #ab1801; 1:5000), mouse anti-polyubiquitinated proteins (clone FK2, Millipore, 1:1000) and anti-Atg8 (1:1000) (Castillo-Quan et al., 2016).

For detection of S6K and tS6K protein levels, 15 fly heads in each sample were prepared by homogenization in 2 × SDS Laemmli sample buffer (4% SDS, 20% glycerol, 120 mM Tris-HCl, pH 6.8, 200 mM DTT with bromophenol blue), and boiled at 95°C for 5 min. Samples were separated on precast 4%–12% Invitrogen Bis-Tris gels (NP0322) and blotted onto nitrocellulose paper in Tris-glycine buffer supplemented with 10% ethanol. They were then blocked as above, and the primary antibodies used were anti-phosphorylated S6K anti-phospho-Thr398-S6K (Cell Signaling Technology, #9209, 1:1000), anti-total-S6K (1:1000) (Sofola-Adesakin et al., 2014). The appropriate secondary antibodies (Abcam) were diluted 1:10,000 in 5% BSA in TBST for 1 h at room temperature. Bands were visualized with Luminata Forte (Millipore).

All blots were imaged with ImageQuant LAS4000 (GE Healthcare Life Science). Quantification was performed using the ImageJ program (National Institutes of Health).

Immunohistochemistry, LysoTracker, confocal imaging, and quantification. For immunohistochemistry, adult brains were dissected in PBS and immediately fixed in cold 4% PFA (v/v) for 20 min at room temperature. After fixation, the samples were washed in PBT (PBS containing 0.3% Triton X-100, v/v) four times for 20 min then blocked in PBT containing 10% BSA (PBT-BSA) for 2 h at 20°C-30°C. For primary antibody treatment, samples were incubated in PBT-BSA containing the primary antibody for 3 d at 4°C. After primary antibody incubation, brains were washed in PBT, four times for 20 min at 20°C-30°C, then incubated in PBT-BSA containing the secondary antibody for 24 h at 4°C. Brains were washed four times with PBT for 20 min at 20°C-30°C. Brains were finally mounted in Vectashield containing DAPI overnight (Vector Laboratories). Antibodies were used at the following dilutions: rabbit anti-Ref(2)P (Abcam) 1:200; mouse anti-polyubiquitinated proteins (FK2, Millipore) 1:200; mouse anti-Bruchpilot (DSHB antibody nc82), 1:100; secondary goat anti-rabbit AlexaFluor-568 1:250, and secondary goat-anti-mouse AlexaFluor-488 1:250.

For Ref(2)P and ubiquitin staining, image stacks of specimens were obtained on a Zeiss LSM700 confocal microscope using a 10 × objective for whole-brain imaging. Stacks of 7.25 μM *Z* distance and 14 images per stack were taken. Images were quantified using ImageJ software. Briefly, confocal stacks were merged into a single plane by using the maximum projection function. A region of each central brain was manually selected (200 μm high, 100 μm wide) from the dorsal to the ventral aspect of the brain. Thresholds were then set for p62/Ref(2)P and ubiquitin, and the area above threshold within this region was measured.

For Bruchpilot staining, image stacks were obtained using a 40 × objective in the region encompassing the ventral edge of the antennal lobe and dorsal edge of the subesophageal ganglion. Stacks of 1.00 μM *Z* distance and 11 images per stack were taken. Images were quantified using ImageJ software. Briefly, confocal stacks were merged into a single plane by using the average projection function. Two regions of each image were manually selected (10 μm high, 10 μm wide), one in the center of the antennal lobe region and one in the center of the suboesphageal ganglion region, by an observer blinded to genotype. The mean intensity of Bruchpilot staining was then measured for each region of interest.

For LysoTracker staining, adult brains were dissected in PBS and immediately transferred to a solution of PBS with 1 μM LysoTracker Red DND-99 (Invitrogen) and 1 μM DAPI. Brains were mounted on slides in this solution and imaged within 15 min of dissection on a Zeiss LSM700 confocal microscope using a 40 × objective. For each replicate within the experiment, one control and one mutant brain were imaged side by side, with identical microscope settings and images taken from the same region of the subesophageal ganglion for each brain. Images were quantified using ImageJ software, by setting a threshold for LysoTracker and measuring the area above threshold.

Electron microscopy of fly brains and image analysis. The flies were decapitated and the proboscis removed to allow penetration of the fixative. They were then processed and visualized using previously described methods (Kinghorn et al., 2015). Cross-sectional mitochondrial and rhabdomere areas were measured manually using ImageJ software.

Statistical analyses. Survival experiments were analyzed using log rank test. Single comparisons were analyzed using the Student's *t* test. Other data were tested by ANOVA, and planned comparisons of means were made using Tukey-Kramer HSD test. Statistical analyses were performed using Excel, GraphPad Prism, or JMP software version 9 (SAS Institute).

Results

Knock-out of the *Drosophila* orthologs of GBA1 using homologous recombination

Drosophila melanogaster has two orthologs of the human *GBA1* gene, CG31148 and CG31414, which we refer to as *dGBA1a* and *dGBA1b*, respectively. These two genes are found on the same chromosome, separated by the *CG31413* gene (Fig. 1*A*), and show differential tissue expression. *dGBA1b* is expressed in the adult brain, albeit at low levels, as well as moderately expressed in the adult fat body. *dGBA1a* is predominantly expressed in the adult fly digestive system and shows no expression in the adult brain (Flyatlas) (Robinson et al., 2013). To study the function of the *dGBA1* genes, we produced loss-of-function mutants lacking *dGBA1a* ($dGBA1a^{-/-}$), d*GBA1b* ($dGBA1b^{-/-}$), or double-mutants lacking both genes ($dGBA1a,b^{-/-}$) using ends-out homologous recombination. The complete open reading frame of *dGBA1a* was knocked out by homologous recombination, whereas *dGBA1b* expression was disrupted by the introduction of a stop codon and a frame shift 12b downstream of the putative ATG start codon (Fig. 1*A*; for more details, see Materials and Methods). Deletion of *dGBA1a* and integrity of the *CG31413* gene were confirmed by PCR on genomic DNA (Fig. 1*B*). Furthermore, introduction of specific point mutations within the *dGBA1b* gene were verified by PCR (Fig. 1*C*) and sequencing. To test whether these mutations affected expression of the *dGBA* genes and the interjacent *CG31413* gene, we measured mRNA transcript levels by qRT-PCR data in female heads and bodies for *dGBA1b* (Fig. 1*D*), in female bodies for *dGBA1a* (Fig. 1*E*), and in male bodies for *CG31413* (Fig. 1*F*). The latter gene is specifically expressed in male accessory glands (Flyatlas) (Robinson et al., 2013). *dGBA1b* transcript levels were barely detected in $dGBA1b^{-/-}$ single-mutant and $dGBA1a,b^{-/-}$ double-mutant flies (Fig. 1*D*), suggesting that the introduced point mutations affect the stability of the *dGBA1b* transcript. *dGBA1a* expression was absent from $dGBA1a^{-/-}$ single-mutant and $GBA1a,b^{-/-}$ double-mutant flies (Fig. 1*E*) and *CG31413* expression was slightly reduced in $dGBA1a,b^{-/-}$ double-mutants (Fig. 1*F*). Thus, the qRT-PCR data suggest that both $dGBA1a^{-/-}$ and $dGBA1b^{-/-}$ are loss-of-function alleles for the respective *dGBA* genes, with the single mutations not affecting expression of the CG31413 gene, and the double mutation very slightly reducing it. Knock-out of *dGBA1a*, *dGBA1b*, or both genes was not associated with any gross changes in body size or obvious differences in morphology (data not shown). In keeping

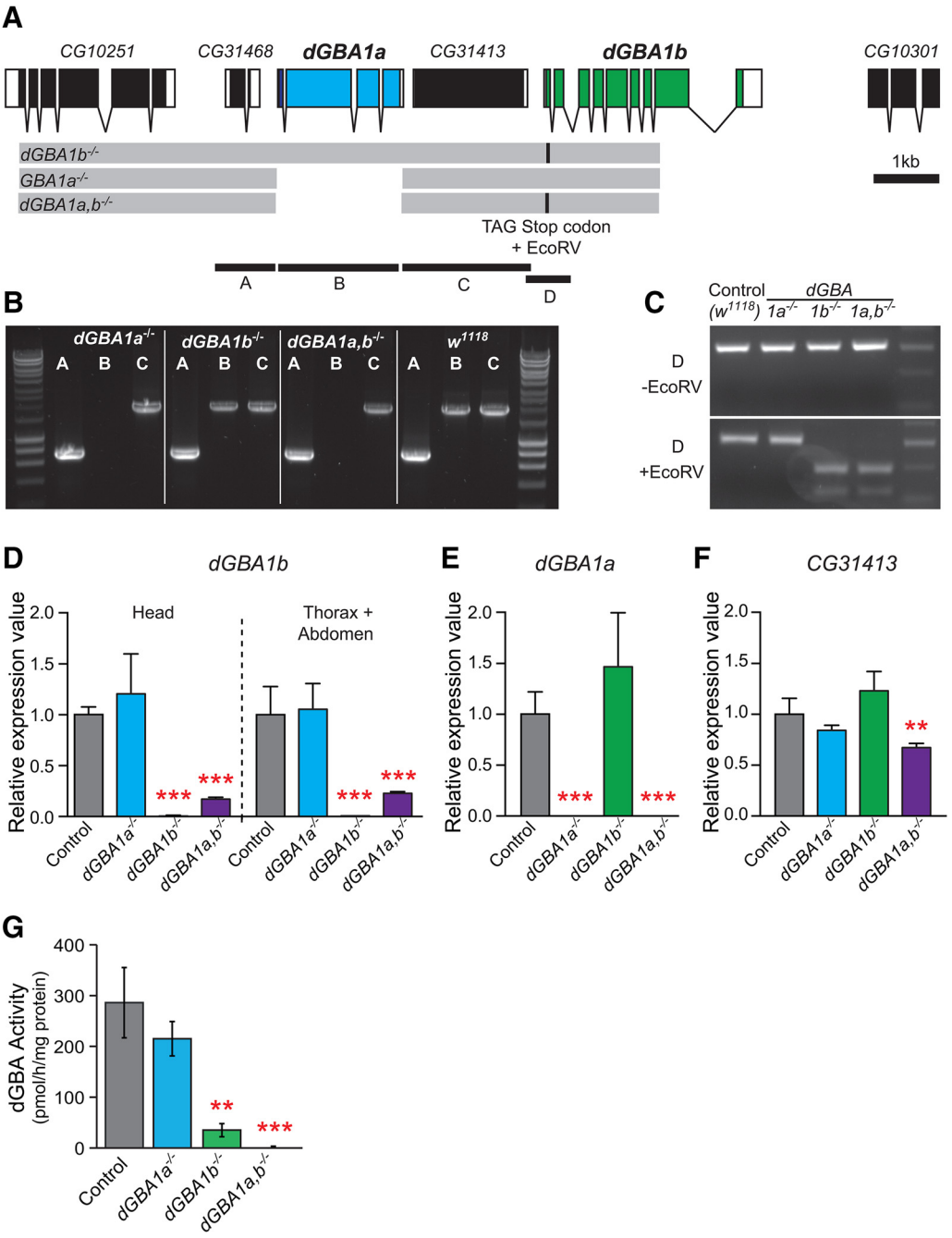

Figure 1. Generation of flies lacking the d*GBA1a* and d*GBA1b* genes. ***A***, Schematic view of the *dGBA1* gene locus. *dGBA1a* and *dGBA1b* are located in close proximity separated by the CG31413 gene, the function of which is unknown. Gray bars represent donor constructs for ends-out homologous recombination. Gaps between gray bars indicate genomic regions replaced by a *white*^{hs} marker gene. Black boxes represent coding parts of exons. White boxes represent noncoding regions. *dGBA1a* was mutated by introduction of a stop codon and a frame shift 12 kb downstream of the ATG start codon. Black bars ***A–D*** represent genomic regions PCR amplified in ***B***, ***C***. ***B***, PCR on genomic DNA of *dGBA1b*$^{-/-}$, *dGBA1a*$^{-/-}$, *dGBA1a, b*$^{-/-}$ mutants and *w*^{1118} control flies. ***C***, PCR verification of point mutations in *dGBA1b* mutants. An EcoRV restriction site accompanied the introduced stop codon and frame shift mutation. Top, Undigested PCR product. Bottom, PCR product restricted with EcoRV. A specific double band is apparent only in *dGBAb*$^{-/-}$ and *dGBA1a, b*$^{-/-}$ mutants. ***D–F***, Quantitative real-time PCR with probes directed against *dGBA1b* (***D***), *dGBA1a* (***E***), and CG31413 (***F***). Total RNA was isolated from female heads (left) and bodies (right) (***D***), female bodies (***E***), and male bodies (***F***). Tissue and gender were chosen corresponding to the endogenous expression of the respective gene. ***D–F***, $^{**}p \leq 0.01$ (one-way ANOVA with Dunnett's test relative to *w*^{1118} controls). $^{***}p \leq 0.001$ (one-way ANOVA with Dunnett's test relative to *w*^{1118} controls). ***G***, dGBA activity in fly heads was decreased by ~95% in *dGBA1b*$^{-/-}$ flies ($^{**}p = 0.01$) and was undetectable in *dGBA1a,b*$^{-/-}$ flies ($^{***}p = 0.006$). Conversely, the dGBA activity measured in *dGBA1a*$^{-/-}$ fly heads was not significantly different from that of controls ($p = 0.39$).

with the expression of *dGBA1b*, and not *dGBA1a*, in the fly brain, dGBA activity levels were decreased by 95% in *dGBA1b*$^{-/-}$ fly heads and were undetectable in the heads of *dGBA1a,b*$^{-/-}$ flies. Conversely, the levels of dGBA activity in *dGBA1a*$^{-/-}$ fly heads were not statistically different from that of controls, consistent with its predominant expression within the fly midgut (Fig. 1*G*).

Flies lacking dGBA displayed reduced lifespan and progressive age-dependent locomotor deficits

The lifespan of flies lacking *dGBA1a* (*dGBA1a*$^{-/-}$), *dGBA1b* (*dGBA1b*$^{-/-}$) or both *dGBA1* genes (*dGBA1a,b*$^{-/-}$) was assessed. *dGBA1b*$^{-/-}$ flies displayed reduced survival compared with control flies. However, *dGBA1a*$^{-/-}$ flies, which lack the *dGBA* isoform ex-

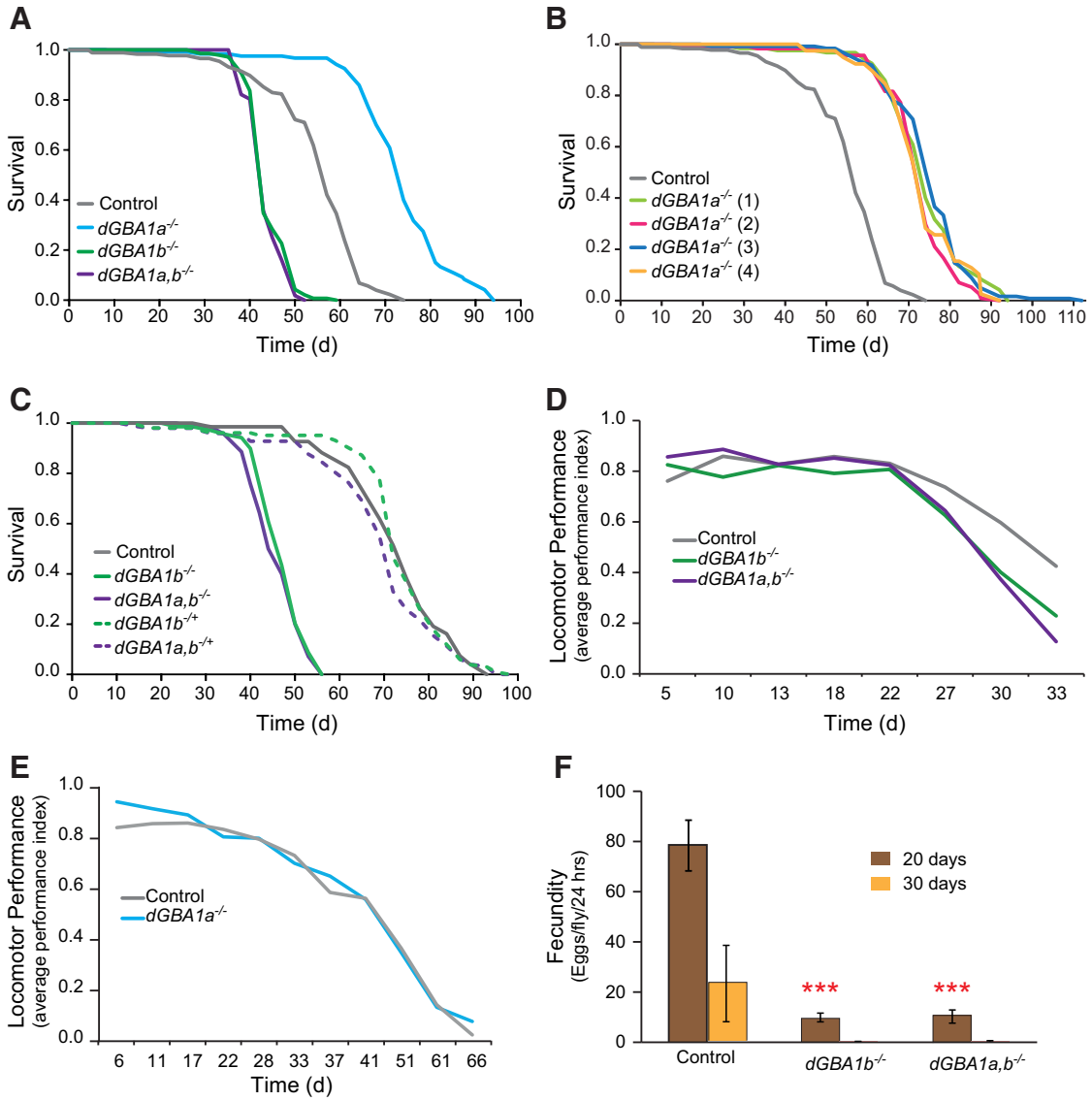

Figure 2. Lack of *dGBA* activity led to reduced survival and locomotor deficits. ***A***, *dGBA1b*$^{-/-}$ and *dGBA1a,b*$^{-/-}$ female flies had significantly reduced lifespan compared with w^{1118} control flies ($p = 3 \times 10^{-39}$ and $p = 7 \times 10^{-27}$). Furthermore, *dGBA1a*$^{-/-}$ flies displayed a significant lifespan extension compared with control flies ($p = 8 \times 10^{-52}$). ***B***, This lifespan extension was consistent using a further 4 independent *dGBA1a*$^{-/-}$ lines (all $p < 6 \times 10^{-12}$, $n = 150$ flies per genotype). ***C***, Flies heterozygous for *dGBA1b* or both *dGBA1* genes (*dGBA1b*$^{-/+}$ and *dGBA1a,b*$^{-/+}$) did not display a lifespan phenotype ($p = 0.69$ and $p = 0.33$). ***D***, *dGBA1b*$^{-/-}$ and *dGBA1a,b*$^{-/-}$ flies showed an age-dependent reduction in climbing ability compared with w^{1118} control flies ($p = 0.0001$ and $p = 0.0004$; $n = 45$ flies per genotype, 3 repeats each). ***E***, The climbing ability of *dGBA1a*$^{-/-}$ flies was indistinguishable from that of controls ($p = 0.38$). ***F***, The fecundity of *dGBA1b*$^{-/-}$ and *dGBA1a,b*$^{-/-}$ flies was significantly reduced at day 20 compared with age-matched control flies. ***$p = 3 \times 10^{-6}$. ***$p = 2 \times 10^{-5}$. They were almost completely infertile at day 30, whereas >20% of the control flies were still able to lay eggs.

pressed mainly in the digestive system, showed a significantly increased survival compared with control flies (Fig. 2*A*), and this trend was seen using 4 additional *dGBA1a* null mutant fly lines (Fig. 2*B*). Interestingly, double-mutant *dGBA1a,b*$^{-/-}$ flies displayed a lifespan that was similar to that of the single *dGBA1b* knock-out line (Fig. 2*A*), suggesting that the detrimental effects of *dGBA1b* deficiency on lifespan cannot be reversed by the prolongevity effects of *dGBA1a* knock-out. Given that *GBA1* mutations are usually found in the heterozygous state in PD and other synucleinopathies, we also assessed *dGBA1b* and *dGBA1a* heterozygote knock-out flies (*dGBA1b*$^{-/+}$ and *dGBA1a*$^{-/+}$) and found that the lifespans of these flies were not significantly different from those of controls (Fig. 2*C*).

In keeping with the lifespan phenotypes, *dGBA1b*$^{-/-}$ and *dGBA1a,b*$^{-/-}$ flies, which lack the *dGBA* isoform expressed in the brain, also displayed progressive age-dependent locomotor deficits, with the climbing ability of *dGBA1b*$^{-/-}$ and *dGBA1a,b*$^{-/-}$ flies in response to light tapping falling below that of controls at older ages (Fig. 2*D*). Knock-out of *dGBA1a*, despite its prolongevity effects, did not have any significant effect on climbing ability over time compared with control flies (Fig. 2*E*). Therefore, because loss of *dGBA1a* was not associated with any lifespan defect or change in locomotor ability, and has no expression in the adult brain, we concentrated on studying the *dGBA1b*$^{-/-}$ and *dGBA1a,b*$^{-/-}$ flies in the subsequent experiments.

We also assessed the fecundity of *dGBA1b*$^{-/-}$ and *dGBA1a,b*$^{-/-}$ female flies as a further measure of healthspan. The number of eggs laid per female significantly declined with age compared with age-matched control flies, and day 30 null mutant

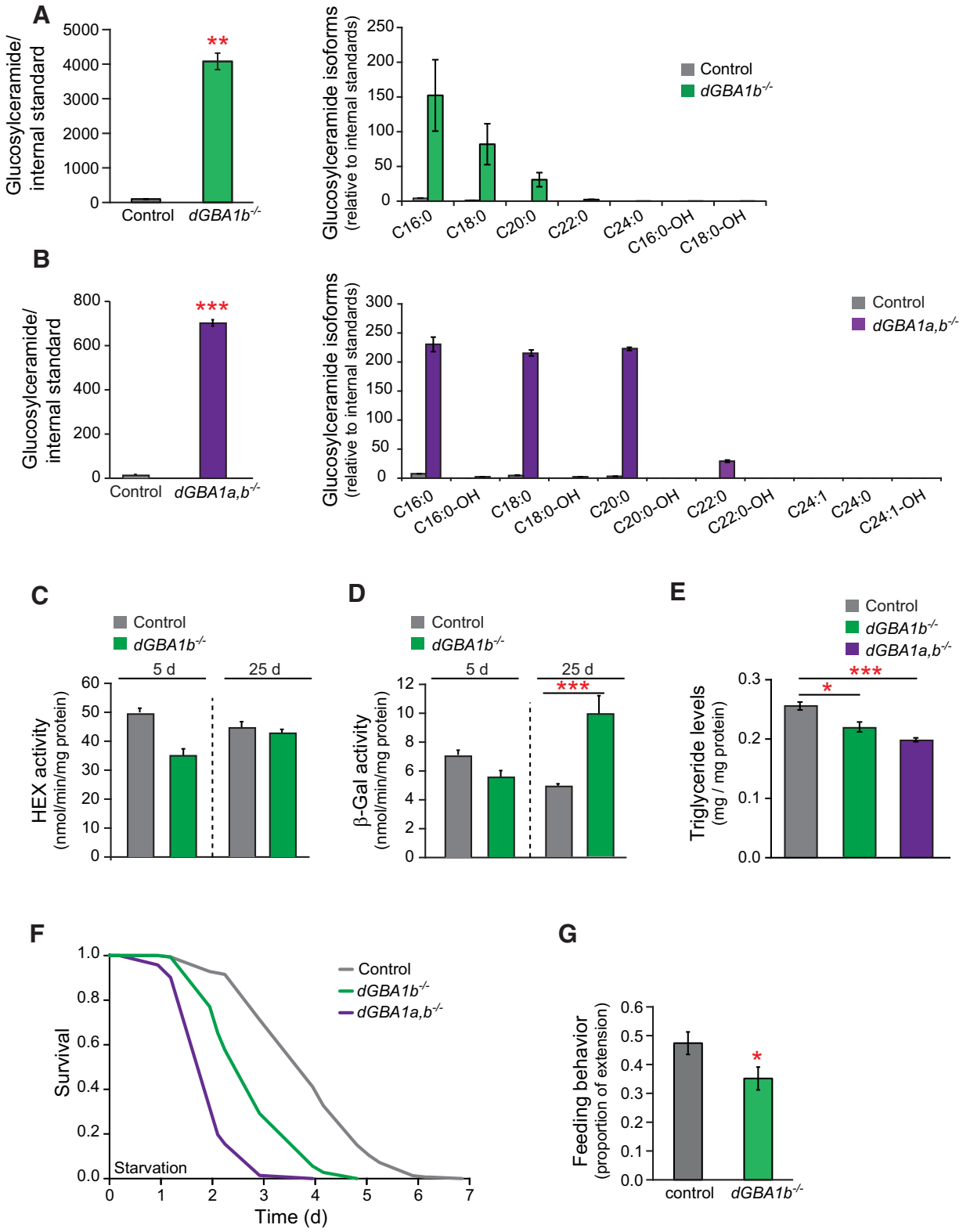

Figure 3. Loss of dGBA activity resulted in lipid defects and substrate accumulation in fly brains. ***A***, Mass spectroscopic analysis revealed an ~7-fold increase in accumulation of the dGBA substrate, glucosylceramide, in the heads ($n = 70$) of 25-d-old *dGBA1b*$^{-/-}$ compared with age-matched w^{1118} control flies. $^{**}p = 0.01$. The isoforms that were predominantly elevated were C16:0, C18:0, and C20:0. ***B***, Similar results were seen in *dGBA1a,b*$^{-/-}$ fly heads ($n = 70$ heads per sample, 3 technical repeats). $^{***}p = 0.0008$. ***C***, There was no age-dependent decrease in hexosaminidase (HEX) activity or (***D***) β-galactosidase (β-GAL) activity in *dGBA1b*$^{-/-}$ fly heads. There was a significant increase in β-GAL activity in older 25-d-old *dGBA1b*$^{-/-}$ fly heads compared with age-matched w^{1118} control flies. $^{***}p = 2 \times 10^{-5}$. Data are the mean ± SEM of three independent experiments. ***E***, The 25-d-old *dGBA1b*$^{-/-}$ and *dGBA1a,b*$^{-/-}$ flies had reduced whole-body levels of TAG compared with age-matched controls. $^{*}p = 0.046$ (paired *t* test). $^{***}p = 0.00082$ (paired *t* test). ***F***, Day 15 *dGBA1b*$^{-/-}$ and *dGBA1a,b*$^{-/-}$ flies were more sensitive to starvation conditions than age-matched w^{1118} control flies ($p = 3 \times 10^{-20}$ and $p = 5 \times 10^{-51}$; $n = 150$ flies per genotype). ***G***, Day 15 *dGBA1b*$^{-/-}$ flies had reduced feeding activity as assessed by the proboscis-extension assay ($n = 55$ flies per genotype). $^{*}p = 0.040$.

dGBA1b and the double-mutant *dGBA1a,b*$^{-/-}$ flies were almost completely infertile (Fig. 2*F*).

Knock-out of *dGBA* resulted in changes in lipid metabolism and accumulation of glucosylceramide

We next assessed whether knock-out of dGBA activity in the fly is associated with accumulation of its substrate, glucosylceramide. Indeed, using lipid mass spectrometry, we found that *dGBA1b*$^{-/-}$ and *dGBA1a,b*$^{-/-}$ flies displayed significant accumulation of glycosylceramide in their heads, whereas the heads of w^{1118} control flies contained very little glycosylceramide (Fig. 3*A*,*B*). Furthermore, the predominant glycosylceramide isoforms produced were C:16, C:18, and C:20 fatty chains (Fig. 3*A*,*B*). To determine whether loss of dGBA caused any change in the activity of other lysosomal enzymes, we also assessed hexosaminidase (Fig. 3*C*) and β-galactosidase (Fig. 3*D*). There was no age-dependent decrease in the activity of these two enzymes in the heads of *dGBA1b*$^{-/-}$ flies compared with controls. Indeed, the activity of β-galactosidase in day 25 *dGBA1b*$^{-/-}$ fly heads was significantly higher than in the controls (Fig. 3*D*).

In addition to specific lipid defects caused by the loss of dGBA we also looked at more general lipid abnormalities. As mentioned above, *dGBA1* is expressed in both the midgut and the fat body of the fly, an organ analog of vertebrate adipose tissue and liver that acts as a major organ of energy metabolism and nutrient storage (Tatar et al., 2014). We therefore assessed whether loss of dGBA in these tissues might result in general defects in lipid metabolism. TAG is the main form of lipid storage in the fly and therefore reflects the ability of flies to respond to starvation conditions (Ballard et al., 2008). Measurement of whole-body TAG levels in day 25 female flies revealed a significant reduction in *dGBA* knock-out flies compared with age-matched controls (Fig. 3*E*). In particular, there was a greater reduction in TAG levels in double-mutant *dGBA1a,b*$^{-/-}$ flies compared with the single-mutant *dGBA1b*$^{-/-}$ flies (Fig. 3*E*). The physiological relevance of the decrease in TAG levels was confirmed in both *dGBA1b*$^{-/-}$ and, to a greater extent, in *dGBA1a,b*$^{-/-}$ flies, which were more sensitive to starvation conditions compared with controls (Fig. 3*F*). Furthermore, assessment of feeding behavior by measuring proboscis-extension (Wong et al., 2009) demonstrated that *dGBA1b*$^{-/-}$ flies had significantly reduced feeding activity compared with controls (Fig. 3*G*). This suggests that reduced food intake may contribute to the reduced TAG levels and hypersensitivity to starvation.

Loss of dGBA activity led to lysosomal-autophagic deficits

To determine whether the accumulation of the dGBA substrate corresponds with abnormal lysosomal pathology, which is characteristic of GD, we stained the brains of *dGBA1b*$^{-/-}$ and *dGBA1a,b*$^{-/-}$ flies with LysoTracker and visualized the lysosomes with confocal microscopy. Aged *dGBA1b*$^{-/-}$ and *dGBA1a,b*$^{-/-}$ flies displayed numerous enlarged and abnormal lysosomes in their brains, which were not seen in age-matched control brains (Fig. 4*A*,*B*). Given that normal lysosomes are required to fuse with autophagosomes to form autophagolysosomes in the process of autophagy (Rubinsztein et al., 2012), we next studied autophagy. During the elongation phase, the cytosolic form of protein microtubule-associated protein 1 light chain 3 (LC3), LC3-I, is conjugated to phosphatidylethanolamine to form LC3-II, which is specifically targeted to the autophagosome membrane, where it remains until fusion with lysosomes. LC3 is therefore considered a good marker for studying autophagy (Ravikumar et al., 2010). We therefore measured the accumulation of Atg8, the fly ortholog of LC3, in both the heads of *dGBA1b*$^{-/-}$ and headless bodies of *dGBA1a,b*$^{-/-}$ flies, respectively (Fig. 5*A*,*B*). Western blot analysis demonstrated that Atg8-I and Atg8-II accumulated in the heads of flies lacking *dGBA1b*$^{-/-}$ (Fig. 5*A*). Atg8-II also accumulated in the headless bodies of flies lacking both *dGBA1* genes (*dGBA1a,b*$^{-/-}$) (Fig. 5*B*) compared with controls. Increased steady-state levels of Atg8-II suggests increased autophagosome number, but the marked increase in Atg8-I also could indicate a stall in flux activity in the brains of *dGBA1b*$^{-/-}$ flies (Fig. 5*A*). Analysis of the Atg8-II/Atg8-I ratio also confirmed increased autophagosome formation and autophagy block in the dGBA knock-out fly heads and bodies (Fig. 5*A*,*B*). Furthermore, Atg8 levels in homogenates of heads from control and *dGBA1b*$^{-/-}$ mutant flies demonstrated that this tissue was unresponsive to nutrient deprivation (Fig. 5*A*), unlike headless bodies, in which a brief 48 h period of prior starvation slightly increased Atg8-II levels, suggestive of autophagy induction (Fig. 5*B*).

p62 and polyubiquitinated proteins accumulated in dGBA-deficient fly brains

To study the downstream effects of autophagic dysfunction, we next performed immunostaining on the brains of dGBA-deficient flies with antibodies against ubiquitin and p62, markers of lysosomal-autophagic degradation (Bartlett et al., 2011). Under normal physiological conditions, p62 can link ubiquitinated proteins to the autophagy machinery (e.g., Atg8-II), targeting them for degradation (Rogov et al., 2014). Moreover, both ubiquitin and p62 accumulate when autophagy is inhibited (Bartlett et al., 2011) and are abundant constituents of protein inclusions associated with neurological diseases, including LBs in PD (Zatloukal et al., 2002; Bartlett et al., 2011). We first dissected *Drosophila* brains and visualized these proteins using antibodies against polyubiquitinated proteins and the fly ortholog of p62, Ref(2)P. Aged *dGBA1b*$^{-/-}$ brains displayed elevated levels of both ubiquitinated proteins and p62/Ref(2)P-containing aggregates under the confocal microscope, which were not seen in age-matched control fly brains (Fig. 6*A*). We also confirmed elevated levels of polyubiquitinated proteins in *dGBA1b*$^{-/-}$ fly heads using Western blot analysis (Fig. 6*B*). Thus, dGBA knock-out led to lysosomal-autophagic defects and the accumulation of ubiquitin and p62/Ref(2)P-containing deposits in the fly brain.

Knock-out of dGBA in the fly brain led to synaptic loss and neurodegeneration

To study the effect of dGBA deficiency on synaptic viability, we performed immunostaining for Bruchpilot, an essential component of synaptic active zones in *Drosophila* (Wagh et al., 2006). This revealed significantly reduced Bruchpilot in the brains of *dGBA1b*$^{-/-}$ flies compared with controls, suggesting synaptic loss (Fig. 7*A*).

We also performed an ultrastructural examination of *dGBA1b*$^{-/-}$ fly brains using transmission electron microscopy. This demonstrated grossly abnormal morphology of the ommatidia, the units of the compound eye, in *dGBA1b*$^{-/-}$ flies compared with controls (Fig. 7*B*). Quantitative analysis showed that the average rhabdomere area within each ommatidium was significantly reduced in the eyes of *dGBA1b*$^{-/-}$ flies (Fig. 7*B*).

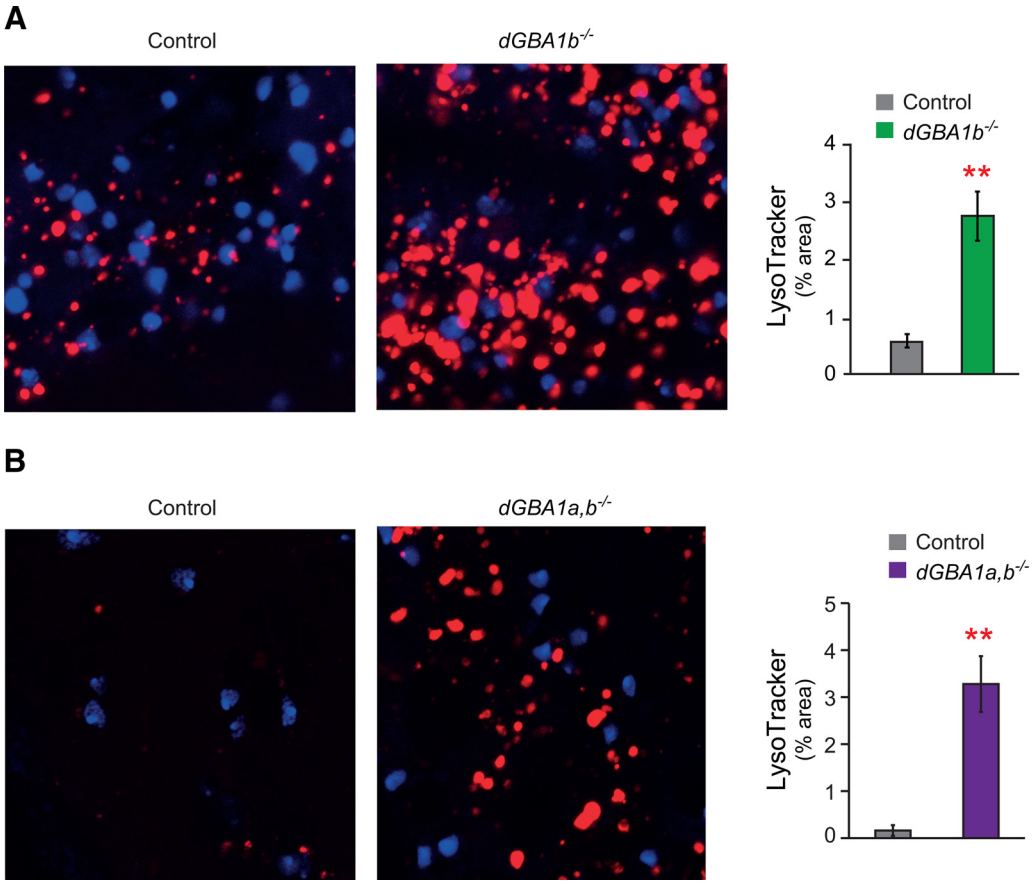

Figure 4. dGBA deficiency was associated with lysosomal defects. ***A***, Brains dissected from 15-d-old w^{1118} control or $dGBA1b^{-/-}$ flies were stained with LysoTracker and imaged live within 15 min of dissection, using the same microscope settings to capture images from the same region of the subesophageal ganglion in each brain. $dGBA1b^{-/-}$ flies displayed abnormal staining with numerous enlarged lysosomes that were not seen in age-matched control flies. For each image, the area of LysoTracker staining above a uniform threshold was quantified, revealing a significantly increased area of LysoTracker staining in $dGBA1a,b^{-/-}$ flies ($n = 6$ experiments with one control and one $dGBA1b^{-/-}$ brain in each experiment). $^{**}p < 0.005$ (paired t test). ***B***, Similar results were also seen in the brains of 25-d-old $dGBA1a,b^{-/-}$ flies compared with age-matched control flies ($n = 6$ experiments with one control and one $dGBA1a,b^{-/-}$ brain in each experiment). $^{**}p < 0.005$ (paired t test).

Knock-out of d*GBA* in the brain was associated with mitochondrial abnormalities and hypersensitivity to oxidative stress

Ultrastructural examination of the brains of flies lacking dGBA using electron microscopy revealed giant mitochondria in day 25 $dGBA1b^{-/-}$ fly brains compared with age-matched controls (Fig. 8*A*) or younger day 5 $dGBA1b^{-/-}$ brains (data not shown), with an ~25% increase in the average mitochondrial area (Fig. 8*B*). The presence of giant mitochondria, in addition to the increase in autophagy substrates and increased Atg8-II, further supported the conclusion that there was impaired autophagic flux.

In keeping with our ultrastructural data, mitochondrial dysfunction has been shown in a mouse model of GBA deficiency (Osellame et al., 2013) and GD human fibroblasts (de la Mata et al., 2015). To assess mitochondrial function, we measured ATP levels and found that they were reduced by ~40% in the brains of $dGBA1b^{-/-}$ flies as well as in the whole bodies of $dGBA1b^{-/-}$ and $dGBA1a,b^{-/-}$ flies compared with controls (Fig. 8*C*,*D*). Mitochondrial dysfunction can lead to decreased resistance to reactive oxygen species, which has been implicated in many neurodegenerative diseases (Kinghorn et al., 2015). To explore the role of d*GBA* in resistance to oxidative stress, we examined the survival of *dGBA*-deficient flies after exposure to the potent oxidizer hydrogen peroxide (H_2O_2) and paraquat, a free radical generator. Consistent with the mitochondrial abnormalities in aged flies, day 15 $dGBA1b^{-/-}$ and $dGBA1a,b^{-/-}$ flies showed increased sensitivity to H_2O_2 and paraquat stress (Fig. 8*E*,*F*).

Targeting downstream autophagy defects with the mTOR inhibitor rapamycin

The nutrient-sensing mTOR pathway regulates lysosomal biogenesis and autophagy (Ravikumar et al., 2010). We hence assessed the activity of mTOR by measuring the phosphorylation level of S6K, which acts downstream of mTOR complex 1 (mTORC1) (Castillo-Quan et al., 2015). Western blot analysis revealed a decrease in S6K phosphorylation in the heads of $dGBA1b^{-/-}$ flies compared with controls, indicating downregulation of mTORC1 (Fig. 9*A*), which would be predicted to lead to an increase in autophagy. We also tested whether rapamycin, a known mTORC1 inhibitor (Bjedov et al., 2010), could further downregulate mTOR in dGBA-deficient flies. Treatment of control flies with 200 μM rapamycin resulted in a >50% decrease in S6K phosphorylation. There was a trend for rapamycin treatment of $dGBA1b^{-/-}$ flies to further decrease S6K phosphorylation, although this was not statistically significant. We therefore tested the effect of rapamycin on the lifespan of $dGBA1b^{-/-}$ flies. Interestingly, we found that rapamycin supplementation to the fly medium (both 200 and 400 μM) from 2 d of age was able to partially ameliorate the lifespan defect in $dGBA1b^{-/-}$ flies (Fig. 9*B*). Consistent with previous work (Bjedov et al., 2010), rapa-

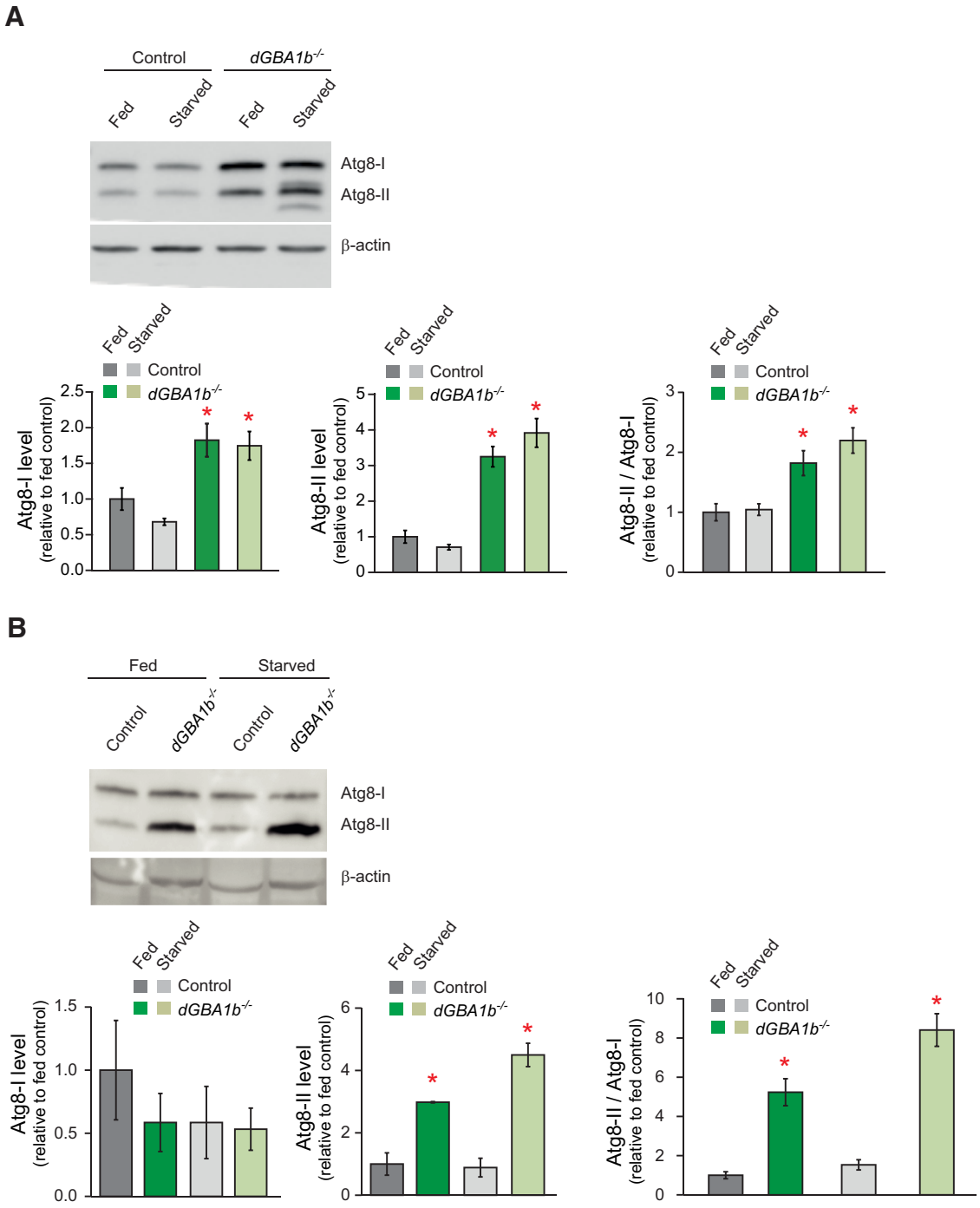

Figure 5. Flies lacking dGBA displayed a block in autophagy. ***A***, Western blot analysis with an antibody against the fly LC 3 ortholog, Atg8, demonstrated increased levels in *dGBA1b*$^{-/-}$ fly heads compared with age-matched w^{1118} control flies. Both Atg8-I and Atg8-II were increased compared with controls, and the ratio of Atg8-II/Atg8-I in *dGBA1b*$^{-/-}$ flies indicated increased autophagosome formation ($n = 3$ experiments). *$p < 0.05$. ***B***, Western blot analysis of Atg8 levels in the headless bodies of *dGBA1a,b*$^{-/-}$ flies demonstrated no significant change in Atg8-I levels, with an increase in Atg8-II levels and an increased Atg8-II/Atg8-I ratio. This effect was more pronounced after starvation in *dGBA1a,b*$^{-/-}$ flies ($n = 3$ experiments). *$p < 0.05$.

mycin also increased the lifespan of control flies (Fig. 9*B*). In keeping with the effect on lifespan, 400 μM rapamycin, but not 200 μM (data not shown), was also able to partially rescue the locomotor deficits in aged *dGBA1b*$^{-/-}$ flies (Fig. 9*C*). An even greater rescue was seen in flies lacking both *dGBA1* genes (*dGBA1a,b*$^{-/-}$). This effect of rapamycin appeared to be specific to dGBA knock-out flies, as rapamycin did not have a significant effect on the climbing ability of age-matched control flies (Fig. 9*C*). We also assessed the effect of rapamycin on the response to oxidative stress. Treatment with 200 μM rapamycin from 2 to 15 d of age subsequently prolonged the survival of *dGBA1b*$^{-/-}$ flies on food containing H_2O_2 (Fig. 9*D*). This effect was also specific to dGBA-deficient flies, as surprisingly rapamycin-treated control flies had reduced lifespan on exposure to H_2O_2 (Fig. 9*D*).

Rapamycin treatment is also associated with an increased resistance to starvation in wild-type flies (Bjedov et al., 2010). We therefore treated *dGBA1b*$^{-/-}$ flies with rapamycin for the

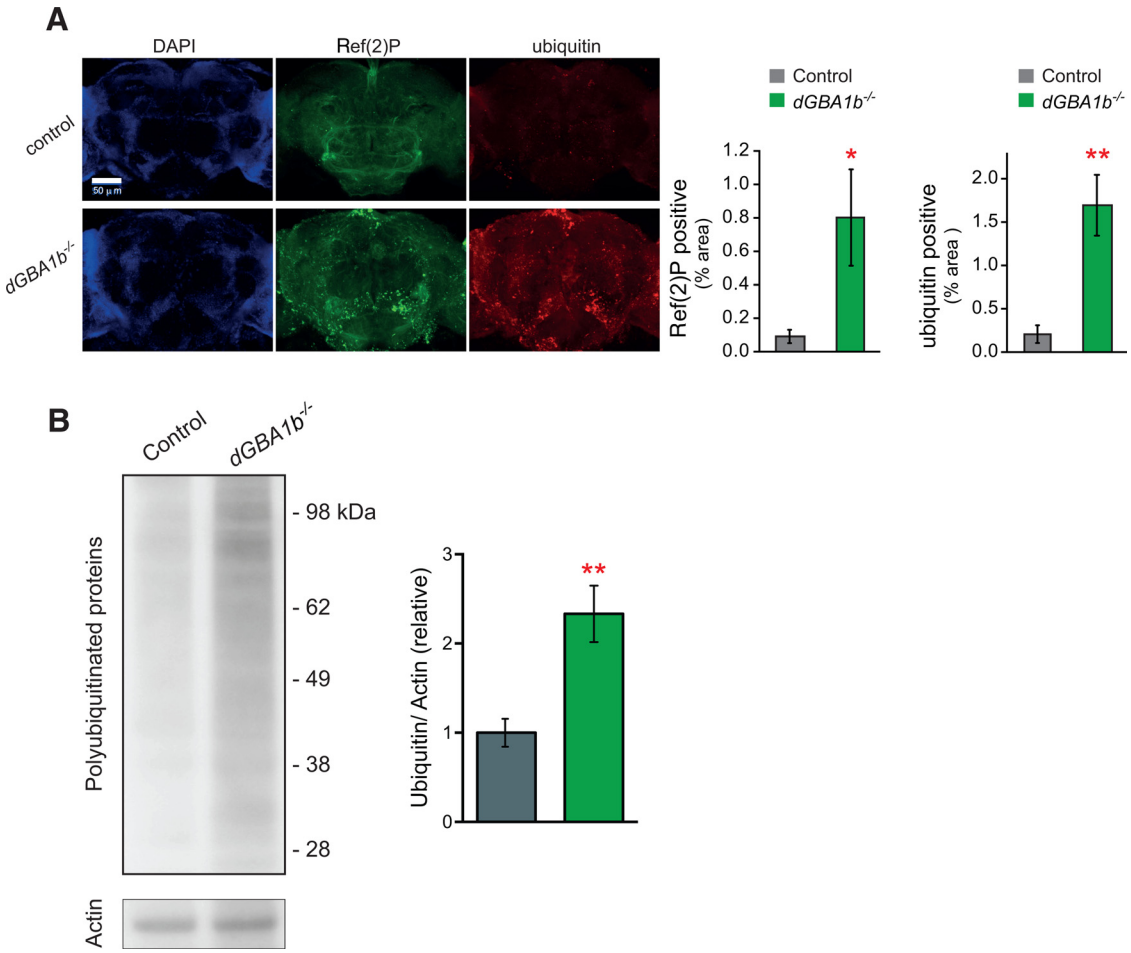

Figure 6. dGBA-deficient flies showed accumulation of p62/Ref(2)P and polyubiquitinated proteins in their brains. ***A***, Immunostaining with antibodies against Ref(2)P, the fly ortholog of p62, and polyubiquitinated proteins demonstrated increased Ref(2)P- and ubiquitin-positive puncta within the $dGBA1b^{-/-}$ fly brains. *$p < 0.05$ (*t* test). **$p < 0.001$ (*t* test). $n = 5$ or 6 brains per genotype. ***B***, Western blotting of Triton-insoluble head extracts confirmed the presence of significantly increased levels of polyubiquitinated proteins in $dGBA1b^{-/-}$ flies. **$p < 0.05$. $n = 4$ samples per genotype, 10–15 heads per sample.

first 15 d of adulthood before exposing them to starvation conditions. The 200 μM rapamycin was able to rescue the survival of $dGBA1b^{-/-}$ flies and control flies under starvation conditions (Fig. 9*E*). These findings suggest that, despite the autophagy block in flies lacking dGBA, rapamycin is still able to exert protective effects on lifespan, locomotor defects, and oxidative and starvation stress responses, likely by exerting a small but functionally significant increase in mTOR inhibition.

Loss of dGBA function in the brain resulted in an upregulation of *Mitf* gene expression and its downstream target gene *Atg8a*

To further study the effects of dGBA deficiency and rapamycin treatment on autophagy, we measured the expression levels of *Mitf* and its downstream target *Atg8a*. *Mitf* is the fly ortholog of the mammalian transcription factor EB (*TFEB*) gene, the master regulator of lysosomal biogenesis and autophagy (Bouché et al., 2016; Tognon et al., 2016). *TFEB* is critical for the autophagic cellular clearance of abnormal proteins and organelles, as well as lipid metabolism. *TFEB* acts by coordinating the expression of a number of genes belonging to the Coordinated Lysosomal Expression and Regulation (CLEAR) network, by directing binding to specific CLEAR-box sequences located near their promoters. *TFEB* is usually cytosolic where it interacts with mTORC1 at the surface of the lysosome (Roczniak-Ferguson et al., 2012), but during starvation it translocates to the nucleus where it induces target gene transcription. Studies have shown that *Mitf* has conserved regulatory mechanisms with mammalian TFEB, translocating to the nucleus when *Drosophila* mTORC1 is inhibited (Bouché et al., 2016).

We first measured *Mitf* gene expression in the heads of $dGBA1b^{-/-}$ flies. qRT-PCR data analysis showed that, in response to the loss of dGBA activity in the brain, there is a highly significant upregulation of *Mitf* gene expression (Fig. 10*A*). We next studied the levels of the *Atg8a* gene, the fly ortholog of the mammalian *GABARAPL1* gene, which acts downstream of *Mitf*. This gene is involved in the main steps of autophagosome formation and maturation. In keeping with the upregulation of *Mitf* in $dGBA1b^{-/-}$ fly heads, *Atg8a* was also upregulated in response to dGBA knockdown in the fly brain (Fig. 10*B*).

We also studied the effect on *Mitf* and *Atg8a* gene expression of treating dGBA-deficient and control flies with 200 μM rapamycin from day 2 (Fig. 10*A*,*B*). Interestingly, we did not see any increase in *Mitf* gene expression in $dGBA1b^{-/-}$ flies treated with rapamycin compared with untreated flies (Fig. 10*A*). Moreover, the levels of *Atg8a* in rapamycin-treated $dGBA1b^{-/-}$ flies were significantly downregulated compared with untreated flies (Fig. 10*B*). Rapamycin significantly increased the expression levels of *Mitf* in control flies (Fig. 10*A*); and although there was a trend

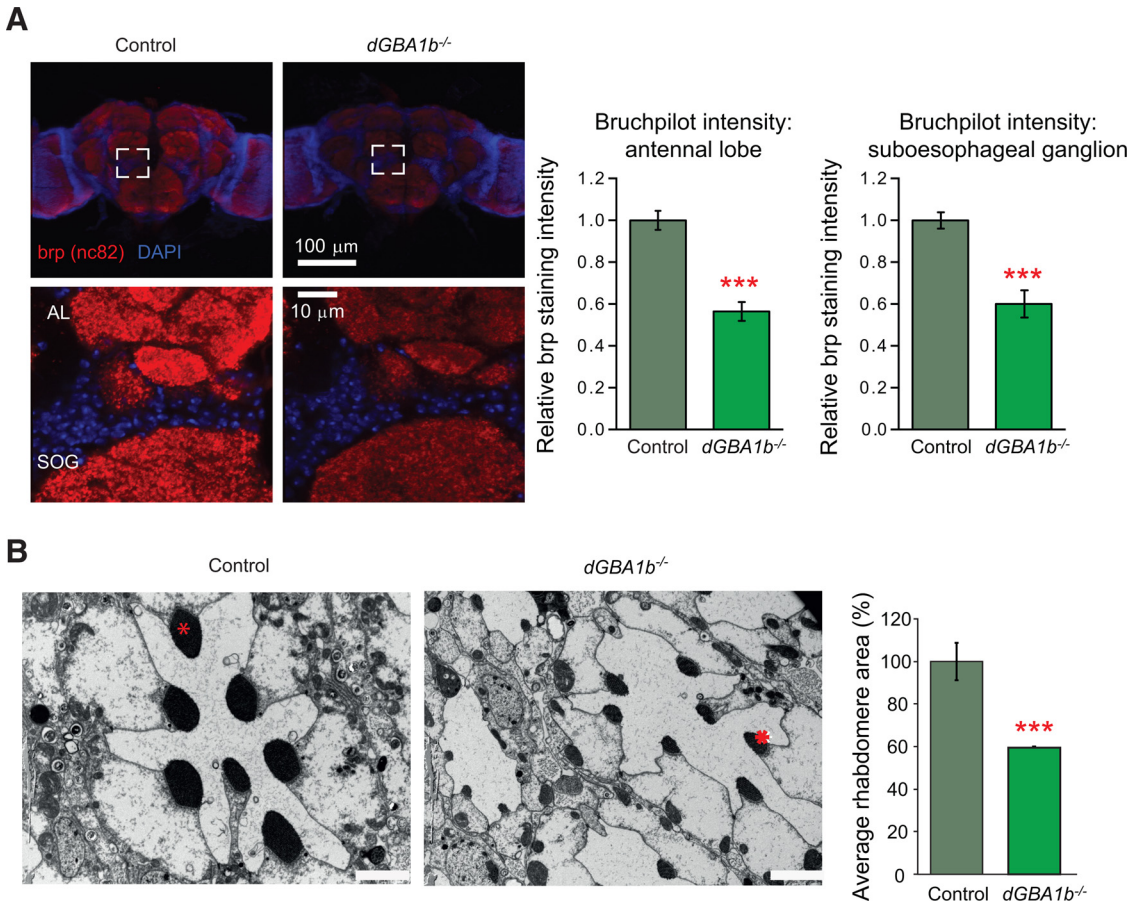

Figure 7. Deficiency of dGBA resulted in synaptic loss and neurodegeneration. ***A***, Immunostaining for Bruchpilot (brp), a critical synaptic component, demonstrated reduced staining (red) in the brains of day 25 *dGBA1b*$^{-/-}$ flies compared with controls. Antennal lobe (AL) and suboesphageal (SOG). $n = 7–8$ brains per genotype. ***B***, EM of the eyes of day 25 *dGBA1b*$^{-/-}$ flies revealed grossly abnormal morphology of the ommatidia compared with age-matched controls (×5600). Scale bars, 2 μm. In addition, quantitative analysis revealed a reduction in average rhabdomere (*) area in *dGBA1b*$^{-/-}$ fly eyes (***$p = 4 \times 10^{-6}$; at least 80 consecutive rhabdomeres studied for each genotype).

toward increasing *Atg8a* levels, it was not statistically significant (Fig. 10*B*). Thus, loss of dGBA activity in the brain is associated with increased expression levels of *Mitf*, and its downstream target gene, *Atg8a*, but upregulation of *Mitf* expression is not responsible for the protective effect of rapamycin on lifespan, locomotor, and oxidative stress phenotypes.

Discussion

We generated a *Drosophila* model of neuronopathic GD. Simple genetics could not be used to precisely excise both *Drosophila GBA1* genes, *dGBA1a* and *dGBA1b,* due to the presence of the CG31413 gene between them. Therefore, we used serial homologous recombination to knock out both *dGBA1* genes separately or together in the fly. Of the two fly GBA orthologs, only *dGBA1b* is expressed in the fly brain (Flyatlas). *dGBA1b*$^{-/-}$ fly heads, lacking dGBA1b expression, displayed accumulation of the dGBA substrate glucosylceramide. Furthermore, the glucosylceramide isoforms (C16:0, C18:0, C22:0) were similar to those found in human spleen tissue (with the addition of hydroxylated or longer chain isoforms including C18:0-OH, C20:0-OH, C24:1, and C24:0 in the human tissue (N. Sebire and S. Paine, unpublished data). Moreover, this is consistent with data showing accumulation of glucosylceramide and glucosylsyphingosine in Types II and III GD patient brains (Orvisky et al., 2002).

Abnormally engorged lysosomes in *dGBA1b*$^{-/-}$ fly brains were visualized with LysoTracker, confirming the validity of this neuronopathic GD fly model. Lysosomal integrity is necessary for normal functioning of the autophagy degradation machinery (Xu and Ren, 2015), and accordingly we observed autophagy dysfunction in *dGBA1b*$^{-/-}$ brains, with accumulation of the autophagolysosomal protein Atg8/LC3. Thus, we demonstrate autophagy defects at the level of the autophagic machinery *in vivo* in a GD *Drosophila* model, following on from *in vitro* studies in GD macrophages and iPSCs showing impaired autophagy (Awad et al., 2015; Aflaki et al., 2016; Fernandes et al., 2016).

Neuronal-specific autophagy deficits, through loss of the mouse autophagy genes *atg7* or *atg5*, result in accumulation of polyubiquitinated proteins, behavioral defects, and reduced longevity (Hara et al., 2006; Komatsu et al., 2006). Consistent with this, we found that *dGBA1b*$^{-/-}$ flies displayed reduced survival and locomotor ability and brain accumulation of p62/Ref(2)P and polyubiquitinated proteins. Both p62 and ubiquitin accumulate in neurodegenerative diseases, such as Alzheimer's disease and PD (Zatloukal et al., 2002; Bartlett et al., 2011), and multiple pathogenic proteins, including p62 and β-amyloid, have been identified in neuronopathic GD mouse brains (Xu et al., 2014).

Surprisingly, knock-out of *dGBA1a*, which is predominantly expressed in the digestive system, significantly increased survival. This finding parallels recent research in *Drosophila* and *Caenorhabditis elegans* demonstrating that the intestine is an important target organ for mediating lifespan extension at the organismal

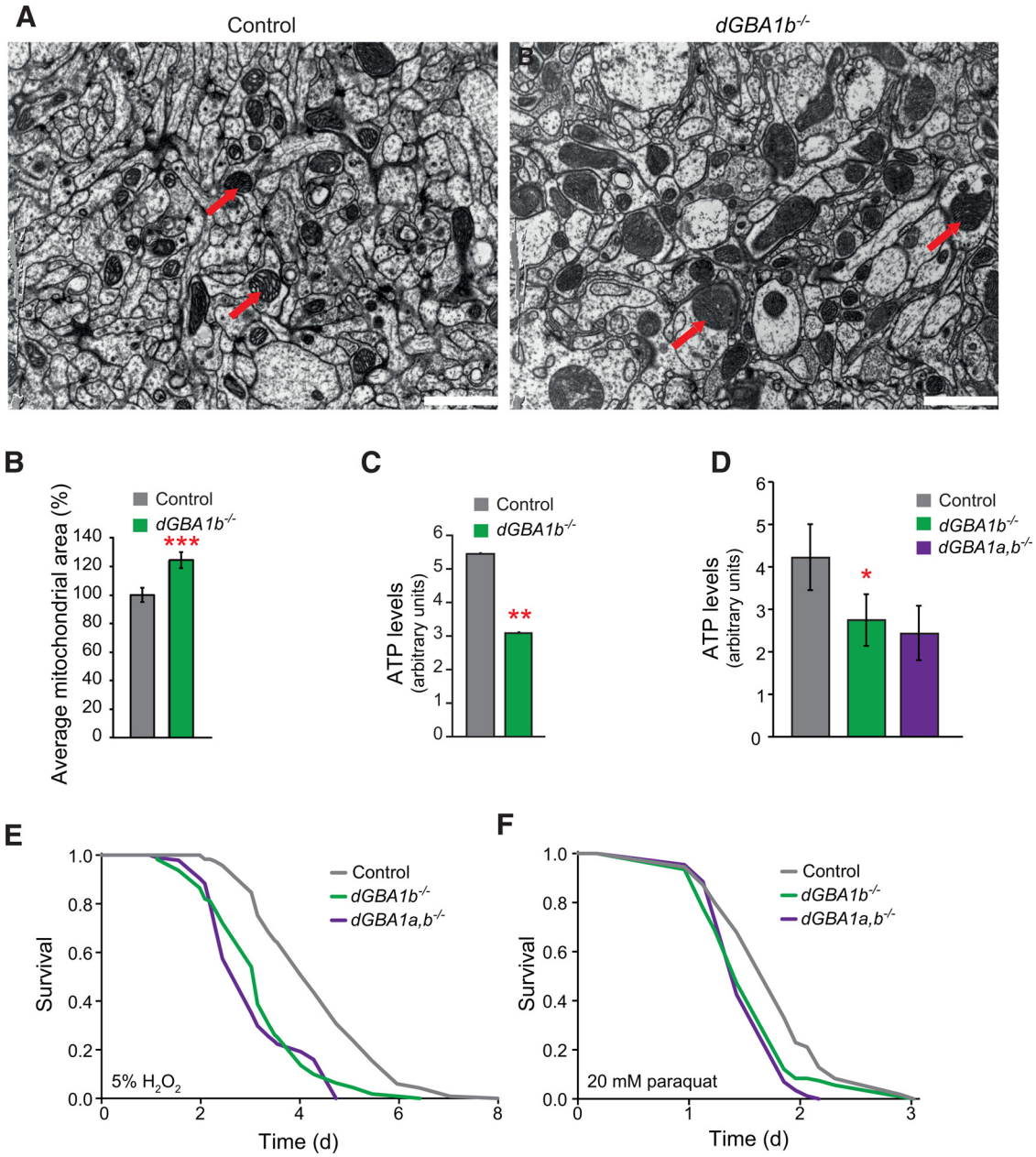

Figure 8. dGBA-deficient fly brains displayed mitochondrial abnormalities. ***A***, EM analysis of the brains of day 25 $dGBA1b^{-/-}$ flies showed giant mitochondria (arrows) compared with mitochondria (arrows) in age-matched w^{1118} control fly brains (×11,500 magnification). Scale bar, 1 μm. ***B***, Average mitochondrial area was increased in $dGBA1b^{-/-}$ flies ($n > 200$ mitochondria per genotype). $^{***}p = 4 \times 10^{-5}$. ***C***, These mitochondrial structural abnormalities were associated with decreased ATP levels in day 25 $dGBA1b^{-/-}$ fly heads ($^{**}p = 0.0016$) and (***D***) in the whole bodies of $dGBA1b^{-/-}$ flies compared with age-matched controls ($^{*}p = 0.02$). There was a trend for reduced ATP levels in the $dGBA1a,b^{-/-}$ flies, but this did not quite reach significance ($p = 0.06$). ***E***, $dGBA1b^{-/-}$ and $dGBA1a,b^{-/-}$ flies displayed reduced survival on exposure to 5% H_2O_2 ($p = 3 \times 10^{-12}$ and $p = 5 \times 10^{-15}$) and (***F***) 20 mM paraquat ($p = 0.003$ and $p = 2 \times 10^{-6}$; $n = 150$ flies per genotype).

level, with single-gene manipulations specifically in the gut prolonging lifespan (Rera et al., 2011; Tatar et al., 2014). The role of dGBA in the gut in regulating lifespan was beyond the scope of this study but is an area that warrants further investigation. We demonstrated, however, that the lifespan extension seen in $dGBA1a^{-/-}$ flies is not associated with any improvement in locomotor ability.

Mitochondrial integrity is necessary for normal autophagy-lysosomal system functioning (Palikaras and Tavernarakis, 2012; Ashrafi and Schwarz, 2013). Indeed, mitochondrial dysfunction occurs in GD mouse models (Osellame et al., 2013; Xu et al., 2014), likely due to defects in the autophagic removal of damaged mitochondria (Osellame et al., 2013). In keeping with this, the deficiency of the *Drosophila* autophagy gene *atg7* is associated with sensitivity to oxidative stressors (Juhász et al., 2007). Accordingly, we demonstrated mitochondrial abnormalities in $dGBA1b^{-/-}$ flies, with giant mitochondria, reduced ATP and hypersensitivity to oxidative stress. Enlarged mitochondria and decreased ATP occur in neuronopathic GD mice (Xu et al., 2014), and giant mitochondria are directly linked to *Drosophila* autophagy defects (Bouché et al., 2016). Therefore, the accumulation of autophagic substrates and giant mitochondria in $dGBA1b^{-/-}$ flies is consistent with autophagy block (Fig. 10*C*).

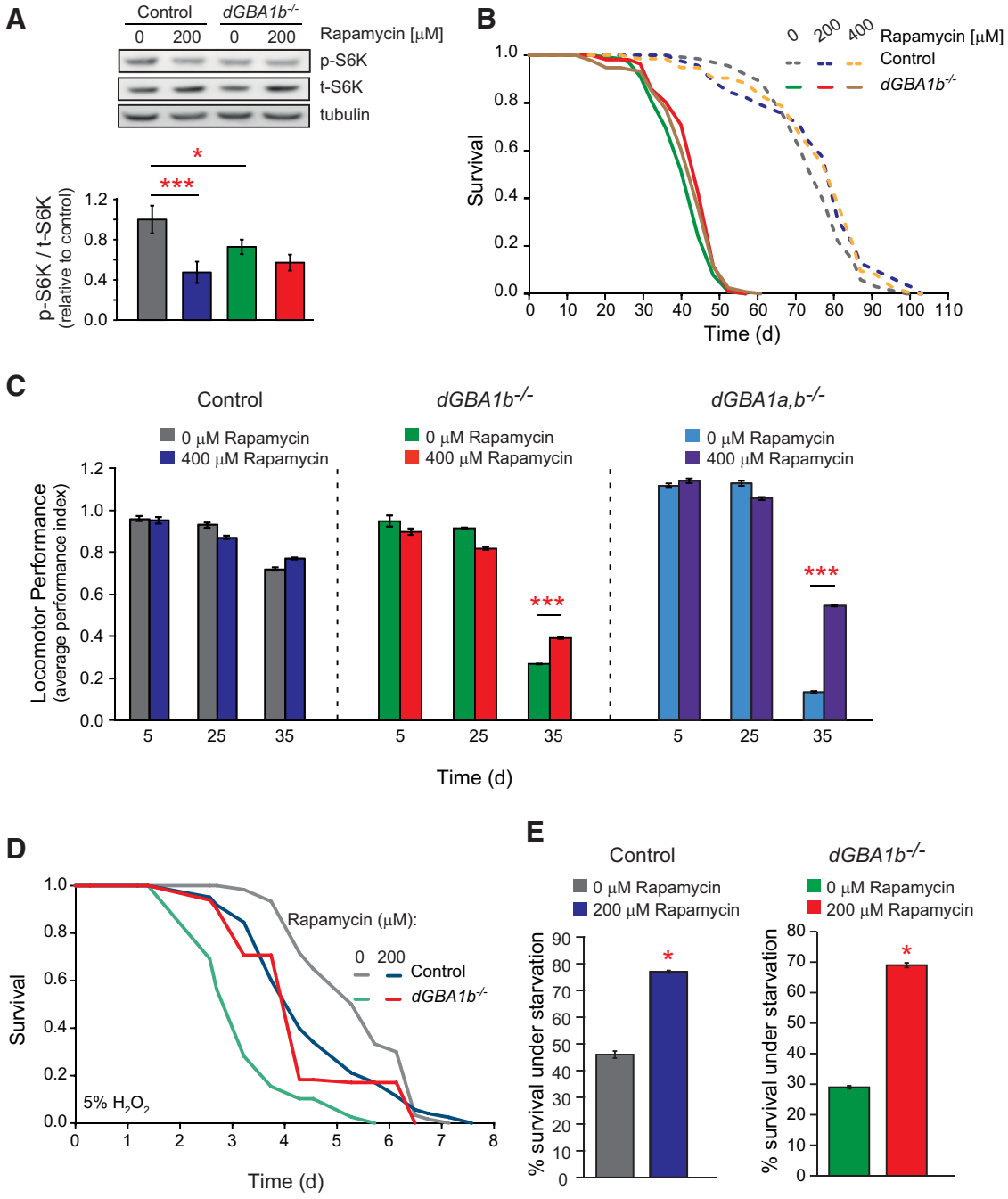

Figure 9. The mTOR inhibitor rapamycin partially ameliorated the lifespan, locomotor, oxidative stress, and starvation phenotypes in dGBA-deficient flies. ***A***, Day 7 *dGBA1b*$^{-/-}$ fly heads had significantly decreased phosphorylated S6K (p-S6K) levels compared with age-matched control flies. *$p = 0.0414$. Treatment of control flies with 200 μM rapamycin led to a reduction in phospho-S6K levels. ***$p = 0.0009$. Although there was a trend for rapamycin to further decrease phospho-S6K levels in *dGBA1b*$^{-/-}$ flies, this was not statistically significant ($p = 0.327$, one-way ANOVA with Bonferroni correction). ***B***, The 200 and 400 μM of rapamycin significantly extended the lifespan of *dGBA1b*$^{-/-}$ flies ($p = 0.005$ and $p < 0.05$; $n = 110–160$ flies per genotype and condition). As previously demonstrated, rapamycin also extended the lifespan of w^{1118} control flies ($p = 0.007$ and $p = 0.02$). ***C***, Treatment with 400 μM rapamycin partially rescued the age-related climbing defects in day 35 *dGBA1b*$^{-/-}$ flies and *dGBA1a,b*$^{-/-}$ flies (***$p = 0.0005$ and ***$p = 0.0006$), but did not have a significant effect on the climbing ability of age-matched control flies ($p = 0.23$; $n = 45$ flies per genotype and condition, average of 3 repeats). ***D***, Treatment of *dGBA1b*$^{-/-}$ flies from 2 to 15 d of age with 200 μM rapamycin partially rescued the survival on subsequent exposure to food containing 5% H_2O_2 ($p = 2.5 \times 10^{-9}$). This protective effect was specific to dGBA-deficient flies as 200 μM rapamycin was toxic to control flies under similar conditions ($p = 0.0007$; $n = 60$ flies per group). ***E***, The 200 μM rapamycin was also able to increase survival of *dGBA1b*$^{-/-}$ flies in response to subsequent exposure to starvation conditions from 15 d of age. *$p = 0.004$. The time point shown is after 3 d of starvation stress ($n = 60$ flies per condition). Under similar conditions, 200 μM rapamycin also rescued the survival of control w^{1118} flies ($n = 60$ flies per group). *$p = 0.023$. The bar chart represents survival after 8 d of exposure to starvation.

Furthermore, we demonstrated that the neuropathological defects in *dGBA1b*$^{-/-}$ flies occur independently of α-synuclein, confirming that dGBA deficiency is sufficient to cause neurodegeneration (Fig. 10*C*). A recent study using a deletion mutant harboring imprecise removal of the *dGBA1b* gene, as well as the incomplete removal of the *dGBA1a* gene and excision of the interjacent *CG31413* gene, provides further validation of our model for studying *GBA1*-associated neurodegeneration. Loss of 60% of GCase activity was also associated with reduced survival and climbing ability in addition to accumulation of autophagy sub-

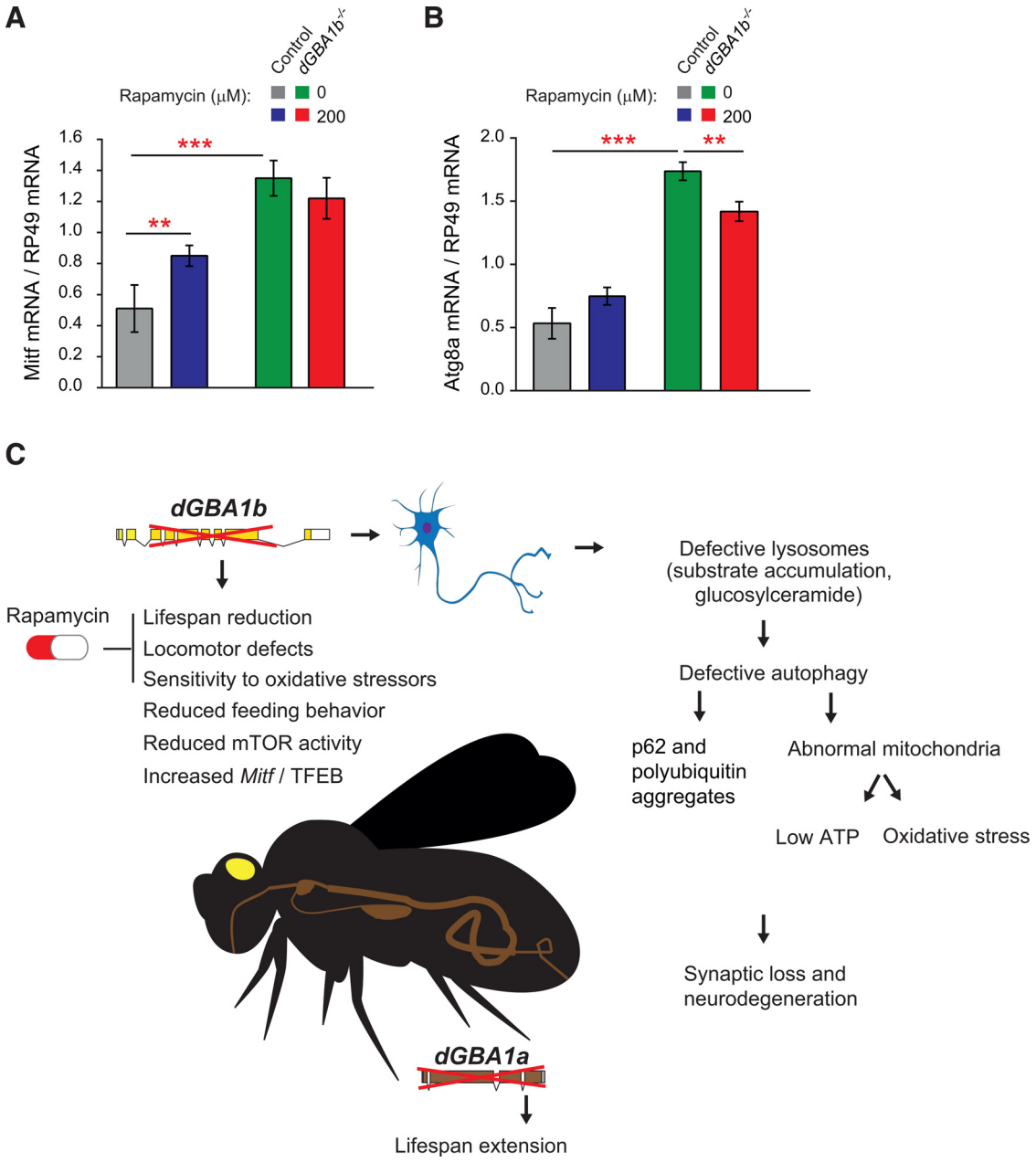

Figure 10. Knock-out of dGBA activity in the fly brain was associated with upregulation of *Mitf* and its downstream target *Atg8a*. ***A***, qRT-PCR data analysis revealed that day 15 $dGBA1b^{-/-}$ fly heads had increased expression levels of *Mitf* compared with controls. $^{***}p = 9.7 \times 10^{-5}$. In addition, treatment with 200 μM rapamycin from 2 d of age had no significant effect on *Mitf* gene expression in $dGBA1b^{-/-}$ flies ($p = 0.32$). However, rapamycin treatment led to a significant increase in the expression levels of *Mitf* in control flies ($^{**}p = 0.016$). ***B***, *Atg8a* gene expression levels were greater in $dGBA1b^{-/-}$ fly heads compared with controls. $^{***}p = 2.8 \times 10^{-7}$. Treatment with 200 μM rapamycin resulted in a decrease in *Atg8a* gene levels in $dGBA1b^{-/-}$ fly heads ($^{**}p = 0.002$); and although there was a trend toward increased *Atg8a* gene expression in control flies with rapamycin treatment, it did not reach statistical significance ($p = 0.054$). The mRNA expression levels of all genes are shown relative to the expression levels of a control gene, *RP49*. ***C***, Schematic diagram showing the downstream effects of impaired autophagy flux in dGBA-deficient flies.

strates (Davis et al., 2016). GCase deficiency was also shown to enhance α-synuclein pathology in the fly (Suzuki et al., 2015; Davis et al., 2016). Our model has the advantage over existing models, as it allows the precise and complete knock-out of each of the *dGBA* genes, and the dissection of the role of dGBA in different tissues. The ability to knock out only brain-specific *dGBA1b* is particularly relevant given our finding that loss of *dGBA* in the gut causes prolongevity effects. Our model also avoids the production of truncated, possibly pathogenic, variants of *dGBA*.

The nutrient-sensing mTOR is localized to the lysosomal surface (Efeyan et al., 2012; Betz and Hall, 2013), where it modulates autophagy (Yu et al., 2010; Zoncu et al., 2011). It has thus been speculated that abnormal lysosomal function leads to activation of autophagy by mTOR downregulation (Li et al., 2013). Indeed, a recent study reported increased expression of mTOR signaling pathway genes in neuronopathic GD mice (Dasgupta et al., 2015). In view of the autophagy defect in $dGBA1b^{-/-}$ flies, we probed mTOR signaling by analyzing S6K phosphorylation downstream of mTORC1. Interestingly, we detected a decrease in S6K phosphorylation and hence downregulation of mTORC1 compared with controls. Furthermore, although not statistically significant, there was a trend for mTOR to be further downregulated in $dGBA1b^{-/-}$ flies treated with rapamycin, a known mTORC1 inhibitor. Because rapamycin has protective effects in animal

models of PD and other neurodegenerative diseases (Malagelada et al., 2010; Cheng et al., 2015), we treated *dGBA1b*$^{-/-}$ flies with rapamycin and found that, despite the autophagy block, it was able to partially ameliorate many neurotoxic phenotypes. Rapamycin treatment led to an improvement in the lifespan and climbing phenotypes, in addition to the hypersensitivity to oxidative and starvation stressors seen in *dGBA1b*$^{-/-}$ flies. These results are somewhat surprising given that rapamycin treatment of iPSC-derived neuronal cells from GD patients caused cell death (Awad et al., 2015), demonstrating that drug effects *in vitro* vary to those at the organismal level. Furthermore, although rapamycin increases the lifespan and protects against starvation conditions in control flies (Bjedov et al., 2010), the rescue of age-related climbing defects and oxidative stress appeared to be specific to dGBA-deficient flies. Indeed, rapamycin had no effect on the climbing ability of control flies, and rapamycin-treated control flies were more sensitive to H_2O_2 than untreated flies. The reason for the opposing effects of rapamycin on the oxidative stress responses of *dGBA1b*$^{-/-}$ and control flies is unclear, but may be related to the differential activation of oxidative stress pathways between *dGBA1b*$^{-/-}$ and healthy controls.

Lastly, we demonstrated that knock-out of dGBA in the brain results in an upregulation of *Mitf* and its downstream target, *Atg8a*, suggesting a compensatory response to the autophagy block. This is in contrast to findings in a recent study showing downregulation of *TFEB* expression in GD iPSC-derived cells (Awad et al., 2015). The reasons for these differing results is not clear, but possible explanations may relate to variations in autophagy block between models, and the fact that neuronal cells are newly differentiated and may reflect early disease compared with adult flies. *Mitf* gene expression may also vary in the presence of mutant dGBA. Our fly model displays very little dGBA expression compared with iPSC cells, which are derived from mutant carriers, and therefore, despite showing very low levels of GCase activity, express mutant GBA. Mutant GCase is known to exert gain-of-function toxic effects, including in *Drosophila*, with upregulation of the unfolded protein response (Maor et al., 2013, 2016). Knockdown of *Mitf* in *Drosophila* leads to similar phenotypes to those in *dGBA1b*$^{-/-}$ flies, including autophagy substrate accumulation, upregulation of Atg8-II, giant mitochondria, as well as enlarged lysosomes (Bouché et al., 2016). Thus, the autophagy defects seen in dGBA deficiency appear to phenocopy *Mitf* downregulation in the fly. This suggests that upregulating *Mitf* as a potential therapeutic strategy in GD and GBA-linked PD may be limited in its efficacy due to the inability of GBA-deficient neuronal tissue to stimulate autophagy. Further studies are warranted to explore the complex interaction between mTORC1 and *TFEB/Mitf* in GD.

Rapamycin treatment of *dGBA1b*$^{-/-}$ flies did not upregulate *Mitf* gene expression, suggesting that rapamycin does not act through *Mitf* signaling to rescue the neurotoxic phenotypes of dGBA-deficient flies. We hypothesize, therefore, that mTOR is downregulated in dGBA-deficient flies as a compensatory response to lysosomal-autophagy block. Possibly as a consequence of lysosomal dysfunction in dGBA-deficient flies, the normal interaction between mTORC1 and TFEB/Mitf at the surface of the lysosome is disrupted, leading to changes in *TFEB/Mitf* gene expression. Therefore, by exerting small additional effects on mTORC1 signaling, rapamycin may mediate its beneficial effects (Fig. 10*C*). Furthermore, *Mitf* also plays a critical role in lipid metabolism and recapitulates the function of *TFEB* in mammals in this regard (Bouché et al., 2016). *Mitf* expression may therefore contribute to the reduced TAG that we see in *dGBA1b*$^{-/-}$ flies.

In conclusion, the autophagy defects seen in our GD flies, likely as a result of failure of the fusion of autophagosomes and lysosomes, may also be relevant to PD linked to *GBA1* mutations. Our results raise the possibility that therapies aimed at ameliorating not only lysosomal dysfunction, but also at autophagic abnormalities, including lowering mTOR activity, may be effective in treating *GBA1*-associated disease. They also suggest that rapamycin may offer significant health benefits in neuronopathic GD and in *GBA1*-related synucleinopathies. Together, our data demonstrate that these *Drosophila* models of dGBA-deficiency are a useful platform to further study the downstream effects of lysosomal-autophagic dysfunction and to identify genetic modifiers and new therapeutic targets in neuronopathic GD and *GBA1*-associated PD.

References

Aflaki E, Moaven N, Borger DK, Lopez G, Westbroek W, Chae JJ, Marugan J, Patnaik S, Maniwang E, Gonzalez AN, Sidransky E (2016) Lysosomal storage and impaired autophagy lead to inflammasome activation in Gaucher macrophages. Aging Cell 15:77–88. CrossRef Medline

Ashrafi G, Schwarz TL (2013) The pathways of mitophagy for quality control and clearance of mitochondria. Cell Death Differ 20:31–42. CrossRef Medline

Auray-Blais C, Blais CM, Ramaswami U, Boutin M, Germain DP, Dyack S, Bodamer O, Pintos-Morell G, Clarke JT, Bichet DG, Warnock DG, Echevarria L, West ML, Lavoie P (2015) Urinary biomarker investigation in children with Fabry disease using tandem mass spectrometry. Clin Chim Acta 438:195–204. CrossRef Medline

Awad O, Sarkar C, Panicker LM, Miller D, Zeng X, Sgambato JA, Lipinski MM, Feldman RA (2015) Altered TFEB-mediated lysosomal biogenesis in Gaucher disease iPSC-derived neuronal cells. Hum Mol Genet 24:5775–5788. CrossRef Medline

Ballard JW, Melvin RG, Simpson SJ (2008) Starvation resistance is positively correlated with body lipid proportion in five wild caught *Drosophila simulans* populations. J Insect Physiol 54:1371–1376. CrossRef Medline

Bartlett BJ, Isakson P, Lewerenz J, Sanchez H, Kotzebue RW, Cumming RC, Harris GL, Nezis IP, Schubert DR, Simonsen A, Finley KD (2011) p62, Ref(2)P and ubiquitinated proteins are conserved markers of neuronal aging, aggregate formation and progressive autophagic defects. Autophagy 7:572–583. CrossRef Medline

Betz C, Hall MN (2013) Where is mTOR and what is it doing there? J Cell Biol 203:563–574. CrossRef Medline

Bjedov I, Toivonen JM, Kerr F, Slack C, Jacobson J, Foley A, Partridge L (2010) Mechanisms of life span extension by rapamycin in the fruit fly *Drosophila melanogaster*. Cell Metab 11:35–46. CrossRef Medline

Bouché V, Espinosa AP, Leone L, Sardiello M, Ballabio A, Botas J (2016) *Drosophila* Mitf regulates the V-ATPase and the lysosomal-autophagic pathway. Autophagy 12:484–498. CrossRef Medline

Castillo-Quan JI, Kinghorn KJ, Bjedov I (2015) Genetics and pharmacology of longevity: the road to therapeutics for healthy aging. Adv Genet 90:1–101. CrossRef Medline

Castillo-Quan JI, Li L, Kinghorn KJ, Ivanov DK, Tain LS, Slack C, Kerr F, Nespital T, Thornton J, Hardy J, Bjedov I, Partridge L (2016) Lithium promotes longevity through GSK3/NRF2-dependent hormesis. Cell Rep 15:638–650. CrossRef Medline

Cheng CW, Lin MJ, Shen CK (2015) Rapamycin alleviates pathogenesis of a new *Drosophila* model of ALS-TDP. J Neurogenet 29:59–68. CrossRef Medline

Cox TM (2010) Gaucher disease: clinical profile and therapeutic developments. Biologics 4:299–313. CrossRef Medline

Dasgupta N, Xu YH, Li R, Peng Y, Pandey MK, Tinch SL, Liou B, Inskeep V, Zhang W, Setchell KD, Keddache M, Grabowski GA, Sun Y (2015) Neuronopathic Gaucher disease: dysregulated mRNAs and miRNAs in brain pathogenesis and effects of pharmacologic chaperone treatment in a mouse model. Hum Mol Genet 24:7031–7048. CrossRef Medline

Davis MY, Trinh K, Thomas RE, Yu S, Germanos AA, Whitley BN, Sardi SP, Montine TJ, Pallanck LJ (2016) Glucocerebrosidase deficiency in *Drosophila* results in alpha-synuclein-independent protein aggregation and neurodegeneration. PLoS Genet 12:1–24. CrossRef Medline

de la Mata M, Cotán D, Oropesa-Ávila M, Garrido-Maraver J, Cordero MD,

Villanueva Paz M, Delgado Pavón A, Alcocer-Gómez E, de Lavera I, Ybot-González P, Paula Zaderenko A, Ortiz Mellet C, García Fernández JM, Sánchez-Alcázar JA (2015) Pharmacological chaperones and coenzyme Q10 treatment improves mutant β-glucocerebrosidase activity and mitochondrial function in neuronopathic forms of Gaucher disease. Sci Rep 5:10903. CrossRef Medline

Efeyan A, Zoncu R, Sabatini DM (2012) Amino acids and mTORC1: from lysosomes to disease. Trends Mol Med 18:524–533. CrossRef Medline

Fernandes HJ, Hartfield EM, Christian HC, Emmanoulidou E, Zheng Y, Booth H, Bogetofte H, Lang C, Ryan BJ, Sardi SP, Badger J, Vowles J, Evetts S, Tofaris GK, Vekrellis K, Talbot K, Hu MT, James W, Cowley SA, Wade-Martins R (2016) ER stress and autophagic perturbations lead to elevated extracellular α-synuclein in GBA-N370S Parkinson's iPSC-derived dopamine neurons. Stem Cell Rep 6:342–356. CrossRef Medline

Gong WJ, Golic KG (2004) Genomic deletions of the *Drosophila melanogaster* Hsp70 genes. Genetics 168:1467–1476. CrossRef Medline

Hara T, Nakamura K, Matsui M, Yamamoto A, Nakahara Y, Suzuki-Migishima R, Yokoyama M, Mishima K, Saito I, Okano H, Mizushima N (2006) Suppression of basal autophagy in neural cells causes neurodegenerative disease in mice. Nature 441:885–889. CrossRef Medline

Hindle S, Hebbar S, Sweeney ST (2011) Invertebrate models of lysosomal storage disease: what have we learned so far? Invert Neurosci 11:59–71. CrossRef Medline

Juhász G, Erdi B, Sass M, Neufeld TP (2007) Atg7-dependent autophagy promotes neuronal health, stress tolerance, and longevity but is dispensable for metamorphosis in *Drosophila*. Genes Dev 21:3061–3066. CrossRef Medline

Kinghorn KJ (2011) Pathological looping in the synucleinopathies: investigating the link between Parkinson's disease and Gaucher disease. Dis Model Mech 4:713–715. CrossRef Medline

Kinghorn KJ, Castillo-Quan JI, Bartolome F, Angelova PR, Li L, Pope S, Cochemé HM, Khan S, Asghari S, Bhatia KP, Hardy J, Abramov AY, Partridge L (2015) Loss of PLA2G6 leads to elevated mitochondrial lipid peroxidation and mitochondrial dysfunction. Brain 138:1801–1816. CrossRef Medline

Komatsu M, Waguri S, Chiba T, Murata S, Iwata J, Tanida I, Ueno T, Koike M, Uchiyama Y, Kominami E, Tanaka K (2006) Loss of autophagy in the central nervous system causes neurodegeneration in mice. Nature 441:880–884. CrossRef Medline

Li M, Khambu B, Zhang H, Kang JH, Chen X, Chen D, Vollmer L, Liu PQ, Vogt A, Yin XM (2013) Suppression of lysosome function induces autophagy via a feedback down-regulation of MTOR complex 1 (MTORC1) activity. J Biol Chem 288:35769–35780. CrossRef Medline

Malagelada C, Jin ZH, Jackson-Lewis V, Przedborski S, Greene LA (2010) Rapamycin protects against neuron death in vitro and in vivo models of Parkinson's disease. J Neurosci 30:1166–1175. CrossRef Medline

Maor G, Rencus-Lazar S, Filocamo M, Steller H, Segal D, Horowitz M (2013) Unfolded protein response in Gaucher disease: from human to *Drosophila*. Orphanet J Rare Dis 8:1–14. CrossRef Medline

Maor G, Cabasso O, Krivoruk O, Rodriguez J, Steller H, Segal D, Horowitz M (2016) The contribution of mutant *GBA* to the development of Parkinson disease in *Drosophila.* Hum Mol Genet. Advance online publication. Retrieved May 9, 2016. doi: 10.1093/hmg/ddw129. CrossRef Medline

Mills K, Eaton S, Ledger V, Young E, Winchester B (2005) The synthesis of internal standards for the quantitative determination of sphingolipids by tandem mass spectrometry. Rapid Commun Mass Spectrom 19:1739–1748. CrossRef Medline

Myllykangas L, Tyynelä J, Page-McCaw A, Rubin GM, Haltia MJ, Feany MB (2005) Cathepsin D-deficient *Drosophila* recapitulate the key features of neuronal ceroid lipofuscinoses. Neurobiol Dis 19:194–199. CrossRef Medline

Orvisky E, Park JK, LaMarca ME, Ginns EI, Martin BM, Tayebi N, Sidransky E (2002) Glucosylsphingosine accumulation in tissues from patients with Gaucher disease: correlation with phenotype and genotype. Mol Genet Metab 76:262–270. CrossRef Medline

Osellame LD, Rahim AA, Hargreaves IP, Gegg ME, Richard-Londt A, Brandner S, Waddington SN, Schapira AH, Duchen MR (2013) Mitochondria and quality control defects in a mouse model of Gaucher disease: links to Parkinson's disease. Cell Metab 17:941–953. CrossRef Medline

Palikaras K, Tavernarakis N (2012) Mitophagy in neurodegeneration and aging. Front Genet 3:297. CrossRef Medline

Ravikumar B, Sarkar S, Davies JE, Futter M, Garcia-Arencibia M, Green-Thompson ZW, Jimenez-Sanchez M, Korolchuk VI, Lichtenberg M, Luo S, Massey DC, Menzies FM, Moreau K, Narayanan U, Renna M, Siddiqi FH, Underwood BR, Winslow AR, Rubinsztein DC (2010) Regulation of mammalian autophagy in physiology and pathophysiology. Physiol Rev:1383–1435.

Rera M, Bahadorani S, Cho J, Koehler CL, Ulgherait M, Hur JH, Ansari WS, Lo T Jr, Jones DL, Walker DW (2011) Modulation of longevity and tissue homeostasis by the *Drosophila* PGC-1 homolog. Cell Metab 14:623–634. CrossRef Medline

Robinson SW, Herzyk P, Dow JA, Leader DP (2013) FlyAtlas: database of gene expression in the tissues of *Drosophila melanogaster*. Nucleic Acids Res 41:D744–D750. CrossRef Medline

Roczniak-Ferguson A, Petit CS, Froehlich F, Qian S, Ky J, Angarola B, Walther TC, Ferguson SM (2012) The transcription factor TFEB links mTORC1 signaling to transcriptional control of lysosome homeostasis. Sci Signal 5:ra42. CrossRef Medline

Rogov V, Dötsch V, Johansen T, Kirkin V (2014) Interactions between autophagy receptors and ubiquitin-like proteins form the molecular basis for selective autophagy. Mol Cell 53:167–178. CrossRef Medline

Rubinsztein DC, Shpilka T, Elazar Z (2012) Mechanisms of autophagosome biogenesis. Curr Biol 22:R29–R34. CrossRef Medline

Shults CW (2006) Lewy bodies. Proc Natl Acad Sci U S A 103:1661–1668. CrossRef Medline

Sidransky E (2004) Gaucher disease: complexity in a "simple" disorder. Mol Genet Metab 83:6–15. CrossRef Medline

Sofola-Adesakin O, Castillo-Quan JI, Rallis C, Tain LS, Bjedov I, Rogers I, Li L, Martinez P, Khericha M, Cabecinha M, Bahler J, Partridge L (2014) Lithium suppresses Ab pathology by inhibiting translation in an adult *Drosophila* model of Alzheimer's disease. Front Aging Neurosci 6:1–10. CrossRef Medline

Suzuki M, Fujikake N, Takeuchi T, Kohyama-Koganeya A, Nakajima K, Hirabayashi Y, Wada K, Nagai Y (2015) Glucocerebrosidase deficiency accelerates the accumulation of proteinase K-resistant α-synuclein and aggravates neurodegeneration in a *Drosophila* model of Parkinson's disease. Hum Mol Genet 24:6675–6686. CrossRef Medline

Tatar M, Post S, Yu K (2014) Nutrient control of *Drosophila* longevity. Trends Endocrinol Metab 25:509–517. CrossRef Medline

Tognon E, Kobia F, Busi I, Fumagalli A, De Masi F, Vaccari T (2016) Control of lysosomal biogenesis and Notch-dependent tissue patterning by components of the TFEB-V-ATPase axis in *Drosophila melanogaster*. Autophagy 12:499–514. CrossRef Medline

Wagh DA, Rasse TM, Asan E, Hofbauer A, Schwenkert I, Dürrbeck H, Buchner S, Dabauvalle MC, Schmidt M, Qin G, Wichmann C, Kittel R, Sigrist SJ, Buchner E (2006) Bruchpilot, a protein with homology to ELKS/CAST, is required for structural integrity and function of synaptic active zones in *Drosophila*. Neuron 49:833–844. CrossRef Medline

Wong R, Piper MD, Wertheim B, Partridge L (2009) Quantification of food intake in *Drosophila*. PLoS One 4:e6063. CrossRef Medline

Xu H, Ren D (2015) Lysosomal physiology. Annu Rev Physiol 77:57–80. CrossRef Medline

Xu YH, Xu K, Sun Y, Liou B, Quinn B, Li RH, Xue L, Zhang W, Setchell KD, Witte D, Grabowski GA (2014) Multiple pathogenic proteins implicated in neuronopathic Gaucher disease mice. Hum Mol Genet 23:3943–3957. CrossRef Medline

Yu L, McPhee CK, Zheng L, Mardones GA, Rong Y, Peng J, Mi N, Zhao Y, Liu Z, Wan F, Hailey DW, Oorschot V, Klumperman J, Baehrecke EH, Lenardo MJ (2010) Termination of autophagy and reformation of lysosomes regulated by mTOR. Nature 465:942–946. CrossRef Medline

Zatloukal K, Stumptner C, Fuchsbichler A, Heid H, Schnoelzer M, Kenner L, Kleinert R, Prinz M, Aguzzi A, Denk H (2002) p62 is a common component of cytoplasmic inclusions in protein aggregation diseases. Am J Pathol 160:255–263. CrossRef Medline

Zoncu R, Bar-Peled L, Efeyan A, Wang S, Sancak Y, Sabatini DM (2011) mTORC1 senses lysosomal amino acids through an inside-out mechanism that requires the vacuolar H(+)-ATPase. Science 334:678–683. CrossRef Medline